
Methods in Cell Biology

VOLUME 71

Neurons: Methods and
Applications for the
Cell Biologist

Edited by

Peter J. Hollenbeck
James R. Bamburg



Prepared under the auspices of the American Society for Cell Biology

Methods in Cell Biology

VOLUME 71

Neurons: Methods and Applications for the Cell Biologist



Series Editors

Leslie Wilson

Department of Biological Sciences
University of California
Santa Barbara, California

Paul Matsudaira

Whitehead Institute for Biomedical Research
Department of Biology
Massachusetts Institute of Technology
Cambridge, Massachusetts

Methods in Cell Biology

Prepared under the auspices of the American Society for Cell Biology

VOLUME 71

Neurons: Methods and Applications for the Cell Biologist

Edited by

Peter J. Hollenbeck

Department of Biological Sciences
Purdue University
West Lafayette, Indiana

James R. Bamberg

Department of Biochemistry and Molecular Biology
Colorado State University
Fort Collins, Colorado



ACADEMIC PRESS

An imprint of Elsevier Science

Amsterdam Boston Heidelberg London New York Oxford
Paris San Diego San Francisco Singapore Sydney Tokyo

Cover Photo Credits:

Upper left: Dual fluorescence overlay on a phase image of a hippocampal neuron expressing a GFP-chimeric protein introduced by an adenoviral vector (see chapter 19). Mitochondria in this cell are labeled with mitotracker red. Image courtesy of Barbara Bernstein.

Upper Right: Neurons from rat hippocampus, fixed during the early stages of axonal elongation and stained for tubulin (green) and F-actin (red) reveal the density of microtubules in the cell bodies and axons, and of the actin filaments in the protrusive regions of the growth cones. (G. Ruthel and P. J. Hollenbeck)

Lower Left: Dual-label immunofluorescence image of axonal network of hippocampal neurons that have been stressed 24 hrs earlier by 30 minutes of ATP depletion. Green Fluorescence is staining of ADF/cofilin in rods. Red fluorescence is staining of phosphorylated neurofilament H. Image courtesy of Laurie Minamide.

Lower Right: Fluorescence overlay of phase contrast image of a cortical neuronal growth cone turning away from a boundary of aggrecan containing fluorescent dextran (red stripe). See chapter 7 for culturing methods of cortical neurons. Image courtesy of Patrick Sarmiere.

This book is printed on acid-free paper. (∞)

Copyright © 2003, Elsevier Science (USA).

All Rights Reserved.

No part of this publication may be reproduced or transmitted in any form or by any means, electronic or mechanical, including photocopy, recording, or any information storage and retrieval system, without permission in writing from the Publisher.

The appearance of the code at the bottom of the first page of a chapter in this book indicates the Publisher's consent that copies of the chapter may be made for personal or internal use of specific clients. This consent is given on the condition, however, that the copier pay the stated per copy fee through the Copyright Clearance Center, Inc. (222 Rosewood Drive, Danvers, Massachusetts 01923), for copying beyond that permitted by Sections 107 or 108 of the U.S. Copyright Law. This consent does not extend to other kinds of copying, such as copying for general distribution, for advertising or promotional purposes, for creating new collective works, or for resale. Copy fees for pre-2003 chapters are as shown on the title pages. If no fee code appears on the title page, the copy fee is the same as for current chapters. 0091-679X/2003 \$35.00

Permissions may be sought directly from Elsevier's Science & Technology Rights Department in Oxford, UK: phone: (+44) 1865 843830, fax: (+44) 1865 853333, e-mail: permissions@elsevier.com.uk. You may also complete your request on-line via the Elsevier Science homepage (<http://elsevier.com>), by selecting "Customer Support" and then "Obtaining Permissions."

Academic Press

An Elsevier Science Imprint.

525 B Street, Suite 1900, San Diego, California 92101-4495, USA

<http://www.academicpress.com>

Academic Press

84 Theobald's Road, London WC1X 8RR, UK

<http://www.academicpress.com>

International Standard Book Number: 0-12-352565-9 (case)

International Standard Book Number: 0-12-352566-7 (paperback)

PRINTED IN THE UNITED STATES OF AMERICA

03 04 05 06 07 08 9 8 7 6 5 4 3 2 1

CONTENTS

Contributors	xi
Preface	xv
1. Comparing the Properties of Neuronal Culture Systems: A Shopping Guide for the Cell Biologist	
<i>Peter J. Hollenbeck and James R. Bamburg</i>	
I. Introduction	2
II. Approaching Experimental Questions Using Neurons	2
III. Choosing a Neuronal Culture System	8
IV. Conclusions	14
References	15
2. Growing and Working with Peripheral Neurons	
<i>Yan He and Peter W. Baas</i>	
I. Introduction	18
II. Methods	19
III. Cultures	31
References	34
3. Dissection and Culturing of Chick Ciliary Ganglion Neurons: A System Well Suited to Synaptic Study	
<i>Barbara W. Bernstein</i>	
I. General Introduction	38
II. Materials	42
III. Methods	43
IV. Variations on Dissection, Dissociation, and Culturing Themes	47
V. Concluding Comments	49
References	49

4. The Culture of Chick Forebrain Neurons	
<i>Steven R. Heidemann, Matthew Reynolds, Kha Ngo, and Phillip Lamoureux</i>	
I. Introduction	52
II. Growth and Development Characteristics	53
III. Isolation of Single Chick Forebrain Neurons	56
IV. Culture Conditions for Chick Forebrain Neurons	59
References	64
5. Growing and Working with Spinal Motor Neurons	
<i>Thomas B. Kuhn</i>	
I. Introduction	68
II. Incubation of Fertilized Chicken Eggs	69
III. Preparation of Chick Embryo	71
IV. Dissection of Intact Spinal Cords and Isolation of Ventral Halves	73
V. Enzymatic and Mechanical Dissociation of Intact Spinal Cords or Ventral Halves	77
VI. Plating Motor Neurons Spinal Cord Neurons	78
VII. Motor Neuron Enrichment by Density Gradient Centrifugation	79
VIII. Experimental Use of Motor Neuron Cultures and Spinal Cord Cultures	80
IX. Preparation of Solutions, Culture Dishes, Media, and Media Supplements	82
References	85
6. Avian Purkinje Neuronal Cultures: Extrinsic Control of Morphology by Cell Type and Glutamate	
<i>Peter L. Jeffrey, Vladimir J. Balcar, Ornella Tollhurst, Ron P. Weinberger, and Jenny A. Meany</i>	
I. Introduction	90
II. Methods and Systems	92
III. Applications	100
References	105
7. Culturing Hippocampal and Cortical Neurons	
<i>Peter J. Meberg and Matthew W. Miller</i>	
I. Introduction	112
II. Acquisition of Hippocampal and Cortical Neurons	113
III. Short-Term Culture Methods	117
IV. Long-Term Culture Methods	121
V. Summary	126
References	127

8.	Working with <i>Xenopus</i> Spinal Neurons in Live Cell Culture	
	<i>Timothy M. Gómez, Dan Harrigan, John Henley, and Estuardo Robles</i>	
	I. Introduction	130
	II. Neuronal Labeling	131
	III. Culturing <i>Xenopus</i> Spinal Neurons	139
	IV. Live Cell Imaging and Manipulations	148
	V. Summary	154
	References	154
9.	Culturing Neurons from the Snail <i>Helisoma</i>	
	<i>Christopher S. Cohan, James L. Karnes, and Feng-Quan Zhou</i>	
	I. Introduction	158
	II. Maintaining Animals	159
	III. Initial Dissection	160
	IV. Culturing Nerve Cells	163
	References	170
10.	The Tibial-1 Pioneer Pathway: An <i>in Vivo</i> Model for Neuronal Outgrowth and Guidance	
	<i>Jennifer Bonner, Kimberly A. Gerrow, and Timothy P. O'Connor</i>	
	I. Introduction	172
	II. Development of the Tibial-1 (Ti1) Pathway	173
	III. Guidance of Ti1 Axons	176
	IV. Analysis of Axon Guidance Mechanisms in Grasshopper Procedures	183
	V. Laboratory Protocols	186
	References	191
11.	Techniques to Dissect Cellular and Subcellular Function in the <i>Drosophila</i> Nervous System	
	<i>Heinrich J. G. Matthies and Kendal Broadie</i>	
	I. Introduction	196
	II. Background Sources of Information	196
	III. <i>Drosophila</i> as a Genetic Model System for Molecular Neurobiology	199
	IV. Biochemistry of the <i>Drosophila</i> Nervous System	203
	V. Cell Biology Techniques in the <i>Drosophila</i> Nervous System	216
	VI. Functional Analysis Techniques in the <i>Drosophila</i> Nervous System	224
	VII. <i>Drosophila</i> Electrophysiology	228
	References	238

12. PC12 Cells as a Model for Studies of Regulated Secretion in Neuronal and Endocrine Cells	
<i>T. F. J. Martin and R. N. Grishanin</i>	
I. Introduction	268
II. Propagation and Culture of PC12 Cells	270
III. Studying Secretion Using PC12 Cells	271
IV. Immunocytochemical Detection of Proteins in Intact and Permeable PC12 Cells	283
References	285
13. B35 Neuroblastoma Cells: An Easily Transfected, Cultured Cell Model of Central Nervous System Neurons	
<i>Carol A. Otey, Malika Boukhelifa, and Patricia Maness</i>	
I. Introduction	288
II. Applications Utilizing B35 and B50 Cells	289
III. Protocols	295
References	302
14. Live-Cell Imaging of Slow Axonal Transport in Cultured Neurons	
<i>Anthony Brown</i>	
I. Introduction	306
II. Culturing Neurons from Superior Cervical Ganglia	306
III. Transfecting Neurons by Nuclear Injection	310
IV. Injecting Neurons with Fluorescent Proteins	314
V. Observing Movement	314
VI. Conclusion	321
References	321
15. Making Proteins into Drugs: Assisted Delivery of Proteins and Peptides into Living Neurons	
<i>Gianluca Gallo</i>	
I. Introduction	326
II. Principles	326
III. Materials	330
IV. Methods	331
V. Conclusions and Perspectives	336
References	337

16. Transfection of Primary Central and Peripheral Nervous System Neurons by Electroporation	
<i>Cecilia Y. Martinez and Peter J. Hollenbeck</i>	
I. Introduction	340
II. Electroporation Theory and Principles	341
III. Electroporation Protocol for Chick Primary Neurons	344
IV. Rationale for Setting Electroporation Parameters	345
V. Discussion	349
References	350
17. Biolistic Transfection	
<i>Paul C. Bridgman, Michael E. Brown, and Irina Balan</i>	
I. Introduction	354
II. Parameters that Affect Success of the Method	355
III. Factors that May Affect Performance but Have Not Been Tested	365
IV. Future Developments or Improvements	365
V. Conclusion	367
References	367
18. Expression of Transgenes in Primary Neurons from Chick Peripheral and Central Nervous Systems by Retroviral Infection of Early Embryos	
<i>Peter J. Hollenbeck and D. M. Fekete</i>	
I. Introduction	370
II. Building Retroviral Vectors and Growing Functional Virus	371
III. Infecting Early Chick Embryos by Injection	379
IV. Dissecting Embryos and Culturing Neurons	382
V. Conclusions	385
References	386
19. Production and Use of Replication-Deficient Adenovirus for Transgene Expression in Neurons	
<i>L. S. Minamide, A. E. Shaw, P. D. Sarniere, O. Wiggan, M. T. Maloney, Barbara W. Bernstein, J. M. Sneider, J. A. Gonzalez, and James R. Bamburg</i>	
I. Introduction	388
II. Preparing Adenoviral Expression Vectors	391
III. Production of Adenovirus in HEK293 Cells	397
IV. Purification and Storage of Adenovirus Stocks	400
V. Titer Assays	402

VI. Safety Issues	405
VII. Infection of Primary Neurons	406
VIII. Conclusions and Perspectives	413
References	414
Index	417
Volume in Series	435

CONTRIBUTORS

Numbers in parentheses indicate the pages on which the authors' contributions begin.

- Peter W. Baas** (17), Department of Neurobiology and Anatomy, Drexel University College of Medicine, Philadelphia, Pennsylvania 19129
- Irina Balan** (353), Department of Anatomy and Neurobiology, Washington University School of Medicine, St. Louis, Missouri 63110
- Vladimir J. Balcar** (89), Institute for Biomedical Research, University of Sydney, Sydney, New South Wales 2600, Australia
- James R. Bamburg** (1, 387), Department of Biochemistry and Molecular Biology, Colorado State University, Fort Collins, Colorado 80523
- Barbara W. Bernstein** (37, 387), Department of Biochemistry and Molecular Biology, Program in Molecular, Cellular, and Integrative Neurosciences, Colorado State University, Fort Collins, Colorado 80523
- Jennifer Bonner** (171), Program in Neuroscience, Department of Anatomy, University of British Columbia, Vancouver, British Columbia, V6T 1Z3 Canada
- Malika Boukhelifa** (287), Department of Cell and Molecular Physiology, University of North Carolina School of Medicine, Chapel Hill, North Carolina 27599
- Paul C. Bridgman** (353), Department of Anatomy and Neurobiology, Washington University School of Medicine, St. Louis, Missouri 63110
- Kendal Broadie** (195), Department of Biological Sciences, Vanderbilt University, Nashville, Tennessee 37235
- Anthony Brown** (305), Neurobiotechnology Center and Department of Neuroscience, Ohio State University, Columbus, Ohio 43210
- Michael E. Brown** (353), Department of Anatomy and Neurobiology, Washington University School of Medicine, St. Louis, Missouri 63110
- Christopher S. Cohan** (157), Division of Anatomy and Cell Biology, University at Buffalo, Buffalo, New York 14214
- Donna M. Fekete** (369), Department of Biological Sciences, Purdue University, West Lafayette, Indiana 47907
- Gianluca Gallo** (325), Department of Neurobiology and Anatomy, Drexel University College of Medicine, Philadelphia, Pennsylvania 19129
- Kimberly A. Gerrow** (171), Program in Neuroscience, Department of Anatomy, University of British Columbia, Vancouver, British Columbia, V6T 1Z3 Canada
- Timothy M. Gómez** (129), Department of Anatomy, Cell and Molecular Biology Training Program, University of Wisconsin Medical School, Madison, Wisconsin, 53706

- J. A. Gonzalez** (387), Department of Biochemistry and Molecular Biology, Program in Molecular Cellular and Integrative Neuroscience, Colorado State University, Fort Collins, Colorado 80523
- R. N. Grishanin** (267), Department of Biochemistry, University of Wisconsin, Madison, Wisconsin 53706
- Dan Harrigan** (129), Department of Anatomy, Cell and Molecular Biology Training Program, University of Wisconsin Medical School, Madison, Wisconsin, 53706
- Yan He** (17), Department of Neurobiology and Anatomy, Drexel University College of Medicine, Philadelphia, Pennsylvania 19129
- Steven R. Heidemann** (51), Department of Physiology, Michigan State University, East Lansing, Michigan 48824
- John Henley** (129), Department of Molecular and Cell Biology, University of California, Berkeley, California
- Peter J. Hollenbeck** (1, 339, 369), Department of Biological Sciences, Purdue University, West Lafayette, Indiana 47907
- Peter L. Jeffrey** (89), Developmental Neurobiology Group, Children's Medical Research Institute, Westmead, New South Wales 2145, Australia
- James L. Karnes** (157), Department of Physical Therapy, D'Youville College, Buffalo, New York 14201
- Thomas B. Kuhn** (67), Department of Pharmaceutical Sciences, University of Montana, Missoula, Montana 59812
- Phillip Lamoureux** (51), Department of Physiology, Michigan State University, East Lansing, Michigan 48824
- M. T. Maloney** (387), Department of Biochemistry and Molecular Biology, Program in Molecular Cellular and Integrative Neuroscience, Colorado State University, Fort Collins, Colorado 80523
- Patricia Maness** (287), Biochemistry and Biophysics, University of North Carolina School of Medicine, Chapel Hill, North Carolina 27599
- Cecilia Y. Martinez** (339), Department of Biological Sciences, Purdue University, West Lafayette, Indiana 47906
- T. F. J. Martin** (267), Department of Biochemistry, University of Wisconsin, Madison, Wisconsin 53706
- Heinrich J. G. Matthies** (195), Department of Biological Sciences, Vanderbilt University, Nashville, Tennessee 37235
- Jennifer A. Meany** (87), Developmental Neurobiology Group, Children's Medical Research Institute, Westmead, New South Wales 2145, Australia
- Peter J. Meberg** (111), Department of Biology, University of North Dakota, Grand Forks, North Dakota 58202
- Matthew W. Miller** (111), Department of Biology, University of North Dakota, Grand Forks, North Dakota 58202
- L. S. Minamide** (387), Department of Biochemistry and Molecular Biology, Program in Molecular Cellular and Integrative Neuroscience, Colorado State University, Fort Collins, Colorado 80523

- Kha Ngo** (51), Department of Physiology, Michigan State University, East Lansing, Michigan 48824
- Timothy P. O'Connor** (171), Program in Neuroscience, Department of Anatomy, University of British Columbia, Vancouver, British Columbia, V6T 1Z3 Canada
- Carol A. Otey** (287), Department of Cell and Molecular Physiology, University of North Carolina School of Medicine, Chapel Hill, North Carolina 27599
- Matthew Reynolds** (51), Department of Physiology, Michigan State University, East Lansing, Michigan 48824
- Estuardo Robles** (129), Neuroscience Training Program, University of Wisconsin Medical School, Madison, Wisconsin, 53706
- P. D. Sarmiere** (387), Department of Biochemistry and Molecular Biology, Program in Molecular Cellular and Integrative Neuroscience, Colorado State University, Fort Collins, Colorado 80523
- A. E. Shaw** (387), Department of Biochemistry and Molecular Biology, Program in Molecular Cellular and Integrative Neuroscience, Colorado State University, Fort Collins, Colorado 80523
- J. M. Sneider** (387), Department of Biochemistry and Molecular Biology, Program in Molecular Cellular and Integrative Neuroscience, Colorado State University, Fort Collins, Colorado 80523
- Ornella Tolhurst** (89), Developmental Neurobiology Group, Children's Medical Research Institute, Westmead, New South Wales 2145, Australia
- Ronald P. Weinberg** (89), Oncology Research Group, Children's Medical Research Institute, Westmead, New South Wales 2145, Australia
- O. P. Wiggan** (387), Department of Biochemistry and Molecular Biology, Program in Molecular Cellular and Integrative Neuroscience, Colorado State University, Fort Collins, Colorado 80523
- Feng-Quan Zhou** (157), Neuroscience Center, University of North Carolina at Chapel Hill, Chapel Hill, North Carolina 27599

This Page Intentionally Left Blank

PREFACE

During the past five decades the practice of cell and tissue culture has become a cornerstone of research in cell biology. Growing cells for use in microscopic or biochemical studies is an entirely routine laboratory procedure. Yet many cell biologists who are comfortable handling immortalized cell lines remain intimidated by the aura surrounding the use of neurons, especially as primary cultures. This is unfortunate because the continual refinement of culture techniques and reagents has produced reliable procedures for obtaining, growing, and studying dozens of neuronal cell types with diverse and useful properties. It is the intention of this volume to stimulate the interest of cell biologists in utilizing neurons in their studies by demystifying the methods necessary to handle them. It is hoped that the collection here of detailed, current cell culture methods for neurons of all sorts will make working with neurons more appealing to the uninitiated.

But why should a cell biologist bother to study neurons in culture? What purpose can the neuron serve that the HeLa cell cannot? In fact, many important cell biological questions have been pursued differently—and sometimes more effectively—in neurons than in other cell types. For example, it is hard to imagine *Drosophila* our current knowledge of cellular morphogenesis, signal transduction, intracellular trafficking, exocytosis, or the cytoskeleton without the critical studies that have been performed in neurons. Even many areas once thought to be special features of neurons are in fact amply worthy of study by cell biologists. Some of these have, upon close analysis, proven to be more general features of cells that simply reach a pinnacle of development—and therefore accessibility—in neurons. It has long been clear, for instance, that fast axonal transport involves the same mechanisms as organelle traffic in other cells. And what is synapse formation except a specialized kind of cell–cell interaction? It behooves us to study neurons anytime that a phenomenon that interests us appears particularly well exposed there. To this end, this volume contains not only methods for growing a variety of neurons, but also procedures for employing them in specific experimental applications. In addition, we have included two *in vivo* systems—one of which is amenable to genetic manipulations—for those who need to study their cell biological question in a developmental or organismal context.

So what is it that makes the use of neurons seem daunting? They are typically primary cultures, and the dissection usually necessary to acquire them can seem laborious compared to thawing a tube of 3T3 cells. But this alone need not be an obstacle—primary culturing of nonneuronal cells, such as fibroblasts, is routine in laboratories around the world. Unlike fibroblasts, however, neurons are postmitotic cells, often with a very limited lifetime in culture, and thus require regular schedules of dissection coordinated with the timing of experiments. But freezing procedures for

primary tissue and the availability of neuronlike transformed cells ameliorate some of these problems, and these are treated in several chapters of this volume. Another part of the lore of neuronal cell culture is that they are difficult cells to transfect. However, in recent years a variety of vectors and procedures have been developed that will allow neurons to be used by most workers whose studies require the introduction and expression of exogenous DNA and proteins, and this volume also contains several chapters on these methods. Finally, there is the perception that the culture media and growth conditions for neurons are more finicky than for other cells, or even that they are incompletely defined. Although we neuronal cell cultists have not always helped to dispel this “eye of newt” reputation, the methods presented in this volume have been chosen for their robustness and reliability. If you can grow BHK cells, you can grow sensory neurons, and the others described here as well. Because there have been other volumes in this series dedicated to cell culture methods, we have chosen not to repeat the general information on biological safety cabinets, media, incubators, etc., an excellent review of which may be found in Volume 57 of this series.

The editors heartily thank the contributors of this volume for sharing their hard-won expertise at using neurons for cell biological studies. We also thank the *Methods in Cell Biology* series editors for their help and advice in assembling this volume.

Peter Hollenbeck
Jim Bamberg

CHAPTER 1

Comparing the Properties of Neuronal Culture Systems: A Shopping Guide for the Cell Biologist

Peter J. Hollenbeck^{*} and James R. Bamberg[†]

^{*}Department of Biological Sciences
Purdue University
West Lafayette, Indiana 47907

[†]Department of Biochemistry and Molecular Biology
Colorado State University
Fort Collins, Colorado 80523

-
- I. Introduction
 - II. Approaching Experimental Questions Using Neurons
 - A. Cell Behavior and Differentiation
 - B. Intracellular Events
 - III. Choosing a Neuronal Culture System
 - A. Basic Biological Properties
 - B. Developmental Properties
 - C. Source, Culture, and Handling Properties
 - D. Ease and Cost of Obtaining and Growing Neurons
 - IV. Conclusions
 - References

Cell biologists of many stripes may find that their question of interest can be studied to advantage in neurons. However, they will also find that “neurons” include many and diverse cell types among which perhaps just one or a few may be ideal for a particular experiment. This chapter discusses the properties, relative complexity, and cost of primary neurons and neuronal cell types from different species and parts of the nervous system and compares their utility for different kinds of cell biological experiments.

I. Introduction

For the purpose of performing cell biological experiments, not all neurons are created equal. Both *in vivo* and *in vitro*, neurons from different parts of the nervous system are at least as varied in their properties as, for instance, epithelial cells. In addition, if we consider different species, including invertebrates, the range of cell biological properties becomes very wide. Choosing the correct neuron to study in culture requires the scrutiny of many cellular features, including cell size; neurite length, diameter, and type; growth cone size and rate of advance; biological responsiveness; and lifetime in culture. Important ancillary features that also figure in the choice of a system include the ease and cost of obtaining and maintaining neurons, and their accessibility to various experimental techniques, such as transfection, microinjection, or protein loading.

It is also worth noting here that not all parts of a single neuron are created equal. For example, axonal and dendritic growth cones of a polarized neuron show different motility behavior, can express unique receptors, and respond quite differently to environmental cues. This degree of spatial differentiation has been compared frequently—and only slightly naively—to the apical and basolateral domains of epithelial cells. Thus, cell biologists seeking to elucidate particular questions using neurons need not only choose the right neuron, but also the right end. In fact, neurons provide a polarized and compartmentalized system in which it is possible to separate and identify molecules that are unique to each domain (Job and Eberwine, 2001), something that cannot be accomplished for the cytoplasmic compartments of other polarized cells.

We attempt here to aid the experimentalist in choosing the right neuronal culture system. We first offer a general review of some major cell biological questions and the cultured neurons in which they have been studied effectively. Then, we survey a number of properties of different neuronal culture systems as a guide to weighing which systems suit particular experimental needs. Much of the information necessary to evaluate different culture systems is summarized in Tables I–IV. For a thorough treatment of the general principles of cell culture, we refer the reader to Volume 57 in this series.

II. Approaching Experimental Questions Using Neurons

Many cell biological problems have been pursued productively in one or more neuronal systems. Some examples follow.

A. Cell Behavior and Differentiation

1. Cell Crawling and Navigation

Many workers have studied the capacity of the neuronal growth cone to advance over a culture substratum and to respond to specific guidance cues such as

Table I
Names and Sources of Neurons and Cell Lines

	Name	Source	Chapter
Peripheral neurons	Sensory	Embryonic chick dorsal root ganglia	2
		Grasshopper embryonic limb	10
	Sympathetic	Embryonic chick paravertebral chain ganglia or embryonic rodent superior cervical ganglion	2 and 14
	Buccal ganglion	Buccal ganglion of freshwater snail, <i>Heliosoma</i>	9
Central neurons	Hippocampal	Embryonic rat brain	7
	Cortical	Embryonic rat brain	7
	Spinal motor	Embryonic chick spinal cord	5
	Spinal neurons	<i>Xenopus</i> neural tube	8
	Ciliary	Embryonic chick ciliary ganglion	3
	Purkinje cells	Embryonic chick brain (cerebellum)	6
	Forebrain	Embryonic chick brain	4
Cell lines	PC12	Pheochromocytoma, originally isolated from rat	12
	B35	Neuroblastoma, originally isolated from rat central nervous system	13

substratum-bound molecules or cell surface molecules of other cells. Most convenient culture systems that produce an active growth cone have been used for this purpose at one time or another, but several have been particularly amenable. For example, vertebrate retinal ganglion cells show clear cell–cell attractions and repulsions in culture (Cox *et al.*, 1990) and their growth cones respond to specific extracellular signaling molecules involved in axonal guidance *in vivo* (Mann and Holt, 2001), as do those of vertebrate sensory neurons (Nakamura *et al.*, 2000). Large invertebrate neurons, such as those of the snails *Aplysia* (Schafer *et al.*, 2002) and *Heliosoma* (Chapter 9), have also been useful because of their large size and ability to recapitulate in culture their patterns of *in vivo* outgrowth. Studies of growth cone guidance and navigation within intact or partially dissected embryos have been carried out successfully in transparent embryos such as zebrafish (Whitlock and Westerfield, 1998), as well as in *Drosophila* (Godenschwege *et al.*, 2002) and the grasshopper, *Schistocerca americana* (Isbister and O'Connor, 2000; Chapter 10). The former two systems have the advantage of genetic manipulation.

2. Protrusive Activity

As with crawling and navigation, many neuronal culture systems have been used for the study of cytoskeletal, membrane, and signaling events in the protrusive activity of the growth cone. The extreme thinness of the growth cone, along with its complex behavior and response to signaling molecules, makes it as attractive as the best lamellipodia of nonneuronal cells. Invertebrate neurons with

Table II
Basic Biological Properties of Cultured Neurons

Name	Cell body diameter	Neurite diameter	Growth rate ^b
Chick sensory (DRG)	20–25 μm	0.5–1 μm	40 $\mu\text{m}/\text{h}$
Chick sympathetic	10–15 μm^a	0.4 μm	40 $\mu\text{m}/\text{h}$
Rat sympathetic (SCG)	20–25 μm^a	0.–1 μm	40 $\mu\text{m}/\text{h}$
Chick ciliary	23 μm^c	0.5–1.5 μm	25–35 $\mu\text{m}/\text{h}$
Chick spinal motor	20–50 μm^c	1–2 μm	25 $\mu\text{m}/\text{h}$
Chick forebrain	15 μm	0.5–1 μm	5–10 $\mu\text{m}/\text{h}^d$
Rat hippocampal	20–25 μm	0.2–1 μm	4–8 $\mu\text{m}/\text{h}^d$
Rat cortical	15–20 μm	0.2–1 μm	4–8 $\mu\text{m}/\text{h}^d$
<i>Xenopus</i> spinal neurons	10–20 μm	0.4–3 μm	2–4 $\mu\text{m}/\text{h}^f$ 40 $\mu\text{m}/\text{h}^f$
Chick purkinje	8–20 μm^e	0.2–1 μm	2 $\mu\text{m}/\text{h}$
<i>Heliosoma</i> buccal ganglion	60–100 μm	5–10 μm^g 0.5–2 μm^h	0 $\mu\text{m}/\text{h}^g$ 15–25 $\mu\text{m}/\text{h}^h$
Grasshopper T11	20 $\mu\text{m} \times 10 \mu\text{m}^a$	0.5–1.5 μm	5–10 $\mu\text{m}/\text{h}^j$
PC12	15–20 μm^a	0.5–1 μm	< 30 $\mu\text{m}/\text{day}$
B35 neuroblastoma	10–20 μm	0.5–1 μm^i	30 $\mu\text{m}/\text{day}$

These values are intended to help distinguish between particularly fast- or slow-moving growth cones in choosing a culture system.

^aBecause these neurons can develop significantly elongated cell bodies, diameters are approximate or listed as length \times width. ^bGrowth rates for axons in culture vary widely with culture conditions, substrata, and time in culture. ^cDifferent classes of neurons in these cultures can be distinguished by their diameters; ciliary neurons average 23 μm in diameter whereas choroid neurons average 13 μm in diameter. ^dA rough net rate for pulsatile growth averaged over 1–2 days. ^ePurkinje neurons start out at about 8 μm in diameter when plated and mature to larger sizes by 21 days in culture. ^fOn a highly adhesive substrate, growth rates are low, but increase >10-fold on laminin. ^gThe primary explanted axon has a large diameter and forms a large growth cone that is not motile. ^hIn a presence of a *Heliosoma* brain extract, small motile growth cones sprout from the soma and axon tip. ⁱDifferentiated with dibutyryl cyclic AMP. ^jThe rate of growth is faster in the region of another neuron or guidepost cell and slower when extending along the epithelium.

very large growth cones such as *Aplysia* (Schaefer *et al.*, 2002) and *Heliosoma* (Chapter 9) have proven useful for light microscope studies. A variety of smaller vertebrate neurons, both central and peripheral, have been used to study protrusive activity, including rodent sensory (Lewis and Bridgman, 1992) and cortical (Boukhelifa *et al.*, 2001) neurons, and chick sympathetic (Dailey and Bridgman, 1989) and spinal motor (Brown *et al.*, 2000) neurons. Because growth cones of some central neurons advance with characteristics different than those of peripheral neurons in culture, rat hippocampal neurons have been useful subjects despite their small size (Ruthel and Banker, 1999).

3. Development of Cell Polarity

Several kinds of neurons can be induced to differentiate into their completely polarized form in culture, producing both an axon and dendrites. These include

Table III
Developmental Properties of Cultured Neurons

Name	No. of cells available	Minimum density of cultures ^a	Maximum time in culture ^b
Chick sensory (DRG)	10 ⁴ per ganglion 20 ganglia per embryo	10,000/cm ²	1–5 days
Chick sympathetic	10 ³ per ganglion 20 ganglia per embryo (in two chains)	10,000/cm ²	1–5 days, longer if differentiated to produce dendrites
Rat sympathetic (SCG)	10 ⁴ per ganglion, two ganglia per rat	< 100/cm ² (with antioxidants)	1–5 days, longer if differentiated to produce dendrites
Chick ciliary	1.75 × 10 ⁴ /ganglion (E8), two ganglia per embryo	8,000/cm ²	14 days
Chick spinal motor	10 ⁶ per spinal cord; 1–2 × 10 ⁵ per ventral half	20,000/cm ²	14 days
Chick forebrain	5 × 10 ⁷ per forebrain	> 5,000/cm ²	5–7 days in air medium; 14 days in CO ₂ medium
Rat hippocampal	5 × 10 ⁵ per rat pup	1,000/cm ²	>3 weeks
Rat cortical	3 × 10 ⁷ per rat pup	10,000/cm ²	>3 weeks
<i>Xenopus</i> spinal neurons	100 per embryo	100/cm ²	2 days
Chick purkinje	1.5 × 10 ⁶ cells per embryo	2,000 cells/mm ²	>3 weeks
<i>Heliosoma</i>	10–12 per ganglion 30–50 per <i>Heliosoma</i> brain	1 cell per plate	12–24 h on poly-lysine 3–7 days conditioned medium
Grasshopper Til	1 per embryo	<i>In vivo</i> system	<i>In vivo</i> system
PC12	Mitotic cell line	1000/cm ²	14 days
B35 neuroblastoma	Mitotic cell line	4,500/cm ²	5 days

^aFor some of these systems, the minimum achievable cell density in culture has not yet been determined; these values are the minimum reported thus far. ^bSome of these systems have not been optimized for long survival in culture. The times listed may be exceeded with future modifications.

rat hippocampal neurons (Fletcher and Banker, 1989; Chapter 7), rat or mouse cortical neurons (Hayashi *et al.*, 2002; Chapter 7), rat sympathetic neurons (Bruckenstein and Higgins, 1988; Lein *et al.*, 1995; Wang *et al.*, 1996), and chick forebrain neurons (Chapter 4). Essentially all neurons grown in culture also establish significant polarity by producing axons or at least the more generic processes referred to as neurites.

B. Intracellular Events

1. Cytoskeletal Transport and Dynamics

The movement, assembly, and disassembly of the cytoskeleton had been studied successfully in cell bodies, axons, and growth cones of a number of common

Table IV
Experimental Properties of Cultured Neurons

Name	Optical properties	Growth conditions	Preparation requirements	Difficulty of preparation	Overall cost
Chick sensory (DRG)	Good	37°C, air incubator	Timed fertile eggs Stereoscope	Easy dissection	Low
Chick sympathetic	Good	37°C, air incubator	Timed fertile eggs Stereoscope	Easy dissection	Low
Rat sympathetic (SCG)	Thin axons Good	37°C, air incubator short term; CO ₂ incubator long term	Timed pregnant rat Stereoscope	Moderate dissection, handling neonates or adult female euthanasia	Moderate
Chick ciliary	Good	37°C, CO ₂ incubator	Timed fertile eggs Stereoscope	Moderate dissection	Low
Chick forebrain	Good	37°C, air incubator	Timed fertile eggs Stereoscope	Easy dissection	Low
Rat hippocampal	Good	37°C, CO ₂ incubator	Timed pregnant rat Stereoscope	Moderate dissection Adult female euthanasia	Moderate if cell stocks are frozen Expensive if only fresh cells are used
Rat cortical	Good	37°C, CO ₂ incubator	Timed pregnant rat Stereoscope	Easy dissection Adult female euthanasia	Low to moderate if cell stocks are frozen Moderate to expensive if only fresh cells are used
<i>Xenopus</i> spinal neurons	Good	Room temperature (20–25°C)	Gravid female, adult male frog Stereoscope	Moderate dissection	Moderate to high
Chick purkinje	Fair to good ^a	37°C, CO ₂ incubator	Timed fertile eggs Stereoscope	Easy dissection	Low

<i>Heliosoma</i>	Excellent for very large growth cones in non motile state ^b	Room temperature (20–25°C)	Adult snail	Moderate dissection	Low for small number of neurons
	Good for small growth cones in motile state ^b	<i>Heliosoma</i> brain extract needed for motile growth cones	Stereoscope		
Grasshopper sensory	Fair— <i>in vivo</i> preparation	Room temperature (20–25°C)	Grasshopper embryos Stereoscope	Moderate dissection	Low for single neuron
PC12	Good	37°C, CO ₂ incubator	Tissue culture hood	None—cell line	Low
B35 neuroblastoma	Good	37°C, CO ₂ incubator	Tissue culture hood	None—cell line	Low

^aAstrocytes required in coculture for Purkinje cell survival and differentiation. Granule cell addition required for obtaining most mature phenotype. Neurons aggregate and processes fasciculate when cocultured with ED8 astrocytes, but single cells predominate when cocultured with ED16 astrocytes. ^bLarge growth cone on primary explanted axon is nonmotile and remains attached to poly-lysine-coated substrate even during collapse of the cytoskeleton. Small motile growth cones develop in the presence of *Heliosoma* brain extract.

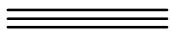
vertebrate neurons in culture. For example, studies involving light and electron microscopy have employed rat sympathetic superior cervical ganglion (SCG) (Wang *et al.*, 2000; Roy *et al.*, 2000; Yu *et al.*, 2000), chick sensory (Bamburg *et al.*, 1986), and *Xenopus* motor neurons (Chang *et al.*, 1999; Chapter 8).

2. Exocytosis, Endocytosis, and Recycling

Endocytosis and endocytic recycling have been studied in the distal axon and growth cones of several cultured neurons, including chick dorsal root ganglia (DRG) (Overly and Hollenbeck, 1996), sympathetic (Bernstein *et al.*, 1998), and ciliary ganglion (Diefenbach *et al.*, 1999) neurons, the frog neuromuscular junction (Betz *et al.*, 1992), and sensory neurons of *Aplysia* (Bailey *et al.*, 1992).

3. Organelle Transport

The squid giant axon, while not strictly speaking an intact cell in culture, has been used extensively to study the fast axonal transport of organelles (Allen *et al.*, 1982). It offers not only a good subject for light microscopy, but its size allows a variety of *in vitro* manipulations and provides adequate axoplasm to reactivate and observe organelle transport *in vitro* (Brady *et al.*, 1985, 1993) and to carry out biochemical studies (e.g., Vale *et al.*, 1985a,b). Organelle traffic has also been studied in the large bag cell neurons of *Aplysia* (Forscher *et al.*, 1987; Savage *et al.*, 1987) and in many smaller vertebrate neurons, including chick sensory and sympathetic (Hollenbeck, 1993; Morris and Hollenbeck, 1993, 1995) and rat sympathetic (Dailey and Bridgman, 1993) neurons. The study of organelle traffic in dendrites has of course been limited to cells such as hippocampal neurons (Overly *et al.*, 1996) that produce dendrites in culture.



III. Choosing a Neuronal Culture System

Studies of the roles of specific proteins in cell differentiation and/or development often benefit from the generation of cell lines with stable expression of transgenes. While this is not possible for postmitotic neurons, several immortalized cell lines can be carried in culture indefinitely but can also be differentiated into neuron-like cells. Two of these, PC12 cells and B35 cells, are discussed in Chapters 12 and 13. While these cells have proven very useful in answering important cell biological questions about neuronal differentiation and development, there are no cell lines that fully differentiate into functional neurons. This section and Tables I–IV summarize the variables that make specific neuronal culture systems practical for various kinds of experiments and which are the most important in choosing which neuronal culture system to work with.

A. Basic Biological Properties

1. Dimensions

The size of the cell body, axon, and growth cone are important to consider for most experimental applications of cultured neurons (see Table II). Whether a neuron has desirable optical qualities and whether it is a good subject for direct manipulations such as electrophysiological measurements will depend at least in part on its dimensions. Commonly used neurons have cell body diameters that vary from the small neurons of the rat hippocampus, chick forebrain, or *Drosophila* embryo, which are around 10 μm , up to large invertebrate cells such as *Heliosoma* buccal ganglion neurons with diameters of 100 μm . Not surprisingly, the cell body diameter is directly related to the axon or neurite diameter, which also varies widely from small vertebrate neurons with axon diameters $<1 \mu\text{m}$ to invertebrates such as *Heliosoma* (5–10 μm) and upward to squid giant axon (500–800 μm). It is important to consider that the projected diameter of the axon can be affected strongly by culture conditions: a wider, flatter axon better suited to light microscopic observation has been obtained by altering substratum conditions for *Xenopus* motor neurons (Chang *et al.*, 1999) and by treating *Drosophila* neuroblasts with cytochalasin B (Saito and Wu, 1991). Growth cones, which can vary 10-fold in size among the neurons considered in this volume, likewise show significant variation in their size, shape, and behavior when the same neurons are grown on different substrata. In general, substrata that give the best spread and most readily observed growth cones also give the slowest outgrowth rates; e.g., the best substratum for observing the very large growth cones of *Heliosoma* allows virtually no motility (Chapter 9).

2. Growth Rate

The feasibility of studies of growth cone navigation, protrusive activity, or the growth cone cytoskeleton can depend on the rate and pattern of growth cone advance. These vary greatly, with growth cones of vertebrate peripheral neurons tending to move faster and more continuously than those of vertebrate central neurons, some of which advance in pulsatile fashion. *Xenopus* motor neurons have a very high rate of outgrowth, *in vitro* as *in vivo*. For a given type of neuron, the growth cone behavior and rate of advance typically depend strongly upon the exact culture substratum used (see later). Appropriate combinations of cell type and culture conditions can elicit the rapid initiation of growth cones after plating out (Chapters 2 and 3).

3. Length and Number of Neurites

Some of the neurons that form axons and dendrites in culture, such as hippocampal, cortical, and forebrain neurons, tend to form one or two long axons, whereas neurons from sympathetic and dorsal root ganglia form variable numbers. This can depend strongly on the culture substratum, which can regulate

not only the number of primary processes, but also the number and pattern of branches (Bray *et al.*, 1987). This is a significant consideration for studies in which the number, geometry, or complexity of processes is deemed important. In addition, for studies of the signaling mechanisms and cytoskeletal events involved in neurite branching (Gallo and Letourneau, 1998), it may be useful to take advantage of intrinsic and induced differences among neurons in the frequency and pattern of branching.

4. Species

Selecting the species that will be the source for cultured neurons or cell lines can determine the effectiveness or cross-reactivity of reagents. Viral vectors, DNA constructs, antibodies, protein-loading procedures, or antisense RNA may work across species lines, but the variety of sources for neurons provides some control over this. The species may also be important if animal-holding facilities are needed. For example, an egg incubator or freshwater aquarium may be more readily available than a rodent facility, and it is certainly less expensive. In addition, genetically tractable species such as *Drosophila* (Chapter 11) or neuron-like cell lines such as PC12 (Chapter 12) or B35 cells (Chapter 13) that are subject to stable transfection can provide superior opportunities for manipulation of gene expression.

B. Developmental Properties

1. Rate of Development

Questions concerning cytoplasmic reorganization, cell polarity, and the origin of growth cones can best be studied using neurons that form growth cones rapidly after plating, such as those from the chick ciliary ganglion (Chapter 3) or the rat SCG (Chapter 2). Neurons that differentiate more slowly or that grow neurites at a slow but sustained pace for many days might be more useful for studies in which newly introduced genes need time to be expressed in sufficient amounts to affect growth properties.

2. Production of Dendrites

For some applications, such as studies of the cytoskeleton or mRNA localization, it is desirable to choose a neuronal cell type that produces bona fide dendrites in culture. As described earlier, the best systems for this application are rat hippocampal neurons (Fletcher and Banker, 1989; Chapter 7), rat cortical neurons (Chapters 7 and 19), rat sympathetic neurons (Lein *et al.*, 1995; Chapter 2), and chick forebrain neurons (Chapter 4). The latter are less well characterized than the others, but their relative simplicity, purity, and high cell yield recommend them nonetheless.

3. Production of Synapses

Studies of cell–cell interaction, stimulated secretion, and synaptic transmission can be pursued in culture using either homologous or heterologous synapse-forming cultures. Chick sympathetic neurons can form axonal–somatic synapses within 2 days in culture, whereas rat hippocampal neurons, once they have developed dendrites with spines (2 weeks in culture), will develop many functional synapses between spines and axonal terminals. Chick ciliary ganglion neurons in high-density cultures will form large numbers of synapses within less than 12 h (Chapter 3).

4. Purity of Neurons in Different Preparations

Some sources of neurons, such as sensory ganglia, contain a significant fraction of glial or fibroblastic cells, even in early embryos. In cultures maintained for more than a day or two, these mitotic cells can overrun the neurons unless an anti-proliferative agent such as cytosine 1- β -arabinofuranoside (AraC) is used. Some neurons are sensitive to these agents, making their long-term use impractical, but most cultures will tolerate low but effective levels of AraC. There are sources of neurons such as chick forebrain or spinal cord that have vanishingly few non-neuronal cells and thus can be maintained as nearly pure cultures of neurons. The purity of primary neuron preparations is often critically dependent on the stage of embryo from which they are obtained. In some systems, nonneuronal cells can be removed efficiently from suspensions of tissue prior to plating out by mechanical methods (Chapter 19) or centrifugation (Chapter 5).

C. Source, Culture, and Handling Properties

1. Quantity of Neurons Available

The yield of neurons from a dissection procedure varies widely with the source (Table III) and must be high if neuronal cultures are to be used in biochemical procedures, metabolic labeling, or immunoblotting. For some applications, such as microscopy or single-cell polymerase chain reaction (PCR), it may actually be advantageous to have small numbers of neurons growing at low densities. Large invertebrate neurons are obtained in very small numbers, but each contains enough mass for PCR reactions and cloning. Some vertebrate sources, such as chick forebrain, can provide 10^8 – 10^9 cells from a relatively brief dissection. Peripheral ganglia, such as rat SCG and rat or chick DRG, as well as central nervous system (CNS) sources, such as chick spinal cord or rat cortex, provide intermediate numbers of cells, whereas rat hippocampus or *Xenopus* neural tube provide fewer still (Table III). Most neurons will grow in culture at a wide range of densities, and applications in this volume range from those requiring maximum cell mass per dish to those that require physically isolated neurons. It is common for neurons to tolerate high densities in culture ($\geq 5 \times 10^4$ cells cm^2), providing

adequate material for biochemical, metabolic labeling, or immunological procedures, as long as the necessary number of cells is available. Chick forebrain (Chapter 4) and rat cortex (Chapters 7 and 19) are particularly good systems for obtaining large numbers of relatively pure neurons and growing them at very high densities. However, many neurons will not grow well at extremely low densities. Hippocampal neurons are an exception, growing and differentiating well at densities as low as 10^3 cells cm^2 . Differentiated rat sympathetic neurons can be maintained at even lower densities. Chick forebrain and ciliary neurons will also grow at densities below 10^4 cells cm^2 . For many other neurons, experiments requiring single cells that have not contacted others must be carried out in the first few hours after plating, before extensive axonal growth causes cells to interact.

2. Culture Substratum

Many neurons can be grown on a variety of different substrata, ranging from tissue culture plastic to glass coated with organic polyions to more complex preparations of extracellular matrix molecules such as collagen or Matrigel. More elaborately prepared substrata may elicit more complex growth patterns and morphology than simpler substrata. However, in some cases, more desirable behavior may be produced by very simple substrata. For many vertebrate neurons, a simple polycation-coated substratum produces desirable properties such as large growth cones or complete differentiation of axons and dendrites. Many extracellular molecules such as laminin or fibronectin exert dramatic growth effects on neurons via receptor-mediated signaling. Thus for neurons cultured on simple substrata but in the presence of fetal bovine serum, the substrata may become altered via fibronectin binding. Many neurons and associated nonneuronal cells secrete materials that adhere to and modify the substrate so that even simple ones may become very complex over time (e.g., Mizel and Bamburg, 1976). These “microexudates” include glycosaminoglycans and proteoglycans.

3. Temperature and Atmosphere

Many vertebrate neurons require carefully controlled temperature for growth in the incubator as well as during observation on a microscope stage. For instance, chick and rodent neurons must be grown and handled at or near 37°C , whereas *Xenopus* and some invertebrate neurons can be maintained near ambient laboratory temperatures (Chapters 8 and 9). Vertebrate neurons also differ in their tolerance for air-buffered vs carbonate-buffered medium; the latter requires a CO_2 incubator and/or observation chamber. While most laboratory tissue culture incubators are excellent at maintaining temperature and appropriate CO_2 levels to hold culture pH, very little attention is usually paid to oxygen levels, which run about 18% in a normal CO_2 incubator. *In vivo*, most vertebrate neurons experience

oxygen concentrations in the 5–8% range, meaning that *in vitro* culture conditions are significantly hyperoxic. Recognition of the oxidative stress on neurons in culture, especially those from the CNS, has led to the development of antioxidant media and supplements that improve the long-term survival and health of the cells. The B27 supplement used commonly in culturing hippocampal and cortical neurons consists of enzymes for reducing superoxide and peroxide levels in addition to stimulants of the cellular antioxidant systems, such as reduced glutathione. However, even these supplements cannot overcome the oxidative stress put on hippocampal neurons cultured under a minimal layer (<3 mm) of medium. Specialized chambers and oxygen monitors are available for maintaining more physiological levels of oxygen through nitrogen displacement (e.g., Pro-ox model 110 from BioSpherix). Such systems are useful for applications in which low volumes of medium are required, such as the testing of expensive peptides or proteins that have to be added to cultures.

D. Ease and Cost of Obtaining and Growing Neurons

For many research questions in cell biology, there is likely to be more than one suitable neuronal culture system. If this is the case, then it only makes sense to use the one that is the least expensive to purchase, least expensive to house, easiest or least destructive to obtain, and easiest to grow and handle. This is an area in which neuronal cell lines look very attractive (Chapters 12 and 13). The following areas are worth considering (Table IV).

1. Suppliers

Most researchers have access to a supplier of timed pregnant rodents or day 0 fertilized chicken eggs. Those at universities with agriculture schools may find the availability and low price of the latter almost irresistible. However, acquiring freshwater snails or *Xenopus* may be just as easy in some locations. Do not underestimate the utility of an organism that is available anytime that you are ready.

2. Ease of Dissection

There is a large range in the relative ease of obtaining neurons by dissection from different sources. Although laboratories equipped with “good hands” will have no trouble learning to dissect out most of the tissues described in this volume, some of the dissections, such as rat hippocampus, are more involved than others. For such dissections, a factor to consider is the availability of an experienced worker to teach the procedure to laboratory members. Obtaining most peripheral ganglia is a skill that can be learned in one or two sittings, whereas the dissection of chick forebrains is so easy that workers with a modest amount of experience can perform it without the aid of a dissecting microscope.

3. Freezing and Recovering Cells

Neuronal cell lines are stored routinely under liquid N₂ and recovered into culture when needed. Although it is much less common to freeze and recover primary neurons, it is possible for some cell types and may be practical if each dissection is difficult or costly and provides far more cells than can be used immediately. The freezing of rat E18 hippocampal and cortical neurons (Chapters 7 and 19) provides from a single dissection a useful supply of neurons for many experiments. For example, one timed pregnant female rat typically carries 10 or more pups. These 10 pups will yield $5\text{--}6 \times 10^6$ hippocampal neurons and $>10^8$ cortical neurons each in a volume of several milliliters. This material can be divided into aliquots and frozen to good effect: the hippocampal dissection provides enough cells for a dozen or more typical cell biological experiments and the cortical preparation for even more, even for biochemical or immunological studies. Frozen hippocampal neurons have been recovered and kept in culture for several weeks and have successfully formed dendritic spines and neuronal networks that are indistinguishable from those made with freshly cultured cells. For some workers, this ability to maximize the products of a single dissection is what makes the rat CNS their system of choice.

4. Facilities

Different neuronal systems place different demands on animal facilities. Rodents require an animal house, chicken eggs only an incubator, and *Xenopus* or *Heliosoma* require freshwater aquaria. As researchers whose funds are consumed by animal maintenance know well, the security and cost of these facilities differ by orders of magnitude.

5. Bureaucracy and Karma

All researchers who employ animals in experiments must ask themselves how much of their time and effort they want to expend on animal care, and on filling out animal forms. Cracking open a fertilized chicken egg, dissecting a frog embryo, and sacrificing a pregnant female mammal are rightly considered to be very different by your institution's laboratory animal program, which may influence the choice of a culture system. In addition, other things being nearly equal, one always chooses a source for neurons that involves the destruction of the minimum number of adult animals, particularly cognizant ones.

IV. Conclusions

A wide range of cell biological and neurobiological questions can be addressed using neurons and neuron-like cell lines grown in culture, but a successful program of experiments requires the selection of the most appropriate culture system. This

volume provides detailed information on the maintenance and use of more than a dozen diverse neuronal systems, and it is hoped that this introduction and its tabular data will allow workers to identify the culture system that most closely matches their needs and resources.

References

- Allen, R. D., Metzals, J., Tasaki, I., Brady, S. T., and Gilbert, S. P. (1982). Fast axonal transport in squid giant axon. *Science* **218**, 1127–1129.
- Bailey, C. H., Chen, M., Keller, F., and Kandel, E. R. (1992). Serotonin-mediated endocytosis of APCAM: An early step of learning-related synaptic growth in *Aplysia*. *Science* **256**, 645–649.
- Bamburg, J. R., Bray, D., and Chapman, K. (1986). Assembly of microtubules at the tip of growing axons. *Nature* **321**, 788–790.
- Bernstein, B. W., DeWit, M., and Bamburg, J. R. (1998). Actin disassembles reversibly during electrically induced recycling of synaptic vesicles in cultured neurons. *Mol. Brain Res.* **53**, 236–250.
- Betz, W. J., Bewick, G. S., and Ridge, R. M. (1992). Intracellular movements of fluorescently labeled synaptic vesicles in frog motor nerve terminals during nerve stimulation. *Neuron* **9**, 805–813.
- Boukhelifa, M., Parast, M. M., Valtschanoff, J. G., LaMantia, A. S., Meeker, R. B., and Otey, C. A. (2001). A role for the cytoskeleton-associated protein palladin in neurite outgrowth. *Mol. Biol. Cell* **12**, 2721–2729.
- Brady, S. T., Lasek, R. J., and Allen, R. D. (1985). Video microscopy of fast axonal transport in extruded axoplasm: A new model for study of molecular mechanisms. *Cell Motil.* **5**, 81–101.
- Brady, S. T., Richards, B. W., and Leopold, P. L. (1993). Assay of vesicle motility in squid axoplasm. In “Methods in Cell Biology,” Vol. 39, pp. 191–202. Academic Press, San Diego.
- Bray, D., Bunge, M. B., and Chapman, K. (1987). Geometry of isolated sensory neurons in culture. *Exp. Cell Res.* **168**, 127–137.
- Brown, M. D., Cornejo, B. J., Kuhn, T. B., and Bamburg, J. R. (2000). Cdc42 stimulates neurite outgrowth and formation of growth cone filopodia and lamellipodia. *J. Neurobiol.* **43**, 352–364.
- Bruckenstein, D. A., and Higgins, D. (1988). Morphological differentiation of embryonic rat sympathetic neurons in tissue culture. II. Serum promotes dendritic growth. *Dev. Biol.* **128**, 337–348.
- Chang, S., Svitkina, T. M., Borisy, G. G., and Popov, S. V. (1999). Speckle microscopic evaluation of microtubule transport in growing nerve processes. *Nature Cell Biol.* **1**, 399–403.
- Cox, E. C., Muller, B., and Bonhoeffer, F. (1990). Axonal guidance in the chick visual system: Posterior tectal membranes induce collapse of growth cones from the temporal retina. *Neuron* **4**, 31–37.
- Dailey, M. E., and Bridgman, P. C. (1989). Dynamics of the endoplasmic reticulum and other membranous organelles in growth cones of cultured neurons. *J. Neurosci.* **9**, 1897–1909.
- Dailey, M. E., and Bridgman, P. C. (1993). Vacuole dynamics in growth cones: Correlated EM and video observations. *J. Neurosci.* **13**, 3375–3393.
- Diefenbach, T. J., Guthrie, P. B., Stier, H., Billups, B., and Kater, S. B. (1999). Membrane recycling in the neuronal growth cone revealed by FM1-43 labeling. *J. Neurosci.* **19**, 9436–9444.
- Fletcher, T. L., and Banker, G. A. (1989). The establishment of polarity by hippocampal neurons: The relationship between the stage of a cell’s development in situ and its subsequent development in culture. *Dev. Biol.* **136**, 446–454.
- Forscher, P., Kaczmarek, L. K., Buchanan, J. A., and Smith, S. J. (1987). Cyclic AMP induces changes in distribution and transport of organelles within growth cones of *Aplysia* bag cell neurons. *J. Neurosci.* **7**, 3600–3611.
- Gallo, G., and Letourneau, P. C. (1998). Localized sources of neurotrophins initiate axon collateral sprouting. *J. Neurosci.* **18**, 5403–5414.
- Godenschwege, T. A., Simpson, J. H., Shan, X., Bashaw, G. J., Goodman, C. S., and Murphey, R. K. (2002). Ectopic expression in the giant fiber system of *Drosophila* reveals distinct roles for roundabout (Robo), Robo2, and Robo3 in dendritic guidance and synaptic connectivity. *J. Neurosci.* **22**, 3117–3129.

- Hayashi, K., Kawai-Hirai, R., Ishikawa, K., and Takata, K. (2002). Reversal of neuronal polarity characterized by conversion of dendrites into axons in neonatal rat cortical neurons in vitro. *Neuroscience* **110**, 7–17.
- Hollenbeck, P. J. (1993). Products of endocytosis and autophagy are retrieved from axons by regulated bidirectional organelle transport. *J. Cell Biol.* **121**, 305–315.
- Isbister, C. M., and O'Connor, T. P. (2000). Mechanisms of growth cone guidance and motility in the developing grasshopper embryo. *J. Neurobiol.* **44**, 271–280.
- Job, C., and Eberwine, J. (2001). Localization and translation of mRNA in dendrites and axons. *Nature Rev. Neurosci.* **2**, 889–898.
- Lein, P., Johnson, M., Guo, X., Rueger, D., and Higgins, D. (1995). Osteogenic protein-1 induces dendritic growth in rat sympathetic neurons. *Neuron* **15**, 597–605.
- Lewis, A. K., and Bridgman, P. C. (1992). Nerve growth cone lamellipodia contain two populations of actin filaments that differ in organization and polarity. *J. Cell Biol.* **119**, 1219–1243.
- Mann, F., and Holt, C. E. (2001). Control of retinal growth and axon divergence at the chiasm: Lessons from *Xenopus*. *Bioessays* **23**, 319–326.
- Mizel, S. B., and Bamberg, J. R. (1976). Studies on the action of nerve growth factor. III. Role of RNA and protein synthesis in the process of neurite outgrowth. *Dev Biol.* **49**, 20–28.
- Morris, R. L., and Hollenbeck, P. J. (1993). Bidirectional transport of mitochondria in neurons is coordinated with axonal outgrowth and metabolism. *J. Cell Sci.* **104**, 917–927.
- Morris, R. L., and Hollenbeck, P. J. (1995). Axonal transport of mitochondria along microtubules and F-actin in living vertebrate neurons. *J. Cell Biol.* **131**, 1315–1326.
- Nakamura, F., Kalb, R. G., and Strittmatter, S. M. (2000). Molecular basis of semaphorin-mediated axon guidance. *J. Neurobiol.* **44**, 219–229.
- Overly, C. C., and Hollenbeck, P. J. (1996). Dynamic organization of endocytic pathways in axons of cultured sympathetic neurons. *J. Neurosci.* **16**, 6056–6064.
- Overly, C. C., Rieff, H. I., and Hollenbeck, P. J. (1996). Axonal and dendritic organelle transport in hippocampal neurons: Differences in organization and behavior. *J. Cell Sci.* **109**, 971–980.
- Roy, S., Coffee, P., Smith, G., Liem, R. K., Brady, S. T., and Black, M. M. (2000). Neurofilaments are transported rapidly but intermittently in axons: Implications for slow axonal transport. *J. Neurosci.* **20**, 6849–6861.
- Ruthel, G., and Banker, G. (1999). Role of moving growth cone-like “wave” structures in the outgrowth of cultured hippocampal axons and dendrites. *J. Neurobiol.* **39**, 97–106.
- Saito, M., and Wu, C. F. (1991). Expression of ion channels and mutational effects in giant *Drosophila* neurons differentiated from cell division-arrested embryonic neuroblasts. *J. Neurosci.* **11**, 2135–2150.
- Savage, M. J., Goldberg, D. J., and Schacher, S. (1987). Absolute specificity for retrograde fast axonal transport displayed by lipid droplets originating in the axon of an identified *Aplysia* neuron in vitro. *Brain Res.* **406**, 215–223.
- Schaefer, A. W., Kabir, N., and Forscher, P. (2002). Filopodia and actin arcs guide the assembly and transport of two populations of microtubules with unique dynamic parameters in neuronal growth cones. *J. Cell Biol.* **158**, 139–152.
- Vale, R. D., Reese, T. S., and Sheetz, M. P. (1985a). Identification of a novel force-generating protein, kinesin, involved in microtubule-based motility. *Cell* **42**, 39–50.
- Vale, R. D., Schnapp, B. J., Reese, T. S., and Sheetz, M. P. (1985b). Organelle, bead, and microtubule translocations promoted by soluble factors from the squid giant axon. *Cell* **40**, 559–569.
- Wang, J., Yu, W., Baas, P. W., and Black, M. M. (1996). Microtubule assembly in growing dendrites. *J. Neurosci.* **16**, 6065–6078.
- Wang, L., Ho, C. L., Sun, D., Liem, R. K., and Brown, A. (2000). Rapid movement of axonal neurofilaments interrupted by prolonged pauses. *Nature Cell Biol.* **2**, 137–141.
- Whitlock, K. E., and Westerfield, M. (1998). A transient population of neurons pioneers the olfactory pathway in the zebrafish. *J. Neurosci.* **18**, 8919–8927.
- Yu, W., Cook, C., Sauter, C., Kuriyama, R., Kaplan, P. L., and Baas, P. W. (2000). Depletion of a microtubule-associated motor protein induces the loss of dendritic identity. *J. Neurosci.* **20**, 5782–5791.

CHAPTER 2

Growing and Working with Peripheral Neurons

Yan He and Peter W. Baas

Department of Neurobiology and Anatomy
Drexel University College of Medicine
Philadelphia, Pennsylvania 19129

- I. Introduction
- II. Methods
 - A. Substrate
 - B. Media
 - C. Dissection
 - D. Preparation of Dissociated Cultures
 - E. Maintenance of Cultures
 - F. Preparation of Explant Cultures
 - G. Reducing Nonneuronal Contamination
- III. Cultures
 - A. Short-Term Chick Dorsal Root Ganglia Culture
 - B. Short-Term Rat Sympathetic Culture
 - C. Long-Term Rat Sympathetic Culture
- References

Cultures of vertebrate peripheral neurons have been used to address a variety of issues related to the cell biology of the neuron. They are particularly amenable to experimental manipulations, such as microinjection, and can be cultured under a variety of different conditions designed to meet the needs of the particular experiment. This chapter focuses on cultures of rat sympathetic neurons from the superior cervical ganglia and on cultures of chick sensory neurons from the lumbosacral dorsal root ganglia. Information is provided on methods for dissection, preparation of culture dishes and substrates, composition of media, relevant growth factors, reduction of nonneuronal contamination, and maintenance of the cultures.

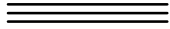
I. Introduction

Over the past several years various different kinds of neurons from the peripheral and central nervous systems of various different kinds of animals have been cultured successfully. These cultures have been used to investigate a number of different issues related to the cell biology of the neuron. Several factors contribute to the selection of a particular type of neuron for a particular study. Although some studies focus specifically on an issue related to one type of neuron, most studies are open to the use of different kinds of neurons. For example, our laboratory studies mechanisms of cytoskeletal organization and axonal transport, and these mechanisms are likely to be preserved across different types of neurons. In these cases, the main factor in choosing which neuron to use is how amenable a particular type of neuron is to the particular experimental manipulations that are required to carry out the study. In our laboratory, we most frequently culture rat hippocampal neurons, rat sympathetic neurons from the superior cervical ganglion, and chick sensory neurons from lumbosacral dorsal root ganglia. Hippocampal neurons, from the central nervous system, have the advantage of undergoing very stereotypical and well-defined stages of axonal and dendritic development. However, they are more tedious to culture, somewhat finicky, and generally die if microinjected. In contrast, the two types of peripheral neurons are easier to culture, more rugged, survive injection, and can be grown under a much wider variety of culture conditions tailored to specific experimental needs. The reason why we use chick for sensory neuronal cultures and rat for sympathetic cultures is simply because of the backlog of knowledge from previous work. It is certainly possible to culture rat sensory neurons and chick sympathetic neurons, but fewer studies have been performed on these cultures, at least in our field.

The cultures of sensory neurons have the advantage of simplicity, they generate axons but not dendrites, and display relatively simple morphologies. However, sympathetic cultures have the advantage of complexity, they generate dendrites as well as axons, and display a much wider range of axonal and dendritic behaviors depending on the culture conditions. Therefore, if the purpose of the study is simply to measure the effects of an experiment on axonal outgrowth or length, sensory neurons would be the better choice. However, if the purpose of the study is to investigate finer features of axogenesis, branch formation, dendrites, or other more complex issues, then sympathetic neurons would be the better choice. As far as we can tell, both types of neurons are about the same in terms of their viability to experimental manipulations, such as microinjection, axotomy, transfection, and application of anticytoskeletal drugs. The dorsal root ganglia (DRG) of chick embryos are much easier to dissect than the superior cervical ganglia of rat pups, but after dissection is completed, subsequent steps in the preparation and care of the cultures are quite similar.

There are superb chapters in other books that outline in great detail various options for generating these cultures (Bray, 1991; Higgins *et al.*, 1991; Mahanthappa and Patterson, 1998; Smith, 1998; Johnson, 2001). Our main

purpose here is not to be exhaustive with regard to options, but rather to share the methods that we have come to rely on in our laboratory, as well as insights that we have gained over the years.



II. Methods

A. Substrate

One of the most important issues for neuronal cell culture is substrate. Neurons are poorly adhesive cells compared to many kinds of cells that can be cultured, and yet adhesion to the substrate is absolutely essential for their viability and their capacity to extend neurites. In general, neurons do not adhere to plain glass or even to plastic culture dishes (except when methylcellulose is added to the medium; see later). There are several possibilities for treating these surfaces that enhance their capacity to adhere to cells. As with the rest of this chapter, we describe the most commonly used approaches in our laboratory. In theory, with appropriate substrate treatments, cultures can be grown either on the surface of tissue culture dishes or on glass coverslips. Glass coverslips offer a more optimal surface for light microscopy, but are hard to manipulate for experiments if they are simply placed inside petri dishes. To circumvent this problem, we routinely grow cultures on glass coverslips that are adhered to the bottom of a 35-mm petri dish into which a hole has been drilled. This permits the cells to be visualized easily using an inverted microscope, microinjected, and marked for relocation. Using terminology originally coined by the Banker laboratory, we refer to these hybrid dishes as “special dishes.” When culturing directly on plastic, it is important to buy dishes that are treated for cell culture, but for the manufacture of special dishes, it is fine to save money by using untreated petri dishes. Sometimes it is useful to prepare special dishes using glass coverslips that have been prepho-toetched for easy relocation of particular cells of interest. Details for cleaning glass coverslips and preparing special dishes are provided in Table 1.

The most common method for promoting the adhesion of neurons is to treat the plastic or glass with a series of positive charges, which are attracted to the negative charges on the surface of the cell membrane. We use poly-D-lysine for this. Several different varieties of polylysine are available; details on the one we use commonly are provided in Table 2. It is necessary to use a relatively low concentration of poly-D-lysine and to rinse very extensively after the glass or plastic is treated. Any excess poly-D-lysine that does not attach to the plastic or glass can be extremely toxic to the cells, as can too much poly-D-lysine that has attached. Generally speaking, we use either 0.1 or 1.0 mg/ml, depending on whether any toxicity arises with the higher concentration. The presence of serum in the medium usually permits the use of the higher concentration, while it is often necessary to use the lower concentration if there is no serum in the medium. Poly-D-lysine alone can be a reasonable substrate for chick sensory neurons (as well as cultures of brain neurons) but generally does not support axonal outgrowth particularly well from

Table I
Preparing Special Dishes

I. Cleaning Glass Coverslips

- A. Place circular glass coverslips (Carolina Biological Supply Company) or etched grid coverslips (Bellco) into ceramic coverslip holders. Immerse the holders under HNO_3 in a glass container. Let coverslips soak in HNO_3 overnight in the dark.
- B. Rinse coverslips once with double-distilled water and wash three more times, 1 hour each time.
- C. Dry coverslips in oven.

Note: Keep HNO_3 in dark at all times because it is light sensitive. If HNO_3 becomes brown rather than colorless, stop using it.

II. Attaching Coverslips to the Special Dishes

- A. Introduce a circular smooth-edged hole into the bottom of a 35-mm petri dish. This can be done using a vertical drill press with a forstner bit or with a lathe. The diameter of the hole can vary depending on the needs of the experiment; we generally use a diameter of 13 mm.
- B. Prepare a mixture of three parts of paraffin and one part of vaseline. Melt in hot water bath.
- C. Using a paint brush, paint a ring of wax around the hole in each dish. Take care not to paint too close to the hole and do not use too much wax. Too much wax can leak onto the region of the coverslip where the cells are to be plated.
- D. Invert the dish and place the clean coverslip on top of the hole.
- E. Put under inverted hot plate, let wax melt, and coverslip fall down evenly. Pull out and let cool before any wax slops into the well.
- F. Sterilize the dish and lid by spraying 70% ethanol evenly on the surface and radiating them under UV light in a tissue culture hood for at least 30 min. After the ethanol evaporates completely, the dishes are ready for plating neurons or coating with different substrates.

Note: If the cultures are ultimately to be used for electron microscopy, it is desirable to use a more heat-resistant adhesive such as epoxy to attach the coverslip to the plastic dish.

sympathetic neurons. The reason for this is unclear, but it may be that the poly-D-lysine is actually “too sticky” for sympathetic neurons.

A more favorable and more physiological substrate is provided by introducing laminin after the poly-D-lysine. The application of laminin, a biologically active matrix molecule, promotes better axonal outgrowth from sensory neurons and extraordinarily rapid and robust axonal outgrowth from the sympathetic neurons (Rivas and Goldberg, 1992; Tang and Goldberg, 2000). Laminin can either be applied over the poly-D-lysine prior to plating the cells or be added to the medium together with or after the cells have been plated. The precise morphology and rate of axonal outgrowth will vary somewhat depending on when the laminin is added. The laminin adheres to the positive charges of the poly-D-lysine and provides a robust substrate for the neurons. Even more robust results can be achieved using a partially defined mixture of substrate-related growth factors called Matrigel rather than laminin (Yu *et al.*, 2002). Additional details are provided in Table 2.

Years ago we commonly used a substrate of rat tail collagen to promote the attachment of sympathetic neurons. We rarely do this anymore because the substrate is rather thick, is rather three-dimensional (which is not good for microscopic analyses), and because axonal outgrowth is very slow on collagen.

Table II
Substrate Coating

I. Poly-D-lysine		
A. Prepare borate buffer (40 ml)		
Ingredient	Amount	Final concentration
Borax (Sigma)	190 mg	4.75 mg/ml
Boric acid (Sigma)	124 mg	3.1 mg/ml
Double-distilled H ₂ O	40 ml	100% (v/v)

Good for up to 1 month at room temperature.

B. To prepare 1 mg/ml stock solution, dissolve 10 mg of poly-D-lysine (Sigma) in 10 ml borate buffer.
C. Filter sterilize using a 0.2- μ m filter. Aliquot desired amount and freeze at -20° C.

D. Add 0.2 ml of poly-D-lysine to the well. Two different methods can be used, one with a higher concentration and the other with a lower concentration of poly-D-lysine. The higher concentration generally provides better adhesion, but sometimes can produce toxicity, particularly if serum-free medium is used. If the latter proves to be the case, then the lower concentration should be used.

Method 1: Coat the glass well with 1 mg/ml poly-D-lysine for 3 h at room temperature. Rinse the dish six times with sterile distilled water, 5 min each time. At the end, add 2 ml of water to the dish and keep the dish in a 37° C incubator overnight. On the next day, rinse the dish with water one more time. Take off water and let dish dry completely. Put the lid back on the dish and keep at room temperature. They are good for up to 1 month.

Method 2: Coat the glass well with 0.1 mg/ml poly-D-lysine (dilute 1 mg/ml stock solution 10 times with borate buffer) overnight at 4° C. On the next day, rinse the dish six times with sterile distilled water, 5 min each time. After the dish dries completely, put the lid back on the dish. They can be kept at room temperature for up to 1 month.

II. Laminin

A. Prepare poly-D-lysine-coated dishes as described previously.

B. On the day of culturing, dilute 10 μ l laminin (Invitrogen) in 1 ml Leibovitz's L-15 medium. Add 200 μ l diluted laminin into each glass-bottomed well that has been precoated with poly-D-lysine.

C. Incubate the dish in a 37° C, CO₂-free incubator for 3 to 4 h.

D. Take off laminin immediately before plating cells into the well.

III. Collagen

A. Purchase collagen derived from rat tail (BD Biosciences). The product will generally be roughly 4 mg/ml in a dilute acetic acid solution.

B. Collagen can be applied directly to the surface of a plastic culture dish. For glass, precoat with poly-D-lysine as described earlier.

C. The amount of collagen to produce a desirable substrate is determined empirically. Generally, 2–3 drops of the undiluted product is sufficient to coat the glass-bottomed well of a special dish. An insufficient amount of collagen will dry unevenly in patches.

D. Allow to air dry.

However, the collagen substrate has one advantage that is particularly helpful for certain types of experiments. Everyone who works with cultured neurons struggles with the fact that the neurons often lose their attachment and simply “float away” if they are extracted too strongly or exposed to anything that might mechanically or otherwise disturb them. When grown on rat tail collagen, sympathetic neurons are extremely well attached, such that they can be extracted with very high

concentrations of detergents such as Triton X-100, and even with high salt concentrations. This permits a clean separation of soluble and insoluble components of the cytoplasm for biochemical studies and also produces “squeaky clean” cytoskeletal polymers for immunostain analyses. We have found this particularly useful for immunoelectron microscopic analyses of tubulin isoforms within microtubules (Baas and Black, 1990). A collagen substrate is relatively easy to work with on plastic (see Table 2), but is somewhat harder to deal with on glass. The problem is that while the neurons are extremely well attached to the collagen, the collagen itself can sometimes roll off the glass or plastic in a sheet, which is more common on glass than on plastic. The glass needs to be pretreated with poly-D-lysine, but even this does not rectify the problem in many cases.

For making substrates of rat tail collagen, we used to prepare our own collagen by plucking collagenous tendons from a rat tail and dissolving them in acetic acid. This is relatively simple and there are published methods for doing so (Johnson and Argiro, 1983). However, it is now more time and cost-efficient to simply purchase sterile collagen solutions for cell culture. A few drops of the product are placed on the glass or plastic and are then smeared evenly using a Pasteur pipette into which a 90° bend has been introduced by placing it in a flame. (For glass, it is first necessary to treat with poly-D-lysine.) The collagen is then allowed to air dry. If insufficient collagen is applied, it will tend to dry in patches. The optimal quantity is best determined empirically. As noted earlier, we rarely use collagen substrates for dissociated cultures because they make for cultures with poor optical qualities for light microscopy and because the axons are very slow to grow. Our protocol for collagen coating is provided in Box 2.

B. Media

We generally use two different types of media, both of which are adequate for either sensory or sympathetic cultures. One of these is a modified L-15-based medium, which has the advantage of maintaining pH in air, but has the disadvantage of supporting cultures only for about 1 or perhaps 2 days. The other medium is an N2-based medium, which is excellent for long-term cultures, but requires a 5% carbon dioxide environment to maintain pH. Long-term cultures can be grown in the N2-based medium and then transferred to the L-15-based medium for short-term experiments on the microscope stage. We have found that peripheral neuronal cultures respond much better to L-15-based media than to media buffered with HEPES, although other laboratories have had good luck with HEPES (Gallo *et al.*, 1997). Formulations for the L-15-based and the N2-based media are provided in Table 3. The L-15-based medium requires serum to be present, whereas the N2-based medium contains supplements that permit it to be used either with or without serum. We have found that serum, although not required, appears to make the cells somewhat more resilient to experimental manipulations such as microinjection. Other laboratories have achieved excellent results with adult rat serum (Wang *et al.*, 2000), but we have not tried this. Both media contain

Table III

I. L-15-Based media		
A. L-15 Incomplete Medium (250 ml)		
Ingredient	Amount	Final concentration
Leibovitz's L-15 medium (GibcoBRL)	242 ml	96.8% (v/v)
D-(+)-Glucose solution (45%) (Sigma)	3.3 ml	0.6% (w/v)
200 mM L-glutamine (GibcoBRL)	2.5 ml	2 mM
Penicillin (10,000 units/ml) streptomycin (10,000 µg/ml) (Sigma)	2.5 ml	100 units/ml penicillin; 100 µg/ml streptomycin
Filter sterilize. Good for up to 3 weeks at 4°C.		
B. L-15 Blocking Medium (50 ml)		
L-15 incomplete medium	45 ml	90% (v/v)
Fetal bovine serum (HyClone)	5 ml	10% (v/v)
Filter sterilize. Good for up to 2 weeks at 4°C.		
C. L-15 Plating Medium (50 ml)		
L-15 incomplete medium	45 ml	90% (v/v)
Fetal bovine serum (HyClone)	5 ml	10% (v/v)
Nerve growth factor (Upstate)	50 µl (from 100 µg/ml stock)	100 ng/ml
Filter sterilize. Good for up to 1 week at 4°C.		
II. N2-Based Media For Short-Term Culture		
N2 Medium (100 ml)		
Ingredient	Amount	Final concentration
DMEM 1 × (Gibco)	49 ml	49% (v/v)
F-12 nutrient mixture (HAM) 1 × (Gibco)	49 ml	49% (v/v)
Bovine serum albumin (BSA) (Calbiochem)	50 mg	0.5 mg/ml
200 mM L-glutamine (GibcoBRL)	1 ml	2 mM
N-2 supplement (Gibco)	1 ml	1 × or 1% (v/v)
Note: BSA is somewhat difficult to dissolve. Initially add the powder to 25 ml DMEM and then pipette up and down several times to dissolve. Combine with the other components and filter sterilize. Then add:		
Nerve growth factor (Upstate)	100 µl (from 100 µg/ml stock)	100 ng/ml
Immediately divide into 10- or 30-ml aliquots in sterile polypropylene tubes and freeze at -80°C for future use.		
III. N2-Based Media For Long-Term Culture		
A. Medium A (100 ml)		
Ingredient	Amount	Final concentration
N2 medium	99.2 ml	99.2% (v/v)
B-27 supplement (Gibco)	0.7 ml	1 × or 0.7% (v/v)
1-β-D-Arabinofuranosylcytosine (Ara-C) (Calbiochem)	100 µl (from 0.24 mg/ml stock)	0.24 µg/ml
B. Medium B (100 ml)		
N2 medium	99.9 ml	99.9% (v/v)
Ara-C (Calbiochem)	100 µl (from 0.24 mg/ml stock)	0.24 µg/ml

(continues)

Table III (Continued)

C. Medium C (100 ml)		
Ingredient	Amount	Final concentration
N2 medium	100 ml	100% (v/v)
OP-1 (Curis) ^a	5 μ l (from 1 mg/ml stock)	50 ng/ml

^aTo the best of our knowledge, OP-1 is only available by collaborating with Curis (www.curis.com).

IV. Maintenance of Sympathetic Neuronal Culture

- A. The day after plating, replace N2 medium with medium A.
- B. The next day, replace two-thirds of medium A with medium B. Repeat every other day.
- C. One week after plating, start feeding the culture with medium C. Each time, replace two-thirds of the medium with medium C.
- D. After 7–10 days in medium C, the cells will have well-developed dendrites.

V. Methylcellulose-Thickened Medium

Inert thickening reagent methylcellulose can be added into either L-15 incomplete medium or N2 medium to facilitate cell attachment to relatively less adhesive substrates, e.g., plain glass. A variety of different types of methylcellulose are available commercially. We use F4M premium grade methocel from Dow Chemical Company (Midland, MI). The procedure for preparing 0.6% methylcellulose containing medium is as follows: Weigh out 0.3 g methylcellulose into a 50-ml polypropylene tube. Autoclave. Add 50 ml L-15 plating medium or N2 medium. Turn the tube upside down and bang the cap against a tabletop to loosen the methylcellulose at the bottom and let it float in the medium. Attach the tube to an electric rotator and rotate at 4°C for at least 12 h to completely dissolve methylcellulose. Warm up when ready to use.

nerve growth factor, which is required for the viability of the cultures, unless replaced with alternative growth factors such as brain-derived neurotrophic factor (Ernst *et al.*, 2000).

Either type of medium can be supplemented with an inert thickening agent called methylcellulose, which has certain advantages but also has disadvantages depending on the specific needs of the experiment. One main advantage is that cells cultured in methylcellulose will adhere to plain glass coverslips or plastic dishes that are not treated with any substrate or positively charged molecule such as poly-D-lysine. The neurons are not adhered tightly under these conditions, but they are sufficiently adhered to support axonal outgrowth. Cultures of this kind are particularly useful for experiments involving axonal retraction, which is more robust when the axons are initially not adhered so tightly to the substrate (see, e.g., Shaw and Bray, 1977; Ahmad *et al.*, 2000; He *et al.*, 2002). Methylcellulose presumably promotes attachment to poorly adherent substrates simply by “weighing” the cells down and permitting them to remain stationary long enough to form attachments. Another advantage of methylcellulose is that it tends to dissuade neuronal cell bodies from clumping together. We have encountered two disadvantages of methylcellulose. First, it is more difficult to exchange media or to introduce drugs into the medium when methylcellulose is present; this must also be done using medium containing methylcellulose so that the two media are miscible. Second, we have found that the cells sometimes extract unevenly in the presence of

methylcellulose; for example, in immunofluorescence preparations. Instructions for including methylcellulose in the medium are also provided in Table 3.

C. Dissection

1. Chick Sensory Ganglia

Fertilized chicken eggs are incubated at 37°C in a humidified egg incubator. Lumbosacral DRGs are dissected from the embryos after 10–11 days of incubation. Eggs are wiped with 70% ethanol and are cracked into a sterile petri dish. The chicken embryo is separated from other contents with sterile forceps and scissors. The head is removed, and the rest of the embryo is placed on a dissecting plate with the ventral side facing up. Syringe needles are used to fix the embryo against the dissecting plate. Legs are stretched laterally to flatten the embryo. The next steps are performed under a dissecting microscope. Two pairs of forceps are used to gently open trunk skin and muscle, and the chest wall. Organs in the chest and abdomen are gently removed with forceps, with care not to damage the spinal column area. The tail is cut off to reduce fluid accumulation in the abdomen. We then increase magnification at the microscope for a better view of the area containing the lumbosacral DRGs. The connective tissue is removed carefully to expose clearly the spinal column, the lumbosacral DRGs, and spinal nerves on both sides (see Fig. 1). The chain of sympathetic ganglia sits along the lateral side of the spinal column and on top of (i.e., ventral to) the DRGs. The chain is removed carefully, with care not to damage the DRGs. The lumbosacral DRGs are dissected using two pairs of fine-tip forceps, with one lifting the spinal nerve bundles and the other disconnecting the DRGs from the spinal cord. The DRGs are then transferred immediately to a petri dish containing Leibovitz's L-15 medium. (For this, we use L-15 directly from the bottle, with no supplements.) The DRGs are then separated from spinal nerves and cleared of any covering tissues. Generally speaking, three to five DRGs can usually be obtained from each side of the embryo.

2. Neonatal Rat Superior Cervical Sympathetic Ganglia

Pregnant female Sprague–Dawley rats generally give birth on the 21st or 22nd day postconception. Litters usually consist of 8–14 pups. We dissect superior cervical sympathetic ganglia from postnatal day 0 or day 1 rat pups. Pups are buried under watery ice for at least 15 min to achieve anesthesia. Pups are then sprayed with 70% ethanol and fixed to a wax dissecting plate with three syringe needles (Fig. 2A). A pair of small scissors is then used to cut the heart (entering through the underarm region). This drains blood from the pup, which is critical for achieving a clear dissecting view for the later procedures. The skin is then cut open along the midline from the midthorax to mandible level and from the lower cervical level to the two upper limbs. Under a dissecting microscope, two large salivary glands are clearly seen along the midline of the neck (Fig. 2B). One of the salivary glands (with surrounding connective tissue) is removed with a pair

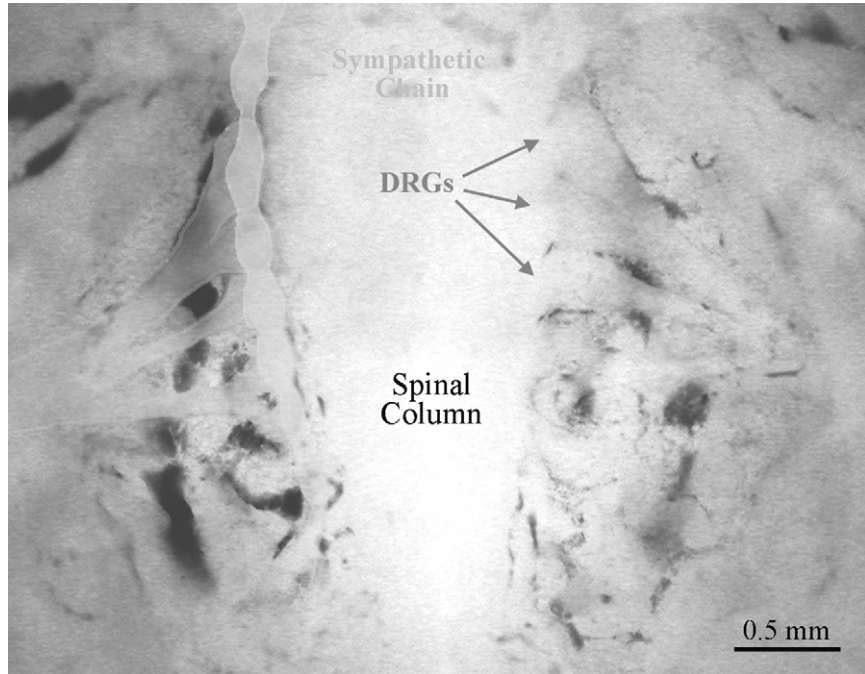


Fig. 1 Dissection of DRGs from a day 10 chicken embryo. After decapitation, the embryo was pinned to the dissection plate with its ventral side up. Organs in the chest and abdomen were removed. Working under a dissecting microscope, connective tissues surrounding the spinal column and DRGs were removed carefully. Shown in the middle of the view in this figure is the lumbosacral region of the spinal column (the top of the photo is rostral). On the left side of the figure, lumbosacral DRGs and their roots are highlighted in pink and the sympathetic chain is highlighted in blue. The sympathetic chain has been removed on the right side of the figure to expose the DRGs beneath. Arrows point to three DRG. (See Color Insert.)

of forceps. This exposes the ipsilateral sternocleidomastoid muscle (Fig. 2C). Transection of this muscle exposes the strap muscles covering the vessels beneath. Dissecting these muscles will then expose the carotid artery. Under higher magnification, bifurcation of the carotid artery can be resolved; the nodose ganglion is located directly lateral to the bifurcation (Fig. 2D). The nodose ganglion is removed to avoid confusion with the sympathetic ganglion later. The superior cervical ganglion sits directly beneath (i.e., dorsal to) the carotid bifurcation. There are two ways to dissect out the sympathetic ganglion. In the first way, the dissector lifts the tail of the ganglion and the carotid artery together with one pair of forceps and then separates the ganglion and the artery from surrounding tissues with another pair of forceps. Once fully detached, the ganglion and the artery are transferred into Leibovitz's L-15 medium in a petri dish. In the second way, the carotid artery and its branches are removed first, which will clearly expose the sympathetic ganglion beneath. Then two pairs of forceps are used to dissect out

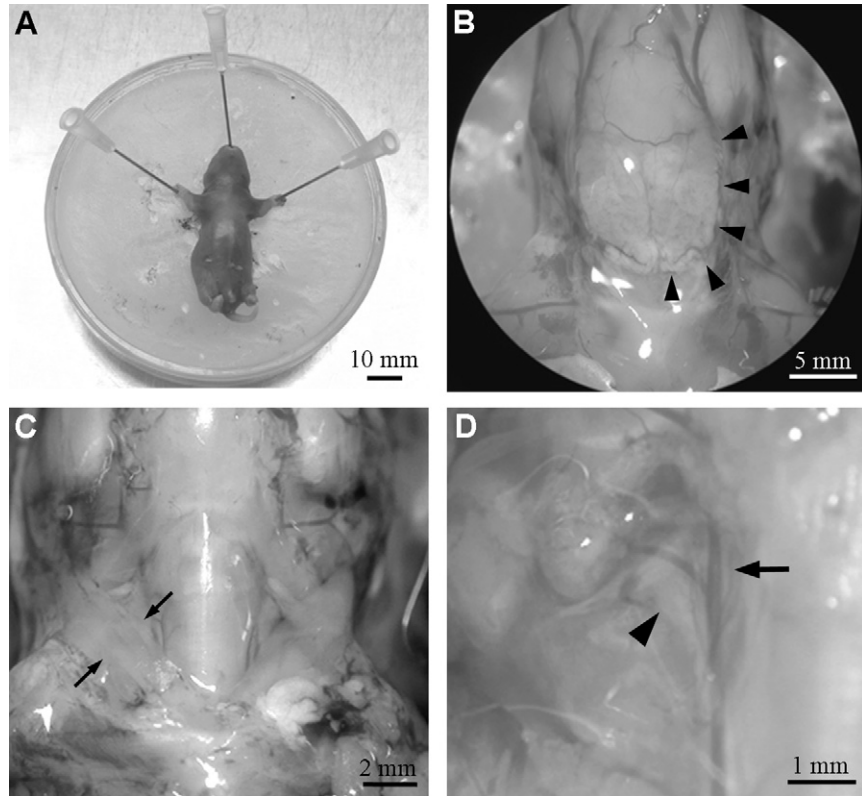


Fig. 2 Dissection of superior cervical ganglion from neonatal rat. (A) A neonatal rat pup was fixed on a dissecting plate with three syringe needles after anesthesia. (B) The two large salivary glands (one of which is outlined by arrowheads) along the midline were exposed after the neck skin was cut open. (C) After the salivary glands were removed, the sternocleidomastoid muscle (bracketed by arrows) was revealed on both sides. (D) Transection of the sternocleidomastoid muscle and strap muscles beneath has exposed the carotid artery and its branch (shown at higher magnification). The nodose ganglion (indicated by the arrowhead) is located directly lateral to the branch point of the carotid artery, and the sympathetic ganglion (indicated by the arrow) is located directly beneath the branch point.

the ganglion and transfer it to Leibovitz's L-15 medium in a petri dish. The ganglion is cleaned of blood vessels and covering connective tissues with two pairs of fine-tip forceps. The nerves from the ganglion are severed from the body of the ganglion. Then, the entire procedure is repeated on the other side of the animal to obtain the second superior cervical ganglion.

D. Preparation of Dissociated Cultures

After dissection from the animals and cleaning of any contaminating tissue, chick DRGs and rat superior cervical ganglia are treated in a very similar way to

obtain cultures of dissociated neurons. The sympathetic ganglia are transferred to a small tube containing 3 ml of 2.5 mg/ml collagenase (Worthington Biochemical), in calcium and magnesium-free phosphate-buffered saline (PBS) and incubated at 37°C for 15 min. The ganglia are then incubated in 2.5 mg/ml trypsin (Worthington Biochemical) in PBS at 37°C for 45 min. (If sympathetic ganglia are dissected from rat fetuses, the collagenase incubation may not be necessary because younger ganglia are easier to dissociate than older ones.) It is important to make sure that all of the ganglia sink to the bottom of the tube, as sometimes they can stick to the edge of the tube or float on a small air bubble. For chick DRGs, we incubate the ganglia with both enzymes at the same time for 20 min at 37°C. At the end of the enzyme treatments, the DRGs or sympathetic ganglia are rinsed twice in L-15 blocking medium (for composition, see Box 3) to neutralize the enzymes. Each rinse is for 5 min. For cultures that will be eventually grown in serum-free N2 medium, the ganglia are rinsed two more times in N2 medium (see Box 3) to remove any residual fetal bovine serum (FBS). We then add about 1 ml of complete L-15 plating medium (see Box 3) or N2 medium. The ganglia are then triturated into a single-cell suspension with a Pasteur pipette whose tip has been fire polished to obtain a narrow opening. The diameter of the pipette opening should be slightly smaller than that of the ganglia so that the ganglia are squeezed through it and dissociated sufficiently. In our experience, trituration should be done roughly five or six times. The concentration of cells in the trituration medium can be counted on a hemocytometer and diluted in L-15 plating medium or N2 medium to the desired concentration for plating. Alternatively, one can determine empirically the number of ganglia required to generate a desired cell density in a certain number of cultures. Cells cultured in L-15 plating medium are kept at 37°C in normal air, whereas cells cultured in N2 medium are kept at 37°C in 5% CO₂. When dividing the cells into dishes, it is important to work quickly because dispersed cells can settle quickly in the test tube or the pipette, resulting in cultures of very different density from one another.

E. Maintenance of Cultures

Neurons cultured for more than 2 days must be “fed” roughly every other day or twice a week. For this, we remove two-thirds of the medium and replace this volume with fresh medium. The inclusion of serum in the medium will promote dendritic differentiation in cultures of sympathetic neurons, but even more rapid and robust dendritic differentiation can be induced by including a member of the transforming growth factor β family called OP-1 (see, e.g., Yu *et al.*, 2000). Cytosine arabinoside (also called Ara-C or 1- β -D-arabinofuranosylcytosine), a deoxycytidine analogue, can be added into the culture to inhibit the growth of dividing nonneuronal cells, which could dominate the culture otherwise. B-27, a commercially available mixture of culture additives, contains a cocktail of antioxidants that reduce reactive oxygen damage and enhance optimal growth and long-term survival of neurons. Details on our standard method for maintaining

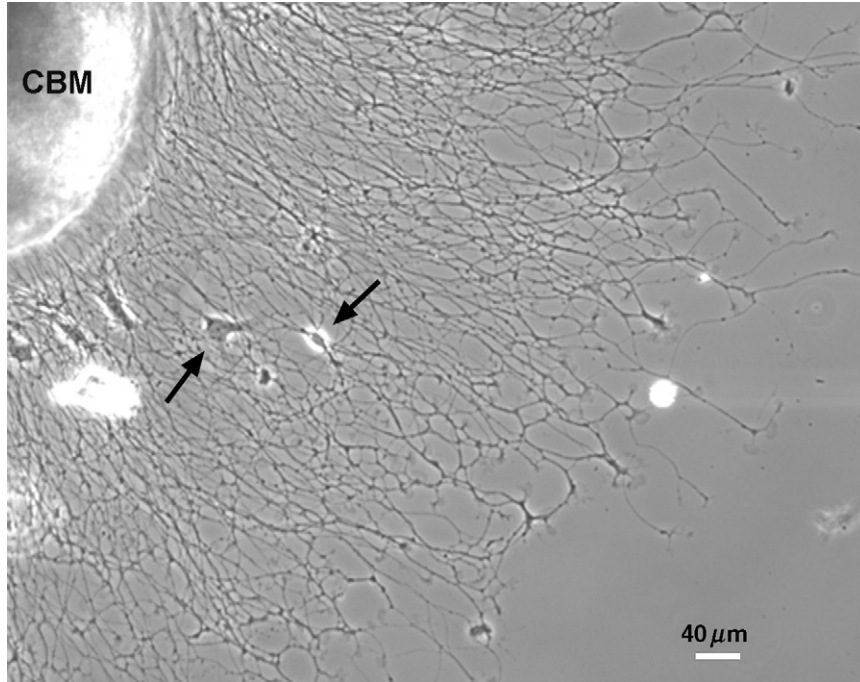


Fig. 3 Sympathetic explant culture. A chunk of neonatal rat sympathetic ganglion was plated on a substrate of poly-D-lysine and laminin. One day after plating, numerous axons had grown radially from the cell body mass (CBM). Arrows point to a few nonneuronal cells.

long-term sympathetic cultures and inducing dendrite formation are provided in Table 3.

F. Preparation of Explant Cultures

Explants are another way to culture neurons. Rather than dissociating the ganglia into individual cells, the ganglia are simply cut into small pieces and cultured as chunks. Axons grow radially away from the “cell body mass.” Cultures of this kind are used far less commonly than dissociated cultures because the morphology of individual neurons cannot be fully discerned. However, there are special applications for which explant cultures are ideally suited. For example, explant cultures can be used for biochemical analyses in which one wishes to compare composition of the axons with that of cell bodies and dendrites. The cell body mass can simply be cut away from the axons under a dissecting microscope and then plucked out of the culture after development of the axonal halo. The axonal halos and cell body masses can then be analyzed separately by biochemical means. The axonal halo contains only axons, whereas the cell body masses contain

cell bodies, proximal regions of the axons, and, in the case of sympathetic neurons, dendrites. For a clean separation, it is necessary that there are no loosened cell bodies within the axonal halo. If this happens, the cell body masses can be plucked out and then cultured a second time, which results in a cleaner axonal halo. Most typically, a collagen substrate is used for explants because the explants do not tend to adhere well unless they have a thick substrate into which to “burrow.” However, smaller explants can be grown successfully on any of the substrates used for dissociated cultures. Fig. 3 shows a small explant grown on laminin for 1 day; axonal outgrowth is apparent, as are a few nonneuronal cells that have detached from the cell body mass. More details on explant cultures are provided in Peng *et al.* (1986).

G. Reducing Nonneuronal Contamination

For most purposes, it is advantageous to have cultures that are as enriched as possible for neurons. However, ganglia are composed of nonneuronal cells (fibroblasts and glial cells), as well as neurons, and hence primary neuronal cultures consist of a mixture of cell types. Because nonneuronal cells undergo mitosis, whereas neurons do not, ganglia from younger animals contain a higher proportion of neurons to nonneuronal cells than ganglia from older animals. One method for routinely obtaining “cleaner” cultures of neurons is to carefully remove the capsule from each ganglion after it has been dissected from the animal. The capsule surrounding each ganglion is essentially invisible to the eye, but can be peeled away (almost like a banana peel) by a talented dissector with some good luck. An attempt should be made, but if the ganglia begin to tear, it is wise to abandon the attempt to remove the capsule and simply live with additional nonneuronal cells in the culture. Tearing a ganglion can result in the death of many neurons. Some workers have found that they can reduce nonneuronal contamination by plating the cells, agitating the culture, and replating the cells that lose their attachment during agitation (Shaw and Bray, 1977). Neurons are more poorly adhered than nonneuronal cells, and hence replating will result in a richer density of neurons. We have not had good luck with this approach, although we have not put substantial effort into it. For long-term cultures, antimetabolic agents such as cytosine arabinoside can be added to the cultures. These agents prevent cells from dividing and slowly kill cells that normally divide, but do not have notable adverse effects on neurons if used at appropriate concentrations. For dissociated cultures, a concentration of 0.24 $\mu\text{g/ml}$ generally works well; this concentration can be increased 10-fold for explant cultures (Peng *et al.*, 1986). For experiments on cultures that are grown for less than 3 days, there is no point in adding such agents. However, for sympathetic cultures grown for over a week, exposure to cytosine arabinoside can result in cultures that consist of over 95% neurons. This is particularly useful for biochemical studies. Eliminating nonneuronal cells from DRG cultures tends to be more problematic, for reasons that we do not understand.

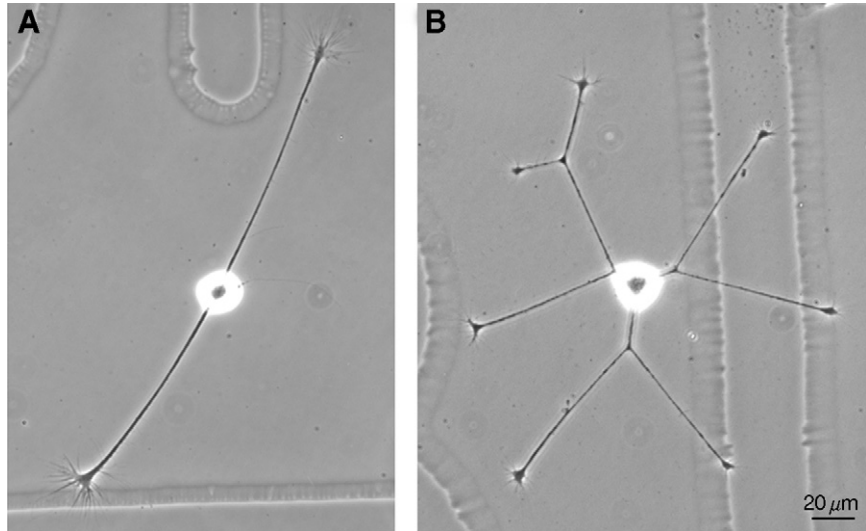


Fig. 4 Dissociated embryonic chick DRG culture. Embryonic day 10 chick DRG neurons were plated on plain glass coverslips in L-15-based medium thickened with methylcellulose. By 16 to 20 h after being plated, DRG neurons had generated axons tipped with growth cones. Some neurons generate several simple axons without branches (A), whereas others generate axons that bifurcate (B).

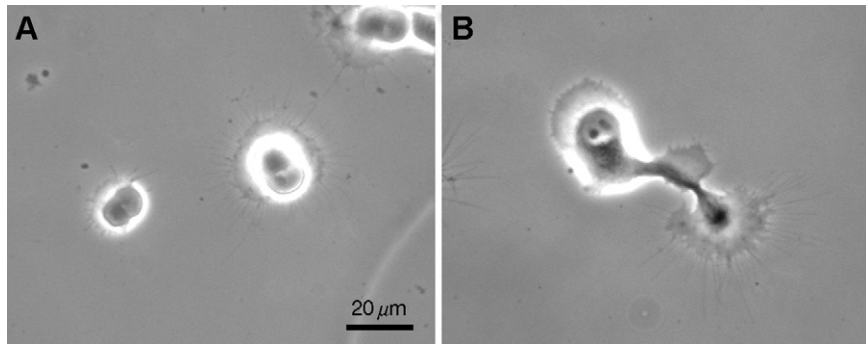
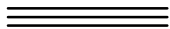


Fig. 5 Rat sympathetic neuronal culture. (A) When plated in L-15-based medium on a poly-D-lysine-coated coverslip, neurons attach firmly to the substrate and generate small lamella and numerous filopodia. Most neurons do not grow processes under these conditions. (B) When plated in N2 serum-free medium, sympathetic neurons show somewhat more robust outgrowth, with broader lamellae and short stumpy processes with large growth cones.



III. Cultures

In closing, this section is devoted to describing the cultures that result from the efforts described earlier.

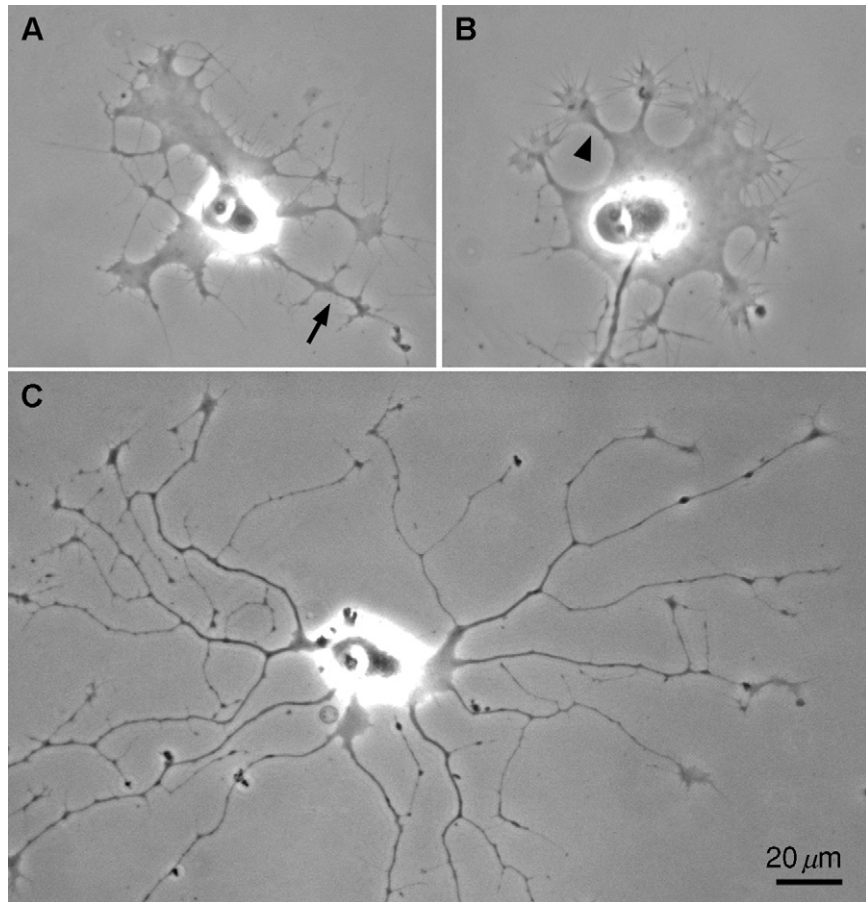


Fig. 6 Laminin-induced axogenesis from sympathetic neurons. Sympathetic neurons were treated with laminin in N2 serum-free medium. (A and B) Thirty minutes after laminin treatment, broad lamellae have extended from the base of the cell bodies. Early processes tipped with large growth cones have begun to protrude from the periphery of the lamellae (arrowhead) and some short axons are already seen (arrow). (C) By 3 h after laminin treatment, sympathetic neurons had generated long, thin axons with complex branches.

A. Short-Term Chick Dorsal Root Ganglia Culture

Chick DRG neurons are generally used for short-term experiments in our laboratory. We typically plate DRG neurons in methylcellulose-thickened L-15 plating medium on plain glass coverslips. Because plain glass is a relatively less adhesive substrate, these conditions are ideal for studying axonal retraction (Ahmad *et al.*, 2000; He *et al.*, 2002). By 16 to 20 h after plating, most DRG neurons have grown several distinguishable axons tipped with growth cones. The axonal identity of these processes is evidenced by their long, thin, and

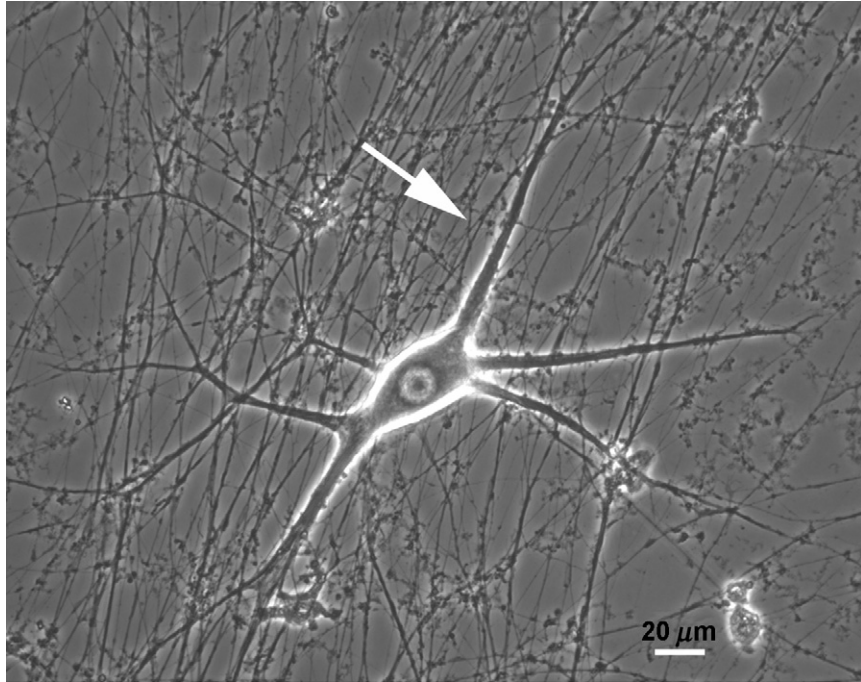


Fig. 7 Long-term rat sympathetic culture. Neonatal rat sympathetic neurons were plated and maintained as described in the text. A typical neuron is shown. After roughly 2 weeks in culture, the neuron has developed several short, thick and tapering dendrites, one of which is marked by an arrow.

uniform-diametered morphology, and also by their expression of axonal marker proteins (Smith, 1998). Some DRG neurons generate several simple primary axons (Fig. 4A), whereas some generate primary axons that bifurcate (Fig. 4B). When cultured for a longer period of time, a typical DRG neuron undergoes significant recrafting of the axonal arbor to produce a morphology that better reflects that of the DRG neurons inside the animal.

B. Short-Term Rat Sympathetic Culture

For most of the short-term experiments in our laboratory, we plate sympathetic neurons on poly-D-lysine-coated glass coverslips in L-15 plating medium. Neurons attach to the bottom of the dish shortly after being plated. Within the first 1 to 2 h after plating the neurons have generated a modest lamella from the base of the cell body, with numerous filopodia extending from the edge of the lamella (Fig. 5A). By this time, neurons have attached to the coverslip firmly. The morphology of the neuron remains essentially the same over the next several hours and even by the next morning. The rapid outgrowth of axons can be induced by the addition of laminin to a final concentration of 25 $\mu\text{g/ml}$ (Invitrogen) to the culture (Rivas *et al.*,

1992; Tang and Goldberg, 2000). A commercially available partially defined mixture of growth factors (which contains laminin as well as other factors) termed Matrigel matrix (BD Biosciences) can be used at 1:40 dilution instead of pure laminin for an even more rapid and robust response (Slaughter *et al.*, 1997; Yu *et al.*, 2002). Alternatively, laminin can be applied directly onto the poly-D-lysine substrate prior to the plating of the cells (see Box 2). This approach produces a rapid outgrowth of axons that begins almost immediately after the firm attachment of the cell body to the substrate (roughly 30 min after plating; see, e.g., Ahmad *et al.*, 1999). When grown in the presence of laminin or matrigel, neurons generate thin and extremely long axons, as shown in Fig. 6. It is our impression that an even broader, more robust lamella is produced on the poly-D-lysine and that an even more robust response to laminin or matrigel can be obtained by using the N2-based medium as opposed to the L-15-based medium (see Fig. 5B). We generally use the L-15-based medium, however, because its capacity to maintain pH in normal air is advantageous for experimental manipulations on the microscope stage.

C. Long-Term Rat Sympathetic Culture

Neurons in culture generate dendrites much later than axons. Therefore we need to maintain rat sympathetic neurons in culture for a longer period of time to study dendrites. Generally speaking, after 7 to 10 days in medium containing OP-1, neurons will have developed robust dendrites (Yu *et al.*, 2000). Each neuron has several dendrites, which are distinguishable from axons on the basis of their short, thick, and tapering morphology (Fig. 7). The axons have become extremely long at this point and have formed a dense network on the culture substrate. It is impossible to discern at this point which axons arise from which cell bodies, but interestingly, the number of axons has been pruned such that each individual neuron typically has a single axon. This can be revealed by microinjecting a fluorescent dye into an individual cell body to reveal its detailed morphology (Higgins *et al.*, 1991).

References

- Ahmad, F. J., Hughey, J., Wittmann, T., Hyman, A., Greaser, M., and Baas, P. W. (2000). Motor proteins regulate force interactions between microtubules and microfilaments in the axon. *Nature Cell Biol.* **2**, 276–280.
- Ahmad, F. J., Yu, W., McNally, F. J., and Baas, P. W. (1999). An essential role for katanin in severing microtubules in the neuron. *J. Cell Biol.* **145**, 305–315.
- Baas, P. W., and Black, M. M. (1990). Individual microtubules in the axon consist of domains that differ in both composition and stability. *J. Cell Biol.* **111**, 495–509.
- Bray, D. (1991). Isolated chick neurons for the study of axonal growth. In “Culturing Nerve Cells” (G. Banker and K. Goslin, eds.), pp. 119–135. MIT, Cambridge, MA.
- Ernst, A. F., Gallo, G., Letourneau, P. C., and McLoon, S. C. (2000). Stabilization of growing retinal axons by the combined signaling of nitric oxide and brain-derived neurotrophic factor. *J. Neurosci.* **20**, 1458–1469.

- Gallo, G., Lefcort, F. B., and Letourneau, P. C. (1997). The trkA receptor mediates growth cone turning toward a localized source of nerve growth factor. *J. Neurosci.* **17**, 5445–5454.
- He, Y., Yu, W., and Baas, P. W. (2002). Microtubule reconfiguration during axonal retraction induced by nitric oxide. *J. Neurosci.* **22**, 5982–5991.
- Higgins, D., Lein, P. L., Osterhout, D. J., and Johnson, M. I. (1991). Tissue culture of mammalian autonomic neurons. In “Culturing Nerve Cells” (G. Banker and K. Goslin, eds.), pp. 177–205. MIT, Cambridge, MA.
- Johnson, M. I. (2001). Primary cultures of sympathetic ganglia. In “Protocols for Neural Cell Culture” (S. Fedoroff and A. Richardson, eds.), 3rd, Ed., pp. 71–94. Humana Press, Totowa, NJ.
- Johnson, M. I., and Argiro, V. (1983). Techniques in the tissue culture of rat sympathetic neurons. *Methods Enzymol.* **103**, 334–347.
- Mahanthappa, N. K., and Patterson, P. H. (1998). Culturing mammalian sympathoadrenal derivatives. In “Culturing Nerve Cells” (G. Banker and K. Goslin, eds.), 2nd Ed., pp. 289–307. MIT, Cambridge, MA.
- Peng, I., Binder, L. I., and Black, M. M. (1986). Biochemical and immunological analyses of cytoskeletal domains of neurons. *J. Cell Biol.* **102**, 252–262.
- Rivas, R. J., Burmeister, D. W., and Goldberg, D. J. (1992). Rapid effects of laminin on the growth cone. *Neuron* **8**, 107–115.
- Shaw, G., and Bray, D. (1977). Movement and extension of isolated growth cone. *Exp. Cell Res.* **104**, 55–62.
- Slaughter, T. S., Wang, J., and Black, M. M. (1997). Transport of microtubules from the cell body into the axons of cultured neurons. *J. Neurosci.* **17**, 5807–5819.
- Smith, C. L. (1998). Cultures from chick peripheral ganglia. In “Culturing Nerve Cells” (G. Banker and K. Goslin, eds.), 2nd Ed., pp. 261–287. MIT, Cambridge, MA.
- Tang, D., and Goldberg, D. J. (2000). Bundling of microtubules in the growth cone induced by laminin. *Mol. Cell. Neurosci.* **15**, 303–313.
- Wang, L., Ho, C. L., Sun, D., Liem, R. K. H., and Brown, A. (2000). Rapid movement of axonal neurofilaments interrupted by prolonged pauses. *Nature Cell Biol.* **2**, 137–141.
- Yu, W., Cook, C., Sauter, C., Kuriyama, R., Kaplan, P. L., and Baas, P. W. (2000). Depletion of a microtubule-associated motor protein induces the loss of dendritic identity. *J. Neurosci.* **20**, 5782–5791.
- Yu, W., Ling, C., and Baas, P. W. (2001). Microtubule reconfiguration during axogenesis. *J. Neurocytol.* **30**, 861–875.

This Page Intentionally Left Blank

CHAPTER 3

Dissection and Culturing of Chick Ciliary Ganglion Neurons: A System Well Suited to Synaptic Study

Barbara W. Bernstein

Department of Biochemistry and Molecular Biology and
Program in Molecular, Cellular, and Integrative Neurosciences
Colorado State University
Fort Collins, Colorado 80523

-
- I. General Introduction
 - A. Neuroanatomy and Development of the Ciliary Ganglion
 - B. Applications of Cultured Cells and Isolated Calyx Terminals
 - II. Materials
 - A. Materials for Dissection
 - B. Materials for Dissociation and Culturing
 - III. Methods
 - A. Dissection: Isolation of Ciliary Ganglion
 - B. Dissociation of the Ganglion
 - C. Culturing of Ciliary Neurons
 - IV. Variations on Dissection, Dissociation, and Culturing Themes
 - V. Concluding Comments
 - References

This chapter describes the function and development of the ciliary ganglion, the potential of ciliary ganglion neurons as a cell biological tool, and their dissection, dissociation, and culturing. Ciliary ganglion neurons grow unusually rapidly on a laminin-based substratum and develop large, thin calyx terminals in culture in less than 12 h. The two neuronal classes present in the cultures can be identified by size alone. The limited number of ganglia per animal renders this ganglion a poor choice for biochemical studies based on the extraction of cultured cells. However, they are ideally suited for studies based on single-cell observation, particularly investigation of presynaptic mechanisms using fluorescence microscopy.

I. General Introduction

Like all other neuronal cell culture preparations, the ciliary ganglion has distinct advantages and disadvantages that must be weighed according to the research needs. One of its primary advantages is the relative homogeneity of its neurons, which is typical of parasympathetic ganglia because of their limited number of targets. There are only two neuronal types, ciliary and choroid, both of which are cholinergic and receive cholinergic input (Marwitt *et al.*, 1971; Chiappinelli and Dryer, 1984).

A. Neuroanatomy and Development of the Ciliary Ganglion

The ganglion lies in the caudal part of the orbital cavity at the junction of the lateral side of the optic nerve and the extraocular muscle, sending a short branch to the oculomotor nerve. Ciliary cells receive midbrain input through single, large calyciform terminals (Martin and Pilar, 1963; Dryer and Chiappinelli, 1987), whereas choroid cells receive multiple small boutons. Ciliary cells control light reflex and visual accommodation through the innervation of striated muscle in the iris and ciliary body, whereas choroid neurons, distinguished easily by their smaller somata diameter ($13 \pm 2 \mu\text{m}$ compared to $23 \pm 3 \mu\text{m}$ of ciliary neurons; McNerney *et al.*, 2000), innervate the smooth muscle of choroid coat blood vessels. If a more stringent identifying criterion of ciliary neurons is required, they can be labeled by incubating the ciliary nerves of the intact ganglion in the fluorescent dye Dil (1,1'-dioctadecyl-3,3,3',3'-tetramethylindocarbocyanine perchlorate; Haugland, 1996; McNerney *et al.*, 2000). These two neuron classes both have (α Bgt)-AChRs, composed of $\alpha 7$ subunits and inhibited by bungarotoxin, and $\alpha 3^*$ -AChRs, composed of $\alpha 3$, $\alpha 5$, and $\beta 4$ subunits and insensitive to bungarotoxin, but choroid and ciliary neurons have distinctively different electrophysiological characteristics (McNerney *et al.*, 2000).

B. Applications of Cultured Cells and Isolated Calyx Terminals

This avian ganglion is a favorite model system for the study of embryonic development (Dryer, 1994; Nishi, 1994) and neurotrophic signaling (Finn and Nishi, 1996; Ip and Yancopoulos, 1992) because of the ease of manipulating target tissue and inputs (accessory part of the oculomotor nucleus; Lee *et al.*, 2001). They undergo a fairly complex pattern of cell death that is coordinated with synapse formation, involves replacement by postmitotic precursor cells, and is target driven rather than programmed (Barde, 1989). Neuronal degeneration starts as early as HH stage 24, i.e., before embryonic day 5 (Lee *et al.*, 2001; Hamburger and Hamilton, 1951).

Investigators have taken advantage of the high efficiency (Borasio *et al.*, 1989; Yamashita *et al.*, 1999) with which proteins can be trituration loaded into these neurons before plating. The efficiency of loading untagged species can be

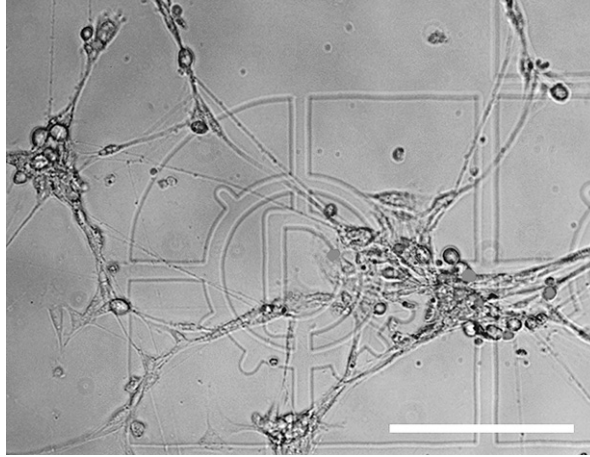


Fig. 1 Forty percent of the neurons were loaded through trituration. The fluorescence image of cells containing rhodamine-tagged cofilin, a protein that regulates actin filament turnover (Bamburg, 1999), was merged with a phase image of the same field. Cells were grown overnight on a glass coverslip etched with a lettered matrix (trade name Cellocate; Brinkmann, Westbury, NY). The matrix allows one to identify and image the same cell area repeatedly even after returning the culture to the incubator. Bar: 175 μm . (See Color Insert.)

monitored with FITC-dextran. In the first study, isotope-tagged RhoA (5 mg/ml) or C3 transferase (0.1 mg/ml) was used to reveal the linkage between p75^{ntr} and actin assembly in neurite outgrowth. Fluorescently tagged cytoskeletal proteins (see Fig. 1), chromophore-tagged antibodies for CALI studies (chromophore-assisted laser inactivation; Beermann and Jay, 1994), and transfecting DNA plasmids can also be trituration loaded efficiently. Introduction of proteins via microinjection should be feasible, as the large soma has a relatively small nucleus compared to many neurons in which the nucleus occupies the entire cell body (see Fig. 2). The large flat, thin calyx terminal formed between ciliary neurons in culture (Fujii and Berg, 1987) provides an ideal structure for presynaptic terminal research with fluorescence microscopy (see Fig. 3). The calyx terminal fits like a bathing cap over the postsynaptic cell body. It can be specifically loaded with a tagged protein via a sequence of hyperosmotic and hypoosmotic medium incubations (see Fig. 4). Instructions and materials for this protocol can be obtained as a kit from Molecular Probes (Influx; Eugene, OR).

Alternatively, the calyx terminal has been studied immediately after cell dissociation as an isolated pre- and postsynaptic structure, *i.e.*, a terminal with an attached cell body, removed intact from the ganglion. This structure can be isolated with a combination of proteolytic enzymes (collagenase, hyaluronidase, dispase; Stanley and Goping, 1991) with more limited activity than trypsin, which is used commonly for ganglion dissociation. This proteolytic combination digests glia/neuron connections more effectively than neuron/neuron connections. The

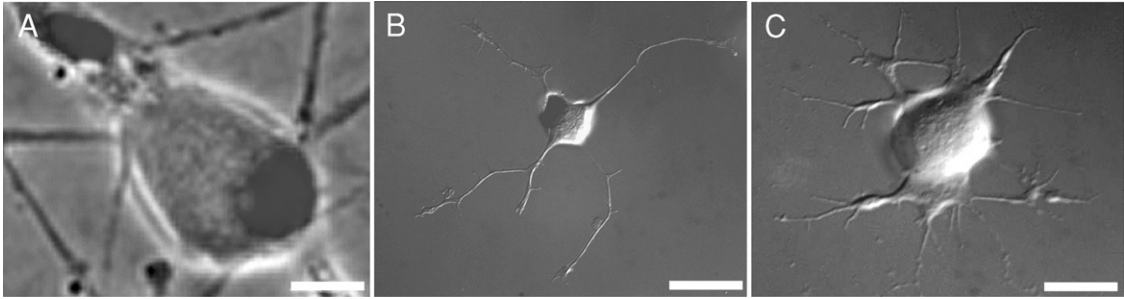


Fig. 2 Ciliary neurons have a relatively small nucleus that occupies $\sim 25\%$ of the somata area. Images, showing fluorescent DAPI staining of the nucleus, were overlaid on phase images of the same field. (A) Overnight culture. Bar: $10\ \mu\text{m}$. (B) Three-hour culture. Bar: $20\ \mu\text{m}$. (C) One-hour culture. Bar: $15\ \mu\text{m}$. (See Color Insert.)

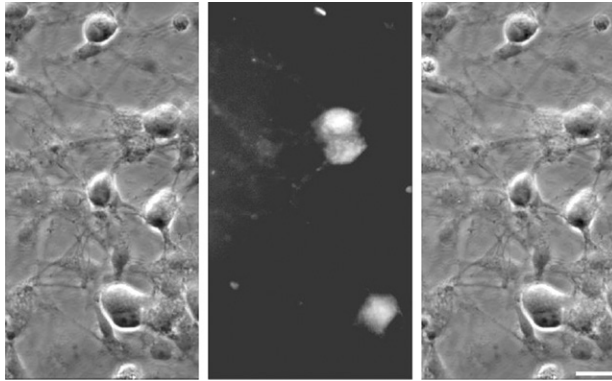


Fig. 3 Active calyx presynaptic terminals are visualized with the fluorescent styryl dye FM1-43 (Cochilla *et al.*, 1999). Cells were incubated in $10 \mu\text{M}$ FM1-43 and were depolarized with an isotonic 75 mM K^+ buffer. FM1-43 is internalized in terminals only when they are depolarized, and neurotransmitter vesicles are formed through endocytosis. (Right) Overlay of a FM1-43 image (center) and phase image (left). Bar: $20 \mu\text{m}$. (See Color Insert.)

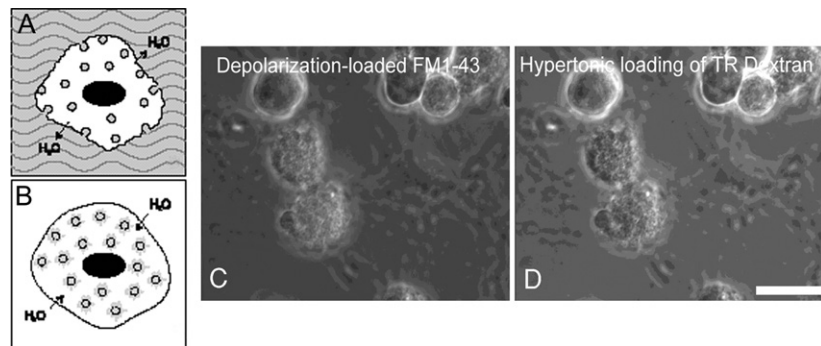


Fig. 4 Membrane-impermeable molecules can be loaded into terminals via Influx (Molecular Probes). A schematic of Influx modified from the “Molecular Probes Handbook” illustrates the mechanism of loading species through incubation first in hypertonic medium containing impermeable molecules (A), which are taken up in endocytotic vesicles that are then lysed by switching the culture to hypotonic medium (B). FM1-43, loaded by depolarization (C), identifies active terminals, which are the same structures loaded with Texas red-tagged dextran (20 kDa) via the Influx kit (D). Bar: $20 \mu\text{m}$. (See Color Insert.)

neuromuscular junction *in vitro* is yet another area of investigation for which this preparation is appropriate (Campagna *et al.*, 1997; Brusés *et al.*, 1995).

A major disadvantage of ciliary ganglia for cell culture studies is the small number of neurons obtainable per animal. There are 17,500/ganglion at embryonic day 8 (E8; see Fig. 5; Lee *et al.*, 2001). Only 2 ganglia are present per animal

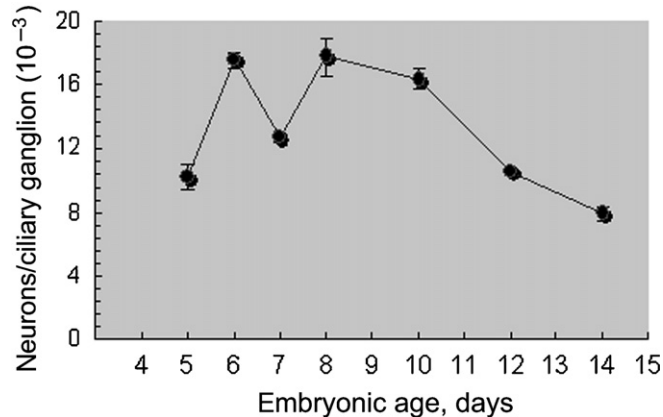


Fig. 5 Time course of neuronal proliferation and degeneration (data from Lee *et al.*, 2001). Data represent the mean of 8–11 ganglia \pm SEM.

as opposed to 10–30 ganglia for other peripheral nervous system tissue, such as sympathetic or dorsal root ganglia.

II. Materials

A. Materials for Dissection

Dissecting microscope with illumination from above (*e.g.*, Nikon SMZ-U 1:10 zoom)

Egg incubator

High-intensity lamp for candling eggs (blood vessel network visible in a healthy, well-developed egg)

Laminar flow hood

Scalpel

Two pairs of Dumont No. 5 forceps

Crocus cloth, grind stone (sharpening and polishing forceps)

Ethanol

~4-in. square dish filled with Sylgard (a silicone plastic; Dow Corning, Midland, MI)

Plastic culture dishes (Falcon; 35, 60, or 100 mm diameter)

B. Materials for Dissociation and Culturing

Trypsin (Sigma-Aldrich, St. Louis, MO; should be kept in frozen aliquots to avoid repeated freeze/thaw cycles)

Matrigel (Becton-Dickinson Labware, Bedford, MA; frozen 11 mg/ml stock)
Penicillin/streptomycin (Sigma-Aldrich)
Neurobasal medium (Invitrogen, Carlsbad, CA; Brewer *et al.*, 1993)
B27 supplement (Invitrogen)
Glutamine (200 mM frozen stock; Sigma-Aldrich)
Hank's balanced salt solution (HBSS; Sigma-Aldrich)
Humidified CO₂ tissue culture incubator
No. 1 glass coverslips

III. Methods

A. Dissection: Isolation of Ciliary Ganglion

For ease of handling, we have chosen E10 ganglia, which have close to the maximum number of neurons (Fig. 5; Lee *et al.*, 2001). However, by E10 there are more nonneuronal cells than at E8. Before starting, all materials are sterilized by autoclaving, rinsing with 70% ethanol, or exposing to ultraviolet (UV) light for >20 min. If culturing cells for <12 h, sterilization is not critical.

1. When growing cells for more than 2 days, precoating No. 1 glass coverslips with 100 $\mu\text{g/ml}$ poly-D-lysine is recommended to prevent cell clumping. Store poly-D-lysine at -20°C (5 mg/ml). Dilute it 50 \times in borate buffer [1.24 g boric acid and 1.90 g sodium tetraborate (borax) in 400 ml H₂O]. Apply 100–150 μl /coverslip ($\sim 130\text{ mm}^2$), incubate for 30 min, remove poly-D-lysine, wash 3 \times ultrapure H₂O, air dry, UV sterilize (20 min), and use coverslips within a week.

2. Warm to room temperature trypsin, Dulbecco's modified Eagle's medium (DMEM)/10% fetal bovine serum (FBS), and HBSS without Ca²⁺ or Mg²⁺; trypsin is inhibited by Ca²⁺. Warm to 37 $^{\circ}\text{C}$ complete neurobasal growth medium (neurobasal medium/1:50 dilution B27 supplement/2 mM glutamine/100 U/ml penicillin/100 $\mu\text{g/ml}$ streptomycin).

3. Apply enough Matrigel (100 $\mu\text{g/ml}$) to No. 1 glass coverslips to cover the area on which cells will be grown, *i.e.*, Matrigel volume approximately equal to the volume of the cell suspension to be plated. Coverslips may be sealed permanently to the bottom of plastic drilled-out dishes or placed in any sterile plastic container (square or round dish of suitable size). Incubate coverslips with Matrigel for 30 min to several hours in a humidified 37 $^{\circ}\text{C}$ /5% CO₂ incubator while preparing cells. Do not allow Matrigel to dry.

4. Ganglia can be collected in a 500- μl microfuge tube containing 50 μl HBSS.

5. Spray egg shell with 70% ethanol. Use the blunt end of forceps to tap through the shell. Repeat tapping to form a circular crack that approximates the air sac perimeter. Use forceps to lift the cracked top off the egg. Gently lift chick from the egg, holding below the head with forceps.

6. Place the whole embryo on a dish filled with black Sylgard (a rubbery material). Surgically decapitate chick with a scalpel. Discard body. Pin the head to Sylgard with beak up. Pins the size of standard sewing pins are appropriate. Push one through the lower neck and one through each eye at an angle away from the dissector and toward the dish sides (see Fig. 6.1). The drawn white circle in Fig. 6.1 indicates the area of eyeball completely covered by tissue that must be removed. Bright white blotches on panels are reflected light from well-wetted surfaces. They can be eliminated by adjusting the polarizing filter on the microscope; unfortunately, this filtering reduces the illumination intensity.

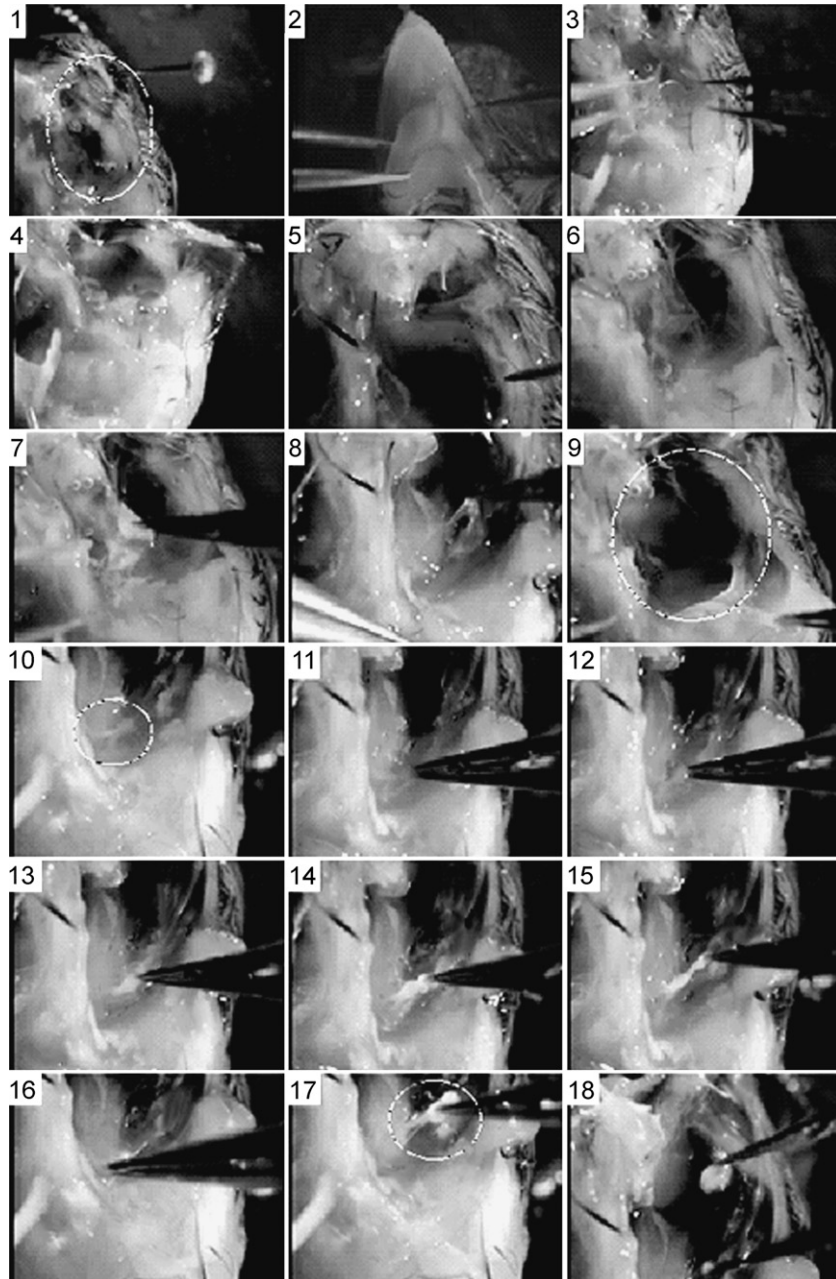
7. Completely peel away the lower beak and then the upper beak (see Fig. 6.2). This can be done under the lowest magnification of a dissecting microscope.

8. Remove connective tissue covering the exposed eye. Try to remove as large a sheet of tissue as possible, which includes the caudal region of the eye. Be careful not to puncture the eyeball. If the eyeball collapses or pigment starts flaking off the eye, it is much more difficult to find the ganglion (see Figs. 6.3–6.9). The drawn white circle in Fig. 6.9 indicates the area of the eye from which the covering tissue has been removed.

9. Remove as much connective tissue as possible from over the extraocular muscles without inadvertently removing the ganglion. Reposition the eye pin so the head of the pin is closer to the bottom of the dish. This can be done by merely loosening the pin attachment to the dish without removing the pin from the eye. The repositioning rotates the dorsal surface of the eye upward, often exposing the ganglion if sufficient connective tissue has been removed. It may help to rinse the intraocular space with HBSS, which removes fragments of connective tissue and floats apart layers of tissues (Fig. 6.6). Increasing microscope magnification slightly is sometimes helpful.

10. The circled area in Fig. 6.10 is the “7 o’clock” position of the circle in Fig. 6.9. Use one pair of forceps to lift the ganglion from the area encircled in Fig. 6.10. The ganglion is located in the “V” formed by the optic nerve and the extraocular muscles. Lifting the ganglion exposes its nerve trunks. The trunks and slightly greater optical density of the ganglion (circled in Fig. 6.17) distinguish it from abundant small chunks of connective tissue (see Figs. 6.11–6.17). Use the other pair of forceps to pluck out the ganglion without crushing it. A fully extracted ganglion is seen at the tip of the forceps (Fig. 6.18) with completely retracted

Fig. 6 Dissection of a left ciliary ganglion from a 13-day chick embryo. Images were captured with Metamorph software (Universal Imaging Corp., West Chester, PA) from a VCR tape recording of the dissection viewed through a dissecting microscope fitted with a DAGE camera. Magnification is the same in all panels. (1) The circled area indicates tissue covering the eyeball through which a pin is positioned. (2) Focus is shifted down to the lower beak, which is removed along with the upper beak. (3–9) Tissue is removed from the eyeball surface. (9) The circle shows cleared surface. (10) The small circled area, positioned at “7 o’clock” on the circle (9), contains a barely visible ganglion, which can often be seen after repositioning the pin through the eye. (11–18) Removal of the ganglion. (17) The circled area is the lifted ganglion attached by only one nerve trunk.



trunks, which make it appear twice as big as in previous panels. If necessary, dip the forceps tip up and down through the HBSS meniscus to wash the ganglion from the tip.

11. The ganglion can be kept at room temperature in HBSS for some time while collecting more. When all are collected (*e.g.*, four ganglia), they can be trypsinized together.

B. Dissociation of the Ganglion

1. Add 10–15 μl 2.5% trypsin to 50 μl HBSS containing ganglia. Incubate for 10–15 min in a 37°C/5% CO₂ incubator (described by Collins and Dawson, 1982).

2. Add 500 μl DMEM/10% FBS to inhibit trypsin. Let the ganglia settle to the bottom of the tube before removing all but \sim 10 μl of the medium.

3. Add \sim 100 μl growth medium: neurobasal medium, 1/50 dilution B27 supplement, 2 mM glutamine, 100 U/ml penicillin, and 100 $\mu\text{g/ml}$ streptomycin. With ganglia on the bottom of tube and at the lowest magnification, adjust the microscope light and focus to visualize ganglia. Draw ganglia repeatedly up and down through the opening of a 200- μl pipette tip (yellow tip) or a fire-polished glass Pasteur pipette held close to the bottom of the tube. Ganglia fall apart, often leaving a piece of undigested capsule; dissociated cells give the solution a granular appearance. It should require 30–70 cycles of repetitive pipetting to dissociate the cells. If fewer cycles are required, it suggests that the enzymatic treatment is too strong to maximize cell survival.

4. Adjust the growth medium volume to plate the cells at a desired density on the coverslip. For example, 1/5–1/10 ganglion may be plated in 50 μl and allowed to adhere to the substratum for 15–30 min in the incubator before bringing the final volume of medium in a 35-mm plastic culture dish to 2 ml.

C. Culturing of Ciliary Neurons

Immediately after dissociating ganglia, remove coverslips from the incubator, withdraw Matrigel, and plate the cell suspension without allowing the Matrigel residue to dry. We have grown cells for 48 h at a cell density as low as 1/16 ganglion/13 mm² (area covered by 50 μl of medium); we have counted 7.4×10^4 cells/ganglion of which 1.6×10^4 are neurons (Lee *et al.*, 2001). After this time, cells that were originally well isolated form large clusters, which for many purposes is unacceptable (see Fig. 7A). Cell aggregation can be prevented by choosing a more tightly adhering substratum than Matrigel, such as poly-D-lysine or a combination of poly-D-lysine and Matrigel. Matrigel is a solubilized basement membrane from a mouse sarcoma; it is predominantly laminin with some collagen and heparin sulfate proteoglycans and lesser concentrations of entactin, nidogen, transforming growth factor β , fibroblast growth factor (FGF) and other growth factors.

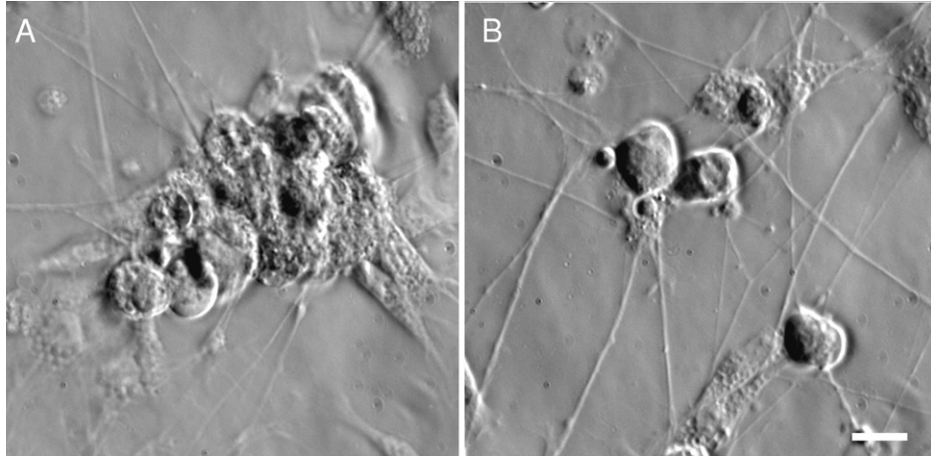


Fig. 7 Ciliary neurons cluster when cultured for 2 days on Matrigel alone (A). This clustering can be avoided by first coating coverslips with poly-D-lysine and then applying Matrigel (B). Bar: 20 μm .

Many possibilities exist for handling coverslips when doing live cell microscopic imaging. Coverslips are available as circles, squares, or rectangles in sizes ranging from 12 mm² to 22 × 70 mm. They can be sealed permanently with 100% silicone aquarium sealant (All-Glass Aquarium Co., Franklin, WI) to drilled-out dishes. To avoid chemical toxicity, sealing should be done the day before plating cells to allow 24 h for the sealant to cure. Alternatively, coverslips can be left floating freely in dishes filled with medium and sealed reversibly to the bottom of drilled-out dishes immediately before transfer to a microscope stage; one can rim the opening of a drilled dish with Dow Corning high vacuum grease and press the dish over the coverslip with growing cells. Silicone gaskets, with or without attached clear plastic covers (Grace Bio-Labs, Bend, OR), can be sealed to dry coverslips before plating. These gaskets restrict the area of cell growth and can be used to limit the volume of incubating solution to <70 μl . Small culture volumes may be important if reagents are limiting or expensive. It is not recommended to use such small volumes for long-term culture. Neuronal growth is preferred with a medium depth of >5 mm (unpublished data; mechanism currently under investigation).

===== IV. Variations on Dissection, Dissociation, and Culturing Themes

Laminin (Collaborative Biomedical, Bedford, MA) combined with poly-D-ornithine, poly-DL-ornithine (Brusés *et al.*, 1995), or poly-D-lysine sustains cultures longer term. These cells have been kept for up to 2 weeks (Chen *et al.*, 2001) when changing the medium every 2–3 days: minimum essential medium (MEM) with penicillin/streptomycin, 2 mM glutamine, 10% (v/v) heat-inactivated horse serum, and 3% embryonic chick eye extract (Nishi and Berg, 1981). Ciliary

ganglion neurons have been cultured under a variety of conditions other than Matrigel alone. They include the following.

a. Poly-D-lysine and laminin coverslips with recombinant ciliary neurotrophic factor ([his]6-chCNTF_{yy} 10 ng/ml) (Lee *et al.*, 2001).

b. Coverslips coated sequentially with poly-L-ornithine and laminin (Becton-Dickinson Labware) and Ham's F-12 medium (Becton-Dickinson Labware) supplemented with 10% fetal calf serum; 50 ng of combined nerve growth factor (NGF), brain-derived neurotrophic factor, neurotrophin-3 (Sigma-Aldrich) (Yamashita *et al.*, 1999). The developmental time course of responsiveness to NGF and other neurotrophins must be considered; for NGF it peaks at E8 (Collins, 1988).

c. Coverslips coated sequentially with poly-D-lysine and Matrigel (see Fig. 7B).

Ciliary neuronal cells from E8 to E14 chick have been cultured. The dissection of chicks at different stages is qualitatively different due largely to the increase in connective tissue and cartilage with age. Dissection of E8 ganglia involves a totally different approach, one in which the eyeball is partially released from the socket (Nishi, 1996).

Dissociation has been accomplished with trypsin concentrations as low as 0.05% with incubation times extended to 20 min or more and ganglia first hemisected with a scalpel, thus circumventing the capsule. Collagenase, a milder and more specific protease than trypsin, has also been used (Chiappinelli *et al.*, 1981).

Additionally, when necessary to achieve a particular research goal, intact ganglia can be maintained in complete neurobasal medium (Section III,A,1) in a humidified CO₂ incubator for 24 h before dissociating and plating the cells. An example of a situation for which the maintenance of intact ganglia is convenient is the adenoviral infection of neurons for exogenous gene expression. One can dissociate ciliary cells immediately after dissection and culture them for 24 h before infecting with adenovirus containing a green fluorescent fusion protein (see Chapter 19). Alternatively, one can hemisect the ganglia with a scalpel to increase the exposed surface area of neurons and infect overnight with the virus before dissociating and plating. A similar holding procedure has been used to label ciliary cells with bungarotoxin (Brusés *et al.*, 2001).

For some purposes, the enrichment of neurons over glia and fibroblasts is necessary. Removal of nerves and mesenchymal tissue before enzymatic incubation helps in this regard. In this case, ganglia should be collected in a small culture dish rather than in a microfuge tube. Nerve and connective tissue are teased away from the ganglion with two forceps. Preplating of dissociated cells is an additional commonly followed procedure, although it reduces neuronal yield. Cells are plated for ~60 min at 37°C; then the neurons, which adhere more weakly than non-neuronal cells, can be shaken off and replated. One can also use horse serum, which is reported to be less mitogenic than fetal calf serum, and FGF, which does not support nonneuronal cell proliferation (Nishi, 1996). Low concentrations of

cytosine arabinoside ($<10^{-5} M$) or $10^{-5} M$ fluorodeoxyuridine plus uridine have been recommended for inhibiting nonneuronal cell division while minimizing neuronal toxicity. A less commonly used protocol to enrich neurons involves centrifugation of the suspension on a discontinuous Percoll gradient (30/60%) for 20 min at $500 \times g$, $4^{\circ}C$ and collection of the neurons at the interface (Brusés *et al.*, 1995).

V. Concluding Comments

This chapter describes in some detail procedures for dissecting, dissociating, and culturing chick ciliary ganglion neurons in some detail. They are methods that we have found appropriate for our research interests. They are presented here merely as a starting point and should be modified according to individual needs. Similarly, while vendors of some materials have been named, these are not necessarily endorsements. In most cases, several suppliers are available.

If large quantities of protein are needed for biochemical studies of cell extracts, the limited number of ganglia per animal makes ciliary ganglion neurons a poor choice. If single cell study is appropriate, *i.e.*, one is using electrophysiology or various forms of electron or light microscopy, then these cells are a good choice. They grow rapidly, are generally robust, are efficiently loaded with macromolecules by trituration, can be loaded with macromolecules via Influx (incubation in a sequence of hyperosmotic and hypoosmotic medium), and form axonal/somatic synapses in culture.

Acknowledgments

I thank Professor James R. Bamberg, in whose laboratory this work was performed, and the agencies who support his research: the Alzheimer's Association (Grant IIRG-01-2730) and National Institutes of Health (Grants GM 35126 and NS40371). Adenovirus was supplied by L.S. Minamide.

References

- Bamberg, J. R. (1999). Proteins of the ADF/cofilin family: Essential regulators of actin dynamics. *Annu. Rev. Cell Dev. Biol.* **15**, 185–230.
- Barde, Y. A. (1989). Trophic factors and neuronal survival. *Neuron* **2**, 1525–1534.
- Beermann, A. E., and Jay, D. G. (1994). Chromophore-assisted laser inactivation of cellular proteins. *Methods Cell Biol.* **44**, 715–732.
- Borasio, G. D., John, J., Wittinghofer, A., Barde, Y. A., Sendtner, M., and Heumann, R. (1989). ras p21 protein promotes survival and fiber outgrowth of cultured embryonic neurons. *Neuron* **2**, 1087–1096.
- Brewer, G. J., Torricelli, J. R., Evege, E. K., and Price, P. J. (1993). Optimized survival of hippocampal neurons in B27-supplemented Neurobasal, a new serum-free medium combination. *J. Neurosci. Res.* **35**, 567–576.
- Brusés, J. L., Chauvet, N., and Rutishauser, U. (2001). Membrane lipid rafts are necessary for the maintenance of the $\alpha 7$ nicotinic acetylcholine receptor in somatic spines of ciliary neurons. *J. Neurosci.* **21**, 504–512.

- Brusés, J. L., Oka, S., and Rutishauser, U. (1995). NCAM-associated polysialic acid on ciliary ganglion neurons is regulated by polysialyltransferase levels and interaction with muscle. *J. Neurosci.* **15**, 8310–8319.
- Campagna, J. A., Ruegg, M. A., and Bixby, J. L. (1997). Evidence that agrin directly influences presynaptic differentiation at neuromuscular junctions in vitro. *Eur. J. Neurosci.* **9**, 2269–2283.
- Chen, M., Pugh, P. C., and Margiotta, J. F. (2001). Nicotinic synapses formed between chick ciliary ganglion neurons in culture resemble those present on the neurons in vivo. *J. Neurobiol.* **47**, 265–279.
- Chiappinelli, V. A., Cohen, J. B., and Zigmond, R. E. (1981). The effects of alpha- and beta-neurotoxins from the venoms of various snakes on transmission in autonomic ganglia. *Brain Res.* **211**, 107–126.
- Chiappinelli, V. A., and Dryer, S. E. (1984). Nicotinic transmission in sympathetic ganglia: Blockade by the snake venom neurotoxin kappa-bungarotoxin. *Neurosci. Lett.* **50**, 239–244.
- Cochilla, A. J., Angleson, J. K., and Betz, W. J. (1999). Monitoring secretory membrane with FM1-43 fluorescence. *Annu. Rev. Neurosci.* **22**, 1–10.
- Collins, F. (1988). Developmental time course of the effect of nerve growth factor on the parasymphatic ciliary ganglion. *Brain Res.* **467**, 111–116.
- Collins, F., and Dawson, A. (1982). Conditioned medium increases the rate of neurite elongation: Separation of this activity from the substratum-bound inducer of neurite outgrowth. *J. Neurosci.* **2**, 1005–1010.
- Dryer, S. E. (1994). Functional development of the parasymphatic neurons of the avian ciliary ganglion: A classic model system for the study of neuronal differentiation and development. *Prog. Neurobiol.* **43**, 281–322.
- Dryer, S. E., and Chiappinelli, V. A. (1987). Analysis of quantal content and quantal conductance in two populations of neurons in the avian ciliary ganglion. *Neuroscience* **20**, 905–910.
- Finn, T., and Nishi, R. (1996). Does ciliary neurotrophic factor serve a different function in the rat versus the chicken? *Perspect. Dev. Neurobiol.* **4**, 91–99.
- Fujii, J. T., and Berg, D. K. (1987). Formation of calyx-like contacts preferentially on appropriate target neurons in culture. *Dev. Biol.* **123**, 346–353.
- Hamburger, V. L., and Hamilton, H. L. (1951). A series of normal stages in the development of the chick embryo. *J. Morphol.* **88**, 49–92.
- Haugland, R. P. (1996). “*Handbook of Fluorescent Probes and Research Chemicals.*” Eugene.
- Ip, N. Y., and Yancopoulos, G. D. (1992). Ciliary neurotrophic factor and its receptor complex. *Prog. Growth Factor Res.* **4**, 139–155.
- Lee, W. M., Smiley, G. G., and Nishi, R. (2001). Cell death and neuronal replacement during formation of the avian ciliary ganglion. *Dev. Biol.* **233**, 437–448.
- Martin, A. R., and Pilar, G. (1963). Transmission through the ciliary ganglion of the chick. *J. Physiol.* **168**, 464–475.
- Marwitt, R., Pilar, G., and Weakly, J. N. (1971). Characterization of two ganglion cell populations in avian ciliary ganglia. *Brain Res.* **25**, 317–334.
- McNerney, M. E., Pardi, D., Pugh, P. C., Nai, Q., and Margiotta, J. F. (2000). Expression and channel properties of α -bungarotoxin-sensitive acetylcholine receptors on chick ciliary and choroid neurons. *J. Neurophysiol.* **84**, 1314–1329.
- Nishi, R. (1994). Target-derived molecules that influence the development of neurons in the avian ciliary ganglion. *J. Neurobiol.* **25**, 612–619.
- Nishi, R. (1996). Autonomic and sensory neuron cultures. *Methods Cell Biol.* **51**, 249–263.
- Nishi, R., and Berg, D. K. (1981). Two components from eye tissue that differentially stimulate the growth and development of ciliary ganglion neurons in cell culture. *J. Neurosci.* **1**, 505–513.
- Stanley, E. F., and Goping, G. (1991). Characterization of a calcium current in a vertebrate cholinergic presynaptic nerve terminal. *J. Neurosci.* **11**, 985–993.
- Yamashita, T., Tucker, K. L., and Barde, Y. A. (1999). Neurotrophin binding to the p75 receptor modulates Rho activity and axonal outgrowth. *Neuron.* **24**, 585–593.

CHAPTER 4

The Culture of Chick Forebrain Neurons

**Steven R. Heidemann, Matthew Reynolds, Kha Ngo, and
Phillip Lamoureux**

Department of Physiology
Michigan State University
East Lansing, Michigan 48824

- I. Introduction
 - II. Growth and Development Characteristics
 - A. Chick Forebrain Neurons Develop into Typical Pyramidal Neurons in Low-Density Culture
 - B. Chick Forebrain Neurons Show Elongation Behaviors Similar to Hippocampal Neurons
 - C. Chick Forebrain Neurons Differ in Important Ways from Hippocampal Neurons
 - III. Isolation of Single Chick Forebrain Neurons
 - A. Obtaining and Maintaining Chick Embryos
 - B. Dissection of the Forebrain
 - C. Dissociation of Forebrain Tissue
 - IV. Culture Conditions for Chick Forebrain Neurons
 - A. Polylysine Treatment of Tissue Culture Surfaces
 - B. Culture Media
 - C. Plating Efficiency and Culture Density
 - D. Improvements for the Future
- References

Dissociation of the forebrain of a single 8-day chick embryo produces $>10^7$ neurons in nearly pure culture. Our methods allow 50–70% of these neurons to develop an axon and typical pyramidal shape after 3–4 days in culture at low density (10^4 cells/cm²) by a stereotyped developmental sequence similar to that of rat hippocampal neurons. The culture method for chick forebrain neurons is unusually rapid, inexpensive, simple, and could be used in undergraduate laboratory exercises. The dissection and dissociation of the tissue are easy and

rapid, requiring less than 30 min from cracking open the chicken egg to plating the cells. Axonal development by these neurons and growth for about a week do not require glial support. The neurons are grown on polylysine-treated culture surfaces in either CO₂-dependent (Medium 199) or -independent (Liebovitz L15) media with 10% fetal bovine serum and a supplement based on the classic N2 supplement for neuronal culture.

I. Introduction

The culture of forebrain neurons from embryonic chicks at day 8 (E8) is notable for the rapidity, ease, and economy of obtaining very large numbers of neurons with highly stereotyped development of a typical pyramidal shape (Fig. 1).

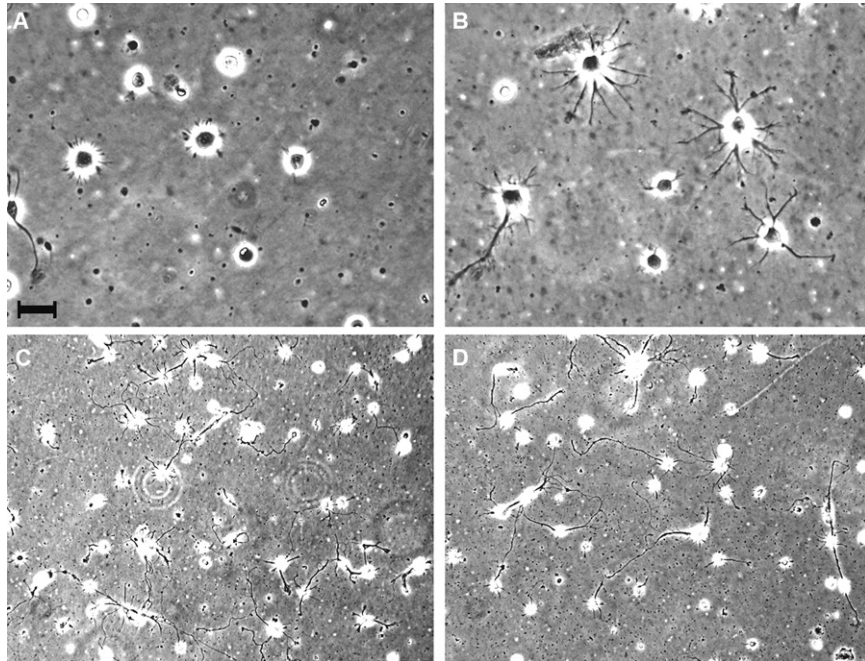


Fig. 1 Axonal morphogenesis by chick forebrain neurons in culture. (A) Phase micrograph of cells approximately 4 h after plating. Most cells have short filopodial and/or lamellipodial extensions surrounding the margin of the cell. We call this stage 1, as for rat embryonic hippocampal neurons. (B) After 1 day in culture, most cells have developed minor processes and thus developed to stage 2. A few neurons have begun axonal outgrowth, e.g., the neuron in the lower left, and so advanced to stage 3. (C) Lower magnification view of a culture after 3 days: 40–50% of neurons have developed an axon and developed to stage 3. (D) After 5 days the fraction of cells developing to stage 3 has leveled off at 50–70% of neurons. After day 5, all neurons begin to degrade when cultured in L15 medium (see Section IV.B). In Medium 199, stage 3 neurons remain healthy for another 5–7 days, but cells that do not develop to stage 3 undergo gradual attrition. Bar: 22 μm (A and B) and 44 μm (C and D).

Indeed, the lack of technical and equipment needs for their most basic culture methodology even suits these neurons for use in undergraduate laboratory classes. With somewhat more refined protocols of culture, we have used them for toxicological assays (Heidemann *et al.*, 2001) and for cell biological studies of axonal development (Chada *et al.*, 1997). Having had experience culturing other neuronal cells, including chick sensory neurons, rat hippocampal neurons, and PC 12 cells, our goal is to draw attention to the substantial advantages of these neurons in terms of ease, animal-use issues, economy, productivity, and authentic neuronal character. That is, we would like to cordially invite the community of cell neurobiologists to consider using and developing these neurons because we believe they would prove highly suitable for many applications of single cell neuronal culture. However, this will require additional studies to further optimize their development and to develop biochemical and genetic markers of the kind that exist for other cultured neurons. Although their culture was introduced in the mid-to-late 1970s by Sensenbrenner and colleagues, including a high-profile report (Pettman *et al.*, 1979), only a few laboratories routinely used chick forebrain neurons in the 1980s and 1990s, notably that of A. Vernadakis in a wide variety of studies. We believe these neurons deserve wider use.

II. Growth and Development Characteristics

In addition to their technical conveniences, we chose to work with chick forebrain neurons because they share several useful growth characteristics with rat E19 hippocampal neurons in low-density culture (Goslin and Banker, 1991). The latter is a standard preparation for a variety of cytological studies in which clear observations of neurites belonging to a particular cell body are needed, e.g., specification of axonal/dendritic polarity (Craig and Banker, 1994) and the role of the cytoskeleton in axonal function (e.g., Fischer *et al.*, 1998). Unlike rat hippocampal neurons, however, chick forebrain neurons do not require “the black magic of nerve cell culture” (Goslin and Banker, 1991) but grow well with simple procedures and conditions.

A. Chick Forebrain Neurons Develop into Typical Pyramidal Neurons in Low-Density Culture

We were initially attracted to chick forebrain neurons because they can be grown at low enough density to clearly identify neurites as axons belonging to a particular cell body, which was needed for cytomorphological work (Chada *et al.*, 1997). We also found that these neurons develop their classical pyramidal shape by a series of stereotyped stages. We used this property to quantitatively assess the inhibition of axonal morphogenesis by sublethal exposure to methylmercury (Heidemann *et al.*, 2001), a potent neurotoxicant that is particularly damaging during early neural development (National Research Council, 2000). The stereotyped progression to axonal outgrowth is similar to that of rat hippocampal

neurons as described by Dotti *et al.* (1988) from whose studies we have adopted our three stages of axonal development and our terminology. Fig. 1 shows the development of chick forebrain neurons during a 5-day period after plating. Shortly after plating (Fig. 1A), chick forebrain neurons show lamellipodial and filopodial motility all along their margin, as do hippocampal and most other neurons in culture. This early stage is called “stage 1.” After a day in culture (Fig. 1B), most neurons have developed to “stage 2,” which is characterized by short tapering neurites called “minor processes.” Some cells remain in stage 2 and never develop axons. However, 50% or more of the cells extend a single (usually) axon and thereby develop to “stage 3” by the third, fourth, and fifth day in culture (Figs. 1C and 1D). This axonal outgrowth occurs via rapid elongation of one of the minor processes, again very similar to axonal growth in hippocampal neurons [see Craig and Banker (1994) for a discussion of the development of axons from minor processes]. As shown in Figs. 1 and 2, individual neurons developing to stage 3 are typical pyramidal brain neurons. This morphology not only allows for clear axonal identification, but is another advantage for student laboratory use because such pyramidal neurons are the typical textbook illustration of a neuron.

B. Chick Forebrain Neurons Show Elongation Behaviors Similar to Hippocampal Neurons

Similar to hippocampal neurons (Ruthel and Banker, 1998, 1999), chick forebrain neurites often elongate via a cycle of retraction and subsequent net elongation accompanying the arrival of a “wave” of motility that propagates along the axon (Fig. 3). A motile growth cone-like structure appears near the proximal end of the neurite (Fig. 3A) and then moves distally toward the true growth cone (Fig. 3B). As the wave approaches the distal end, the neurite retracts (Fig. 3C), but then elongates again over the following 10–15 min (Fig. 3D) showing a net elongation of about the length of a growth cone. The motile behavior of the wave, retraction, and elongation behavior, as well as the time course and step size of elongation, are all very similar to rat hippocampal axons (see Fig. 2; Ruthel and Banker, 1999).

C. Chick Forebrain Neurons Differ in Important Ways from Hippocampal Neurons

The foregoing developmental, growth, and general shape similarities of hippocampal and chick forebrain neurons suggest to us that both cell types share certain properties that are probably conserved among embryonic forebrain pyramidal neurons. There are also differences with hippocampal neurons in culture. Although one’s first impression is the morphological similarity of the two neurons, direct comparison shows that chick forebrain neurons (Fig. 2A) have slightly larger, more rounded cell bodies and their neurites are a larger caliber than hippocampal neurons (Fig. 2B). Also, the sequence of development of chick forebrain neurons is slower by about a day compared to optimal cultures of hippocampal neurons. For our work, at least, these two differences proved useful insofar as larger cells are easier to manipulate and slower development allows for a

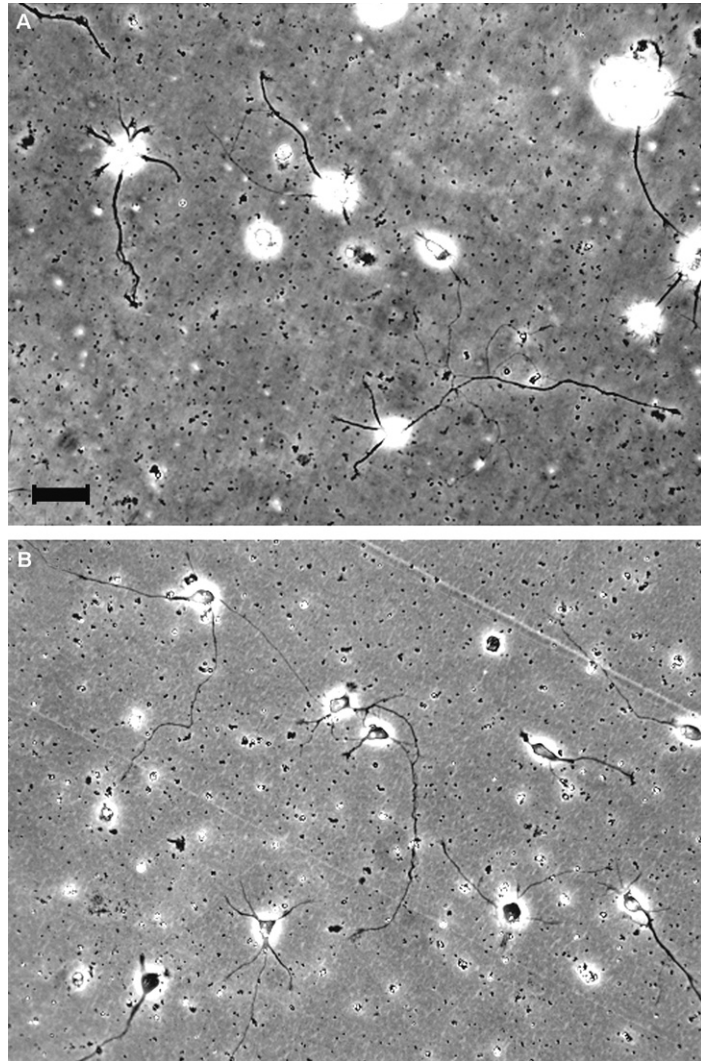


Fig. 2 Morphological comparison of chick forebrain neurons and embryonic rat hippocampal neurons in early stage 3. (A) Chick forebrain neurons show typical pyramidal morphology with a single axon, usually, and several nongrowing minor processes. These neurons have a particularly rounded cell body and are thus obscured by the halo that is characteristic of Zernike phase optics. (B) Rat hippocampal neurons also show a typical pyramidal shape, but both the cell body and the neurites are more delicate than those of chick forebrain neurons. Both neuronal types were cultured on polylysine-treated tissue culture plastic. Bar: 20 μm .

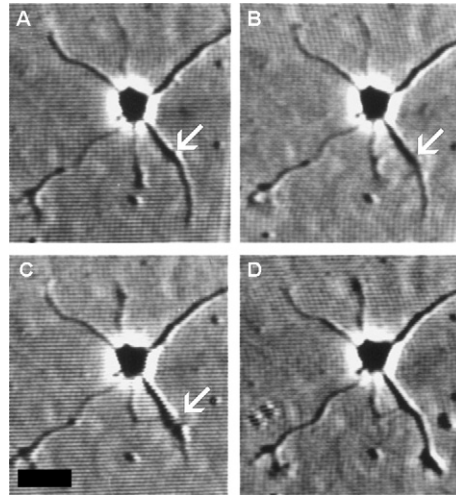


Fig. 3 Motile growth cone-like waves accompany neurite elongation in chick forebrain neurons, as reported for hippocampal neurons. Frames are taken from analog time-lapse video recordings of a chick forebrain neuron in culture. (A) A motile wave (arrow) develops in the proximal region of a minor process. The lamellipodial activity of this thickening is clear in time lapse. (B) Three minutes later, this wave has moved distally along the neurite. (C) As the motility wave approaches the distal end of the neurite (4 min after B), the neurite retracts, which is followed some 8 min later (D) by net elongation and thickening of the neurite. These motility behaviors associated with outgrowth are similar in appearance, size, and time scale to those reported for rat hippocampal neurons by Ruthel and Banker (1999). These behaviors accompany approximately 40% of elongation bouts by chick forebrain neurons. Bar: 15 μm .

longer time window to investigate initial axonal morphogenesis. Morphologically, at least, the minor processes of stage 3 chick forebrain neurons do not subsequently grow into well-developed dendrites and thus fail to develop to stages 4 and 5, as do hippocampal neurons (Dotti *et al.*, 1988). Although chick forebrain neurons will grow at sufficiently low densities to count, manipulate, and image individual cells, they will not develop at the very low density reported for hippocampal neurons (1000 cells/cm²; Goslin and Banker, 1991). Plating efficiency and cell density results for chick forebrain neurons are discussed in Section IV,C.

III. Isolation of Single Chick Forebrain Neurons

The ease of locating, identifying, and dissecting the telencephalon of E8 chicks is one of the most attractive features of this preparation. Typical, brief trypsin treatment and dispersion or just simple mechanical dispersion of this tissue layer produces a mixture of single cells and larger cell aggregates. A simple settling procedure then produces a reasonably uniform suspension of single neurons of 90–99% purity. A single embryo produces enough neurons for approximately fifty

60-mm plates at low density (300,000 cells/dish). In our hands, the entire procedure from cracking open the egg to a suspension of cells ready for plating takes less than 30 min, another feature that suits this culture system to undergraduate student laboratories.

A. Obtaining and Maintaining Chick Embryos

We obtain our chick embryos from our university's poultry farm. Workers at or near other "ag schools" will likely enjoy the same convenient source, and others can use such academic poultry operations to obtain information about local poultry farms/hatcheries as suppliers of fertilized eggs and/or later embryos. Government agricultural agents are also a good source for such information. Fertilized chicken eggs are more widely available than later embryos because the former are produced for the organic food market. While fertilized, unincubated eggs in the retail store are not suitable for culture use, eggs from a local wholesale source usually are.

Conveniently, unincubated eggs (<24 h by the hen) can be stored at 15–18°C in an airtight food container for 7–10 days, which curtails embryonic development completely without damaging subsequent development (North and Bell, 1990). By placing these eggs into incubation every 1–2 days, a single purchase of fertilized eggs can provide 8-day-old embryos throughout a week. Longer term storage at lower temperatures progressively inhibits any subsequent development, which is presumably the reason refrigerated fertilized eggs from a retail store do not develop well. In contrast to unincubated eggs, eggs incubated by the hen for >24 h cannot be stored conveniently for useful lengths of time, although a reduced incubation temperature (34°C) will slow development.

The egg incubator we use to support normal development is an inexpensive styrofoam box with a fan and thermostatted heater that accepts the standard cardboard tray for 30 eggs (Hov-a-bator, G.Q.F. Mfg. Co, Savannah, Georgia; www.gqfmfg.com). At the bottom of this unit, there is a reservoir channel for water to humidify the eggs, which also should be turned every day. These or similar units can often be purchased from a local agricultural supply house ("feed-and-seed store").

As the foregoing suggests, chick embryos are obtained and used under agricultural guidelines and practices. Their price reflects the economy of an agricultural commodity, and chicken eggs raise fewer animal-use issues than mammalian embryos. In cases where forebrain neurons can substitute for mammalian neurons, the use of chick embryos fulfills an ethical desire to substitute simpler animals for more complex in studies of primary neurons in culture.

B. Dissection of the Forebrain

In addition to standard tissue culture items, such as serological pipettes and sterile tubes, the only tools we use for dissection include two pairs of watchmakers

forceps (Dumont #5, inexpensive “electronic grade” suffice) and a sterile Pasteur pipette that has been scored and broken off to produce a 3- to 5-mm orifice and then fire polished and sterilized by a gas flame. Anesthesia of the embryo at E8 is impractical: the embryo begins to die after cracking the egg because rupture of the extraembryonic vasculature causes blood pressure to fall to near zero. The egg is cracked open into the top of a 100-mm petri plate, and the embryo is isolated with the forceps from the yolk and extraembryonic tissue. The embryo is decapitated quickly as near to the trunk as possible to allow the head to be immobilized on a wax-filled dissection plate by a pin through the neck. (We make our dissection dishes by filling a petri plate with melted histological embedding wax and allowing the wax to harden.) All waste is deposited into a plastic bag and disposed of as for food.

For dissection, magnification (from simple reading glasses to a dissecting scope) is helpful, but not absolutely required. The two forebrain hemispheres form an easily observed triangle of grayish tissue at the most forward portion of the head: one point is located just behind the beak; two sides of the triangle are next to each of the large eyes. The third side is formed by the left-to-right brain fissure separating the two forebrain hemispheres from the midbrain, which is seen easily by the vasculature running through this fissure. The neural tissue is overlain by two, thin almost transparent layers (later to become skin and bone) that should be removed individually with watchmakers forceps. All of the tissue of the embryo is quite soft at this early stage and both layers can be removed as if one were tearing wet tissue paper with forceps. It is helpful to begin the dissection at the central fissure of the forebrain so that the forceps pierce the two overlying layers in a gap between neural tissues, thus minimizing the risk of a stab wound to the brain hemispheres. Once the overlying tissue is removed, each telencephalon is removed by bringing open forceps down around and beneath the hemisphere. Subsequent squeezing and lifting of the forceps should release the hemisphere like removing a grape at the stem.

We process the isolated tissue through two 35-mm culture dishes containing Ca^{2+} , Mg^{2+} -free Hanks balanced saline (HBSS) buffered to pH 7.4 with 5 mM HEPES and containing 100 U/ml of penicillin G and 100 $\mu\text{g/ml}$ streptomycin sulfate. In the first dish, we remove the overlying meninges, some of which may have been removed by previous dissection maneuvers. This very thin layer of cells on the outside (pial surface) of the hemispheres is highly vacularized and can be seen by its red tinge compared to the nearly white neural tissue. Complete and careful removal of the meninges (“never a trace of red”) is the most important step in ensuring cultures of nearly pure neurons. After removal of the meninges, the tissue is moved to the second dish of HBSS and minced with the forceps. Up until this point in the procedure, we have sterilized the forceps several times by a brief rinsing in alcohol and brief flaming. The tissue fragments are harvested from the dish by the broken Pasteur pipette. By allowing the tissue fragments to settle in this pipette, a drop or two will place all of the tissue at the bottom of a sterile 15-ml tube for dissociation.

C. Dissociation of Forebrain Tissue

Tissue dissociation is performed in HBSS. The simplest method is to vigorously vortex the tube containing the tissue fragments in 2 ml of HBSS and then gently aspirate through a 10-ml pipette. However, we routinely use a typical trypsin dissociation. We add 2 ml of 0.1% crude trypsin (“1:250 trypsin,” Sigma) in HBSS to the tube containing the brain fragments and incubate in a 37°C water bath with vortexing every 2 min for about 8 min. After 8 min, the tissue is aspirated five or six times through a sterile 10-ml serological pipette and is then incubated another 2–5 min with occasional vortexing. Some tissue fragments usually remain and we let these settle to the bottom of the tube for a few minutes. Then, using a sterile Pasteur pipette, we transfer the supernatant suspension of single cells into another sterile tube. Simple swirling of this tube allows quite uniform aliquots of cells to be delivered from this tube into each culture vessel.

Not surprisingly, all cultures have some level of detritus and dead or abnormal cells. Unfortunately, some of this contamination is not removed easily because it sticks to the polylysine-treated culture surface (see later). However, living cells in the culture are nearly pure neurons, as claimed originally by Pettman *et al.* (1979), which is consistent with the finding that glia do not develop in the chick forebrain until E10 (Tsai *et al.*, 1981). After dissociation and settling, we count the number of cells in a hemocytometer and find that we obtain $2\text{--}5 \times 10^7$ neurons of 90–95% viability (as shown by trypan blue exclusion) from the two hemispheres of a single embryo.

IV. Culture Conditions for Chick Forebrain Neurons

Chick forebrain neurons are grown on polylysine-treated culture surfaces, either glass or plastic. Like all other neurons we have cultured, chick forebrain neurons grow better on tissue culture plastic than on equivalently treated glass. We find that two “classic” culture media are particularly suitable for these neurons: Medium 199 is CO₂ dependent and Leibovitz’s L-15 is CO₂ independent. We routinely supplement both with a variety of growth promoters, as discussed later. Like most brain neurons, chick forebrain neurons grow better at higher density, but good development and good single cell access are achieved at a plating density of 1×10^4 cells/cm². In our hands, two widely used methods of improving the survival and development of brain neurons have in fact proven inhibitory to forebrain neurons: high K⁺ in the medium and coculture with glial-derived factors.

A. Polylysine Treatment of Tissue Culture Surfaces

Five to 10 min prior to the dissection of the embryo, we begin polylysine treatment of the culture surfaces. For plastic tissue culture surfaces, our protocol is to flood the surface with 0.1% poly-L-lysine hydrobromide (1 mg/ml, Sigma) in Dulbecco’s phosphate-buffered saline (PBS) containing Ca²⁺ and Mg²⁺. Many

laboratories use polylysine dissolved in 0.1 M sodium borate buffer, pH 8.5, which works equally well. We pipette off most of the solution, leaving only a thin layer of solution on the surface. The recovered solution is then used to flood the next surface, and so on. At the earliest opportunity we cover the culture vessel. Near the end of the trypsin dissociation outlined earlier, we rinse the culture surface three times in sterile H₂O. Typically, the polylysine solution is in contact with the dish for approximately 30 min. At least on tissue culture plastic, longer treatment times do not improve attachment or development of these neurons.

For glass coverslips, we sterilize and clean ordinary glass coverslips by soaking them in absolute ethanol for 10 min. Using Dumont #5 forceps, we drain each coverslip and then ignite the ethanol by passing through a gas flame. (A high rate of coverslip cracking is usually due to insufficient drainage of the ethanol prior to ignition.) Polylysine treatment is similar to that described earlier except that rather than flooding the surface, we place approximately 1 ml of the same polylysine solution onto the coverslip. With care, the solution remains restricted to the coverslip by surface tension.

B. Culture Media

In terms both of longevity of culture and of the fraction of cells developing axons to stage 3, our best results have been obtained in Medium 199 (Table I), which was originally developed to support chick embryo fibroblasts (Morgan *et al.*, 1955). This medium is superior to other CO₂-dependent media we tried, including MCDB, RPMI 1640, Hams F12, DMEM, MEM, and neurobasal medium (Life Technologies Inc.). When using Medium 199, we equilibrate the medium in a 5% CO₂ atmosphere prior to plating because chick forebrain neurons (like hippocampal neurons) are quickly damaged by exposure to alkaline conditions.

We also routinely use Leibovitz's L15 medium, which is buffered by its constituent amino acids, not CO₂-bicarbonate, because our work has often involved extended periods of manipulation on a microscope stage in the ambient atmosphere (Chada *et al.*, 1997). This medium supports slightly less robust axonal

Table I
Fraction of Chick Forebrain Cells Developing an Axon (Stage 3)

Media tested	Third day of growth	Fifth day of growth
199 ($n = 8$) ^a	45.5	73.3
L15 + ($n = 6$)	26.9	52.6
DMEM ($n = 4$)	40.3	39.3
MEM ($n = 2$)	39.6	18.8
Ham F12 ($n = 4$)	20.9	29.7
MCDB ($n = 4$)	25.0	42.8

^a n = Number of dishes in which cell counts were taken in 1-mm circles etched shortly after plating [see Heidemann *et al.* (2001) for more on the method of quantitation of development]. All media contained 10% fetal bovine serum and the N9 supplement.

development than Medium 199 (Table I) and cultures stay healthy only for 5–7 days. However, this medium is clearly superior to the use of HEPES buffering in any of the aforementioned CO₂-dependent media or CO₂-independent medium (Life Technologies Inc.). L15 would appear to be advantageous for undergraduate laboratories in that it requires only a space heated to 37°C, not the CO₂ tank, regulator, and incubator typically used. Also useful for the constraints of undergraduate laboratories, respectable axonal development (15% in stage 3 at day 3) can be achieved with only L15+ or Medium 199 and serum without the additional supplements outlined later.

Our current optimal conditions for growth and development include a large number of supplements, but which we have combined so that culture preparation is not onerous. We prepare both media from dry powder to which we add 100 U/ml of penicillin and 100 µg/ml streptomycin. We also add 0.6% glucose and 2 mM glutamine to L15 (Bray, 1991), which we call L15+. Just prior to use, mix either L15+ or Medium 199 with three additional liquid components: (a) 10% fetal bovine serum (horse serum does not support robust axonal development), (b) 7S nerve growth factor (100 ng/ml from a 1-mg/ml stock, Harlan Bioscience Inc.,

Table II
Preparation of N9 Neuronal Growth Supplement

A. Individual component stock solutions

Selenium dioxide ^a	37.5 µg/ml	in phosphate-buffered saline (PBS)
Putrescine dihydrochloride	16.1 mg/ml	in PBS
BSA	10 mg/ml	in PBS
Partially iron-saturated human holo-transferrin (not apo-transferrin)	10 mg/ml	in PBS
Insulin	10 mg/ml	in 0.01 M HCL
Tri-iodothyronine	200 µg/ml	in 0.01 M NaOH
Progesterone	0.63 mg/ml	in EtOH absolute
Corticosterone	2 mg/ml	in EtOH absolute
β-Estradiol	100 µg/ml	in EtOH absolute

B. Preparing 50 ml of 10 × N9 supplement from component stock solutions

To 40 ml of preferred medium (we use L15+), add the following volumes of the individual component stocks

Selenium dioxide	1 ml
Putrescine	1 ml
BSA	1 ml
Transferrin	5 ml
Insulin	1 ml
Tri-iodothyronine	50 µl
Progesterone	50 µl
Corticosterone	50 µl
β-Estradiol	0.5 ml

^aA 20× prestock solution of SeO₂ is prepared at 0.75 mg/ml and then diluted in PBS.

Indianapolis, IN), and (c) 10% by volume of a supplement mixture we call N9 (Table II). This supplement mixture was developed from the basic N2 supplement (Bottenstein and Sato, 1979), but several component concentrations have been changed, and we have added tri-iodothyronine, estradiol, and corticosterone (Akuzawa and Wakabayashi, 1985; Ferreira and Caceres, 1991). The final concentrations of N9 components (all from Sigma) in the medium are bovine serum albumin (20 $\mu\text{g/ml}$), corticosterone (200 ng/ml), β -estradiol (100 ng/ml), insulin (20 $\mu\text{g/ml}$), progesterone (63 $\mu\text{g/ml}$), putrescine dihydrochloride (32 $\mu\text{g/ml}$), selenium dioxide (75 ng/ml), partially iron-saturated human holo-transferrin (not apo-transferrin) (100 $\mu\text{g/ml}$), and tri-iodothyronine (20 ng/ml). As outlined in Table II these supplements are prepared by making and freezing concentrated stocks of each component in appropriate solvents. These are then used to mix 10 \times concentrated supplement in unsupplemented L15+ medium, which in turn is frozen in aliquots for addition to the basic medium. This supplement was substantially better at supporting axonal development of chick forebrain neurons than commercially available N2 or B27 supplements used according to the supplier's directions (Life Technologies Inc.). Needless to say, we have not tried every potential growth supplement; we found that the addition of ascorbic acid or its metabolites (Makar *et al.*, 1994) or pyruvate (Bottenstein and Sato, 1979) to the supplement mixture did not improve neuronal development. The addition of gangliosides to synthetic medium has been reported to improve axonal outgrowth (Ferrari *et al.*, 1983; Cestelli *et al.*, 1985), and our original formulation for N9 (Heidemann *et al.*, 2001) included a crude mixture of bovine brain gangliosides (Sigma). However, this particular product is no longer available, and we found that higher purity ganglioside preparations, which are expensive, inhibited growth. Insofar as the addition of the original ganglioside preparation improved growth only marginally, we have not pursued gangliosides further. The chick embryo extract, both commercial and laboratory prepared, did not improve the development of forebrain neurons at 0.5% concentration and inhibited development at higher concentrations.

Many brain neurons in culture benefit from medium containing high $[\text{K}^+]$ (Franklin and Johnson, 1992), but not chick forebrain neurons. Added at 12, 20, or 25 mM in either L15+ or medium 199-supplemented media, K^+ reduced the frequency of cells developing axons to approximately half that seen in control cultures lacking added K^+ , and by the fifth day nearly all cells were dead.

As we have described, chick forebrain neurons share several growth characteristics with rat hippocampal neurons. The latter are usually cultured with glia or with glia-conditioned medium. Curiously, our experience coculturing chick forebrain neurons with either rat or chick glia has been uniformly negative. Far from helping to support development, in our hands, the addition of glia on an overlying coverslip or growth in glia-conditioned medium substantially inhibited axonal development and hastened cell death even during the first day of culture. It should be noted that Pettman *et al.* (1979) emphasized the lack of need for glia to support development in chick forebrain neurons.

C. Plating Efficiency and Culture Density

As mentioned earlier, chick forebrain neurons will not develop axons at the very low densities (1000 cells/cm²) of which hippocampal neurons are capable (Goslin and Banker, 1991). We have conducted most of our work with $8\text{--}10 \times 10^3$ cells/cm² as an actual density of cells on the dish or coverslip surface. This is low enough to allow for most axons to be clearly associated with a particular cell body but high enough to support axonal development by >50% of cells. In general, the apparent health of the culture increases with increasing density, and we get little or no axonal development at densities below 5×10^3 cells/cm².

As with most primary cell cultures, there is a substantial loss of cells at early times after plating. After allowing 2–4 h for cell settling and attachment, only 60–70% of neurons added to the dish can be accounted for on the dish surface. By the third day after plating, attrition has reduced the cell number to approximately 50% of those plated. Thus, we typically add twice the number of cells that would otherwise be expected to achieve the desired plating density. After day 4 or 5, we find that those cells that have not yet elaborated an axon begin to die and lose adhesion to the culture surface. Thus, cell density decreases while the fraction of cells in stage 3 increases at longer times of culture, particularly in Medium 199 in which stage 3 neurons remain healthy for about 10 days if the medium is changed every other day. After the elaboration of axons, the fasciculation of axons from different neurons occurs to varying extents. In some cultures, cell bodies also have a tendency to clump after 5 days in culture. Based on anecdotal observations from time-lapse video, this is due in part to neurites contacting other cell bodies, and subsequent contraction of the neurite pulls the cell bodies together.

D. Improvements for the Future

The economy, ease, and simplicity of obtaining freshly prepared chick forebrain neurons would appear to be nearly optimal. However, it is hoped that improvements in culture conditions can be developed for this preparation that would increase their resemblance to rat hippocampal neurons in culture, particularly at longer times. That is, hippocampal neurons cocultured with astrocytic glia can be routinely maintained for 3–5 weeks (Goslin and Banker, 1991), whereas chick forebrain neurons remain healthy only for 10 days in the conditions described earlier. Hippocampal neurons develop axons at a very low plating density and also develop dendrites after about a week in culture, although this is less routine than axonal development (Goslin and Banker, 1991; G. Ruthel, personal communication). These growth characteristics of cultured hippocampal neurons are highly dependent on coculture with rat glial cells. In the absence of glia, hippocampal neurons develop much less well than chick sensory neurons. For this reason, we were particularly disappointed by our lack of success in improving culture conditions for chick forebrain neurons using the glial coculture (Section IV,B). In our own work, the limitations of chick forebrain neurons compared to rat hippocampal neurons have not been serious. For this reason, we

have made several, but by no means exhaustive, efforts to improve the culture of these cells. It is hoped in the future that additional growth supplements and/or culture conditions can be identified that improve the development and health of chick forebrain neurons. As noted in the introduction, the advantages of these neurons seem to us to make improvements in their culture very worthwhile, and cooperation among users would be most welcome. Thus, we would be grateful to workers who use chick embryonic neurons if they would share their experiences with us and, for our part, we would be pleased to answer queries from scientists regarding our experiences with these neurons.

Acknowledgment

Our work on chick forebrain neurons was supported by NSF Grant IBN 9603640.

References

- Akuzawa, K., and Wakabayashi, K. (1985). A serum-free culture of the neurons in the septal, pre-optic and hypothalamic region: Effects of tri-iodothyronine and estradiol. *Endocrinol. Japan* **32**, 163–173.
- Bottenstein, J. E., and Sato, G. H. (1979). Growth of rat neuroblastoma cell line in serum-free supplemented medium. *Proc. Natl. Acad. Sci. USA* **76**, 514–517.
- Bray, D. (1991). Isolated chick neurons for the study of axonal growth. In “Culturing Nerve Cells” (G. Banker and K. Goslin, eds.), pp. 119–135. MIT Press, Cambridge, MA.
- Cestelli, A., Savettieri, G., Ferraro, G., and Vitale, F. (1985). Formulation of a novel synthetic medium for selectively culturing rat CNS neurons. *Dev. Brain Res.* **22**, 219–227.
- Chada, S., Lamoureux, P., Buxbaum, R. E., and Heidemann, S. R. (1997). Cytomechanics of neurite outgrowth from chick brain neurons. *J. Cell Sci.* **110**, 1179–1186.
- Craig, A. M., and Banker, G. (1994). Neuronal polarity. *Annu. Rev. Neurosci.* **7**, 267–310.
- Dotti, C. G., Sullivan, C. A., and Banker, G. A. (1988). The establishment of polarity by hippocampal neurons in culture. *J. Neurosci.* **8**, 1454–1468.
- Ferrari, G., Fabris, M., and Gorio, A. (1983). Gangliosides enhance neurite outgrowth in PC12 cells. *Dev. Brain Res.* **8**, 215–221.
- Ferreira, A., and Caceres, A. (1991). Estrogen-enhanced neurite growth: Evidence for a selective induction of tau and stable microtubules. *J. Neurosci.* **11**, 392–400.
- Fischer, M., Kaeck, S., Knutti, D., and Matus, A. (1998). Rapid actin-based plasticity in dendritic spines. *Neuron* **20**, 847–854.
- Franklin, J. L., and Johnson, E. M., Jr. (1992). Suppression of programmed neuronal death by sustained elevation of cytoplasmic calcium. *Trends Neurosci.* **15**, 501–508.
- Goslin, K., and Banker, G. (1991). Rat hippocampal neurons in low-density culture. In “Culturing Nerve Cells” (G. Banker and K. Goslin, eds.), pp. 251–281. MIT Press, Cambridge, MA.
- Heidemann, S. R., Lamoureux, P., and Atchison, W. D. (2001). Inhibition of axonal morphogenesis by nonlethal, submicromolar concentrations of methylmercury. *Toxicol. Appl. Pharmacol.* **174**, 49–59.
- Makar, T. K., Nedergaard, M., Preuss, A., Gebard, A. S., Perumal, A. S., and Cooper, A. J. L. (1994). Vitamin E, ascorbate, glutathione, glutathione disulfide, and enzymes of oxidative metabolism in cultures of chick astrocytes and neurons: Evidence that astrocytes play an important role in oxidative processes in the brain. *J. Neurochem.* **62**, 45–53.
- Morgan, J. F., Campbell, M. E., and Morton, H. J. (1955). The nutrition of animal tissues cultivated in vitro. I. A survey of natural materials as supplements to synthetic Medium 199. *J. Natl. Cancer Inst.* **16**, 557–566.

- National Research Council. (2000). "Toxicological Effects of Methylmercury," National Academy Press, Washington, DC.
- North, M. O., and Bell, D. D. (1990). In "Commercial Chicken Production Manual," 4th Ed., pp. 96–100. Van Nostrand Reinhold, New York.
- Pettmann, B., Louis, J. C., and Sensenbrenner, M. (1979). Morphological and biochemical maturation of neurones cultured in the absence of glial cells. *Nature* **281**, 378–380.
- Ruthel, G., and Banker, G. (1998). Actin-dependent anterograde movement of growth-cone-like structures along growing hippocampal axons: A novel form of axonal transport? *Cell Motil. Cytoskel.* **40**, 160–173.
- Ruthel, G., and Banker, G. (1999). Role of moving growth cone-like "wave" structures in the outgrowth of cultured hippocampal axons and dendrites. *J. Neurobiol.* **39**, 97–106.
- Tsai, H. M., Garber, B. B., and Larramendi, L. M. H. (1981). ³H-thymidine autoradiographic analysis of telencephalic histogenesis in the chick embryo. I. Neuronal birthdates of telencephalic compartments in situ. *J. Comp. Neurol.* **198**, 275–292.

This Page Intentionally Left Blank

CHAPTER 5

Growing and Working with Spinal Motor Neurons

Thomas B. Kuhn

Department of Pharmaceutical Sciences
University of Montana
Missoula, Montana 59812

- I. Introduction
- II. Incubation of Fertilized Chicken Eggs
 - A. Materials
 - B. Procedure
- III. Preparation of Chick Embryo
 - A. Materials
 - B. Procedures
- IV. Dissection of Intact Spinal Cords and Isolation of Ventral Halves
 - A. Materials
 - B. Procedures
- V. Enzymatic and Mechanical Dissociation of Intact Spinal Cords or Ventral Halves
 - A. Materials
 - B. Procedure
- VI. Plating Motor Neurons or Spinal Cord Neurons
 - A. Materials
 - B. Procedure
- VII. Motor Neuron Enrichment by Density Gradient Centrifugation
 - A. Materials
 - B. Procedure
- VIII. Experimental Use of Motor Neuron Cultures and Spinal Cord Cultures
- IX. Preparation of Solutions, Culture Dishes, Media, and Media Supplements
- References

The chick embryo has a long tradition as a model organism in developmental biology as well as embryology. A year-round supply of fertilized eggs, accessibility to all stages of development, and the ease of manipulation of the embryo all

contribute to the advantages of investigations using chick embryos. A plethora of culture systems have been developed over the past century allowing to culture intact embryos from as early as 2 days of development. Other culture systems include whole embryo slices, organotypic cultures, tissue explants, and dissociated cultures. Studies utilizing the chick embryo, and in particular spinal motor neurons, were crucial for our present knowledge of the development but also adult physiology, injury, and disease of the nervous system. Extensive studies on spinal motor neurons revealed many molecular mechanisms underlying fundamental events, such as neural induction, axon guidance, programmed cell death, and neuron–target interaction. Cultures of dissociated spinal motor neurons represent one important experimental paradigm. This chapter describes two alternative procedures to establish dissociated spinal motor neuron cultures with virtually no contamination by nonneuronal cells.

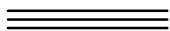
I. Introduction

The common domestic chick (*Gallus gallus*) has a long history as one of the most intensely studied model organisms in embryology and developmental biology, dating as far back as Aristotle (384–323 B.C.E.). William Harvey (1578–1657) resumed Aristotle’s work, followed by many great scientists such as Marcello Malphigi (1628–1694, first microscopic study of chick development), Kaspar Friedrich Wolff (1733–1794), Karl Ernst von Baer (1792–1876), Frank Rattray Lillie (1870–1947), and Viktor Hamburger (1900–2001). Motor neurons of the chick spinal cord represent the best characterized population of central nervous system (CNS) neurons. Extensive studies have covered every aspect of CNS development, ranging from neural induction, cell fate, axon guidance, trophic factors, and target interactions all the way to function, disease, and injury in the adult organism.

The spatial and temporal induction of motor neurons in the chick spinal chord under the regulation of the notochord, the axial mesoderm organizing center, represents one of the best understood systems of neurogenesis during early embryonic development (Tanabe and Jessell, 1996; Pituello, 1997). The pivotal role of sonic hedgehog, a prototypic morphogen, was recognized in the induction and organization of the first postmitotic motor neurons (Roelink *et al.*, 1995). Fundamental principles of axon guidance and target interaction were derived from studies on motor neurons (Yaginuma *et al.*, 1994; deLapeyriere and Henderson, 1997). For instance, distinct subsets of LIM homeodomain transcription factors are crucial for the establishment of the motor neuron subpopulation with distinct innervation patterns (Pfaff *et al.*, 1996). Axon guidance studies on motor neurons revealed the simultaneous integration of attractive and repulsive guidance cues as diverse as target derived, deposited in the extracellular matrix, exposed on the surface of other neurons or nonneuronal cells, or soluble. Other studies have addressed autocrine, paracrine, and even systemic effects of growth factors and androgens and underlying synergisms

at different stages during development (Oppenheim, 1996; Gould *et al.*, 1999; Bibel and Barde, 2000). Formation of the neuromuscular junction is by far the best understood neuron–target interaction in the CNS (Lance-Jones, 1988). Investigations on the naturally occurring cell death of motor neurons during development have contributed significantly to our understanding of programmed cell death (Hamburger, 1975; Houenou *et al.*, 1994). As many as 50% of all motor neurons are eliminated during spinal cord development in vertebrates. Motor neurons are also the study object for various injury models, as well as diseases (Camu and Henderson, 1994; Guale and Burrows, 1997; Bar, 2000). The ease of manipulation of the developing chick embryo contributes significantly to the understanding of the complexity of spinal cord injury (Keirstead *et al.*, 1995; Lu *et al.*, 2000). Also, many inherited and sporadic diseases derive from the selective vulnerability of different motor neuron populations reflected by dysfunction, atrophy, degeneration, and cell death (e.g., amyotrophic lateral sclerosis, juvenile spinal muscle atrophy, Kennedy’s disease).

Numerous experimental paradigms, such as dissociated neurons, organotypic culture system, and even *in ovo* experiments, have been utilized to study the aspects of motor neuron development, adult physiology, injury, and disease (Gaehwiler *et al.*, 1997; Kuhn *et al.*, 1999). The homogeneity of a neuronal population is often critical for understanding neuronal responses to extrinsic cues or insults. For motor neurons, two principal approaches achieve this goal: (1) retrograde labeling of motor neurons in the living chick embryo followed by selective isolation (Calof and Reichardt, 1984; Honig and Hume, 1986) and (2) enrichment of motor neurons based on their unique characteristics (Masuko *et al.*, 1979; Juurlink *et al.*, 1990; Kuhn *et al.*, 1998). In retrograde labeling, spinal cord tissue is dissociated and labeled motor neurons are isolated by cell sorting. Although this approach results in a highly purified, homogeneous population of motor neurons, the yields are low and thus pose a significant limitation. The latter approach takes advantage either of the defined anatomy of motor neurons residing in the ventral spinal cord or the unique buoyant density of motor neurons in conjunction with a virtual absence of nonneuronal cells at early developmental stages. The enrichment of motor neurons based on their restricted localization in the ventral spinal cord or their unique buoyant density are technically simple, result in high yields, and achieve considerable enrichment of motor neurons (approximately 95% motor neurons) with very little to no contamination with other neuronal or nonneuronal cell types. These procedures are described in detail. Protocols for the preparation of solutions, media, sera, culture dishes, and more are summarized in Section IX.



II. Incubation of Fertilized Chicken Eggs

Fertilized chicken eggs can be obtained from many different breeds of chicken, but white leghorns are the most common source for research. Fertilized white

leghorn eggs can be purchased from local farms or from several commercial suppliers, e.g., Carolina Biological (www.carolina.com). Chicken breed independent of seasons and thus fertilized eggs are available year round and in almost any quantity. A good start to finding local suppliers of fertilized eggs, incubators, and anything related to breeding various avian species can be found on the web site of the Poultry Connection (<http://www.poultryconnection.com>).

A. Materials

Humidified incubator (Carolina Biological Supply Company, Burlington, NC; Humidaire Incubator Company, New Madison, OH; G.F.Q. Manufacturing Company, Savannah, CA)

Fertilized white leghorn eggs

Egg candler

Refrigerator

Controlled parameters for the incubation of fertilized eggs comprise correct humidity, stable temperature, and regular rotation of the eggs to prevent sticking of the embryo and are imperative for proper embryonic development. Numerous models of incubators are available, ranging from inexpensive to very expensive, and several texts provide useful information regarding egg incubation (Stromberg, 1975; Demming and Ferguson, 1992; Mason, 1999). Fertilized eggs can be stored for up to 14 days in a refrigerator ($10 \pm 1^\circ\text{C}$); however, fertility declines pro-portionally to storage length.

B. Procedure

It is best not to wash or rinse eggs prior to incubation to avoid clogging of the tiny pores in the eggshell, which are required for proper gas exchange between the embryo and its environment. Although immediate incubation is recommended, fertilized eggs can be stored at $10 \pm 1^\circ\text{C}$ (refrigerator) for up to 14 days. Longer storage should be avoided as fertility declines significantly. Place fertilized eggs into egg cartons or egg trays blunt end up and mark the set date on the egg with a pencil. Incubation should be performed in a forced-air, humidified incubator at $37.5\text{--}38^\circ\text{C}$ and with 50–60% relative humidity. Eggs will tolerate incubation temperatures from 35° to 40°C but will affect the time course of embryonic development. Humidity is maintained easily utilizing an open water reservoir, which has to be filled daily. During incubation, eggs should be turned several times a day to a 45° angle off the vertical. Turning is important as this prevents the embryo from becoming stuck to the eggshell.

To test whether development occurs, eggs can be candled using a specific egg candler or an improvised light source inside a box containing an egg-sized opening. While moving the egg around, it is held against the light source. Victor Hamburger has established a detailed atlas of defined stages of chick embryo

development according to several morphological criteria (Hamburger and Hamilton, 1951). Correct incubation time can be determined according to this atlas. Other excellent texts also refer to chick embryo development (Romanoff, 1960; Freeman and Vince, 1974; Stern, 1994; Bellairs and Osmond, 1998). Motor neurons are obtained from stage 30 embryos (approximately 6-day-old chick embryos). As a rule of thumb, the number of days of incubation taken from the set time correlates well with later stages of embryonic development. Chick embryos older than 6 days are not well suited due to significant motor neuron cell death between embryonic day 6 and 9 and an increased proliferation of nonneuronal cells. Note that chickens hatch at 21 days after incubation.

III. Preparation of Chick Embryo

Spinal cord tissue containing motor neurons is obtained from 6-day-old chick embryos. Removing the chick embryo from the egg requires some practice as at this developmental stage, the embryo is very fragile. To avoid any contamination, all procedures should be carried out in a laminar flow hood. Stainless steel dissection tools can be obtained from several suppliers, including Fine Science Tools (www.finescience.com), World Precision Instruments (www.wpiinc.com), Stoelting (www.stoeltingco.com), Carolina Biological (www.carolina.com), and others. The lifetime of dissection tools can be extended greatly by carefully protecting tips and blades with covers. Bent tips of forceps and scissors can be straightened and sharpened using a sharpening stone.

A. Materials

Fertilized eggs incubated for 6 days

Egg carton

70% ethanol in a spray bottle

Waste receptacle lined with a plastic bag

Box of tissue paper

Dissection instruments (sterile): one straight forceps, one curved forceps, one fine scissors, and one spring scissors

Hank's balanced salt solution (HBSS, Gibco)

Pasteur pipette cotton plugged with a small rubber bulb (sterile)

100-mm glass petri dishes (sterile)

50-ml glass beaker containing 70% ethanol

Dissecting instruments are sterilized either by autoclaving or by immersing into 70% ethanol and very brief flaming in a gas burner. Do not hold instruments into the flame for extended periods of time, as overheating will turn the fine tips of forceps and scissors brittle and useless. A typical setup for the dissection of embryonic chick spinal motor neurons is shown in Fig. 1.

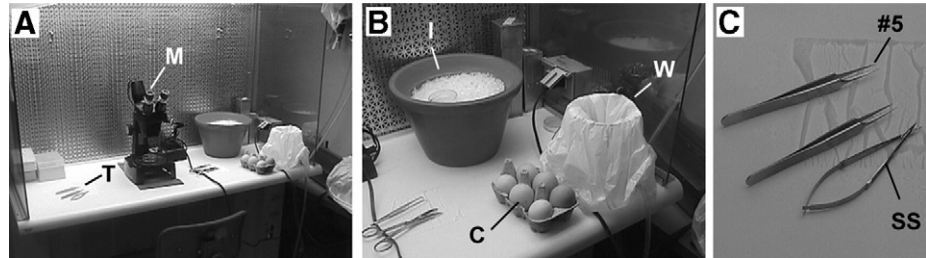


Fig. 1 Setup for spinal motor neuron dissection. Initial setup for the dissection of motor neurons. (A) A stereo zoom microscope (M) is placed in a laminar flow and wiped with 70% alcohol. Dissection tools (T) are flamed with 70% alcohol. A beaker with 70% alcohol (not shown) is used to sterilize tools during the dissection. (B) An ice bucket (I) carries a 60-mm glass petri dish containing HBSS for the collection of spinal cord ventral halves. Six eggs incubated for 6 days have been placed in an egg carton (C) and are rinsed with 70% alcohol. A wastebasket (W) is ready for the disposal of eggs and remains of embryos after dissection. (C) The most important dissection tools include two forceps (#5) and spring scissors (SS). The tips of these instruments have to be sharp and straight. (See Color Insert.)

B. Procedures

1. Accessing the Chick Embryo

Remove fertilized eggs from the incubator after 6 days of incubation and put, blunt end up, into an egg holder (part of an egg carton). Do not remove more than six eggs at one time. Briefly spray eggs with 70% alcohol, which cleans the shell sufficiently but does not sterilize it completely. Using the straight forceps, punch a hole through the blunt end of the shell (Figs. 2A and 2B), which is where the air space of the egg is located. Insert one tip of the forceps into the hole and remove the eggshell by breaking off pieces around the entire air space (Fig. 2C). At this time, the embryo is hidden under the inner shell membrane, a thick white membrane. It is the easiest to do this right over the waste receptacle. Resterilize the straight forceps by soaking in the beaker filled with 70% ethanol.

2. Isolation of Chick Embryo

The following procedure allows a quick removal of the chick embryo from the egg and minimizes both stress and discomfort of the animal. All methods adhere to the guidelines set by the International Animal Care and Use Committee and a report on euthanasia (*Journal of the American Veterinary Medical Association*, Vol. 202, No. 2, pp. 229–249, 1993). Using the bent forceps, peel the inner shell membrane off; the embryo becomes visible enclosed in the highly vascularized, chorioallantoic membrane. Pierce this membrane with the bent forceps or make an incision with the fine scissors to create an opening. Hook the embryo around the neck and lift it out very gently (Fig. 2D). All the extraembryonic membranes, including amnion, yolk sac, allantois, and chorion, are still connected to the embryo. Lifting the embryo out too quickly will inevitably rupture its neck. Place the embryo on its side in the dissecting dish and remove the head immediately by

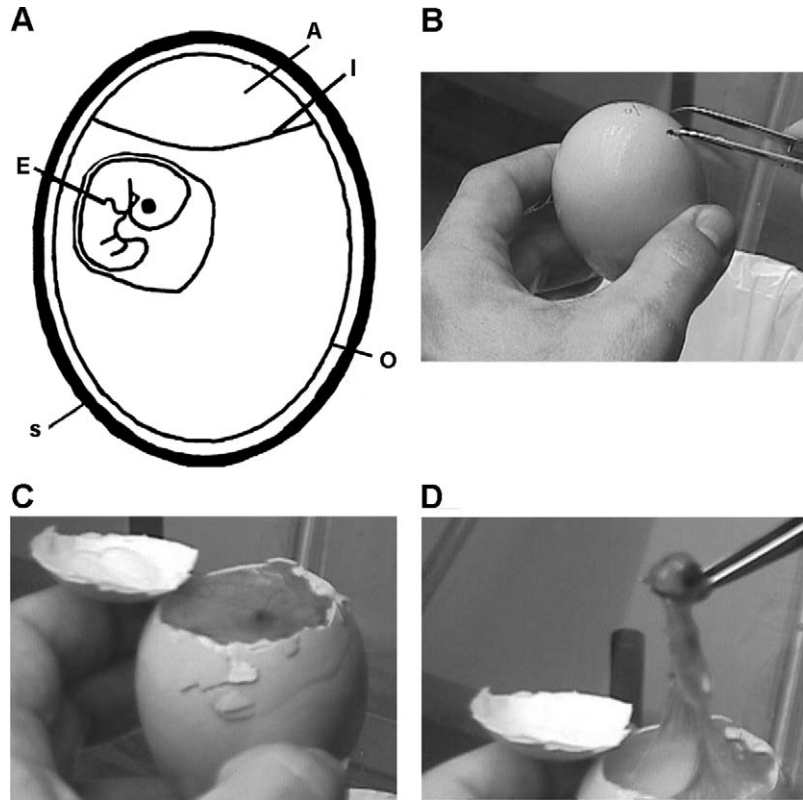


Fig. 2 Removal of the chick embryo from the egg. (A) Schematic drawing of a chicken egg incubated for 6 days. A robust eggshell (S) protects the embryo. The outer shell membrane (O) and the inner shell membrane (I) enclose the embryo (E), albumen, and yolk. The blunt end of the egg contains the air space (A), which lies between the outer and the inner shell membranes. (B) Using forceps (straight or bent types work well), a hole is punched through the blunt end of the egg. (C) The eggshell is removed piece by piece all around the entire air space. After peeling off the thick, white inner shell membrane, the embryo is readily visible. (D) The highly vascularized chorioallantoic membrane, which encloses the embryo, is pierced with #5 forceps or cut with fine scissors, and the embryo is lifted out at its neck using the bent forceps. If the embryo is lifted out too quickly, its neck will rupture. (See Color Insert.)

either using fine scissors or firmly grasping the neck just caudal of the head with the bent forceps and squeezing. Finally, using the fine scissors, remove all the extraembryonic membranes and rinse the embryo thoroughly with HBSS.

IV. Dissection of Intact Spinal Cords and Isolation of Ventral Halves

The enrichment of motor neurons by isolating the ventral halves of the spinal cords takes advantage of the unique anatomy of motor neurons, their exclusive

residence in the ventral hemichords (Masuko *et al.*, 1979; Kuhn *et al.*, 1998). With a little practice, it is surprisingly easy to isolate the intact spinal cord from 6-day-old chick embryos.

A. Materials

Dissection instruments (sterile): two #5 forceps, one fine scissors, one spring scissors, and one scalpel (blade #10, handle #3).

Dissecting microscope (a stereo zoom microscope with incident and/or transmitted light works well)

HBSS (Gibco)

Pasteur pipette cotton plugged with a small rubber bulb (sterile)

60-mm glass petri dish (sterile, kept on ice) filled with 3 ml ice-cold HBSS

Ice bucket with ice

70% ethanol in a spray bottle

Box of tissue paper

50-ml glass beaker containing 70% ethanol

Prior to dissecting, wipe the stereomicroscope with tissues soaked in 70% alcohol. Sterilize all dissecting instruments by rinsing with 70% alcohol and flaming briefly. Instruments can be resterilized during the dissection by soaking in a beaker containing 70% alcohol. Always keep the embryo moist during the dissection using ice-cold HBSS. As general rules for microscopy, adjust your optics properly for each eye, use low light levels, and work with the least magnification. These precautions all reduce stress on your eyes.

B. Procedures

1. Dissection of Intact Spinal Cords

At this point, the head and all the extraembryonic membranes of the embryo have been removed. To eviscerate the embryo, cut along the ventral side of the spine without touching the spine from neck to tail, (spring scissors) remove all internal organs, cut off limb buds and wing buds (Fig. 3A). Hold the embryo in place by grabbing the skin on the back with #5 forceps. Turn the remainder of the embryo onto the ventral side. Starting at the neck, remove the epidermis on the back by pulling to the sides using one #5 forceps in each hand and clip the very end of the tail with the spring scissors. Care should be taken not to puncture or break the spine. Now the two dorsal halves of the spinal cord are visible as two solid, light strands separated by a thin, dark midline. Make a deep incision into the spinal cord along the midline (Fig. 3B). Starting at the tail, insert one tip of the spring scissors into the central canal of the spinal cord and cut (Fig. 4A). Continue along the midline toward the neck while holding the embryo in place using #5 forceps. This incision should separate the dorsal hemicordes, yet leave the ventral halves intact. Gently push each side of the cut apart from each other (use #5 forceps closed), both

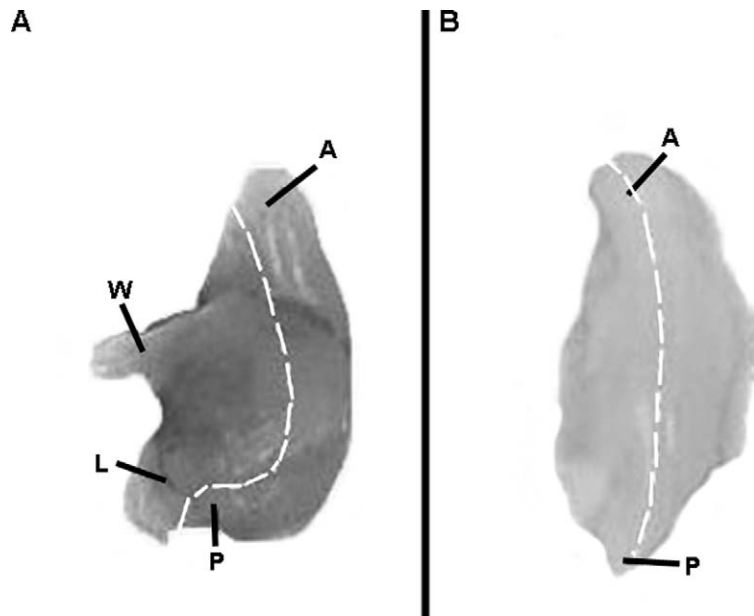


Fig. 3 Preparation of the embryo for spinal cord dissection. (A) After the embryo is lifted out of the egg, it is placed on its side in a 100-mm glass petri dish and the head is removed immediately. The dashed line along the ventral side of the spine indicates where the incision is made using fine scissors to eviscerate the embryo. Anterior end or neck (A). Posterior end or tail (P). Wing buds (W). Limb buds (L). (B) After the embryo has been eviscerated, the back containing the spine and all surrounding tissue is turned onto the ventral side. The dashed line indicates the midline along which the incision is made. (See Color Insert.)

hemicordes of the spinal cord are now clearly visible (Fig. 4B). Insert #5 forceps (keep closed) between the spinal cord and the surrounding tissue and gently move along each lateral surface of the spinal cord to separate the spinal cord from meninges and dorsal root ganglia (Fig. 4C). Rinse and cover the preparation well with HBSS. Lift the spinal cord carefully out of its cavity by inserting closed #5 forceps between the spinal cord and underlying tissue starting from the neck (Fig. 4D). If enough HBSS is used, the spinal cord will actually float, which facilitates this procedure greatly. Isolate the entire spinal cord without breaking or twisting. To establish dissociated neuronal cultures from whole spinal cords or when enriching for motor neuron utilizing density gradient centrifugation, transfer the intact spinal cord to a 60-mm petri dish containing ice-cold HBSS (use a Pasteur pipette) and continue with Section V. Otherwise proceed with isolating ventral halves.

2. Isolation of Ventral Halves of Spinal Cords

The intact isolated spinal cord now lies flat with the dorsal halves facing outward and the two adjacent ventral halves (open-book preparation). It is

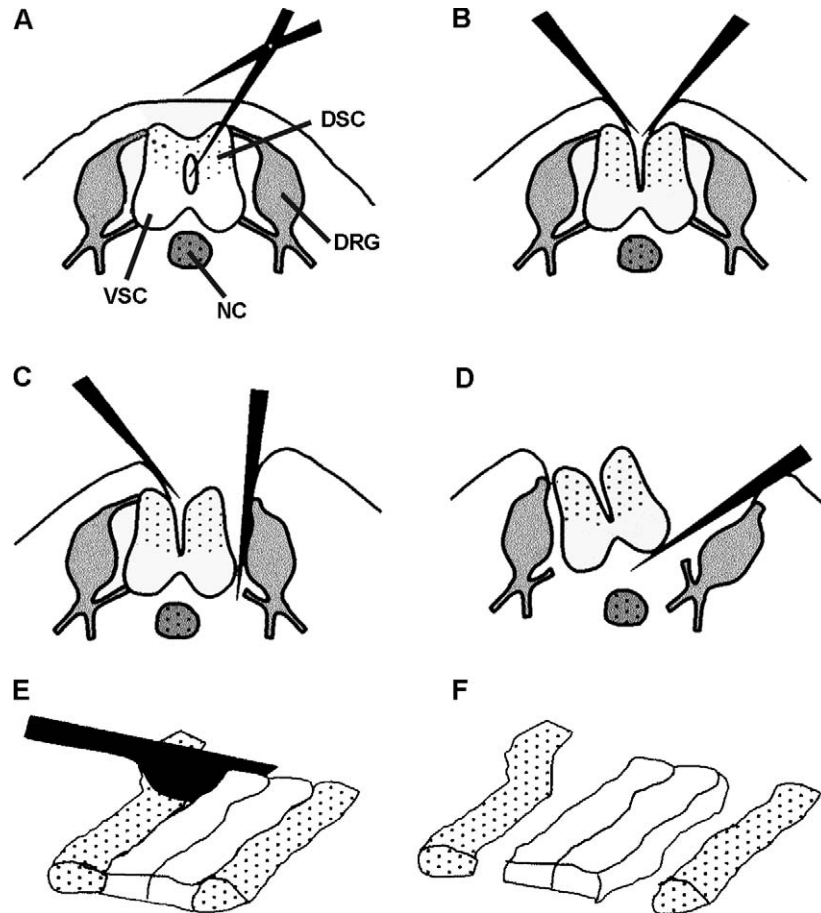


Fig. 4 Isolation of the ventral spinal cord. (A) After the skin is removed, an incision is made along the midline using spring scissors. This incision reaches all the way into the central canal of the spinal cord, thus separating the dorsal halves but leaving the ventral halves connected. (B) With closed #5 forceps, the incision is enlarged by pushing each side outward. (C) The meninges and the nerve fiber bundles of the dorsal root and ventral root are severed by gently moving closed #5 forceps anterior to posterior along the surface of the spinal cord. (D) With #5 forceps, the spinal cord is separated carefully from the underlying tissue and lifted out. Plenty of HBSS facilitates this step greatly, as the loosened spinal cord will float. (E) Once the entire spinal cord is isolated (open-book preparation), the dorsal halves (dotted areas) are removed from the ventral halves (white area) using a scalpel. Each spinal cord hemisphere displays characteristic morphologies and is easily distinguished. (F) Ventral halves are collected in ice-cold HBSS.

imperative to keep the intact isolated spinal cord always covered with ice-cold HBSS. Any attached meninges or dorsal root ganglia can be removed using #5 forceps. Using the scalpel, separate the dorsal halves by pushing down between dorsal and ventral halves, moving stepwise from anterior to posterior (Figs. 4E

and 4F). Slicing will inevitably rupture the spinal cord. The two halves of the spinal cord exhibit distinct morphology and are easily distinguishable. While dorsal halves display an opaque, coarse morphology, the ventral halves are homogeneous and almost transparent. Transfer ventral spinal cord halves into a 60-mm petri dish containing ice-cold maintenance solution using a Pasteur pipette. Isolated ventral halves or whole spinal cords can be kept on ice in maintenance solution for up to 4 h.

===== V. Enzymatic and Mechanical Dissociation of Intact Spinal Cords or Ventral Halves

Chelating free Ca^{2+} ions in combination with tryptic digestion significantly weakens many cell–cell and cell–matrix adhesion interactions and facilitates the mechanical dissociation by shear forces. Neuronal viability is compromised by prolonged exposure to trypsin.

A. Materials

15-ml conical centrifuge tubes (sterile)
Pasteur pipette cotton plugged with a small rubber bulb (sterile)
5-ml serological pipettes (sterile)
Clinical centrifuge (swing-out rotor up to $2000 \times g_{\text{max}}$ is sufficient)
Ice
Cell dissociation solution (Gibco; 10× stock aliquots)
2% DNase I (Roche Diagnostics Corp.; 100× sterile stock solution)
Horse serum (HS), sterile and heat inactivated (Hyclone)
Fetal bovine serum (FBS), sterile and heat inactivated (Hyclone)
Water bath heated to 37°C
Dulbecco's modified Eagle medium (DMEM) high glucose (Gibco)
DMEM/10% FBS

B. Procedure

Transfer intact spinal cords or ventral halves to a 15-ml conical tube and rinse twice with HBSS by gently swirling and removing the supernatant after tissue has settled. Adjust volume with HBSS using 1 ml HBSS for each four ventral halves or whole spinal cords. Add cell dissociation solution (1/10 of final volume) and DNase I (1/100 of final volume) and incubate for 10 min at 37°C (water bath). Extensive tryptic digestion will result in considerable cell debris and significant cell death. Add horse serum (10% final concentration) and swirl the tissue gently.

Remove the supernatant after tissue has settled and resuspend in DMEM. Mechanically dissociate tissue (triturate) by pushing tissue through a Pasteur pipette pressed against the bottom of a conical tube. The resulting shearing forces will dissociate the tissue quickly, resulting in a slightly pale cell suspension. Allow any remaining fragments to settle before collecting the cell suspension in a 15-ml conical tube. Pellet cells ($200 \times g_{\max}$, 2 min) and resuspend in 2 ml DMEM/10% FBS for each four ventral or whole spinal cords. Section VII describes the enrichment of spinal motor neurons by density gradient centrifugation utilizing cell suspensions obtained from intact spinal cords.

VI. Plating Motor Neurons or Spinal Cord Neurons

Motor neurons or spinal cord neurons can be grown in either serum-containing or serum-free medium. Long-term cultures (5 days or longer) require the presence of serum. It is recommended to adjust cell density prior to plating by counting cells in a hemacytometer. Motor neurons or spinal cord neurons exhibit robust neurite outgrowth and excellent survival when plated on laminin-coated dishes.

A. Materials

- Pasteur pipette cotton plugged with a small rubber bulb (sterile)
- 5-ml serological pipettes (sterile)
- Pipettors with tips
- Hemacytometer
- Clinical centrifuge (swing-out rotor up to $2000 \times g_{\max}$)
- 15-ml conical tubes
- Drilled tissue culture dishes (35 mm) equipped with a laminin-coated glass coverslip
- Laminin-coated glass coverslips inserted into 35-mm tissue culture dishes
- Laminin-coated 35- or 60-mm tissue culture dishes
- Spinal cord medium (see Section VIII)
- Defined medium (see Section VIII.)

Plate motor neurons or spinal cord neurons into either of the tissue culture dishes listed earlier depending on the purpose of the experiment. Drilled dishes (see Section XI) are ideal for live video observations at high magnification, whereas glass coverslips inserted into 35-mm dishes work well for immunocytochemical staining. For biochemical assays, plate cells directly into 35- or 60-mm tissue culture dishes. Although laminin is suggested as a substrate for growing motor neurons or spinal cord neurons, other substrates can be substituted, such as fibronectin or poly-D-lysine (Section XI).

B. Procedure

Place cell suspensions of dissociated ventral halves or whole spinal cords in a 60-mm tissue culture dish (four ventral halves of whole spinal cord, 2 ml DMEM/10% FBS) and preplate for 1 h (CO₂ incubator, 37°C, 5% CO₂). This preplating step depletes nonneuronal cells due to their preferential adhesion to tissue culture plastic while neuronal cells remain in suspension.

Carefully recover the supernatant, pellet cells ($200 \times g_{\max}$ for 5 min), and resuspend the cell pellet in spinal cord medium or defined medium using 1 ml medium for four spinal cords or ventral halves. Determine the cell density using a hemacytometer. One intact spinal cord yields approximately 1×10^6 neurons, whereas ventral halves of one spinal cord should yield around $1-2 \times 10^5$ motor neurons. For live video observation, of individual neurons, plate cells at 75,000 cells/ml (plating volume 500 μ l) onto a laminin-coated glass coverslip glued over a 1-cm hole drilled into the bottom of a 35-mm tissue culture dish. For immunocytochemical staining, plate cells at 1.5×10^5 cells/ml (plating volume 500 μ l) onto laminin-coated glass coverslips inserted into 35-mm tissue culture dish. For biochemical assays, cells are best plated into laminin-coated 35-mm tissue culture dishes ($0.5-1 \times 10^6$ cells/ml, plating volume 2 ml) or into 60-mm tissue culture dishes ($0.5-1 \times 10^6$ cells/ml, plating volume 4 ml).

VII. Motor Neuron Enrichment by Density Gradient Centrifugation

Density gradient centrifugation takes advantage of the buoyant density of large motor neurons. Although this technique does not require isolation of the intact spinal cord, the yield of motor neuron enrichment is slightly less compared to the isolation of ventral halves. The technique described in this section is adapted with modifications (Juurlink, 1992).

A. Materials

- 3.5% BSA
- 6.4% metrizamide
- DMEM
- Clinical centrifuge (swing-out rotor up to $2000 \times g_{\max}$)
- Pasteur pipette cotton plugged with small rubber bulb (sterile)
- 5-ml serological pipettes (sterile)
- Ice

B. Procedure

After enzymatic and mechanical dissociation of whole spinal cords (see Section V), centrifuge the resulting cell suspension for 5 min ($200 \times g_{\max}$). Resuspend the

cell pellet in 5 ml DMEM (15-ml centrifuge tube), carefully layer on top of a 5-ml cushion of 3% BSA, and spin for 10 min at $200 \times g_{\max}$. The BSA cushion traps much of the small debris. Remove the entire supernatant and resuspend the cell pellet in 5 ml DMEM. Layer the cell suspension onto 5 ml 6.4% metrizamide. Add the cell suspension slowly along the side of the tube slightly above the meniscus and avoid considerable intermixing of the cell suspension and metrizamide. After centrifugation at $500 \times g_{\max}$ for 30 min, a band of cells becomes visible at the DMEM/metrizamide interface consisting mostly of motor neurons. Aspirate this fraction, which contains the motor neurons (Pasteur pipette), dilute with twice the volume of DMEM, and centrifuge at $200 \times g_{\max}$ for 10 min. Resuspend the cell pellet in spinal cord medium or defined medium using 1 ml per four spinal cords (ventral halves or intact). No preplating is necessary, and plate recovered motor neurons as described in Section VI.

VIII. Experimental Use of Motor Neuron Cultures and Spinal Cord Cultures

Using the conditions described previously, motor neurons, as well as spinal cord neurons, extend neuronal processes within 8–10 h after plating. Neurite outgrowth on laminin is very vigorous with little bifurcations. In contrast, motor neurons on fibronectin or poly-D-lysine grow slower and display more bifurcations. The differentiation of neuronal processes into axons and dendrites can be detected after 3 days *in vitro* using double indirect immunocytochemical staining. Axons can be revealed using anti-Tau, whereas dendrites are identified using anti-MAP2 (Kuhn *et al.*, 1998). Neurons will survive for over 14 days with regular changes of serum-containing medium every 3 days. Inclusion of 5-fluoro-2'-deoxyuridine, an irreversible inhibitor of thymidylate synthase, interferes with the proper DNA replication of mitotically active nonneuronal cells, such as astrocytes and fibroblasts, which account for less than 5% of total cells in motor neuron cultures (Fig. 5A). Low-density motor neuron cultures allow for investigating the responses of individual neurons or even individual neuronal growth cones to extrinsic cues (Fig. 5B). Preferentially, motor neurons are cultured in a defined, serum-free medium. However, at very low densities, motor neurons survive for about 4 to 6 days. The covalent coupling of extrinsic cues to small polystyrene beads and their presentation to advancing growth cones represents an elegant assay system used to elucidate growth cone responses in detail. For this assay, motor neurons are best cultured on drilled dishes, which allow the use of high magnification objectives for both visible light (phase contrast, DIC) and fluorescence observations. For instance, upon contacting laminin-coated beads, the growth cones of dorsal root ganglia neurons turn toward beads and exhibit increased rates of advance for a considerable time period after passing the beads (Kuhn *et al.*, 1995). Moreover, growth cones are repelled by beads coated with semaphorin3A, and collateral branching results

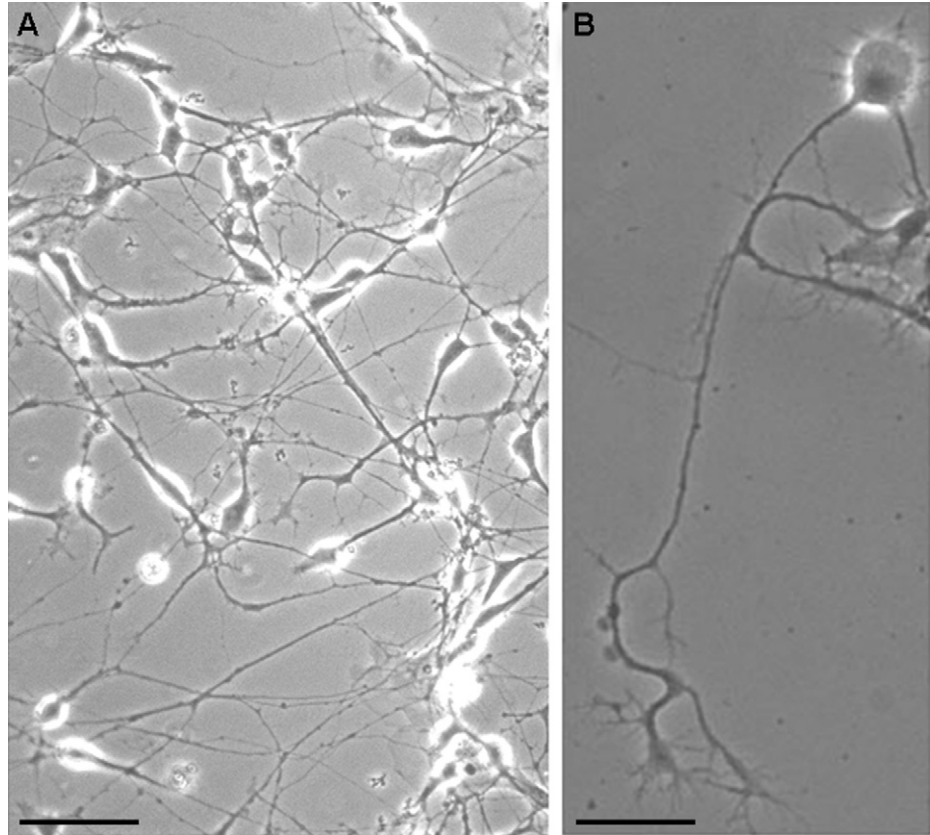


Fig. 5 Cultures of spinal motor neurons. (A) A typical high-density culture of spinal motor neurons obtained from 6-day-old chick embryos. Motor neurons were grown for 5 days on laminin in spinal cord medium containing 10% FBS. Preplating and incorporation of FdU_r in the medium virtually depletes these cultures of any contaminating nonneuronal cells, such as fibroblasts and astrocytes. (B) Low-density cultures provide an excellent assay system to investigate individual neurons, their processes, and growth cones. A motor neuron after 1 day in culture on laminin extends a neuronal process (most likely an axon). Bifurcation is readily visible by two individual growth cones. Scale bars: 100 μm .

from contact to nerve growth factor-coated beads (Fan and Raper, 1995; Gallo and Letourneau, 1998). As shown in Fig. 6, a motor neuron growth cone encounters a bead coupled covalently with tumor necrosis factor (TNF) α , a proinflammatory cytokine. Over a time period of 30 min, the growth cone displays a series of morphological changes and ultimately loses its morphology and ceases advance, i.e., the typical behavioral pattern of growth cone collapse. It is possible that the failure of motor neurons to reestablish neuronal processes following acute injury results partially from the growth inhibitory properties of proinflammatory cytokines such as TNF α . Live video observation of motor

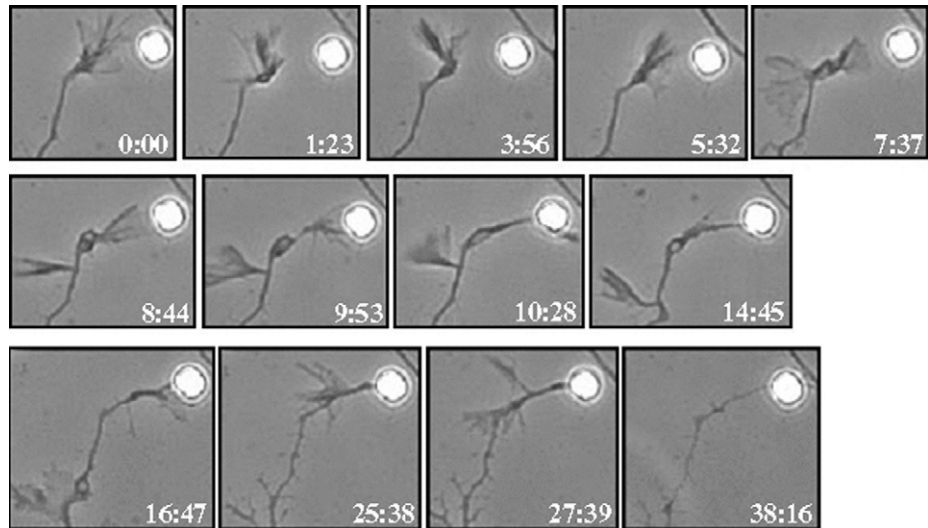


Fig. 6 Interaction of a motor neuron growth cone with an extrinsic cue. An individual motor neuron growth cone encounters the extrinsic cue tumor necrosis factor α , coupled covalently onto a small polystyrene bead ($5\ \mu\text{m}$ in diameter). Upon initial filopodia contact, the growth cone displays changes in behavior and morphology over a time period of 30 min. Finally the growth cone collapses, which is indicated by a complete loss of morphology and cessation of advance.

neurons is accomplished using defined medium with Leibovitz' L15 medium replacing DMEM. Leibovitz' L15 medium (Gibco) is phosphate buffered and thus maintains a pH of 7.4 irrespective of room atmosphere. A heating system is required to maintain cultures on the microscope table at 37°C .

IX. Preparation of Solutions, Culture Dishes, Media, and Media Supplements

1. Sterilization Procedures

Sterilize all glassware by autoclaving (20 min, 121°C , 1 bar). Label all items with autoclave indicator tape. Sterilize large volumes of solutions (100 ml or more) by filtration over $0.22\text{-}\mu\text{m}$ filter membranes using disposable bottle-top filters. Small volumes of solutions are best sterilized using disposable syringes and $0.22\text{-}\mu\text{m}$ syringe filters.

2. Glass Coverslips

Insert glass coverslips in a holding device ($22 \times 22\ \text{mm}^2$, #1, German glass, Carolina Biological Supply Company, Burlington, NC). Teflon holders or wafer baskets used to wash computer chips work well (Entegris Inc., Chaska, MN, www.entegris.com). Wash coverslips in 2% Micro-90 (VWR, 10 ml detergent per

500 ml water) heated to 50–55°C for 30 min. Rinse glass coverslips 10 times with double distilled water and twice with MilliQ water. Place glass coverslips onto a filter paper (Whatman #1, Millipore) to dry in a convection oven at 65°C overnight. Sterilize washed coverslips under ultraviolet light (UV) for 15 min in a laminar flow hood and store at room temperature indefinitely in a sterile container. Coverslips can be either glued onto the bottom of drilled dishes or inserted into a 35-mm tissue culture dish.

3. Drilled Dishes

Drill a 1-cm-diameter hole into the bottom of 35-mm tissue culture dishes using a drill press equipped with an 11/16-in. drill bit. For protection, wear gloves and goggles. Clean debris from hole and smooth rims using a scalpel. Apply aquarium glue (local pet store) around the hole using a 1-ml disposable syringe. Firmly press a washed glass coverslip over the hole and dry dishes at room temperature overnight (dishes can be stored indefinitely). For sterilization, expose dishes to UV light for 15 min in a laminar flow hood.

4. Hanks' Balanced Salt Solution

HBSS is a phosphate buffer that maintains pH 7.4 in normal air. HBSS (Gibco) is purchased as a 10 × sterile liquid and is stored at room temperature. Dilute 1 volume of 10 × HBSS with 9 volumes of sterile MilliQ water. Store 1 × HBSS (working solution) at 4°C.

5. Cell Dissociation Solution

Cell dissociation solution (Gibco, 10× stock solution) contains 0.5% trypsin and 5.3 mM Na₄EDTA. Prepare and store aliquots (1 ml and 100 μl) at –20°C.

6. 2% DNase I

Dissolve DNase I (200 mg, Roche Diagnostics Corp., Indianapolis, IN) in HBSS (10 ml) and store aliquots (0.5 ml) –20°C.

7. Horse Serum and Fetal Bovine Serum

Thaw horse serum (Hyclone, Logan, UT), or fetal bovine serum (Hyclone) at 4°C. Gently swirl and heat inactivate liquid serum by placing in a 56°C warm water bath for 30 min. After cooling in a laminar flow hood, prepare 5- and 10-ml aliquots and store aliquots at –20°C.

8. DMEM (High Glucose, Gibco)

Dissolve contents of one bag in 900 ml MilliQ water, add 3.7 g NaHCO₃, and adjust pH to 7.4. Adjust volume to 1 liter with MilliQ water, sterilize by filtration over a 0.22-μm membrane, and store at 4°C.

9. DMEM/10% FBS

Mix 10 ml heat-inactivated FBS with 90 ml DMEM, sterilize by filtration through 0.22- μ m membranes, and store at 4°C.

10. 100 × N3 Supplement

Prepare aliquots of each component (100× stock solutions) and store at -20°C without prior sterilization by filtration over 0.22- μ m membranes.

- 10 mg/ml BSA fraction V (Sigma) in HBSS (500- μ l aliquots)
- 100 mg/ml Apo-transferrin human (Calbiochem) in HBSS (500- μ l aliquots)
- 25 mg/ml insulin (Sigma) in 0.01 M HCl (200- μ l aliquots)
- 80.55 μ g/ml putrescin (Sigma) in HBSS (200- μ l aliquots)
- 200 μ g/ml tri-iodothyronin (Sigma) in 0.01 M NaOH (50- μ l aliquots)
- 10.4 μ g/ml selenium (Sigma) in HBSS (500- μ l aliquots)
- 125.8 μ g/ml progesterone (Sigma) in absolute ethanol (50- μ l aliquots)
- 2 mg/ml corticosterone (Sigma) in absolute ethanol (50- μ l aliquots)

For a 100× stock of the N3 supplement, place 2 ml HBSS in a 15-ml conical tube and add 1 aliquot of each component. Mix gently by swirling the tube and adjust the volume to 5 ml with HBSS. Prepare N3 aliquots (500 μ l and 1 ml) and store at -20°C.

11. 100 × 5-Fluoro-2'-deoxyuridine (FdUr)

Dissolve 29.544 mg FdUr (Sigma) and 73.26 mg uridine (Sigma) in 10 ml HBSS. Prepare 500- μ l and 1-ml aliquots and store at -20°C.

12. Spinal Cord Medium

Add 5 ml FBS and 0.5 ml of each 100× N3 supplement and 100× FdUr to DMEM for a total volume of 50 ml. Sterilize by filtration over a 0.22- μ m membrane using a syringe filter and a 50-ml disposable syringe. Store at 4°C.

13. Defined Medium

Dissolve 50 mg BSA (fraction V) in 49 ml DMEM. Add 0.5 ml of each 100× N3 supplement and 100× FdUr and sterilize by filtration over a 0.22- μ m membrane using a syringe filter and a 50-ml disposable syringe. Store at 4°C. For live video observations, replace DMEM with Leibovitz' L15 (Gibco).

14. Substrate Coating

Dissolve 1.24 g boric acid (Sigma) in 400 ml MilliQ water. Dissolve 1.9 g tetrasodium borate (Sigma), adjust pH to 8.4, and store buffer at 4°C. Add 1 mg

poly-D-lysine (Sigma) to 10 ml borate buffer (100 $\mu\text{g}/\text{ml}$) and store 0.5-ml aliquots at -20°C . Apply 500 μl poly-D-lysine solution onto glass coverslip for each drilled dish and incubate for 30 min at room temperature. Rinse dishes three times with MilliQ water and air dry in a laminar flow hood. Sterilize dishes with UV light for 15 min. Dishes can be stored at room temperature indefinitely. Laminin (Roche Diagnostics Corp., a 1-mg sterile solution) is prepared in aliquots (1 $\mu\text{g}/\mu\text{l}$, 100 μl) at -20°C . For coating, apply 20 μl laminin for each poly-D-lysine-treated glass coverslip and add 200 μl HBSS. Incubate dishes for at least 2 h in a CO_2 incubator. Prior to plating cells, rinse glass coverslips with 500 μl HBSS.

15. 3.5% BSA Fraction V (Sigma)

Add 875 mg BSA to 25 ml DMEM. Simply allow the BSA to go into solution (no vortexing). Sterilize over a 0.22- μm filter membrane using a syringe filter. Store 5-ml aliquots at -20°C .

16. 6.4% Metrizamide

Dissolve 6.4 g of metrizamide (Sigma) in 10 ml MilliQ water and adjust volume to 20 ml. Store this solution (32% metrizamide) at 4°C . Prior to use, place 1 ml of 32% metrizamide into a 15-ml conical centrifuge tube and add 4 ml DMEM. Mix well and keep on ice until use.

17. Web Sites

A plethora of useful information about developmental biology can be found at the following web sites: Zygote (<http://zygote.swarthmore.edu/>), Gilbert-Developmental Biology (www.devbio.com), Society for Developmental Biology (http://sdb.bio.purdue.edu/Other/VL_DB.html), and Virtual Embryo (<http://www.ucalgary.ca/UofC/eduweb/virtualembryo>).

Acknowledgments

Research related to this manuscript was supported in part by The Christopher Reeve Paralysis Foundation (Grant KAC1-0004), The Special Neuroscience Research Program (1U54NS41069), and NCCR COBRE Grant RR15583.

References

- Bar, P. R. (2000). Motor neuron disease in vitro: The use of cultured motor neurons to study amyotrophic lateral sclerosis. *Eur. J. Pharmacol.* **405**, 285–295.
- Bellairs, R., and Osmond, M. (1998). “Atlas of the Chick Development.” Academic Press, San Diego.
- Bibel, M., and Barde, Y. A. (2000). Neurotrophins: Key regulators of cell fate and cell shape in the vertebrate nervous system. *Genes Dev.* **14**, 2919–2937.
- Calof, A. L., and Reichardt, L. F. (1984). Motoneurons purified by cell sorting respond to two distinct activities in myotube-conditioned medium. *Dev. Biol.* **106**, 194–210.

- Camu, W., and Henderson, C. E. (1994). Rapid purification of embryonic rat motoneurons: An in vitro model for studying MND/ALS pathogenesis. *J. Neurol. Sci.* **124**(Suppl), 73–74.
- deLapeyriere, O., and Henderson, C. E. (1997). Motoneuron differentiation, survival and synaptogenesis. *Curr. Opin. Genet. Dev.* **7**, 642–650.
- Demming, D., and Ferguson, M. (eds.) (1992). *Egg Incubation: Its Effects on Embryonic Development in Birds and Reptiles*. Cambridge University Press, New York.
- Fan, J., and Raper, J. (1995). Localized collapsin cues can steer growth cones without inducing their full collapse. *Neuron* **14**, 263–274.
- Freeman, B., and Vince, M. (1974). “Development of the Avian Embryo.” Wiley, New York.
- Gaehwiler, B. H., Capogna, M., Debanne, D., McKinney, R. A., and Thompson, S. M. (1997). Organotypic slice cultures: A technique has come of age. *Trends Neurosci.* **20**, 471–477.
- Gallo, G., and Letourneau, P. (1998). Localized sources of neurotrophins initiate axon collateral sprouting. *J. Neurosci.* **18**, 5403–5414.
- Gould, T. W., Burek, M. J., Ishihara, R., Lo, A. C., Prevet, D., and Oppenheim, R. W. (1999). Androgens rescue avian embryonic lumbar spinal motoneurons from injury-induced but not naturally occurring cell death. *J. Neurobiol.* **41**, 585–595.
- Guale, F. G., and Burrows, G. E. (1997). Evaluation of chick embryo spinal motoneuron cultures for the study of neurotoxicity. *Nature Toxins* **5**, 115–120.
- Hamburger, V. (1975). Cell death in the development of the lateral motor column of the chick embryo. *J. Comp. Neurol.* **160**, 535–546.
- Hamburger, V., and Hamilton, H. L. (1951). A series of normal stages in the development of the chick embryo. *J. Morphol.* **88**, 49–92.
- Honig, M. G., and Hume, R. I. (1986). Fluorescent carbocyanine dyes allow living neurons of identified origin to be studied in long-term cultures. *J. Cell Biol.* **103**, 171–187.
- Houenou, L. J., Li, L., Lo, A. C., Yan, Q., and Oppenheim, R. W. (1994). Naturally occurring and axotomy-induced motoneuron death and its prevention by neurotrophic agents: A comparison between chick and mouse. *Prog. Brain Res.* **102**, 217–226.
- Juurlink, B. H., Munoz, D. G., and Devon, R. M. (1990). Calcitonin gene-related peptide identifies spinal motoneurons in vitro. *J. Neurosci. Res.* **26**, 238–241.
- Juurlink, B. H. J. (1992). Chick spinal somatic motoneurons in culture. In “Protocols for Neural Cell Culture” (S. F. A. A. Richardson, ed.), pp. 39–51. Humana Press, Totowa, NJ.
- Keirstead, H. S., Dyer, J. K., Sholomenko, G. N., McGraw, J., Delaney, K. R., and Steeves, J. D. (1995). Axonal regeneration and physiological activity following transection and immunological disruption of myelin within the hatchling chick spinal cord. *J. Neurosci.* **15**, 6963–6974.
- Kuhn, T., Brown, M., Wilcox, C., Raper, J., and Bamburg, J. (1999). Myelin and collapsin-1 induce motor neuron growth cone collapse through different pathways: Inhibition of collapse by opposing mutants of *rac1*. *J. Neurosci.* **19**, 1965–1975.
- Kuhn, T. B., Brown, M. D., and Bamburg, J. R. (1998). *Rac1*-dependent actin filament organization in growth cones is necessary for $\beta 1$ -integrin-mediated advance but not for growth on poly-D-lysine. *J. Neurobiol.* **37**, 524–540.
- Kuhn, T. B., Schmidt, M. F., and Kater, S. B. (1995). Laminin and fibronectin guideposts signal sustained but opposite effects to passing growth cones. *Neuron* **14**, 275–285.
- Lance-Jones, C. (1988). Development of neuromuscular connections: Guidance of motoneuron axons to muscles in the embryonic chick hindlimb. *Ciba Found. Symp.* **138**, 97–115.
- Lu, J., Ashwell, K., and Waite, P. (2000). Advances in secondary spinal cord injury. *Spine* **25**, 1859–1866.
- Mason, I. (1999). The avian embryo—an overview, and chick embryos—incubation and isolation. In “Molecular Embryology Methods and Protocols: Methods in Molecular Biology” (P. Sharpe and I. Mason, eds.), pp. 215–224. Humana Press, Totowa, NJ.
- Masuko, S., Kuromi, H., and Shimada, Y. (1979). Isolation and culture of motoneurons from embryonic chicken spinal cords. *Proc. Natl. Acad. Sci. USA* **76**, 3537–3541.
- Oppenheim, R. W. (1996). Neurotrophic survival molecules for motoneurons: An embarrassment of riches. *Neuron* **17**, 195–197.

- Pfaff, S. L., Mendelsohn, M., Stewart, C. L., Edlund, T., and Jessell, T. M. (1996). Requirement for LIM homeobox gene *Isl1* in motor neuron generation reveals a motor neuron-dependent step in interneuron differentiation. *Cell* **84**, 309–320.
- Pituello, F. (1997). Neuronal specification: Generating diversity in the spinal cord. *Curr. Biol.* **7**, R701–R704.
- Roelink, H., Porter, J. A., Chiang, C., Tanabe, Y., Chang, D. T., Beachy, P. A., and Jessell, T. M. (1995). Floor plate and motor neuron induction by different concentrations of the amino-terminal cleavage product of sonic hedgehog autoproteolysis. *Cell* **81**, 445–455.
- Romanoff, A. (1960). “The Avian Embryo.” Macmillan, New York.
- Selleck, M. (1996). Culture and microsurgical manipulation of the early avian embryo. In “Methods in Cell Biology,” pp. 1–21. Academic Press, San Diego.
- Stern, C. D. (1994). The chick. In “Embryos: Color Atlas of Development” (J. B. L. Bard, ed.), pp. 167–182. Wolfe, London.
- Stromberg, J. (1975). A guide to better hatching.
- Tanabe, Y., and Jessell, T. M. (1996). Diversity and pattern in the developing spinal cord. *Science* **274**, 1115–1123.
- Yaginuma, H., Shiga, T., and Oppenheim, R. W. (1994). Early developmental patterns and mechanisms of axonal guidance of spinal interneurons in the chick embryo spinal cord. *Prog. Neurobiol.* **44**, 249–278.

This Page Intentionally Left Blank

CHAPTER 6

Avian Purkinje Neuronal Cultures: Extrinsic Control of Morphology by Cell Type and Glutamate

**Peter L. Jeffrey,* Vladimir J. Balcar,[†] Ornella Tolhurst,*
Ron P. Weinberger,[‡] and Jenny A. Meany***

*Developmental Neurobiology Group
Children's Medical Research Institute
Westmead, New South Wales 2145
Australia

[†]Institute for Biomedical Research
University of Sydney
Sydney, New South Wales 2600
Australia

[‡]Oncology Research Unit
Children's Hospital at Westmead
Westmead, New South Wales 2145
Australia

-
- I. Introduction
 - II. Methods and Systems
 - A. Cerebellar Cell Culture
 - B. Coculture Systems
 - C. Immunohistochemistry
 - D. Morphological Analysis
 - E. Glutamate Uptake in Purkinje Neurons
 - III. Applications
 - A. Astrocyte Effects on Purkinje Neurons
 - B. Granule Cell Effects on Purkinje Neurons
 - C. Glutamate Transport in Developing Purkinje Neurons
 - References

An *in vitro* coculture system is described to study the avian Purkinje neuron and the interactions occurring with astrocytes and granule cells during development in the cerebellum. Astrocytes initially and granule cells later regulate Purkinje neuron morphology. The coculture system presented here provides an excellent system for investigating the morphological, immunocytochemical, and electrophysiological differentiation of Purkinje neurons under controlled conditions and for studying cell–cell interactions and extrinsic factors, e.g., glutamate in normal and neuropathological conditions.

I. Introduction

The myriad neuronal interactions, both cellular and synaptic, that occur in a particular central nervous system (CNS) region, both during development and in the mature system, can be better understood by first distinguishing the components of the area. This is the strength of being able to study individual elements of a particular neuronal region *in vitro* and also to study combinations of these elements.

The cerebellum is a layered and foliated structure, consisting of the molecular layer, the Purkinje neuron monolayer, and the internal granule cell layer (Ramon y Cajal, 1995). Because it is easy to recognize and dissect out, it lends itself to *in vitro* study. There are two main *in vitro* systems used: dissociated cell culture, where neurons can be investigated individually in a two-dimensional layer after preparation from a tissue source, and slice culture (Haydar *et al.*, 1999), where the system better reflects the *in vivo* situation, but limits resolution of visualizing individual neurons and glia. Experiments using dissociated culture followed by slice culture would give a more complete analysis of a particular neuronal cell type. A more recently reported method of *in vitro* analysis involves the FACS analysis of green fluorescent protein-labeled neurons (Tomomura *et al.*, 2001).

Dissociated Purkinje neuron cultures from both mammalian mouse and rat cerebellum have been prepared and refined by various laboratories (Baptista *et al.*, 1994; Brorson *et al.*, 1991; Furuya *et al.*, 1988; Gillard *et al.*, 1997; Gruol and Franklin, 1987; Hockberger *et al.*, 1994; Linden *et al.*, 1991; Mintz and Bean, 1993; Okubo *et al.*, 2001; Schilling *et al.*, 1991; Tabata *et al.*, 2000).

Preparation of the mammalian dissociated Purkinje neuron culture is an uncomplicated procedure, and the end product is a mixed neuronal culture where Purkinje neurons comprise approximately 5% of the culture (Baptista *et al.*, 1994). Mammalian cultures that require a higher density of Purkinje neurons require more complicated procedures. This is where our unique chick Purkinje neuron *in vitro* system offers advantages when compared to the mammalian system. The chick cerebellum has a higher *in vivo* Purkinje neuron density than either mouse or rat (Ito, 1984). This also means that at the time of dissection (embryonic day 8, ED8), high-density cultures of Purkinje neurons can be prepared that do not require multiple purification steps, and there is little contamination by other cerebellar neuronal cell types (Feirabend, 1990; Feirabend *et al.*, 1985). In

addition, astrocytes of varying ages, and granule cells, can be purified and added to the initial Purkinje cell cultures to study cell–cell interactions and outcomes (Jeffrey *et al.*, 1996).

The cerebellum offers an ideal model for neurobiological research: neuronal migration (Koster and Fraser, 2001; Yang *et al.*, 2002), pattern formation (Armstrong and Hawkes, 2000; Karram *et al.*, 2000) development (Blanco *et al.*, 2002; Cingolani *et al.*, 2002), mouse mutants (Marti *et al.*, 2002; Fernandez-Gonzalez *et al.*, 2002), electrophysiology (Bushell *et al.*, 2002; Shinmei *et al.*, 2002), glutamate uptake (Brasnjo and Otis, 2001; Reichelt and Knopfel, 2002), synaptic interactions (Hirono *et al.*, 2001; Lossi *et al.*, 2002), and regeneration of axotomized Purkinje neuron axons (Dusart *et al.*, 1997).

Various diseases are also associated with Purkinje neuron pathology. Ataxia telangiectasia (AT) is an autosomal recessive disorder where progressive ataxia is accompanied by Purkinje neuron degeneration (Paula-Barbosa *et al.*, 1983). Inactivation of the ATM gene causes a large decrease in numbers of Purkinje neurons and granule neurons. Without the ATM protein, oxidative stress is increased markedly in Purkinje neurons, elevating superoxide levels (Quick and Dugan, 2001). Spinocerebellar ataxia types 1 and 6 (SCA1 and SCA6) are part of a family of disorders induced by polyglutamine repeats (Gomez *et al.*, 1997; Cummings *et al.*, 2001). SCA1 has been studied using a transgenic mouse model (Burright *et al.*, 1995). SCA6 is an autosomal disorder that encodes the P/Q type Ca^{2+} channel in the CNS, particularly in Purkinje neurons and granule neurons in the cerebellum (Piedras-Renteria *et al.*, 2001). Synaptic alterations in the cerebellum have also been associated with Alzheimer's disease (Baloyannis *et al.*, 2000). Besides the well-known deleterious effects of Creutzfeldt–Jakob disease, Hsp72 accumulates in Purkinje neurons, possibly conferring a protective mechanism on these neurons (Kovacs *et al.*, 2001). All these pathologies present obvious studies with an *in vitro* Purkinje neuron system.

We have used our chick *in vitro* Purkinje neuron system to study the distribution of glutamate transporters, and also glutamate uptake in developing Purkinje neurons, and found that GLT-1, the glutamate transporter normally associated with astrocytes, has a neuronal function at early developmental stages in the chick cerebellum. We also showed that inhibition of glutamate transport reduced neurite outgrowth greatly in immature chick Purkinje neurons, inferring a relationship between the transport of L-glutamate and the morphological development of Purkinje neurons (Meaney *et al.*, 1998).

The link between neuronal sensitivity to excess glutamate and the function of glutamate transporters has implications for neuronal and glial homeostasis at the individual cell level, and also at the level of the whole tissue. Several studies have demonstrated that L-glutamate transport (GluT) is of crucial importance both for the maintenance of low extracellular levels of neurotransmitter L-glutamate and for the normal functioning of neurotransmitter metabolism (for reviews, see Rae *et al.*, 2000; Danbolt, 2001; Balcar, 2002). Inhibition of GluT has been shown to be neurotoxic both in culture and *in vivo* (Danbolt, 2001; Balcar, 2002), and

circumstantial evidence shows that deficient or altered GluT is associated with neurological disease. Thus Scott *et al.* (1995) reported subtle changes in the characteristics of GluT in the brains of patients dying from Alzheimer disease, and Rothstein *et al.* (1995) noticed severe deficits in one of the transporters mediating GluT (GLT) in spinal cords of patients who had died of amyotrophic lateral sclerosis. More recent findings show that glutamate uptake is reduced in astrocytes derived from human AD patients, but that estrogen treatment can increase glutamate uptake (Liang *et al.*, 2002). Experimental autoimmune encephalomyelitis (EAE) results in activation of the AMPA glutamate receptor (Ohgoh *et al.*, 2002). The connection between the AMPA receptor and the expression of glutamate transporters in the spinal cord of the Lewis EAE model has shown that EAAC1 protein and mRNA is upregulated dramatically in the EAE model, whereas other transporters, GLT-1 and GLAST, were both downregulated in the spinal cord. In a rat portacaval anastomosis model, analysis of expression of glutamate transporters in the cerebellum showed that transient alterations in the transporters GLAST and GLT-1 caused an accumulation of excess glutamate in the extracellular space (Suarez *et al.*, 2000). Maric *et al.* (2002) also identified a cytoplasmic LIM protein, *Ajuba*, that interacts with the aminoterminal of the GLT protein, proposing it as the scaffolding protein that allows interactions among it, GLT, and the cytoskeleton. Other transporter-associated proteins have been identified (for a review, see Balcar *et al.*, 2001), but at present there is no evidence that such proteins have any effect on the activity of GluT.

II. Methods and Systems

A. Cerebellar Cell Culture

1. Materials

- Trypsin (type XII-S)
- DNase I
- Dulbeccos Modified Eagles Medium (DMEM)
- Fetal calf serum (FCS)
- Chick embryo extract (CEE)
- Poly-L-lysine
- Laminin
- Cytosine β -D-arabinoside (AraC)
- Phosphate-buffered saline (PBS), calcium and magnesium free
- Millicell (30mm, 0.4- μ m pore size) culture plate inserts
- Poly-D-lysine
- Matrigel
- Percoll

2. Purkinje Neuron Culture

Cerebellar Purkinje neuron cultures were prepared from chick embryos (ED8). This time was chosen as the inner cortical cell layer, the source of Purkinje neurons appears at this time and the layer is subdivided into Purkinje neuron clusters between days 8 and 11 (Feirabend, 1990).

1. Dissect out ED8 cerebellum in aseptic conditions using sterile instruments in a biohazard hood.
2. Incubate in 0.25% (w/v) trypsin in PBS for 30 min at 37°C.
3. Triturate in 0.15% DNase I (including 0.25% MgSO₄).
4. Coat 25-mm glass coverslips with 1 mg/ml poly-L-lysine and 100 µg/ml laminin dissolved in sterile distilled water and dried in a tissue culture hood.
5. Plate the coverslips at a density of 2000 cells/mm² with cells in DMEM containing 5% FCS, 2.5% CEE, and 25 mM KCl (neuronal medium) in 7.5% CO₂ at 37°C.
6. After 2 days in culture, add the mitotic inhibitor, AraC, at $5 \times 10^{-6}M$ for 3 days to inhibit astrocyte proliferation on the coverslips.

Fifteen ED8 embryos yield enough cells for 18 coverslips at a density of 2000 cells/mm².

3. Astrocytes

1. Dissect cerebellum from ED16 chickens under aseptic conditions.
2. Cut into small pieces.
3. Produce a single cell suspension by dissociation with 0.25% trypsin in PBS and triturate with 0.15% DNase I containing 0.25% (w/v) MgSO₄ in PBS.
4. Culture for 4 days in six-well, 35-mm Corning plates in DMEM plus 15% FCS in 7.5% CO₂ at 37°C to produce an astrocyte monolayer.
5. Coat Millicells (30 mm, 0.4-µm pore size) culture plate inserts with 1/10 Matrigel and allow to air dry.
6. Prepare a single cell suspension from astrocyte monolayers by subculturing in 0.25% trypsin and 0.15% DNase I containing 0.25% (w/v) MgSO₄.
7. Coat astrocytes onto Millicells at a density of 2800 cells/mm² and culture in neuronal medium overnight.

Three embryos will yield enough cells for 18 Millicells. Astrocytes were characterized using antibody to glial fibrillary acidic protein (GFAP). Astrocytes can be prepared from any age using this procedure.

4. Granule Cells

Purified granule cells were isolated utilizing the procedure of Hatten (1985) developed for mice.

1. Dissect cerebellum from chicks of ED13 or ED15, chop into small pieces, and incubate in 0.25% trypsin, and triturate in 0.15% DNase I, including 0.25% (w/v) MgSO_4 for 20 min at 37°C.
2. Prepare 30% Percoll (1.5 ml Percoll plus 3.5 ml DMEM) and 60% Percoll (3 ml Percoll plus 2 ml DMEM) gradient in a centrifuge tube.
3. Layer the single cell suspension onto the Percoll gradient and centrifuge at 3000 rpm ($2000 \times g_{\text{max}}$) for 30 min in a Beckman GS-6 centrifuge.
4. Collect cells from the 30/60% Percoll interface and wash twice with PBS at a 5/1 volume ratio to cell pellet by centrifugation at 2200 rpm for 5 min ($1000 \times g_{\text{max}}$).
5. Plate granule cells onto tissue culture plastic dishes coated with 100 $\mu\text{g}/\text{ml}$ poly-D-lysine dissolved in sterile distilled water for 20 min. Collect nonadherent granule cells by centrifugation.
6. Store in neuronal medium at high density ($>2 \times 10^6$ cells/ml) until the addition to coverslips.

Purified avian granule cells stain positive for the amino acid neurotransmitter glutamate and negative for parvalbumin and calbindin D-28. The cell size (6 μm) and immunohistochemical profile define these cells as granule cells (Gruol and Crimi, 1988).

B. Coculture Systems

1. Purkinje Neurons Plus Astrocytes

A Purkinje neuron coverslip was placed into each well of a six-well 35-mm culture dish, followed by an astrocyte-coated Millicell covered with neuronal medium and cultured for various times.

2. Isochronic Culture with Granule Cells

Granule cells at a ratio of 5/1 to Purkinje neurons were added onto Purkinje neuron coverslips, which had been incubated for either 5 or 7 days *in vitro* culture (DIV). Isochronic cultures were prepared by adding granule cells from either ED13 or ED15 cerebellum so that granule cells added were the same age as Purkinje neurons on the coverslip, e.g., ED8 plus 5 or 7 DIV.

C. Immunohistochemistry

1. Materials

PBS
Triton X-100
BSA
–20°C methanol

2% paraformaldehyde

Antibodies to:

Neurofilament 200 (NF200), 68 (NF68), monoclonal antibodies from Amersham, Australia

Cyclic GMP protein kinase, polyclonal antibody, a kind gift from Professor P. Greengard, Rockefeller University

Parvalbumin, MAP 2, calbindin D-28, glutamate, monoclonal antibodies from Sigma, Chemical Co.

Neuron-specific enolase (NSE), polyclonal antibody from Sigma Chemical Co.

Thy-1 (French and Jeffrey, 1986)

Alkaline phosphatase, horseradish peroxidase, FITC and RITC-conjugated secondary antibodies from Jackson ImmunoResearch Laboratories or Bio-Rad Laboratories

NBT/BCIP

DAB – chromogen

Leitz or Olympus optical microscope

Goat serum

2. Neuronal Characterization

Purkinje neurons were identified by markers and morphological characteristics following days *in vitro* culture. Coverslips were fixed in either -20°C methanol for 30 min prior to immunostaining for neurofilament 200 (NF200 1/100), cyclic GMP protein kinase (G-kinase 1/1000), parvalbumin (1/250), MAP2 (1/100), and neurofilament 68 (NF68 1/50) or in 2% paraformaldehyde in PBS at room temperature for 30 min prior to immunostaining for calbindin D-28 (1/100), NSE (1/100), amino acid glutamate (1/100), GABA (1/100), and Thy-1 (1/100) (French and Jeffrey, 1986).

1. Following fixation, wash three times with PBS.
2. Block with 1% BSA in PBS for 45 min.
3. Wash three times with PBS.
4. Partially permeabilize with 0.5% Triton X-100 in PBS for 2 min.
5. Add primary antibodies in dilutions determined specifically for the antibody source. Sample dilutions from this laboratory were given earlier.
6. Visualization is by enzyme-linked antibodies, either alkaline phosphatase or horseradish peroxidase with NBT/BCIP or DAB chromogen, respectively.
7. View under a high-quality optical microscope.

Double fluorescent staining, to identify Purkinje neurons, was performed using rabbit antibody to NSE, a neuronal marker, and a mouse monoclonal antibody to calbindin D-28, a Purkinje neuron marker, for 1 h at room temperature or

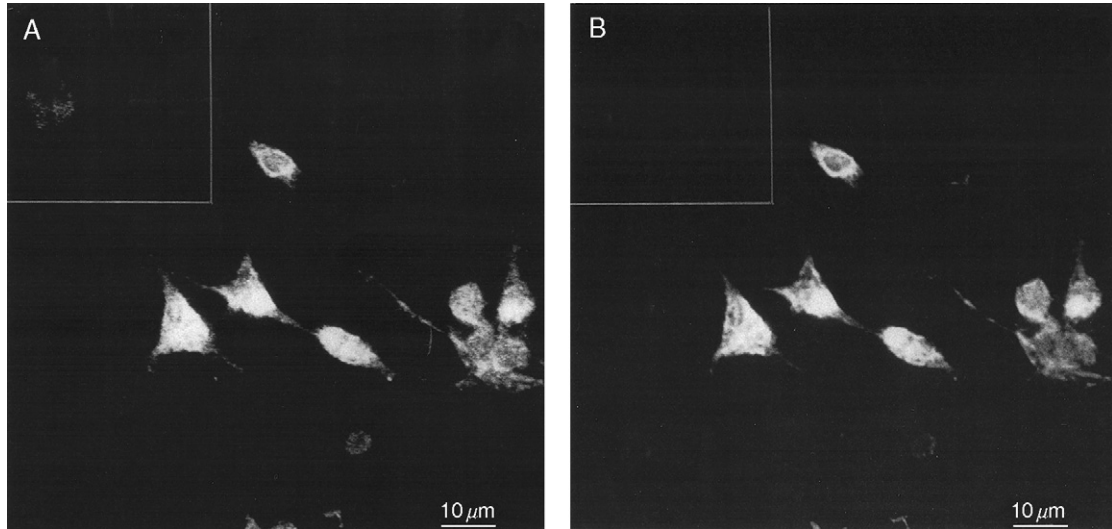


Fig. 1 Identification of the neuronal population as Purkinje neurons. Cells cultured from ED8 chick cerebellum after 14 DIV (equivalent to hatch) are positive for both the Purkinje neuron-specific marker calbindin D-28 (A) linked to an FITC-labeled secondary antibody and the pan-neuronal marker NSE (B) linked to an RITC-labeled secondary antibody. The majority of cells were double labeled. Inserts contain the negative control for each primary antibody. Scale bar 10 μm . Reprinted from Jeffrey *et al.* (1996), with permission.

overnight at 4°C (Fig. 1). Coverslips were washed three times in PBS and incubated for 1 h in the dark with antimouse FITC (1:100) or antirabbit RITC (1:100), made up in 1% goat serum in PBS. Coverslips were mounted in FluorSave Reagent (Calbiochem Corp) and viewed under a confocal laser-scanning microscope (Wild Leitz Instrument, Heidelberg, Germany). Incubations were performed in a humidified chamber.

D. Morphological Analysis

1. Materials

Ethanol/acetic acid
Ethanol
Polyester wax

2. Morphological Types

The stages of Purkinje neuron development were first described by Armengol and Sotelo (1991) in the rat. This system of classification was applied to the development of avian Purkinje neurons in the *in vitro* culture and for comparison to the *in vivo* situation.

The basic features of the neuronal types described for the rat have been modified to formulate five morphological categories of avian Purkinje neurons in the developing avian cerebellum: type I, bipolar cells with smooth oval cell body and processes at opposite ends; type II, cells with less than four processes growing from all parts of the cell body; type III, cells with processes that are being withdrawn or regressing; and type IV, stellate cells characterized by the progressive outgrowth of processes. Another category has been added for avian analysis: type V, cells with a primary dendrite and secondary dendritic branching.

a. In Vivo Purkinje Neuron Morphology

Cerebellar tissue from ED10, ED13, ED15, ED17, and hatch chicks was fixed in ethanol/acetic acid (95/5, v/v) on ice and embedded in soft polyester wax as described previously by Sheppard *et al.* (1988). Sections ($4\mu\text{m}$) were blocked in 10% normal goat serum for 15 min and were stained with antibodies parvalbumin (1:100) or calbindin (1:150) for 1 h, followed by the secondary antibody of rabbit antimouse-conjugated alkaline phosphatase (1:1000) and NBT/BCIP. Only nucleated Purkinje neurons in sections were counted. Counts were determined on 20 sections of each age between ED10 and ED17. The morphological types can be recognized in the developing chick cerebellum (type I, bipolar with two processes, Fig. 2A; type II, greater than four processes emanating from the cell body, Fig. 2B; type III, processes are regressive, Fig. 2C; type IV, stellates form where new processes grow out of the cell body, Fig. 2D; and type V, formation of the primary dendrite, Fig. 2E). The quantitation of this conversion from type I at ED10 to type V at ED17 is presented in Fig. 3B.

b. In Vitro Purkinje Neuron Morphology

In vitro morphological types can be quantitated in simple cultures with different aged astrocytes or in coculture with isochronic granule cell addition. Counts were carried out at four time points—2, 8, 16, and 21 DIV—using coverslips stained with either calbindin D-28 or NF200. Only single Purkinje neurons were counted, with data expressed as a percentage of total counts at each particular time point (Figs. 2F–2I; Fig. 3A).

E. Glutamate Uptake in Purkinje Neurons

1. Materials

Phosphate-buffered Krebs–Ringer solution (PBKR)

L- ^3H glutamate, 28 Ci/mmol

D- and L-Threo-3-hydroxyaspartic acids (D- and L-t-3OHA)

L-*trans*-Pyrrolidine-2,4-dicarboxylic acid (L-t-PDC)

Antibody to GLT-1, a generous gift from Dr. J. D. Rothstein

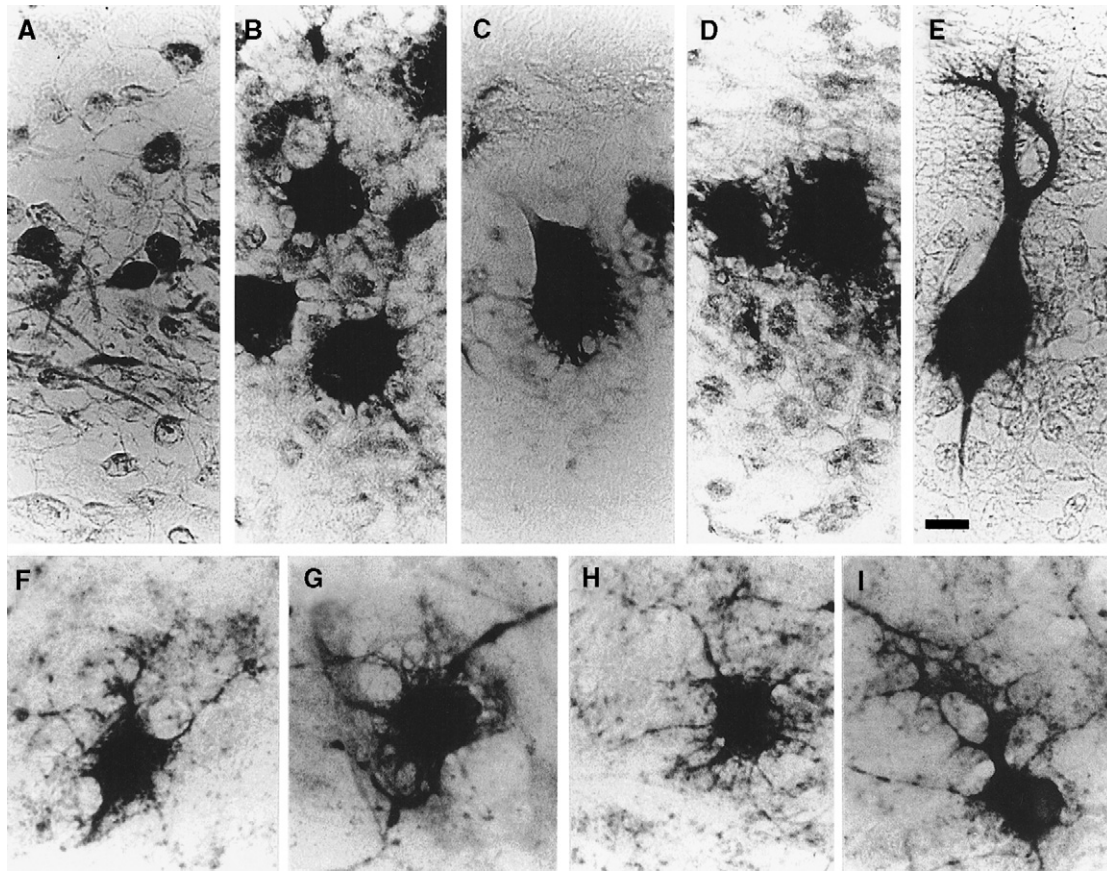


Fig. 2 Identification of the morphological phenotypes of avian Purkinje neurons according to the modified criteria of Armengol and Sotelo (1991) *in vivo* (A–E) and *in vitro* (F–I). (A) Type I with process at opposite ends of the cell body. (B) Type II, with less than four processes emanating from the cell body. (C) The regressive form, when the processes are retracted. The emergence of new fibers, and also the beginning of the primary dendrite, is seen *in vivo* (D and E) and *in vitro* (F–I) from coculturing with granule cells. *In vitro* neurons are stained for NF200. *In vivo* sections of ED10 Purkinje neurons are stained for parvalbumin, but all other embryonic ages are stained for calbindin-D (Fig. 3B). Scale bar: 10 μ m. Reprinted from Jeffrey *et al.* (1996), with permission.

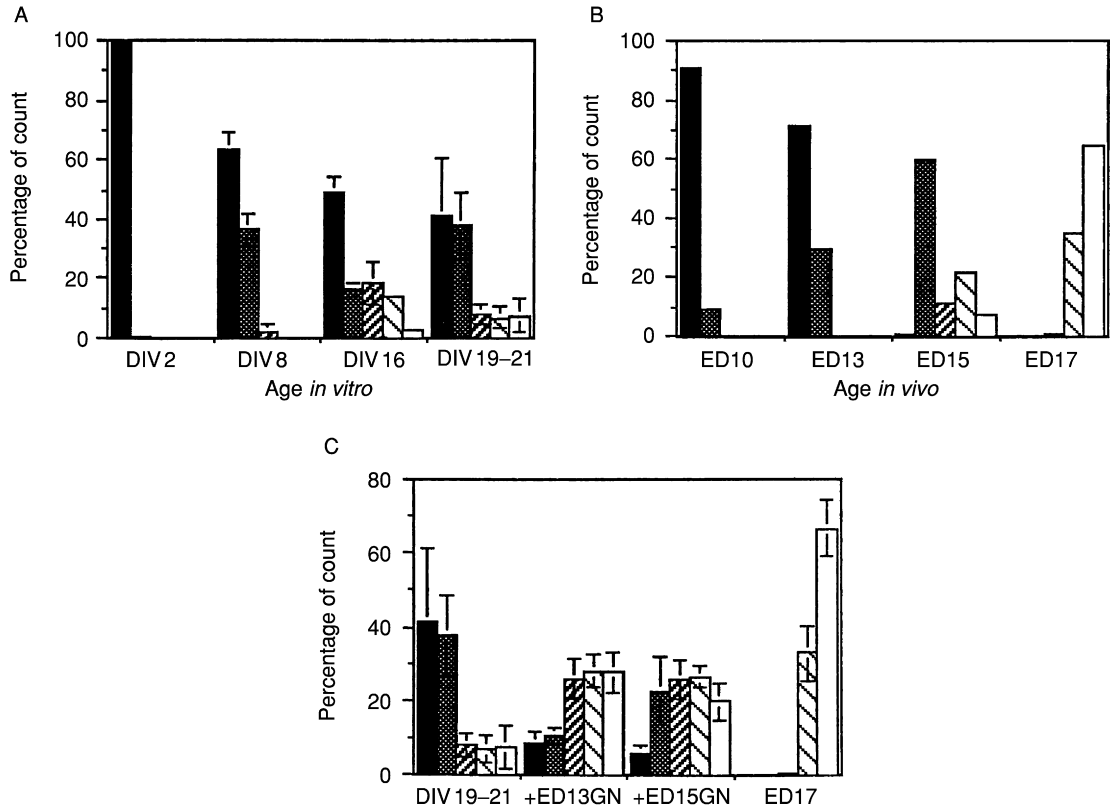


Fig. 3 Quantitation of Purkinje neuron morphological types under various experimental conditions. Purkinje neuron types were quantitated as described in the text and graphed as a percentage of the total count at each time point. Black bars refer to type I, type II is represented by dark striped bars, crosshatched bars show type III, and type IV is represented as a light striped diagonal. The type V type, which is mature with prominent primary dendrites, is shown by open bars. (A) Temporal distribution of the different types of immature Purkinje neurons over a period of 21 DIV in the presence of ED16 astrocytes. Error bars are the mean \pm SD from four individual experiments. (B) Temporal distribution of the different types of Purkinje neurons present in the developing avian cerebellum from ED10 to ED17. Purkinje were identified in sections by calbindin-D28 staining, except ED10, which were stained for parvalbumin. (C) The effect of the addition of granule cells from ED13 (ED13GN) and ED15 (ED15GN) on Purkinje neuron morphology after 21 DIV. Purkinje neurons from ED8 cerebellum were cultured in the presence of ED16 astrocytes for 5 and 7 DIV before the addition of ED13 and ED15 granule cells, respectively. Results are given as mean \pm SD for 3 individual experiments for each age of granule cells. For comparison, the distribution after 21 DIV in the presence of ED16 astrocytes and in the absence of granule cells and the *in vivo* avian ED17 data are given. Reprinted from Jeffrey *et al.* (1996), with permission.

2. Uptake of L-[³H]Glutamate

1. Place three small drops mounting medium (Euparal, GBI Laboratories, Manchester, UK) on the bottom of petri dishes and allow to harden for a few days. This prevents coverslips containing Purkinje neurons from adhering too closely to the bottom of the petri dish and makes the removal of coverslips at the end of incubation much simpler.
2. Remove coverslips containing 7 DIV and 14 DIV Purkinje neurons from neuronal culture medium.
3. Wash by dipping into 80 ml of PBKR (Balcar *et al.*, 1994) (PBKR: 120 mM NaCl, 4.5 mM KCl, 1.8 mM MgCl₂, 1.8 mM CaCl₂, 5.5 mM glucose, pH 7.4) at room temperature (23–25°C).
4. Store in same PBKR medium for 5–15 min before use.
5. Transfer coverslips to 35-mm petri dishes containing 1 μM L-[³H]glutamate in 2 ml incubation medium (PBKR), with or without inhibitors. For best results, it is suggested that the specific activity be set at 0.5 to 1 μCi/ml if 1 μM L-glutamate uptake is used or higher if L-[³H]glutamate uptake is studied at higher concentrations.
6. Incubate for 8 min in a 25°C water bath.
7. After the incubation period, wash coverslips by rapidly dipping twice into three 100-ml beakers filled with PBKR and finally place in 1 ml water.
8. For best results, the washing procedure should be completed within 5 s.
9. After 24 h, determine tritium radioactivity in a 1-ml aqueous sample by liquid scintillation counting.
10. Determine protein on coverslips by solubilizing protein from parallel coverslips in 0.25 M NaOH and using the Lowry protein assay (Lowry *et al.*, 1951). Alternatively, it is possible to determine water-soluble protein in the aqueous extract. It is possible to extract the cultures with 0.1–0.5 M NaOH to solubilize the proteins and then use the Lowry protein assay.
11. Process data with Prism software (Graphpad, San Diego) or any other suitable high-power statistical package.

III. Applications

The method presented here has allowed the study of the development of avian Purkinje neurons in a controlled coculture system. The system is rapidly manipulated, and two approaches already published from this laboratory are presented as examples of the suitability of the system for investigating the morphological, immunocytochemical, and electrophysiological differentiation of Purkinje neurons (Jeffrey *et al.*, 1996; Meaney *et al.*, 1998; Jeffrey *et al.*, 1998).

A. Astrocyte Effects on Purkinje Neurons

1. Survival and Limited Morphological Development Requires the Presence of Astrocytes

Purkinje neurons are identified by markers and morphological characteristics following days *in vitro* culture. Following 14 DIV, which is roughly equivalent to hatch, Purkinje neurons are positive for the pan-neuronal marker, neuronal-specific enolase, and the specific Purkinje neuron marker, calbindin D-28 (Fig. 1), and other markers, cyclic GMP kinase, MAP 2, NF68, NF200, and Thy-1. The size of neuronal soma increases from 8 μm at 7 DIV to $19.0 \pm 1.7 \mu\text{m}$ at 21 DIV.

Astrocyte monolayers present on Millicells were necessary to promote neuronal survival by providing essential factors, as Purkinje neuron survival was extremely low in the absence of Millicell astrocyte monolayers at even a high plating density (6–8000 cells/ mm^2).

Astrocytes derived from two embryonic ages caused different effects on the Purkinje neurons. Purkinje neurons in the presence of ED8 astrocytes exhibited increased fasciculation of neurites and the number of neurons in aggregates. With ED16 astrocytes, Purkinje neurons remain predominately as single cells with minimal aggregation and with a slightly more mature phenotype and are hence a better source for morphological studies. These findings implicate temporally regulated astrocyte factors affecting neuronal aggregation and fasciculation. Purkinje neurons grown for 5 DIV with ED16 astrocyte layers on Millicells form long simple neurites. Removal of Millicells at 5 DIV and further culturing for a further 9 DIV resulted in a dramatic retraction of the processes. Cell bodies remained normal and no cell death was noted. Thus following an initial period of culture in the presence of astrocytes, their removal does not affect survival but causes a retraction of processes, indicating different factors being present with increasing time in culture.

2. Limited Development of Purkinje Neuron Morphology by Astrocyte-Conditioned Media

Coculture with ED16 astrocytes over a period of 21 DIV results in a maturation block in Purkinje neuron development at the type II phenotype. This limited differentiation clearly evident at 21 DIV was seen routinely up to 28 DIV (2 weeks posthatch *in vivo*) in our culture system and is quantitated in Fig. 3A. The limited Purkinje neuron development was independent of the age of the cerebellar astrocytes present on Millicells.

B. Granule Cell Effects on Purkinje Neurons

1. Formation of Mature Purkinje Neuron Phenotype Requires Isochronic Addition of Granule Cells

In order to keep the *in vitro* coculture system as close a possible to the *in vivo* situation with regard to the avian developmental timetable (Feirabend, 1990), isochronic granule cells purified from cerebellum were added to the cultures.

Adding ED13-purified granule cells (ratio 5/1 to Purkinje neurons) to Purkinje neuron cultures from ED8 cerebellum following 5 DIV produced a dramatic effect on the morphology, inducing a more mature phenotype where types III – V predominate (Fig. 3C), and was less dramatic with ED15 granule cells. The effect was dependent on the number of granule cells added; ratios of granule cells to Purkinje neurons less than 1/1 had no effect on maturation, whereas ratios of 10/1 showed no increased maturation over the 5/1 ratio but analysis became difficult. Representative profiles of mature Purkinje neurons are shown (Figs. 2F–2I) and quantitated in Fig. 3C.

The importance of granule neuron interactions with developing Purkinje neurons has been reported in mouse where plating of immature Purkinje neurons onto networks of parallel fibers enhances Purkinje neuron maturation (Baptista *et al.*, 1994).

The shift to the mature phenotype is not complete, reflecting the role of other neuronal cell types in the cerebellum on Purkinje dendritic tree development and the two-dimensional nature of this culture system.

Clearly, two phases of *in vitro* avian Purkinje neuron development can be defined by this system.

1. Survival and limited morphological development requires astrocytes.
2. Attainment of mature phenotypes is dependent on the presence of granule cells added in an isochronic manner.

C. Glutamate Transport in Developing Purkinje Neurons

The coculture of cerebellar Purkinje cells and glial monolayers provides an excellent model system for studying the effects of epigenetic factors on the differentiation of neurons.

Excitatory amino acids, specifically L-glutamate, have been proposed as cofactors essential for the development and differentiation of Purkinje neurons, particularly in relation to the morphology of the dendrites (Cohen-Cory *et al.*, 1991; Mount *et al.*, 1993). The actions of L-glutamate could be mediated by ionotropic or metabotropic receptors (iGluR, mGluR) that are usually positioned on the outer surface of the cytoplasmic membrane. Interaction of L-glutamate with its receptors (GluR) can, however, contribute not only to the mechanisms of neuronal signalling or morphogenesis, but, in the case of uncontrolled GluR activity, could trigger a cascade of events resulting in the death of the neurons. Extracellular concentrations of L-glutamate therefore have to be regulated precisely.

The actions of L-glutamate released at excitatory glutamatergic synapses in the adult brain are limited temporally and spatially by sodium-dependent transport (GluT) that is located usually, but not always, in the cytoplasmic membrane of neighboring astrocytes (Danbolt, 2001). Transporters mediating GluT are expressed in brain tissue at very high densities both in the forebrain and in the cerebellar cortex (Danbolt, 2001). GluT can thus very efficiently “sweep” the

synaptic cleft, as well as the perisynaptic extracellular space, remove any excess L-glutamate, transport it against very steep concentration gradients (Danbolt, 2001), and include it in normal glial metabolism (Rae *et al.*, 2000; Moussa *et al.*, 2002). At least five distinct transporters (not counting numerous splice variants present in brain; Robinson, 1998) can handle L-glutamate in a Na⁺-dependent manner: GLAST (EAAT1), GLT (EAAT2), EAAC1 (EAAT3), EAAT4, and EAAT5 [see Danbolt (2001) or Balcar (2002) for the explanation of nomenclature]. While GLT is the principal glutamate transporter in astrocytes of the forebrain, GLAST is found at very high densities in glial cells of the cerebellar cortex (Danbolt, 2001). EAAC1 is found in neurons throughout the CNS, but EAAT4 and EAAT5 have very specific locations: EAAT4 exists in significant amounts only in cerebellar Purkinje cells, whereas EAAT5 is expressed appreciably only in the retina (Pow, 2001; Rauen, 2000).

1. Glutamate Uptake by Developing Purkinje Neurons

There seems to be a period of time during neuronal differentiation when glutamate transporters, such as GLT and GLAST, which are, in the adult brain, found only in glial cells, appear transiently in developing neurons. Sutherland *et al.* (1996) reported increased densities of glutamate transporter mRNA in regions with high synaptogenesis and, subsequently, the expression of GLT was demonstrated both in developing hippocampal neurons (Mennerick *et al.*, 1998) and in Purkinje cells of the chick cerebellum (Meaney *et al.*, 1998). It has also been shown that expression of the transporter protein is associated with the appearance of a vigorous uptake of L-[³H]glutamate (Meaney *et al.*, 1998; Gaillet *et al.*, 2001). The 7 DIV culture of ED8 chick Purkinje neurons accumulates 1 μ M L-[³H]-glutamate by a high-affinity transport system that could be inhibited in order of potency L-t-DOC~L-t-3-OHA>D-t-3OHA. The IC₅₀ decreased for D-t-3OHA between 7 and 14 DIV, indicating the appearance of heterogeneity for transport sites at later times. Furthermore, hippocampal neurons were shown to coexpress GLAST together with GLT (Plachez *et al.*, 2000).

2. Inhibition of High-Affinity Glutamate Transport Results in Changes in Purkinje Neuron Morphology

The hypothesis that L-glutamate acts as an epigenetic factor during neuronal morphogenesis can be tested using cultured Purkinje cells, and we have done so by inhibiting either GluT or GluR of the NMDA type. Typical results of such experiments are displayed in Fig. 4. While the extracellular levels of L-glutamate would be expected to rise as a consequence of GluT inhibition, thus increasing the stimulation of GluR, MK-801 would have an exactly opposite effect, causing a potent inhibition of NMDA receptors. Inhibition of GluT by L-*trans*-pyrrolidine-2,4-dicarboxylate reduces the number of neurites (Fig. 4), whereas MK-801 has, in fact, an opposite effect. Therefore, it appears that L-glutamate, acting on GluR of the NMDA type, actually tends to downregulate the growth and branching of the

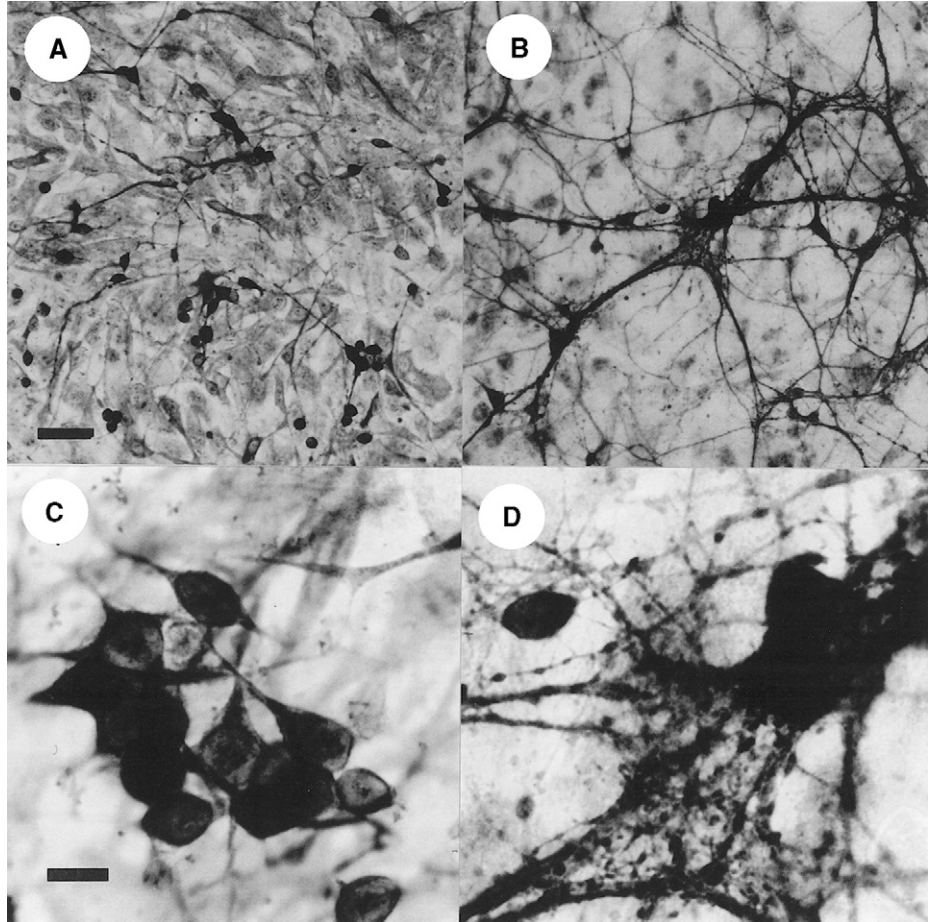


Fig. 4 Effects of L-t-PDC on Purkinje neuron morphology. The addition of L-t-PDC, a potent inhibitor of glutamate transport (IC_{50} 116 μ M at 7 DIV) to Purkinje neuron cultures, causes a massive regression of neurites. L-t-PDC was added at 1 DIV (1–250 μ M) and grown for 9 DIV and was fixed and stained for NF200. Neuronal coverslips are presented in B and D, where D is a higher power magnification showing extensive neurite outgrowth and fasciculation. Contrast to A and C, following the addition of L-t-PDC over an 8 DIV period, results in almost complete neurite retraction. Scale bars: 50 μ m (A and B) and 10 μ m (C and D). Reprinted from Meaney *et al.* (1998), with permission.

neurites of Purkinje cells. Stimulation of NMDA receptors would increase the concentration of Ca^{2+} in the cytosol, thus activating numerous enzymes such as Ca^{2+} -dependent proteases and kinases that could affect either synthesis or post-translational processing of proteins important for the development of the neuritic tree. Whether such mechanisms are also active *in vivo* and contribute to the process of “sculpting” the developing dendrites to develop the large, complex, and precisely oriented tree-like structure so characteristic of Purkinje neurons in

the adult cerebellar cortex is not known, but a strong transient expression of GLT has since been reported in the ovine cerebellum *in utero* (Northington *et al.*, 1999).

GLT and GLAST are, however, not the only glutamate transporters found on or in the vicinity of Purkinje neurons, and there are at least two other glutamate transporters that could be important in the differentiation of Purkinje cells: EAAT3 and EAAT4. Little is known of the expression of EAAT3 either by the adult or developing Purkinje neurons, but findings from hippocampal neurons suggest that EAAT3 could move rapidly between the cytoplasm and the cytoplasmic membrane in response to changing neuronal activity, and one might conjecture that such intracellular movements are part of the mechanism involved in synaptic plasticity (Danbolt, 2001; Robinson, 2002). As such phenomena have also been studied in Purkinje neurons (in the form of long-term depression, LTD), the presently discussed coculture system would seem to represent an excellent experimental model for studies involving both morphological and molecular aspects of the hypothesis.

Probably the most enigmatic glutamate transporter expressed by Purkinje neurons is EAAT4. In the adult brain it is found mainly in a precise arrangement close to the dendritic spines (Danbolt, 2001). Like most other transporters, EAAT4, when transporting L-glutamate, also permits passive passage of chloride ions across the neuronal membrane (Fairman *et al.*, 1995). This could influence depolarization of the neuronal membrane caused by ionotropic glutamate receptors and thus further modify the activity of glutamatergic synapses on Purkinje neurons (Auger and Attwell, 2000; Otis *et al.*, 1997). EAAT4 is distributed heterogeneously not only within cells, but also across the cerebellar cortex; it has been reported that it codistributes with zebrin II, thus forming characteristic parasagittal “stripes” (Dehnes *et al.*, 1998).

Several potent GluT inhibitors have been identified and/or synthesized over the past three decades (review Balcar *et al.*, 2001), and the structural specificity of GluT has been studied in great detail (review Balcar, 2002). Moreover, clear differences exist between the pharmacological characteristics of GluT in the forebrain and the cerebellar cortex, respectively (Takamoto *et al.*, 2002; Balcar, 2002), thus leaving hope that substrates and inhibitors specific for GluT in Purkinje neurons could be identified and tested in systems such as the glial/neuronal coculture discussed here.

Acknowledgments

Work in this laboratory is supported by the NH&MRC. The authors thank Dr. Christine Smythe for excellent work on the confocal microscope.

References

- Armengol, J. A., and Sotelo, C. (1991). Early dendritic development of Purkinje cells in the rat cerebellum. A light and electron microscopic study using axonal tracing in *in vitro* slices. *Dev. Brain Res.* **64**, 95–114.

- Armstrong, C. L., and Hawkes, R. (2000). Pattern formation in the cerebellar cortex. *Biochem. Cell Biol.* **78**, 551–562.
- Auger, C., and Attwell, D. (2000). Fast removal of synaptic glutamate by postsynaptic transporters. *Neuron* **28**, 547–558.
- Balcar, V. J. (2002). Molecular pharmacology of the Na⁺-dependent transport of acidic amino acids in the mammalian central nervous system. *Biol. Phar. Bull. (Japan)* **25**, 291–301.
- Balcar, V. J., Shen, J., Bao, S., and King, N. J. C. (1994). Na⁺-dependent high affinity uptake of L-glutamate in primary culture of human fibroblasts isolated from three different types of tissue. *FEBS Lett.* **339**, 50–54.
- Balcar, V. J., Takamoto, A., and Yoneda, Y. (2001). Neurochemistry of L-glutamate transport in the CNS: A review of thirty years of progress. *Collect. Czech. Chem. Commun.* **66**, 1315–1340.
- Baloyannis, S. J., Manolidis, S. L., and Manolidis, L. S. (2000). Synaptic alterations in the vestibulocerebellar system in Alzheimer's disease: A Golgi and electron microscope study. *Acta Otolaryngol.* **120**, 247–250.
- Baptista, C. A., Hatten, M. E., Blazeski, R., and Mason, C.A (1994). Cell-cell interactions influence survival and differentiation of purified Purkinje cells *in vitro*. *Neuron* **12**, 243–260.
- Blanco, M. J., Pena-Melian, A., and Angela Nieto, M. (2002). Expression of EphA receptors and ligands during chick cerebellar development. *Mech. Dev.* **114**, 225–229.
- Brasnjo, G., and Otis, T. S. (2001). Neuronal glutamate transporters control activation of postsynaptic metabotropic glutamate receptors and influence cerebellar long-term depression. *Neuron* **31**, 607–616.
- Brorson, J. R., Bleakman, D., Gibbons, S. J., and Miller, R. J. (1991). The properties of intracellular calcium stores in cultured rat cerebellar neurons. *J. Neurosci.* **11**, 4024–4043.
- Burright, E. N., Clark, H. B., Servadio, A., Matilla, T., Feddersen, R. M., Yunis, W. S., Durick, L. A., Zoghbi, H. Y., and Orr, H. T. (1995). SCA1 transgenic mice: A model for neurodegeneration caused by an expanded CAG trinucleotide repeat. *Cell* **82**, 937–948.
- Bushell, T., Clarke, C., Mathie, A., and Robertson, B. (2002). Pharmacological characterization of a non-inactivating outward current observed in mouse cerebellar Purkinje neurons. *Br. J. Pharmacol.* **135**, 705–712.
- Cingolani, L. A., Gymnopoulos, M., Boccaccio, A., Stocker, M., and Pedarzani, P. (2002). Developmental regulation of small conductance Ca²⁺ activated K⁺ channel expression and function in rat Purkinje neurons. *J. Neurosci.* **22**, 4456–4467.
- Cohen-Cory, S., Dreyfus, C. F., and Black, I. B. (1991). NGF and excitatory neurotransmitters regulate survival and morphogenesis of cultured cerebellar Purkinje cells. *J. Neurosci.* **11**, 462–471.
- Cummings, C. J., Sun, Y., Opal, P., Antalffy, B., Mestril, R., Orr, H. T., Dillmann, W. H., and Zoghbi, H. Y. (2001). Over-expression of inducible HSP70 chaperone suppresses neuropathology and improves motor function in SCA1 mice. *Hum. Mol. Genet.* **10**, 1511–1518.
- Danbolt, N. C. (2001). Glutamate uptake. *Prog. Neurobiol.* **65**, 1–105.
- Dehnes, Y., Chaudry, F. A., Ullensvang, K., Lehre, K. P., Storm-Mathisen, J., and Danbolt, N. C. (1998). The glutamate transporter EAAT4 in rat cerebellar Purkinje cells: A glutamate-gated chloride channel concentrated near the synapse in parts of the dendritic membrane facing astroglia. *J. Neurosci.* **18**, 3603–3619.
- Dusart, I., Airaksinen, M. S., and Sotelo, C. (1997). Purkinje cell survival and axonal regeneration are age dependent: An *in vitro* study. *J. Neurosci.* **17**, 3710–3726.
- Fairman, W. A., Vandenberg, R. J., Arriza, J. L., and Amara, S. G. (1995). An excitatory amino acid transporter with properties of a ligand-gated chloride channel. *Nature* **375**, 599–603.
- Feirabend, H. K. P. (1990). Development of longitudinal patterns in cerebellum of the chick *Gallus domesticus*: A cytoarchitectural study on the genesis of cerebellar modules. *Eur. J. Morphol.* **28**, 169–223.
- Feirabend, H. K. P., Van Luxemburg, E. A., Van Denderen-Van Dorp, H., and Voogd, J. (1985). A ³H-thymidine autoradiographic study of the development of the cerebellum of the white leghorn (*Gallus*

- domesticus*): Evidence for longitudinal neuroblast generation patterns. *Acta Morphol. Neerl. Scand.* **23**, 115–126.
- Fernandez-Gonzalez, A., La Spada, A. R., Treadaway, J., Higden, J. C., Harris, B. S., Sidman, R. L., Morgan, J. I., and Zuo, J. (2002). Purkinje cell degeneration (pcd) phenotypes caused by mutations in the axotomy-induced gene, *Nna1*. *Science* **295**, 1904–1906.
- French, P. W., and Jeffrey, P. L. (1986). Partial characterization of chicken Thy-1 glycoprotein by monoclonal antibodies. *J. Neurosci. Res.* **16**, 479–489.
- Furuya, S., Makino, A., and Hirabayashi, Y. (1988). An improved method for culturing cerebellar Purkinje cells with differentiated dendrites under a mixed monolayer setting. *Brain Res. Protocols* **3**, 192–198.
- Gaillet, B., Plachez, C., Malval, F., Bezine, M. F., and Recasens, M. (2001). Transient increase in the high affinity [³H]L-glutamate uptake activity during *in vitro* development of hippocampal neurons in culture. *Neurochem. Int.* **38**, 293–301.
- Gillard, S. E., Volsen, S. G., Smith, W., Beattie, R. E., Bleakman, D., and Lodge, D. (1997). Identification of pore-forming subunit of P-type calcium channels: An antisense study on rat cerebellar Purkinje cells in culture. *Neuropharmacology* **36**, 405–409.
- Gomez, C. M., Thompson, R. M., Gammack, J. T., Perlman, S. L., Dobyns, W. B., Truwit, C. L., Zee, D. S., Clark, H. B., and Anderson, J. H. (1997). Spinocerebellar ataxia type 6: Gaze-evoked and vertical nystagmus, Purkinje cell degeneration, and variable age of onset. *Ann. Neurol.* **42**, 933–950.
- Gruol, D. L., and Crimi, C. P. (1988). Morphological and physiological properties of rat cerebellar neurons in mature and developing cultures. *Dev. Brain Res.* **41**, 135–146.
- Gruol, D. L., and Franklin, C. L. (1987). Morphological and physiological differentiation of Purkinje neurons in cultures of rat cerebellum. *J. Neurosci.* **7**, 1271–1293.
- Hatten, M. E. (1985). Neuronal regulation of astroglial morphology and proliferation *in vitro*. *J. Cell Biol.* **100**, 384–396.
- Haydar, T. F., Bambrick, L. L., Krueger, B. K., and Rakic, P. (1999). Organotypic slice cultures for analysis of proliferation, cell death and migration in the embryonic neocortex. *Brain Res. Protocols* **4**, 425–437.
- Hirono, M., Yoshioka, T., and Konishi, S. (2001). GABA(B) receptor activation enhances mGlu-R mediated responses at cerebellar excitatory synapses. *Nature Neurosci.* **4**, 1207–1216.
- Hockberger, P. E., Yousif, L., and Nam, S. C. (1994). Identification of acutely isolated cells from developing rat cerebellum. *Neuroimage* **1**, 276–287.
- Ito, M. (1984). Purkinje cells: Morphology and development. In “The Cerebellum and Neural Control,” pp. 21–39. Raven Press, New York.
- Jeffrey, P. L., Meaney, J., Tolhurst, O., and Weinberger, R. P. (1996). Epigenetic factors controlling the development of avian Purkinje neurons. *J. Neurosci. Methods* **67**, 163–175.
- Jeffrey, P. L., Meaney, J. A., Tolhurst, O., and Weinberger, R. P. (1998). Avian cerebellar Purkinje neurons: Monolayer/coculture approach. *Methods Neurosci.* **18**, 481–486.
- Karam, S. D., Burrows, R. C., Logan, C., Koblar, S., Pasquale, E. B., and Bothwell, M. (2000). Eph receptors and ephrins in the developing chick cerebellum: Relationship to sagittal patterning and granule cell migration. *J. Neurosci.* **20**, 6488–6500.
- Koster, R. W., and Fraser, S. E. (2001). Direct imaging of *in vivo* neuronal migration in the developing cerebellum. *Curr. Biol.* **11**, 1858–1863.
- Kovacs, G. G., Kurucz, I., Budka, H., Adori, C., Muller, F., Acs, P., Kloppel, S., Schatzl, H. M., Mayer, R. J., and Luszlo, L. (2001). Prominent stress response of Purkinje cells in Creutzfeldt-Jakob disease. *Neurobiol. Dis.* **8**, 881–890.
- Liang, Z., Valla, J., Sefidvash-Hockley, S., Rogers, J., and Li, R. (2002). Effects of estrogen treatment on glutamate uptake in cultured human astrocytes derived from cortex of Alzheimer’s disease patients. *J. Neurochem.* **80**, 807–814.
- Linden, D. J., Dickinson, M. H., Smeyne, M., and Connor, J. A. (1991). A long-term depression of AMPA currents in cultured cerebellar Purkinje neurons. *Neuron* **7**, 81–89.

- Lossi, L., Mioletti, S., and Merighi, A. (2002). Synapse independent and synapse-dependent apoptosis of cerebellar granule cells in postnatal rabbits occur at two subsequent but partly overlapping developmental stages. *Neuroscience* **112**, 509–523.
- Lowry, O. H., Rosebrough, N. J., Farr, A. L., and Randal, R. J. (1951). Protein measurement with the Folin phenol reagent. *J. Biol. Chem.* **193**, 265–275.
- Maric, H., Billups, D., Bedford, F. K., Dumoulin, A., Goyal, R. K., Longmore, G. D., Moss, S. J., and Attwell, D. (2002). The amino terminus of the glial glutamate transporter GLT-1 interacts with the LIM protein Ajuba. *Mol. Cell. Neurosci.* **19**, 152–164.
- Marti, J., Wills, K. V., Ghetti, B., and Bayer, S. A. (2002). Regional differences in the Purkinje cells settled pattern: A comparative autoradiographic study in control and homozygous weaver mice. *Exp. Neurol.* **175**, 168–181.
- Meaney, J. A., Balcar, V. J., Rothstein, J. D., and Jeffrey, P. L. (1998). Glutamate transport in cultures from developing avian cerebellum: Presence of GLT-1 immunoreactivity in Purkinje neurons. *J. Neurosci. Res.* **54**, 595–603.
- Mennerick, S., Dhond, R. P., Benz, A., Xu, W., Rothstein, J. D., Danbolt, N. C., Isenberg, K. E., and Zorumski, C. F. (1998). Neuronal expression of glutamate transporter GLT-1 in hippocampal microcultures. *J. Neurosci.* **18**, 4490–4499.
- Mintz, I. M., and Bean, B. P. (1993). GABA_B receptor inhibition of P-type Ca²⁺ channels in central neurons. *Neuron* **10**, 889–898.
- Mount, H. T. J., Dreyfus, C. F., and Black, I. B. (1993). Purkinje cell survival is differentially regulated by metabotropic and ionotropic excitatory acid receptors. *J. Neurosci.* **13**, 3173–3179.
- Moussa, C. E., Mitrovic, A. D., Vandenberg, R. J., Provis, T., Rae, C., Bubb, W. A., and Balcar, V. J. (2002). Effects of L-glutamate transport inhibition by a conformationally restricted glutamate analogue (2S,1''s,2'R)-2-(carboxycyclopropyl)glycine (L-CCG III) on metabolism in brain tissue *in vitro* analysis by NMR spectroscopy. *Neurochem. Res.* **27**, 27–35.
- Northington, F. J., Traystman, R. J., Koehler, R. C., and Martin, L. J. (1999). GLT-1, glial glutamate transporter, is transiently expressed in neurons and develops astrocyte specificity only after midgestation in the ovine foetal brain. *J. Neurobiol.* **39**, 515–526.
- Ohgoh, M., Hanada, T., Smith, T., Hashimoto, T., Ueno, M., Yamanishi, Y., Watanabe, M., and Nishizawa, Y. (2002). Altered expression of glutamate transporters in experimental autoimmune encephalomyelitis. *J. Neuroimmunol.* **125**, 170–178.
- Okubo, Y., Kalazawa, S., Hirose, K., and Iino, M. (2001). Visualisation of IP₃ dynamics reveals a novel AMPA receptor-triggered IP₃ production pathway mediated by voltage-dependent Ca²⁺ influx in Purkinje cells. *Neuron* **32**, 113–122.
- Otis, T. S., Kavanaugh, M. P., and Jahr, C. E. (1997). Postsynaptic glutamate transport at the climbing fibre Purkinje cell synapse. *Science* **277**, 1515–1518.
- Paula-Barbosa, M. M., Ruela, C., Tavares, M. A., Pontes, C., Saraiva, A., and Cruz, C. (1983). Cerebellar cortex ultrastructure in ataxia-telangiectasia. *Ann. Neurol.* **13**, 297–302.
- Piedras-Renteria, E. S., Watase, K., Harata, N., Zhuchenko, O., Zoghbi, H. Y., Lee, C. C., and Tsien, R. W. (2001). Increased expression of alpha IA Ca²⁺ channel currents arising from expended trinucleotide repeats in spinocerebellar ataxia type 6. *J. Neurosci.* **21**, 9185–9193.
- Plachez, C., Danbolt, N. C., and Recasens, M. (2000). Transient expression of the glial glutamate transporters GLAST and GLT in hippocampal neurons in primary culture. *J. Neurosci. Res.* **59**, 587–593.
- Pow, D. V. (2001). Amino acids and their transporters in the retina. *Neurochem. Int.* **38**, 463–484.
- Quick, K. L., and Dugan, L. L. (2001). Superoxide stress identifies neurons at risk in a model of ataxia-telangiectasia. *Ann. Neurol.* **49**, 627–635.
- Rae, C., Lawrance, M. L., Dias, L. S., Provis, T., Bubb, W. A., and Balcar, V. J. (2000). Strategies for studies of neurotoxic mechanisms involving deficient transport of L- glutamate: Antisense knockout in rat brain *in vivo* and changes in the neurotransmitter metabolism following inhibition of glutamate transport in guinea pig brain slices. *Brain Res. Bull.* **53**, 373–381.

- Ramon y Cajal, S. (1995). Histology of the nervous system: The cerebellum. In "Histology of the Nervous System of Man and Vertebrates," pp. 3–27. Translated from the French in series "History of Neuroscience No. 6." Oxford University Press, New York.
- Rauen, T. (2000). Diversity of glutamate transporter expression and function in the mammalian retina. *Amino Acids* **19**, 53–62.
- Reichelt, W., and Knopfel, T. (2002). Glutamate uptake controls expression of a slow postsynaptic current mediated by mGluRs in cerebellar Purkinje cells. *J. Neurophysiol.* **87**, 1974–1980.
- Robinson, M. B. (1998). The family of sodium-dependent glutamate transporters: A focus on GLT-1/EAAT-2 type. *Neurochem. Int.* **33**, 479–491.
- Robinson, M. B. (2002). Regulating trafficking of neurotransmitter transporters: Common notes but different melodies. *J. Neurochem.* **80**, 1–11.
- Rothstein, J. D., Van Kammen, M., Levey, A. I., Martin, L. J., and Kuncl, R. W. (1995). Selective loss of glial glutamate transporter GLT-1 in amyotrophic lateral sclerosis. *Ann. Neurol.* **38**, 73–84.
- Schilling, K., Dickinson, M. T., Conner, J. A., and Morgan, J. I. (1991). Electrical activity in cerebellar cultures determines Purkinje cell dendritic growth patterns. *Neuron* **7**, 891–902.
- Scott, H. L., Tannenberg, A. E., and Dodd, P. R. (1995). Variant forms of neuronal glutamate transporter sites in Alzheimer's disease cerebral cortex. *J. Neurochem.* **64**, 2193–2202.
- Sheppard, A. M., Konopka, M., and Jeffrey, P. L. (1988). The developmental appearance of Thy-1 in the avian cerebellum. *Dev. Brain Res.* **40**, 181–192.
- Shinmei, Y., Yamanobe, T., Fukushima, J., and Fukushima, K. (2002). Purkinje cells of the cerebellar dorsal vermis: Simple-spike activity during pursuit and passive whole-body rotation. *J. Neurophysiol.* **87**, 1836–1849.
- Suarez, I., Bodega, G., and Fernandez, B. (2000). Modulation of glutamate transporters (GLAST, GLT-1 and EAAC1) in the rat cerebellum following portacaval anastomosis. *Brain Res.* **859**, 293–302.
- Sutherland, M. L., Delaney, T. A., and Noebels, J. L. (1996). Glutamate transporter mRNA expression in proliferative zones of the developing and adult murine CNS. *J. Neurosci.* **16**, 2191–2207.
- Tabata, T., Sawada, S., Araki, K., Bono, Y., Furuya, S., and Kano, M. (2000). A reliable method for culture of dissociated mouse cerebellar cells enriched for Purkinje neurons. *J. Neurosci. Methods* **104**, 45–53.
- Takamoto, A., Quiggin, L. B., Lieb, I., Shave, E., Balcar, V. J., and Yoneda, Y. (2002). Differences between D- and L-aspartate binding sites on glutamate transporters in frozen sections of rat brain. *Life Sci.* **70**, 991–1001.
- Tomomura, M., Rice, D. S., Morgan, J. I., and Yuzaki, M. (2001). Purification of Purkinje cells by fluorescence-activated cell sorting from transgenic mice that express green fluorescent protein. *Eur. J. Neurosci.* **14**, 57–63.
- Yang, H., Jensen, P., and Goldowitz, D. (2002). The community effect and Purkinje cell migration in the cerebellar cortex: Analysis of scrambler chimeric mice. *J. Neurosci.* **22**, 464–470.

This Page Intentionally Left Blank

CHAPTER 7

Culturing Hippocampal and Cortical Neurons

Peter J. Meberg and Matthew W. Miller

Department of Biology
University of North Dakota
Grand Forks, North Dakota 58202

- I. Introduction
- II. Acquisition of Hippocampal and Cortical Neurons
 - A. Dissections
 - B. Cell Dissociation and Storage
- III. Short-Term Culture Methods
 - A. Plating of Neurons
 - B. Culture Characteristics
- IV. Long-Term Culture Methods
 - A. Preparation of Glia Stocks
 - B. Long-Term Maintenance of Neurons Using Glia-Conditioned Medium
 - C. Culture Characteristics
- V. Summary
- References

Primary cultures of rat and mouse hippocampus and cerebral cortex are widely used to study neuronal properties such as axonal extension, synaptic transmission, and excitotoxicity. Short-term culturing of these neurons can be very straightforward and is perhaps easier than culturing cell lines once dissections are made and cell stocks are frozen. Long-term cultures of relatively pure neuronal populations require slightly more effort, but protocols are described that are less complicated than most published protocols. These include simpler ways to clean and coat coverslips, as well as using glia-conditioned medium to eliminate the need to make individual cocultures of neurons and glia. These methods consistently yield hippocampal and cortical cultures expressing dendritic spines and synapses that survive over 3 weeks in culture. For investigators employing biochemical

assays where a fairly large amount of protein is necessary, cortical neurons may be especially attractive to use as large amounts of tissue are obtained and available for culture.

I. Introduction

Cultured neurons from rodent hippocampus and cerebral cortex have been popular for studying a variety of cell functions. Short-term cultures of these neurons are useful for studying neurite initiation and extension, as well as the establishment of cell polarity. The ability of these neurons to survive for weeks in culture and form synapses allows for studies of synaptogenesis and synaptic transmission. At all stages these neurons have been used for studies of mRNA and protein trafficking and targeting, signal transduction, and excitotoxicity. Part of the popularity of these cultures stems from their physiological relevance. Both the cortex and the hippocampus are primary sites for acquisition and storage of memories, and are regions significantly affected by neurodegenerative diseases such as Alzheimer's disease, epilepsy, and stroke. The corticospinal tract is also damaged after spinal cord injury, for example. These properties make these cultures excellent and accessible models for studies of normal neuronal development, as well as neurodegeneration.

Hippocampal and cortical neurons are also good models because the synapses formed in culture are not completely unnatural. In the intact hippocampus, pyramidal cells send out recurrent collaterals, which form synapses on other pyramidal cells. In the intact cerebral cortex, a large proportion of cortical neurons also normally synapse on cortical neurons in other layers of the cortex.

The majority of cells in hippocampal cultures obtained from embryonic rats or mice are pyramidal neurons having a highly characteristic morphology, plus a smaller component of interneurons and glia. A drawback of these cultures is the relatively small amount of tissue obtained from hippocampal dissections. A much greater amount of tissue is available from cortical cultures, which is important if doing biochemical assays or Western blots. A drawback of cortical cultures is the greater cell heterogeneity, but there still remain a large fraction of neurons having classical pyramidal neuron morphology.

In general, short-term cultures (<5 days) do well grown in a variety of media, either with serum or in serum-free medium with growth supplements. However, because longer term cultures lose viability, give inconsistent results, or become overrun with glia if grown in this manner, studies requiring long-term cultures and synapse formation have used more complex culture methods that involve the presence of differentiated glia. The most commonly used method is the classic "Banker method" (Goslin *et al.*, 1998), which involves growing hippocampal neurons on coverslips placed in close apposition to a bed of glia. The Banker method can give beautiful cultures and allows for the harvest of fairly pure neuronal cultures, but is a relatively complicated method. Another commonly

used method for long-term cultures is to grow a confluent culture of glia and then plate neurons directly on the glial bed. This method has been useful for electrophysiological studies (e.g., Bekkers and Stevens, 1989) and studying individual neurons. However, glia contamination prevents biochemical analyses of neurons alone.

Our goal is to describe methods for culturing hippocampal and cortical neurons that are relatively simple, but which give consistent, healthy cultures. The first method described is useful for cultures grown for a few days. The second method, using glia-conditioned medium, is useful for longer term cultures grown more than 10 days, when synapses form. These methods are modifications of culture methods described previously by several laboratories (Mattson and Kater, 1988; Brewer *et al.*, 1993; Goslin *et al.*, 1998). We have used the short-term culture methods for rat hippocampal and cortical neurons to study signal transduction/phosphorylation (Meberg *et al.*, 1998), effects of adenovirus-mediated overexpression of ADF/cofilin on neurite outgrowth (Meberg and Bamburg, 2000), and effects of neurodegenerative stimuli on actin inclusion body formation (Minamide *et al.*, 2000). We are currently using the long-term cultures to characterize the function of ADF/cofilin at synaptic sites. Protocols are described in detail for rat neurons, but these methods should work equally well for mice, as many laboratories have published studies using similar methods for mouse hippocampal and cortical neurons (e.g., Xiang *et al.*, 1996; Ferreira *et al.*, 2000; Hasbani *et al.*, 2001).

II. Acquisition of Hippocampal and Cortical Neurons

Both cortical and hippocampal neurons can be obtained from the dissection of a single pregnant rat. Preparation, dissections, cell dissociation, and freezing of cell stocks can be completed in less than 3 h. With this relatively minimal time investment you can have cells ready for experiments for several weeks to follow, especially if using cortical tissue. Dissections are not difficult after minimal practice, if dissection tools are of good quality and a decent dissecting microscope is available.

A. Dissections

Fetal rats are obtained from timed-pregnant Sprague–Dawley rats (Charles River Laboratories) at a gestational age of 18 days (E18). Charles River Laboratories considers day 1 as the morning a vaginal plug is present after introduction of the mate the previous day. At this age, pyramidal cells, not granule cells, are present in the hippocampus (Bayer, 1980) and astrocytes are small in number compared to neurons. Cortical neurons can be obtained from earlier fetal ages (E16–E18), which may reduce glia numbers, but at this time hippocampal dissections are too difficult. Because mouse development is more rapid, cortical neurons from mice should be obtained at E15–E16 (e.g., Hasbani *et al.*, 2001) and hippocampal neurons at E16 (e.g., Ferreira *et al.*, 2000).

We typically obtain 10–14 fetuses/pregnant rat and acquire both cortical and hippocampal neurons in the same dissection. The protocol for the dissections is described and shown in Table I and Fig. 1. We find the best illumination for dissections is from beneath the tissue; dark-field (indirect illumination with a dark background) illumination may work best for early parts of the dissection and then direct illumination through a diffuser for cutting out the hippocampus.

Table I
Dissections of Hippocampal and Cortical Neurons

Equipment and supplies
Halothane (anesthetic) and sealable jar
Scissors, scalpel, straight forceps (medium size)
70% ethanol
Two 100-mm and 6–8 60-mm sterile petri dishes containing Hank's balanced salt solution (HBSS)
Dissecting microscope in a laminar flow hood
Two pair fine forceps (Dumont #5)
Fine spring scissors (Fine Science Tools)
Solutions
HBSS (500 ml)
50 ml 10× HBSS without Ca ⁺⁺ or Mg ²⁺ (Invitrogen/Life Technologies)
1 mM HEPES
adjust pH to 7.3
Protocol
1. Pour ~1 ml halothane onto small Kimwipe in small plastic beaker; place beaker in jar.
2. Place pregnant rat into jar to euthanize. Leave rat exposed to halothane for 1 min after breathing stops. Rat should not respond to toe pinch.
3. Ensure death of rat by lung puncture (insert scalpel underneath ribs to puncture lungs).
4. Place rat on back and use squirt bottle to spray abdomen with 70% ethanol. All tools should also be rinsed with 70% ethanol.
5. Lift skin and cut across abdomen with scissors to expose muscle beneath. Again rinse scissors in 70% ethanol.
6. Hold abdominal muscle up with forceps and cut through muscle with scissors to expose uterine horns.
7. Grab uterus with forceps and gently pull upward while cutting away connective tissue and fat with scissors. Ideally the uterus will not touch any external part of the rat!
8. Place uterus in 100-mm dish containing cold HBSS and transfer to a laminar flow hood for brain dissections.
9. Dip fine forceps and spring scissors into ethanol to sterilize and then flame off ethanol.
10. To remove fetuses, tear uterus above each fetus by pinching with two pair of fine forceps close together and then pulling apart. When fetus is exposed, pull up on umbilical cord with forceps to sever the cord and transfer fetus to a new 100-mm dish with HBSS.
11. Quickly cut head from fetus with scissors and transfer head to a 60-mm dish with HBSS.
12. Remove brain (see Figs. 1A and 1B).
13. Transfer brains to a 60-mm dish (we usually place 3/dish), making sure that brain tissue is always completely covered with HBSS in subsequent steps.
14. Separate cortical hemispheres from brain (Fig. 1C).
15. Remove meninges from hemispheres (Fig. 1D).
16. Cut hippocampus away from the medial surface of the cortex with spring scissors and place in a 60-mm dish (Fig. 1E). Place cortices in a separate dish.

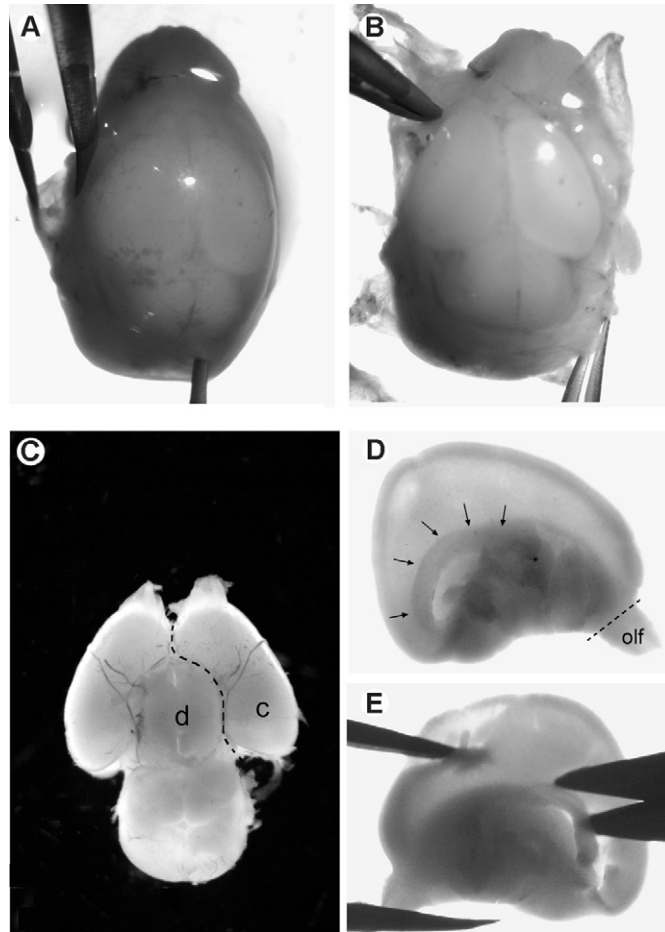


Fig. 1 Dissection of the cerebral cortex and hippocampus. (A) The dorsal view of the head is shown before dissection. To remove the brain, first pinch skull over brain with two pairs of forceps positioned close together and then gently pull them apart to tear away skin/skull covering the brain. Continue this process, always pulling at the same time in diametrically opposed directions with the two forceps until the brain is exposed. (B) The exposed brain can be removed by holding forceps tips together and then sliding them under the brain to gently lift it up while holding the nose down with another forceps. (C) The ventral surface of the brain is shown here, with the dashed line indicating fissure between the diencephalon (d) and the cerebral cortex (c). To remove the cortical hemispheres, use spring scissors to gently cut/tease apart the cortices from the diencephalon while holding the diencephalon with forceps. Be careful not to damage the medial portion of the cortex, which is where the hippocampus is located. (D) The medial surface of the cortical hemispheres is shown after the meninges (the outer covering of the brain containing visible blood vessels) have been removed. The meninges are removed by gently pulling horizontally apart with two pairs of forceps to not damage the cortex. When slightly loose, pull upward on the meninges, out of the liquid, and they should pull free from the brain. Make sure none of the meninges remain! After the meninges are removed the hippocampus should be readily visible as a crescent on the medial surface (noted by arrows). (E) Use a small scissors to cut along the dorsolateral edge of the hippocampus to free the hippocampus. For cortical cultures the olfactory bulb (olf) should be removed, indicated by the dashed line in (D).

B. Cell Dissociation and Storage

Because the methods of dissociating hippocampal and cortical neurons are nearly identical, both are summarized in Table II. The difference is additional initial steps for corticals that involve first chopping the hemispheres into small pieces before trypsin treatment and the inclusion of DNase I in the trypsin solution to break down DNA released by damaged cells. An important aspect of the dissociation is the vigor and number of trituration strokes. Too little trituration will result in incomplete dissociation, which is not bad if there are simply a

Table II
Dissociation of Hippocampal and Cortical Neurons

Equipment and supplies
Razor blade and medium forceps (corticals only)
15-ml sterile tubes (Corning)
Sterile transfer pipettes (Fisher)
Cotton-plugged Pasteur pipettes, autoclaved
Water bath heated to 37°C
Dimethyl sulfoxide (DMSO)
Freezing tubes (Corning)
Cryo freezing container (Nalgene) filled with isopropanol
Solutions
HBSS (see Table I)
10 × trypsin (2.5%; Invitrogen/Life Technologies)
DNase solution (10 ml)
100 mg DNase (Sigma)
10 ml HBSS
pH to 7.0–7.8, sterile filter, store aliquots at –20°C
DMEM/10% FBS
90 ml DMEM (Invitrogen/Life Technologies)
10 ml defined fetal bovine serum (Hyclone)
Protocol
1a. <i>Cortical</i> . Chop into small pieces (~1 mm) with a razor blade that has been ethanol/flame sterilized (hold razor blade with forceps). Transfer pieces to two 15-ml sterile tubes using plastic transfer pipettes. Bring volume to 8 ml in each tube and add 1 ml DNase solution and 1 ml 10 × trypsin to each tube.
1b. <i>Hippocampal</i> . Transfer hippocampi to a 15-ml tube using plastic transfer pipettes. Bring volume to 4.5 ml with HBSS. Add 0.5 ml 10 × trypsin solution.
2. Incubate for 15 min at 37°C.
3. Remove supernatant and rinse two to three times with DMEM/10% FBS (allow tissue to sink to bottom between rinses). After final rinse, add DMEM/10% FBS to a final volume <2 ml.
4. Triturate 6–10 strokes with the tip of a Pasteur pipette at the bottom of the tube until large chunks are diminished.
5. Triturate an additional 6–10 strokes with a fire-polished pipette (to fire polish, rotate tip of Pasteur pipette in gas flame a few seconds until tip opening is just slightly smaller than originally).
6. If freezing cells, dilute cells to the appropriate volume with DMEM/10% FBS and add DMSO to 8% of total volume. Aliquot and freeze slowly by placing vials in cryo freezing containers and leaving at –80°C overnight. Long-term storage should be in liquid nitrogen.

few clusters of <10 cells left sporadically, but too much trituration will increase cell death. Hippocampal cultures require less vigorous trituration than cortical cultures. Occasionally there will be some cortical tissue that is resistant to trituration, but it is not worth trying to overtriturate to break them down! Simply avoid/discard those pieces when plating or aliquoting neurons for freezing or pass the cells through a sterile cell strainer (Falcon) if needed.

Cells can be plated immediately after dissociation or can be frozen and stored for later use. We bring the dissociated hippocampal neurons from 10 to 12 rats up in 3 ml Dulbeccos modified Eagles medium (DMEM)/fetal bovine serum (FBS) before freezing ($\sim 2 \times 10^6$ cells/ml) and freeze in 0.5-ml aliquots. Corticals are brought to 15 ml DMEM/FBS before freezing ($\sim 2 \times 10^7$ cells/ml). Cells are viable for a month when stored at -80°C and viable for years when stored in liquid nitrogen (or vapor phase). Typically, about two-thirds of frozen cells are viable after being thawed, as determined by trypan blue staining.

III. Short-Term Culture Methods

A. Plating of Neurons

For studies on neurons grown less than 10 days in culture, culture methods are simple and cells survive well by plating in Neurobasal/FBS and then switching the medium to neurobasal containing B27 supplements (Table III). Because we typically use these cultures within 4 days, no feeding is necessary. Otherwise they should be fed by replacing one-half of the medium every 4–7 days. Cells are plated

Table III
Plating of Neurons on Coverslips and Culture Dishes

Supplies and protocol

Hemocytometer

Poly-D-lysine-coated coverslips or culture dishes (Table V)

Neurobasal/B27

100 ml neurobasal medium (Invitrogen)

2 ml B27 serum-free supplement (50 \times) (Invitrogen)

1 ml 200 mM glutamine stock (~ 2 mM final)

Neurobasal/FBS (add 10 ml FBS instead of 2 ml B27)

1. If using frozen cells, thaw briefly in a 37°C water bath.
 2. Dilute cells in Neurobasal/FBS and perform cell counts. Further dilute cells in Neurobasal/FBS for the appropriate cell number.
 3. Plate cells on a poly-D-lysine-coated cell culture dish or coverslip. For 35-mm dishes, plate 100,000–500,000 viable cells in 2 ml Neurobasal/FBS. For each coverslip plate 10,000–40,000 viable cells in 0.5 ml Neurobasal/FBS (2000–8000 cells/cm²). Surface tension keeps the cell solution on the coverslip, but care is required to not bump the dish and send cells over the edge of the coverslip!
 4. After 4 h remove Neurobasal/FBS and replace with 2 ml Neurobasal/B27 medium.
-

on cleaned coverslips (Table IV) or plastic dishes, which are then coated with poly-D-lysine (Table V).

The coverslip holder we use is made for silicon wafers, but holds twenty-four 22-mm coverslips. For poly-D-lysine coating, the coverslips are either placed flat on a piece of filter paper or inside a 35-mm dish before adding the solution. Coverslips can be rinsed either by sequential dipping in beakers, or by adding ultrapure H₂O directly to the surface. We typically use the coated coverslips or dishes the same day for cultures, but have seen no adverse effects on short-term cultures when they are stored dry for a few days. However, long-term hippocampal or high-density cortical cultures occasionally exhibit fasciculation of processes if plated on dried and then UV-irradiated poly-D-lysine. To prevent this, the poly-D-lysine coating protocol (Table V) can be modified. Coverslips are UV irradiated prior to the addition of a sterile-filtered poly-D-lysine solution. The dishes or coverslips are

Table IV
Cleaning of Coverslips

Equipment and supplies

Glass coverslips (Carolina Biological Supply)^a
Plate heater
Teflon holder for 24 coverslips (Fluoroware, Inc.)
Pyrex crystallizing dish (Corning)

Protocol

1. Warm the 2% micro wash solution in a Pyrex dish on a plate heater at setting #2 (near boiling).
 2. Soak coverslips in a coverslip holder in the micro solution for ~20 min.
 3. Rinse in complete changes of ultrapure H₂O at least 10 times.
 4. Put coverslips/holder in a 160° C oven for ~30 min to dry.
-

^aWe normally use 22-mm coverslips, which fit nicely into 35-mm petri dishes.

Table V
Poly-D-Lysine Coating of Culture Dishes or Glass Coverslips

Supplies and solutions

35-mm tissue culture dishes (Falcon) or cleaned glass coverslips (Table IV) in petri dishes (Falcon)
Poly-D-lysine solution (100 µg/ml)
400 µl of 5 mg/ml poly-D-lysine mol wt 70,000–150,000 (Sigma) frozen aliquot
20 ml borate buffer
Borate buffer, pH 8.4
1.24 g boric acid
1.90 g sodium tetraborate (Borax)
to 400 ml distilled H₂O

1. Add the poly-D-lysine solution to a culture dish (1.5 ml) or as a 500-µl bubble covering a cleaned 22-mm glass coverslip, and incubate for 30 min.
 2. Rinse three times with ultrapure H₂O.
 3. UV 10–20 min (if using coverslips, place the coverslip in a petri dish and then UV)
-

then rinsed three times with sterile H₂O and once with the plating medium. The medium is removed immediately before plating neurons.

A useful type of dish for the live imaging of fluorescence can be made by attaching a glass coverslip to the bottom of a petri dish with a hole in it. Simply drill a 16-mm hole in a 35-mm petri dish and then attach a cleaned 22-mm glass coverslip to the bottom using a thin bead of silicone aquarium sealant (Dow Corning). Because poly-D-lysine does not attach well to glass under acidic conditions, it is important to use borate buffer during poly-D-lysine coating to buffer the acetic acid that is released from the drying aquarium sealant.

For studies involving oxidative damage to neurons, the B27 supplement used in the neurobasal medium may be inappropriate to use as it contains high levels of antioxidants. For this reason, B27 without antioxidants (Invitrogen) is available. Alternatively, cultures can be grown in N2 (Invitrogen) or N2.1 supplements. A recipe for the N2.1 supplement is described in Chapter 5. DMEM/N2.1 or neurobasal/N2 media support the growth of hippocampal and cortical neurons fairly well, but there is a slightly lower level of cell survival, and these media are not recommended for cultures kept longer than 3 days.

B. Culture Characteristics

Both cortical and hippocampal cultures contain primarily neurons, as we typically find <15% nonneuronal cells 3 days after plating, as assayed by cell morphology together with glial fibrillary acidic protein (GFAP) immunoreactivity, an astrocyte marker. Therefore, these cortical cultures are excellent for biochemical assays as the vast majority of the cells are neurons and there is a large supply of them. For visualization of individual neurons, we typically plate 3000–5000 viable cells/cm² on glass coverslips. At lower densities, neurons grow poorly, and at higher densities, neurites begin growing across each other relatively quickly. For protein isolation we typically plate ~500,000 viable cells in 35-mm culture dishes and get approximately 30 μg of total protein from 3-day cultures. Protein levels increase with time in these cultures as neurite extension and arborization continue.

Hippocampal cultures initially look cleaner than cortical cultures, with a higher percentage of neurons having classical pyramidal cell morphology. Pyramidal cells initially have a single, obviously longer neurite, the axon, and several much shorter, unbranched dendrites. After several days in culture, these dendrites will begin to grow and branch. Cortical cultures tend to have some cell debris present and slightly more neurons that are not pyramidal cells, but a large proportion will still be pyramidal (Fig. 2A). The differences we find in frozen cultures compared to fresh are minor, but include a somewhat delayed initiation of neurites and the initial presence of slightly more cell debris, but glia seem less numerous (or proliferate more slowly).

Compared to many other neuronal types, such as spinal motoneurons or dorsal root ganglia, axonal extension in cortical neurons is relatively slow. Axon lengths after 3 days of growth in culture typically range from 100 to 1000 μm. This slow

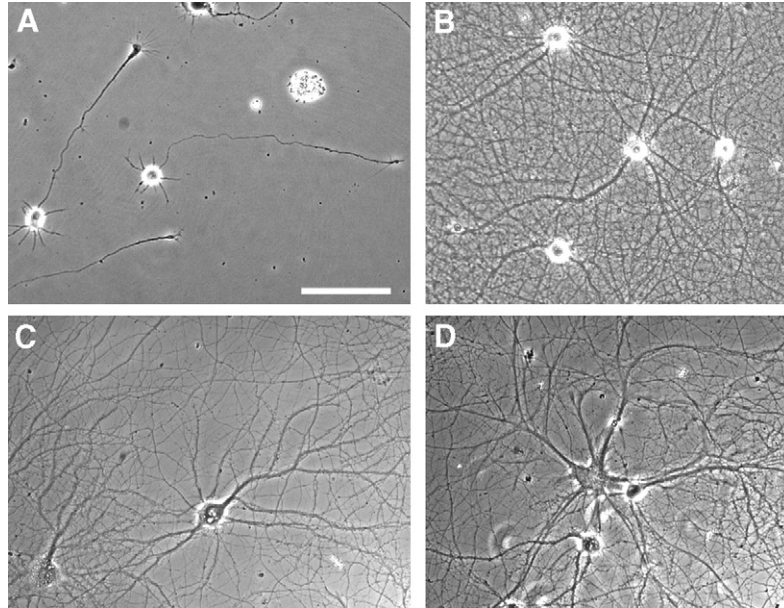


Fig. 2 Hippocampal and cortical cultures. Live cultures of cortical neurons are shown at 3 (A) and 21 (B) days after plating. (B) The long-term culture is a high-density culture, which yields plentiful protein for protein analysis. (C and D) Fixed cultures of 21-day hippocampal neurons are shown. Pyramidal cells are characterized by a primary apical dendrite with multiple branches along with several other less arborized dendrites (C). Some astrocytes (<10% of cells) having long branched processes can be found in these cultures (D), especially if they are not treated with AraC a few days after plating. An astrocyte is shown near the center, with two smaller neuronal cell bodies adjacent to it. This is an obvious astrocyte, based on its large cell body and greater width at process branch points, but many others are more difficult to discern unless astrocyte markers such as GFAP are labeled. Scale bar: 100 μm .

growth rate can be advantageous in certain circumstances. For example, if there is a lag time between introduction of a gene and sufficient levels of protein expression, axons will not be overgrown and impossible to follow in the culture before the expressed protein has an effect. However, the relatively slow growth makes it difficult to measure growth rates with live imaging unless it is done for hours. If a faster growth rate is needed, it does appear that the addition of glia-conditioned medium speeds growth rates (see Section IV,B).

Use of the serum-free neurobasal/B27 medium is not supposed to support cell division, but we find that glia do proliferate, albeit at a slow rate. Glia proliferation appears negligible for several days after plating, but even a slow rate of division becomes a problem if exponential growth occurs! Glial proliferation does become a problem after 7–14 days in culture, depending on the dissection, because neuronal protein content in these cultures becomes overwhelmed by contaminating glia. Also, even though neurons exhibit spines and synapse formation, it can be difficult to obtain clear images of individual neuronal arbors due to crowding

astrocytes. To kill glia and other dividing cells, cultures can be treated with either 5-fluorodeoxyuridine/uridine (FDUR) or cytosine β -D-arabinofuranoside (AraC), inhibitors of DNA synthesis. However, concentrations of AraC that prevent glia proliferation also kill neurons cultured in the described manner. FDUR seems less toxic to the neurons, but loss of the glia leads to either neurons that do not regularly form spines or unhealthy neurons that begin dying off after 10 days. We are able to avoid these problems and get more consistent long-term culture results by using the following methods.

IV. Long-Term Culture Methods

We wanted to have neurons in culture that consistently formed active synapses and spines without contaminating glia so that we could readily visualize dendritic arbors and do biochemical assays with neuronal protein, not glial protein. We also did not want the time commitment and complication involved in the many steps of the Banker method and wanted to be able to plate many neurons on 35- or 60-mm tissue culture dishes. To accomplish this, neurons are initially plated as described for short-term neuronal cultures. The only differences are that cultures are then fed with glia-conditioned medium and an AraC treatment is given that spares neurons and decreases the number of nonneuronal cells.

A. Preparation of Glia Stocks

As described for neuronal cultures, large stocks of glia cells can be prepared from a single dissection and then frozen for future use in many experiments. Glia are obtained from cerebral cortices in a manner similar to that described earlier for cortical neurons, but cortices are taken from postnatal animals. The dissociated cells are then grown in culture to allow glia to proliferate. The glia cultures are grown on uncoated culture dishes so that neurons do not attach well. After amplification of the glia number in culture, the cells are lifted and frozen in aliquots for future use as feeder cultures. This protocol for preparing glia cultures (Table VI) closely follows that described by Goslin *et al.* (1998). The protocol, described for three rat pups, provides sufficient cells for 20–30 frozen aliquots, and each aliquot is sufficient for feeding more than two dozen neuronal cultures for 3 weeks (see later).

B. Long-Term Maintenance of Neurons Using Glia-Conditioned Medium

Neurons are plated in Neurobasal/FBS as described for short-term cultures in Table III and are then fed with glia-conditioned medium on the day of plating (day 0) and again on days 4, 7, 14, and (if needed) 21 (Table VII). This feeding schedule has also been used successfully by other laboratories for both rat and mouse hippocampal cultures (Morales *et al.*, 2000). The glia-conditioned medium

Table VI
Preparation of Glia Stocks

Equipment and supplies

Scissors, blunt forceps, fine forceps (Dumont #5)
 50-ml sterile centrifuge tubes
 Five 10-ml sterile pipettes
 Primaria 75-cm² culture flasks (Falcon)
 Cell strainer, 70 μ m (Falcon)

Solutions

70% ethanol
 HBSS (Table I)
 10 \times trypsin (2.5%; Invitrogen)
 10 \times trypsin-EDTA solution (Sigma) diluted to 1X
 DNase solution (Table II)
 PBS (without Ca²⁺ and Mg²⁺)
 Glial DMEM (GMEM)
 500 ml DMEM
 50 ml heat-inactivated horse serum
 5 ml 100X penicillin/streptomycin (Invitrogen)
 GMEM/10%DMSO

Protocol

1. Decapitate newborn or 1-day-old rat pups, letting heads fall into a sterile dissection dish.
 2. Dissect out cortices as described for neuronal dissections (Table I, steps 11–15).
 3. Chop tissue with a razor blade into small pieces.
 4. Transfer tissue to a 50-ml sterile tube and bring volume to \sim 12 ml with warm HBSS.
 5. Add 1.5 ml of DNase and 1.5 ml of 10 \times trypsin solutions.
 6. Incubate tube for 10 min in a 37°C water bath, swirling the tube continuously.
 7. Triturate with a 10-ml pipette \approx 12 times.
 8. Return to the water bath and swirl another 5 min.
 9. Triturate with a 5-ml pipette 15 times.
 10. Draw cell suspension up in a pipette and pour through a sterile screen into a 50-ml centrifuge tube containing 15 ml GMEM.
 11. Pellet cells at 200 \times g for 3 min.
 12. Remove supernatant, tap tube on bench to loosen cells, and add 2 ml GMEM.
 13. Stir gently with a pipette tip, add 13 ml GMEM, and pipette up and down a few times.
 14. Plate approximately 7.5×10^6 cells in 15 ml total GMEM in Primaria flasks.
 15. The next day remove GMEM from four dishes and add 12 ml fresh GMEM.
 16. Feed every other day with GMEM. To do so, first shake/whack flasks before each feeding to remove loosely adhered cells, remove medium, and replace with fresh GMEM.
 17. When nearly confluent (7–10 days), lift cells by rinsing once in warm PBS, adding 2 ml 1 \times trypsin-EDTA and incubating for 2–3 min at 37°C. Add 8 ml GMEM and pipette over the flask surface to dislodge cells. Transfer cells to a 15-ml centrifuge tube and pellet by centrifugation at 200 \times g for 3 min.
 18. Remove supernatant and resuspend cells in 3 ml GMEM/10% DMSO. Freeze 0.5-ml aliquots in cryotubes and place in a Nalgene freezing box containing isopropanol. Freeze at -80°C overnight and then transfer to liquid nitrogen.
-

Table VII
Long-Term Maintenance of Neurons Using Glia-Conditioned Medium

Reagents and solutions
 Neurobasal/FBS (Table III)
 Neurobasal/B27 (Table III)
 Glia-conditioned medium (Table VIII)
 AraC (Sigma)

Protocol

1. Plate neurons as described in Table III.
2. Replace Neurobasal/FBS with 50% neurobasal/B27 and 50% glia-conditioned medium (Table VIII) instead of simply Neurobasal/B27.
3. On day 4 postplating, replace one-half of the medium with glia-conditioned medium containing 2–4 μM AraC (final concentration of 1–2 μM).
4. On day 7, and every 7 days thereafter, replace one-half of the medium with fresh glia-conditioned medium.

Table VIII
Plating and Maintenance of Glia Feeder Cultures

Reagents and solutions
 GMEM (Table VI)
 Neurobasal/B27 (Table III)
 AraC (Sigma)
 Primaria 75-cm² culture flasks (Falcon)

Protocol

1. Briefly thaw the cryovial containing 0.5 ml glia in a 37°C water bath.
2. Transfer cells to a 15-ml centrifuge tube containing 5 ml GMEM. Pellet cells at 200 × g for 3 min.
3. Remove supernatant and resuspend cells in 6 ml GMEM.
4. Add 3 ml of cell suspension to each of two Primaria flasks containing 9 ml of GMEM.^a
5. Feed cultures with GMEM every other day until they reach confluence (~7 days).
6. When cultures reach confluence, replace GMEM with neurobasal/B27 containing 5 μM AraC to glia cultures to halt cell proliferation.
7. Continue feeding approximately twice weekly with neurobasal/B27 only.
8. For glia-conditioned medium add fresh neurobasal/B27 and leave on cells 24 h. When removed, this “glia-conditioned medium” should be added directly to neuronal cultures.

^aThe cells will look quite sparse initially. The 0.5-ml glia aliquots can also be split among four flasks, rather than two, and will just take longer (10–14 days) to reach confluence.

is prepared by adding fresh Neurobasal/B27 medium to glia cultures for 24 h and then removing that medium and adding it to the neurons (Table VIII). On day 4, AraC is added to the glia-conditioned medium right before addition to the neuronal cultures to kill dividing cells. For some unknown reason, the AraC addition to glia-conditioned medium does not harm neurons, but the addition

to unconditioned Neurobasal/B27 is toxic to neurons. Because the effective concentration for AraC that we use is lower than commonly reported by other laboratories, it is possible that variations in lots or storage conditions may affect its efficacy, and this should be tested.

The glia-conditioned medium is made by growing frozen stocks of glia in DMEM/horse serum for approximately a week until glia form a confluent layer and then the growth medium is switched to Neurobasal/B27 (Table VIII). At this time, glia are also treated with AraC to prevent the continued proliferation of unwanted cell types such as microglia right before using them for the production of glia-conditioned medium. These cultures should be comprised primarily of type 1 astrocytes (Goslin *et al.*, 1998) and will look somewhat like confluent fibroblasts, being flattened, spread cells without significant extensions. These feeder cultures can be used for approximately 3 weeks after switching to neurobasal/B27, but should be discarded if bare areas begin appearing in the dish or smaller cells start appearing over the monolayer.

Our typical schedule is (i) start the glia 7–10 days before the neurons; (ii) replace the medium with 12 ml fresh neurobasal/B27 the day before plating neurons; (iii) completely remove the medium and add to neurons on the next day; and (iv) replace glia growth medium with fresh neurobasal/B27 until the day before the next feeding. The 12 ml of conditioned medium/flask is sufficient to feed 12 cultures. Therefore, one aliquot of frozen glia can be used to feed 24–48 neuronal culture dishes (see Table VIII). Glia can be grown in Primaria flasks, but we also use regular 100-mm tissue culture dishes. If not using Primaria-treated plastic, glia will just achieve confluence more slowly (~10 days versus 7).

C. Culture Characteristics

Cortical and hippocampal neurons treated with AraC and grown in the glia-conditioned medium have good long-term survivability (>21 days), develop extensive axonal and dendritic arbors (Figs. 2B and 2C), and exhibit hallmarks of mature excitatory synapses, such as dendritic spines and pre- and postsynaptic markers in close apposition (Fig. 3). In these cultures, <10% of the cells are nonneuronal, based on morphology together with GFAP labeling in 21-day cultures.

This low level of glia means that the glia contamination of neuronal protein is minimal in these cultures, especially considering the protein content of the extensive axonal and dendritic arbors. When 300,000 viable neurons are plated on 35-mm dishes, we typically harvest 75–100 μg of total protein/dish. If additional amounts of protein are needed, larger dishes can be used, but the cell densities should not be increased. At higher neuronal densities, the fasciculation of processes can occur and adhesion to the substrate is reduced.

Factors released from glia may be essential for promoting synapse formation in certain neurons (Ullian *et al.*, 2001). One of the factors that promotes synaptogenesis is cholesterol (Mauch *et al.*, 2001). Glia-conditioned medium also appears

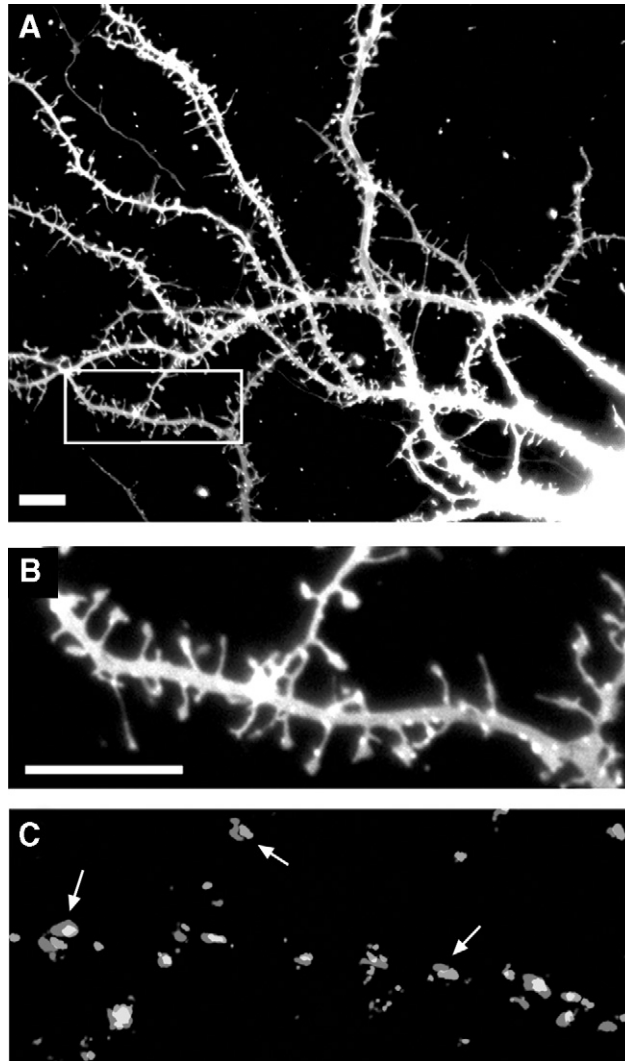


Fig. 3 Dendritic spines and synapses in long-term cultures. (A and B) A portion of a dendritic arbor is shown for a hippocampal neuron labeled with DiI (Molecular-Probes). Numerous spines are evident throughout the dendrites. The boxed area is shown enlarged (B). (C) The presence of synapses is demonstrated along dendrites of another neuron by the presence of pre- and postsynaptic markers in close apposition. Synaptophysin (presynaptic) is shown in red and PSD-95 (postsynaptic) in green, with overlapping fluorescence yellow. Many synapses can be seen; three are indicated by arrows. For immunocytochemistry, cells were fixed in 4% paraformaldehyde and permeabilized with Triton X-100 before the addition of synaptophysin (Zymed, rabbit polyclonal, no dilution) and PSD-95 (Upstate Biotechnology clone K28/43, 1:100 dilution). Scale bars: 10 μ m; scale is the same in B and C. (See Color Insert.)

to increase the rate of neurite extension, as the average lengths of axons and dendrites in the cortical cultures are increased by about 30% after 3 days in the presence of glia-conditioned medium. Therefore, when studying neurite outgrowth in cortical neurons, it may be advantageous to include glia-conditioned medium if a faster growth rate is desired. The glia-conditioned medium does not appear to increase neuronal survival, as neuron densities 3 days after plating are equivalent to that of neurons grown in neurobasal/B27 alone.

Do not make the mistake of cursorily looking at cultures at low magnification and assuming that you are seeing extensive networks of axons and dendrites when the apparent neurites are in fact astrocyte processes when observed more carefully! Differentiated type 2 astrocytes can look somewhat like neurons, having extensive and branched processes (Fig. 2D). Astrocytes can usually be discerned from neurons because the cells bodies are flatter, larger, or more irregular than the round, phase-bright neuronal cell bodies. Dendrites and axons also taper or retain their diameter as you move away from the cell body, whereas astrocytic processes often get wider, especially at branch points. Of course, the best way to distinguish astrocytes from neurons is by GFAP immunostaining of astrocytes or by using neuronal markers. To label astrocytes, fix cells in 4% paraformaldehyde, permeabilize with Triton X-100, and label with a GFAP antibody (Chemicon mAB3402, 1:4 dilution). Astrocyte proliferation should not be a problem when treating the cultures with AraC, but should still be monitored in case frozen AraC aliquots begin to lose their efficacy.

V. Summary

We have described protocols for the short- and long-term culture of healthy hippocampal and cortical neurons. The protocols for cleaning and coating coverslips or culture dishes are faster and simpler than many commonly used protocols. The use of frozen stocks of neurons and glia also greatly reduces the frequency of required dissections. Finally, the use of glia-conditioned medium is (1) effective in producing long-lived neurons with spines and synapses and (2) easier and less complicated than coculturing coverslips of neurons over beds of glia. While short-term cultures do not require glia-conditioned medium, it appears essential that long-term cultures be exposed to factors released from glia. It is also important that glia in neuronal cultures be reduced by AraC treatments if immunocytochemical or biochemical assays are to be performed.

Acknowledgments

Thanks to Steve Schmidt and Kelsey Thibert for performing assays on glia number, neurite lengths, and cell survivability. This work was supported in part by the National Institutes of Health (NS40760) and a Basil O'Connor Starter Scholar Research Award (5-FY99-850) from the March of Dimes Birth Defects Foundation.

References

- Bayer, S. A. (1980). Development of the hippocampal region in the rat. II. Morphogenesis during embryonic and early postnatal life. *J. Comp. Neurol.* **190**, 115–134.
- Bekkers, J. M., and Stevens, C. F. (1989). NMDA and non-NMDA receptors are co-localized at individual excitatory synapses in cultured rat hippocampus. *Nature* **341**, 230–233.
- Brewer, G. J., Torricelli, J. R., Evege, E. K., and Price, P. J. (1993). Optimized survival of hippocampal neurons in B27-supplemented Neurobasal, a new serum-free medium combination. *J. Neurosci. Res.* **35**, 567–576.
- Ferreira, A., Kao, H. T., Feng, J., Rapoport, M., and Greengard, P. (2000). Synapsin III: Developmental expression, subcellular localization, and role in axon formation. *J. Neurosci.* **20**, 3736–3744.
- Goslin, K., Asmussen, H., and Banker, G. (1998). Rat hippocampal neurons in low-density culture. In “Culturing Nerve Cells” (G. Banker and K. Goslin, eds.), 2nd Ed., pp. 339–370. MIT Press, Cambridge, MA.
- Hasbani, M. J., Schlieff, M. L., Fisher, D. A., and Goldberg, M. P. (2001). Dendritic spines lost during glutamate receptor activation reemerge at original sites of synaptic contact. *J. Neurosci.* **21**, 2393–2403.
- Mattson, M. P., and Kater, S. B. (1988). Isolated hippocampal neurons in cryopreserved long-term cultures: Development of neuroarchitecture and sensitivity to NMDA. *Int. J. Dev. Neurosci.* **6**, 439–452.
- Mauch, D. H., Nagler, K., Schumacher, S., Goritz, C., Muller, E. C., Otto, A., and Pfrieger, F. W. (2001). CNS synaptogenesis promoted by glia-derived cholesterol. *Science* **294**, 1354–1357.
- Meberg, P. J., and Bamberg, J. R. (2000). Increase in neurite outgrowth mediated by overexpression of actin depolymerizing factor. *J. Neurosci.* **20**, 2459–2469.
- Meberg, P. J., Ono, S., Minamide, L. S., Takahashi, M., and Bamberg, J. R. (1998). Actin depolymerizing factor and cofilin phosphorylation dynamics: Response to signals that regulate neurite extension. *Cell Motil. Cytoskel.* **39**, 172–190.
- Minamide, L. S., Streigl, A. M., Boyle, J. A., Meberg, P. J., and Bamberg, J. R. (2000). Neurodegenerative stimuli induce persistent ADF/cofilin-actin rods that disrupt distal neurite function. *Nature Cell Biol.* **2**, 628–636.
- Morales, M., Colicos, M. A., and Goda, Y. (2000). Actin-dependent regulation of neurotransmitter release at central synapses. *Neuron* **27**, 539–550.
- Ullian, E. M., Sapperstein, S. K., Christopherson, K. S., and Barres, B. A. (2001). Control of synapse number by glia. *Science* **291**, 657–661.
- Xiang, H., Hochman, D. W., Saya, H., Fujiwara, T., Schwartzkroin, P. A., and Morrison, R. S. (1996). Evidence for p53-mediated modulation of neuronal viability. *J. Neurosci.* **16**, 6753–6765.

This Page Intentionally Left Blank

CHAPTER 8

Working with *Xenopus* Spinal Neurons in Live Cell Culture

Timothy M. Gómez, Dan Harrigan,* John Henley,[†] and Estuardo Robles[‡]

*Department of Anatomy
Cell and Molecular Biology Training Program
University of Wisconsin Medical School
Madison, Wisconsin 53706

[†]Department of Molecular and Cell Biology
University of California
Berkeley, California 94720-3200

[‡]Neuroscience Training Program
University of Wisconsin Medical School
Madison, Wisconsin 53706

-
- I. Introduction
 - II. Neuronal Labeling
 - A. Injection Sample Preparation
 - B. Blastomere Injection
 - C. Lipofection
 - D. Single Cell Injection
 - III. Culturing *Xenopus* Spinal Neurons
 - A. Dissociated Mixed Cultures
 - B. Neural-Enriched Cultures
 - C. Cocultures
 - D. Culture Substrata
 - IV. Live Cell Imaging and Manipulations
 - A. Imaging Chambers
 - B. Live Cell Imaging
 - C. Rapid Fixation and Staining
 - D. Ultraviolet Photolysis
 - V. Summary
 - References

Neurons from the *Xenopus* spinal cord are highly versatile and easily manipulated, making them an ideal model system to answer questions regarding the cellular and molecular basis of early neural development and function. *Xenopus* has been a productive model system in studies ranging from axon growth and guidance to synaptic plasticity. Exogenous molecules, such as proteins, fluorescent tracers, and nucleic acids, can be injected into early blastomeres to load tracers in all neurons or into late blastomeres to target specific classes of neurons based on established lineage maps. *Xenopus* spinal neurons also provide an excellent culture system, as neurons extend processes on a variety of substrata and develop at room temperature in minimal salt solutions. Live fluorescent neurons can be imaged for hours with fluorescence microscopy at room temperature in static cultures without neurotrophic support or serum. This highly reduced culture system minimizes variables that can confound interpretation of results. Cultures can be prepared at various stages of development as dissociated neurons or as spinal cord explants. Both excitatory and inhibitory neurons develop in culture, and synaptic contacts among neurons and between neurons and nonneuronal targets form naturally. The simple anatomy and rapid rostral-to-caudal development of the *Xenopus* spinal cord also make this an excellent *in vivo* model system to analyze axon guidance by identifiable classes of neurons. This chapter focuses on techniques that exploit both *in vitro* and *in vivo* qualities of this system.

I. Introduction

Xenopus laevis has proven to be an extremely productive embryological model system for over a century due in large part to the accessibility, size, rapid development, and ease in which large numbers of embryos are generated and manipulated at room temperature. Much of our understanding of the mechanisms of early vertebrate development comes from studies using *Xenopus*. Advantages offered by this organism continue to aid investigators using modern approaches, such as fluorescent fusion protein expression, electrophysiological recordings, and *in vivo* imaging. However, two disadvantages have made this system less popular than genetic model systems such as *Drosophila* and *Zebrafish*; *Xenopus* has a protracted generation time (1–2 years) and it is an allotetraploid (four copies of each chromosome). However, even these shortcomings are being challenged by the development of *Xenopus* transgenesis techniques based in sperm nuclear transplantation (Kroll and Amaya, 1996) and the use of *X. tropicalis*, the diploid cousin of *X. laevis* that has a 5-month generation time (Amaya *et al.*, 1998). *Xenopus* transgenesis techniques have been described elsewhere (Offield *et al.*, 2000; Sive *et al.*, 2000) so are not discussed here. Instead this chapter focuses on techniques designed for the short-term modification of *Xenopus* neurons, which are well suited for the study of early developmental events.

The techniques described in this chapter take advantage of the ability to rapidly and efficiently label or operationally alter many neurons in a population and then

examine those manipulations 24–36 h later in culture or *in vivo*. Particularly useful manipulations include the expression of fluorescent fusion proteins and dominant-negative (DN) or constitutively active (CA) mutant proteins. Our particular interest is in growth cone motility and axon guidance, thus the particular manipulations and assays described here reflect this interest, but our techniques are not limited to this focus. This chapter is divided into three sections. We begin with manipulations to label or modified neurons that are made to early embryos prior to culturing or *in vivo* imaging. The next section discusses several spinal cord culture techniques aimed at either isolating individual neurons or promoting interactions among neurons or between neurons and target cells in mixed cultures. The last section describes imaging and manipulating cells in culture.

II. Neuronal Labeling

This section describes labeling or functionally modifying neurons with molecules such as fluorescent tracers, physiological indicators, or mutant proteins using several alternative approaches at different stages of development. Molecules are introduced most easily into large numbers of neurons by the microinjection of individual precursor cells of cleavage-stage embryos. This approach is simple and appropriate for many types of reagents (Table 1), however, it can be problematic for molecules that alter some aspect of development prior to their intended function. For example, blastomere injection of DN or CA proteins or RNA/DNA encoding mutant proteins can, in some cases, affect developmental events prior to neurogenesis or axon outgrowth. Control injections and titering the amount of injected material are often necessary to assure the specificity or localization of the molecules being tested. In instances where early expression non-specifically alters embryogenesis, methods for delayed introduction of molecules are presented.

Table 1
Compounds Injected Effectively into Blastomere Stage *Xenopus* Embryos

Compound	Effective quantity (ng)	Reference
Fluorescent dextrans	10–50	Davidson and Keller (1999); Gomez and Spitzer (1999)
Calcium indicator dextrans	10–100	Muto <i>et al.</i> (1996)
Fluorescent proteins	1–250	Tanaka and Kirschner (1995)
Functional proteins (peptides)	1–250	Olafsson <i>et al.</i> (1995); Rettig <i>et al.</i> (1997)
Function-blocking ABs	1–50	Lin and Szaro (1995); Kume <i>et al.</i> (1997)
RNA	0.1–5	Tessier-Lavigne and Stein (2000)
DNA	0.01–0.1	Fu <i>et al.</i> (1998)
Antisense RNA	1–20	Heasman <i>et al.</i> (2000); Nutt <i>et al.</i> (2001)

A. Injection Sample Preparation

1. Dextran and Proteins

Many useful reagents are available commercially from sources such as Molecular Probes or Cytoskeleton, Inc., and can be injected directly into blastomeres. For example, fluorescent tracers, calcium indicators, and proteins are used to mark and measure dynamic changes in live cells. Because the volume injected into blastomeres is typically a small fraction of the total, most dextrans can be diluted in DEPC water or phosphate-buffered saline (PBS) prior to injection. Glycerol-free proteins should also be centrifuged at $100,000 \times g$ for 20 min to remove precipitates in the solution using a Beckman airfuge or equivalent. We have found that most fluorescent tracers and indicators do not alter normal development if injected at reasonable levels into blastomeres (Table 1), including, FITC-dextran, caged-FITC dextran, TRITC-dextran, and Oregon green BAPTA dextran. Fluorescent tracers are often used to examine cell motility, axon outgrowth, and calcium signaling in live cells (Collazo *et al.*, 1993; Davidson and Keller, 1999; Gomez and Spitzer, 1999; Wallingford *et al.*, 2001) or to identify cells after fixation using lysine-fixable forms of fluorescent dextrans (Lin and Szaro, 1995; Moran-Rivard *et al.*, 2001). Fluorescent fusion proteins are also injected readily into blastomeres and combine with endogenous proteins to allow examination of dynamic protein distribution in living cells (Tanaka and Kirschner, 1995; Noguchi and Mabuchi, 2001). However, with the cloning of the green and red fluorescent proteins (GFP and RFP, respectively) (Prasher *et al.*, 1992; Matz *et al.*, 1998), and the molecular engineering of several spectral variants (Heim and Tsien, 1996), new possibilities involving molecular expression rather than direct protein injection exist.

2. DNA and RNA

The injection of DNA or RNA encoding for fluorescent (GFP, RFP, etc.), functional, or fluorescence resonance energy transfer (FRET)-based reporter proteins is one of the most useful, versatile, and cost-effective ways to label, modify, or make physiological measurements in developing *Xenopus* neurons. A particularly effective plasmid for driving expression in *Xenopus* is the pCS2 plasmid. The pCS2 expression vector, originally designed by Dave Turner and Ralph Rupp, was based on the backbone of pBluescript II KS+. This vector combines the simian CMV IE94 promoter with the SV40 polyadenylation site and two polylinker regions. An SP6 promoter in the 5'-untranslated region of the CMV promoter allows for the *in vitro* RNA synthesis of sense sequences inserted into the first polylinker. The second polylinker provides several choices to linearize the vector for the transcription of sense RNA and for subcloning in different transcripts. A T7 promoter site outside the second polylinker allows for the transcription of antisense RNA sequences. RNA transcribed from the SP6 promoter through the SV40 poly(A) site produces highly stable mRNA that is translated efficiently when injected into *Xenopus* embryos. Alternatively, expression

from injected pCS2 DNA is also possible, but results in delayed and highly mosaic expression (see later). Numerous additions to the basic CS2 vector exist, including variants expressing myc, β -galactosidase, and fluorescent protein tags.

Plasmid DNA and mRNA each provide unique opportunities to ectopically express proteins in developing embryos. Dilute solutions of mini-prep DNA in DEPC water (~ 100 pg/nl) is normally pure enough to inject; however, less than 100 pg per blastomere should be introduced, as DNA can be toxic above this level. 5'-capped mRNA is transcribed *in vitro* from linearized CS2 DNA using the SP6 mMessage machine kit (Ambion) and is diluted in DEPC water (~ 1 ng/nl). Up to 5 ng per blastomere mRNA can be tolerated; however, the level of expression is often so great that reducing the amount of injected RNA is necessary. For example, to express GFP fusion proteins, we typically inject just 100–300 pg mRNA. Because early *Xenopus* embryos express proteins exclusively from maternally derived mRNA, injected DNA does not begin to be expressed until the early gastrula stages at around 9 h postfertilization (hpf). Therefore, DNA injections result in a highly mosaic expression that is delayed as compared to RNA (Fig. 1). This delayed and limited expression can be useful if the expressed protein has deleterious effects on early embryos. However, even by 24 hpf, the level of protein expression from DNA injections is less than that after RNA injections. Contrary to DNA, RNA begins being expressed within 1 h of injection and is expressed homogeneously at high levels in all cells derived from the injected blastomere.

Embryos can be injected with plasmid DNA or mRNA at the single cell stage and beyond. Early stage injections lead to a greater proportion of labeled cells but at the cost of increased developmental defects and embryo death. Injections at the 1 to 4 cell stage are favorable for *in vitro* and cell transplantation experiments where large numbers of expressing cells of varying types are desired. However, embryo injections at the 32 and 64 cell stage are well suited for the labeling of particular classes of neurons based on established lineage maps (Jacobson and Hirose, 1981; Moody, 1989). Specific regions of the spinal cord and brain can be targeted, leaving individual classes of neurons in these regions identifiable *in vivo*. The dorsoventral pigmentation patterns of blastomeres are used to identify the precursors of particular cell types.

B. Blastomere Injection

On the day of injections, fresh eggs obtained from ovulating female frogs are fertilized *in vitro* using isolated testes taken from sexually mature male frogs. Detailed methods of how to obtain and fertilize *Xenopus* eggs have been described elsewhere (Sive *et al.*, 2000). This section describes the injection of blastula stage embryos between the 2 and the 64 cell stages. The initial cell divisions proceed rapidly over the first 3.5/hpf at room temperature, but can be slowed slightly by cooling embryos between 16 and 22°C. However, because healthy ovulating females often lay eggs throughout the day, we prefer to fertilize multiple batches of eggs staggered by 1–2 h.

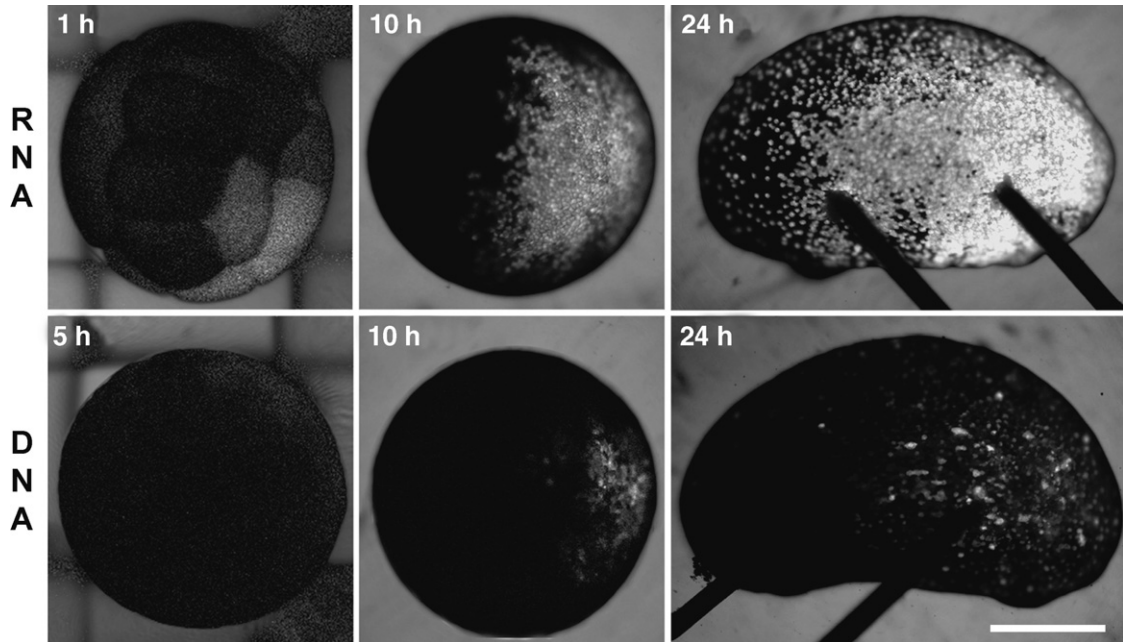


Fig. 1 Comparison of GFP expression in embryos at times after DNA and RNA injection. DNA (100 pg) or RNA (1 μ g) was injected into a single blastomere of 4 cell stage embryos. Confocal images of GFP fluorescence were taken periodically over the first 24 h of development. One hour after RNA injection, GFP expression is already detected in a 16 cell stage embryo, whereas after 5 h of development, GFP fluorescence was still not detectable in DNA-injected embryos. After 10 h of development, DNA expression is detected; however, it is much less widespread as compared to RNA. After 24 h of development, GFP expression is highly mosaic in DNA-injected embryos, but is widespread and uniformly high in RNA-injected embryos. Scale: 500 μ m.

1. Equipment, Materials, and Common Solutions

Stereo microscope (Leica), micromanipulator (WPI), pressure injection system (Parker), Flaming Brown P-97 micropipette puller (Sutter Instrument Co.)

Blunt forceps (Dumont #5 standard tip) to handle and move embryos and a fine forceps (Dumont #55 biology tip) to break micropipette tips

Homemade embryo holding dish made from a 60-mm culture dish with 1-mm nylon mesh (Small Parts Inc.) cut to size and secured to the bottom of the dish with plastcine

Thin-walled borosilicate capillary tubing (with omega dot fiber, 1.0 mm O.D. \times 0.75 mm I.D.; FHC) pulled to a fine tip using an electrode puller

Modified Ringers solution (MR in mM), 100 NaCl, 1.8 KCl, 2.0 CaCl₂, 1.0 MgCl₂, 5.0 HEPES, pH 7.6, using NaOH and filter sterilize or autoclave

2% L-cysteine (Sigma) made fresh in 10% MR. pH 8.0–8.1 using 10 M NaOH
5% Ficoll PM400 (Amersham) in 10% MR and autoclave
One cell to 64 cell stage embryos

2. Procedure

a. Dejelly Embryos

Freshly fertilized embryos can be dejellied chemically after cortical rotation (0.5 hpf), although survival seems to improve if performed after the first cell division at 1.5 hpf. Transfer embryos into freshly prepared 2% cysteine and swirl for 3–5 min until jelly coats, but not vitelline membranes, have been removed. Wash embryos extensively in 10% MR.

b. Prepare Pipette Tips

Pull capillary tubes to a tip diameter of $\sim 1 \mu\text{m}$ and then break manually using fine forceps leaving a tip diameter of $\sim 5 \mu\text{m}$. Backload micropipettes by placing small drop (0.5–1 μl) of solution to the back end.

c. Calibrate Injection Volume

Using a transfer pipette, transfer dejellied embryos into the holding dish containing 5% Ficoll solution. Mount loaded micropipette onto the capillary holding device attached to a micromanipulator and pressure injection system. House air is usually sufficient to drive the pressure injection system (output set ~ 20 psi with ejection duration ~ 1 s). Position micropipette tip above the medium in the center of the image field. Eject a volume of solution, and at a known magnification factor, measure the diameter of the suspended drop. If the drop does not stay on the tip of the micropipette, it is sometimes helpful to penetrate an embryo several times. Adjust the duration of the pressure ejection to achieve the desired drop size (volume).

d. Injection

Embryos with the most regular cleavage patterns should be arranged in the holding dish to allow rapid injection in succession. If specific blastomeres are being targeted, it is helpful to arrange four cell stage embryos with the most ideal pigmentation pattern in the same dorsal–ventral orientation. Position the tip of the micropipette just above the blastomere being injected and then lower it rapidly into the blastomere and then out slightly to relieve dimpling of the cell membrane. Inject a known volume of solution into a blastomere and then remove the tip rapidly. Repeat injections for at least two times the desired number of embryos to account for embryo loss. After 5–10 injections, remove tip from solution and reexamine drop diameter as clogging can reduce drop size. Rebreak tip and recalibrate if necessary. Transfer injected embryos into a fresh dish containing 5% Ficoll and allow them to recover several hours to overnight. After recovery, transfer all embryos into 10% MR without Ficoll and allow them to develop to the desired stage.

C. Lipofection

One of the principal shortcomings of expression by blastomere injection is that this leads to early and widespread expression in embryos (Fig. 1). This problem can be reduced with DNA injections; however, the expression of ectopic protein still begins well before neurogenesis. Therefore, defects that result from these early manipulations could be secondary effects of earlier abnormal events. An ideal manipulation for experiments testing the cell autonomous function of a particular gene product later in development is to express the protein in a limited number of cells at the time the event is being studied. For example, in studies examining axonal pathfinding, ectopic genes would ideally be expressed only in the specific neurons at times of particular guidance behaviors. One approach that has allowed late expression in a limited number of cells in the developing retina is lipofection (Holt *et al.*, 1990; Ruchhoeft *et al.*, 1999; Nakagawa *et al.*, 2000).

We have modified the original *Xenopus in vivo* lipofection technique (Holt *et al.*, 1990) to ectopically express proteins during and after neurogenesis in the developing neural tube. The delay between lipofection and the earliest axon outgrowth in the spinal cord can be very short. For this reason, we prefer RNA transfection to DNA as it results in more rapid expression and, unlike DNA, does not require mitotic cells. DNA can be substituted in this protocol with the possible advantage of providing longer lasting and higher levels of expression over time; however, the lipofection solution must be injected into a region of the dividing neuroepithelium. *In vivo* lipofection is similar to blastomere injection except that neural plate stage through neural tube stage embryos (stages 14 to 20; 16.5 to 21.75 hpf) are used and a liposomal carrier reagent is included with the

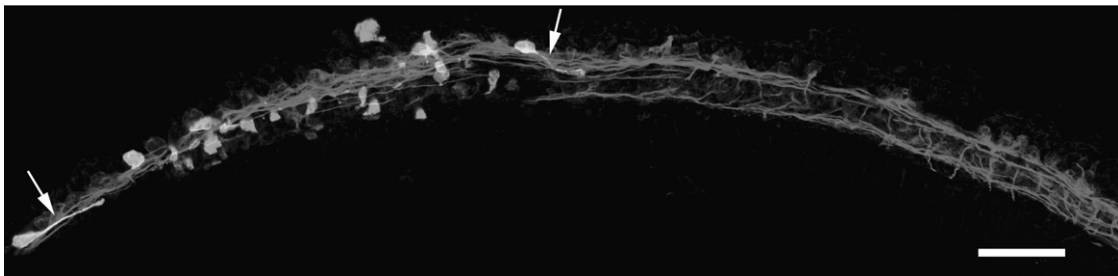


Fig. 2 Expression in the spinal cord by RNA lipofection. Five hundred micrograms of RNA encoding a myc-tagged protein along with DOTAP was injected into the caudal region of the neural folds on the right side of a stage 17 embryo. After an additional 7.5 h of development, this stage 24 embryo was fixed in 4% paraformaldehyde/4% sucrose overnight. This embryo was then washed extensively with CMF-PBS, dissected to expose the spinal cord, and double labeled for myc (green) and neural-specific tubulin (red). Lateral view of a spinal cord showing two myc-positive neurons that have extended axons (arrows), although many other neurons are labeled in the caudal spinal cord. Dorsal is up and caudal is left. Scale: 100 μ m. (See Color Insert.)

genetic material. We have successfully lipofected embryos from stages 14–18 with this approach and believe this range can be extended. However, it is most reliable to target the spinal neurons using older embryos (stages 16–18), and because RNA is expressed so rapidly, delayed lipofection may be necessary for studies involving axon growth and guidance, which does not begin until stage 21. Lipofection into the developing neural tube has the added advantage of allowing targeted expression into different anterior–posterior positions along the developmentally graded axis of the spinal cord (Fig. 2). Our technique utilizes the transfection reagent DOTAP, although other lipofection agents that have been developed more recently have not been tested. This technique for expression is best suited for studies done *in vivo*, as typically a small population of cells are transfected.

1. Materials

DOTAP liposomal transfection reagent (Roche). DOTAP is bottled under argon as it oxidizes rapidly; keep vial sealed at 4°C but do not freeze. Due to the instability of DOTAP, vials typically last for less than 6 months.

500 µg/ml Fast Green dye in DEPC water

1-ml syringe with a 27-gauge needle

Stage 15–20 embryos

2. Procedure

a. Prepare RNA/DOTAP

Chill several small Eppendorf tubes on ice. Remove a small amount of DOTAP with a syringe and transfer to a chilled Eppendorf tube. The optimum DOTAP-to-DNA ratio was determined to be 3:1 by weight (Holt *et al.*, 1990), and we assume that a comparable optimum ratio exists for RNA, although this has not been tested. Dilute RNA to 0.33 mg/ml and transfer 1 µl of RNA to a clean and chilled Eppendorf tube. Add 1 µl DOTAP (1 mg/ml) to 1 µl RNA to achieve 3:1 and flick to mix. Keep solution on ice, as RNA and DNA will precipitate. If a white precipitate does form, new DOTAP may be required. Add 1 µl chilled Fast Green solution to 2 µl of RNA/DOTAP solution and flick to mix. Dilution of RNA with Fast Green helps visualize the injected solution in embryos and facilitates the backloading of micropipettes, which often load poorly with concentrated DOTAP/RNA solutions.

b. Prepare Pipette Tips

Pull, break tips, and load micropipettes as described previously. Calibrate drop volume to at least 5 nl. Tips may need to be rebroken occasionally between injections as they clog more easily when loaded with DOTAP.

c. Injection

Place dejellied, stage 14–19 embryos (16.25 to 21 hpf at 23°C) in a holding dish with 5% Ficoll. Inject 5 or more nanoliters into the dorsal region of the developing neural plate, neural folds, or neural tube. Transfer injected embryos into a fresh dish containing 5% Ficoll and allow them to develop to desired stage.

D. Single Cell Injection

The delivery of molecules by a single cell injection represents an extreme example of delayed and targeted labeling or manipulation as this procedure is designed for individual neurons in culture. This technique is well suited for the injection of nucleic acids, proteins, or fluorescent dextrans into neurons that have extended processes. The main benefit of this approach is that the acute and cell autonomous effects of proteins on function can be assessed. Further, fluorescent tracers or physiological indicators that may alter aspects of normal cell development or function chronically can be introduced acutely. The primary drawback of this approach is that it is time-consuming and requires specialized and relatively expensive equipment.

1. Equipment and Materials

Cultured neurons (see later)
Phase-contrast microscope with 20 or 40× long working distance objectives
Eppendorf transjector 5246 or Narishege IM-200 microinjector
K T Brown type micropipette beveler (Sutter Instrument Co.)
Nanosep microconcentrators (Pal Filtron)
Ultracentrifuge (Beckman TL100 rotor or equivalent)

2. Procedure

a. Prepare Injection Solutions

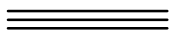
Injection reagents are diluted or dialyzed and, if necessary, concentrated in microinjection buffer [5 mM HEPES (pH 7.2), 72 mM KCl, 12 mM NaCl, 0.05 mM EGTA] using the appropriate molecular weight cutoff microconcentrators. An alternate microinjection buffer that works well for *Xenopus* spinal neurons is 1.34 mM K₂HPO₄, 0.44 mM NaH₂PO₄, 2.0 mM HEPES (pH 7.4), 110 mM KCl, 10 mM NaCl, 2 mM glucose, 1 mM Na pyruvate, 1 mM ATP, 0.1 mM GTP. Injection solutions must be clarified by ultracentrifugation at >40,000 × *g* for 20 min before loading to minimize plugging of the microneedle. Fluorescent conjugates of various molecular weight dextrans (~400 μM) are added to all solutions to verify successful injections as well as identify and track injected cells by fluorescence microscopy.

b. Prepare Pipette Tips

Pull microneedles to a tip diameter of $\sim 0.2 \mu\text{m}$. It is important to make microneedles from thin-walled capillaries with omega dot fiber to minimize plugging of the needle tip and to ensure that injection solutions reach the tip without air bubbles. Microneedles are loaded either by adding injection solutions directly to the back of the microneedle or by using a drawn-out Pasteur pipette as a back-loading micropipette. For injections of viscous solutions, such as concentrated protein ($>10 \text{ mg/ml}$), it is necessary to first bevel microneedles (tip diameter $\sim 0.3 \mu\text{m}$) using a micropipette beveler.

c. Injection

Microinjections of isolated *Xenopus* spinal neurons growing in culture (see later) are done at room temperature on a microscope stage, and cells are allowed to recover for 1–4 h prior to subsequent manipulations. Back pressure is maintained to the injection needle to prevent dilution of the injection solution with culture medium through capillary action and to help prevent clogging. Injection times ($\sim 0.2 \text{ s}$) and pressures (usually 150% of the back pressure) are adjusted to minimize cell damage during microinjection. Using the Eppendorf microinjector, we position the microneedle tip adjacent to the cell soma and in the same focal plane as the nucleus to set the z limit. The needle is then moved up a few micrometers and is positioned directly over the soma and to one side of the nucleus. This is the starting position. During automatic injection, the needle tip will travel at an angle to the same x and y coordinates and down to the preset z limit, which should be near the middle of the soma. This is the preferred method as injection time is constant and damage to the cell is minimized. Injections can also be done by moving the microneedle down manually to penetrate the cell body adjacent to the nucleus. This method must be used if using the Narishege IM-200 injector.

**III. Culturing *Xenopus* Spinal Neurons**

Xenopus spinal neurons as a culture system offer several advantages over other model systems. First, *Xenopus* neurons and nonneuronal cells survive for more than 24 h in culture at room temperature without additives in simple buffered physiological salt solutions. Second, spinal neuron cultures contain a mixture of functionally distinct neuronal types that extend axons over a variety of substrata. Third, *Xenopus* neurons form functional synapses between neurons and with nonneuronal cells within 24 h in culture. The extent of interactions among neurons and with nonneuronal cells is dependent on the culture technique used. Culture methods exist that generate (1) isolated neurons with few interactions with other neurons, (2) neurons in tissue explants with extensive synaptogenesis with other neurons within the explant, and (3) mixed cultures containing neurons that synapse upon muscle and/or skin cells. In addition to varying the density and composition of cells cultured, our work has benefited from the ability to grow

Xenopus spinal neurons on a variety of different extracellular matrix proteins (laminin, fibronectin, tenascin, etc.), cell adhesion molecules (L1, N-cadherin), and artificial substrata (tissue culture plastic, poly-D-lysine, glass). The following sections outline the basic technique for isolating *Xenopus* neural tissue from different age embryos, along with variations in culture composition mentioned earlier.

Toward the end of *Xenopus* gastrulation, induction of the dorsal ectoderm results in formation of the neural plate, a spatially distinct population of neuronal precursors. Around 16 hpf the neural plate begins to invaginate (NF14; Nieuwkoop and Faber, 1967), taking on a cylindrical conformation. Closure of the neural tube in the *Xenopus* embryo occurs through stage 20 (21.75 hpf) and coincides with pioneering axon outgrowth. After closure of the neural tube, the intact spinal cord can be isolated easily from the somites (lateral tissue, which is the source of muscle cells in mixed cultures), notochord, and skin. These tissues contribute the majority of nonneuronal cells in culture, including myocytes, fibroblasts, melanocytes, and unidentified round cells. Following mechanical isolation, the neural tube may be dissociated and streaked onto the culture substrate as isolated cells or plated as large explants containing dozens of cells. The neural tube at this stage is composed of postmitotic primary neurons, mitotically active neuronal precursors that generate secondary neurons, and glial cells. For an in-depth description of neuronal proliferation and differentiation in the *Xenopus* spinal cord, see Hartenstein (1989, 1993).

By 48 hpf the *Xenopus* neural tube is composed of nonneuronal cells (glia and fibroblasts), mitotic secondary neurons, and fully differentiated postmitotic primary neurons. This neuronal population consists of eight distinct subtypes *in vivo*, including cholinergic motor neurons, substance P immunoreactive sensory neurons (Rohon-Beard cells), several classes of GABAergic and glycinergic inhibitory interneurons, and glutamatergic excitatory interneurons. The identity of neurons in the tadpole spinal cord and their functional circuitry have been reviewed by Roberts (2000). If development proceeds normally in culture, a 24-h-old culture from 24 hpf neural tissue should yield these eight types of neurons; however, it is likely that the differentiation of spinal neurons is altered in culture. Although it has been reported that many aspects of differentiation proceed normally *in vitro*, this has not been established for all neuronal subtypes. Undoubtedly cellular interactions that induce the differentiation of specific neuron types are lost during the culture process. One way to reduce and possibly help characterize these necessary and mostly undefined inductive cues is to culture spinal cords at later times in development.

Despite the uncertainties presented by a mixed neuronal population, cultured *Xenopus* spinal neurons offer many advantages for the study of cell biological mechanisms controlling motility, adhesion modulation, cytoskeletal dynamics, and the signaling mechanisms underlying these phenomena. These aspects of cell function appear to be well conserved among different neuronal types in culture. For example, our work examining the role of spontaneous and induced calcium

transients and their effects on local adhesion and subsequent cytoskeletal rearrangements has not revealed subpopulations with divergent responses to calcium signals. The benefits of this system, which include the ability to easily introduce exogenous nucleic acids and proteins into developing neurons by blastomere injection and the rapid and robust growth of neurons at room temperature, greatly outweigh any limitations.

A. Dissociated Mixed Cultures

This type of culture has been used extensively in studies of the cellular and physiological mechanisms underlying synaptic development and plasticity. Using mixed cultures, electrophysiological recordings and imaging can be conducted easily due to the accessibility and accurate identification of presynaptic neuronal cell bodies and postsynaptic muscle cells. Mixed cultures also support studies of the development of the neuromuscular junction; however, it should be noted that neurons in mixed cultures, unlike neural-enriched cultures, are exposed to unidentified factors likely originating from myocytes that stimulate neurite outgrowth (Holliday and Spitzer, 1993). This approach has proven useful for examining the development of axons and myocytes, as well as synapses between them. The dissection and culture technique is used on embryos ranging from stage 15 to 24, although complete dissociation of spinal neurons past stage 20 is difficult and may require the addition of 5 mg/ml trypsin, as reported previously (Anderson and Cohen, 1977).

1. Materials

CMF-MR (same as MR, except CA^{2+}/Mg^{2+} free with 1 mM EDTA)

Stage 15–24 embryos

Untreated or coated culture dishes (with or without acid-washed glass coverslips)

Antibiotics (penicillin/streptomycin and gentamycin, Sigma)

2. Procedure

a. Embryo Preparation

Transfer the required number of stage 15–22 embryos (Figs. 3A and 3B) into a 35-mm petri dish containing 100% MR for initial dissection. We normally use one dorsal section for each culture dish, although a higher or lower density can be achieved using more or less than one dorsal section per dish. All dissections are carried out at 10–50 \times magnification using a standard dissection microscope equipped with a fiber optic external light source (Leica Optical). The jelly coat and vitelline membrane surrounding embryos are removed manually by pinning the jelly coat with blunt forceps while piercing and pulling away the surrounding membranes with a fine forceps.

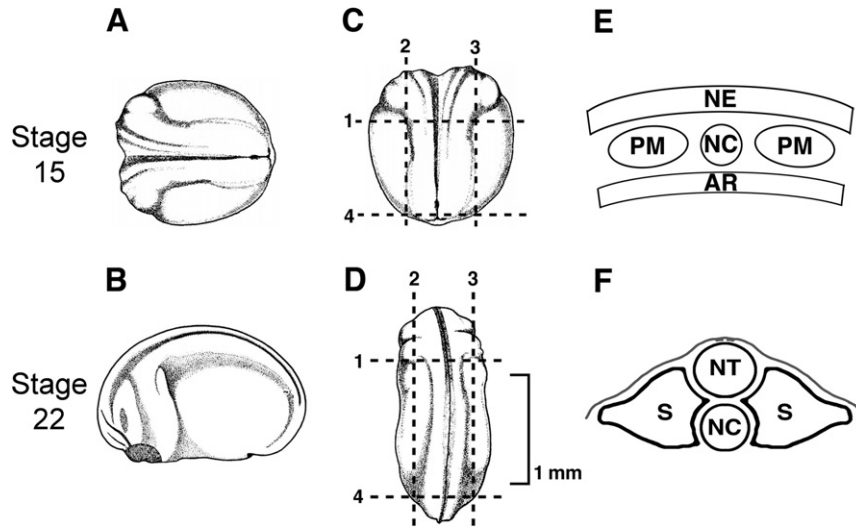


Fig. 3 Schematic diagrams of neural plate and neural tube dissections. (A) Dorsal view of a stage 15 *Xenopus* embryo. (B) Lateral view of a stage 22 *Xenopus* embryo. Dorsal views of stage 15 (C) and stage 22 (D) embryos with dashed lines indicating the major incisions performed to separate the dorsal aspect of the embryo. (E) Schematic cross section of a neural plate indicating the location of the neuroectoderm (NE) relative to the paraxial mesoderm (PM), notochord (NC), and archenteron roof (AR). All germ layers can be cultured together in mixed cultures or NE can be isolated and plated separately as neural-enriched cultures. (F) Schematic cross section of a neural tube (NT) and associated tissues, including the somitic mesoderm (S), notochord (NC), and the surrounding dorsal pigmented epidermis (gray line).

b. Dissect Dorsal Region

Isolation of the dorsal aspect of the embryo is achieved through a series of precise incisions using fine forceps. An initial incision perpendicular to the longitudinal axis and immediately caudal to the hindbrain (Figs. 3C and 3D) serves to expose the hollow interior of the embryo. The entire dorsal region of the neural plate or tube can now be isolated by making two parallel incisions along either side. This is accomplished by inserting one forcep into the interior of the embryo adjacent to the neural tissue and pinching longitudinally in the posterior direction. A final cut near the posterior end of the embryo results in a rectangular, multi-layered piece of tissue containing the neuronal cells (Figs. 3E and 3F).

c. Dissociate Cells

Transfer all dorsal sections into a 60-mm petri dish containing 100% CMF-MR solution for a 30- to 60-min incubation period. Stage 15 neural plates should not require more than 30 min to dissociate; however, longer incubation times and possibly additional mechanical disruption are necessary to dissociate older dorsal sections. Dorsal sections should be noticeably disassociated prior to plating.

d. Prepare Culture Dishes

Each dorsal section is plated onto culture substrata in 100% MR containing antibiotics (50 $\mu\text{g}/\text{ml}$ penicillin/streptomycin and gentamycin). Culture substrata should be prepared ahead of time. Many cell types contained within dissociated dorsal sections will morphologically differentiate on a variety of substrata ranging from tissue culture plastic and glass left untreated to these same surfaces coated with ECM molecules. If ECM proteins are used, we typically coat them at $\sim 10 \mu\text{g}/\text{ml}$ in $1\times$ PBS for at least 1 h prior to culturing.

e. Cell Plating

Unlike most primary cell cultures, dissociated *Xenopus* cells must be plated directly onto the culture substratum using a drawn-out glass pipette to adhere. Plating pipettes are made by flaming the neck of a 9-in. sterile Pasteur pipette over a Bunsen burner and pulling the softened glass about 3 to 6 in. to a less than $\sim 1\text{-mm}$ shaft diameter. The tip is broken off repeatedly to achieve an even, beveled tip. Cells can now be plated by sucking up a dissociated dorsal section into the pulled glass pipette and carefully streaking the cells out onto the culture dish in parallel lines. Plating pipettes can also be used to triturate incompletely dissociated neural tubes. Repeat for the remaining dorsal sections onto separate culture dishes. Dishes should be maintained near 23°C and not moved for at least 30 min after plating. Neurite outgrowth can be observed within 6 h of plating on laminin (LN), although this is influenced heavily by the tissue culture substrata, as discussed later.

B. Neural-Enriched Cultures

Isolation of the *Xenopus* neural tube in tissue culture provides a useful method for eliminating large numbers of nonneuronal cell types that can confound the analysis of cell autonomous functions. Dissection techniques described earlier and elsewhere (Tabti and Poo, 1990) provide a framework for this culture method. Examination of growth cone motility and other processes *in vitro* is often less complicated using isolated primary neurons free from potential postsynaptic targets (mainly myocytes) or other cell types that influence neurite outgrowth. This requires that neural tissue be isolated mechanically from other tissue, such as the somatic mesoderm, epidermis, and notochord.

Neural-enriched cultures can be prepared either as dissociated neurons or as spinal cord explants. Dissociated cultures allow for a more precise examination of properties such as axonal and dendritic length, intracellular protein localization, and neuronal morphology. In contrast, the cell bodies of growth cones extending from within explants are difficult to identify, and both cell bodies and neurites often interact with neighboring neurons. However, explant cultures are advantageous as they allow the simultaneous examination of many growth cones that typically extend out in close association. The ability to monitor aspects of cellular physiology, such as growth rate, calcium dynamics, protease activity, or membrane potential in multiple cells simultaneously, makes this system amenable to

high-throughput approaches. In particular, this approach could aid in the analysis of the specific effects of various pharmacological agents, diffusible signals, or substratum molecules.

Neural tissue can be isolated as early as stage 15; however, at this time in developmental, the neural epithelium consists of a bilayer of pigmented superficial cells and nonpigmented cells that lay atop the deeper endoderm and paraxial mesoderm (Fig. 3E). Mechanical isolation of the neural tissue requires separation of these tissues with collagenase. At the other extreme, the dissection of embryos beyond stage 23 becomes increasingly difficult due to the tight association the spinal cord forms with the axial somites. At this stage, the spinal cord itself also seems to become incased in matrix molecules and embryos begin to have reflex movements. For our purposes, isolation of the neural tube between stages 21 and 23 is ideal, providing a self-contained, cylindrical neural tube that is separated easily from the surrounding epidermis, notochord, and somites (Fig. 3F).

1. Materials

Electrolytically sharpened tungsten wire mounted on holding tool
Collagenase B (Boehringer Mannheim)

2. Procedure

a. Common Procedures

The isolation of dorsal sections can be carried out as in steps **a** and **b** of the protocol for mixed nerve–muscle cultures.

b. Collagenase Treatment

Using a Pasteur pipette, transfer dorsal sections to a 35-mm dish containing 1 mg/ml collagenase B in 100% MR and incubate for 5 min. Subsequent dissection of neural tubes may be carried out in this collagenase solution; however, if a large number of neural tubes are being dissected, they should be done in batches, as prolonged collagenase exposure may be detrimental to cell survival.

c. Isolate Neural Tissue

Shortly after collagenase treatment, neural tissue will begin to separate from adjacent nonneuronal tissues. An electrolytically sharpened tungsten wire with a right angle bend is useful in facilitating tissue separation. When dissecting neural plate stage embryos, use the curved edge of the hooked wire to assist neural ectoderm division from underlying tissues. When dissecting neural tube stage embryos, first peel back the dorsal pigmented epithelia by pulling or hooking the edges that have begun to separate from the deeper tissue layers. Skin is removed most easily if peeled back intact. Upon removal of the epidermis, the neural tube and lateral somitic mesoderm are clearly visible (see Fig. 3F cross section). Somites can now be flaked away using a forceps or the curved edge of the

tungsten wire, thus exposing the spinal cord and underlying notochord (small cylindrical structure ventral to the neural tube). Separate the notochord from the spinal cord by pushing the curved edge of the tungsten wire between these tissues, starting at sites where the collagenase has already loosened the attachment.

d. Plate Neural Tissue

For dissociated neural-enriched cultures, neural tissue should be transferred to 100% CMF-MR and plated as described earlier, taking extra caution when plating such a small amount of tissue. If neural tube explant cultures are being made, transfer all spinal cords back to 100% MR. Each neural tube must be cut into small pieces with a diameter of $\sim 100 \mu\text{m}$ prior to plating. A typical stage 22 spinal cord is approximately 1 mm in length and $100 \mu\text{m}$ in diameter. Using a sharpened tungsten wire, cross section this tissue into at least 10 pieces followed by perpendicular cuts to yield ~ 20 individual explants. Transfer all explant pieces using a Pipetman onto prepared culture substrata submerged in medium as described previously. Explants should be spaced adequately and may be repositioned within the dish during plating; however, cultures should not be moved for several hours after plating to allow adhesion and preserve explant spacing. Outgrowth on laminin occurs as early as 4–6 h following culture and continues for more than 24 h after plating.

C. Cocultures

Although mixed cultures will often result in stochastic interactions between neurons and target cells (Stoop and Poo, 1995), synaptic connections are enhanced by coculturing neural tube explants near target tissue explants. Cocultures between neurons and targets, such as muscle and possibly skin, can be created *in vitro* (Fig. 4). Coculturing neurons with target cells proceeds essentially as described earlier, except that during the initial dissection, portions of skin or myotomal tissue are kept aside for coculturing. Once spinal cords have been isolated, transfer each tissue type separately into fresh 100% MR. Next, nonneuronal tissues are cut into small pieces as was done for neural tube explants. After all tissues have been cut into appropriate-sized pieces, transfer neural explants into a culture dish, taking care to place pieces in an orderly fashion. Finally, place target tissue explants in close proximity to spinal explants such that extending axons are likely to encounter target cells. Synaptically connected *Xenopus* spinal neurons in culture are also a very useful and often studied model system of synaptic physiology. Although neural tube explants contain functional synapses within the explant, these types of connections are studied most easily in dissociated cultures.

D. Culture Substrata

Xenopus neuronal cultures are well suited for investigations of cellular mechanisms regulating growth cone motility and guidance, as neurons extend axons on many biological and artificial tissue culture substrata that have different adhesive

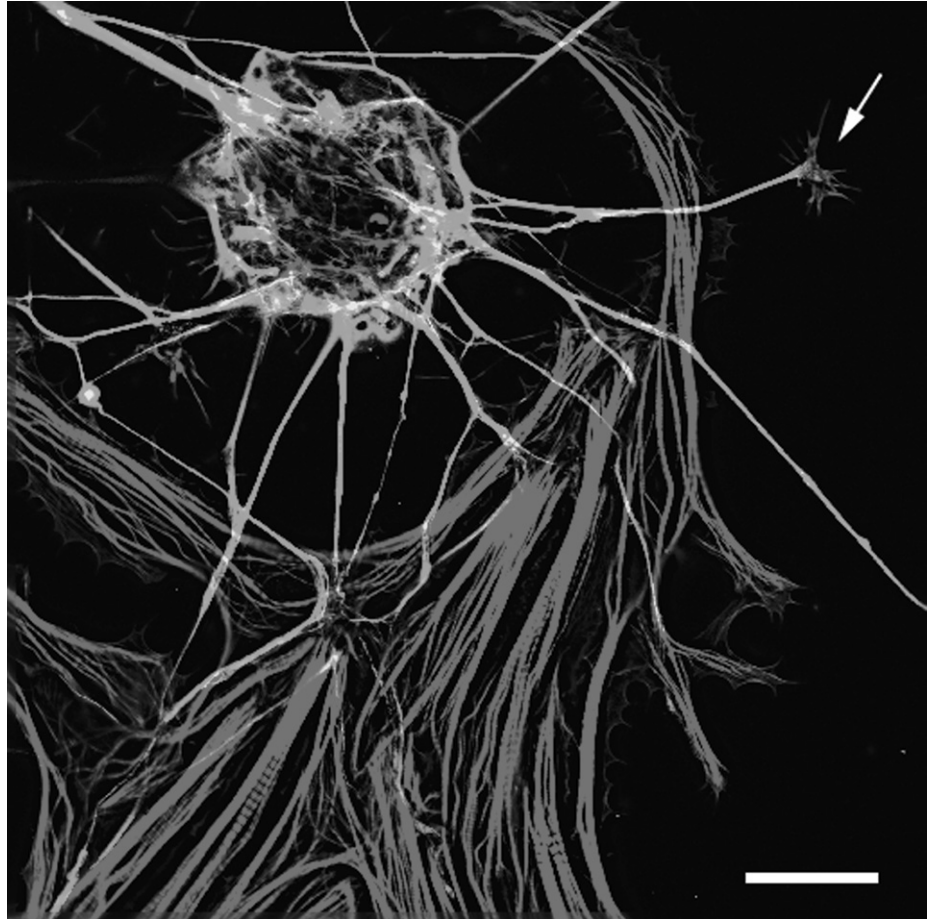


Fig. 4 Cocultured spinal cord explant with surrounding myocytes. After 24 h in culture, cells were fixed and stained for neural-specific β -tubulin (green) and actin (red; Alexa-546 phalloidin). Isolated growth cones (arrow) can be identified, as well as functional synaptic contacts between neurons and muscle cells (as suggested by α -bungarotoxin staining of clustered acetylcholine receptors, not shown). Scale: 50 μm . (See Color Insert.)

and growth-promoting properties. We have tested a variety of tissue culture substrata, including laminin, fibronectin, tenascin-C, vitronectin, N-cadherin, L1, polylysine, tissue culture plastic, and untreated glass. Substrata-specific requirements exist for coating proteins onto culture dishes and glass coverslips, as well as limitations with respect to the types of cultures that will extend axons on a given substratum. For example, in order to bind cell adhesion molecules such as L1 and N-cadherin onto glass coverslips or plastic, these surfaces must be precoated with nitrocellulose as described previously (Payne *et al.*, 1992).

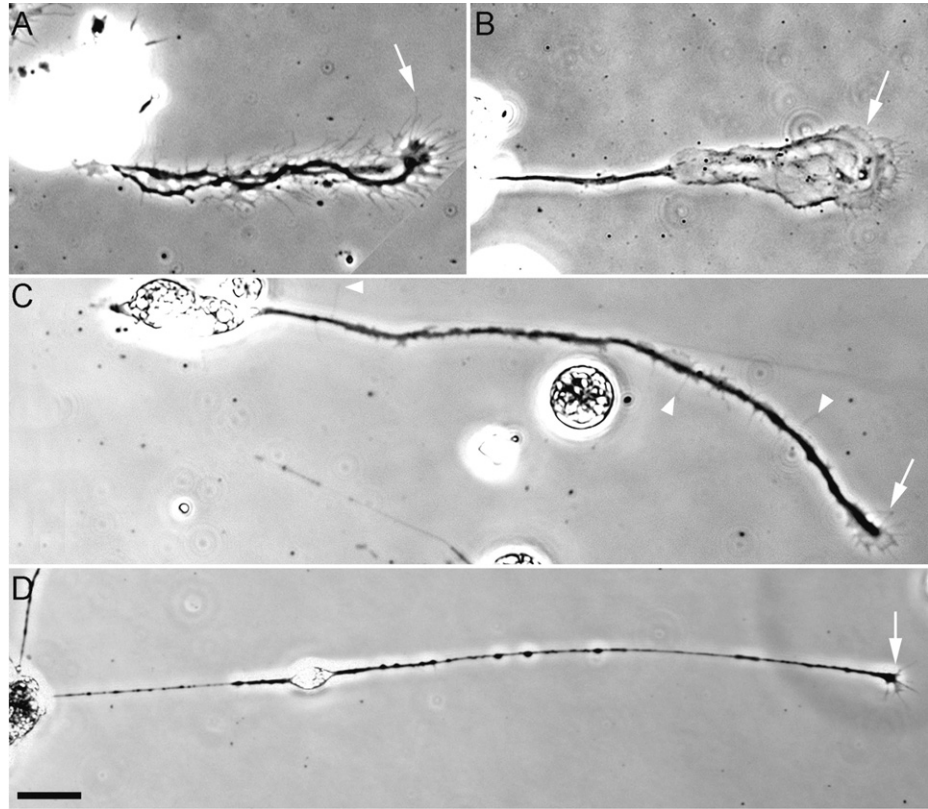


Fig. 5 *Xenopus* spinal neuronal morphology varies depending on culture substrata. (A) Neurons plated on $10\ \mu\text{g}/\text{ml}$ tenascin-C have short axons and highly adherent growth cones with many filopodia (arrow). (B) Neurons plated on $250\ \mu\text{g}/\text{ml}$ poly-D-lysine have short axons and highly adherent growth cones with broad lamellipodial (arrow). (C) Neurons plated on $10\ \mu\text{g}/\text{ml}$ fibronectin extend moderate-length, unbranched axons with many filopodia along their length (arrowheads) and small, highly motile growth cones (arrow). (D) Neurons plated on $10\ \mu\text{g}/\text{ml}$ laminin extend very long, smooth axons that tend to be adherent only at their small, highly motile terminal growth cones (arrow). Scale: $10\ \mu\text{m}$ for A–C and $20\ \mu\text{m}$ for D.

Xenopus growth cones cultured on laminin, fibronectin, tenascin-C, and polylysine exhibit unique morphologies, and there is a marked difference in both the rate and the extent of axonal outgrowth (Fig. 5). In particular, spinal neurons extend short neurites on highly adhesive substrata such as tenascin-C, polylysine, and tissue culture plastic (on the order of $50\text{--}100\ \mu\text{m}$ at 24 h in culture under control conditions) exhibiting highly filopodial and lamellipodial morphologies on tenascin and polylysine, respectively. In contrast, on laminin and other growth-permissive substrata, neuronal growth cones are highly motile and exhibit more

balanced filopodial and lamellipodial morphologies, resulting in increased neurite lengths of up to 1 mm at 24 h in culture.

Growth-permissive substrata such as laminin and, to a lesser extent, fibronectin are suitable for neural tube explant cultures, as a large number of neurites project from the explant and form an extensive halo of radiating neurites. However, highly adhesive or inhibitory substrata, such as those mentioned earlier, should not be used for explant cultures. On surfaces that tend to be less growth permissive, explants rarely adhere and those that do stick often do not extend neurites out of the explant, probably due to the explant providing a more permissive environment for growth. Therefore, when working with less growth permissive substrata, mixed or enriched dissociated neuronal cultures should be used; however, even here increased axon fasciculation and growth upon nonneuronal cells are expected.

IV. Live Cell Imaging and Manipulations

One of the biggest advantages of working with *Xenopus* neurons in culture is the ability to examine cells expressing a particular mutant or marker protein less than 36 h after embryo fertilization with live cell imaging. This benefit has been advanced further with the explosion of fluorescent fusion protein technologies. As is clear from many studies, viewing the dynamic distribution of proteins in live cells can be much more informative and accurate as compared to viewing the same proteins distributed in fixed, static cells. With different color protein variants, it is now possible to view the dynamic distribution of several proteins simultaneously in living cells. The color variants of fluorescent proteins have also greatly expanded the utility of fusion proteins by taking advantage of the overlaps of fluorophore excitation and emission spectra and close intra- and intermolecular interactions of fusion proteins. Based on the properties of FRET, new expressible proteins are being designed daily that not only report the location of proteins in live cells, but also report protein function or some aspect of cell physiology (Pollok and Heim, 2000). This type of work is particularly useful when studying motile cells, as protein distribution and function, as well as cell physiology, can each be correlated with cellular behavior.

A. Imaging Chambers

Live cell imaging studies often require the rapid exchange of culture solutions. The perfusion of solutions containing pharmacological agents, function blocking antibodies, vital dyes, or fixatives allows the examination of behavioral and physiological changes during and after treatment. In addition, combining rapid solution changes with high temporal and spatial resolution imaging allows for time-resolved measurements of intracellular ion and fluorescent protein dynamics. To this end, we have developed a technique for mounting cells plated on loose

glass coverslips onto glass slides that allows for the fast perfusion of culture medium in combination with confocal imaging on an upright microscope. Our technique results in a culture chamber volume $\sim 120 \mu\text{l}$, which allows for a complete solution exchange in less than 5 s and the use of limited quantities of reagents. Using thinner spacers or small openings will create even lower volume chambers. These chambers are useful for live cell imaging as well as rapid fixation followed by immunocytochemistry.

1. Materials

Neuronal cultures on loose 22×22 -mm glass coverslips
300- to 500- μm -thick plastic shims (Small Parts, Inc.)
Prcleaned glass microscope slides (Fisher)
High vacuum grease (Dow Corning)
18-mm volume-reducing ring (Thomas Scientific)

2. Procedure

a. Preassemble Chamber

Seal precut plastic shim (Fig. 6A) onto a glass slide using a small bead of high vacuum grease applied to all sides of the plastic spacer. Apply a second bead of high vacuum grease to the outer surface of the plastic spacer that will seal with a glass coverslip. Four small spacer squares can be sealed onto the glass slide with high vacuum grease in positions to meet the corners of the glass coverslip as an alternative to a complete precut-shaped plastic spacer.

b. Remove Submerged Coverslip

Glass coverslips containing cultured cells must be lifted from culture dish without exposing cells to air (Fig. 6B), which for *Xenopus* cells leads to an immediate disruption of membranes and cell death. To remove a submerged coverslip, we use an 18-mm glass ring with two spots of vacuum grease placed at either side to seal onto a coverslip surrounding cultured cells. Next, use a forceps to carefully pull the glass ring with the attached coverslip from the culture dish and place it onto a clean glass ring, which functions as a mounting stage.

c. Seal Chamber

Remove the glass ring from the loose coverslip, being careful not to tip the culture as medium will flow off and expose cells to air. Quickly place the aligned greased side of the preassembled glass slide with a spacer onto the glass coverslip. If the slide is tilted slightly when sealed onto the coverslip, air bubbles will be forced out of one open end. Note that the two remnants of grease on the glass coverslip should be placed at the sides rather than the ends of the chamber to prevent interference with medium flow. With the coverslip sealed in place, the

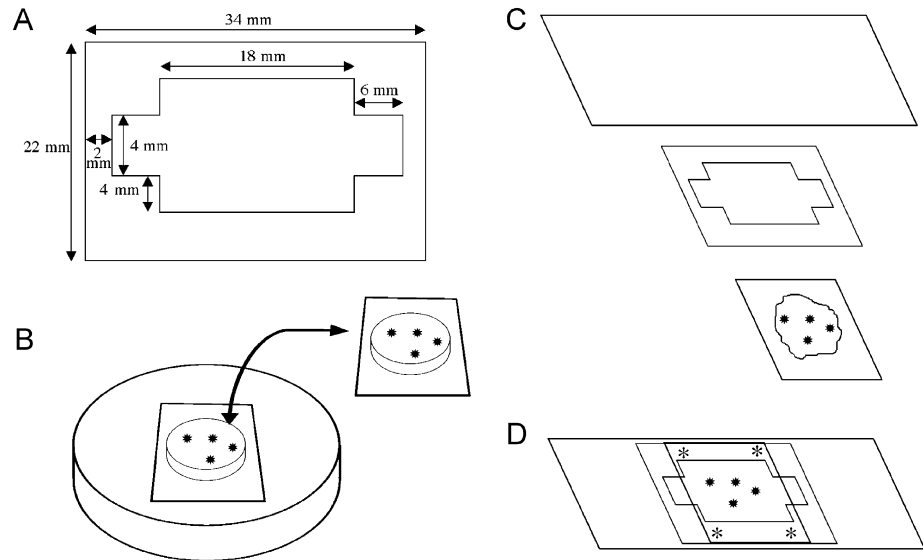


Fig. 6 Schematic diagram of perfusion chamber assembly. (A) A spacer cut from a 400- μm -thick plastic shim with the dimensions indicated yields a chamber volume of 120 μl when sealed with a coverslip. First attach the spacer to a glass slide with high vacuum grease and then grease the outer surface of the spacer in preparation to receive a coverslip containing cultured cells. (B) Use a greased glass volume-reducing ring to remove the submerged coverslip. (C) Remove the volume-reducing ring from the coverslip and seal quickly with a glass slide, taking care to avoid introducing air bubbles. (D) Turn the slide right side up and press on all sides to tighten the seal. Mount the slide on a microscope stage using slide clips on coverslip corners (asterisks) to prevent coverslip movement during perfusion.

chamber may now be inverted, revealing the inlet and outlet ports on either side. To assure a complete seal, press all sides of the coverslip down with forceps. If small square spacers were used instead of complete chamber mold, all sides of coverslip, except inlet and output ports, must be sealed with vacuum grease. Test the chamber by adding medium to the inlet side and suctioning from the output side, taking care not to suction the chamber dry.

d. Mount Chamber on Stage

These chambers are designed for use with an upright microscope using oil, water, or air objectives; however, they could also be used with an inverted microscope using long working distance air or water objectives. Place the slide onto the microscope stage and clamp down all four corners of the glass coverslip using slide clamps. It is important to clamp directly onto the glass coverslip rather than the glass slide, as this will prevent movement of the coverslip during perfusion. We use specially designed slide clamps that precisely meet the four corners of the mounted glass slide. Finally, position a hypodermic needle or fine tubing with constant suction near the edge of coverslip within the output port. A properly

positioned suction tubing will not suck a chamber dry when input stops, but will draw off fluid rapidly when flow begins.

B. Live Cell Imaging

For most live cell imaging we prefer to use a confocal microscope for the increased clarity, speed, sensitivity, and versatility offered by these systems. We use a three-channel Olympus Fluoview 500 laser-scanning confocal equipped with an argon ion gas laser (488 nm), a green helium neon laser (543 nm), and a red helium neon laser (633 nm). This laser combination allows us to excite GFP and RFP, as well as many commercially available fluorophores. In addition to scanning lasers, our system is equipped with a 100-W mercury light source focused along a separate light path for simultaneous imaging and UV uncaging of photosensitive compounds (see later).

The conditions used to collect confocal images vary depending on what is being examined. In general, when imaging fluorescence signals from vital dyes, such as Fluo-4 or CM DiI, we are less concerned about spatial resolution and more concerned about the viability of living cells, especially if we are collecting many images over a short period of time (high-temporal resolution). However, when imaging fluorescent fusion proteins with the intent of analyzing dynamic protein localization, high-spatial resolution is essential (~ 200 nm/pixel). To maximize the detected signal while minimizing laser power to the sample, we open the confocal aperture beyond the optimal Airy disc size. The photo multiplier tube (PMT) gain is also set high (50–75% of maximum), allowing laser power to be left below 5% of maximum. These values will vary for different confocal systems. For high-temporal, low-spatial resolution imaging, we also scan fast (2 ms/line) and reduce the scan region in the vertical dimension to fewer than 40 horizontal lines. Under these conditions, images can be captured at frequencies up to 8–12 Hz. We collect images at this rate to detect brief calcium signals that often persist for less than 200 ms. Even higher frequency imaging can be achieved by performing one-dimensional line scans along the length of individual filopodia. In this mode, a 2-ms temporal resolution is attained at the sacrifice of spatial resolution and signal to noise. In contrast, fluorescent proteins are typically imaged at a higher spatial and lower temporal resolution using a high NA oil objective, a near optimal pinhole diameter, and a lower PMT gain to increase the signal-to-noise level. Slower scan speeds (5 ms/line) are also used when imaging fluorescent proteins.

C. Rapid Fixation and Staining

Rapid fixation followed by immunocytochemical labeling after live cell imaging allows for the correlation of cellular behaviors, protein localization, or physiological activity with receptors and other key signaling molecules associated with cell motility. This is done by directly perfusing fixative through the imaging chamber on the microscope stage immediately following acquisition of a

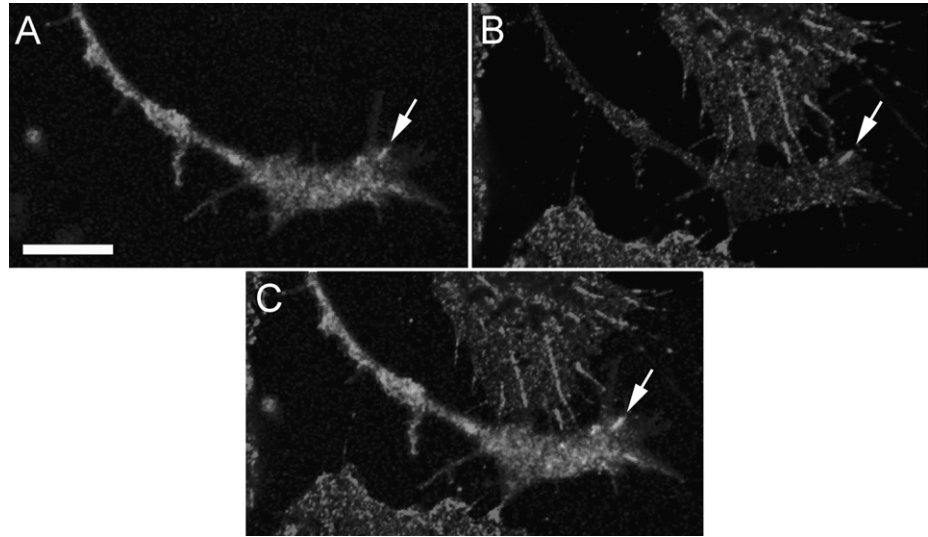


Fig. 7 GFP- $\alpha 5$ integrin receptors in a live growth cone growing on fibronectin colocalize with $\beta 1$ integrin receptors after fixation. (A) GFP- $\alpha 5$ integrin distribution in a growth cone just prior to fixation. Note streaks of $\alpha 5$ integrin receptor clusters resembling focal contacts (arrow). (B) Immunofluorescent staining for $\beta 1$ integrin receptors after fixation reveals that GFP- $\alpha 5$ integrin clusters in the live growth cone colocalize $\beta 1$ integrin clusters (arrow). Neighboring nonneuronal cells that were not expressing the GFP- $\alpha 5$ integrin also express clustered $\beta 1$ integrin receptors. (C) A merged live GFP image with a fixed immunofluorescence image reveals colocalizations (arrow). Scale: $10 \mu\text{m}$. (See Color Insert.)

time-lapse sequence. *Xenopus* neurons and nonneuronal cells are fixed by the rapid perfusion of room temperature 4% paraformaldehyde/4% sucrose, followed by standard immunocytochemical procedures. Rapid fixation results in only moderate changes in cell morphology during this process but should be performed immediately following live imaging. We have used this technique to localize integrin receptor clusters to sites of Ca^{2+} transient activity in growth cone filopodia (Gomez *et al.*, 2001) and because Fluo-4 fluorescence is lost upon fixation, this wavelength remains available, along with others, to localize multiple cellular elements with immunofluorescence. This approach also serves as an excellent test for the proper localization of fluorescent fusion proteins, as proteins tracked in live cells can be stained subsequently with specific antibodies after fixation (Fig. 7).

D. Ultraviolet Photolysis

Manipulation of cell physiology by UV photolysis of caged compounds is a powerful method used to study the acute effects of well-defined stimuli on cell motility. Many photosensitive reagents are available commercially, such as caged Ca^{2+} (MP-EGTA) and cAMP (Molecular Probes), and still others are being

synthesized by individual investigators using a variety of techniques (Marriott, 1998). Caged Ca^{2+} has been a particularly useful tool in studying the effects of user-defined Ca^{2+} transients on growth cone motility. This approach allows one to examine the downstream effectors of spatially and temporally distinct Ca^{2+} signals. Imposed Ca^{2+} transients are detected by coloaded Fluo-4, whereas the effects on growth cone behaviors can be studied with DIC optics or with various expressed fluorescent proteins. However, caution must be taken when using caged compounds, as growth cones are sensitive to UV light. Therefore, UV-only controls are important to determine the Ca^{2+} -dependent component of behavioral changes in response to photorelease.

UV photolysis of caged compounds is simplified on a confocal microscope, as these systems typically have separate light paths for laser-scanning imaging and wide-field fluorescence excitation. We use an Olympus AX-70 upright microscope equipped with a fiber-launched 100-W mercury arc lamp on our Fluoview 500 laser-scanning confocal system. Excitation and neutral density filters to select and attenuate photolysis wavelengths, respectively, are positioned in the optical path. We use narrow bandpass filters (either 360 ± 25 or 380 ± 6.5) to release Ca^{2+} efficiently while minimizing UV damage. The region exposed to UV light is adjusted using the field diaphragm, an aperture iris located at the conjugate focal plane between the illuminator and the specimen. UV exposure can typically be restricted to areas as small as 10–15 μm in diameter when using a 100 \times objective and can be determined by imaging a solution of caged-FITC dextran (Molecular Probes) sandwiched between coverslips. A dichroic mirror (Chroma) reflects light shorter than 400 nm toward the sample while transmitting longer wavelengths. A programmable shutter (Uniblitz) controls both the duration of single UV pulses and the delay between a series of pulses. It is worth noting that the total power of light delivered to the UV spot appears slightly higher toward the center, which may be due to the mechanism of iris opening and increased light defraction near the edge of the field diaphragm.

Photoactivation of caged Ca^{2+} provides higher spatial and temporal control of stimuli compared to alternative techniques (i.e., local or bath perfusion of Ca^{2+} channel activators). We use caged Ca^{2+} to locally generate Ca^{2+} transients at the tips of filopodia to determine the effects of these signals on growth cone guidance. Growth cones typically have many filopodia distributed in a fan shape at the leading edge of the advancing neurite. Thus, a growth cone can be positioned such that only filopodia on one side are exposed to the uncaging stimulus (Gomez *et al.*, 2001). We use local release of caged Ca^{2+} to determine how imposed Ca^{2+} transients at the tips of filopodia on one side of the growth cone affect the direction of neurite outgrowth. We position NP-EGTA-loaded growth cones so their direction of growth is toward a $\sim 12\text{-}\mu\text{m}$ spot of pulsed UV light. To generate brief Ca^{2+} transients, we program the shutter to open for 100–200 ms at a frequency of 3–6/min. Fluorescent images of GFP expressing growth cones or DIC images of untransfected growth cones are collected every 15–60 s for 30 min of growth. Using this paradigm, we find that growth cones loaded with NP-EGTA

consistently turn to avoid the region of pulsed UV light and typically do so after only filopodia enter the spot. In contrast, unloaded growth cones do not exhibit significant turning, although some UV-dependent responses are observed.

V. Summary

This chapter described techniques that distinguish *X. laevis* as a unique and highly effective model system, which we use to study the development of spinal neurons in culture. The principal advantages of *Xenopus* as a model system are the speed and ease of ectopic gene expression, as well as the versatility and amenability of its neuronal culture. Work with fluorescent fusion proteins seems particularly well suited for studying the mechanism of growth cone motility using *Xenopus* neurons, as labeled neurons can be examined within 36 h of fertilization. The molecular tools available to label or modify cells are expanding rapidly with no end in sight. Color variants of fluorescent fusion proteins engineered to utilize FRET to report physiological activity or protein function continue to be developed. These unique reporter constructs, as well as tailor-made DN and CA receptors, signaling components, and effector molecules, can be expressed easily in *Xenopus* to study the molecular mechanisms governing growth cone motility in culture. Although this chapter focused principally on *in vitro* studies, the *Xenopus* spinal cord is also an excellent model for studying *in vivo* axon guidance. Many of the tools developed and used *in vitro* can ultimately be tested *in vivo*. With such versatility and so many technical advances, it seems that this developmental model system will continue to be a productive organism of study over the next century.

References

- Amaya, E., Offield, M. F., and Grainger, R. M. (1998). Frog genetics: *Xenopus tropicalis* jumps into the future. *Trends Genet.* **14**, 253–255.
- Anderson, M. J., and Cohen, M. W. (1977). Nerve-induced and spontaneous redistribution of acetylcholine receptors on cultured muscle cells. *J. Physiol.* **268**, 757–773.
- Collazo, A., Bronner-Fraser, M., and Fraser, S. E. (1993). Vital dye labelling of *Xenopus laevis* trunk neural crest reveals multipotency and novel pathways of migration. *Dev. Suppl.* **118**, 363–376.
- Davidson, L. A., and Keller, R. E. (1999). Neural tube closure in *Xenopus laevis* involves medial migration, directed protrusive activity, cell intercalation and convergent extension. *Devel. Suppl.* **126**, 4547–4556.
- Fu, Y., Wang, Y., and Evans, S. M. (1998). Viral sequences enable efficient and tissue-specific expression of transgenes in *Xenopus*. *Nature Biotechnol.* **16**, 253–257.
- Gomez, T. M., Robles, E., Poo, M.-M., and Spitzer, N. C. (2001). Filopodial calcium transients promote substrate-dependent growth cone turning. *Science* **291**, 1983–1987.
- Gomez, T. M., and Spitzer, N. C. (1999). *In vivo* regulation of axon extension and pathfinding by growth-cone calcium transients. *Nature* **397**, 350–355.
- Hartenstein, V. (1989). Early neurogenesis in *Xenopus*: The spatio-temporal pattern of proliferation and cell lineages in the embryonic spinal cord. *Neuron* **3**, 399–411.
- Hartenstein, V. (1993). Early pattern of neuronal differentiation in the *Xenopus* embryonic brainstem and spinal cord. *J. Comp. Neurol.* **328**, 213–231.

- Heasman, J., Kofron, M., and Wylie, C. (2000). Beta-catenin signaling activity dissected in the early *Xenopus* embryo: A novel antisense approach. *Dev. Biol.* **222**, 124–134.
- Heim, R., and Tsien, R. Y. (1996). Engineering green fluorescent protein for improved brightness, longer wavelengths and fluorescence resonance energy transfer. *Curr. Biol.* **6**, 178–182.
- Holliday, J., and Spitzer, N. C. (1993). Calcium regulates neuronal differentiation both directly and via co-cultured myocytes. *J. Neurobiol.* **24**, 506–514.
- Holt, C. E., Garlick, N., and Cornel, E. (1990). Lipofection of cDNAs in the embryonic vertebrate central nervous system. *Neuron* **4**, 203–214.
- Jacobson, M., and Hirose, G. (1981). Clonal organization of the central nervous system of the frog. II. Clones stemming from individual blastomeres of the 32- and 64-cell stages. *J. Neurosci.* **1**, 271–284.
- Kroll, K. L., and Amaya, E. (1996). Transgenic *Xenopus* embryos from sperm nuclear transplantations reveal FGF signaling requirements during gastrulation. *Dev. Suppl.* **122**, 3173–3183.
- Kume, S., Muto, A., Inoue, T., Suga, K., Okano, H., and Mikoshiba, K. (1997). Role of inositol 1,4,5-trisphosphate receptor in ventral signaling in *Xenopus* embryos. *Science* **278**, 1940–1943.
- Lin, W., and Szaro, B. G. (1995). Neurofilaments help maintain normal morphologies and support elongation of neurites in *Xenopus laevis* cultured embryonic spinal cord neurons. *J. Neurosci.* **15**, 8331–8344.
- Marriott, G. (ed.) (1998). “Caged Compounds.” Academic Press, San Diego.
- Matz, M., Tarabykin, V., Usman, N., Shagin, D., Zaráisky, A., Lukyanov, S., and Matz, M. V. (1998). Fluorescent proteins from nonbioluminescent Anthozoa species. *Dev. Biol.* **194**, 172–181.
- Moody, S. A. (1989). Quantitative lineage analysis of the origin of frog primary motor and sensory neurons from cleavage stage blastomeres. *J. Neurosci.* **9**, 2919–2930.
- Moran-Rivard, L., Kagawa, T., Saueressig, H., Gross, M. K., Burrill, J., and Goulding, M. (2001). *Evx1* is a postmitotic determinant of $v0$ interneuron identity in the spinal cord *Lbx1* is required for muscle precursor migration along a lateral pathway into the limb. *Neuron* **29**, 385–399.
- Muto, A., Kume, S., Inoue, T., Okano, H., and Mikoshiba, K. (1996). Calcium waves along the cleavage furrows in cleavage-stage *Xenopus* embryos and its inhibition by heparin. *J. Cell Biol.* **135**, 181–190.
- Nakagawa, S., Brennan, C., Johnson, K. G., Shewan, D., Harris, W. A., and Holt, C. E. (2000). Ephrin-B regulates the ipsilateral routing of retinal axons at the optic chiasm. *Neuron* **25**, 599–610.
- Nieuwkoop, J. M., and Faber, J. (1967). “Normal Table of *Xenopus laevis* (Daudin),” 2nd Ed. North-Holland, Amsterdam.
- Noguchi, T., and Mabuchi, I. (2001). Reorganization of actin cytoskeleton at the growing end of the cleavage furrow of *Xenopus* egg during cytokinesis. *J. Cell Sci.* **114**, 401–412.
- Nutt, S. L., Bronchain, O. J., Hartley, K. O., and Amaya, E. (2001). Comparison of morpholino based translational inhibition during the development of *Xenopus laevis* and *Xenopus tropicalis*. *Genesis. J. Genet. Dev.* **30**, 110–113.
- Offield, M. F., Hirsch, N., and Grainger, R. M. (2000). The development of *Xenopus tropicalis* transgenic lines and their use in studying lens developmental timing in living embryos. *Dev. Suppl.* **127**, 1789–1797.
- Olafsson, P., Wang, T., and Lu, B. (1995). Molecular cloning and functional characterization of the *Xenopus* Ca(2+)-binding protein frequenin. *Proc. Natl. Acad. Sci. USA* **92**, 8001–8005.
- Payne, H. R., Burden, S. M., and Lemmon, V. (1992). Modulation of growth cone morphology by substrate-bound adhesion molecules. *Cell Motil. Cytoskel.* **21**, 65–73.
- Pollok, B. A., and Heim, R. (2000). Using GFP in FRET-based applications. *Trends Cell Biol.* **2000**, 57–60.
- Prasher, D. C., Eckenrode, V. K., Ward, W. W., Prendergast, F. G., and Cormier, M. J. (1992). Primary structure of the *Aequorea victoria* green-fluorescent protein. *Gene* **111**, 229–233.
- Rettig, J., Heinemann, C., Ashery, U., Sheng, Z. H., Yokoyama, C. T., Catterall, W. A., and Neher, E. (1997). Alteration of Ca²⁺ dependence of neurotransmitter release by disruption of Ca²⁺ channel/syntaxin interaction. *J. Neurosci.* **17**, 6647–6656.

- Roberts, A. (2000). Early functional organization of spinal neurons in developing lower vertebrates. *Brain Res. Bull.* **53**, 585–593.
- Ruchhoeft, M. L., Ohnuma, S., McNeill, L., Holt, C. E., and Harris, W. A. (1999). The neuronal architecture of *Xenopus* retinal ganglion cells is sculpted by rho-family GTPases in vivo. *J. Neurosci.* **19**, 8454–8463.
- Sive, H. L., Grainger, R. M., and Harland, R. M. (eds) (2000). “Early Development of *Xenopus laevis*: A Laboratory Manual.” Cold Spring Harbor Laboratory Press, Cold Spring Harbor, NY.
- Stoop, R., and Poo, M. M. (1995). Potentiation of transmitter release by ciliary neurotrophic factor requires somatic signaling. *Science* **267**, 695–699.
- Tabti, N., and Poo, M. M. (1990). Spontaneous synaptic activity at developing neuromuscular junctions. *Prog. Brain Res.* **84**, 63–72.
- Tanaka, E., and Kirschner, M. W. (1995). The role of microtubules in growth cone turning at substrate boundaries. *J. Cell Biol.* **128**, 127–137.
- Tessier-Lavigne, M., and Stein, E. (2000). Hierarchical organization of guidance receptors: Silencing of netrin attraction by slit through a Robo/DCC receptor complex. *Science* **289**, 1365–1367.
- Wallingford, J. B., Ewald, A. J., Harland, R. M., and Fraser, S. E. (2001). Calcium signaling during convergent extension in *Xenopus*. *Curr. Biol.* **11**, 652–661.

CHAPTER 9

Culturing Neurons from the Snail *Helisoma*

Christopher S. Cohan,^{*} James L. Karnes,[†] and Feng-Quan Zhou[‡]

^{*}Division of Anatomy and Cell Biology
University at Buffalo
SUNY
Buffalo, New York 14214

[†]Department of Physical Therapy
D'Youville College
Buffalo, New York 14201

[‡]Neuroscience Center
University of North Carolina at Chapel Hill
Chapel Hill, North Carolina 27599

-
- I. Introduction
 - II. Maintaining Animals
 - III. Initial Dissection
 - A. Reagents and Supplies
 - B. Protocol
 - C. Comments
 - IV. Culturing Nerve Cells
 - A. Reagents and Supplies
 - B. Protocols
 - C. Types of Cultures
 - D. Comments
 - References

The large neurons of the freshwater snail *Helisoma trivolvis* provide a unique preparation to study cytoskeletal mechanisms involved in neuronal growth and axon guidance. When placed into culture, these neurons form large growth cones in which cytoskeletal components and their dynamics can be analyzed with high-spatial resolution. Moreover, these growth cones display all of the dynamic features characteristic of growing axons, including advance, pause, collapse, and turning, allowing the correlation of cell biological mechanisms with growth cone

motility. This chapter describes complete procedures for culturing *Helisoma* neurons, including snail dissection, enzymatic treatments, removal of neurons, and necessary solutions, equipment, and supplies. Techniques are presented to culture *Helisoma* neurons by the extraction and transfer of individual neurons to culture dishes. A newer technique to dissociate neurons from whole ganglia is also described. In addition, methods to culture neurons on two substrates are presented. Culturing on polylysine in defined medium produces large, but nonmotile growth cones for cytoskeletal analysis, whereas culturing on polylysine in conditioned medium allows growth and motility for behavioral analysis. Recent tests suggest a new, simpler formulation for the medium used to culture *Helisoma* neurons that does not require the special-order medium that was previously used for cultures. These procedures make it feasible for someone inexperienced to successfully culture *Helisoma* neurons for use in a variety of experiments.

I. Introduction

Neurons of the freshwater pond snail *Helisoma trivolvis* exhibit the unusually large size characteristic of the molluscan phylum. The large diameter of neuronal cell bodies (up to 100 μm) and axons makes them uniquely accessible for the microscopic study of the neuronal structure and for the injection of probes to test neuronal function. In addition, the smaller number of neurons and their constant position in ganglia have allowed identification of many of the morphological, physiological, and molecular properties of individual neurons. This provides an opportunity to test repeatedly the responses of individual neurons with known identity and eliminates the variability inherent in populations of phenotypically mixed neurons. These neurons are also less dependent on growth factors for their short-term survival, which can be eliminated for some experiments. These properties make these neurons uniquely suited to a wide variety of cell biological questions, including growth cone formation during axon regeneration (Welnhofer *et al.*, 1997; Ziv and Spira, 1997, 1998), mechanisms of growth cone motility during axon guidance (Zhou *et al.*, 2002), synaptogenesis (Haydon, 1988), and cytoskeletal structure and dynamics (Cohan *et al.*, 2001; Welnhofer *et al.*, 1999; Zhou and Cohan, 2001).

Identified neurons from *Helisoma* buccal ganglia can be extracted with their original axons still attached to their cell bodies (Kater, 1974). When these neurons are plated onto polylysine-coated coverslips and cultured in defined medium (no growth factors), large growth cones (diameter about 50 μm) form within minutes at the tips of the axons. In addition, because of the high adhesion of the cell membrane to the substrate, these growth cones are not motile and do not collapse even when the actin filaments, which support the growth cone structure, are completely depleted (Zhou and Cohan, 2001). These properties allow a high-resolution study of cytoskeletal changes associated with growth cone responses to extracellular cues. In contrast, when the same identified neurons are cultured in medium conditioned

with *Helisoma* brain, which provides growth factors and extracellular matrix, neurites emerge from the neuron cell body and the tip of the original axon. Small but motile growth cones are present at the tips of these newly formed neurites. The growth cones in conditioned medium share similar morphology and motile properties to vertebrate growth cones, which extend, turn, or collapse depending on the microenvironment they encounter. Previous studies have shown that growth cones formed on polylysine substrate or in conditioned medium respond to applied molecules with similar cytoskeletal changes (Williams and Cohan, 1994; Zhou *et al.*, 2001, 2002). Therefore, by studying cytoskeletal rearrangement in the larger, nonmotile growth cones, it is possible to reveal the cytoskeletal mechanisms underlying the responses of the motile growth cones to environmental cues, such as collapse and turning (Zhou and Cohan, 2001; Zhou *et al.*, 2002). Furthermore, after identifying the cytoskeletal changes in large nonmotile growth cones, the same changes can be verified in motile growth cones, bringing both findings together in one condition. Thus, by comparing the cytoskeletal reorganization of large nonmotile growth cones with cellular responses of motile growth cones, it is now possible to gain insight into cytoskeletal mechanisms underlying complex growth cone responses to extracellular factors with high resolution.

II. Maintaining Animals

Helisoma are maintained easily in 5-gal. aquaria, which provide good access to food and are easily handled and cleaned. All supplies can be obtained at local aquarium stores. Plastic aquaria with accompanying tops are convenient and have the advantages of resistance to breakage and they also provide a preferred surface (plastic) for egg laying, but glass aquaria are also used. Tanks should contain a layer of oyster shell or crushed coral about 1 cm thick on the bottom, which provides a source of calcium for shell development. Fill tanks with high-quality deionized water to which artificial salts (Instant Ocean) are added (1 g/gal.). The tanks should be aerated continuously, and a simple filter (corner or bubble type) should be used to remove debris from the water. Motorized filters should not be used because the vigorous water intake will remove newly hatched snails from the tank. The animals should be maintained on a 12-h light–dark cycle using a light timer and fluorescent lighting. Animals are fed Romaine lettuce and carrot slices as necessary. Water should be changed and the gravel rinsed at 2- to 3-month intervals, which encourages egg laying. Eggs are laid as small, circular patches on smooth surfaces. Embryos undergo a larval stage in the eggs and then hatch as small snails in about 8 days (Goldberg *et al.*, 1988).

III. Initial Dissection

In preparation for cultures, snails are anesthetized, their body wall is opened, and ganglia containing nerve cells are removed. Then ganglia are trypsin treated before the final dissection to remove nerve cells.

A. Reagents and Supplies

Helisoma saline (Table I) is used for animal dissections

0.15% trypsin (source: bovine pancreas; Sigma Chemical) diluted in medium in a 35-mm petri dish

0.2% trypsin inhibitor (source: soybean type I-S; Sigma Chemical) diluted in medium in a 35-mm petri dish.

Medium—Leibovitz L-15 is prepared so that the salt concentrations are appropriate for *Helisoma* (Table II). This has required a special order (Gibco; see later) in which L-15 powder is obtained without inorganic salts, which are then added at appropriate levels. Antibiotics (Gentamicin) may be added for long-term cultures. Because the L-15 special order is inconvenient (there is a 200-liter minimum order

Table I
Helisoma Saline^a

NaCl	51.3
KCl	1.7
CaCl ₂	4.1
MgCl ₂	1.5
HEPES	10

^aConcentrations of components (in mM). Adjust pH to 7.5 and sterilize.

Table II
Recipe for *Helisoma* L-15 Medium^a

L-15 (without inorganic salts)	50% dilution
NaCl	40
KCl	1.7
CaCl ₂	4.1
MgCl ₂	1.5
HEPES	10
L-Glutamine	0.15 mg/ml

^aThe components (in mM) are added to L-15 (special order), which is purchased without inorganic salts. pH is adjusted to 7.5 and then the medium is sterile filtered.



Fig. 1 Position of snail at start of dissection. The foot of the snail is placed against the dissecting pad, and pins are placed in two anterior and one posterior position to stabilize it. The incision (dotted line) is started at the ridge of skin just posterior to the foot and is extended anteriorly to the front edge. The cut is placed off midline to protect structures close to the surface.

at a cost of \$400–\$500 or more), an easier formulation has been tested. Standard L-15 medium is diluted to one-third strength, which has the appropriate concentrations of Na and K ions for *Helisoma*. Other salts are supplemented to their correct concentrations by adding 3.7 mM CaCl₂, 1.2 mM MgCl₂, 10 mM HEPES, and 0.15 mg/ml L-glutamine and pH is adjusted to 7.5. Initial tests indicate that this medium supports viable *Helisoma* neurons. Growth cones that form in this medium in polylysine-attached cultures (see Section IV,C,1) are indistinguishable from those in special-order L-15.

Cell extraction medium—add 2 μ l/ml of 1 M CaCl₂ to *Helisoma* medium

Small scissors (12 cm length) for shell cutting

Vannas spring scissors—an inexpensive student grade such as #15100-09 from Fine Science Tools is adequate

Minutien pins 0.1 and 0.2 mm in diameter are available from Fine Science Tools (#26002-10 and #26002-20, respectively)

Dissecting dishes—Sylgard (Dow Corning) elastomer is an excellent dissection surface for pinning specimens. It can be purchased with black pigment, which provides the contrast necessary for visualizing specimens during dissection. A larger dish (60 or 100 mm petri) can be made for animal dissections and a smaller dish (35 mm petri) can be made for ganglia dissection.

B. Protocol

1. Snails about 1 cm shell diameter are deshelled by cutting through their shell following its spiral curvature for one revolution. Cut with the tips of the scissors to avoid cutting the soft tissue of the snail body adjacent to the shell. The shell is then separated into halves and the snail is removed by gentle prodding with the tips of scissors, which must sever the attachment between the small columellar muscle and the shell.

2. The snail is placed in a solution of 25% Listerine (Pfizer) in saline for 20 min. In addition to antibacterial agents in Listerine, the menthol component acts as an anesthetic.

3. The snail is placed in a large, sylgard dissecting dish with its foot oriented downward and pinned (Fig. 1).

4. An incision is started about midway back on the dorsal surface of the snail where the skin (mantle) forms a lip. The incision is extended anteriorly to the front edge of the snail, progressing off the midline so that ganglia near the surface are not damaged.

5. The penis retractor muscle is cut and the penis is pinned to the side to allow access to ganglia. The esophagus is located as it originates from the buccal mass and passes through the brain (circumesophageal ganglia). It is cut posterior to the brain as it enters the area of the digestive system and then it is gently pulled forward through the brain and pinned anteriorly. This exposes the buccal ganglia and salivary glands that are positioned on the dorsal surface of the buccal mass (Fig. 2).

6. The last step involves cutting the attachments to remove the buccal ganglia and brain. The nerves and muscles that attach the buccal ganglia to the snail are cut, leaving as long a length as possible to facilitate pinning the ganglia later. However, the esophageal trunks, two nerves that innervate the esophagus (Fig. 2), should not be cut. They should remain attached to the esophagus, but their branches that innervate the salivary glands should be severed. Then the esophagus

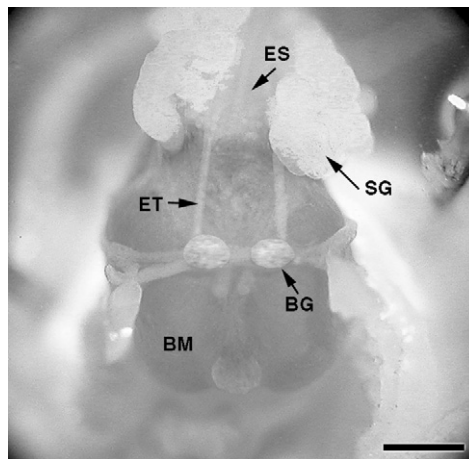


Fig. 2 Diagram showing the placement of buccal ganglia (BG) and salivary glands (SG) on the buccal mass (BM). Nerves and muscle exit the buccal ganglia at its anterior, lateral, and posterior edges to connect to the buccal mass and other areas. Two long nerves, the esophageal trunks (ET), send branches to innervate the esophagus (ES) and salivary glands. Branches innervating the esophagus should remain intact, but those innervating the salivary glands should be cut. Bar: 700 μ m. (See Color Insert.)

should be cut at its junction with the buccal mass and the buccal ganglia and the esophagus is removed from the snail. Finally, the brain is removed by severing all its connections with the snail.

7. Ganglia are placed in the trypsin solution at room temperature. Buccal ganglia are incubated for 30 min and brains are incubated for 60 min.

8. After the incubation period, transfer the ganglia to the trypsin inhibitor solution and incubate for 25 min.

9. At the end of the trypsin inhibitor period, transfer the ganglia to cell extraction medium. Ganglia can remain in this medium for several hours before subsequent dissection, if necessary.

C. Comments

The initial dissection, from beginning of anesthesia to placement in trypsin, requires about 30 min for a snail and about 1.5 to 2 h until the end of enzyme treatments. The effect of trypsinization is to allow the detachment of axons and nerve processes from connections in the neuropil of the ganglion during the extraction. Shorter incubation times (less than 20 min) result in cell bodies separating from their emerging axons as cells are extracted from the ganglia, which usually results in cell death. Although extensive testing with the new medium formulation (one third standard L-15) has not been conducted yet, initial results are positive. Neurons in polylysine-attached cultures are similar to neurons cultured in the special-order formulation. However, conditioned medium using the new formulation has not been tested yet, but it will be examined in the near future.

IV. Culturing Nerve Cells

A. Reagents and Supplies

Polylysine-coated coverslips—Coverslips are treated with polylysine to facilitate cell attachment. Acid-washed coverslips are incubated in a solution of 0.5% poly-L-lysine (MW 15,000–30,000, Sigma Chemical) in 0.15 M Tris, pH 8.4, in a petri dish with gentle shaking for 60 min. Coverslips are then rinsed well one at a time in deionized water and subsequently incubated in phosphate-buffered saline (PBS) in a petri dish with gentle shaking for 60 min. The PBS is replaced and the incubation is repeated. Finally, coverslips are rinsed in deionized water individually and tilted against the edge of a large petri dish in a culture hood to dry. They may be stored as a single layer on filter paper at -20°C for 6–7 weeks.

Glass-bottom dishes—High-resolution optical studies require that cells be viewed on a coverglass substrate. Polylysine-coated coverslips may be attached to a suitable culture chamber in a variety of ways. A 15-mm hole can be bored in the bottom of a 35-mm petri dish or a chamber may be fabricated with a suitable hole. The coverslip can be attached to the chamber using a thin layer of silicon

high vacuum grease. For more durable attachment, a thin line of 100% silicon rubber adhesive (Dow Corning) can be used (only types without mold inhibitors should be used). Alternatively, petri dishes with coverslips already attached may be purchased from MatTek Corp.

Micrometer syringe and assembly—This is necessary for delivering controlled amounts of positive and negative pressure during cell extraction. It can be purchased from Gilmont Instruments (0.2 ml size). The syringe is mounted on a short ring stand that also holds a three-dimensional micromanipulator (MM-33 or similar, Fine Science Tools). The syringe is attached to a hypodermic needle and plastic tubing that is connected to a glass micropipette. A plexiglass electrode holder in the micromanipulator clamps the micropipette in place. The micropipette is made from 1.5-mm O.D. borosilicate glass in a micropipette puller. The settings are adjusted so that the micropipette has a fairly long shank (1 cm), which can be placed close to ganglia without visual distortion. The end of the micropipette should be scored with a diamond scribe and broken so that the tip measures about 80–100 μm in diameter. It should be fire polished in a microforge (similar to those used for patch clamping) to obtain a smooth edge. The syringe, tubing, and micropipette must be filled completely with cell extraction medium without any air bubbles so that pressures can be applied instantly in the absence of a compressible filling. This is best accomplished by back-filling the syringe and tubing, attaching the syringe plunger, and then connecting the micropipette to the tubing.

B. Protocols

1. Extracting Single Neurons from Ganglia

a. Ganglia (dorsal side up) are pinned to the black sylgard pad of a 35-mm petri dish using 0.1-mm minutien pins (Fig. 3). The black background provides the necessary contrast for visualizing the nerve cell bodies situated at the ganglionic surface, which are yellow within the orange background of ganglia. The best illumination is provided by a fiber-optic light source, which can be positioned close to ganglia. Ganglia should be stabilized well with pins to minimize movement during the subsequent dissection. Extracting nerve cells is a straightforward procedure, but it requires concentration and patience.

b. For smaller buccal ganglia, a small hole is made in the connective tissue capsule around the ganglia by pinching and gently tearing the capsule near the center of a ganglion using fine forceps (Dumont #5, Biologie tip). This procedure is critical for obtaining viable cells. It is important not to exert too much force so that the cells bulge out from the hole, which often results in death of cell bodies. Due to the strength of the capsule, it usually is not possible to tear it from one side to the other in one motion. Rather, the initial hole is enlarged periodically to access more neurons.

c. As neurons are exposed by this hole, the tip of the micropipette is positioned near a cell body and gentle suction is applied using the micrometer screw (Fig. 4). If suction is applied too quickly, cell bodies will separate from their emerging

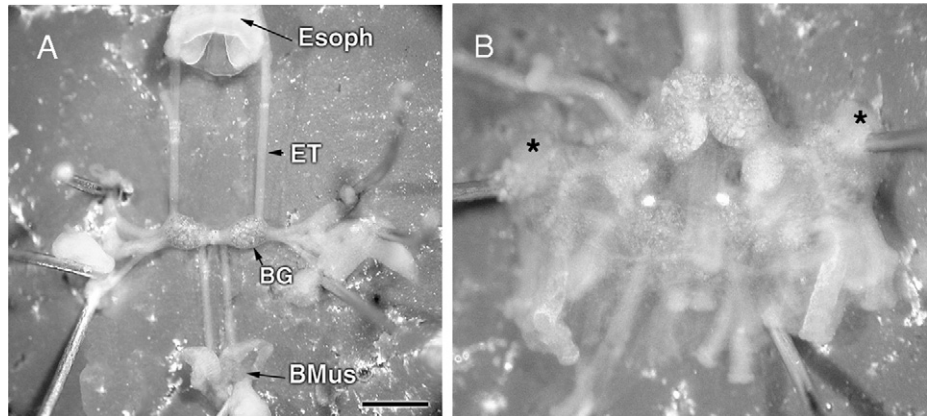


Fig. 3 Preparing the buccal ganglia and brain for the extraction of neurons. (A) Buccal ganglia are removed from the snail and stabilized with pins through nerves, small portions of muscle (BMus), and esophagus attached to the ganglia. Neurons appear as large yellow spheres on the surface of ganglia, which have a background orange color. (B) After cutting the short cerebral commissure (*), the brain is pinned flat against the sylgard pad. Bars: (A) 500 μm and (B) 300 μm . (See Color Insert.)

axons and the cells will die. Suction is applied periodically while the micropipette tip is moved backward as the cell body is drawn out of the ganglion, still attached by its axon. Eventually, the axon may break and the cell body will move into the micropipette (Fig. 4B). Otherwise, the axon can be severed by advancing the micropipette (with the cell body and length of axon in its tip) into the sylgard pad.

d. After the cell body and axon are brought into the micropipette the nerve cell is transferred to the culture dish by positioning the micropipette tip near the coverslip bottom and applying positive pressure gently to expel the neuron (Figs. 4C and 4D). Then, another attempt to extract a new cell is made. The most successful technique for transferring nerve cells from ganglia to a coverslip involves a stationary culture chamber placed adjacent to the dissecting dish and a moveable microscope head and micromanipulator stand. After a cell body is taken into the micropipette, the microscope and micropipette are repositioned over the culture chamber so that the neuron can be expelled under visual observation.

e. Extracting neurons from the brain is performed similarly. However, the brain, which consists of nine, closely arranged ganglia, is larger, has a greater number of nerve cells, and the average size of a cell body is larger. This provides a greater opportunity for cultures and it can facilitate training in these procedures. The commissure connecting the cerebral ganglia should be cut so that ganglia can be pinned in a stable position (Fig. 3B). These ganglia contain a thicker, outer layer of connective tissue that should be removed with forceps. However, after this is accomplished, the ganglionic capsule can be torn more completely and more easily than the buccal ganglion capsule without damaging underlying nerve cells.

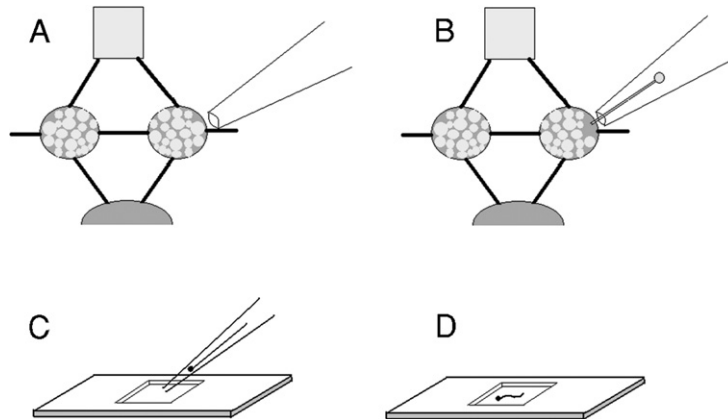


Fig. 4 Diagram of the procedure to extract individual neurons from ganglia. (A) A pipette tip is positioned near a hole in the ganglionic capsule. (B) Suction applied to the pipette draws a cell body and axon into the pipette tip. (C) The pipette tip is repositioned over the coverslip chamber. (D) Positive pressure through the pipette expels the neuron from the pipette and allows it to settle onto the coverslip where it adheres to the surface. (See Color Insert.)

2. Dissociation of Whole Ganglia

We have developed a technique to dissociate the contents of entire ganglia, in contrast to extracting individual neurons as detailed in Section IV,B. Although the time required for preparing dissociated cultures is similar to that for extracting single neurons, dissociated cultures require less technical expertise and can be performed with little practice. To maximize the number of neurons in the cultures, *Helisoma* brains were used.

a. Two brains are removed from snails, the cerebral commissure is cut, and the brains are pinned so they lie flat in a sylgard dissecting dish. The outer, thick connective tissue surrounding the ganglia is removed partially with forceps or by cutting. Do not pierce the thin capsule that confines the neurons in each ganglion. Removing the thick connective tissue will facilitate dissociation later.

b. Brains are incubated in 0.3% collagenase (type XI, Sigma) in medium for 90 min at 37°C.

c. Brains are incubated in 0.15% trypsin for 30–60 min at room temperature.

d. Brains are incubated in 0.2% trypsin inhibitor for 30 min at room temperature.

e. Brains are transferred to 0.5 ml cell extraction medium (2 μ l/ml of 1 M CaCl₂) for 15 min.

f. Brains are transferred to a tube containing 1 ml of medium and they are dissociated mechanically by passing them through the opening of a Pasteur pipette (tip reduced in diameter by fire polishing) 15–20 times.

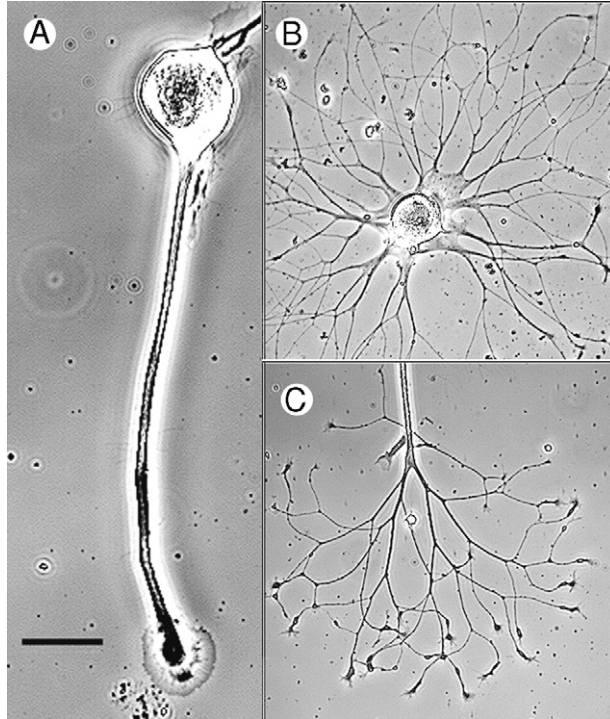


Fig. 5 Neurons cultured on different substrates. (A) In polylysine-attached cultures, cell bodies and axons adhere quickly to the polylysine coating. A large growth cone forms at the cut end of the axon within 1 h. (B) Conditioned medium cultures promote neurite outgrowth from cell bodies and axons (C) over a 6- to 12-h period. Bar: 50 μm .

g. The suspended neurons are transferred into one or more culture dishes, depending on the desired cell density.

C. Types of Cultures

1. Polylysine-Attached Cultures

In the simplest cultures, neurons are plated onto a polylysine-coated coverslip (Williams and Cohan, 1994; Welnhof *et al.*, 1997; Zhou *et al.*, 2001, 2002) in medium in the absence of other extracellular matrix molecules or growth factors. Neurons with their attached axons stick immediately when they contact the coverslip and develop growth cones at the severed, distal end of their axons within a 1- to 2-h period (Fig. 5A). These growth cones are large (60–80 μm in diameter), do not advance, and their membrane remains attached to the coverslip even when their cytoskeleton is disassembled (Zhou *et al.*, 2001, 2002). These properties make it

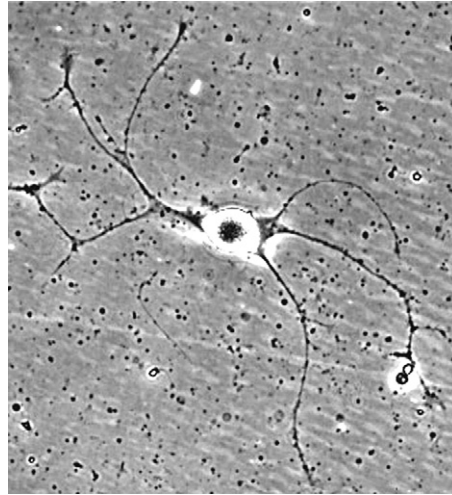


Fig. 6 Cultures of dissociated neurons. When neurons are dissociated from whole ganglia and placed into conditioned medium cultures, they form growth cones and neurites similar to neurons that are extracted individually from ganglia.

possible to perform high-resolution analyses of the neuronal cytoskeleton that are difficult or impossible in other preparations (Welnhofer *et al.*, 1999; Zhou *et al.*, 2002).

2. Conditioned Medium Cultures

When grown in conditioned medium cultures, *Helisoma* neurons produce neurites (Figs. 5B, 5C, and 6) and display the full complement of motile growth cone behaviors, including advance, collapse (Zhou and Cohan 2001), turning (Zhou *et al.*, 2002), and synapse formation (Haydon, 1988). Growth cones in these cultures usually are significantly smaller than in polylysine-attached cultures, but they provide the important property of motility. Previous studies (Miller and Hadley, 1991; Barker *et al.*, 1982; Wong *et al.*, 1981, 1984) indicate that extracellular matrix molecules provide the signal for growth, similar to vertebrate neurons, but little is known about the identity of these molecules. Therefore, a conditioned medium that promotes growth is made by incubating brain ganglia for 72 h in coverslip-bottom (polylysine-coated) 35-mm petri dishes that contain four brains in 2 ml of *Helisoma* L-15. After the incubation period, the brains are removed and neurons are plated directly onto the coverslip in these dishes. To facilitate cell attachment, which occurs more slowly in these cultures, neurons should remain undisturbed for the 8- to 12-h period required for outgrowth. Because sterility is an important consideration in these cultures, gentamicin can be added at a concentration of 50 $\mu\text{g/ml}$ (Wong *et al.*, 1981) at the start of the incubation period.

D. Comments

After neurons are placed into the culture chamber, adhesion to the substrate must occur for further development. Adhesion occurs quickly in polylysine-attached cultures but slowly in conditioned medium cultures. Adhesion is aided by maintaining the culture chamber in a fixed position so that neurons are not disturbed after they are deposited on the coverslip. Transferring neurons individually to a fixed culture chamber requires that the dissecting microscope is situated on a boom stand, which has an arm that can swing from dissection dish to the adjacent culture chamber. If this arrangement is not available, it may be possible to move the culture chamber gently in the case of polylysine-attached cultures, but this may be a problem for conditioned medium cultures.

Single neurons are deposited onto the coverslip surface by expelling them from the micropipette tip close to the coverslip. In polylysine-attached cultures, the intended result is growth cone formation at the tip of the axon. However, the manner in which neurons are expelled from the micropipette affects the position of the neuron as it attaches to the substrate and thus the ability to form growth cones. Due to the greater mass of the cell body compared to the axon, cell bodies will sink toward the coverslip faster and adhere on contact, causing the axon to project up into the medium. In this situation, growth cones will not form. However, by expelling neurons closer to the coverslip, small streams of positive or negative pressure can be used to orient the axon and its tip to ensure contact and adhesion to the substrate. Precise placement of neurons is not necessary for conditioned medium cultures because growth cones and ensuing neurite outgrowth occur from the cell body as well as from axons in these cultures (Figs. 5B and 5C). Visualization of cell bodies and axons on the coverslip is enhanced by indirect illumination, which allows neurons to appear bright against a dark background.

Finally, it is also important to consider potential difficulties with these cultures. Cross-reactivity of *Helisoma* antigens to antibodies from vertebrate species can limit immunocytochemistry in these cultures. In addition, due to the smaller number of neurons in the snail nervous system, these cultures contain fewer nerve cells. Cultures prepared by extracting individual neurons typically contain less than 15 neurons. However, this smaller number of cells is justified given the depth of cytoskeletal analysis that can be attained. This may be a disadvantage for other types of experiments that require assays of large populations of neurons. Dissociated *Helisoma* cultures containing larger numbers of neurons may overcome some of these difficulties. Finally little information exists on genetic manipulations necessary for the expression of molecules in snail neurons, although this methodology should be feasible as shown for a wide variety of species. Despite these limitations, *Helisoma* cultures provide one of the few neuronal preparations where cytoskeletal mechanisms can be visualized and manipulated to gain insight into many cell biological questions.

Acknowledgments

The authors acknowledge the pioneering work of Dr. S. B. Kater who initially developed *Helisoma* as a model system to study neuronal function. This work was supported by funds from the NIH and NSF to CSC.

References

- Barker, D., Wong, R., and Kater, S. (1982). Separate factors produced by the CNS of the snail *Helisoma* stimulate neurite outgrowth and choline metabolism in cultured neurons. *J. Neurosci. Res.* **8**, 419–432.
- Cohan, C. S., Welnhof, E. A., Zhao, L., Matsumura, F., and Yamashiro, S. (2001). Role of actin bundling protein fascin in growth cone morphogenesis: Localization in filopodia and lamellipodia. *Cell Motil. Cytoskel.* **48**, 109–120.
- Goldberg, J. I., McCobb, D. P., Guthrie, P. B., Lawton, R. A., Lee, R. E., and Kater, S. B. (1988). Characterization of cultured embryonic neurons from the snail *Helisoma*. In “Cell Culture Approaches to Invertebrate Neuroscience” (D. J. Beadle and S. B. Kater, eds.), Academic Press, pp. 85–108.
- Haydon, P. G. (1988). The formation of chemical synapses between cell-cultured neuronal somata. *J. Neurosci.* **8**, 1032–1038.
- Kater, S. B. (1974). Feeding in *Helisoma trivolvis*: The morphological and physiological bases of a fixed action pattern. *Am. Zool.* **14**, 1017–1036.
- Miller, J. D., and Hadley, R. D. (1991). Laminin-like immunoreactivity in the snail *Helisoma*: Involvement of a ~300kD extracellular matrix protein in promoting outgrowth from identified neurons. *J. Neurobiol.* **22**, 431–442.
- Welnhof, E. A., Zhao, L., and Cohan, C. S. (1997). Actin dynamics and organization during growth cone morphogenesis in *Helisoma* neurons. *Cell Motil. Cytoskel.* **37**, 54–71.
- Welnhof, E. A., Zhao, L., and Cohan, C. S. (1999). Calcium influx alters actin bundle dynamics and retrograde flow in *Helisoma* growth cones. *J. Neurosci.* **19**, 7971–7982.
- Williams, D. K., and Cohan, C. S. (1994). The role of conditioning factors in the formation of growth cones and neurites from the axon stump after axotomy. *Dev. Brain Res.* **81**, 89–104.
- Wong, R., Barker, D., Kater, S., and Bodnar, D. (1984). Nerve growth-promoting factor produced in culture media conditioned by specific CNS tissues of the snail *Helisoma*. *Brain Res.* **292**, 81–91.
- Wong, R. G., Hadley, R. D., Kater, S. B., and Hauser, G. C. (1981). Neurite outgrowth in molluscan organ and cell cultures: The role of conditioning factors. *J. Neurosci.* **1**, 1008–1021.
- Zhou, F.-Q., and Cohan, C. S. (2001). Growth cone collapse through coincident loss of actin bundles and leading edge actin without actin depolymerization. *J. Cell Biol.* **153**, 1071–1083.
- Zhou, F.-Q., Waterman-Storer, C. M., and Cohan, C. S. (2002). Focal loss of actin bundles causes microtubule redistribution and growth cone turning. *J. Cell Biol.* **157**, 839–849.
- Ziv, N. E., and Spira, M. E. (1997). Localized and transient elevations of intracellular Ca^{2+} induce the dedifferentiation of axonal segments into growth cones. *J. Neurosci.* **17**, 3568–3579.
- Ziv, N. E., and Spira, M. E. (1998). Induction of growth cone formation by transient and localized increases of intracellular proteolytic activity. *J. Cell Biol.* **140**, 223–232.

CHAPTER 10

The Tibial-1 Pioneer Pathway: An *in Vivo* Model for Neuronal Outgrowth and Guidance

Jennifer Bonner, Kimberly A. Gerrow, and Timothy P. O'Connor

Program in Neuroscience
Department of Anatomy
University of British Columbia
Vancouver, British Columbia V6T 1Z3
Canada

- I. Introduction
- II. Development of the Tibial-1 (Ti1) Pathway
 - A. Grasshopper Limb Development
 - B. Anatomy of Ti1 Neurons
 - C. The Path of Ti1 Pioneer Neurons: From the Periphery to the Central Nervous System
- III. Guidance of Ti1 Axons
 - A. Mechanisms
 - B. Guidance Molecules
- IV. Analysis of Axon Guidance Mechanisms in Grasshopper Procedures
 - A. Staging Grasshopper Embryos from 29 to 35% of Development
 - B. Culturing Grasshopper Embryos
 - C. Blocking the Function of Known Molecules (Antibodies and Peptides)
 - D. Ectopic Expression in the Developing Limb Bud
 - E. Microinjection and Labeling Ti1 Neurons
- V. Laboratory Protocols
 - A. Embryo Dissection
 - B. Embryo Cultures
 - C. Immunocytochemistry
 - D. Preparation of Glass Bottom Culture Dishes for Microinjection and Time-Lapse Imaging
 - E. Preparation of Poly-L-Lysine-Coated Coverslips

- F. Filleting Grasshopper Limb Buds to Gain Access to the Ti1 Pathway
- G. Labeling and Injecting Ti1 Neurons *in Situ*
- H. Ectopic Overexpression in the Developing Limb Bud
- I. Blocking Protein Function

References

As neurons extend axons to their targets during development, growth cones must reorient their direction of migration in response to extracellular guidance cues. A variety of model systems have been employed in order to dissect the cellular and molecular mechanisms that underlie this complex process. One preparation, the developing grasshopper limb bud, has proved to offer a number of advantages in which to examine mechanisms of growth cone guidance and motility *in vivo*. First, the relatively large size of the embryonic nervous system allows for straightforward imaging of both fixed and live neurons *in vivo*. Second, the peripheral nerves generated in the limb bud are highly stereotyped. Third, intact embryos can be cultured for a period of days, allowing for fairly easy perturbations at precise developmental stages. Fourth, due to the ease of dissection, numerous cell biological and molecular techniques can be utilized in the limb bud. Finally, axon guidance molecules and mechanisms are conserved between grasshoppers and other organisms, including vertebrates.

I. Introduction

The nervous system is composed of a complex arrangement of individual neurons that make very specific functional connections. During development, neuronal cell bodies extend neurites that navigate through the embryonic environment in response to a variety of directional cues. An integral component of this navigation, also termed “pathfinding,” is the anatomical specialization at the distal tip of the outgrowing neurite, called the growth cone. The growth cone is a highly motile and dynamic, actin-filled structure that actively surveys the environment by extending and retracting filopodial and lamellipodial protrusions. Upon reaching their targets, the migrating growth cones will undergo a transformation in order to form a stable connection with their target. A fundamental question in neuroscience is how the migrating tip distinguishes between the various guidance cues to forge an accurate path to the appropriate target. Generally speaking, there are two broad classes of guidance cues, attractive and repulsive; and growth cones exhibit contrasting behaviors depending on which they are in contact with. In the complex molecular landscape of the developing embryo, growth cones often encounter these diverse cues simultaneously and must therefore be able to process seemingly contradictory information in order to arrive at a pathfinding response. While a great deal of information can be collected from studying growth cone responses to cues in isolation (i.e., *in vitro*), it is crucial to also analyze these behaviors *in vivo*.

For the neuroscientist interested in the mechanisms underlying axonal guidance, the development of the grasshopper embryo provides several notable benefits. First, the relatively large size of the embryonic nervous system allows for straightforward imaging of both fixed and live neurons *in vivo*, including visualization of the neuronal cytoskeleton. Second, the ability to culture grasshopper embryos up to a period of 2 days combines the advantage of maintaining an intact organism with the benefits of cell culture techniques. In addition, analysis of molecules can be carried out at precise developmental stages in order to ascertain their role in axon guidance rather than their contribution to earlier developmental events. Third, the highly accessible and relatively simple nervous system is amenable to various cell biological manipulations, which are outlined later. Finally, the simplicity of the nervous system is not undermined by a lack of functional and molecular conservation, as axon guidance mechanisms in grasshoppers are conserved in vertebrates. This chapter outlines some of the methodologies pertinent to answering questions relating to axon guidance. Specifically, the focus is on one neuronal projection found in the developing grasshopper limb bud, called the Tibial-1 (Ti1) pathway.

II. Development of the Tibial-1 (Ti1) Pathway

A. Grasshopper Limb Development

Grasshopper embryogenesis is divided into stages based on the percentage of development. Embryos develop roughly 5% per day with the earliest born neurons in the peripheral nervous system (PNS) and central nervous system (CNS) appearing at approximately 30% of development. The Ti1 pathway is established from 30 to 35% of embryonic development. During this time, the developing limb bud also undergoes molecular and morphological changes. At 30% of development, during the time when the Ti1 cell bodies are differentiating and delaminating from the distal tip of the limb bud, the limb bud consists of an epithelial tube that is loosely filled with mesoderm. A basal lamina separates the epithelium from the mesoderm. At this stage, the mesoderm is relatively undifferentiated, consisting largely of various cell specific precursors (e.g., muscle precursors) and hemocytes. The epithelium is rapidly dividing at this stage and is unsegmented. Over the next 5% (24 h) of embryonic development, as the Ti1 pathway is established, muscle cells begin to differentiate (Ho *et al.*, 1983), limb segmentation proceeds, and an abundant heterogeneous basal lamina is produced (Anderson and Tucker, 1988, 1989).

B. Anatomy of Ti1 Neurons

Neurons are highly polarized cells whose cell bodies may lie great distances from their terminal processes. As a result, neurons have specialized compartments. When a neuron differentiates from the surrounding epithelium, it consists solely of

a cell body. During axonogenesis, the plasma membrane extends asymmetrically to generate a growth cone and axon. The growth cone is the most distal structure of the neuron; it is highly motile and “reads” the surrounding environment for directional cues. Emanating from the growth cone are long finger-like processes called filopodia (Fig. 1A) and dynamic veil-like membranous protrusions called lamellipodia, which lie between individual filopodia. Elongation of the axon occurs as the growth cone extends and the most proximal region of the growth cone is converted to an axon. In general, the growth cone exhibits a consistent size, although predictable changes occur in growth cone shape and size depending on the substrate encountered (O’Connor *et al.*, 1990). Not surprisingly, the growth cone and the axon contain distinct cytoskeletal elements. The relatively immobile axon consists mainly of highly packed microtubules (Fig. 1A; Sabry *et al.*, 1991), whereas the highly motile growth cone is composed of both actin filaments and microtubules (Fig. 1A; Sabry *et al.*, 1991; O’Connor and Bentley, 1993). Filopodia and lamellipodia are composed of F-actin bundles (O’Connor and Bentley, 1993). In the central core of the growth cone, microtubule bundles extend from the axon shaft (Fig. 1A). Unlike the tightly packed array of microtubules in the axon, microtubules are splayed out in the growth cone and often form transient microtubule loops that may extend into lamellipodia (Sabry *et al.*, 1991).

C. The Path of Ti1 Pioneer Neurons: From the Periphery to the Central Nervous System

Consisting of two neurons, the Ti1 pathway is established early in development when the limb bud is relatively undifferentiated. Ti1 neurons are considered to be pioneer neurons because they are the first peripheral neurons to establish a projection into the CNS. The growth cones of migrating Ti1 axons make contact with several substrates, including the basal lamina (Anderson and Tucker, 1988; Bonner and O’Connor, 2001), intrasegmental epithelium, segment boundary epithelium, and several intermediate neuronal targets (Keshishian and Bentley, 1983; O’Connor, 1999). At 30% of development, Ti1 cell bodies delaminate from the epithelium and initiate axon extension toward the CNS. Ti1 cell bodies are located at the distal tip of limb epithelium when they first initiate axons. As the morphology of the limb changes and the segmental boundaries are generated, the cell bodies typically end up in the tibia, just distal to the femur–tibial segment boundary (hence the Ti1 designation; Fig. 1B). Much of the pathway is pioneered along epithelium that forms the femur limb segment. As the Ti1 growth cones extend along the midfemur, they may contact a neuronal guidepost cell, the Fe1 cell, although often this cell has not differentiated at this stage. After proximal extension across the femur, Ti1 growth cones contact another preaxonogenesis neuron, the Tr1 cell, which is located in the trochanter epithelium. After contact with the Tr1 cell, the Ti1 axons make an abrupt ventral turn (Fig. 1B). Near the ventral midline of the limb bud, the growth cones contact another intermediate target, the Cx1 preaxonogenesis neurons, which lie proximal to the trochanter limb segment in the coxa limb segment. Upon contact with the Cx1 neurons, the Ti1 axons cease

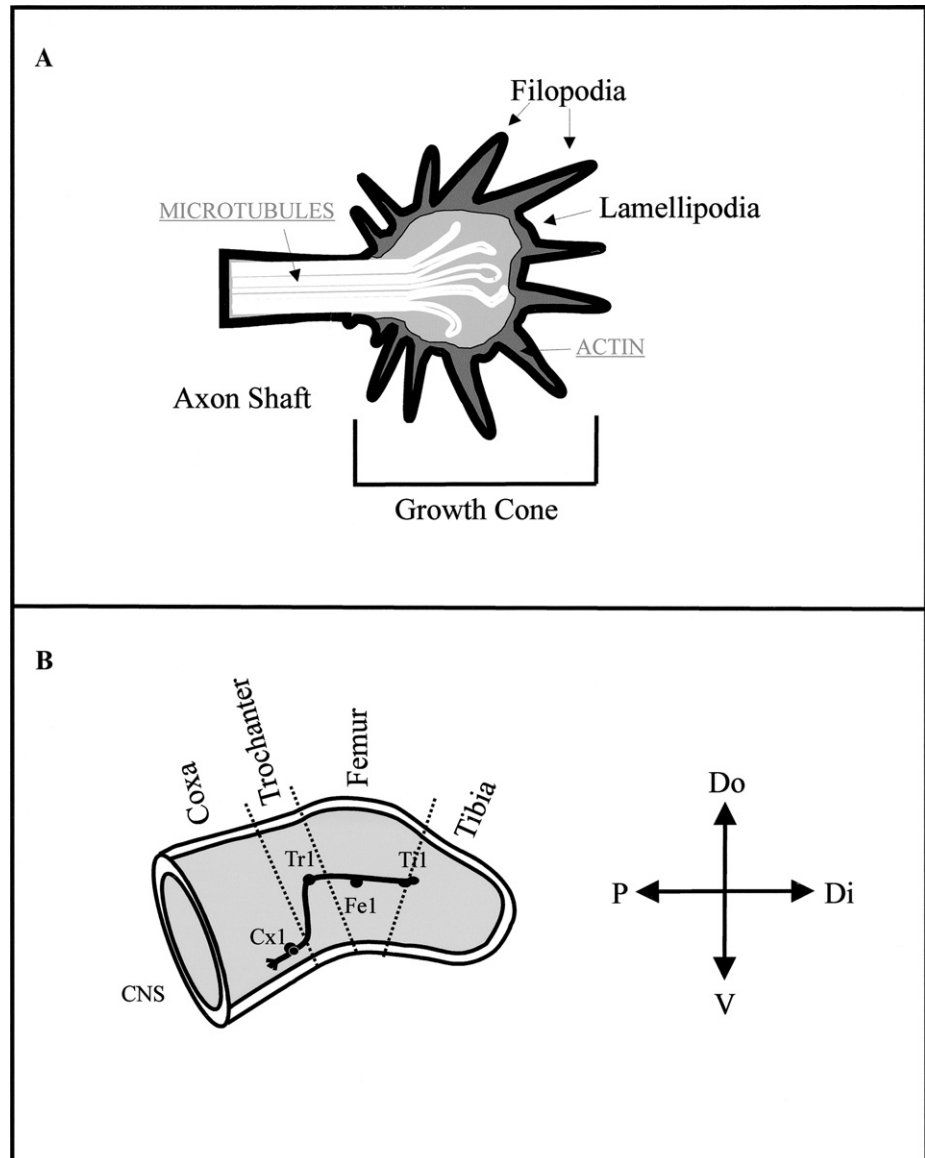


Fig. 1 Schematic representation of a growth cone and the Ti1 pioneer neuron pathway. (A) The growth cone extends from the distal axon shaft and consists of lamellipodia and filopodia, which are motile. The axon shaft, as well as the proximal growth cone, is filled predominantly with microtubules (white), whereas the filopodia and lamellipodia consist of actin filaments (gray). (B) The Ti1 pioneer pathway in the developing grasshopper limb bud is depicted at approximately 34% of development. Limb segments and the axis are given; details on the pathway are found in the text. Do, dorsal; Di, distal; P, proximal; V, ventral.

ventral extension along the trochanter and turn proximally to extend into the CNS (Fig. 1B; Keshishian and Bentley, 1983; Bentley and O'Connor, 1992.) Later in development the Ti1 pioneer pathway serves as a scaffold for the axons of sensory neurons that are born in the periphery. Distinct from pioneer neurons, these later arising neurons fasciculate with the established Ti1 pathway to gain entry into the CNS (Klose and Bentley, 1989; Wong *et al.*, 1997; O'Connor, 1999).

III. Guidance of Ti1 Axons

A. Mechanisms

We have described three important substrates (basal lamina, epithelium, and guidepost cells) encountered by the Ti1 growth cones that have distinct effects on their behavior. How does a single apparatus, the growth cone, discriminate from these different substrates? Although the Ti1 neurons follow a relatively simple trajectory, time-lapse imaging of the neurons reveals complex growth cone behaviors depending on the substrate encountered. When traversing the femur limb segment, Ti1 growth cones typically advance by extending lamellipodia between filopodia, which is characterized by an accumulation of actin filaments in filopodia and lamella that are extended in the direction of growth (O'Connor *et al.*, 1990; O'Connor and Bentley, 1993). Often, at the trochanter, Ti1 axons extend microtubule-filled branches both dorsally (the incorrect decision) and ventrally (the correct decision). The dorsal projection is subsequently retracted and ventral projection proceeds (O'Connor *et al.*, 1990; Sabry *et al.*, 1991). The decision to proceed ventrally is characterized by a greater accumulation of F-actin in filopodia on the ventral side of the growth cone (or in the ventral branch) compared to dorsally extending filopodia (O'Connor and Bentley, 1993). Also, ventral extending filopodia start to show an increase in net extension just prior to growth cone turning, possibly indicating that individual filopodia can sense guidance cues (Isbister and O'Connor, 1999).

A somewhat different growth cone behavior is observed when they contact guidepost cells. Reorientation of Ti1 growth cones in response to guidepost cells can be accomplished by contact with a single filopodium (O'Connor *et al.*, 1990). Upon contact, the proximal shaft of the filopodium expands, with high amounts of F-actin accumulation followed by microtubule invasion (O'Connor *et al.*, 1990; Sabry *et al.*, 1991; O'Connor and Bentley, 1993). Although the extracellular signal(s) responsible for events such as filopodial formation has not been identified, downstream effectors of filopodia formation likely converge on an increase of local Ca^{2+} , as release of caged Ca^{2+} results in filopodia formation in Ti1 neurons (Lau *et al.*, 1999).

The Ti1 growth cones encounter several guidepost cells (preaxonogenesis neurons) during their migration. Guidepost cells appear to provide a high-affinity substrate for the Ti1 growth cones as they appear to always turn toward the cells after making filopodial contact. For example, the Ti1 axons contact and

momentarily stall on the Tr1 cell in the trochanter limb segment before turning ventrally. In addition, after ventral extension, the Ti1 growth cones turn proximally after contacting the Cx1 cells. These contacts are also specialized in that the growth cones typically form gap junctions with the guidepost cells while they do not with other cell types (Bentley *et al.*, 1991). However, it appears that Fe1 and Tr1 guidepost cells play a nonessential role in guiding the Ti1 growth cones. Examination of precocious developing embryos where the Ti1 growth cones extend past the Fe1 cell prior to its differentiation showed little effect on growth cone guidance (Caudy and Bentley, 1986). Similarly, we have observed numerous examples of Ti1 pathways that show no evidence of contact with the Tr1 guidepost cell, suggesting that these cells are not necessary for accurate pathfinding (unpublished observations). In contrast, ablation studies have demonstrated that Cx1 cells are necessary for the proximal turn made by Ti1 growth cones as they extend toward the CNS (Bentley and Caudy, 1983).

Removal of the basal lamina with enzymatic digestion revealed an adhesive role of the basal lamina, as shown by the retraction of Ti1 axons back to the cell bodies. (Condic and Bentley, 1989c). Surprisingly, when the enzymes were washed out, the Ti1 axons again initiated axons and navigated without error to the trochanter limb segment and commenced the ventral turn (Condic and Bentley, 1989a). These experiments suggest that Ti1 axons rely on the basal lamina at least initially for adhesion, but that the epithelium is capable of compensating for the loss of the basal lamina. Interestingly, however, the reliance of Ti1 adhesion to the basal lamina is dependent on location in the limb bud. For example, when the basal lamina is removed when the growth cones are in the trochanter limb segment, the axons do not retract, instead, the Ti1 cell bodies are displaced distally, toward the growth cones (Condic and Bentley, 1989b). Similarly, after disassembling the F-actin in filopodia, those filopodia in contact with the trochanter epithelium retract significantly slower than filopodia contacting the femur epithelium, suggesting greater filopodial:substrate adhesion in the trochanter (Isbister and O'Connor, 1999). Thus, with respect to adhesion properties, the limb bud is heterogeneous. Not surprisingly, several molecules are found to be expressed in restricted bands of epithelium and may be potential mediators of differential adhesion (see later).

B. Guidance Molecules

1. Semaphorins

Although the Ti1 pathway appears to be relatively simple, the expression profile of known guidance cues in the limb bud is rather complex. For example, semaphorin family members are expressed in restricted epithelial domains that change as development proceeds. Semaphorins are a family of conserved glycoproteins that are distinguished by a common semaphorin domain. Widely accepted as repulsive guidance cues, semaphorins repel neurons. Members of two classes of semaphorins are expressed in the developing grasshopper limb bud and contribute to Ti1 pathfinding (reviewed by Bonner and O'Connor, 2000).

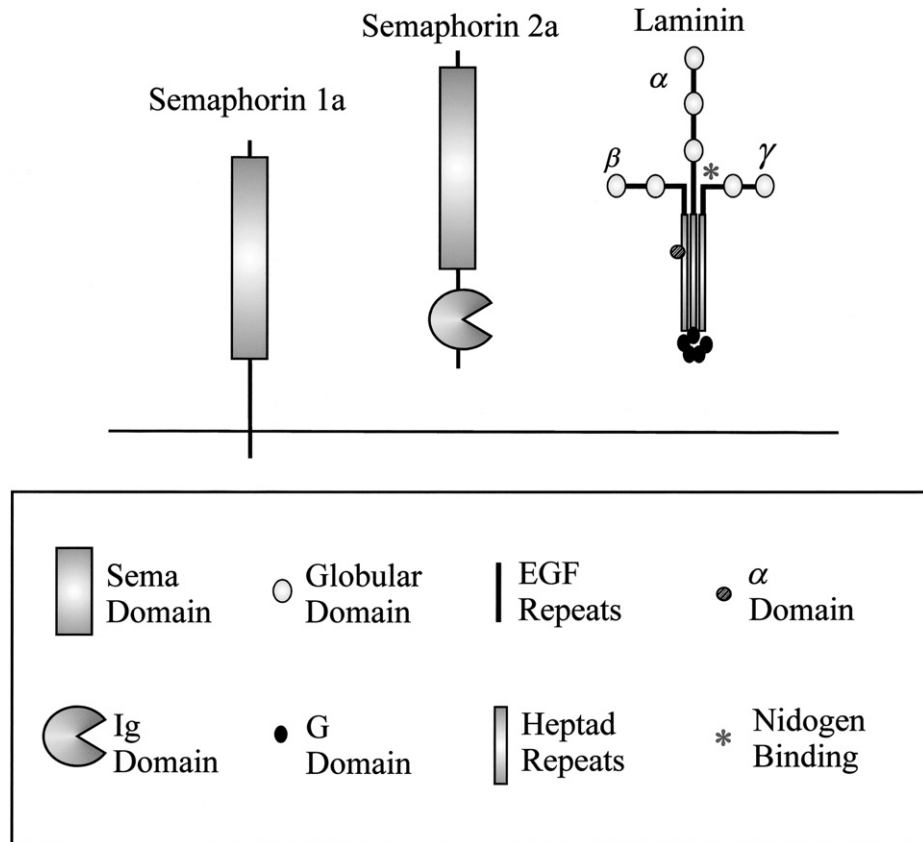


Fig. 2 Domain structures of semaphorins and laminin. Semaphorin 1a is a transmembrane glycoprotein that consists of a sema domain and a short intracellular tail. Semaphorin 2a is secreted and also has a sema domain, as well as an Ig domain. Laminin is a major constituent of the basal lamina and is made up of three subunits: α , β , and γ . The following domains are common to all laminin chains: globular domains, helical domains, and EGF repeats. The α chain also has several G domains, and the β chain has an α domain.

Grasshopper semaphorin 2a, (Sema-2a), a secreted class 2 semaphorin, is composed of a conserved sema domain and an Ig domain (Fig. 2). A candidate repulsive cue, Sema-2a is expressed in two overlapping epithelial gradients in the limb bud: a distal-to-proximal gradient and a dorsal-to-ventral gradient (Fig. 3; Isbister *et al.*, 1999). Consistent with a repulsive role in T11 axon guidance, a high expression of Sema 2a correlates with areas of the limb bud that T11 axons avoid. In the presence of antibodies that recognize the sema domain, T11 neurons extend axons into the limb epithelium, which expresses high levels of Sema-2a, areas they usually avoid (Fig. 3; Isbister *et al.*, 1999). Importantly, the repulsive activity of

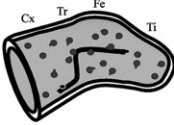
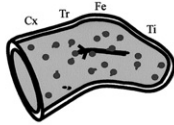
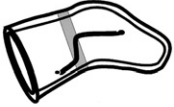


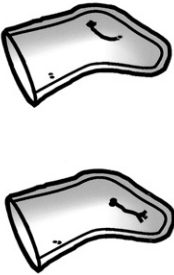
GUIDANCE MOLECULE	EXPRESSION PROFILE	DISTRIBUTION	BLOCKING DEFECT
LAMININ γ Permissive	Basal lamina, (uniform) hemocytes		
SEMAPHORIN 1A Adhesive/ Attractive	Restricted Trochanter Epithelium		
SEMAPHORIN 2A Repulsive	Restricted Epithelial gradient, subsets of mesodermal cells		

Fig. 3 Laminin and semaphorins are important guidance cues for T11 neurons. The schematic summarizes the expression pattern and defects resulting from blocking distinct semaphorin family members and the laminin γ chain. For details, see text.

Sema-2a is restricted to the sema domain, as antibodies recognizing regions at the C terminus of Sema-2a had little effect on axon pathfinding (Isbister *et al.*, 1999). While these experiments demonstrated the repulsive activity of Sema-2a, they did not address relevance of the graded distribution of Sema-2a. Comparisons of the slope of the Sema-2a gradient and T11 pathfinding error indicate that the slope of the gradient rather than the absolute concentration is important for T11 steering (Isbister *et al.*, 2003).

While the role of Sema-2a is to discourage T11 axons from making incorrect guidance decisions through repulsion, an alternative role was found for another semaphorin family member in the developing limb bud. Semaphorin-1a (Sema-1a) is distinct from Sema-2a in that it is membrane bound through a transmembrane domain (Fig. 2; Kolodkin *et al.*, 1992). The intracellular domain is relatively short and contains no identifiable signaling motifs, with the possible exception of a

putative PDZ-binding site (Fig. 2; Wong *et al.*, 1999). During Ti1 outgrowth, *Sema-1a* expression is restricted to a circumferential band of epithelium in the trochanter segment where the Ti1 pioneer neurons make the ventral turn (Fig. 2; Kolodkin *et al.*, 1992). Later in development, the *Sema-1a* expression pattern expands to include complete circumferential epithelial bands in the tibia [just proximal to subgenual organ (SGO) neurons] and proximal tarsus (Singer *et al.*, 1995; Wong *et al.*, 1997; Isbister *et al.*, 1999).

To block *Sema-1a* function during establishment of the Ti1 pathway, a monoclonal antibody was applied to grasshopper embryos. This treatment resulted in marked defasciculation and axon branching of Ti1 axons in the region of the trochanter epithelium (Fig. 3; Kolodkin *et al.*, 1992). Notably, although the axons were defasciculated, they were still capable of turning ventrally and completing the pathway to the CNS. Interpretation of these results could lead to either an attractive or a repulsive function for *Sema-1a*. As discussed earlier, compared to other regions in the developing limb bud, *Sema-1a* expressing epithelium appears to be more adhesive for Ti1 growth cones, suggesting the possibility that *Sema-1a* may, in part, be mediating this adhesiveness (Condic and Bentley, 1989b; Isbister and O'Connor, 1999). Alternatively, mass defasciculation at the trochanter could also be interpreted as a loss of function of an inhibitory molecule. In this scenario, the repulsiveness of *Sema-1a* may normally act to promote Ti1 axon fasciculation (Kolodkin *et al.*, 1992). However, it is unlikely that *Sema-1a* functions as a repulsive cue that collapses growth cones or retards their growth, as observations suggest that *Sema-1a* may be an attractive cue. For example, a later arising neuronal group, the SGO neurons, initiate axons that travel within and extend across *Sema-1a* expressing epithelium until contact with the Ti1 pathway is established (Wong *et al.*, 1997). In the absence of Ti1 neurons (removed by either heat shock or mechanical ablation), SGO neurons grow to the edge of the *Sema-1a* expressing epithelium but do not continue further. When *Sema-1a* blocking antibodies are applied, SGO outgrowth is entirely inhibited. These results strongly suggest that *Sema-1a* is not only adhesive (SGO neurons cannot leave the *Sema-1a* expressing epithelium) but also may be required for axon initiation (Wong *et al.*, 1997). In addition, when ectopic *Sema-1a* is expressed by S2 or COS cells in the limb bud, Ti1 axons repeatedly choose to reorient growth toward *Sema-1a* expressing cells (Wong *et al.*, 1999). Thus, *Sema-1a* may be functionally complex, acting as a preferred or high-affinity guidance cue, while maintaining sufficient repulsive activity to encourage axon fasciculation.

In the developing limb bud, semaphorin family members have distinct roles in establishment of the Ti1 pathway. When both *Sema-1a* and *Sema-2a* are blocked simultaneously, the results are additive as opposed to synergistic. For example, some neurons exhibit a *Sema-2a*-specific defect, whereas others exhibit *Sema-1a*-specific defects (Isbister *et al.*, 1999). This suggests a stepwise process of Ti1 axon guidance to the CNS. First, after axonogenesis, a distal-to-proximal gradient of *Sema-2a* repels Ti1 axons proximally toward the CNS. Before the turn in the trochanter, a dorsal-to-ventral *Sema-2a* gradient is partially responsible for

directing the ventral turn of the axons. Upon turning in the trochanter, Sema-1a may encourage the ventral outgrowth of Ti1 axons while ensuring that they do not wander proximally or distally in the limb before contacting the Cx1 cells.

2. Laminin

The basal lamina is a thin extracellular array that separates tissue types, withstands tension, acts as a molecular sieve for secreted molecules, and is a scaffold for migrating cells during embryonic development. A complex network of several molecules, the basal lamina includes type IV collagen, perlecan, nidogen, and laminin (Timpl and Brown, 1996). The structure of the basal lamina relies on highly ordered physical interactions of individual components that are required in order to serve the functions described earlier. Laminin binds to a number of proteins in the basal lamina, such as perlecan and nidogen (Timpl and Brown, 1996). Importantly, laminin binds to itself, resulting in polymerization that is calcium and concentration dependent (Yurchenco *et al.*, 1985; Cheng *et al.*, 1997). Type IV collagen also self-assembles, forming a collagen network (Yurchenco and Furthmayr, 1984). The laminin and collagen networks are spatially distinct within the basal lamina; however, linker molecules, such as perlecan and nidogen, connect the two networks. Within the context of the basal lamina, laminin exists as a heterotrimer within a network that associates with many other molecules, suggesting a complex conformation that may have functional ramifications.

The laminin heterotrimer consists of three distinct subunits, α , β , and γ (Fig. 2). Each subunit has a similar domain structure of heptad repeat-containing domains I and II, followed by an EGF repeat-containing domain III, a globular domain IV, another EGF repeat-containing domain V, and a final globular domain VI (Fig. 2). This general structure has a few subunit-specific modifications: the α chain contains a globular domain adjacent to domain I, as well as duplications of domain III and IV. The β chain has an α domain between I and II. Also, several variant chains of α , β , and γ have been cloned that have truncations in various domains (Colognato and Yurchenco, 2000). The mature laminin molecule has a cruciform structure characterized by long and short arms (Fig. 2). Domains I and II of all three subunits come together to form a coiled-coil, which is strengthened by disulfide bonding. All laminin isoforms examined to date contain one each of the three subunits.

a. Basal Lamina Establishment

In grasshopper, laminin β and γ chains are distributed in the limb bud basal lamina as early as 30% of embryonic development (Bonner and O'Connor, 2001). This stage corresponds to Ti1 differentiation and axonogenesis. Laminin is distributed uniformly within the basal lamina and appears to be tightly adherent to the epithelium throughout the duration of Ti1 pathway establishment (Fig. 3). However, the epithelium does not secrete laminin, as this tissue is negative with both *in situ* hybridization and laminin immunocytochemistry (Bonner *et al.*, 2002).

Interestingly, laminin is secreted into the basal lamina by randomly migrating hemocytes. Thus the basal lamina is established by a tissue that is only transiently associated with it at any given moment. This is in stark contrast to establishment of the basal lamina in vertebrates and other invertebrates such as *Drosophila*. In these organisms, laminin is secreted by tissue that stably abuts the basal lamina and this tissue likely plays a role in its assembly and anchorage.

b. Role of Laminin in Ti1 Axon Guidance

To determine the role of laminin during Ti1 outgrowth and pathfinding, the nidogen-binding site on the γ chain of laminin was disrupted with blocking antibodies and blocking peptides (Fig. 2). Disruption of the nidogen recognition site on laminin γ had a profound effect on Ti1 pathfinding. Whereas Ti1 neurons in control cultures were capable of completion of the pathway to the CNS, Ti1 neurons cultured in the presence of blocking antibodies could not navigate the ventral turn, resulting in stalled axons (Fig. 3; Bonner and O'Connor, 2001). Axons stalled predominantly in the trochanter limb segment, at the site of the ventral turn. This result was specific for the turn as Ti1 neurons of laminin-blocked cultures arrived at the trochanter at the same time as control cultures and stalled Ti1 axons could not overcome the cessation of growth with a longer culture period. Important in the interpretation of these results is the uniform distribution of laminin compared to the specificity of the location of the defect. While it is likely that Ti1 axons require laminin and other guidance cues simultaneously, it appears that when laminin is blocked, Ti1 growth cones are still responding to *Sema-2a* signals from the distal epithelium, as evidenced by the fidelity of the proximal extension. As the trochanter limb epithelium is more adhesive for Ti1 neurons compared to more distal limb bud regions (Condic and Bentley, 1989c; Isbister and O'Connor, 1999), it is possible that laminin is required in this region to overcome this adhesion and to turn ventrally. Thus, perhaps laminin is required for the integration of other guidance signals at the turn, such as a cue that directs the ventral turn. Although the identity of a functional laminin interactor is unknown, there are several molecules whose function remains to be determined in the guidance of Ti1 axons.

3. Other Molecules

Although the functions of laminin and semaphorins have been partly elucidated, the roles of other molecules expressed in the limb bud remain to be determined. Annulin, a transglutaminase, is restricted to epithelial bands in the developing limb bud (Singer *et al.*, 1992; Bastiani *et al.*, 1992; Singer *et al.*, 1995). G-innexin-1, a connexin gap junction protein, is expressed at the trochanter-coxa segment boundary (Ganforina *et al.*, 1999). REGA-1, an Ig superfamily member, is dynamically expressed by the mesoderm and is also found on the epithelium in the developing limb bud (Seaver *et al.*, 1996). A second Ig superfamily member, lachesin, and lazarrillo, which encodes a novel member of the lipocalin family, are

found on the Ti1, Fe1, and Tr1 neurons (Karlstrom *et al.*, 1993; Sanchez *et al.*, 1995). A promoter of Ti1 fasciculation, fasciclin I is expressed by Ti1 neurons and is also found in the epithelium (Bastiani *et al.*, 1987; Diamond *et al.*, 1993).

IV. Analysis of Axon Guidance Mechanisms in Grasshopper Procedures

A. Staging Grasshopper Embryos from 29 to 35% of Development

Our staging protocol is essentially from Bentley *et al.* (1979) with some changes that reflect the difference in species used (*Schistocerca americana* vs *Schistocerca gregaria*). The shape of the limb bud changes substantially from 29 to 35% of embryonic development. At 29%, the distal tip of the limb bud is only slightly pointed and the overall shape of the limb bud is rounded and unsegmented. At this stage, Ti1 cell bodies are delaminating from the distal epithelium (Fig. 4). At 30% (the appropriate culturing stage for examination of the Ti1 pathway), the distal tip becomes slightly squared (Fig. 4). In addition, the Ti1 neurons have completely delaminated but have not initiated axonogenesis. By 33% of development, the Ti1 growth cones have reached the trochanter limb segment. At this stage the limb is more tubular and the squared distal tip is more definite, with a slight invagination evident at the distal tip of the epithelium (Fig. 4, arrow). By 35%, the Ti1 pathway is established and the distal tip invagination is more evident. Segmentation is more pronounced, particularly at the tibia–femur boundary and the femur–trochanter boundary (Fig. 4).

B. Culturing Grasshopper Embryos

Pods of grasshopper eggs are removed from the sand in which they were laid and are cleaned gently with room temperature water to remove excess sand or dirt. The cleaner the eggs, the lower the chance of fungal and bacterial contamination. Pods can be stored on moist towels (Kimwipes; Kimberly-Clark) in Tupperware containers in a 30°C incubator. Eggs should be sprayed with water daily to avoid desiccation. At 30°C, embryos develop at approximately 5% per day. If desired, eggs can be stored at room temperature to slow their development.

Grasshopper embryos can be cultured for up to several days without affecting nervous system development. Adult female grasshoppers lay anywhere from 30 to 80 eggs at a time, and each clutch of eggs is referred to as a pod. Because each embryo from the same pod is roughly the same age and differs by only 1% (Bentley *et al.*, 1979), large numbers of embryos can be experimented on reproducibly. Furthermore, as each embryo has six limbs, each embryo provides six Ti1 pathways for analysis. Typical culture periods are 24 h, which allows for completion of the Ti1 pathway. At 30% of embryonic development, dorsal closure has not occurred, allowing culture media and reagents to penetrate the embryo readily. In order to label, microinject, and conduct time-lapse imaging of Ti1 growth

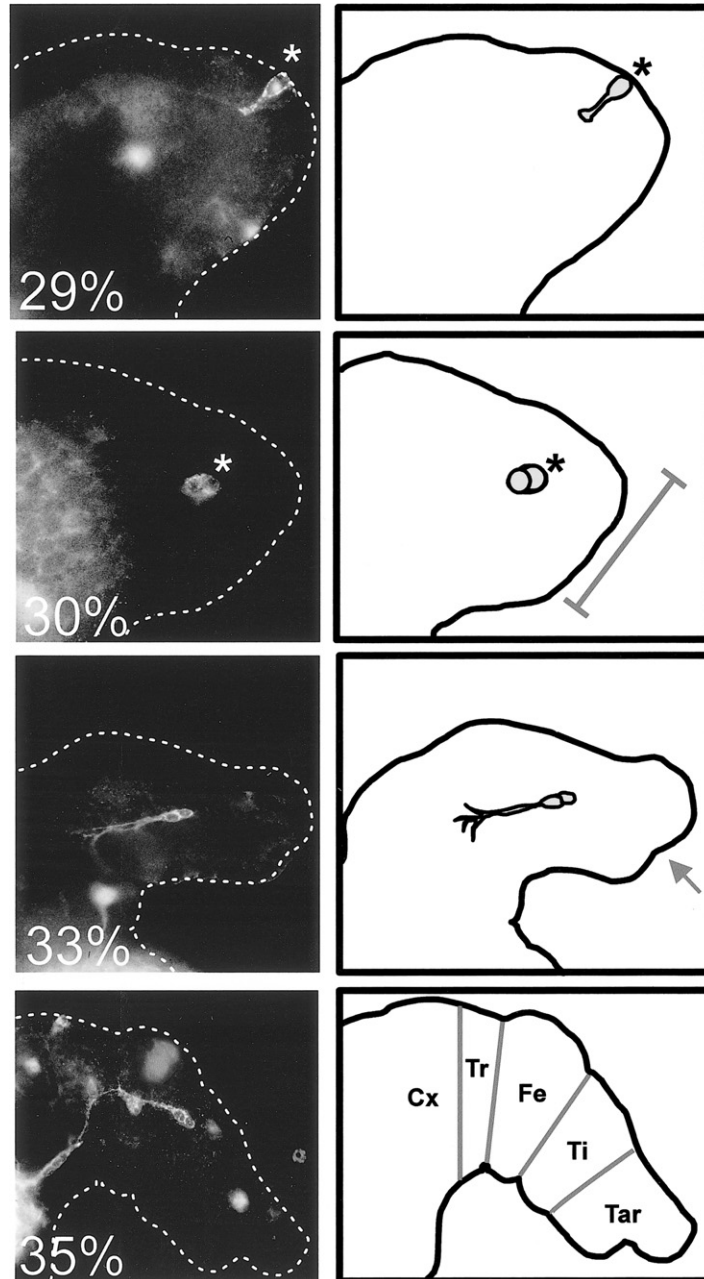


Fig. 4 Anti-HRP immunofluorescence depicts the T1l pioneer neuron pathway in various stages. The shape of the limb has been outlined indicating the limb changes during these developmental stages and the location of the T1l pioneer growth cones. Asterisks indicate T1l neurons.

cones, grasshopper limbs are filleted open and the mesoderm is removed. Using Nomarski optics the Ti1 neuronal cell bodies are readily identifiable and accessible for labeling and injecting (see Section V).

C. Blocking the Function of Known Molecules (Antibodies and Peptides)

To specifically inactivate the function of a protein, antibody blocking or peptide blocking can be employed. Site-specific antibodies (either polyclonal or monoclonal) have been used successfully to inactivate transmembrane, secreted, and basal lamina molecules. Access of blocking antibodies can be monitored accurately by simply adding the appropriate secondary antibody for visualization. Antibodies can be cleared enzymatically in order to produce Fab fragments for use in culture. An alternative method to antibody blocking is peptide blocking. If functional motifs have been identified on a molecule, for example, receptor interaction sites, then peptides can be generated that mimic this site to compete for receptor interaction. Both of these techniques have been used successfully in the past to study Ti1 axon guidance (Kolodkin *et al.*, 1992; Wong *et al.*, 1997, 1999; Isbister *et al.*, 1999; Bonner and O'Connor, 2001). Often, the best strategy is to combine these techniques with overexpression or ectopic expression studies.

D. Ectopic Expression in the Developing Limb Bud

The current method for ectopic overexpression in the developing limb bud requires the use of transfected cell lines. Ectopic expression by this method has been successful with insect cell lines (S2 and Sf21 cells) and a mammalian cell line (COS cells) (Wong *et al.*, 1999). To introduce transfected cells into the limb, one of two methods can be used. If Ti1 neurons are to be visualized with real time microscopy, the limb fillet preparation can be used. In this case, after the limbs have been filleted, transfected cells are placed on top of the limb fillet. When using an intact embryo, cells can be introduced into the lumen of the limb bud by entering the medial aspect of the limb bud with a micropipette containing the transfected cells. Cells are then expelled gently into the limb lumen with a mouth pipette. The location of transfected cells can be detected by GFP expression, immunocytochemical labeling of the recombinant protein, or membrane labeling of the transplanted cells with the lipophilic carbocyanine dyes with DiI or DiO (Molecular Probes).

E. Microinjection and Labeling Ti1 Neurons

One of the most powerful advantages of the grasshopper limb bud system is the ability to directly observe the growing neurons using time-lapse imaging as they extend their axons and respond to guidance cues *in situ* (O'Connor *et al.*, 1990; Sabry *et al.*, 1992, 1995; O'Connor and Bentley, 1993; Isbister and O'Connor, 1999). Using this system the behaviors of growth cones at precise locations in the Ti1 pathway have been analyzed to determine how neurons make steering decisions

(O'Connor *et al.*, 1990), and the role of differential adhesion in growth cone steering has been tested (Isbister *et al.*, 1999). In addition, microtubules (Sabry *et al.*, 1991, 1995) and actin dynamics (O'Connor and Bentley, 1993) have been imaged to examine the cytoskeletal dynamics that are important for neuronal growth and growth cone steering. This work has contributed, in part, to the basis of a variety of cytoskeletal models of growth cone guidance (O'Connor and Bentley, 1993; Tanaka and Sabry, 1995; Isbister and O'Connor, 2000). Presently we are developing this system to allow for the ectopic expression of recombinant proteins in T11 neurons.

V. Laboratory Protocols

A. Embryo Dissection

1. Under a dissecting microscope, in a 35-mm culture dish containing grasshopper saline (150 mM NaCl, 10 mM KCl, 4 mM CaCl₂, 2 mM MgSO₄, 5 mM TES, and 140 mM sucrose, pH 7.1), embryos are removed from their egg cases by puncturing the opposite end of the egg that contains the embryo to relieve pressure (the dark pigment at one end of the egg indicates the presence of an embryo); some yolk will be expelled from the egg.
2. Using micro scissors, the very tip of the end of the egg containing the embryo is cut off and the embryo is removed by applying gentle pressure to the center of the egg case. The embryo and some yolk will be expelled. Separate the embryo from the yolk and move embryo to a yolk-free area of the dish.
3. To allow access of culture media and reagents, the amniotic membrane is removed on the dorsal and ventral sides. This membrane is easiest removed by pinning the head or abdomen of the embryo with one set of forceps while running a second set of forceps along the midline of the animal to tear and remove the amnion.
4. Whenever embryos need to be transferred, the best method is to use a Pasteur pipette and gently pipette the embryos to their new location. Because the embryos will stick to the inside of the glass pipette, it is best to coat the inside of the pipette with grasshopper saline [containing 0.3% bovine serum albumen (BSA) or some egg yolk from the dissection dish] by pipetting up and down a few times before pipetting the embryos. This should be done every time embryos are pipetted.

B. Embryo Cultures

1. Prior to dissection, eggs are brushed clean in grasshopper saline and sterilized in 70% ethanol for 1 min followed by rinsing twice in sterile grasshopper culture medium [RPMI (Gibco-BRL), 4 μ M 20-hydroxyecdysone, 0.4 mM CaCl₂, 0.4 mM MgSO₄, 2 units/ml insulin, 100 units/ml penicillin, 100 μ g/ml streptomycin, 2 mM L-glutamine, 0.45 mM sodium pyruvate, 1 mM oxaloacetic acid, 0.45% D-glucose, 0.12 M sucrose, and 10 mM TES, pH 6.9].

2. Place eggs in fresh sterile culture media for dissection under a dissecting microscope in a laminar flow hood.

3. Using sterile technique, embryos are dissected as described earlier, except that when culturing, embryos should be dissected in grasshopper culture medium instead of grasshopper saline.

4. After dissection, embryos can be placed in a well of a 96-well culture dish. To assess the Ti1 pathway, embryos are cultured for 24 h, but can be cultured for as long as 48 h, with a change of culture medium after 24 h. Embryos are cultured in a 30°C incubator (without CO₂).

C. Immunocytochemistry

1. Embryos are dissected in grasshopper saline as described earlier.

2. Embryos are fixed by immersion in PEM-FA [0.1 M PIPES (pH 6.95) 2.0 mM EGTA, 1.0 mM MgSO₄, and 3.7% formaldehyde] for 30 min to 1 h.

3. Embryos are washed three times for 1 min and three times for 10 min in PBT [1× phosphate-buffered saline (PBS), 0.1% Triton X-100, 0.1% BSA].

4. Embryos are incubated overnight at 4°C in primary antibody. Dilutions ranging from 1:500 to 1:1200 are appropriate for both rabbit and goat anti-HRP (horseradish peroxidase) (depending on individual lots; Jackson ImmunoResearch).

5. After primary antibody incubation, embryos are again washed three times for 1 min and three times for 10 min in PBT.

6. Secondary antibodies are incubated for 1 h at room temperature, followed by three times for 1 min and three times for 10 min in PBT.

7. For mounting, we typically use the antifade reagent SlowFade (Molecular Probes).

8. In order to visualize the Ti1 pathway and the limb bud properly, further dissection of the embryos after labeling is employed. Embryos are pipetted gently on glass slides with a minimal amount of SlowFade antifade. Using forceps, separate the three pairs of limb buds gently by making incisions under each pair of limb buds across the width of the body and spreading out the pieces on the slide.

D. Preparation of Glass Bottom Culture Dishes for Microinjection and Time-Lapse Imaging

In order to culture and image filleted embryos, specialized culture dishes must be prepared in advance.

1. A 15-mm hole is bored into a 35-mm sterile polystyrene tissue culture dish using a drill press.

2. To ensure proper contact between the coverslip and the petri dish plastic, the edges of the hole are smoothed using sandpaper. The petri dish is then soaked briefly with 70% ethanol, rinsed with distilled water, and allowed to dry. Dishes can be sterilized further by overnight ultraviolet light exposure.

3. With the petri dish upside down, the outside of the hole is ringed with a melted mixture of beeswax and petroleum jelly (80:20), and then a rinsed round (22-mm diameter, No. 1) coverslip that has been pretreated with 5 mg/ml poly-L-lysine (see Section V,E) is placed on top of the wax so that the coverslip covers the hole.

4. Because the wax hardens rapidly, it is typically necessary to place the upside-down petri dish in an 80°C oven for 3–5 min to allow the wax to melt and seal the coverslip. Dishes prepared in this manner allow for visualization of the T1 neurons at high magnification on a compound microscope.

E. Preparation of Poly-L-Lysine-Coated Coverslips

1. Using sterile conditions, one drop of filter sterilized 5 mg/ml poly-L-lysine is placed into a 35-mm tissue culture dish.

2. A sterile 22-mm-round coverslip (number 1) is placed on top of the drop of poly-L-lysine.

3. Another drop of poly-L-lysine is placed on top of the coverslip, followed by another coverslip, and this process is repeated until the desired number of coated coverslips is achieved.

4. To avoid evaporation, the bottom of the tissue culture dish is filled with poly-L-lysine and is wrapped in Parafilm.

5. The coverslips are incubated at 37°C overnight followed by storage at 4°C. In general, the longer the coverslips are incubated at 4°C, the more adherent the coverslips become.

F. Filleting Grasshopper Limb Buds to Gain Access to the T1 Pathway

1. Sterilize and dissect embryos as described earlier and prepare a glass bottom dish.

2. Transect the embryo between the second and third limb pairs with forceps, retaining the third limb pair and tail for fillet. The transection can be made more anteriorly if it is desired to fillet the T1 or T2 limbs.

3. Using a glass pipette, transfer the embryo to the edge of the glass bottom dish filled with hopper saline.

4. At low magnification, pick up the embryo by the tail with forceps ventral side down and transfer onto the poly-L-lysine coverslip.

5. Let the tips of the limbs touch and attach, and then flip the abdomen 180° so that the ventral side is up. This ensures that the anterior surface of the limbs, and consequently the T1 neurons, is adjacent to the coverslip.

6. Dissection of the limb is carried out at high magnification using dark-field optics.

7. Using a tamp [a fire-polished pulled solid glass tube (1 mm diameter) that has been passed through the flame of a match to give it a smooth tip], ensure that the limbs are attached firmly to the coverslip by pressing them against the coverslip gently.

8. Using a sharp dissecting tip (a solid 1-mm-diameter glass needle that has been pulled on a gravity micropipette puller), a cut is made along the length of the limb down the center of the posterior epithelium (Fig. 5), being careful only to pierce the top epithelium. Each freshly pulled glass needle is sharp enough to finely cut two limbs. Pipettes should be repulled for additional use.

9. Using the tamp, roll out the epithelium flat on the coverslip and apply gentle pressure to the edges of the limb to promote adhesion to the coverslip (Fig. 5).

10. Changing to bright field, the mesoderm is discernible as an irregular mass of cells on top of a homogeneous layer of epithelium.

11. Using a micromanipulator, position a thin-walled, pulled micropipette (with a broken tip) over the limb and aspirate the mesoderm off using gentle suction with a mouth pipette (Fig. 5). Removal of all the mesoderm may require several passes.

12. Replace hopper saline with grasshopper culture medium.

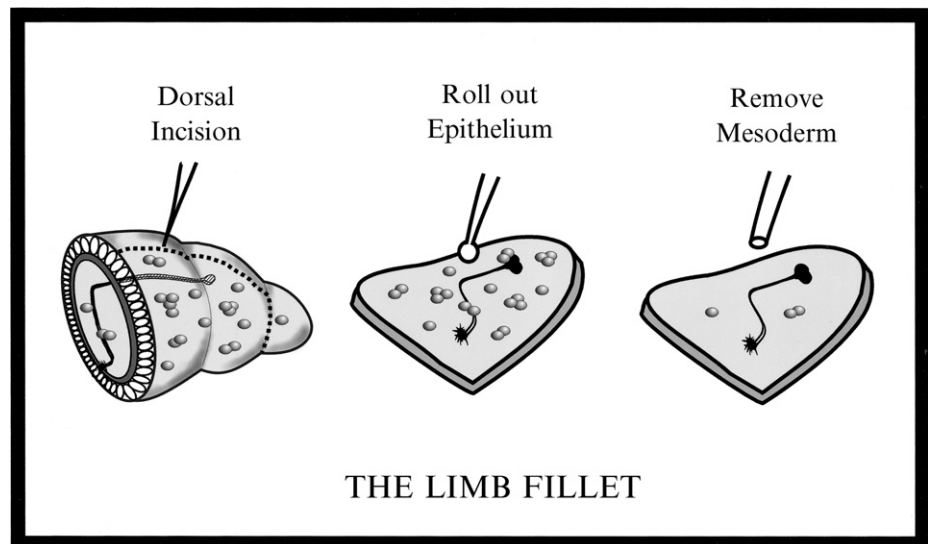


Fig. 5 Schematic representation of the limb fillet technique. An incision is made along the posterior aspect of the limb bud, and the limb epithelium is flattened. After removal of the mesoderm, the T11 pathway is exposed and can be visualized. See text for details.

G. Labeling and Injecting Ti1 Neurons *in Situ*

1. Limb fillets are prepared as described in Section V,F.
2. To label Ti1 cell membranes with a lipophilic dye (e.g., DiI or DiO), Ti1 cell bodies are located with Nomarski optics and then a dye-coated solid microelectrode is gently pushed up against the cell membrane using a micromanipulator. The electrode is left in contact with the Ti1 cell membrane for 10 s to 1 min, depending on the rate of transfer of dye from the electrode to the cell membrane.
3. Lipophilic dye-coated electrodes can be prepared a variety of ways; however, we find the following method to be the most reliable. A small solid piece of DiI or DiO (Molecular Probes) is placed in a small ($\sim 700 \mu\text{l}$) Eppendorf tube and 300–400 μl of distilled water is added. The tube is then sonicated for 3–4 min in a pen-cleaning sonicator until there is an even dispersal of the dye. While sonicating, 5–10 solid micropipettes are arranged with their tips converging at the same point. Approximately 10 μl of the sonicated dye is then placed on the pipette tips, and water is allowed to evaporate (15 to 20 min), resulting in a fine coating of dye. The solution of dye can be maintained in a -20°C freezer between applications; however, we find sonicating before application to be beneficial. In addition, coated pipettes become increasingly more effective with the frequency of coating.
4. Microinjection of Ti1 neurons is performed with a picospritzer. For the injection of large proteins and plasmids, we find that beveled electrodes are beneficial. In addition, because the electrode has to penetrate through the Ti1 cell membrane and the overlying basal lamina, we find that beveled electrodes do not clog as easily during injection attempts. Typically we find that a continuous flow at low pressure and a slight tap of the microscope will result in reliably injected cells. A disadvantage to this approach is that it is difficult to determine the volume of injected material.

H. Ectopic Overexpression in the Developing Limb Bud

1. Dissect embryos for culturing using sterile conditions as described and prepare a glass bottom dish.
2. For intact limbs, embryos are placed ventral side down onto an attached coverslip in a glass bottom dish filled with grasshopper culture medium as described earlier. The limbs are splayed away from the body wall. For filleted limbs, prepare as described previously.
3. Transfer transfected cells into a freshly pulled mouth micropipette (or, for a limb fillet, clustered cells can be transferred directly to the culture dish with a 10- μl pipette tip). We use thin-walled, 1-mm-diameter pulled micropipettes placed in a micromanipulator. The very tip is broken off to allow for the gentle expulsion of cells.

4. For intact limbs, insert the tip through the dorsal closure into a limb in a medial-to-lateral orientation. Cells are released into the limb with gentle pressure. Pipette placement and delivery of cells are monitored with a dissecting microscope.

5. For limb fillets, cells are expelled on, or near, the filleted limbs, and the clumps of cells are maneuvered individually with hand-held solid needles and tampers. This allows for precise placement of the cells along the T11 pathway. Cell placements are monitored with a dissecting microscope.

I. Blocking Protein Function

1. Antibodies

1. In general, antibodies should be affinity or IgG purified, followed by dialysis against grasshopper culture medium (see the aforementioned recipe). If desired, Fab fragments of antibodies can be prepared. The concentration of antibody used depends on numerous factors, including affinity for antigen and ability to bind *in vivo*. Previously, the 1–5 μM range has been effective at blocking.

2. Embryos are dissected and added to culture medium containing various concentrations of antibodies. Preliminary experiments using a range of antibody concentrations are used to establish the effective concentrations. Control antibodies should be used at the same concentrations and ideally should consist of antibodies generated to different regions of the same protein.

2. Peptides

1. Peptides are dissolved in sterile H₂O or suitable solvent.

2. It is assumed that peptides compete with endogenous protein activity. Effective concentrations vary and are generally established empirically.

Acknowledgments

We would like to thank members of the O'Connor lab for the critical reading of the manuscript. Work described in this chapter is supported by grants from the Canadian Institutes of Health Research (MOP-13246), the Natural Sciences and Engineering Research Council (OGP0171387) and the National Neurotrauma/Rick Hansen Institute (#99019990). TOC is an EJLB research scholar.

References

- Anderson, H., and Tucker, R. P. (1989). Spatial and temporal variation in the structure of the basal lamina in embryonic grasshopper limbs during pioneer neuron outgrowth. *Development* **106**, 185–194.
- Anderson, H., and Tucker, R. P. (1988). Pioneer neurones use basal lamina as a substratum for outgrowth in the embryonic grasshopper limb. *Development* **104**, 601–608.

- Bastiani, M. J., de Couet, H. G., Quinn, J. M., Karlstrom, R. O., Kotrla, K., Goodman, C. S., and Ball, E. E. (1992). Position-specific expression of the annulin protein during grasshopper embryogenesis. *Dev. Biol.* **154**, 129–142.
- Bastiani, M. J., Harrelson, A. L., Snow, P. M., and Goodman, C. S. (1987). Expression of fasciclin I and II glycoproteins on subsets of axon pathways during neuronal development in the grasshopper. *Cell* **48**, 745–755.
- Bentley, D., and Caudy, M. (1983). Pioneer axons lose directed growth after selective killing of guidepost cells. *Nature* **304**, 62–65.
- Bentley, D., Guthrie, P. B., and Kater, S. B. (1991). Calcium ion distribution in nascent pioneer axons and coupled preaxonogenesis neurons *in situ*. *J. Neurosci.* **11**, 1300–1308.
- Bentley, D., Keshishian, H., Shankland, M., and Toroian-Raymond, A. (1979). Quantitative staging of embryonic development of the grasshopper, *Schistocerca nitens*. *J. Embryol. Exp. Morphol.* **54**, 47–74.
- Bentley, D., and O'Connor, T. P. (1992). Guidance and steering of peripheral pioneer growth cones in grasshopper embryos. In “The Nerve Growth Cone” (P. C. Letourneau, S. B. Kater, and E. R. Macagno, eds.), pp. 265–281. Raven Press, New York.
- Bonner, J., Auld, V. J., and O'Connor, T. P. (2002). Migrating mesoderm establish a uniform distribution of laminin in the developing grasshopper embryo. *Dev. Biol.* **249**, 57–73.
- Bonner, J., and O'Connor, T. P. (2000). Semaphorin function in the developing invertebrate peripheral nervous system. *Biochem. Cell Biol.* **78**, 603–611.
- Bonner, J., and O'Connor, T. P. (2001). The permissive cue laminin is essential for growth cone turning *in vivo*. *J. Neurosci.* **21**, 9782–9791.
- Caudy, M., and Bentley, D. (1986). Pioneer growth cone morphologies reveal proximal increases in substrate affinity within leg segments of grasshopper embryos. *J. Neurosci.* **6**, 364–379.
- Cheng, Y. S., Champlaud, M. F., Burgeson, R. E., Marinkovich, M. P., and Yurchenco, P. D. (1997). Self-assembly of laminin isoforms. *J. Biol. Chem.* **272**, 31525–31532.
- Colognato, H., and Yurchenco, P. D. (2000). Form and function: The laminin family of heterotrimers. *Dev. Dyn.* **218**, 213–234.
- Condic, M. L., and Bentley, D. (1989a). Pioneer neuron pathfinding from normal and ectopic locations *in vivo* after removal of the basal lamina. *Neuron* **3**, 427–439.
- Condic, M. L., and Bentley, D. (1989b). Removal of the basal lamina *in vivo* reveals growth cone-basal lamina adhesive interactions and axonal tension in grasshopper embryos. *J. Neurosci.* **9**, 2678–2686.
- Condic, M. L., and Bentley, D. (1989c). Pioneer growth cone adhesion *in vivo* to boundary cells and neurons after enzymatic removal of basal lamina in grasshopper embryos. *J. Neurosci.* **9**, 2687–2696.
- Diamond, P., Mallavarapu, A., Schnipper, J., Booth, J., Park, L., O'Connor, T. P., and Jay, D. G. (1993). Fasciclin I and II have distinct roles in the development of grasshopper pioneer neurons. *Neuron* **11**, 409–421.
- Ganformina, M. D., Sanchez, D., Herrera, M., and Bastiani, M. J. (1999). Developmental expression and molecular characterization of two gap junction channel proteins expressed during embryogenesis in the grasshopper *Schistocerca americana*. *Dev. Genet.* **24**, 137–150.
- Ho, R. K., Ball, E. E., and Goodman, C. S. (1983). Muscle pioneers: Large mesodermal cells that erect a scaffold for developing muscles and motoneurons in grasshopper embryos. *Nature* **301**, 66–69.
- Isbister, C. M., and O'Connor, T. P. (1999). Filopodial adhesion does not predict growth cone steering events *in vivo*. *J. Neurosci.* **19**, 2589–2600.
- Isbister, C. M., and O'Connor, T. P. (2000). Mechanisms of growth cone guidance and motility in the developing grasshopper embryo. *J. Neurobiol.* **44**, 271–280.
- Isbister, C. M., Tsai, A., Wong, S. T., Kolodkin, A. L., and O'Connor, T. P. (1999). Discrete roles for secreted and transmembrane semaphorins in neuronal growth cone guidance *in vivo*. *Development* **126**, 2007–2019.
- Isbister, C. M., MacKenzie, P. J., To, K. C. W., and O'Connor, T. P. (2003). Gradient steepness influences the pathfinding decisions of neuronal growth *in vivo*. *J. Neurosci.* **23**, 193–202.

- Karlstrom, R. O., Wilder, L. P., and Bastiani, M. J. (1993). Lachesin: An immunoglobulin superfamily protein whose expression correlates with neurogenesis in grasshopper embryos. *Development* **118**, 509–522.
- Keshishian, H., and Bentley, D. (1983). Embryogenesis of peripheral nerve pathways in grasshopper legs. I. The initial nerve pathway to the CNS. *Dev. Biol.* **96**, 89–102.
- Klose, M., and Bentley, D. (1989). Transient pioneer neurons are essential for formation of an embryonic peripheral nerve. *Science* **245**, 982–984.
- Kolodkin, A. L., Matthes, D. J., O'Connor, T. P., Patel, N. H., Admon, A., Bentley, D., and Goodman, C. S. (1992). Fasciclin IV: Sequence, expression, and function during growth cone guidance in the grasshopper embryo. *Neuron* **9**, 831–845.
- Lau, P. M., Zucker, R. S., and Bentley, D. (1999). Induction of filopodia by direct local elevation of intracellular calcium ion concentration. *J. Cell Biol.* **145**, 1265–1275.
- O'Connor, T. P. (1999). Intermediate targets and segmental pathfinding. *Cell. Mol. Life Sci.* **55**, 1358–1364.
- O'Connor, T. P., and Bentley, D. (1993). Accumulation of actin in subsets of pioneer growth cone filopodia in response to neural and epithelial guidance cues *in situ*. *J. Cell Biol.* **123**, 935–948.
- O'Connor, T. P., Duerr, J. S., and Bentley, D. (1990). Pioneer growth cone steering decisions mediated by single filopodial contacts *in situ*. *J. Neurosci.* **10**, 3935–3946.
- Sabry, J. H., O'Connor, T. P., Evans, L., Toroian-Raymond, A., Kirschner, M., and Bentley, D. (1991). Microtubule behavior during guidance of pioneer neuron growth cones *in situ*. *J. Cell Biol.* **115**, 381–395.
- Sabry, J., O'Connor, T. P., and Kirschner, M. W. (1995). Axonal transport of tubulin in Til pioneer neurons *in situ*. *Neuron* **14**, 1247–1256.
- Sanchez, D., Ganfornia, M. D., and Bastiani, M. J. (1995). Developmental expression of the lipocalin Lazarillo and its role in axonal pathfinding in the grasshopper embryo. *Development* **121**, 135–147.
- Seaver, E. C., Carpenter, E. M., and Bastiani, M. J. (1996). REGA-1 is a GPI-linked member of the immunoglobulin superfamily present on restricted regions of sheath cell processes in grasshopper. *Development* **122**, 567–578.
- Singer, M. A., Hortsch, M., Goodman, C. S., and Bentley, D. (1992). Annulin, a protein expressed at limb segment boundaries in the grasshopper embryo, is homologous to protein cross-linking transglutaminases. *Dev. Biol.* **154**, 143–159.
- Singer, M. A., O'Connor, T. P., and Bentley, D. (1995). Pioneer growth cone migration in register with orthogonal epithelial domains in the grasshopper limb bud. *Int. J. Dev. Biol.* **39**, 965–973.
- Tanaka, E., and Sabry, J. (1995). Making the connection: Cytoskeletal rearrangements during growth cone guidance. *Cell* **83**, 171–176.
- Timpl, R., and Brown, J. C. (1996). Supramolecular assembly of basement membranes. *Bioessays* **18**, 123–132.
- Wong, J. T., Wong, S. T., and O'Connor, T. P. (1999). Ectopic semaphorin-1a functions as an attractive guidance cue for developing peripheral neurons. *Nature Neurosci.* **2**, 798–803.
- Wong, J. T., Yu, W. T., and O'Connor, T. P. (1997). Transmembrane grasshopper semaphorin I promotes axon outgrowth *in vivo*. *Development* **124**, 3597–3607.
- Yurchenco, P. D., and Furthmayr, H. (1984). Self-assembly of basement membrane collagen. *Biochemistry* **23**, 1839–1850.
- Yurchenco, P. D., Tsilibary, E. C., Charonis, A. S., and Furthmayr, H. (1985). Laminin polymerization *in vitro*: Evidence for a two-step assembly with domain specificity. *J. Biol. Chem.* **260**, 7636–7644.

This Page Intentionally Left Blank

CHAPTER 11

Techniques to Dissect Cellular and Subcellular Function in the *Drosophila* Nervous System

Heinrich J. G. Matthies and Kendal Broadie

Department of Biological Sciences
Vanderbilt University
Nashville, Tennessee 37235

- I. Introduction
 - II. Background Sources of Information
 - III. *Drosophila* as a Genetic Model System for Molecular Neurobiology
 - A. Rapid Reverse Genetic Approaches for Initial Assessment of Gene Function
 - B. Generation of Mutations in a Gene of Interest
 - IV. Biochemistry of the *Drosophila* Nervous System
 - V. Cell Biology Techniques in the *Drosophila* Nervous System
 - A. The *Drosophila* Life Cycle
 - B. Protein Expression Studies with Immunocytochemistry
 - C. Transgenic Protein Expression Studies
 - D. Clonal Techniques for Mutant Analyses
 - VI. Functional Analysis Techniques in the *Drosophila* Nervous System
 - A. Imaging and Manipulating Calcium Levels in *Drosophila* Neurons
 - B. Monitoring Membrane Dynamics with Stryl Dyes
 - C. Monitoring Protein Dynamics in Living *Drosophila* Neurons
 - VII. *Drosophila* Electrophysiology
 - A. Recording from Cultured Neurons
 - B. Recording from the Neuromuscular Junction
 - C. Recording from Central Motor Neurons
 - D. The Characterized *Drosophila* Circuit: Giant Fiber System
 - E. Recording from Sensory Systems
 - F. Future Directions: Recording from the Adult Brain
- References

I. Introduction

Drosophila melanogaster has been a fruitful model for studying neurobiology, greatly increasing our understanding of neuronal fate determination, pathfinding, synapto-(genesis), ion channel function, neurotransmission (endocytosis and exocytosis), and synaptic plasticity. The primary strength of the *Drosophila* system is the ability to identify new molecules by systematic forward genetic screens; the only other model system where this approach is fully developed is *Caenorhabditis elegans*. The blind mutagenesis approach produces mutants in a process or pathway of interest without any bias based on preconceived ideas and is only limited by the speed and precision of the mutant screen (for review, see St. Johnston, 2002). A complementary approach, called reverse genetics, disrupts the activity of known proteins by the directed mutagenesis of genes (for review, see Adams and Sekelsky, 2002). In the past few years, much more rapid reverse genetic approaches have begun to be developed in *Drosophila*, including putative methods for targeted gene disruption (Rong and Golic, 2000; 2001; Bibikova *et al.*, 2002) and RNA interference (RNAi; Kennerdell and Carthew, 1998; Misquitta and Patterson, 1999; Carthew *et al.*, 2001; Schmid *et al.*, 2002; Eaton *et al.*, 2002; Allikian *et al.*, 2002; Giordano *et al.*, 2002). These new approaches allow more rapid tests of targeted gene function. Once mutants are generated, the fly nervous system is amenable to a wide range of cell biology approaches to elucidate the function of the gene product. A particularly powerful benefit of the *Drosophila* system is the ability to work with individually identified neurons, or small populations of neurons, derived through a known developmental lineage (Doe, 1992; Luer and Technau, 1992; for review, see Doe and Technau, 1993; Bossing and Technau, 1994; Bossing *et al.*, 1996a,b; Chu-LaGraff *et al.*, 1991, 1993, 1995; Landgraf *et al.*, 1997; Schmidt *et al.*, 1997, 2000; Schmid *et al.*, 1999). This chapter provides an overview of how an investigator can move from mutant to gene to gene product function using *Drosophila* as a genetic model system for cellular neurobiology. This chapter provides an outline of the resources and experimental approaches available to the *Drosophila* neurobiologist. Selected methods of particular interest are discussed in detail and protocols are provided.

II. Background Sources of Information

A number of volumes have been written about fly development, genetics, husbandry, and general molecular/cellular protocols (listed in Table I). The primary references are provided here: (1) "The Genome of *Drosophila melanogaster*," by Lindsley and Zinn; (2) "*Drosophila*: A Laboratory Manual" and "*Drosophila*: A Laboratory Handbook," both by Ashburner; (3) "*Drosophila*, A Practical Approach," edited by D. B. Roberts; (4) Fly Pushing: The Theory and Practice of *Drosophila* Genetics by R. J. Greenspan; (5) "The Embryonic Development of *Drosophila melanogaster*," by J. A. Campos-Ortega and V. Hartenstein; (6) a two

Table I
List of Important Resources for *Drosophila melanogaster*

-
- Books: Comprehensive information about *Drosophila* development, genetics, husbandry, and protocols
- “The Genome of *Drosophila melanogaster*,” by L. Lindsley and G. G. Zimm (1992)
 - “*Drosophila*: A Laboratory Manual,” edited by M. Ashburner (1989)
 - “*Drosophila*: A Laboratory Handbook,” edited by M. Ashburner (1989)
 - “*Drosophila*, a Practical Approach,” edited by D. B. Roberts, (1998)
 - “Fly Pushing: The Theory and Practice of *Drosophila* Genetics,” by R. J. Greenspan (1997)
 - “The Embryonic Development of *Drosophila melanogaster*,” by J. A. Campos-Ortega and V. Hartenstein (1998)
 - “The Development of *Drosophila melanogaster*,” Vol. I and II, edited by M. Bate and A. Martinez Arias, (1993)
 - “*Drosophila melanogaster*: Practical Uses in Cell and Molecular Biology,” edited by L. S. B. Goldstein and E. A. Fyrberg (1994)
 - “*Drosophila* Protocols,” edited by W. Sullivan, M. Ashburner and R. S. Hawley (2000)
- Specific chapters on *Drosophila* neurobiological techniques
- In “*Drosophila* Protocols,” edited by W. Sullivan, M. Ashburner, and R. Scott Hawley, (2000).
 - H. Bellen and V. Budnik: The Neuromuscular Junction
 - T. Wolff: Histological Techniques for the *Drosophila* Eye. Part I: Larva and Pupa
 - T. Wolff: Histological Techniques for the *Drosophila* Eye. Part II: Adult
 - K. S. Broadie: Electrophysiological Approaches to the Neuromusculature
 - K. S. Broadie: Functional Assays of the Peripheral and Central Nervous Systems
 - S. Sweeney, A. Hidalgo, J. S. deBelle, and H. Keshishian: Functional Cell Ablation
 - J. Hirsch: Exposing *Drosophila* to Neuroactive Drugs
 - In “*Drosophila*: A Practical Approach,” edited by D. B. Roberts (1998)
 - Connolly, J. G., and T. Tully: Behaviour, Learning, and Memory.
 - In “*Drosophila melanogaster*: Practical Uses in Cell and Molecular Biology,” edited by L. S. B. Goldstein and E. A. Fyrberg (1994)
 - N. H. Patel: Imaging Neuronal Subsets and Other Cell Types in Whole-Mount *Drosophila* Embryos and Larvae Using Antibody Probes
- Specific volumes and chapters on *Drosophila* developmental neurobiology
- “Neuromuscular Junctions in *Drosophila*,” edited by V. Budnik and L. S. Gramates (1999)
 - In “The Development of *Drosophila melanogaster*,” Vol. I, edited by M. Bate and A. Martinez Arias (1993)
 - M. Bate.: The Mesoderm and Its Derivatives
 - C. S. Goodman and C. Q. Doe: Embryonic Development of the *Drosophila* Central Nervous System
 - Y. N. Jan and L. Y. Jan: The Peripheral Nervous System
- Useful internet sites
- <http://flybase.bio.indiana.edu/>
 Extensive information about *Drosophila* biology and research. Information on maps, genes, proteins, alleles, stocks, vectors, and references; addresses for researchers in the fly community
 - <http://www.fruitfly.org/>
 Berkeley *Drosophila* Genome Project (BDGP). Information about the genomic projects at the center and how to obtain reagents, including ESTs, genomic clones, and multiple P-element collections. Also a site for *Drosophila* protocols
 - <http://edgp.ebi.ac.uk/>
 European *Drosophila* Genome Project (EDGP). Information about the genomic projects at the center and how to obtain reagents, including ESTs, genomic clones, and multiple P-element collections. Also a site for *Drosophila* protocols
-

(Continues)

Table I (Continued)**List of Important Resources for *Drosophila melanogaster***

http://flybrain.neurobio.arizona.edu/
Interactive site specializing in anatomy of the fly brain
http://flybrain.uni-freiburg.de/Flybrain/html/atlas/index.html
Interactive site specializing in anatomy of the fly brain
http://flybrain.nibb.ac.jp/
Interactive site specializing in anatomy of the fly brain
http://www.fly-trap.org/
Searchable database for expression patterns of Gal4 lines
http://www.its.caltech.edu/~zinnlab/motoraxons/fma%20home%20page.html
Anatomy, development, and methods for <i>Drosophila</i> neuromuscular junction; Kai Zinn web page
http://www.neuro.uoregon.edu/doelab/doelab.html
A description of neuroblast maps and lineages, including 3D and DiI labeling; Chris Doe web page
http://www.biochem.northwestern.edu/carthew/manual/Manual.html
Carthew laboratory protocols, including RNAi in <i>Drosophila</i> embryos; Richard Carthew web page

volume set “The Development of *Drosophila melanogaster*,” edited by M. Bate and A. Martinez Arias; (7) “*Drosophila melanogaster*: Practical Uses in Cell and Molecular Biology,” edited by L. S. B. Goldstein and E. A. Fryberg; and (8) “*Drosophila* Protocols,” edited by W. Sullivan, M. Asburner, and R. S. Hawley. Several of these sources have chapters written specifically about *Drosophila* neurobiological techniques, including (1) a chapter on immunocytochemistry of subsets of neurons (“*Drosophila melanogaster*: Practical Uses in Cell and Molecular Biology,” edited by L. S. B. Goldstein and E. A. Fryberg); (2) a chapter on immunocytochemistry at the neuromuscular junction (H. J. Bellen); (3) two chapters on histological techniques for the eye (T. Wolff); (4) two chapters on electrophysiological techniques at the neuromuscular junction (NMJ) and the central nervous system (CNS) (K. Broadie); (5) a chapter on neuronal cell ablation (S. Sweeney *et al.*); and (6) a chapter on exposing *Drosophila* to neuroactive drugs (J. Hirsch). These latter five chapters are all in “*Drosophila* Protocols,” edited by W. Sullivan, M. Asburner, and R.S. Hawley. These chapters give extensive detail about many methods used by fly neurobiologists. A review of various aspects of the most commonly used neuronal system in flies, the neuromuscular junction, may be found in “Neuromuscular Junctions in *Drosophila*,” edited by V. Budnik and L. S. Gramates.

An online database about *Drosophila* can be found at <http://flybase.bio.indiana.edu/>, which contains extensive information about many aspects of *Drosophila* biology and research. Information about maps, genes, proteins, alleles, stocks, vectors, and references can be found at this site, as well as addresses for people in the fly community. Different information can be found at the Berkeley *Drosophila* Genome Project (BDGP, <http://www.fruitfly.org/>) and European *Drosophila* Genome Project (EDGP, <http://edgp.ebi.ac.uk/>). These sites contain information about the genomic projects at these centers and information about obtaining

various reagents, including expressed sequence tags (ESTs), genomic clones, and multiple P-element collections. These sites also host an array of *Drosophila* protocols.

III. *Drosophila* as a Genetic Model System for Molecular Neurobiology

The entire genome of *Drosophila* has been sequenced (Adams *et al.*, 2000), and EST cDNAs are available from multiple libraries representing different stages of development (BDGP, <http://www.fruitfly.org/>). The availability of both genomic sequence and cDNA clones has increased the efficiency of forward and reverse genetic approaches (for review, see Adams and Sekelsky, 2002). Mutant screens for novel genes remain a primary tool of *Drosophila* neurobiologists (for examples of reviews, see Broadie, 1998; Garcia-Alonso, 1999; Wager-Smith and Kay, 2000; Featherstone and Broadie, 2000; Waddell and Quin, 2000; Sokolowski, 2001; Jin, 2002; for general review about the methods and rationale of *Drosophila* screens, see St. Johnston, 2002). Screens involve mutagenizing the genome with transposable elements (e.g., P-element), chemical mutagens or ionizing radiation, and screening for desired phenotypes. A new method of screening is through the use of a double element consisting of a transposable element (Hobo) bracketed by two genetic markers all in a “carrier” P element (Huet *et al.*, 2002). Once in flies, it can be mobilized to make nested deletions, and is desirable because it does not suffer from the site specificity of P-element insertion (Spradling *et al.*, 1999). Comprehensive collections of deletions spanning the genome are continually being developed for mapping genomic regions and to allow a focus on smaller regions of interest (Huet *et al.*, 2002).

P-element-generated mutants allow one to rapidly identify the relevant gene, as many versions of P-elements have been designed to make it relatively simple to recover the genomic sequences flanking the site of insertion [for details, see the two chapters by Wolfner and Goldberg (1994) and by Hamilton and Zinn (1994), a chapter by Huang *et al.*, (2000), sections of the book by R.J. Greenspan, Adams, and Sekelsky, (2002) and the BDGP, <http://www.fruitfly.org/>]. However, new methods for identifying the site of chemically induced mutations, which are less time-consuming, are currently being refined (Bentley *et al.*, 2000; Teeter *et al.*, 2000; Hoskins *et al.*, 2001; Berger *et al.*, 2001). A recently developed method that is particularly sensitive, but relatively expensive, is called denaturing high-performance liquid chromatography (DHPLC) and is based on polymerase chain reaction (PCR) analyses of heterozygous flies leading to both homoduplexes and heteroduplexes of the mutagenized regions (Bentley *et al.*, 2000). The heteroduplexes have altered heat stability and are separated on an HPLC column at the temperature causing partial denaturation. This method is reliable but requires a large investment of equipment. Another method of mapping mutants is called single

nucleotide polymorphism (SNP) mapping, and a description of the project developing this method may be found at BDGP (<http://www.fruitfly.org/SNP/index.html>). This method is in the process of rapid development in *Drosophila* (Teeter *et al.*, 2000; Hoskins *et al.*, 2001; Berger *et al.*, 2001; Martin *et al.*, 2001) and relies on single base pair polymorphisms between specific laboratory strains of flies.

A. Rapid Reverse Genetic Approaches for Initial Assessment of Gene Function

Although forward genetic screens are a real power of *Drosophila*, the detailed knowledge of the genome is rapidly increasing the need for and use of reverse genetic methods to test the function of genes previously identified in vertebrates or through the analysis of human diseases (for review, see Link, 2001). Several approaches can be used to determine if a target gene is involved in a process of interest. First, one may look to see if a mutant strain already exists by searching available stocks at *Drosophila* stock centers (<http://flybase.bio.indiana.edu/stocks/>). Because cDNAs can be obtained (or generated) easily, *in situ* RNA hybridization (Tautz and Pfeifle, 1989; Lehman and Tautz, 1994) will quickly tell one where and when the gene is expressed in the nervous system. Second, a tool recently developed to rapidly assess the function of a gene is RNA interference (RNAi) (Fire *et al.*, 1999; Kennerdell and Carthew, 1998; Misquitta and Patterson, 1999; Li *et al.*, 2000; Wianny and Zernicka-Goetz, 2000; for review, see Sharp, 2001; Fjose *et al.*, 2001; Schmid *et al.*, 2002; Hutvagner and Zamore, 2002). RNAi effectively silences genes at a posttranscriptional stage. Application of double-stranded RNA (dsRNA) corresponding to a single gene leads to the enzymatic degradation of the relevant mRNA having the same sequence. This technique was first used in *C. elegans* and more recently in several other organisms (Fire *et al.*, 1999; Kennerdell and Carthew, 1998; Li *et al.*, 2000; Wianny and Zernicka-Goetz, 2000). Bathing (Eaton *et al.*, 2002) or injection of double-stranded RNA into embryos (Misquitta and Patterson, 1999) or even adult abdomens (Dzitoyeva *et al.*, 2001) can quickly give preliminary data indicating the likelihood of a gene playing a neurobiological role. RNAi can also be used via transgenic methods; however, it takes months to create the flies and is not always as reliable as classical mutants, but it does allow for tissue-specific RNAi dissection (Lam and Thummel, 2000; Kennerdell and Carthew, 2000; Fortier and Belote, 2000; Piccin *et al.*, 2001; Allikian *et al.*, 2002; Kalidas and Smith, 2002; see later).

A chapter outlining the technique of RNAi injection can be found in Misquitta and Patterson (2000). An example of a test of the rapid injection approach has been described by Schmidt *et al.* (2002). In this study, the role of five neural receptor tyrosine phosphatases (RTP) in axon development was tested by injecting various combinations of double-stranded RNAs into embryos and subsequent injection of a lipophilic dye (DiI) into identified neuroblasts. This allowed visualization of identified neurons derived from known progenitors and the effects

of RPTP RNAi on these cells. These experiments were particularly beneficial because mutations in three of the five RPTPs are embryonic lethal and the other two show no phenotype. This method allowed them to easily address the issue of functional redundancy. Using RNAi, quadruple mutants were generated, allowing the demonstration that all four RPTPs play a role in axon guidance. In this report, it was clear that identifying the correct dose of RNAi to yield high efficiency of gene silencing and at the same time avoiding nonspecific toxic effects is not trivial. Additionally, this method relies on protein turnover to approach a “protein null” phenotype at the time when one observes the RNAi-treated cell. For these reasons, among others, the next step after this type of RNAi experiment should be to generate or obtain mutants of the relevant gene(s).

More recently, several laboratories have used RNAi by transgenic methods to assay function for a given gene because injected dsRNA does not interfere reliably with gene function later in development (Lam and Thummel, 2000; Kennerdell and Carthew, 2000; Fortier and Belote, 2000; Piccin *et al.*, 2001; Allikian *et al.*, 2002; Kalidas and Smith, 2002). This allows for efficient targeting of RNAi in adult tissues. This new method depends on the creation of transgenic flies carrying constructs that drive the transcription of RNAs with inverted repeats separated by a linker, such as an intron. These RNAs then fold back on themselves to form dsRNA molecules. Expression of the dsRNA can be driven by the Gal4UAS system described later. The Gal4UAS system drives expression in a tissue-specific manner, and recent permutations allow for finer temporal regulation of expression (Bieschke *et al.*, 1998; Bello *et al.*, 1998; Osterwalder *et al.*, 2001; Roman *et al.*, 2001; Stebbins and Yin, 2001; Stebbins *et al.*, 2001; Landis *et al.*, 2001). These newer methods rely on the control of transcription by agents fed to flies, such as RU486 or doxycycline, and therefore allows for the timing of RNAi expression to be controlled temporally and spatially in a dose-dependent manner (Allikian *et al.*, 2002).

B. Generation of Mutations in a Gene of Interest

There are several standard methods of generating mutants, each with its own advantages and disadvantages. Many P-element collections exist, and information regarding these lines is available via a searchable database at BDGP [for a review of methods, see chapter by Mistra *et al.*, (2000) and review by Adams and Sekelsky (2002)]. Standard methods can be used to mobilize a P-element into your gene or generate precise/imprecise P-element excisions [for details, see the two chapters by Wolfner and Goldberg (2000), by Hamilton and Zinn (2000), sections in R. J. Greenspan’s book and Adams and Sekelsky (2002)]. However, occasionally the insertion of a P-element into a particular gene occurs with very low frequency because P-elements display a bias for certain sequences (Spradling *et al.*, 1999). In the event that this occurs, larger deletions can be made from the sites of nearby insertions (Adams and Sekelsky, 2002), but the risk is that other genes are likely to be deleted. Precise excisions restore the original sequence and are critical because

they demonstrate that the observed phenotype is due to the P-element insertion; imprecise excisions generate mutants ranging from nulls to hypomorphs (reduced function). A note of warning: one has to be careful with any P-element line, as a P-element can be mobilized more than once in the germ line, thereby disrupting the function of another gene that may not be easy to identify. Thus, the best policy is to outcross the mutant line with a wild-type reference line that should eliminate second site hits. Generally, P-elements insertions lead to hypomorphs or mutants with low gene activity because of the tendency of P-elements to insert into 5' regions, leading to reduced expression (Spradling *et al.*, 1999). Typically, imprecise excisions of P-elements result in null alleles.

Chemical mutagen-induced point mutations are more likely to generate informative hypomorphs and null alleles. Classical methods of mutagenesis in flies have relied on either chemical mutagens or ionizing radiation [for radiation methods, see Sankaranarayanan and Sobels (1976) and Grigliatti (1998); for chemical mutagens, see Lee (1976), Grigliatti (1998), and Adams and Sekelsky (2002)]. Chemical mutagens [ethyl methanesulfonate (EMS) or, more recently, *N*-ethyl-*N*-nitrosourea (ENU)] tend to give point mutations, whereas irradiation gives deletions and other chromosomal aberrations. ENU (Vogel and Natarajan, 1979; Batzer *et al.*, 1998; Lee *et al.*, 1990) has gained popularity because it produces fewer translocations and appears to be more potent than EMS (Vogel and Natarajan, 1979; Lee *et al.*, 1990). Both EMS and ENU are very useful because these mutagens yield high mutation rates with a high probability of hitting any given gene. Therefore, the frequency of mutagenizing any particular gene depends essentially on the size of the gene, unlike P-elements, which insert into distinct "hot spots" (Spradling *et al.*, 1999). Chemical mutagens generally do lead to mutations at specific bases, but these bases are found in all genes. Another advantage of chemical mutagens is that one can potentially identify unknown critical domains in a protein by identifying point mutations by sequence analysis. Ionizing radiation produces a full spectrum of mutations, including deletions (Sankaranarayanan and Sobels, 1976; Grigliatti, 1998). It might be best used as a method of generating deletions in a gene in which it is difficult to obtain a P-element in the region.

Another method of generating a mutation in a gene of choice is by using random mutagenesis on flies heterozygous for a deficiency spanning the region covering the gene and then screening for a predicted phenotype. Flies have been treated by various means leading to chromosomal aberrations, including those with deletions of portions of chromosomes (deficiencies, Gubb, 1998). Flies carrying deficiencies covering the genome (deficiency kit) can be found by searching Flybase and are available from the Bloomington stock (<http://flystocks.bio.indiana.edu/>). These methods using deletions rely on being able to predict the mutant phenotype (Saxton *et al.*, 1991; Renden *et al.*, 2001) or detecting the loss of or modification of the protein by Western blotting (Katz *et al.*, 1988; Van Vactor *et al.*, 1988; Dolph *et al.*, 1993).

IV. Biochemistry of the *Drosophila* Nervous System

Although genetics is the well-known strength of *Drosophila*, biochemical studies are feasible in this system and represent a vital research avenue. The quantities of neuronal/brain extract required for many biochemical studies can be readily obtained from flies. Initially, fly head extracts were used to study the biochemical, pharmacological, and electrical properties of various ion channels previously identified and characterized in vertebrate systems (Schmidt-Nielson *et al.*, 1977; Pauron *et al.*, 1987; Pelzer *et al.*, 1989). The idea was to verify the similar nature of the *Drosophila* proteins and then to identify the *Drosophila* gene and generate mutants. In other studies, enzyme activity was measured in head extracts to verify the biochemical nature of mutants [e.g., (dnc) Byers *et al.*, 1981; (rdgA) Inoue *et al.*, 1989; (norpA) Inoue *et al.*, 1985; Toyoshima *et al.*, 1990]. More recently, head extracts have been used for many purposes, including identifying proteins playing roles in synaptic transmission (Schulze *et al.*, 1994; van de Goor *et al.*, 1995; Littleton *et al.*, 1998; Phillips *et al.*, 2000), enzyme activity (glutamic acid decarboxylase; Phillips *et al.*, 1993; Featherstone *et al.*, 2000), and RNA metabolism (Zhang *et al.*, 2001). This section describes the method used to generate adult head extracts, first published by the Hall laboratory (Schmidt-Nielson *et al.*, 1977).

Briefly, flies (~1 mg/fly) are frozen, and heads (~0.1 mg/head) are collected, homogenized, and then centrifuged as detailed later. This preparation is advantageous because reasonably large quantities of neuronal tissue can be obtained. One disadvantage of this preparation is that a large portion of the material is of retinal origin rather than from other regions of the brain. To circumvent this problem, one may utilize mutants (e.g., *eya* mutants), which lack compound eyes (although ocelli are present; Stark *et al.*, 1993; Bonini *et al.*, 1998). However, a substantial portion of the fly brain is the optic lobe, and in flies lacking eyes, these neurons are presumably less active, which could be a problem if the biochemical property of interest is regulated by neuronal activity. Another method exists that involves freeze drying using acetone, lyophilization, and the manual separation of eyes and heads (Fujita *et al.*, 1987). This method was used to demonstrate that a substantial portion of the total phosphatidic acid is found in eyes as opposed to the remaining tissue (Fujita *et al.*, 1987). In a later study of *rdgA*, a mutation in a diacylglycerol kinase, the surprising result was obtained that the substrate (diacylglycerol) levels are normal, while as predicted the level of the product (phosphatidic acid) is reduced. By using the freeze-drying method, the authors demonstrated that this effect of the mutation on phosphatidic acid levels was due to altered phospholipid metabolism in the eye. A take-home message of this study is that the biochemical analysis of flies carrying a mutation in a gene with a predicted function can be beneficial for identifying the true basis of the phenotype (Inoue *et al.*, 1989). This procedure involves freezing flies in a flask with acetone, anhydrous Na₂SO₄, and liquid nitrogen. This flask is then moved to a freezer (−20 to −25°C) for several days and allowed to dry at room temperature. Under these conditions, the eyes are

separated readily from the head, and the quantitative recovery of both proteins and lipids has been demonstrated (Fujita *et al.*, 1987). Many enzymes are not active under these conditions, as the acetone removes the water, yielding most enzymes inactive until one rehydrates the sample. This allows more time for the dissection; however, less material is readily obtained because manual dissection is time-consuming. This method will not necessarily be useful for all procedures but is ideal for lipid biochemistry, especially if the wild-type gene is specifically expressed in either the eye or the brain. In this case, if the substrate of the mutant gene is a molecule(s) that exists and is metabolized in both tissues, then this method allows one to study the effect of the gene on the relevant neuronal tissue in isolation. However, some enzymes do not recover full activity after the acetone treatment and rehydration (Fujita *et al.*, 1987).

A powerful tool for fly neurobiologists is the use of temperature-sensitive paralytics (Suzuki *et al.*, 1971; Grigliatti *et al.*, 1973; Siddiqi and Benzer, 1976). Some examples mutants are in channels upstream of the synaptic cycle or in components of the synaptic vesicle cycle. Some examples include temperature-sensitive alleles of cacophony (α 1-calcium channel subunit, von Schilcher, 1976, 1977; Heisenberg and Götz, 1975; Homyk and Pye, 1989; Smith *et al.*, 1996, 1998; Kawasaki *et al.*, 2002), para (sodium channel subunit; Suzuki *et al.*, 1971), shibire (dynamin; Poodry *et al.*, 1973; Poodry and Edgar, 1979; Koenig and Ikeda, 1989; Poodry, 1990; Kawasaki *et al.*, 2000), comatose (NSF; Ordway *et al.*, 1994; Pallanck *et al.*, 1995; Kawasaki *et al.*, 1998; Littleton *et al.*, 1998), and syntaxin (Littleton *et al.*, 1998). Use of the aforementioned mutants allow one to arrest the synaptic vesicle cycle at various stages (van de Goor *et al.*, 1995; Phillips *et al.*, 2000; Littleton *et al.*, 1998). Using these mutants, flies are shifted to the restrictive temperature (typically 37°C but in some cases 29°C) and fractionated, and the subcellular fractionation pattern the protein of interest is determined. These experiments can be used to begin to decipher at which stage of the vesicle cycle a protein functions (Littleton *et al.*, 1998, 2001). Flies carrying the shibire mutation have been used most frequently in this method. Shibire codes for a temperature-sensitive mutant version of dynamin, a GTPase with a major role in endocytosis (Poodry *et al.*, 1973; Poodry and Edgar, 1979; Koenig and Ikeda, 1989; Poodry, 1990; Kawasaki *et al.*, 2000a,b). When active neurons carrying the shibire mutation are shifted to the restrictive temperature, synaptic vesicles continue to fuse with the plasma membrane but can no longer be endocytosed. This leads to a depletion of synaptic vesicles and accumulation of synaptic vesicle proteins in the plasma membrane. One example of using this tool has been described by Phillips *et al.* (2000). In this study, the authors sought to determine if stonedB, a protein with a role in vesicle recycling (Stimson *et al.*, 1998; Fergestad *et al.*, 1999), bound to synaptic vesicles before or after endocytosis (Phillips *et al.*, 2000). Previous publications indicated that Stoned was likely to be involved in the synaptic vesicle endocytic pathway and that stonedB is enriched in the P3 fraction, which contains synaptic vesicles (Stimson *et al.*, 1998; Fergestad *et al.*, 1999). The hypothesis was that stonedB associates with synaptic vesicles after endocytosis.

The authors reasoned that if this were the case, stonedB should not be found on vesicles in heat-treated shibire mutants. They took advantage of the use dependency of shibire. Because shibire blocks exocytosis only after endocytosis, shibire only blocks in a use-dependent manner (Salkoff and Kelly, 1978; Salkoff, 1979). If flies are heat shocked in the dark, the visual system will not be depleted of synaptic vesicles, but neurons communicating with other sensory systems will be depleted of synaptic vesicles. However, if stonedB only associates with recycling vesicles, one would expect to see stonedB fail to associate with synaptic vesicles. Contrary to the expectation, in dark-adapted heat shock-treated flies, stonedB remained associated with synaptic vesicles. This study indicated that stonedB associates with synaptic vesicles prior to exocytosis. These studies also indicate that when one uses shibire, one must be aware of the level of synaptic activity in the shibire neuron (Salkoff and Kelly, 1978; Salkoff, 1979; Phillips *et al.*, 2000).

Changes in neuronal activity can alter a biochemical process or protein function. One can purposely alter neuronal activity in flies by using mutants in potassium channels such as double mutants of ether a go-go (*eag*) and *Sh* (Shaker), which cause hyperactivity in most of the nervous system (for review, see Wu and Ganetzky, 1992). Reduced activity in select neurons can be achieved using transgenic flies that express a mutagenized Shaker potassium channel (White *et al.*, 2001a,b; Osterwalder *et al.*, 2001) via an inducible GAL4/UAS system. Other ways of selectively reducing neuronal activity are to express the temperature-sensitive version of shibire (Kitamoto, 2001) or tetanus toxin (Sweeney *et al.*, 1995) under control of the GAL4/UAS system. The benefit of these inducible GAL4/UAS systems is that one can feed the inducing agent to the adult fly, allowing development to advanced stages so that head extracts could be generated.

Flies have been used to study proteins involved in the synaptic vesicle cycle (for reviews, see Littleton and Bellen, 1995; Broadie, 1995; Keshishian *et al.*, 1996; Fernandez-Chacon and Sudhof, 1999; Zhang and Zehhof, 2002) and some of these studies used subcellular fractionation of fly heads (e.g., Schulze *et al.*, 1994; van de Goor *et al.*, 1995; Littleton *et al.*, 1998; Phillips *et al.*, 2000). One such protocol simply uses a glycerol gradient to separate vesicles from the plasma membrane (van de Goor *et al.*, 1995) and is described next.

Method A: Mass Isolation of Fly Heads and Preparation of Head Extract

Approximately 100 mg of heads is generated per gram of flies. Start by expanding flies in bottles or large population cages (Sisson, 2000) to a degree appropriate for the application. Flies are anesthetized (e.g., with CO₂) and collected in preweighed 50-ml conical tubes, thereby allowing easy measurement of the weight of the collected flies. The weighed tubes are submerged in liquid nitrogen and stored at -80°C. In a 4°C cold room, each tube is vortexed, causing the heads to detach from the body. The tubes are then emptied onto a stack of prechilled sieves. The stack consists of two brass and stainless-steel sieves with a 710 and 300 μm mesh, a lid, and a base. Metal sieves can be purchased from

companies such as VWR or Fischer [710 μm , U.S. Standard sieve designation No. 25; 300 μm , U.S. Standard sieve designation No. 50; brass receiver pan (depth 2 in.)]. Sieves can be prechilled in a -80°C freezer before the experiment is begun or simply cooled by first pouring liquid nitrogen over them. Once all of the flies are on the top sieve, the stack of sieves is shaken vigorously for roughly 30 s, which causes dissociation of the heads from the flies, depositing the heads onto the second screen while the bodies remain on the top screen. The top sieve should be examined for flies with their heads still attached. If necessary, another round of shaking will increase the yield. The frozen heads are then collected into a preweighed tube or homogenizer. The heads can then be either stored at -80°C or homogenized at the desired ratio of buffer to total weight of heads. For example, for total soluble protein extraction, the best yield is obtained at the highest ratio of buffer to total dry weight of heads, but in order to avoid loss of protein activity or nonspecific binding to containers, a ratio of 5 ml buffer/g of heads is a good starting point for satisfactory yields of soluble extract. However, if the first step after the generation of the extract is a method that does not yield concentration and where application of a concentrated sample is critical, such as sucrose or glycerol gradients or gel-filtration chromatography, a lower ratio of buffer to tissue such as 1:1 or 2:1 might be considered.

To begin to generate the head lysate, heads are placed into a mortar prechilled with liquid nitrogen and ground with a frozen pestle until a fine powder is generated. Add more liquid nitrogen as needed. Once a uniform powder is achieved by grinding, weigh the powder in a Dounce homogenizer and add the lysis buffer. Homogenize with the loose-fitting pestle using 5–10 strokes, followed by 10 strokes with the tighter fitting pestle. One can homogenize the heads directly, skipping the mortar and pestle step, but cracking the cuticle using this method is more difficult. Once the lysate is generated, spin for 10 min at $1000 \times g$ at 4°C , separating nuclei, cuticle, and unbroken cells from the extract. This post-nuclear extract can then be used for various experiments. If smaller quantities of heads are sufficient, one may simply remove the head from the body by manual dissection using forceps or razor blades under a dissecting microscope. Collect the heads in an Eppendorf tube on ice, and homogenize 10 heads in 100 μl lysis buffer. For a typical Western, one head per lane on a minigel is a good starting point.

Method B: Subcellular Fractionation of Fly Heads

An initial step at uncovering the function of a protein might be to identify the membrane fraction where the protein is localized. For example, synaptic vesicles and plasma membranes can be separated readily by at least two methods. The first method of fractionating fly heads is by standard methods of differential centrifugation. For this method, isolated heads are homogenized at a ratio of 10 ml buffer to 1 g of heads in order to achieve the best separation of membranes and soluble material in the initial steps. Heads (100 mg) are homogenized in 1 ml of buffer [in mM: 10 HEPES, pH 7.4, 1 EGTA, 0.1 MgCl_2 , 0.1 phenylmethylsulfonyl fluoride

(PMSF)] or in the same buffer except containing Ca^{+2} instead of EGTA (in mM: 10 HEPES, pH 7.4, 1, CaCl_2 , 0.1 MgCl_2 , 0.1 PMSF). A comparison of the distribution of the protein in these two buffers will test for the effects of calcium on the subcellular compartmentalization of the protein of interest. This test might be used if it is suspected that the protein may function in calcium-dependent events such as synaptic activity or cell adhesion. Alternatively, if the effects of calcium are not to be tested, magnesium can be left out of the buffer, and if a higher ionic strength buffer is desired, 150 mM NaCl or K glutamate may be added. Higher ionic strength buffers can be used, for example, if one intends to use various fractions for immunoprecipitations; however, if one intends on using fractions for an ion-exchange column, for example, leaving out the salts is desirable. Homogenates are then centrifuged at $1000 \times g$ to produce the P1 pellet fraction. The supernatant (S1) is centrifuged at $25,000 \times g$ at 4°C for 40 min to produce the P2 (heavy membrane) pellet fraction. The resulting S2 supernatant is then centrifuged at 4°C at $125,000 \times g_{\text{ave}}$ for 1 h to obtain the P3 (light membrane and synaptic vesicle) pellet and the final supernatant, S3 (soluble fraction).

If the distribution of all proteins and membrane relative to each other is desired, then head extracts can be fractionated on a density gradient. Powdered heads (1 g) can be resuspended in 1 ml of lysis buffer (in mM: 150 NaCl, 10 HEPES, pH 7.4, 1 EGTA) and homogenized 5–10 strokes using the loose Dounce pestle, followed by 10 strokes with the tight-fitting pestle. The postnuclear supernatant (10 min at $1000 \times g$) is layered carefully onto a 5–25% glycerol gradient made in lysis buffer, overlaying a 50% sucrose cushion also made in lysis buffer. For optimal separation, use a volume of supernatant corresponding to less than 5–10% of the volume of the gradient and a cushion representing 10% of the gradient volume. This gradient can be made most simply in the following manner (e.g., for a Beckman SW41 rotor): Place 1 ml 50% sucrose in lysis buffer at the bottom of the gradient. Make 5 and 25% glycerol solutions in lysis buffer. Make a 1:1 mixture of the 5 and 25% stocks and then a 1:1 mixture of this solution and either the 5 or 25% stocks. Layer 2.1 ml of each of these five solutions sequentially on top of the cushion, beginning with the 25% glycerol solution and ending with the 5% glycerol solution. Be careful to add these solutions slowly to avoid mixing. After pouring, allow the gradient and cushion to sit in the cold room for at least 2 h prior to adding the supernatant. Add 0.5 ml of the postnuclear fraction on the top of the gradient and spin for 2 h in a swinging bucket rotor at $160,000 \times g_{\text{ave}}$ (36,000 rpm in a Beckman SW41Ti). Fractionate the gradient by removing 0.5-ml fractions, and assay each by Western analysis. Alternatively, if a tabletop ultracentrifuge is available, this separation using glycerol gradients is more rapid. For example, the gradients can be spun at 50,000 rpm in a TLS-55 rotor using a Beckman tabletop ultracentrifuge for 30 min. Fractions containing synaptic vesicles are identified using antibodies specific for cysteine string protein or synaptobrevin, whereas fractions containing plasma membrane are identified using antibodies against syntaxin, HRP, or the Na/K ATPase (see Table II). The

Table II
List of Antibodies to *Drosophila* Proteins Found in Neurons and Glia

Protein	Source/type	Expression pattern	Reference
Acheate	Mouse mAB	Nuclei of four neuroblasts	Skeath and Carroll (1992)
α -Adaptin	Rabbit pAB	Presynaptic	Gonzalez-Gaitan and Jackle (1997)
α PS1	Mouse mAB DK1A4	NMJ postsynaptic	Brower <i>et al.</i> (1984); Beumer <i>et al.</i> (1999)
α PS2 integrin	Rat mAB PS2hc2	NMJ postsynaptic	Bogaert <i>et al.</i> (1987); Beumer <i>et al.</i> (1999)
α spectrin	Mouse mAB	NMJ, pre- and postsynaptic	Dubreuil <i>et al.</i> (1997); Featherstone <i>et al.</i> (2001)
Amnesiac	Rabbit pAB	Two neurons around mushroom body	Waddell <i>et al.</i> (2000)
Dankyrin2	Mouse pAB	Embryonic nerve tracts	Bouley <i>et al.</i> (2000)
APP	Rabbit #332	Neuropil, NMJ boutons	Buxbaum <i>et al.</i> (1990); Torroja <i>et al.</i> (1999)
APPL	Rabbit pABAb952	Neuropil, NMJ boutons	Torroja <i>et al.</i> (1996); Torroja <i>et al.</i> (1999)
APP 2 (4G8)	Mouse mAB (Syntek)	CNS neurons, NMJ axons, boutons	Gunawardena and Goldstein (2001)
APP (22C11)	Mouse mAB (Chemicon)		Gunawardena and Goldstein (2001)
Atonal	Rabbit pig pAB	Chordotonal and photoreceptors cells	Jarman <i>et al.</i> (1995)
	Guinea pig pAB	Subset of neuroblasts, subset of CNS cells	Hassan <i>et al.</i> (2000)
β spectrin h.c.	Rabbit pAB	NMJ pre- and postsynaptic	Byers <i>et al.</i> (1989); Featherstone <i>et al.</i> (2001)
β -PS integrin	Mouse mABCF6G11	NMJ pre- and postsynaptic	Brower <i>et al.</i> (1984); Beumer <i>et al.</i> (1999)
	Rabbit pAB 185E	NMJ pre- and postsynaptic	Zusman <i>et al.</i> (1993); Beumer <i>et al.</i> (1999, 2002)
BiP	Mouse mAB SPA-827 (StressGen)	Endoplasmic reticulum	Huovila <i>et al.</i> (1992); Baumann (2000) Diagana <i>et al.</i> (2002)
BP102	Mouse mAB BP102	CNS axons	Seeger <i>et al.</i> (1993)
BP104 (see neuroglian)	Mouse mAB BP104	CNS cell membranes	Hortsch <i>et al.</i> (1990)
N-cadherin	Rat mABs and rat pAB	Axons; R cell axons and targets	Iwai <i>et al.</i> (1997); Lee <i>et al.</i> (2000a,b)
CaMKII	Rabbit pAB	Synapses	Koh <i>et al.</i> (1999)
CAPS (calcium-activated protein for secretion)	Rabbit pAB	Presynaptic terminals	Renden <i>et al.</i> (2001)
CCAP	Rabbit pAB	Subset of ventral nervous system	McNeil <i>et al.</i> (1998)
CHAT	Mouse mAB	Neuropil	Ikeda and Salvaterra (1989); Yasuyama <i>et al.</i> (1995)
	Mouse mAB	Neuropil	Takagawa and Salvaterra (1996)
	Rabbit pAB	Neuropil	Munoz-Maines <i>et al.</i> (1988)
Clathrin h.c.	Goat pAB CG034 (Sigma)	Presynaptic membrane and cytoplasm	Zhang <i>et al.</i> (1998)
Cut	Rabbit pAB	Nuclei of all external sensory organ precursors and some CNS cells	Blochlinger <i>et al.</i> (1990)
Cystein string protein	Mouse mAB	Presynaptic; vesicle-associated	Zinsmaier <i>et al.</i> (1994, 1990)
DAP160	Rabbit pAB	Presynaptic membrane	Roos and Kelly (1998, 1999)
Dopamine decarboxylase	Rabbit pAB	Subset of neurons	Scholnick <i>et al.</i> (1991)

Discs large (DLG)	Rabbit and rat pABs	Type 1 boutons, pre- and postsynaptic, SSR	Woods and Bryant (1991); Lahey <i>et al.</i> (1994)
Dock	Rabbit pAB	Growth cones, ISN nerve	Clemens <i>et al.</i> (1996); Desai <i>et al.</i> (1999)
Dynamin,	Three rabbit pABs	Presynaptic type 1 boutons	Estes <i>et al.</i> (1996); Roos and Kelly (1998)
	Rabbit pAB	Presynaptic endocytic sites	Guichet <i>et al.</i> (2002)
Dynein h.c. (PIH4)	Mouse mAB		McGrail and Hays (1997)
Dynein i.c. (IC74.1)	Mouse mAB		Bowman <i>et al.</i> (1999); Dillman and Pfister (1994)
Eagle	Rabbit pAB	Subset of neuroblasts	Dittrich <i>et al.</i> (1997)
Elav	Rabbit pAB	Nuclei of all neurons	Robinow <i>et al.</i> (1988)
	Mouse mAB44C11	Nuclei of all neurons	Bier <i>et al.</i> (1988)
Engrailed	Mouse mAB	Nuclei of all row 6 and 7 neuroblasts and neuroblasts of row 1	Patel <i>et al.</i> (1989)
	Rabbit pAB		Dinardo <i>et al.</i> (1985)
Endophilin A	Two guinea pig pABs		Verstreken <i>et al.</i> (2002)
	Rabbit pAB	Presynaptic exocytotic sites	Guichet <i>et al.</i> (2002)
Even-skipped	Rabbit pAB	Nuclei of a small subset of neurons	Frasch <i>et al.</i> (1987)
	Mouse mABs3C10	Nuclei of a small subset of neurons	Patel <i>et al.</i> (1992)
	Mouse mAB 2B8	Nuclei of a small subset of neurons	Patel <i>et al.</i> (1994)
Fasciclin I (5H7, 2A2, 1B8, 5E1)	Mouse mAbs	Neuroepithelial cells and neuroblasts, axons glia	Hortsch and Goodman (1990); Desai <i>et al.</i> (1994)
Fasciclin II (1D4)	Mouse mAB	Subsets of neurons and axons in the CNS, motorneuron growth cones and axons in the PNS pre and postsynaptic SSR type I and II	Seeger <i>et al.</i> (1993); Van Vactor <i>et al.</i> (1993); Schuster <i>et al.</i> (1996)
	Mouse mAB1D4G9)		Zito <i>et al.</i> (1999)
Fasciclin III	Rabbit pAB	Surface of a subset of neurons	Genningloh <i>et al.</i> (1991)
	Mouse mAb 2D5		Patel <i>et al.</i> (1987)
	Mouse mAB 1D4		Van Vactor <i>et al.</i> (1993)
Flamingo	Mouse mAB	Axons, dendrites	Usui <i>et al.</i> (1999); Gao <i>et al.</i> (2000)
FMRFamide	Rabbit pAB	Subset of neurons; in cell body axons and terminals	Taghert and Schneider (1990); Schneider <i>et al.</i> (1993)
d-Fragile-X	Mouse mAB	Cell body and axons	Wan <i>et al.</i> (2001); Zhang <i>et al.</i> (2001)
Frazzled	Rabbit pAB	Axons	Kolodziej <i>et al.</i> (1996)
Frequenin	Rabbit pAB	Presynaptic	Pongs <i>et al.</i> (1993)
Futsch (Mab 22C10)	Mouse mAB	Subset of neurons, axonal cytoskeleton and portions of synaptic cytoplasm	Fujita <i>et al.</i> (1982), Zipursky <i>et al.</i> (1984); Hummel <i>et al.</i> (2000)
GABA	Mouse mAB	Neuropil	Featherstone <i>et al.</i> (2000)
GABA receptor (LCCH3=GABAA)		Neuroblasts, cell bodies	Aronstein <i>et al.</i> (1996)

(Continues)

Table II (Continued)

Protein	Source/type	Expression pattern	Reference
GABA receptor (Rdl) (novel GABA receptor)	Several rabbit pAB	Neuropil	Aronstein and Ffrench-Constant (1995); Mudmerer <i>et al.</i> (2002)
GAD	Two rabbit pABs	GABAergic and some glutaminergic cell bodies, axons, and boutons	Featherstone <i>et al.</i> (2000)
Glued	Two rabbit pABs	NMJ boutons	Waterman-Storer and Holzbaur (1996) Eaton <i>et al.</i> (2002); Fan and Ready (1997)
Glutamate Glutamate receptor (DGLUR-IIA)	Rabbit pAB (Chemicon) Rabbit pAB DM2	Presynaptic; all boutons Postsynaptic membrane	Johansen <i>et al.</i> (1989) Saitoe <i>et al.</i> (1997, 2001)
Glutamate receptor (DGLUR-IIA)	Mouse mAB 8B4D2	Postsynaptic membrane	Featherstone <i>et al.</i> (2002)
Glutamate receptor (DGLUR-IIA,B,C)	Rabbit pABAS5	Postsynaptic membrane	Saitoe <i>et al.</i> (2001)
Glutamate-gated chloride channel (DmGluClalpha)	Rabbit pAB		Mudmerer <i>et al.</i> (2002)
Golgi (Calbiochem)	Mouse mAB345865	Golgi	Stanley <i>et al.</i> (1997); Diagana <i>et al.</i> (2002)
Gooseberry	Rabbit pAB	Subset of neurons	Gutjahr <i>et al.</i> (1993)
Highwire	Mouse mAB	Synapses, neuropil	Wan <i>et al.</i> (2000)
Hiraku genki	Rat pAB	Presynaptic and cleft in pupae and adult; NMJ M8 in larvae	Hoshino <i>et al.</i> (1996)
Homer	Rat pAB	Dendrites and ER	Diagana <i>et al.</i> (2002)
HRP	Mouse mAb Mouse and goat pABs	Numerous glycoproteins on neuronal plasma membrane	Jan and Jan (1982); Snow <i>et al.</i> (1987) Katz <i>et al.</i> (1988); Desai <i>et al.</i> (1994); Cappel Lab, Sigma, Molecular Probes
Hunchback	Rabbit pAB	Nuclei of all neuroblasts during early neurogenesis	Tautz <i>et al.</i> (1987)
Kinesin heavy chain	Rabbit pAB	Axons	Saxton <i>et al.</i> (1988); Hurd <i>et al.</i> (1996); Gindhardt <i>et al.</i> (1998)
Kinesin l.c.	Rabbit pAB	Axons	Gindhadt <i>et al.</i> (1998)
Kinesin II	Rabbit pAB	Chordotonal organs	Pesavento <i>et al.</i> (1994); Ray <i>et al.</i> (1999)
Leonardo	Two rabbit pAB	Mushroom body and NMJ boutons	Skoulakis and Davis (1996); Broadie <i>et al.</i> (1997)
Leucokinin (1992)	Rabbit pAB	Subset of neurons	Cantera and Nassel (1992)
LAP (Like-AP180)	Rat pAB	Presynaptic	Zhang <i>et al.</i> (1998)
DLAR	Mouse	Embryonic axons, axon termini of R1–R6	Sun <i>et al.</i> (2000); Clandrinin <i>et al.</i> (2001)
Dliprin	Rabbit pAB	Neuropil; weak cell body, NMJ pre- and postsynaptic	Kaufmann <i>et al.</i> (2002)
Lola	Rabbitt pAB	CNS, PNS subset of cells	Giniger <i>et al.</i> (1994); Crouner <i>et al.</i> (2002)

Na/K ATPase α sub.	Mouse mAB	Neuronal plasma membrane	Lebovitz <i>et al.</i> (1989)
Na/K ATPase β sub.	Mouse mAB	Neuronal plasma membrane	Sun and Salvaterra (1995); Sun <i>et al.</i> (1998)
NetrinA (Dunc6)	Goat pAB	Midline glia	Harris <i>et al.</i> (1996)
NetrinB (Dunc6)	Goat pAB	Midline glia	Harris <i>et al.</i> (1996)
Neurexin	Rabbit pAB	Midline glia	Baumgartner <i>et al.</i> (1996)
Neuroglian ¹⁸⁰ (BP104 and 1B7)	Mouse mAB BP104	CNS cell membranes	Bieber <i>et al.</i> (1989); Hortsch <i>et al.</i> (1990)
DNSF1			Pullikuth and Gill (1999)
Octopamine	Rabbit pAB	Presynaptic type II boutons	Monastiriot <i>et al.</i> (1995)
PACAP-38	Rabbit pAB	Presynaptic type I boutons	Zhong and Pena (1995)
PAK	Rabbit pAB	Postsynaptic region surrounding synapse	Hing <i>et al.</i> (1999)
PC2 (amontillado)	Rabbit pAB	Peptidergic neurons, endocrine cells	Hwang <i>et al.</i> (2000)
Pigment dispersing factor (PDF)	Rabbit pAB	Subset of neurons	Dirksen <i>et al.</i> (1987); Helfrich-Förster (1995)
ProPDF	Guinea pig pAB	Subset of neurons	Renn <i>et al.</i> (1999)
Peptidylglycine α -hydroxylating monooxygenase (PHM)	Rabbit pAB	Peptidergic neurons, neurosecretory cells	Kolhekar <i>et al.</i> (1997)
Pox-neuro	Rabbit pAB	Nuclei, polyinnervated external sensory cells	Dambly-Chadiere <i>et al.</i> (1992)
Proctolin	Rabbit pAB	Presynaptic in many endings	Anderson <i>et al.</i> (1988)
Prospero	Mouse mAB		
Ras opposite (ROP-dunc18)	Rabbit pAB and mouse mAB	Presynaptic and axonal	Salzberg <i>et al.</i> (1993); Harrison <i>et al.</i> (1994)
			Schulze <i>et al.</i> (1995)
Repo	Rat pAB	Glial cell marker	Campbell <i>et al.</i> (1994)
	Rabbit pAB	Glial cells	Halter <i>et al.</i> (1995)
Robo (13C9)	Mouse mAB		Kidd <i>et al.</i> (1998a,b)
Roadblock/LC7 (dynein light chain)	Rabbit pAB		Bowman <i>et al.</i> (1999)
α -SAP	Mouse mAB	Presynaptic	Reichmuth <i>et al.</i> (1995)
Scam	Rabbit pAB	Axons	Schmucker <i>et al.</i> (2000)
	Rabbit pAB		Worby <i>et al.</i> (2001a,b)
Semaphorin			Kolodkin <i>et al.</i> (1993); Matthes <i>et al.</i> (1995)
Serotonin	Rabbit pAB and mouse mAB	Subset of neurons in cell body, axons, and terminals	White and Valles (1985)
Slit (555.4, C555.6D)	Mouse mABs and rabbit pAB	Midline glia	Rothberg <i>et al.</i> (1988, 1990)

(Continues)

Table II (Continued)

Protein	Source/type	Expression pattern	Reference
Small synaptic bouton antigen (SSB)	Rabbit pAB	Type II boutons; made against but does not recognize dunce protein	Budnik and Gorczyca (1992); Nighorn <i>et al.</i> (1991)
SNAP24	Two rabbit pABs		Niemeyer and Schwarz (2000)
SNAP25 (CI.71.1)	Mouse mAB	Presynaptic and axonal	Otto <i>et al.</i> (1997); Chapman <i>et al.</i> (1994)
	Rabbit pAB		Rao <i>et al.</i> (2001)
Still life	Rat pAB	Presynaptic	Sones <i>et al.</i> (1997)
Stoned A	Rabbit pAB	Presynaptic terminals	Andrews <i>et al.</i> (1996); Stimson <i>et al.</i> (1998); Fergestad <i>et al.</i> (1999)
Stoned B	Rabbit pAB	Presynaptic terminals	Andres <i>et al.</i> (1996); Stimson <i>et al.</i> (1998); Fergestad <i>et al.</i> (1999)
SV2	Mouse mAB	Presynaptic terminals	Fergestad <i>et al.</i> (1999)
Synapsin	Mouse mAB	Presynaptic	Klagges <i>et al.</i> (1996)
n-Synaptobrevin	Four rabbit pABs	Presynaptic; vesicles and membrane	DiAntonio <i>et al.</i> (1993), van de Goor <i>et al.</i> (1995); Sweeney <i>et al.</i> (1995); Deitcher <i>et al.</i> (1998)
Synaptotagmin 1	Two rabbit pABs	Presynaptic and axonal	Littleton <i>et al.</i> (1993, 1994)
	Rabbit pAB and mouse mAB	Presynaptic and axonal	Dubuque <i>et al.</i> (2001)
Synaptotagmin IV	Rabbit pAB and mouse mAB		Littleton <i>et al.</i> (1999)
Syntaxin 1A	Three mouse mABs	Presynaptic and axonal	Fujita <i>et al.</i> (1982); Schulze <i>et al.</i> (1995)
		Presynaptic and axonal	Cerezo <i>et al.</i> (1995)
Dunc5 (netrin)	Rabbit pAB	Motor neurons and glial cells	Keleman and Dickson (2001)
Dunc13	Rabbit pAB	Presynaptic terminals	Avamundrun and Broadie, accepted
VAP-33A	Guinea pig pAB	Presynaptic terminals	Pennetta <i>et al.</i> (2002)
Volado (α -PS integrin)	Rabbit pAB	MB, neuropil; NMJ subset of boutons	Grotewiel <i>et al.</i> (1998); Rohrbough <i>et al.</i> (2000)
Wingless	Rabbit pAB	Row 5 neuroblasts, neuroectoderm	Chu-LaGriff and Doe (1993)
Wit (23C7) (wishful thinking BMP type II receptor)	Mouse mAB	Subset of neurons	Aberle <i>et al.</i> (2002)
Wrapper (10D3)	Mouse mAB	Midline glia	Noordermeer <i>et al.</i> (1998)

position of the gene product of interest in the gradient can then be compared to these markers.

Method C: Coimmunoprecipitation for Identifying Interacting Proteins

The entire genome of flies is known, and several projects overseen by the BDGP have the goal of generating mutants in virtually all of the genes. The next step is to identify the function of all these genes and to identify physically interacting proteins. The latter question can be approached by immunoprecipitations using antibodies recognizing native proteins or epitope-tagged fusion proteins. The benefits of each of these approaches are discussed further in the section on protein expression.

An example of the utility of this approach is a recent study demonstrating the surprising result that certain GABA and glutamate gated-channels may heterodimerize *in vivo*. A GABA-gated channel had been identified previously, but when expressed in a heterologous system, the pharmacology was distinct from the native channel (Zhang *et al.*, 1995) and glutamate was known to regulate ligand binding (Smith *et al.*, 2000). Coimmunoprecipitation from membranes prepared from head extracts demonstrated that a GABA and glutamate gated-channel can coassemble using two radiolabeled ligands and antibodies to both subunits.

For immunoprecipitations, antibodies should be bound to protein A, G, or A/G beads depending on the host species of the antibody (see manufacturers instructions) to as high a stoichiometry as possible. This allows for fewer beads to be used, thereby lowering nonspecific background binding. Antibodies should be affinity purified (see Harlow and Lane, 1999) and incubated overnight with protein A- or g-linked beads at 4°C. Nonspecific rabbit IgG, preimmune IgG, and/or beads alone should be used as controls for the affinity-purified antibodies. For the best results, IgGs are linked covalently to the protein A beads using 5–20 mM dimethylpimelimidate or 0.5–4 mM disuccinimidyl suberate (DSS) as described (Harlow and Lane, 1999). Covalent coupling prevents the IgG subunits from masking interacting proteins during analysis and allows the reuse of the beads. The beads are then washed with high salt (1 M NaCl or 4 M MgCl₂) and detergent-containing buffers (up to 1% TX-100) to release unbound antibodies followed by a wash in phosphate-buffered saline (PBS) with 0.1% bovine serum albumen (BSA). The lysate can then be incubated with control beads to preclear the extract (Harlow and Lane, 1999). The specific antibody beads are mixed with the precleared lysate (SI) or subcellular S2-P3 fractions in equivalent volumes for 2 h (or overnight) at 4°C, washed with 0.1% BSA in PBS, and finally in PBS. Bound material is eluted by 0.1 M glycine, pH 2.5, or by boiling in reducing SDS sample buffer. The immunoprecipitate is electrophoresed on SDS-PAGE and is Western blotted for the antigen and suspected interactors. Alternatively, analysis of the immunoprecipitate by two-dimensional gels followed by matrix-assisted laser desorption/ionization time-of-flight mass spectroscopy (MALDI-TOF MS) can be used to identify interacting proteins (for review, see Nordhoff *et al.*, 2001).

Two-dimensional gels allow one to separate proteins based on molecular weight and isoelectric point on large gels. This makes it more likely to pick a spot containing a single protein, and mass spectrometric analyses (MALD-TOF) can allow the identification of the protein. A good control, if it is available, is an immunoprecipitation reaction for a true protein null or one in which the epitope is truncated.

Some biochemical studies of *Drosophila* proteins have utilized S2 cells to study neuronal proteins. These cells tend to express a large set of proteins, including neuronal ones. RNAi (for review, see Worby *et al.*, 2001) and biochemical experiments have been very successful in these cells, including looking for or demonstrating protein/protein interactions (Hwang *et al.*, 2000; Worby *et al.*, 2001b, 2002). These studies can also serve as a starting point for the choice of generating mutants in newly identified interacting proteins and subsequent determination of their *in vivo* function in flies (Schmucker *et al.*, 2000). A nice example of this latter approach is a series of studies of DOCK, an adaptor protein that functions in axonal guidance. Immunoprecipitation of DOCK from S2 cells and embryos led to the observation that DOCK interacts with several phosphotyrosine-containing proteins, including p270 (Clemen *et al.*, 1996). Further coimmunoprecipitations of a tagged version of DOCK (SH2) expressed in S2 cells demonstrated several interacting proteins, including the phosphotyrosine containing Down syndrome cell adhesion molecule (Dscam-p270) (Schmucker *et al.*, 2000; Worby *et al.*, 2001a). Mutants of DSCAM were isolated and shown to also have a role in axon guidance (Schmucker *et al.*, 2000) consistent with coimmunoprecipitation data of Dock and Dscam. Dock and Dscam also interact genetically (Schmucker *et al.*, 2000).

Method D: Lipid Analyses

The effect of diet on lipid metabolism has been studied in flies, and mutants have been isolated that putatively should disrupt lipid metabolism in the nervous system (Yoshioka *et al.*, 1983; Fujita *et al.*, 1987; Inoue *et al.*, 1989; Stark *et al.*, 1993; Pavlidis *et al.*, 1994). To address these issues, methods of extracting and analyzing lipids in fly heads have been developed. Lipids have been found to modify many parameters of a neural cell, but still the role of lipid composition in membranes is not well understood. Genetic approaches in yeast have been helpful at addressing this issue, and an example of addressing the role of lipids in neuronal function is the study of the *easily shocked* gene, which encodes an ethanolanine kinase. Mutants in this gene are paralyzed easily by brief, intense electrical stimulation (Pavlidis *et al.*, 1994). Phospholipid analysis indicated that phosphatidylethanolamine levels were depressed. Synthesis of phosphatidylethanolamine requires ethanolanine kinase and highlights the importance of phospholipid metabolism for neuronal function. PIP₂ has been shown to play critical roles in the nervous system. PIP and PIP₂ levels can be analyzed readily in the *Drosophila* head by thin-layer chromatography coupled to immunological detection and using labeled inorganic phosphate as described later. A complementary approach to the

direct measurement of PIP₂ has been demonstrated by a biosensor of PIP₂ (Hardie *et al.*, 2001). With this technique, one can determine relative levels of PIP₂ *in vivo*.

Briefly, 20 fly heads are homogenized in 400 μ l of 0.32 M sucrose, 50 mM Tris, pH 7.4, and 1 mM EDTA for 60 s in 1.5-ml Eppendorf tubes. Then 0.8 ml of chloroform/methanol (2:1 v/v) is added, and the tissue is further homogenized for 60 s. Another 0.8 ml is added and vortexed for 2 min. This mixture is centrifuged at $2500 \times g$ for 5 min and the lower organic phase is removed and saved. Two more extractions are done with 2 volumes of acidic chloroform/methanol/12 N HCL (2:1:0.0125, v/v/v) and the lipid containing lower phases are pooled and neutralized with one drop of 4 N NH₄OH. The organic phase is dried under nitrogen gas and the sides of the container are rinsed with chloroform/methanol (2:1). Samples are resuspended in chloroform/methanol (2:1) and either stored at -80°C or applied to a thin-layer chromatography (TLC) plate. The TLC plates (Whatman, aluminum backed) are prepared by treating with 1% potassium oxalate in methanol, removing the excess, and heating at 110°C for 1 h. Samples are applied to the plates based on the number of heads extracted or by quantitating total phospholipids by measuring phosphorus content (Ames, 1966). The TLC plates are then developed by solvents depending on the desired separation (Inoue *et al.*, 1989; Stark *et al.*, 1993). For example, PIP and PIP₂ can be analyzed by developing in 65% isopropanol and 35% 2 M acetic acid. Once the solvent front reaches the top of the plate, the TLC plate is allowed to dry in a hood. After drying, the TLC plate can be analyzed by several methods. For example, one can analyze both PIP and PIP₂ levels by antibody binding and detection. When the TLC plate is completely dry (no acetic acid odor), the plates are blocked in PBS-B-PVP (PBS with 1% BSA and 1% polyvinylpyrrolidone, an average molecular weight of 10,000). The PIP (1:1000 Assay Designs, Ann Arbor, MI) and PIP₂ (1:1000 Assay Designs or Echelon Labs, Salt Lake City, UT) antibodies are applied and incubated for 2 h. The plates are washed four times in PBS-B-PVP, incubated with either HRP or alkaline phosphatase-coupled secondary antibodies for 1 h, and then rinsed again as for primary antibodies. The plates are developed in the appropriate reagents (Lane and Harlow).

Few phospholipid-specific antibodies exist, but methods based on the incorporation of radioactive precursors can be used (Inoue *et al.*, 1989; Stark *et al.*, 1993). For example, flies can be fed 1–12% sucrose containing ³²P-labeled inorganic phosphate for up to 24 h. Labeled flies are frozen in liquid nitrogen, vortexed, and their heads collected. Lipids are extracted as described earlier and are then analyzed by various methods on TLC plates (Inoue *et al.*, 1989; Stark *et al.*, 1993). Identification of specific molecules is made by using standards and detected using iodine or ninhydrin vapors (Skipski and Barclay, 1969). Quantitation can be achieved by scraping the radioactive spots identified by autoradiography, and the radioactivity measured using a liquid scintillation counter. Alternatively, one can use a phosphoimager such as the one made by Molecular Dynamics and its associated software.

V. Cell Biology Techniques in the *Drosophila* Nervous System

Among the forward genetic systems, methods for the analysis of neurons *in situ* are the most advanced in *Drosophila*. Immunocytochemical methods are developed for all stages of the life cycle and many antibodies are available (see Table II). In *C. elegans*, creating transgenic animals expressing marked proteins is much faster, but regulating the expression levels is fairly difficult. In flies, however, transgenic protein expression is a standard method and many variations of controlling expression can be used. Genomic (Spradling, 1986) or ectopic expression (Brand and Perrimon, 1993; Brand *et al.*, 1994; van Roessel and Brand, 2002) is routine, and inducible systems have also been introduced (Bieschke *et al.*, 1998; Bello *et al.*, 1998; Osterwalder *et al.*, 2001; Roman *et al.*, 2001; Stebbins and Yin, 2001; Stebbins *et al.*, 2001; Landis *et al.*, 2001). Newly developed gene targeting methods should also allow “knockins” of tags and mutations (Rong and Golic, 2000, 2001; Bibikova *et al.*, 2002), leading to mutated proteins expressed under the control of the endogenous genomic promoter. Finally, in flies it is possible to study the phenotypes of early lethal mutations by several clonal analysis techniques in neural tissues. Before these methods are discussed, the *Drosophila* life cycle is outlined briefly.

A. The *Drosophila* Life Cycle

During its holometabolous life cycle, *Drosophila* passes through several developmental stages, each of which has distinct advantages (and disadvantages) for a neurobiologist. The development of *Drosophila* is highly temperature dependent. The times given here represent development at 25°C, at which eggs are laid under optimal conditions. The eggs are laid soon after fertilization and subsequently undergo 17 defined embryonic stages, together lasting 20–22 h. During this time embryos develop and ultimately hatch into first instar (L1) larvae. The larvae undergo two molts, leading to a succession of three larval instar states (L1, L2, and L3) lasting ~96 h. Mature third instar larvae enter a “wandering stage,” leaving the food in search of a suitable site for pupariation. Adults eclose from the pupal case after 4–4.5 days. Adult flies typically live 30–60 days. For an account of the development of the structure and electrical properties of neurons during development, see Budnik and Gramates (1999).

B. Protein Expression Studies with Immunocytochemistry

Many antibodies are available to probe identified classes of *Drosophila* neurons and glia in the embryo, larva, and adult. Many of these antibodies may be used to identify subcellular compartments within neurons or glia. A list of available antibodies is provided in Table II. Many of these antibodies are available from the Developmental Studies Hybridoma Bank at the University of Iowa (DSHB: <http://www.uiowa.edu/~dshbwww/>). Because fixation and staining protocols must

be worked out empirically for any given antibody, a simple set of immunocytochemistry instructions is not feasible. Variations in fix type/duration, dilutions, and other specific protocols may be found in the original papers, as indicated in Table II.

Method A: Immunolabeling the Embryonic Nervous System

For optimal egg collection, maintain young (<7 days), healthy male and female flies (20–40) on fresh laying pots for 2–3 days. Laying pots consist of 100-ml plastic beakers (Tri-Pour) perforated to provide adequate air circulation, covering a 60-mm agar plate. Agar plates contain apple or grape juice hardened with agar. Several recipes exist, but one example is as follows: 700 ml of water, 25–30 g agar, 300 ml of juice concentrate (grape or apple), 0.5 g methyl paraben (*p*-hydroxymethylbenzoate), and 30 g sugar. Autoclave the water and agar and, separately, boil the *p*-hydroxymethylbenzoate with the sugar and juice. Mix the agar and juice solutions and quickly pour into 60-mm plates, removing bubbles. Prior to egg collection, flies are fed daily with yeast paste (7 g baker's yeast in 9 ml of water stored at 4°C) on fresh plates twice a day. By day 3, a good pot will produce 100–200 eggs per hour. Better egg laying is observed on a pot maintained on its side with the agar in the plate scratched. Many embryos will be laid in or next to the scratches.

For embryo collection, gently transfer the embryos from the juice plate and into a basket using a paintbrush. A basket can be made with a 15- or 50-ml centrifuge tube. Cut off the bottom, leaving enough surface area to trap a screen (70 μm mesh) between the lid and the top of the tube. Rinse the embryos with dH₂O and put into a petri dish of fresh 50 to 100% bleach to remove the outer chorion. Dechoriation can take from 30 s to 2 min and should be monitored under the microscope. Removal of the chorion exposes the shiny, transparent vitelline membrane. The next step is to permeabilize the vitelline membrane, which is achieved simultaneously with fixation. Fixation protocols may vary for different antibodies. For a standard fixation procedure, place 2 ml of heptane and 2 ml of 4% paraformaldehyde fix in a glass vial (paraformaldehyde is best made fresh, but for routine experiments we store 5-ml aliquots in the freezer). Drop the embryo basket into the vial, shake off the embryos, and remove the screen. Fix for 20 min at room temperature with agitation. Remove the lower phase containing the paraformaldehyde and add 2 ml 100% methanol. Shake vigorously for 30 s to rupture the vitelline membrane. Allow embryos to settle (only the devitellinized embryos sink to the bottom of the vial). Aspirate the upper heptane phase and remove most of the methanol, and wash embryos three times with methanol. At this point, embryos can be stored in methanol for many weeks to months at –20°C.

Antibody staining protocols vary, but a standard approach is given here. Transfer embryos to a microcentrifuge tube and rehydrate in 50% methanol. Rinse three times in PBS-TX (0.02 M phosphate buffer and 0.1 M NaCl, pH 7, 0.1% Triton X-100; note that detergent use can also vary with different antibodies) and

three more times in PBS-T-BSA (PBS, 0.1% Tween 20, 4% BSA). Block by incubating for 1 h in PBS-T-BSA. After 1 h, remove PBS-T-BSA and add antibodies diluted in PBS-T-BSA. Incubate at least 2 h at room temperature or overnight at 4°C. Allow embryos to settle, and remove and save antibody by adding 0.01% azide. For routine studies, these antibodies can generally be used five times if quantitation is not the main issue being examined. Rinse embryos four times in PBS-T-BSA over a period of 1 h. Add an appropriate dilution of secondary antibody conjugated to a fluorescent chromophore, an enzyme (HRP), or biotin. For fluorescent secondary antibodies, dilute (typically 1:100–500) in PBS-T-BSA and incubate 1–2 h at room temperature in tubes covered with aluminum foil. Wash twice with PBS-T-BSA for 30 min and four times with PBS over a period of 30 min. Mount in a protective medium (e.g., Vectorshield) and observe by light or confocal microscopy.

For HRP-conjugated antibodies or biotin-labeled secondary antibodies, dilute (typically 1:100–500) in PBS-T-BSA and incubate for 1–2 h or overnight at 4°C. Wash the embryos twice with PBS-T-BSA for 30 min and four times with PBS over a period of 30 min. If amplification via the avidin/biotin-HRP system is used (Vectastain kit, Vector Laboratories), prepare a 1:200 dilution of avidin (reagent A) and biotinylated-HRP (reagent B) in PBS-T-BSA. Incubate the embryos in this mixture at room temperature for 1 h. Wash the embryos twice with PBS-T-BSA for 30 min and four times with PBS-TX over a period of 30 min. Begin developing in 600 μ l PBS-TX by adding 20 μ l of 2% NiCl₂, and then bring the sample to 0.06% H₂O₂ using a freshly made 30% stock of H₂O₂. Put embryos into a watchglass and add 30 μ l of 10 mg/ml diaminobenzidine (DAB). One at a time, add to each sample 20 μ l of 1:500 H₂O₂, swirl, and watch reaction in the microscope. Wait until the NMJ becomes visible and then stop the reaction by replacing buffer with fresh PBS-TX. Rinse three times with PBS-TX. Prepare samples in the manner allowing one to mount the samples in your favorite permanent mounting medium (e.g., Permount).

Method B: Embryonic and Larval Dissection for Immunolabeling

Embryos can be dechorionated with bleach and devitellinated manually, and the developmental stage determined either temporally or using morphological criteria. Homozygous mutant embryos can be selected from siblings based on the absence of balancer chromosome markers (e.g., yellow, GFP). Balancer chromosomes are dominantly marked, multiply inverted chromosomes, which allow one to maintain heterozygous stocks of lethal mutants (Greenspan, 1997). This tool is another strength of *Drosophila* that makes maintaining stocks and generating crosses simple. For embryonic lethal mutations, one-quarter of the eggs are homozygotes, one-quarter will have two balancer chromosomes, and half will be heterozygotes. Embryos lacking the balancer will be unmarked. The most readily scored marker is the green fluorescent protein (GFP) (Tsien, 1998), and

balancer chromosomes marked with GFP can be obtained from the Bloomington stock center.

For dissection, it works best if staged embryos are glued (Histoacryl Blue, Braun Germany) to Sylgard-coated coverslips under physiological saline (Sylgard resin from Dow Corning, Corning, NY). The saline contains (in mM): 135 NaCl, 5 KCl, 4 MgCl₂, 1.8 CaCl₂, 72 sucrose, 5 TES, pH 7.2; however, alternative salines are also used (for a complete list of salines and comparison with hemolymph measurements, see Broadie, 2000a). The addition of sucrose approximates the osmotic strength reported in a natural hemolymph (Stewart *et al.*, 1994). Following gluing of the head and tail, a slit is made along either the dorsal or the ventral midline, using a glass capillary pulled to a sharp point or metal needle. The body walls are then glued flat to the coverslip, and the internal organs (gut, fat body, and salivary glands) are removed to expose the neuromusculature.

Dissected animals may then be fixed for 30 min in freshly made 4% paraformaldehyde in PBS. Preparations are washed in PBS-TX several times over a period of 1 h and are then incubated for 1 h with the appropriate blocking agent (i.e., PBS-T-BSA). After blocking, the dissected embryos are incubated with the primary antibody (in PBS-T-BSA) for 2 h at room temperature or overnight at 4°C. Fillets are then rinsed four times over a period of 1 h (PBS-T-BSA) and are then incubated with diluted secondary antibodies (in PBS-T-BSA) for 1–2 h at room temperature. The secondary antibody solution is rinsed off (four washes of PBS-T-BSA), and the embryos are mounted and viewed by light or confocal microscopy.

Larval neuromuscular preparations (CNS and body wall) and the stereotypic pattern of innervation of the larval body wall muscles have been described previously (Jan and Jan, 1976a; Johansen *et al.*, 1989a,b). For dissection, the larvae are placed dorsal side up on a 35-mm-diameter petri dish containing a thin layer of Sylgard resin, pinned down at the head and tail using fine insect pins (Fine Science Tools), and cut along the dorsal midline using fine microdissecting scissors. The filleted larva is pinned out flat, and viscera are carefully removed, taking care to leave the CNS intact. In the final preparation, segmentally repeated larval muscles innervated by axons from the CNS are clearly visible (Johansen *et al.*, 1989a,b; Broadie and Bate, 1993). These larvae can then be immunolabeled as described earlier for embryos.

Immunolabeling of the larval and adult CNS often requires sectioning because some antibodies do not readily penetrate these thicker tissues. Paraffin or cryo-sectioning by standard methods are used (see, for example, Buchner *et al.*, in Ashburner, 1989b; Yang *et al.*, 1995), and methods of sectioning and labeling the retina are described in Wolff (2000a,b). A method describing how to make a tool to mount many heads simultaneously, thereby allowing one to section rapidly, can be found in Ashburner (1989b).

Drosophila neurons have been studied by electron microscopy methods when higher resolution is beneficial. For example, fly NMJs have been analyzed by transmission electron microscopy (TEM; Jia *et al.*, 1993; Atwood *et al.*, 1993 and for methods see chapter by Bellen and Budnik, 2000), scanning electron

microscopy (SEM; Yoshihara *et al.*, 1997), HRP-enhanced immuno-EM (Lin *et al.*, 1994; Zito *et al.*, 1999), immuno-EM using gold particles (Wan *et al.*, 2000; Pennetta *et al.*, 2002), and immuno-SEM (Broadie and Bate, 1993; Yoshihara *et al.*, 1997). TEM has been used to study the effects of mutations on the steady-state distribution and size of synaptic vesicles in many neuronal mutants. It is useful tool for understanding the role of a protein in the vesicle cycle in conjunction with other assays used to study the presynaptic terminal (i.e., calcium measurements and vesicle dynamics using GFP markers, styryl dyes, and electrophysiology; for methods, see later). Immuno-EM can also be invaluable for determining the subcellular location of a protein; however, one problem is that conditions that preserve tissue morphology the best are frequently too harsh for maintaining optimal antigenicity (see chapter about TEM examination including immuno-EM of *Drosophila* by McDonald *et al.*, 2000). Immuno-SEM using anti-HRP has been used successfully to outline neurons (Broadie and Bate, 1993; Yoshihara *et al.*, 1997). This method allows one to observe at high resolution the structure and position of dendrites and axons.

C. Transgenic Protein Expression Studies

It is relatively simple to express normal and tagged versions of proteins in the fly nervous system, but it is time-consuming. Genomic and ectopic (heat shock or GAL4/UAS systems) vectors have been utilized extensively for gene expression in *Drosophila*, and methods of generating transgenic animals are detailed in many chapters (Spradling, 1986; Brand *et al.*, 1994; Phelps and Brand, 1998). Currently, most laboratories use the GAL4/UAS system to create transgenic flies to express proteins in a tissue-specific manner (Brand *et al.*, 1994; Phelps and Brand, 1998). This system is very powerful and easy to use and consists of a yeast transcription factor, GAL4, that can activate transcription in flies (Fischer *et al.*, 1988) but has no endogenous gene targets. Many lines exist in which GAL4 without an enhancer was inserted randomly into the genome by P-element transposition (Spradling, 1986). Lines containing a single insertion have been isolated in which this element is downstream of an enhancer, leading to expression of GAL4 in a temporal and tissue-specific manner depending on when and where the specific enhancer is activated. To utilize this system, another strain of flies is generated with the gene of interest downstream of an upstream activating sequence (UAS), which allows for transcription of the gene in cells where GAL4 is expressed. Once one has a strain with a gene under the control of UAS, one can cross those flies to flies from a large collection of GAL4 lines. Lines can be obtained that drive expression in a panneuronal manner or in a subset of cells (Brand *et al.*, 1994; Phelps and Brand, 1998; van Roessel and Brand, 2000).

There are several advantages to this system compared to older systems used previously to drive expression by heat shock or genomic promoters. First, one can use the UAS line to drive expression in the cells of choice simply by crossing this line to various GAL4 lines, as opposed to generating multiple transgenic lines each

with their own specific promoter. Second, a constitutively expressing genomic construct could potentially be toxic in the wild-type background. However, using the GAL4/UAS system, GAL4 and target gene-bearing flies can be maintained as separate stocks. One point to consider with the GAL4/UAS system is that GAL4 expression is both temperature sensitive and positional sensitive. Because all transgenes, whether driven by a genomic or the GAL4 line, drive expression depending on where they are inserted in the genome, many insertions need to be tested to determine the level of expression induced by the line. The GAL4/UAS system temperature sensitivity can also be taken advantage of as protein expression can be modulated by growing flies at temperature of 18 to 29°C, with 29°C yielding maximum expression. This, for example, can be useful for gain-of-function tests, but may contribute to the variability of expression sometimes seen between flies. A disadvantage of the GAL4/UAS system is that the GAL4 element is inserted in the 5' region of a gene that is expressed exactly where the gene of interest will be driven. These GAL4 insertions could have phenotypes on their own, and in particular, it may be difficult to predict how a GAL4-induced hypomorph may interact with other perturbations in the genome (mutants, over-expression of a protein, etc.). To avoid this problem, one can either generate new lines with an insert of the 5' regulatory region into the construct driving the expression of GAL4. Alternatively, classical methods of using a genomic construct to drive expression have the benefit of possibly driving expression in an otherwise virtually wild-type background.

The transgenic expression of tagged proteins is commonly used to determine the expression pattern and localization of proteins and is useful for the biochemical purification of a protein. The best method for doing this would be to utilize tools of the new gene targeting methods (Rong and Golic, 2000, 2001; Bibikova *et al.*, 2002). Knock-ins of GFP, HA, FLAG, or myo-tagged proteins would generate flies potentially expressing fusion proteins at wild-type levels and with wild-type timing. However, these methods are not yet used routinely because they require more time investment than the generation of lines carrying simple expression constructs. Thus, alternatively one can insert the tagged cDNAs or the genomic region covering the cDNA into vectors with a UAS (UAST) or into vectors requiring the insertion of promoter regions (5'UTR) and 3'-untranslated regions (e.g., Casper series, see Flybase for references and sequences of vectors). Tagged versions of proteins driven by these constructs may not necessarily accurately reflect exact wild-type levels, distribution, or timing of expression, but are nonetheless useful. Biochemical experiments, such as immunoprecipitations using commercially available antibodies specific to the tags and gentle elution with the peptides corresponding to the tag, are good methods of identifying interacting proteins (see, for example, Zheng *et al.*, 1995). A complex can then be demonstrated after immunoprecipitation by gel filtration or subcellular fractionation on sucrose and/or glycerol gradients (Zheng *et al.*, 1995, 1998). Specific antibodies are sometimes function blocking, meaning that they could disturb native interactions but tagging a protein could also potentially disrupt function. Elution of

coimmunoprecipitants from antibodies made against large regions of a protein usually requires harsh treatment, making it more difficult to demonstrate that the interacting proteins are part of a complex. The best approach is to generate specific antibodies and tagged versions of your protein allowing for a confirmation of results by independent methods.

D. Clonal Techniques for Mutant Analyses

Many genes required for neuronal function in *Drosophila* cause early lethality if they are mutated. One can then either study the embryonic phenotype or use specific methods that allow study of the mutant phenotype in the adult nervous system. Also, if one is interested in studying the role of a protein on the structure or development of neurons in adult tissues, it is difficult because the adult CNS is densely packed with neurons. Silver staining overcomes this issue but can only be used for mutants that allow an adult CNS to develop. Methods addressing both of these issues can be used in flies. To overcome the issue of early lethality, several techniques for generating mutant clones in the nervous system have been described using mitotic recombination (Ashburner, 1989a) via the FLP/FRT system (Golic and Lindquist, 1989). This system leads to expression of the yeast FLP recombinase enzyme that catalyzes the recombination between two 34-bp recognition target sites (FRT sites) (Golic and Lindquist, 1989). Flies are generated with FRT sites on one chromosome and a specific mutation on the homologous chromosome (i.e., flies are heterozygous for the lethal mutation). If recombination is induced after DNA replication, then after mitosis, one sister cell will become homozygous mutant while the other will be wild type. Using this idea, methods of generating eyes composed primarily of mitotic clones of a single genotype have been described, allowing one to study the developmental or physiological consequences of mutation in an adult tissue that would otherwise be lethal (Stowers and Schwarz, 1999; Newsome *et al.*, 2000). The visual system is excellent for the study of neural fate decisions (for review, see Kumar and Moses, 2000) or neuronal pathfinding (for review, see Chiba, 2001). Simple electrophysiological methods also allow one to study both phototransduction and synaptic activity in the retina (see later) (Kelly and Suzuki, 1974; Stowers and Schwarz, 1999). Another recently developed clonal method is mosaic analysis with a repressible cell marker (MARCM; for review, see Lee and Luo, 2001). This method addresses both the issue of early lethality and the one concerning the visualization of individual neurons. This method combines several tools of the fly geneticist, resulting in GFP-marked adult mutant clones in the nervous system. The MARCM system has been used to study autonomous developmental processes in defined neuronal populations in the adult brain, such as axonal pathfinding and dendritic arbor formation (Lee and Luo 1999; Lee *et al.*, 1999, 2000a,b; Scott *et al.*, 2001; Lee and Luo, 2001; Hitier *et al.*, 2001; Jefferis *et al.*, 2001; Grueber *et al.*, 2002; Sweeney *et al.*, 2002).

The MARCM method allows one to analyze the effects of a homozygous mutation in an otherwise wild-type background at a single cell resolution (for

review, see Lee and Luo, 2001). Briefly, homozygous mutant clones are generated by mitotic recombination (Ashburner, 1989) via the FLP/FRT system (Golic and Lindquist, 1989). First, a recombinant chromosome is generated during meiosis containing both the recessive mutant gene and a membrane-targeted GFP (mCD8-GFP) on the same arm. The membrane-targeted GFP is a fusion of the mouse T-cell membrane protein, CD8, with eGFP. The expression of mCD8-GFP is under the Gal4/UAS binary system described in Section IV, E (Brand and Perrimon 1993; Brand *et al.*, 1994; Phelps and Brand, 1998; Brand, 1999). Second, two strains of flies are crossed: one Gal4 line, which drives the expression of the yeast transcription factor, and the other driving the expression of the UAS-driven mCD8-GFP fusion protein. This allows one to drive the expression of a transgene by Gal4 in a tissue-specific manner depending on the timing of that promoter. However, in the MARCM system, Gal4 initially cannot lead to transcription of the GFP marker because the other homologous chromosome carries a Gal4 repressor (GAL80) under a ubiquitous driver. This means that all cells that are heterozygous for these two chromosomes will not express the GFP marker. Upon FLP/FRT-mediated mitotic recombination, only one daughter cell receives the repressor (homozygous for repressor) and the other cell is homozygous mutant and expresses mCD8-GFP, but lacks the chromosome containing GAL80. The mCD8-GFP will now be transcribed, translated, and inserted into the membrane outlining the entire cell. FLP expression can be controlled in time and space using a heat shock promoter, which is a promoter that leads to transcription at elevated temperatures. The timing of a particular neuroblast division is known, thereby allowing one to mark only clones actively dividing at the time of FLP expression.

Formation of the *Drosophila* nervous system occurs by the division of identified neuroblasts that give rise to specific clones of neurons via asymmetric divisions. Each division regenerates a neuroblast and a ganglion mother cell. The ganglion mother divides, yielding two neurons (Goodman and Doe, 1993). Therefore, depending on whether mitotic recombination occurs in a neuroblast, ganglion mother cell, or a dividing ganglion mother cell, a multicellular, two cell, or one cell clone might become GFP marked, respectively. The MARCM system is very powerful but has several drawbacks. If the gene is expressed in a precursor cell, then one has to be aware of the half-life of the protein or mRNA in order to be sure of studying the null rather than a hypomorphic phenotype. By the same token, the mCD8-GFP may not get turned on until the GAL80 level is low enough for GAL4 activation, and then after GFP is expressed, one has to wait for the GFP chromophore to develop (for review, see Tsien, 1998). Despite these slight disadvantages, the MARCM approach has already been used successfully for the study of many genes (Lee and Luo 1999, 2001; Lee *et al.*, 1999; 2000a,b; Scott *et al.*, 2001; Hitier *et al.*, 2001; Jefferis *et al.*, 2001; Grueber *et al.*, 2002; Sweeney *et al.*, 2002) and also for a screen (Lee *et al.*, 2000c).

VI. Functional Analysis Techniques in the *Drosophila* Nervous System

Many mutants modifying the nervous system will alter the communication between neurons and their target cells. To rigorously determine how a particular gene product affects the activity of an excitable cell *in vivo*, several methods directly monitoring neuronal physiological function are used in *Drosophila* and described in this section. Elevation of intracellular calcium is the trigger for the exocytosis of synaptic vesicles, and the released transmitter typically leads to a postsynaptic electrical response. Methods that can monitor the neuron at all of these stages of neuronal communication are discussed, i.e., measurements of (1) calcium levels, (2) vesicle dynamics, (3) protein dynamics, and (4) electrical signals.

A. Imaging and Manipulating Calcium Levels in *Drosophila* Neurons

Calcium is the primary trigger of neuronal activity and as such is the most important ion to be imaged dynamically. In *Drosophila*, $[Ca^{2+}]$ has been measured in cultured giant neurons (see later; Berke *et al.*, 2002), larval NMJs (Karunanithi *et al.*, 1997; Umbach *et al.*, 1998a,b; Dawson-Scully *et al.*, 2000; Kuromi and Kidokoro, 2002), adult photoreceptors (Ranganathan *et al.*, 1994; Peretz *et al.*, 1994; Hardie, 1996), and kenyon cells of the adult brain mushroom body (MB) (Rosay *et al.*, 2001; Wang *et al.*, 2001). These studies used various methods to generate calcium measurements, including a transgenically expressed calcium-sensitive protein (proaequorin; Rosay *et al.*, 1997, 2001), and either injected (Hardie, 1996) or extracellularly loaded calcium-sensitive fluorescent dyes (Karunanithi *et al.*, 1997; Umbach *et al.*, 1998a,b; Dawson-Scully *et al.*, 2000; Wang *et al.*, 2001; Berke *et al.*, 2002; Kuromi and Kidokoro, 2002). Controlled photoactivation of caged calcium has also been achieved in larval motorneurons (Kuromi and Kidokoro, 2002). In these studies, neuronal activity was stimulated by several means, including application of high $[K^+]$ to depolarize cells (Berke *et al.*, 2002), application of α -latrotoxin (Umbach *et al.*, 1998), direct electrical stimulation (Karunanithi *et al.*, 1997; Umbach *et al.*, 1998a; Dawson-Scully *et al.*, 2000; Kuromi and Kidokoro, 2002), light (Peretz *et al.*, 1994; Ranganathan *et al.*, 1994; Hardie, 1996), odors (Wang *et al.*, 2001), or endogenous neuronal activity (Rosay *et al.*, 2001).

Each method has its own advantages and disadvantages. If intact tissues are to be used, none of these methods are useful except for visualizing cells close to the surface because light penetration and reliable, accurate fluorescence capturing is efficient only at the surface. However, an interesting structure, the mushroom body, is close to the surface of the *Drosophila* brain, and calcium measurements have demonstrated interesting properties of some of the surface cells in this region (Rosay *et al.*, 2001; Wang *et al.*, 2001). Extracellular AM-calcium dyes (ester forms of the dyes allowing membrane permeability) are used frequently in other organisms, but they take 1 h to load and then some time for the endogenous

esterase to cleave the side group from the membrane permeable version. If one proceeds without this last maturation step, misleading results could be obtained as the dye is restored to its Ca-binding form only after cleavage. Therefore, this method requires maintaining a preparation healthy for prolonged periods prior to the initiation of the experiment, and some mutant neurons may be less hardy than wild-type neurons. In addition, in order to achieve good sensitivity, high concentrations of intracellular dyes ($100\ \mu\text{M}$) are sometimes required and some damping of the calcium spikes cannot be avoided as these dyes are potent calcium buffers (Requena *et al.*, 1991; Takahashi *et al.*, 1999). A range of dyes with different kinetics and K_d values for calcium exist, and combinations of dyes have been used by vertebrate investigators to extend the dynamic range (Voets, 2000). A distinct advantage of some of these dyes is that they are ratiometric, thereby minimizing the need to obtain equivalent dye loading and eliminating errors due to photoinactivation of the dye or dye escaping the cells. Also in live samples that occasionally move, a ratiometric dye will help minimize errors due to movement of the sample. Many of the calcium dyes are measured by sampling at two wavelengths, and typically the measurements at the two wavelengths are inversely proportional to the calcium level. This amplifies the signal and eliminates concerns about dye loss.

Calcium imaging via proaequorin requires loading of the prosthetic group colentraxine (Brini *et al.*, 1995; Rosay *et al.*, 1997, 2001; for review, see Chiesa *et al.*, 2001). Because this can take 1 to 6 h and equivalent levels may not necessarily be achieved, loading is done as rapidly as possible to avoid degradation of the sample (Brini *et al.*, 1995; Rosay *et al.*, 1997, 2001). Aequorin gives off luminescence and is therefore relatively insensitive, as each molecule can undergo only one reaction (for review, see Chiesa *et al.*, 2001). Typically, luminometers are used to measure the output, but photon-counting methods can also be used. Bio-Rad confocals have excellent photon-counting abilities and could be used. However, an advantage of aequorin is that it is a poor calcium buffer, and intracellular calcium levels are not perturbed dramatically by this calcium probe (Chiesa *et al.*, 2001). Aequorin has also been fused to different proteins, leading to the targeting of the chimera to different intracellular compartments (Marsault *et al.*, 1997; see review by Chiesa *et al.*, 2001). It has been demonstrated that fusion of aequorin and its native partner in the jellyfish, GFP, allows for fluorescence detection that is more sensitive than luminescence (Waud *et al.* 2001). In theory, if such a construct were introduced into flies, more sensitive Ca imaging could be assayed by measuring fluorescence. Another advantage of aequorin is its naturally wide dynamic range ($0.5\text{--}30\ \mu\text{M}\ \text{Ca}^{2+}$), and a genetically modified version can measure calcium up to the $300\text{-}\mu\text{M}$ range (Llinas *et al.*, 1992). This feature of aequorin has been taken advantage of by Marsault *et al.*, (1997). In this study, they were able to obtain calcium measurements in the range of $100\text{--}200\ \mu\text{M}$ calcium close to the membrane using a SNAP-25–aequorin chimera (Marsault *et al.*, 1997).

Our laboratory and others have also attempted FRET using cameleon, a protein fusion of two versions of GFP with different fluorescent properties, fused to calmodulin and to the myosin light chain kinase calmodulin-binding domain

(see Reiff and Schuster, 2000). As has been reported for this fusion in *C. elegans* (Kerr *et al.*, 2000), this method is quite difficult because the ratio does not change to a great degree, resulting in a poor signal-to-noise ratio. However, better GFP-based calcium-sensing probes are being developed (Truong *et al.*, 2001; Nagai, 2001), which, if introduced into flies, would avoid any incubation prior to initiation of the experiments.

B. Monitoring Membrane Dynamics with Stryl Dyes

The kinetics of vesicle dynamics may be monitored by members of a family of fluorescent lipophilic stryl dyes (Betz and Bewick, 1992). These dyes are useful tools for studying synaptic vesicle exocytosis and recycling because they reversibly stain membranes, they are membrane impermeant, and they fluoresce. They are a complementary technique to electrophysiological methods in that the distribution of vesicles can be observed directly and rates of endocytosis and exocytosis can be measured. This method also does not depend on measuring a postsynaptic response, which is the typical assay of electrophysiological methods and therefore potentially allowing one to dissect pre- and postsynaptic effects of a mutation. However, dye-loading experiments do not provide the resolution of electrophysiology. Several variants have been made with different fluorescent properties (FM1-43, fluorescein-like; FM4-64, rhodamine-like). Modifications of the original dye have yielded products with altered hydrophobic properties, and therefore with different washout kinetics (Betz *et al.*, 1996; Ryan *et al.*, 1996; Klingauf *et al.*, 1998). For example, FM2-10 dissociates much faster from the membrane, allowing one to distinguish populations of vesicles with different recycling properties (Ryan *et al.*, 1996; Klingauf *et al.*, 1998; Schote and Seelig, 1998; Pyle *et al.*, 2000). Vesicle recycling is monitored by labeling the plasma membrane via dye in the extracellular media, and subsequent stimulation of exocytosis. Stimulation of exocytosis causes fusion of the vesicular membrane with the plasma membrane, thereby allowing binding of the dye to the exocytosing membrane. The stained membrane is then internalized. Washout of the dye from the plasma membrane in the absence of synaptic activity is performed using calcium-free buffers. At this point one can either measure the amount of membrane internalized by measuring the total fluorescence or one can restimulate the cell, causing the dye to unload, thereby allowing the measurement of exocytosis. Another useful feature of the dye FM1-43 that has been underutilized by fly neurobiologists is that it can be photoconverted into an electron-dense precipitate, allowing EM detection of the marked vesicle (Henkel *et al.*, 1996; Richards *et al.*, 2000; Schikorski and Stevens, 2001; Harata *et al.*, 2001).

The first use of FM1-43 by fly neurobiologists at the larval NMJ was to demonstrate that a mutation in the gene *shibire* blocks endocytosis, and that endocytosis requires extracellular calcium (Ramaswami *et al.*, 1994). Since those experiments, FM1-43 has been used to characterize vesicle cycling in wild-type motoneurons (Kuromi *et al.*, 1997; Kuromi and Kidokoro, 1999, 2000, 2002)

and in many synaptic mutants (Gonzales-Gaitan and Jackle, 1997; Ranjan *et al.*, 1998; Kuromi and Kidokoro, 1998; Delgado *et al.*, 2000; Fergestad and Broadie, 2001; Stimson *et al.*, 2001; Verstreken *et al.*, 2002; Guichet *et al.*, 2002; Roche *et al.*, 2002).

To label *Drosophila* with stryly dyes, embryos or third-instar larvae are dissected (as described in Section IV,D) in calcium-free saline and are loaded with FM1-43. Generally, the dye is loaded for 5 min using elevated extracellular potassium (50–90 mM) containing 0.8–10 μ M FM1-43 (Ramasawami *et al.*, 1994; Gonzalez-Gaitan and Jackle, 1997; Fergestad and Broadie, 2001). A more physiological approach can be achieved via stimulation by a suction electrode leading to labeling of only a subset of neurons. Wash the fillets twice rapidly and then four to six times in Ca-free buffer for 5 min. One can now quantitate the amount of fluorescence retained by the bouton. To measure exocytosis, one can also unload the dye using either elevated potassium or electrical stimulation. By using different staining/destaining protocols, the size and dynamics of subpopulations of vesicles can be determined.

C. Monitoring Protein Dynamics in Living *Drosophila* Neurons

Various aspects of *Drosophila* cell biology can be monitored in mutants using available GFP markers of subcellular compartments (Brand, 1995, 1999; Hazelrigg, 2000). New GFP variants or other fluorescent proteins spanning the visible range have been produced, allowing multicolor labeling and FRET between the appropriate GFP pairs (for reviews, see Tsien, 1998; van Roessel and Brand, 2002), but to date no published reports using *Drosophila* have taken advantage of these new tools. Many transgenics expressing GFP-tagged proteins are available, including a general membrane marker (mCD8-GFP), a postsynaptic marker (Shaker-GFP), cytoskeletal markers (actin, Verkhusha *et al.*, 1999; moesin, Edwards *et al.*, 1997; Tau, Brand, 1995; and tubulin, Grieder *et al.*, 2000), a mitochondrial marker (cytochrome C-GFP, Pilling and Saxton, 1999), synaptic vesicle markers (synaptobrevin-GFP, Estes *et al.*, 2000; Zhang *et al.*, 2002 and synaptotagmin-GFP, Zhang *et al.*, 2002), and a densecore vesicle marker (ANF-GFP, Rao *et al.*, 2001). These GFP reporters label compartments that are highly dynamic and can be used to assess the effect of a mutation on an organelle and to determine the earliest point of deviation from the wild type. For example, the biogenesis, axonal transport, and localization of synaptic vesicles are regulated by many proteins (Rodesch and Broadie, 2000), and the effect of mutations in these proteins could be studied through the use of GFP markers of the cytoskeleton and vesicles. Bleaching and then observing recovery of the fluorescence (FRAP) has been shown to be feasible at the larval *Drosophila* NMJ (Zhang *et al.*, 2002), and similar methods should allow one to also look at the effect of mutations on both the dynamics and distribution of vesicles and the underlying cytoskeleton. A word of caution about these markers is that some may not fully rescue null mutants and some markers may even lead to their own phenotypes (Williams *et al.*, 2000).

The process of bouton development has been studied at the neuromuscular junction using a GFP fusion of CD8 with the postsynaptic targeting domain of Shaker (Shaker PDZ domain). The NMJ could be imaged live, and the process of bouton duplication was examined (Zito *et al.*, 1999). New boutons appeared to be added at the end of existing boutons or are “inserted” between existing ones. This division could be symmetric or asymmetric similar to yeast budding. This observation led to a later study testing the idea that yeast budding and bouton division share some machinery in common (Eaton *et al.*, 2002).

All of these GFP markers could also be used for genetic screens and soluble GFP (Kraut *et al.*, 2001) and Shaker-GFP have been used for this purpose. In *C. elegans*, a GFP-synaptobrevin strain was used to find proteins with roles in synaptogenesis (Jin, 2002) by screening for mutants with an altered distribution of the GFP marker.

VII. *Drosophila* Electrophysiology

Of the forward genetic systems (*C. elegans*, *Drosophila*, and zebrafish), physiological assays of neuronal function are the most advanced and sophisticated in *Drosophila*. However, relative to nongenetic systems, the range of recording configurations in *Drosophila* is decidedly limited, and there remains a great need for expansion and refinement. The lion's share of *Drosophila* recording has been done at the neuromuscular junction in the embryo, larva, and adult (giant fiber system). Neuronal properties have been characterized most fully in primary culture cells derived mostly from gastrula-stage embryos, but also from the larval and adult brain. The first tentative steps have been made to record from neurons *in situ* in both the embryo and larva. In addition, a number of sensory systems have been characterized, including the eye, antenna, and mechanosensory structures. This section provides a brief overview of the electrophysiological approaches available in flies. A more comprehensive treatment of these methods is provided in Broadie (2000a,b).

A. Recording from Cultured Neurons

Drosophila neurobiologists have used primary neuronal cultures for decades (Seecof, 1979; Seecof *et al.*, 1971, 1973). The most common method is to collect cells from gastrulating embryos that are then grown in dissociated cell culture in serum-supplemented media. *Drosophila* embryonic cultures are unique in that neurons arise from precursors that undergo mitosis and differentiation *in vitro*. Neuroblasts repeatedly divide and differentiate to form clonal lineages of neurons, which extend neurite processes during the first 24 h (Seecof *et al.*, 1971, 1973). A single identified neuroblast grown in culture can give rise to progeny that express the molecular markers and functional properties expected for that lineage *in vivo* (Luer and Technau, 1992; Schmidt *et al.*, 2000). Multinucleate myocytes will also

differentiate in conjunction with neurons, and extracellular stimulation of neurite bundles terminating on myocytes can result in muscular contraction, indicating functional neuromuscular synaptic connections (Seecof *et al.*, 1972).

A disadvantage of traditional “Seecof-type” cultures is that neurons are small ($\sim 4 \mu\text{m}$ in diameter) and fragile. However, with whole cell patch-clamp recording, it is feasible to examine voltage-gated ion channels in these cultured neurons (Byerly and Leung, 1988; O’Dowd and Aldrich, 1988; Leung *et al.*, 1989; O’Dowd *et al.*, 1989; Germeraad *et al.*, 1992; Tsunoda and Salkoff, 1995). Mutations that eliminate or severely reduce the function of essential neuronal genes result in embryonic lethality. Such mutations can be assayed in cultured neurons prepared from single embryos obtained from heterozygous parental stocks, each having one copy of the mutation or deficiency over a “balancer” chromosome. Homozygous single embryo cultures are identified by the absence of expression of reporter genes present on the balancer chromosomes. Initial studies employed lacZ-marked balancers; however, it is now easier to use balancer chromosomes containing green fluorescent protein coding sequences, under the control of various promoters, which make it possible to identify the genotype of living single embryo cultures prior to recording.

The small size of cultured neurons has made recording problematic. A variant method has been to use “giant” neurons (10–15 μm in diameter) formed following cytochalasin B treatment of neuroblasts to block cell division (Wu *et al.*, 1990). These large, multinucleate cells display neuronal morphology and express voltage-gated currents; moreover, it is possible in whole cell patch clamp to record evoked and spontaneous action potentials in these neurons (Saito and Wu, 1991; Yao and Wu, 1999). The most recent embryonic culture system uses a defined, serum-free, bicarbonate-buffered medium (O’Dowd, 1995; O’Dowd *et al.*, 1995). In this medium, neurons are somewhat larger (up to 8–12 μm diameter) than those in serum-supplemented medium ($\sim 4 \mu\text{m}$ diameter). In contrast to recordings from serum-supplemented medium, neurons in this new culture medium appear electrically excitable, exhibit a variety of evoked firing phenotypes, and some also generate action potentials spontaneously (Hodges *et al.*, 2002).

Neurons differentiating in all of these culture systems express synaptic vesicle molecular markers localized to varicosities that resemble synaptic boutons and also express functional acetylcholine (ACh) receptor channels (Rohrbough *et al.*, 2002). It is therefore surprising that synaptic transmission in culture has not been well established. However, spontaneous autaptic synaptic currents in a “giant” neuron have been reported in a whole cell patch-clamp recording configuration (Yao *et al.*, 2000). Moreover, two studies from defined medium cultures demonstrate fast synaptic transmission between neurons, but as yet only in the form of spontaneous vesicle fusion events (Lee and O’Dowd, 1999, 2000). Pharmacological analyses reveal that fast excitatory synaptic currents are cholinergic and mediated by cationic AChRs, whereas fast inhibitory synaptic currents are GABAergic and mediated by picrotoxin-sensitive chloride channel receptors.

Because *Drosophila* behavioral studies are performed on adult flies, an important goal is to record from neurons known to mediate specific behaviors. Adult neurons are born during larval instars and differentiate during early/midpupal stages. These differentiating neurons can be dissociated from the CNS and grown in disassociated cell cultures. Using a lacZ reporter in cultures prepared from third instar brain, it has been possible to specifically identify and record from mushroom body (MB) neurons (Wright and Zhong, 1995; Delgado *et al.*, 1998) a brain area that coordinates olfactory learning and memory (Davis, 2001). Cultured MB neurons express a number of voltage-gated potassium currents in whole cell patch-clamp recordings, but there are no reports describing sodium currents, sodium-dependent action potentials, or synaptic transmission in these neurons. However, studies from the laboratory of O'Dowd demonstrate that neurons harvested from late pupae (P9 through preecllosion adults) do express voltage-gated sodium, calcium, and potassium currents, and a subset are electrically excitable (Rohrbough and Broadie, 2002). Functional synaptic connections also appear to form between neurons (H. Su and D. K. O'Dowd, in preparation). These studies suggest that synaptic transmission and modulation studies in identified adult neurons in culture may soon be feasible.

B. Recording from the Neuromuscular Junction

The NMJ has been the primary site of recording in *Drosophila* and has provided a wealth of information on synaptic development, function, and plasticity. The embryonic NMJ is accessible to whole cell patch-clamp recording throughout its differentiation. At 25°C, the motor neurons first contact their target muscles at 12–14 h after fertilization (AF) and elaborate synaptic terminals until hatching from the egg case at 20–22 h AF (Broadie and Bate, 1993). Embryos can be prepared for electrophysiology as outlined in Section IV.D.

In later-stage embryos (>16 h AF at 25°C) the muscles are covered by a sheath that must be removed enzymatically prior to recording, using 1- to 2-min exposure to 1 mg/ml collagenase (type IV) in divalent cation-free saline. For recording, embryos in a Plexiglas recording chamber are viewed from above with an upright compound microscope fitted with Nomarski (DIC) optics and a 40–63× water-immersion lens with a long working distance. Conventional whole cell patch-clamp recordings are made at 18°C with patch pipettes pulled from fiber-filled borosilicate glass (tips heat polished to ~1 μm I.D.). Current records are made from identified multinucleate muscle fibers in a voltage clamp (standard holding potentials –60 to –80 mV) (Broadie and Bate, 1993; Broadie *et al.*, 1997; Fergestad *et al.*, 1999; Featherstone *et al.*, 2002). The patch pipette solution contains (in mM): 120 KCl, 20 KOH, 4 MgCl₂, 0.25 CaCl₂, 5 EGTA, 4 Na₂ATP, 36 sucrose, and 5 TES, buffered at pH 7.2. Recordings are usually performed at identified NMJs of the large ventral interior–longitudinal muscle 6 or the dorsal interior–longitudinal muscle 1 in anterior abdominal segments (e.g., A2–A4).

For excitatory junctional current (EJC) recordings, a stimulator (e.g., Grass S48 or S88) is used to deliver 2–6 V, 0.1-ms pulses to a loop of the segmental motor nerve via a glass suction pipette. To assay glutamate receptor function directly, glutamate can be applied directly by a short (e.g., 10–100 ms) pulse of positive current (e.g., 1–10 V) or positive pressure (e.g., 2–4 psi) from a small-tipped ($\sim 5 \mu\text{m}$ opening) pipette containing 1 mM glutamate dissolved in bath solution. A similar application procedure can be used for a variety of other substances, such as hyperosmotic saline, latrotoxin, and calcium ionophores (Aravamudan *et al.*, 1999; Fergestad *et al.*, 1999; Featherstone *et al.*, 2000, 2002). Signals are recorded with a standard patch-clamp amplifier (e.g., Axopatch 1D), filtered (usually at 1–2 kHz), converted to a digital signal using an analog-to-digital interface (e.g., DigiData 1200, Axon Instruments), and acquired with a computer using appropriate software (e.g., pClamp 8, Axon Instruments).

Similar recordings are possible throughout larval development. However, due to the ever-increasing size of the muscles, whole cell patch-clamp recording is not feasible past the first instar. For recording in second and third instars, most laboratories use either very simple intracellular voltage recordings or, as we strongly recommend, two-electrode voltage-clamp (TEVC) recordings (Jan and Jan, 1976a; Zhong and Wu, 1991; Rohrbough *et al.*, 1999, 2000). Larvae are dissected (similar to embryos described earlier, but much easier) and viewed with DIC optics and a 40 \times water-immersion lens. Segmental motor nerves are severed near the CNS to eliminate junctional responses originating from CNS activity, and EJCs are evoked by stimulating (0.25–1 ms) the severed nerve with a suction electrode filled with external saline. For maximum stability, we recommend recording at 18 $^{\circ}\text{C}$ or lower.

Electrophysiological records are usually obtained from muscle 6 or muscle 12 in the anterior ventral abdomen (A2–A5) of wandering third instar larvae (~ 5 –6 days AF at 25 $^{\circ}\text{C}$) using standard TEVC techniques. EJCs are recorded in the range of -60 to -80 mV in the voltage-clamped muscle. Voltage-recording electrodes are filled with 3M KCl and have resistances of 10–40 M Ω . Current-passing electrodes are filled with a 3:1 mixture of 3M K $^{+}$ acetate:KCl and have resistances of 10–25 M Ω . Current and voltage signals are amplified in TEVC mode with an appropriate amplifier (e.g., Axoclamp 2B, Axon Instruments). After establishing TEVC, a command pulse should be applied so that amplifier gain, capacitance neutralization, and speed controls of the peak amplitude and kinetics of the current transient are maximal without introducing oscillations or excess noise. For lower Ca $^{2+}$ concentrations (<0.4 mM), at which most recordings should be done, EJCs are small (2–40 nA) and maximum voltage deviations are a few millivolts or less. At higher [Ca $^{2+}$] (0.4–1.0 mM), voltage deviations (5–6 mV) require a properly set compensator at the amplifier. Under these conditions only, the clamp quality and voltage control should be monitored to be adequate to reliably allow observations of larger EJCs. Current signals are normally filtered at 500–1000 Hz and digitized using appropriate acquisition hardware and software (Rohrbough *et al.*, 1999, 2000).

An extracellular “loose-patch” electrode can be used to examine properties of a single NMJ bouton (Mallart *et al.*, 1991; Kurdyak *et al.*, 1994; Rivosecchi *et al.*, 1994). Note that this is not a single synapse recording, as each bouton contains multiple (>10) active zones. Recording electrodes are pulled from glass capillary tubes (e.g., 75 μ l, 1.5 mm O.D.) and are then fire polished and shaped on a microforge. The final electrode should have an inner diameter of 5–10 μ m, which is sufficient to encircle a single bouton, and resistances in the range of 0.5–2 M Ω . Boutons in NMJ terminals can be targeted using either Nomarski optics or a vital fluorescent dye (e.g., 4-Di-2-Asp). Synaptic arbors that permit a perpendicular approach are easier to use to obtain high-resistance seals. For this reason, muscle 13 terminals have been used in preference to normally targeted muscles 6, 7, and 12, which have a more lateral innervation (Kurdyak *et al.*, 1994). A seal around the bouton is made with the “macro-patch” electrode by applying mild suction, usually increasing the resistance two to six times (seal factor; Rivosecchi *et al.*, 1994). Records are made with a loose-patch clamp amplifier. Records contain a calibration pulse for electrode series and seal resistances to correct for attenuated current amplitudes at the electrode tip.

C. Recording from Central Motor Neurons

Despite the dauntingly small size of the *Drosophila* CNS at all stages of development, this system nevertheless provides advantages for recording from central neurons. Many neurons can be identified individually based on their clonal lineage, soma position, axonal projections, and dendritic morphology (Landgraf *et al.*, 1997). Using the Gal4/UAS system, targeted GFP expression can be used to visualize individual neuronal populations or to target transgene expression to specific identified neurons (Baines *et al.*, 1999). The only recording studies published to date have concentrated on a group of five superficial dorsal neurons within the embryonic and larval ventral nerve cord (VNC): four motor neurons (aCC and RP1-4) and the interneuron pCC. The cell bodies of these identified neurons are accessible to whole cell patch-clamp recording electrodes following brief focal treatment of the overlying neurolemma with protease (Baines and Bate, 1998; Baines *et al.*, 1999; Rohrbough and Broadie, 2002).

Electrophysiological analyses of these neurons during embryogenesis reveal the sequential appearance of voltage-gated ionic currents, including several distinct outward K⁺ conductances and inward Ca²⁺ and Na⁺ conductances (Baines and Bate, 1998; Baines *et al.*, 2001). These cells also manifest the ability to fire repetitive action potentials and exhibit agonist-gated responses and synaptically mediated activity (Baines *et al.*, 2001). Closely correlated with functional synaptic activity is the appearance and subsequent maturation of cholinergic synaptic terminals on these neurons, visualized using cell-specific labeling coupled to electron microscopy. These cells first become responsive to ACh at 13–16 h AF (at 25°C), and by hatching (21 h AF) also respond to the inhibitory transmitter GABA ((Baines and Bate, 1998; Rohrbough and Broadie,

unpublished data). By 16–19 h AF, in parallel with the onset of locomotory movement, synaptic input to motor neurons is recorded in the form of both fast AP-mediated spontaneous excitatory synaptic currents (sEPSCs) and periodic, sustained (up to 1 s duration) episodes of excitatory input occurring several times or more per minute (Baines *et al.*, 1999, 2001). This sustained excitatory activity requires cholinergic synaptic input for its generation, as it is eliminated either by conditionally blocking ACh synthesis in cholinergic neurons or by the general blockade of spontaneous and evoked neuronal synaptic vesicle release (Baines *et al.*, 2001). Strong, sustained episodes of cholinergic presynaptic input lead to the activation of voltage-gated currents and large excitatory potentials accompanied by a burst of motor neuron AP firing. The motor output of this centrally generated activity is recorded at the NMJ as patterned bursts of high-frequency excitatory (glutamatergic) transmission that drive the peristaltic muscle contraction underlying coordinated locomotion (Broadie and Bate, 1993; Baines *et al.*, 2001; Cattaert and Birman, 2001).

Dorsal neuronal cell bodies in the larval VNC can also be exposed with focal protease application, similar to the approach described in the embryo by Baines *et al.* (1998). In the larva, the CNS sheath material is drawn by suction into the tip of a large-diameter patch pipette ($\sim 50 \mu\text{m}$) containing 0.5–1% protease (type XIV) in recording saline. When the sheath visibly ruptures (1–2 min), alternating pressure will clear away overlying sheath material and free underlying cell bodies. This procedure can be repeated to enlarge the window and increase the number of soma accessible to a recording pipette. Under these conditions, groups of five superficial dorsal neurons (similar to those observed in the embryo) can be distinguished under Nomarski optics. Neuronal labeling studies confirm that two of these dorsal neurons correspond to the embryonic aCC and RP3 neurons, but the motor projections of the remaining three larval neurons may differ from those in the embryo (Hoang and Chiba, 2001; L. Griffith, personal communication). To confirm cellular identity during recordings, lucifer yellow (dipotassium salt, 1–2 mg/ml) can be added to the patch solution in order to visualize the position and morphology of the cell.

Standard whole cell voltage- and current-clamp recordings can be made from these larval soma (Rohrbough and Broadie, 2002). The external recording saline contains (in mM): 140 NaCl, 3 KCl, 2 CaCl₂, 4 MgCl₂, 5 HEPES, 10 sucrose, 2 NaOH (pH 7.2). The patch solution contains (in mM): 140 K-acetate, 2 MgCl₂, 0.1 CaCl₂, 10 HEPES, 1.1 EGTA, 2 Na₂-ATP, ~ 6 KOH (pH 7.2). Voltage-clamp recordings are made at holding potentials of -60 mV at 18°C. Typical unadjusted resting potentials are in the range of -45 to -65 mV (-52.9 ± 7.5 mV, mean \pm SD, $n = 78$). Action potential firing in response to intracellular injection of depolarizing current reveals the characteristic biphasic current at holding potentials of -30 to -40 mV. Endogenous synaptic activity and analogous evoked responses can be recorded continuously for up to 30 min. Synaptic responses are evoked electrically using several alternate techniques. A suction pipette (10- to 20- μm tip) filled with external saline can be used in one of two configurations: (1)

stimuli (3–40 V, 1–10 ms) are applied to an anterior peripheral nerve, or nerve stump, close to its exit from the CNS or (2) stimuli can be applied directly to the lateral neuropil region anterior to the soma. The neuropil can also be stimulated via a sharp microelectrode filled with 1 M KCl. Similar results are obtained for each approach. Fast EPSCs are evoked most successfully using smaller diameter (5–10 μm) pipettes. Stimulation pipettes are placed into the neuropil either ipsi- or contralateral to the selected soma, approximately one segment anterior or posterior to the expected location of the presumed dendritic region. Electrophysiological data are filtered (0.5–2 kHz), **written to disk (5–10 kHz)**, and analyzed using appropriate acquisition and analysis hardware.

Drugs and agonists can be focally applied to the soma of recorded cells either iontophoretically or via a pressure pipette ($\sim 1\text{-}\mu\text{m}$ -diameter tip). Motor neurons in mature larval VNC respond to multiple neurotransmitter agonists: they are strongly excited by ACh and respond more weakly to GABA and glutamate, both of which elicit inhibitory responses mediated primarily by picrotoxin-sensitive Cl^- currents (Rohrbough and Broadie, 2002). The VNC central neuropil is densely packed with cholinergic axonal fibers with synaptic-like boutons, which overlap the dendritic arbors of these neurons (Rohrbough *et al.*, 2000). Larval motor neurons exhibit endogenous forms of synaptic activity analogous to that present in the mature embryo, including fast sEPSCs, and sustained excitatory “rhythmic” currents (Rohrbough and Broadie, 2002). Electrical stimulation triggers sustained responses with the same features and pharmacology as endogenous forms of activity, indicating that they share the same cholinergic synaptic basis. Furthermore, focal electrical stimulation of defined regions of the neuropil adjacent to the motor neuron dendritic regions excites fast EPSCs, indicating that transmission at single excitatory synaptic inputs can be driven experimentally, a crucial prerequisite for ongoing detailed functional synaptic plasticity assays.

D. The Characterized *Drosophila* Circuit: Giant Fiber System

The best defined neuronal circuit in *Drosophila* is the adult giant fiber (GF) escape circuit linking the brain and the jump/flight muscles in the thorax (Tanouye and Wyman, 1980; Koto *et al.*, 1981; Tanouye and King, 1983; Tanouye and Ferrus, 1985). This circuit is composed of the giant neuron, with soma in the brain and axon running into the thoracic nerve cord (TNC), mixed electrical/chemical synapses on identified interneurons and motor neurons in the TNC, and motor output onto identified thoracic muscles. To record currents, flies are lightly anesthetized (e.g., cooling) and mounted on a standard dissection microscope platform immobilized with a low-melting point wax (e.g., myristic acid or Tackiwax). The orientation is adjusted to allow the passage and circulation of air in the tracheal system during recording, but the remaining body is best immersed in saline. The thoracic and abdominal spiracles can be aerated as reported by Ikeda and Kaplan (1974). No dissection is required for the recording. However, for better access and more controlled recordings, the preparation can be dissected. An incision is made

in the dorsal or lateral thorax to expose the dorsal longitudinal flight muscles (DLM). These six fibers receive thousands of en passant-type synapses from a single excitatory motor neuron (Ikeda *et al.*, 1980; Ikeda and Koenig, 1988). The motor neuron axons extend through the posterior dorsal mesothoracic nerve (PDMN). The dorsal-lateral surfaces of the DLM and the PDMN are exposed through dissection. The tergochanteral (TTM) jump muscle shares innervation with the DLM and can be recorded from in a similar fashion (Engel and Wu, 1992, 1994).

The giant fiber circuit may be stimulated in two ways (Wu *et al.*, 1978; Elkins and Ganetzky, 1988; Koenig *et al.*, 1989): (1) through extracellular tungsten electrodes (10–50 V; 0.1–0.5 ms), placed in each eye, or (2) intracellularly with depolarizing current passed through an impaling electrode. Recording sites are identified physiologically based on the fact that the giant fiber drives the DLM in a one-to-one fashion; the muscle is not driven one to one by any other cervical connective axon (Ikeda *et al.*, 1980; Tanouye and Wyman, 1980; Koto *et al.*, 1981; Tanouye and King, 1983; Tanouye and Ferrus, 1985). Alternatively, the PDMN may be cut with fine scissors 20–40 μm from the thoracic ganglion, and the nerve can be stimulated (1–5 V, 0.1–0.5 ms) with a glass suction electrode (5–10 μm I.D.) filled with bath saline. This technique is similar to the larval NMJ preparation (given earlier). A tungsten electrode is inserted in the abdomen to measure reference potential. Excitatory junctional potential (EJP) recordings are made with an intracellular electrode in a DLM fiber filled with 3 M KCl (resistances of 10–40 M Ω) (Wu *et al.*, 1978; Koenig *et al.*, 1989). The electrode may be beveled using silicon carbide grit to reduce resistance to 5–10 M Ω and for easier penetration. Healthy cells should have a resting potential greater than –70 mV. Additionally, a two electrode voltage and current clamp can be used as in the larval preparation (Elkins and Ganetzky, 1988). Voltage-clamp records have been made at 4°C (preparation cooled with a Peltier plate) or near room temperature (16–21°C). This preparation can be stable for several hours.

Intracellular recordings can also be made from neuronal cells in the GF circuit. Giant fiber recordings are made with sharp glass electrodes with resistances of 40–60 M Ω . The giant fiber resting potential is normally in the range of 60–80 mV, whereas adjacent cervical axons are difficult to stably penetrate and have substantially lower values (\sim –30 mV). GF action potentials average 60–70 mV in amplitude and overshoot zero approximately 50% of the time (Tanouye and Ferrus, 1985). Using the contour of ganglia and nerves as a guide, a number of motor neurons can be identified and impaled for intracellular recording. These cells include flight and leg motor neurons, such as the DLM motor neurons, tergochanteral motor neuron (TTMn), steering motor neurons (e.g., B1mn), and the fast extensor tibiae motor neuron (FETi; Ikeda and Koenig, 1988; Trimarchi and Schneiderman, 1994; Trimarchi and Murphey, 1997). Intracellular recording from the motor neurons is achieved with sharp glass electrodes of high resistance filled with 3 M KCl. The ability to successfully impale an identified motor neuron is relatively low (<20%) and so recording is usually coupled with an intracellular dye

injection technique that permits unequivocal identification of the cell following recording.

E. Recording from Sensory Systems

A great deal of electrical recording has been obtained from the adult eye, mostly to study phototransduction, but also, to a lesser extent, to examine central synaptic transmission (photoreceptor to lamina neurons; Pak *et al.*, 1969; Kelly and Suzuki, 1974; Broadie, 2000b; Zhang *et al.*, 2001). The oldest and simplest technique is the electroretinogram (ERG), which provides a measurement of whole retina extracellular electrical response to light stimuli. The on- and off-ERG transients provide a crude, massed measurement of synaptic activity downstream of photoreceptor activation (Kelly and Suzuki, 1974). To record ERGs, young adults are anesthetized (e.g., cooling, CO₂), accessibly embedded (e.g., in low melting point wax) to prevent movement and so that the head is rigidly held in place, and viewed with a low magnification (20–40×) dissection microscope. A reference electrode (e.g., tungsten wire or glass electrode filled with standard saline) is inserted into the back of the head (or thorax). A recording electrode filled with 3 M KCl is inserted into the center of the fly eye to a variable (controlled) depth. Flies may be dark adapted prior to recording. Illumination can be provided by the collimated beam of a 12-V, 75- to 100-W QI bulb passed through neutral density filters and a yellow filter (e.g., Schott OG530) to ensure that only responses from one class of photoreceptor (R1–R6) are recorded. Light stimuli can be supplied by a variety of sources with a computer-controlled shutter/timer driver, and light-evoked traces are recorded using an appropriate intracellular amplifier (e.g., Dagan IX1) and analyzed using appropriate acquisition and analysis hardware. Electrical responses to light represent summed extracellular activity from the photoreceptor field (Hotta and Benzer, 1969; Pak *et al.*, 1969; Kelly and Suzuki, 1974). Although not discussed here, similar extracellular recordings can be made from the antenna to study odorant responses.

For the detailed study of phototransduction, records are best obtained from isolated photoreceptors. To harvest photoreceptors, both late pupal and adult eyes are dissected in chilled (4°C) bath saline solution and then transferred quickly to a bath solution containing 10% fetal calf serum (FCS) (Hardie, 1991a,b). Some investigators use enzymatic treatment (2 mg/ml collagenase IV) in divalent-cation free saline for 3–4 min to begin **dissociation** of the retina (Hevers and Hardie, 1995). To dissociate ommatidia mechanically, the retina is triterated gently with an unsiliconized glass pipette fire polished to a diameter of approximately 100–150 μm. This treatment causes the ommatidia to break off at the basement membrane and pigment cells surrounding the photoreceptors to disintegrate (Hardie, 1991a,b). The dissociated cells can be recorded from immediately or stored in FCS saline at 4°C for several hours prior to experimentation. A semi-intact preparation in which the retina is still attached to the lamina can be

generated with milder treatment (Hevers and Hardie, 1995). In both cases, the ommatidia are accessible for patch-clamp recording under Nomarski (DIC) optics on an inverted microscope. Recordings are made with patch pipettes pulled from borosilicate glass (fiber filled) with resistances of 3–5 M Ω for whole cell recordings or 6–12 M Ω for isolated patch recording (Hardie, 1991a,b; Hardie *et al.*, 1991). Seal resistances are typically 5–10 G Ω . In whole cell records, series resistance is in the range of 6–25 M Ω and input resistance 100–2000 M Ω (pupal) or 50–100 M Ω (adult). Cell capacitance increases with age from \sim 3 pF at stage p8 to \sim 30 pF in stage p15 (mature preeclosure pupae; Hardie, 1991a,b; Hardie *et al.*, 1991). Both late pupal and adult cells produce electrical response to light, but this light-activated current typically runs down within a few minutes. The resting potential also tends to decay with time from \sim 50–60 mV to zero. However, voltage-gated currents appear normal under these conditions.

A variety of recording configurations have been established to assay mechanotransduction. Extracellular recordings of mechanically evoked bristle responses have been measured as a transepithelial potential (TEP), a voltage difference between the apical and basal sides of the sensory epithelium (Kernan *et al.*, 1994). One electrode is placed over the cut end of a thoracic bristle (humeral or anterior notopleural macrochaete bristle) and the reference electrode is inserted into the thorax so that it contacts the hemolymph. To stimulate the bristle, the electrode is mounted on a piezoelectric microstage that deflects the bristle. The generation of the TEP serves as a general assay of mechanoreception (Kernan *et al.*, 1994). The adult wing contains a set of eight campaniform sensilla—sensory structures that detect the mechanical deformation of the wing cuticle. It is possible to record the extracellular activity from these campaniform sensory axons as they run through the wing vein (Palka *et al.*, 1986; Dickinson and Palka, 1987). To prepare, the base of the wing is cut so that a small portion of the thorax remains attached and the distal tip of the wing is removed. The wing is then placed with a saline well for the thoracic tissue and another for the cut outer edge of the wing. The wing should now be stretched between two drops of saline with an open passage through the third wing vein. To record extracellular activity of the campaniform neurons, a high impedance differential amplifier is used with one electrode in each of the saline wells (Dickinson and Palka, 1987). Stimulation can be provided with a piezoelectric probe to precisely control the degree and duration of wing depression. This provides another general assay of mechanoreception (Dickinson and Palka, 1987).

F. Future Directions: Recording from the Adult Brain

Recording in the embryonic and larval CNS has advanced to allow the characterization of basic electrical and synaptic transmission properties in identified neurons. The important next step will be to develop approaches for assaying synaptic plasticity relevant to behavioral modulation. Specifically needed are methods to assay the short-term and long-term activity-dependent modulation

of synaptic transmission. These methods include paired-pulse and short-term facilitation and posttetanic potentiation. It is also important to determine whether frequency-dependent synaptic depression is an important component of plasticity in *Drosophila* circuits. A major objective will be to determine whether long-term potentiation and/or long-term depression are active at central *Drosophila* synapses, as suggested in other insects (Oleskevich, 1997).

A sizable gulf remains between recent advances in the embryonic and larval CNS and successful recording in adult CNS areas. One obvious target is the mushroom body, a paired L-shaped structure of $\sim 80\ \mu\text{m}$ diameter containing ~ 2500 neurons per hemisphere. This structure regulates olfactory learning and memory behavior (Armstrong *et al.*, 1998; Waddell and Quinn, 2001; Pascual and Preat, 2001; reviews by Davis, 2001; Roman and Davis, 2001). Extracellular field recordings in the (much larger) MBs of honeybees have demonstrated both cholinergic synaptic transmission (Oleskevich, 1999) and long-term synaptic plasticity (Oleskevich *et al.*, 1997). Synaptic function in the central brain and MBs of *Drosophila*, however, has so far been addressed only indirectly. For example, Ca^{2+} -imaging experiments have shown odorant-induced MB activity (Wang *et al.*, 2001) and altered Ca^{2+} activity in learning mutants (Rosay *et al.*, 2001; reviewed by Davis, 2001; Carlson, 2001). To date, such optical methods represent the only practical means of obtaining physiological access to the *Drosophila* brain.

Acknowledgments

We thank Jeff Rohrbough for critical contributions to this chapter. We also thank numerous members of the Broadie laboratory for discussion and input. We are grateful to Villu Maricq, Mike Bastiani, Ralf Mohrmann, and Sean Speese for their critical reading of this chapter. The authors were supported by grants from the National Institutes for Health.

References

- Aberle, H., Haghghi, A. P., Fetter, R. D., McCabe, B. D., Magalhaes, T. R., and Goodman, C. S. (2002). Wishful thinking encodes a BMP type II receptor that regulates synaptic growth in *Drosophila*. *Neuron* **33**, 545–558.
- Acebes, A., and Ferrus, A. (2000). Cellular and molecular features of axon collaterals and dendrites. *Trends Neurosci.* **23**, 557–565.
- Acharya, J. K., Jalink, K., Hardy, R. W., Hartenstein, V., and Zuker, C. S. (1997). InsP3 receptor is essential for growth and differentiation but not for vision in *Drosophila*. *Neuron* **18**, 881–887.
- Adams, M. D., Celniker, S. E., Holt, R. A., Evans, C. A., Gocayne, J. D., Amanatides, P. G., Scherer, S. E., Li, P. W., Hoskins, R. A., Galle, R. F., George, R. A., Lewis, S. E., Richards, S., Ashburner, M., Henderson, S. N., Sutton, G. G., Wortman, J. R., Yandell, M. D., Zhang, Q., Chen, L. X., Brandon, R. C., Rogers, Y. H., Blazej, R. G., Champe, M., Pfeiffer, B. D., Wan, K. H., Doyle, C., Baxter, E. G., Helt, G., Nelson, C. R., Gabor, G. L., Abril, J. F., Agbayani, A., An, H. J., Andrews-Pfannkoch, C., Baldwin, D., Ballew, R. M., Basu, A., Baxendale, J., Bayraktaroglu, L., Beasley, E. M., Beeson, K. Y., Benos, P. V., Berman, B. P., Bhandari, D., Bolshakov, S., Borkova, D., Botchan, M. R., Bouck, J., Brokstein, P., Brottier, P., Burtis, K. C., Busam, D. A., Butler, H., Cadieu, E., Center, A., Chandra, I., Cherry, J. M., Cawley, S., Dahlke, C., Davenport, L. B., Davies, P., de Pablos, B., Delcher, A., Deng, Z., Mays, A. D., Dew, I., Dietz, S. M., Dodson, K., Doup, L. E.,

- Downes, M., Dugan-Rocha, S., Dunkov, B. C., Dunn, P., Durbin, K. J., Evangelista, C. C., Ferraz, C., Ferreira, S., Fleischmann, W., Fosler, C., Gabrielian, A. E., Garg, N. S., Gelbart, W. M., Glasser, K., Glodek, A., Gong, F., Gorrell, J. H., Gu, Z., Guan, P., Harris, M., Harris, N. L., Harvey, D., Heiman, T. J., Hernandez, J. R., Houck, J., Hostin, D., Houston, K. A., Howland, T. J., Wei, M. H., Ibegwam, C., Jalali, M., Kalush, F., Karpen, G. H., Ke, Z., Kennison, J. A., Ketchum, K. A., Kimmel, B. E., Kodira, C. D., Kraft, C., Kravitz, S., Kulp, D., Lai, Z., Lasko, P., Lei, Y., Levitsky, A. A., Li, J., Li, Z., Liang, Y., Lin, X., Liu, X., Mattei, B., McIntosh, T. C., McLeod, M. P., McPherson, D., Merkulov, G., Milshina, N. V., Mobarry, C., Morris, J., Moshrefi, A., Mount, S. M., Moy, M., Murphy, B., Murphy, L., Muzny, D. M., Nelson, D. L., Nelson, D. R., Nelson, K. A., Nixon, K., Nusskern, D. R., Pacleb, J. M., Palazzolo, M., Pittman, G. S., Pan, S., Pollard, J., Puri, V., Reese, M. G., Reinert, K., Remington, K., Saunders, R. D., Scheeler, F., Shen, H., Shue, B. C., Siden-Kiamos, I., Simpson, M., Skupski, M. P., Smith, T., Spier, E., Spradling, A. C., Stapleton, M., Strong, R., Sun, E., Svirskas, R., Tector, C., Turner, R., Venter, E., Wang, A. H., Wang, X., Wang, Z. Y., Wassarman, D. A., Weinstock, G. M., Weissenbach, J., Williams, S. M., Woodage, T., Worley, K. C., Wu, D., Yang, S., Yao, Q. A., Ye, J., Yeh, R. F., Zaveri, J. S., Zhan, M., Zhang, G., Zhao, Q., Zheng, L., Zheng, X. H., Zhong, F. N., Zhong, W., Zhou, X., Zhu, S., Zhu, X., Smith, H. O., Gibbs, R. A., Myers, E. W., Rubin, G. M., and Venter, J. C. (2000). The genome sequence of *Drosophila melanogaster*. *Science* **287**, 2185–2195.
- Adams, M. D., and Sekelsky, J. J. (2002). From sequence to phenotype: reverse genetics in *Drosophila melanogaster*. *Nature Rev. Genet.* **3**, 189–198.
- Agarwala, K. L., Ganesh, S., Amano, K., Suzuki, T., and Yamakawa, K. (2001). DSCAM, a highly conserved gene in mammals, expressed in differentiating mouse brain. *Biochem. Biophys. Res. Commun.* **281**, 697–705.
- Agarwala, K. L., Nakamura, S., Tsutsumi, Y., and Yamakawa, K. (2000). Down syndrome cell adhesion molecule DSCAM, mediates homophilic intercellular adhesion. *Brain Res. Mol. Brain Res.* **79**, 118–126.
- Allikian, M. J., Deckert-Cruz, D., Rose, M. R., Landis, G. N., and Tower, J. (2002). Doxycycline-induced expression of sense and inverted-repeat constructs modulates phosphogluconate mutase (Pgm) gene expression in adult *Drosophila melanogaster*. *Genome Biol.* **3**.
- Ames, B. N. (1966). Assay of inorganic phosphate, total phosphate and phosphatases. *Methods Enzymol.* **8**, 115–118.
- Andrews, J., Smith, M., Merakovsky, J., Coulson, M., Hannan, F., and Kelly, L. E. (1996). The stoned locus of *Drosophila melanogaster* produces a dicistronic transcript and encodes two distinct polypeptides. *Genetics* **143**, 1699–1711.
- Aravamudan, B., Fergestad, T., Davis, W. S., Rodesch, C. K., and Broadie, K. (1999). *Drosophila* UNC-13 is essential for synaptic transmission. *Nature Neurosci.* **2**, 965–971.
- Armstrong, J. D., de Belle, J. S., Wang, Z., and Kaiser, K. (1998). Metamorphosis of the mushroom bodies; large-scale rearrangements of the neural substrates for associative learning and memory in *Drosophila*. *Learn Mem.* **5**, 102–114.
- Aronstein, K., Auld, V., and Ffrench-Constant, R. (1996). Distribution of two GABA receptor-like subunits in the *Drosophila* CNS. *Invert Neurosci.* **2**(2), 115–120.
- Aronstein, K., and Ffrench-Constant, R. (1995). Immunocytochemistry of a novel GABA receptor subunit Rdl in *Drosophila melanogaster*. *Invert. Neurosci.* **1**, 25–31.
- Ashburner, M. (1989a). “*Drosophila*: A Laboratory Handbook.” Cold Spring Harbor Laboratory Press, Cold Spring Harbor, NY.
- Ashburner, M. (1989b). “*Drosophila*: A Laboratory Manual.” Cold Spring Harbor Laboratory Press, Cold Spring Harbor, NY.
- Atwood, H. L., Govind, C. K., and Wu, C.-F. (1993). Neuromuscular junction ultrastructure of ventral abdominal muscles in *Drosophila* larvae. *J. Neurobiol.* **24**, 1008–1024.
- Auld, V. J., Fetter, R. D., Broadie, K., and Goodman, C. S. (1995). Gliotactin, a novel transmembrane protein on peripheral glia, is required to form the blood-nerve barrier in *Drosophila*. *Cell* **81**, 757–767.

- Baines, R. A., and Bate, M. (1998). Electrophysiological development of central neurons in the *Drosophila* embryo. *J. Neurosci.* **18**, 4673–4683.
- Baines, R. A., Robinson, S. G., Fujioka, M., Jaynes, J. B., and Bate, M. (1999). Postsynaptic expression of tetanus toxin light chain blocks synaptogenesis in *Drosophila*. *Curr. Biol.* **9**, 1267–1270.
- Baines, R. A., Uhler, J. P., Thompson, A., Sweeney, S. T., and Bate, M. (2001). Altered electrical properties in *Drosophila* neurons developing without synaptic transmission. *J. Neurosci.* **21**, 1523–1531.
- Bastmeyer, M., and O’Leary, D. D. (1996). Dynamics of target recognition by interstitial axon branching along developing cortical axons. *J. Neurosci.* **16**, 1450–1459.
- Bate, M. (1990). The embryonic development of the larval muscles in *Drosophila*. *Development* **110**, 791–804.
- Bate, M., and Martinez Arias, A. (ed.) (1993a). “The Development of *Drosophila melanogaster*,” Vol. I., Cold Spring Harbor Laboratory Press, Cold Spring Harbor, NY.
- Bate, M., and Martinez Arias, A. (ed.) (1993b). “The Development of *Drosophila melanogaster*,” Vol. II., Cold Spring Harbor Laboratory Press, Cold Spring Harbor, NY.
- Batzer, M. A., Tedeschi, B., Fossett, N. G., Tucker, A., Kilroy, G., Arbour, P., and Lee, W. R. (1998). Spectra of molecular changes induced in DNA of *Drosophila* spermatozoa by 1-ethyl-1-nitrosourea and X-rays. *Mutat. Res.* **199**(1), 255–268.
- Baumann, O. (2000). Distribution of ryanodine receptor Ca(2+) channels in insect photoreceptor cells. *J. Comp. Neurol.* **421**, 347–361.
- Baumgartner, S., Littleton, J. T., Broadie, K., Bhat, M. A., Harbecke, R., Lengyel, J. A., Chiquet-Ehrismann, R., Prokop, A., and Bellen, H. J. (1996). A *Drosophila* neurexin is required for septate junction and blood-nerve barrier formation and function. *Cell* **87**(6), 1059–1068.
- Begg, M., and Cruickshank, W. J. (1963). A partial analysis of *Drosophila* larval haemolymph. *Proc. R. Soc. Soc. Edinburgh.* **68**, 215–236.
- Berger, J., Suzuki, T., Senti, K. A., Stubbs, J., Schaffner, G., and Dickson, B. J. (2001). Genetic mapping with SNP markers in *Drosophila*. *Nature Genet* **29**, 475–481.
- Bellen, H., and Budnik, V. (2000). The neuromuscular function. In “*Drosophila* Protocols” (W. Sullivan, M. Ashburner, and R. S. Hawley eds.), pp. 175–200. Cold Spring Harbor Laboratory Press, Cold Spring Harbor, NY.
- Bello, B., Resendez-Perez, D., and Gehring, W. J. (1998). *Development* **125**, 2193–2202.
- Bentley, A., MacLennan, B., Calvo, J., and Dearolf, C. R. (2000). Targeted recovery of mutations in *Drosophila*. *Genetics* **156**(3), 1169–1173.
- Berke, B., and Wu, C. F. (2002). Regional calcium regulation within cultured *Drosophila* neurons: Effects of altered cAMP metabolism by the learning mutations *dunce* and *rutabaga*. *J. Neurosci.* **22**(11), 4437–4447.
- Betz, W. J., and Bewick, G. S. (1992). Optical analysis of synaptic vesicle recycling at the frog neuromuscular junction. *Science* **255**, 200–203.
- Betz, W. J., Mao, F., and Smith, C. B. (1996). Imaging exocytosis and endocytosis. *Curr. Opin. Neurobiol.* **6**(3), 365–371.
- Beumer, K., Matthies, H. J., Bradshaw, A., and Broadie, K. (2002). Integrins regulate DLG/FAS2 via a CaM kinase II-dependent pathway to mediate synapse elaboration and stabilization during post-embryonic development. *Development* **129**(14), 3381–3391.
- Beumer, K. J., Rohrbough, J., Prokop, A., and Broadie, K. (1999). A role for PS integrins in morphological growth and synaptic function at the postembryonic neuromuscular junction of *Drosophila*. *Development* **126**(24), 5833–5846.
- Bibikova, M., Golic, M., Golic, K. G., and Carroll, D. (2002). Targeted chromosomal cleavage and mutagenesis in *Drosophila* using zinc-finger nucleases. *Genetics* **161**(3), 1169–1175.
- Bieber, A. J., Snow, P. M., Hortsch, M., Patel, N. H., Jacobs, J. R., Traquina, Z. R., Schilling, J., and Goodman, C. S. (1989). *Drosophila* neuroglian: A member of the immunoglobulin superfamily with extensive homology to vertebrate neural adhesion molecule L1. *Cell* **59**(3), 447–460.

- Bier, E., Ackerman, L., Barbel, S., Jan, L., and Jan, Y. N. (1988). Identification and characterization of a neuron-specific nuclear antigen in *Drosophila*. *Science* **240**(4854), 913–916.
- Bieschke, E. T., Wheeler, J. C., and Tower, J. (1998). Doxycycline-induced transgene expression during *Drosophila* development and aging. *Mol. Genet.* **258**, 571–579.
- Billuart, P., Winter, C. G., Maresh, A., Zhao, X., and Luo, L. (2001). Regulating axon branch stability: The role of p190 RhoGAP in repressing a retraction signaling pathway. *Cell* **107**(2), 195–207.
- Blochlinger, K., Bodmer, R., Jan, L. Y., and Jan, Y. N. (1990). Patterns of expression of cut, a protein required for external sensory organ development in wild-type and cut mutant *Drosophila* embryos. *Genes Dev.* **4**(8), 1322–1331.
- Bloor, J. W., and Brown, N. H. (1998). Genetic analysis of the *Drosophila* alphaPS2-integrin subunit reveals discrete adhesive, morphogenetic and sarcomeric functions. *Genetics* **148**, 1127–1142.
- Bogaert, T., Brown, N., and Wilcox, M. (1987). The *Drosophila* PS2 antigen is an invertebrate integrin that, like the fibronectin receptor, becomes localized to muscle attachments. *Cell* **51**, 929–940.
- Bonini, N. M., Leiserson, W. M., and Benzer, S. (1998). Multiple roles of the eyes absent gene in *Drosophila*. *Dev. Biol.* **196**(1), 42–57.
- Bossing, T., and Technau, G. M. (1994). The fate of the CNS midline progenitors in *Drosophila* as revealed by a new method for single cell labelling. *Development* **120**, 1895–1906.
- Bossing, T., Technau, G. M., and Doe, C. Q. (1996a). huckebein is required for glial development and axon pathfinding in the neuroblast 1–1 and neuroblast 2–2 lineages in the *Drosophila* central nervous system. *Mech. Dev.* **55**, 53–64.
- Bossing, T., Udolph, G., Doe, C. Q., and Technau, G. M. (1996b). The embryonic central nervous system lineages of *Drosophila melanogaster*. I. Neuroblast lineages derived from the ventral half of the neuroectoderm. *Dev. Biol.* **179**, 41–64.
- Bouley, M., Tian, M. Z., Paisley, K., Shen, Y. C., Malhotra, J. D., and Hortsch, M. (2000). The L1-type cell adhesion molecule neuroglian influences the stability of neural ankyrin in the *Drosophila* embryo but not its axonal localization. *J. Neurosci.* **20**(12), 4515–4523.
- Bowman, A. B., Kamal, A., Ritchings, B. W., Philip, A. V., McGrail, M., Gindhart, J. G., and Goldstein, L. S. (2000). Kinesin-dependent axonal transport is mediated by the sunday driver (SYD) protein. *Cell* **103**(4), 583–594.
- Bowman, A. B., Patel-King, R. S., Benashski, S. E., McCaffery, J. M., Goldstein, L. S., and King, S. M. (1999). *Drosophila* roadblock and Chlamydomonas LC7: A conserved family of dynein-associated proteins involved in axonal transport, flagellar motility, and mitosis. *J. Cell Biol.* **146**(1), 165–180.
- Brand, A. (1995). GFP in *Drosophila*. *Trends Genet.* **11**, 324–325.
- Brand, A. (1999). GFP as a cell and developmental marker in the *Drosophila* nervous system. *Methods Cell Biol.* **58**, 165–181.
- Brand, A. H., Manoukian, A. S., and Perrimon, N. (1994). Ectopic expression in *Drosophila*. *Methods Cell Biol.* **44**, 635–654.
- Brand, A. H., and Perrimon, N. (1993). Targeted gene expression as a means of altering cell fates and generating dominant phenotypes. *Development* **118**, 401–415.
- Brini, M., Marsault, R., Bastianutto, C., Alvarez, J., Pozzan, T., and Rizzuto, R. (1995). Transfected aequorin in the measurement of cytosolic Ca²⁺ concentration ([Ca²⁺]_i): A critical evaluation. *J. Biol. Chem.* **270**(17), 9896–9903.
- Broadie, K. (1998). Forward and reverse genetic approaches to synaptogenesis. *Curr. Opin. Neurobiol.* **8**, 128–138.
- Broadie, K. (2000a). Electrophysiological approaches to the neuromusculature. In “*Drosophila* Protocols” (W. Sullivan, M. Ashburner, and R. S. Hawley, eds.), pp. 273–296. Cold Spring Harbor Laboratory Press, Cold Spring Harbor, NY.
- Broadie, K. (2000b). Functional assays of the peripheral and central nervous systems. In “*Drosophila* Protocols” (W. Sullivan, M. Ashburner, and R. S. Hawley, eds.), pp. 297–312. Cold Spring Harbor Laboratory Press, Cold Spring Harbor, NY.

- Broadie, K., and Bate, M. (1993a). Development of the embryonic neuromuscular synapse of *Drosophila melanogaster*. *J. Neurosci.* **13**, 144–166.
- Broadie, K., and Bate, M. (1993b). Development of larval muscle properties in the embryonic myotubes of *Drosophila melanogaster*. *J. Neurosci.* **13**, 167–180.
- Broadie, K., and Bate, M. (1993c). Activity-dependent development of the neuromuscular synapse during *Drosophila* embryogenesis. *Neuron* **11**, 607–619.
- Broadie, K., and Bate, M. (1993d). Synaptogenesis in the *Drosophila* embryo: Innervation directs receptor synthesis and localization. *Nature* **361**, 350–353.
- Broadie, K., Bellen, H. J., DiAntonio, A., Littleton, J. T., and Schwarz, T. L. (1994). The absence of Synaptotagmin disrupts excitation-secretion coupling during synaptic transmission. *Proc. Natl. Acad. Sci. USA* **91**, 10727–10731.
- Broadie, K., Prokop, A., Bellen, H. J., O’Kane, C. J., Schulze, K. L., and Sweeney, S. T. (1995). Syntaxin and Synaptobrevin function downstream of vesicle docking in *Drosophila*. *Neuron* **15**, 663–673.
- Broadie, K., Rushton, E., Skoulakis, E. C. M., and Davis, R. (1997). Leonardo, a 14–3–3 protein involved in learning, regulates presynaptic function. *Neuron* **19**, 391–402.
- Broadie, K., Skaer, H., and Bate, M. (1992). Whole-embryo culture of *Drosophila*: Development of embryonic tissues in vitro. *Roux’s Arch. Dev. Biol.* **201**, 364–375.
- Broadie, K. S. (1995). Genetic dissection of the molecular mechanisms of transmitter vesicle release during synaptic transmission. *J. Physiol. Paris.* **89**, 59–70.
- Broadus, J., Skeath, J. B., Spana, E. P., Bossing, T., Technau, G., and Doe, C. Q. (1995). New neuroblast markers and the origin of the aCC/pCC neurons in the *Drosophila* central nervous system. *Mech. Dev.* **53**, 393–402.
- Brower, D. L., Wilcox, M., Piovant, M., Smith, R. J., and Reger, L. A. (1984). Related cell-surface antigens expressed with positional specificity in *Drosophila* imaginal discs. *Proc. Natl. Acad. Sci. USA* **81**, 7485–7489.
- Brunet, J. F., and Ghysen, A. (1999). Deconstructing cell determination: Proneural genes and neuronal identity. *Bioessays* **21**(4), 313–318.
- Budnik, V., and Gorczyca, M. (1992). SSB, an antigen that selectively labels morphologically distinct synaptic boutons at the *Drosophila* larval neuromuscular junction. *J. Neurobiol.* **23**, 1054–1065.
- Budnik, V., and Gramates, L. S. (1999). “Neuromuscular Junctions in *Drosophila*.” Academic Press, New York.
- Buxbaum, J. D., Gandy, S. E., Cicchetti, P., Ehrlich, M. E., Czernik, A. J., Fracasso, R. P., Ramabhadran, T. V., Unterbeck, A. J., and Greengard, P. (1990). Processing of Alzheimer A4 amyloid precursor protein: Modulation by agents that regulates protein phosphorylation. *Proc. Natl. Acad. Sci. USA* **87**, 6003–6006.
- Byerly, L., and Leung, H. T. (1988). Ionic currents of *Drosophila* neurons in embryonic cultures. *J. Neurosci.* **8**(11), 4379–4393.
- Byers, D., Davis, R. L., and Kiger, J. A. Jr. (1981). Defect in cyclic AMP phosphodiesterase due to the dunce mutation of learning in *Drosophila melanogaster*. *Nature* **289**, 79–81.
- Byers, T. J., Hussain-Chishti, A., Dubreuil, R. R., Brantom, D., and Goldstein, L. S. (1989). Sequence similarity of the amino-terminal domain of *Drosophila* beta spectrin to alpha actinin and dystrophin. *J. Cell Biol.* **109**, 1633–1641.
- Campbell, G., Goring, H., Lin, T., Spana, E., Andersson, S., Doe, C. Q., and Tomlinson, A. (1994). RK2, a glial-specific homeodomain protein required for embryonic nerve cord condensation and viability in *Drosophila*. *Development* **120**(10), 2957–2966.
- Campos-Ortega, J., and Hartenstein, V. (1985). “The Embryonic Development of *Drosophila melanogaster*.” Springer, Berlin.
- Cantera, R., and Nassel, D. R. (1992). Segmental peptidergic innervation of abdominal targets in larval and adult dipteran insects revealed with an antiserum against leucokinin I. *Cell Tissue Res.* **269**(3), 459–471.
- Carlson, J. R. (2001). Viewing odors in the mushroom body of the fly. *Trends Neurosci.* **24**(9), 497–498.

- Carthew, R. W. (2001). Gene silencing by double-stranded RNA. *Curr. Opin. Cell Biol.* **13**, 244–248.
- Cattaert, D., and Birman, S. (2001). Blockade of the central generator of locomotor rhythm by noncompetitive NMDA receptor antagonists in *Drosophila* larvae. *J. Neurobiol.* **48**(1), 58–73.
- Cerezo, J. R., Jimenez, F., and Moya, F. (1995). Characterization and gene cloning of *Drosophila* syntaxin I (Dsynt1): The fruit fly homologue of rat syntaxin I. *Brain Res. Mol. Brain Res.* **29**(2), 245–252.
- Chang, H., and Kidokoro, Y. (1996). Kinetic properties of glutamate receptor channels in cultured embryonic *Drosophila* myotubes. *Jpn. J. Physiol.* **46**, 249–264.
- Chapman, E. R., An, S., Barton, N., and Jahn, R. (1994). SNAP-25, a t-SNARE which binds to both syntaxin and synaptobrevin via domains that may form coiled coils. *J. Biol. Chem.* **269**(44), 27427–27432.
- Chen, H., He, Z., Bagri, A., and Tessier-Lavigne, M. (1998). Semaphorin-neuropilin interactions underlying sympathetic axon responses to class III semaphorins. *Neuron* **21**, 1283–1290.
- Chiba, A. (2001). *Precision networking: A look through the eyes of a fly neuron.* **32**(3), 381–384.
- Chiesa, A., Rapizzi, E., Tosello, V., Pinton, P., de Virgilio, M., Fogarty, K. E., and Rizzuto, R. (2001). Recombinant aequorin and green fluorescent protein as valuable tools in the study of cell signalling. *Biochem. J.* **355**(Pt 1), 1–12.
- Chu-Lagraff, Q., and Doe, C. Q. (1993). Neuroblast specification and formation regulated by wingless in the *Drosophila* CNS. *Science* **17**, 261(5128) 1594–1597.
- Chu-LaGraff, Q., Schmid, A., Leidel, J., Bronner, G., Jackle, H., and Doe, C. Q. (1995). huckebein specifies aspects of CNS precursor identity required for motoneuron axon pathfinding. *Neuron* **15**(5), 1041–1051.
- Chu-Lagraff, Q., Wright, D. M., McNeil, L. K., and Doe, C. Q. (1991). The prospero gene encodes a divergent homeodomain protein that controls neuronal identity in *Drosophila*. *Development* **2**, 79–85.
- Clandinin, T. R., Lee, C. H., Herman, T., Lee, R. C., Yang, A. Y., Ovasapyan, S., and Zipursky, S. L. (2001). *Drosophila* LAR regulates R1-R6 and R7 target specificity in the visual system. *Neuron* **32**(2), 237–248.
- Clark, I. E., Jan, L. Y., and Jan, Y. N. (1997). Reciprocal localization of Nod and kinesin fusion proteins indicates microtubule polarity in the *Drosophila* oocyte, epithelium, neuron and muscle. *Development* **124**(2), 461–470.
- Cogoni, C., and Macino, G. (2000). Post-transcriptional gene silencing across kingdoms. *Curr. Opin. Genet. Dev.* **10**, 638–643.
- Connolly, J. B., Roberts, I. J., Armstrong, J. D., Kaiser, K., Forte, M., Tully, T., and O’Kane, C. J. (1996). Associative learning disrupted by impaired Gs signaling in *Drosophila* mushroom bodies. *Science* **274**, 2104–2107.
- Connolly, J. B., and Tully, T. (1998). Behaviour, learning and memory. In “*Drosophila: A Practical Approach*” (D. B. Roberts, ed.), 2nd Ed., pp. 265–318. Oxford University Press.
- Creton, R., Steele, M. E., and Jaffe, L. F. (1997). Expression of apo-aequorin during embryonic development; how much is needed for calcium imaging? *Cell Calcium* **22**(6), 439–446.
- Crittenden, J. R., Skoulakis, E. M., Han, K. A., Kalderon, D., and Davis, R. L. (1998). Tripartite mushroom body architecture revealed by antigenic markers. *Learn Mem.* **5**, 38–51.
- Croghan, P. C., and Lockwood, A. P. M. (1960). The composition of the haemolymph of the larva of *Drosophila melanogaster*. *J. Exp. Biol.* **37**, 339–343.
- Crowner, D., Madden, K., Goeke, S., and Giniger, E. (2003). Lola regulates midline crossing of CNS axons in *Drosophila*. *Development* **129**, 1317–1325.
- Currie, D., Milner, M., and Evans, C. (1988). The growth and differentiation in vitro of leg and wing imaginal disc cells from *Drosophila melanogaster*. *Development* **102**, 805–814.
- Dambly-Chaudiere, C., and Ghysen, A. (1986). The sense organs in the *Drosophila* larva and their relation to the embryonic pattern of sensory neurons. *Roux Arch. Dev. Biol.* **195**(4), 222–228.
- Davis, G. W., Schuster, C. M., and Goodman, C. S. (1996). Genetic dissection of structural and functional components of synaptic plasticity. III. CREB is necessary for presynaptic functional plasticity. *Neuron* **17**, 669–679.

- Davis, R. L. (2001). Mushroom bodies, Ca²⁺ oscillations, and the memory gene amnesiac. *Neuron* **30**(3), 653–656.
- Dawson-Scully, K., Bronk, P., Atwood, H. L., and Zinsmaier, K. E. (2000). Cysteine-string protein increases the calcium sensitivity of neurotransmitter exocytosis in *Drosophila*. *J. Neurosci.* **15**, 20(16) 6039–6047.
- de Belle, J. S., and Heisenberg, M. (1994). Associative odor learning in *Drosophila* abolished by chemical ablation of mushroom bodies. *Science* **263**, 692–695.
- Deitcher, D. L., Ueda, A., Stewart, B. A., Burgess, R. W., Kidokoro, Y., and Schwartz, T. L. (1998). Distinct requirements for evoked and spontaneous release of neurotransmitter are revealed by mutations in the *Drosophila* gene neuronal-synaptobrevin. *J. Neurosci.* **18**, 2028–2039.
- Delgado, R., Davis, R., Bono, M. R., Latorre, R., and Labarca, P. (1998). Outward currents in *Drosophila* larval neurons: Dunce lacks a maintained outward current component downregulated by cAMP. *J. Neurosci.* **18**(4), 1399–1407.
- Delgado, R., Maureira, C., Oliva, C., Kidokoro, Y., and Labarca, P. (2000). Size of vesicle pools, rates of mobilization, and recycling at neuromuscular synapses of a *Drosophila* mutant, shibire. *Neuron* **28**, 941–953.
- Desai, C. J., Garrity, P. A., Keshishian, H., Zipursky, S. L., and Zinn, K. (1999). The *Drosophila* SH2-SH3 adapter protein Dock is expressed in embryonic axons and facilitates synapse formation by the RP3 motoneuron. *Development* **126**, 1527–1535.
- Desai, C. J., Popova, E., and Zinn, K. (1994). A *Drosophila* receptor tyrosine phosphatase expressed in the embryonic CNS and larval optic lobes is a member of the set of proteins bearing the “HRP” carbohydrate epitope. *J. Neurosci.* **14**(12), 7272–7283.
- Diagana, T. T., Thomas, U., Prokopenko, S. N., Xiao, B., Worley, P. F., and Thomas, J. B. (2002). Mutation of *Drosophila* homer disrupts control of locomotor activity and behavioral plasticity. *J. Neurosci.* **22**(2), 428–436.
- DiAntonio, A., Burgess, R. W., Chin, A. C., Deitcher, D. L., Scheller, R. H., and Schwarz, T. L. (1993). Identification and characterization of *Drosophila* genes for synaptic vesicle proteins. *J. Neurosci.* **13**, 4924–4935.
- Dickinson, M. H., and Palka, J. (1987). Physiological properties, time of development, and central projection are correlated in the wing mechanoreceptors of *Drosophila*. *J. Neurosci.* **7**, 4201–4208.
- Dillman, J. F., and Pfister, K. K. (1994). Differential phosphorylation in vivo of cytoplasmic dynein associated with anterogradely moving organelles. *J. Cell Biol.* **127**, 1671–1681.
- DiNardo, S., Kuner, J. M., Theis, J., and O’Farrell, P. H. (1985). Development of embryonic pattern in *D. melanogaster* as revealed by accumulation of the nuclear engrailed protein. *Cell* **43**(1), 59–69.
- Dirckson, H., Zahnow, C. A., Gaus, G., Keller, R., Rao, K. R., and Riehm, J. P. (1987). The ultrastructure of nerve endings containing pigment-dispersing hormone (PDH) in crustacean sinus glands: Identification by antiserum against synthetic PDH. *Cell Tissue Res.* **250**, 377–387.
- Dittrich, R., Bossing, T., Gould, A. P., Technau, G. M., and Urban, J. (1997). The differentiation of the serotonergic neurons in the *Drosophila* ventral nerve cord depends on the combined function of the zinc finger proteins Eagle and Hucklebein. *Development* **124**(13), 2515–2525.
- Doe, C. Q. (1992). Molecular markers for identified neuroblasts and ganglion mother cells in the *Drosophila* central nervous system. *Development* **116**, 855–863.
- Doe, C. Q., and Goodman, C. S. (1985). Early events in insect neurogenesis. II. The role of cell interactions and cell lineage in the determination of neuronal precursor cells. *Dev. Biol.* **111**, 206–219.
- Doe, C. Q., Kuwada, J. Y., and Goodman, C. S. (1985). From epithelium to neuroblasts to neurons: The role of cell interactions and cell lineage during insect neurogenesis. *Philos. Trans. R. Soc. Lond. Biol. Sci.* **312**, 67–81.
- Doe, C. Q., and Skeath, J. B. (1996). Neurogenesis in the insect central nervous system. *Curr. Opin. Neurobiol.* **6**, 18–24.
- Doe, C. Q., and Technau, G. M. (1993). Identification and cell lineage of individual neural precursors in the *Drosophila* CNS. *Trends Neurosci.* **16**, 510–514.

- Dolph, P. J., Ranganathan, R., Colley, N. J., Hardy, R. W., Socolich, M., and Zuker, C. S. (1993). Arrestin function in inactivation of G protein-coupled receptor rhodopsin in vivo. *Science* **260**, 1910–1916.
- Dubreuil, R. R., Maddux, P. B., Grushko, T. A., and Mac Vicar, G. R. (1997). Segregation of two spectrin isoforms: Polarized membrane-binding sites direct polarized membrane skeleton assembly. *Mol. Biol. Cell* **8**, 1933–1942.
- Dubuque, S. H., Schachtner, J., Nighorn, A. J., Menon, K. P., Zinn, K., and Tolbert, L. P. (2001). Immunolocalization of synaptotagmin for the study of synapses in the developing antennal lobe of *Manduca sexta*. *J. Comp. Neurol.* **441**(4), 277–287.
- Dzitoyeva, S., Dimitrijevic, N., and Manev, H. (2001). Intra-abdominal injection of double-stranded RNA into anesthetized adult *Drosophila* triggers RNA interference in the central nervous system. *Mol. Psychiatr.* **6**, 665–670.
- Eaton, B. A., Fetter, R. D., and Davis, G. W. (2002). Dynactin is necessary for synapse stabilization. *Neuron* **34**, 729–741.
- Eaton, S., Auvinen, P., Luo, L., Jan, Y. N., and Simons, K. (1995). CDC42 and Rac1 control different actin-dependent processes in the *Drosophila* wing disc epithelium. *J. Cell Biol.* **131**(1), 151–164.
- Edwards, K. A., Demsky, M., Montague, R. A., Weymouth, N., and Kiehart, D. P. (1997). GFP-moesin illuminates actin cytoskeleton dynamics in living tissue and demonstrates cell shape changes during morphogenesis in *Drosophila*. *Dev. Biol.* **191**(1), 103–117.
- Elkins, T., and Ganetzky, B. (1988). The roles of potassium currents in *Drosophila* flight muscles. *J. Neurosci.* **8**, 428–434.
- Engel, J. E., and Wu, C.-F. (1992). Interactions of membrane excitability mutants affecting potassium and sodium currents in the flight and giant fiber escape systems of *Drosophila*. *J. Comp. Physiol.* **171**, 93–104.
- Engel, J. E., and Wu, C.-F. (1994). Altered mechanoreceptor response in *Drosophila* bang-sensitive mutants. *J. Comp. Physiol. A* **175**, 267–278.
- Estes, P. S., Ho, G. L., Narayanan, R., and Ramaswami, M. (2000). Synaptic localization and restricted diffusion of a *Drosophila* neuronal synaptobrevin: Green fluorescent protein chimera in vivo. *J. Neurogenet.* **13**(4), 233–255.
- Fan, S., and Ready, D. (1997). Glued participates in distinct microtubule-based activities in *Drosophila* eye development. *Development* **124**, 1497–1507.
- Fashena, D., and Westerfield, M. (1999). Secondary motoneuron axons localize DM-GRASP on their fasciculated segments. *J. Comp. Neurol.* **406**, 415–424.
- Featherstone, D. E., and Broadie, K. (2000). Surprises from *Drosophila*: Genetic mechanisms of synaptic development and plasticity. *Brain Res. Bull.* **53**, 501–511.
- Featherstone, D. E., Davis, W. S., Dubreuil, R. R., and Broadie, K. (2001). *Drosophila* alpha- and beta-spectrin mutations disrupt presynaptic neurotransmitter release. *J. Neurosci.* **21**, 4215–4224.
- Featherstone, D. E., Rushton, E., and Broadie, K. (2002). Developmental regulation of glutamate receptor field size by nonvesicular glutamate release. *Nature Neurosci.* **5**(2), 141–146.
- Featherstone, D. E., Rushton, E. M., Hilderbrand-Chae, M., Phillips, A. M., Jackson, F. R., and Broadie, K. (2000). Presynaptic glutamic acid decarboxylase is required for induction of the postsynaptic receptor field at a glutamatergic synapse. *Neuron* **27**(1), 71–84.
- Fergestad, T., and Broadie, K. (2001). Interaction of stoned and synaptotagmin in synaptic vesicle endocytosis. *J. Neurosci.* 1218–1227.
- Fergestad, T., Davis, W. S., and Broadie, K. (1999). The stoned proteins regulate synaptic vesicle recycling in the presynaptic terminal. *J. Neurosci.* 5847–5860.
- Fergestad, T., Wu, M. N., Schulze, K. L., Lloyd, T. E., Bellen, H. J., and Broadie, K. (2001). Targeted mutations in the syntaxin H3 domain specifically disrupt SNARE complex function in synaptic transmission. *J. Neurosci.* **21**(23), 9142–9150.
- Fernandez-Chacon, R., and Sudhof, T. C. (1999). Genetics of synaptic vesicle function: Toward the complete functional anatomy of an organelle. *Rev. Physiol.* **61**, 753–776.
- Fire, A. (1999). RNA-triggered gene silencing. *Trends Genet.* **15**, 358–363.

- Fischer, J. A., Giniger, E., Maniatis, T., and Ptashne, M. (1988). GAL4 activates transcription in *Drosophila*. *332*, 853–856.
- Fjose, A., Ellingsen, S., Wargelius, A., and Seo, H. C. (2001). RNA interference: Mechanisms and applications. *Biotechnol. Annu. Rev.* **7**, 31–57.
- Fortier, E., and Belote, J. M. (2000). Temperature-dependent gene silencing by an expressed inverted repeat in *Drosophila*. *Genesis*. **26**, 240–244.
- Frasch, M., Hoey, T., Rushlow, C., Doyle, H., and Levine, M. (1987). Characterization and localization of the even-skipped protein of *Drosophila*. *EMBO J.* **6**(3), 749–759.
- Fremion, F., Darboux, I., Diano, M., Hipeau-Jacquotte, R., Seeger, M. A., and Piovant, M. (2000). Amalgam is a ligand for the transmembrane receptor neurotactin and is required for neurotactin-mediated cell adhesion and axon fasciculation in *Drosophila*. *EMBO J.* **19**(17), 4463–4472.
- Fujita, S. C., Inoue, H., Yoshioka, T., and Hotta, Y. (1987). Quantitative tissue isolation from *Drosophila* freeze-dried in acetone. *Biochem. J.* **243**, 97–104.
- Fujita, S. C., Zipursky, S. L., Benzer, S., Ferrus, A., and Shotwell, S. L. (1982). Monoclonal antibodies against the *Drosophila* nervous system. *Proc. Natl. Acad. Sci. USA* **79**, 7929–7933.
- Gallo, G., and Letourneau, P. C. (1998). Localized sources of neurotrophins initiate axon collateral sprouting. *J. Neurosci.* **18**, 5403–5414.
- Ganetzky, B., and Wu, C.-F. (1982). *Drosophila* mutants with opposing effects on nerve excitability: Genetic and spatial interactions in repetitive firing. *J. Neurophys.* **47**, 501–514.
- Gao, F. B., Kohwi, M., Brenman, J. E., Jan, L. Y., and Jan, Y. N. (2000). Control of dendritic field formation in *Drosophila*: The roles of flamingo and competition between homologous neurons. *Neuron* **28**(1), 91–101.
- Garcia-Alonso, L. A. (1999). Postembryonic sensory axon guidance in *Drosophila*. *Cell Mol. Life Sci.* **55**, 1386–1398 Review.
- Germeraad, S. E., O'Dowd, D., and Aldrich, R. W. (1992). Functional assay of a putative *Drosophila* sodium channel gene in homozygous deficiency neurons. *J. Neurogenet.* **8**(1), 1–16.
- Gindhart, J. G. Jr., Desai, C. J., Beushausen, S., Zinn, K., and Goldstein, L. S. (1998). Kinesin light chains are essential for axonal transport in *Drosophila*. *J. Cell Biol.* **141**(2), 443–454.
- Giniger, E., Tietje, K., Jan, L. Y., and Jan, Y. N. (1994). *lola* encodes a putative transcription factor required for axon growth and guidance in *Drosophila*. *Development* **120**, 1385–1398.
- Giordano, E., Rendina, R., Peluso, I., and Furia, M. (2002). RNAi triggered by symmetrically transcribed transgenes in *Drosophila melanogaster*. *Genetics* **160**, 637–648.
- Golby, J. A., Tolar, L. A., and Pallanck, L. (2001). Partitioning of N-ethylmaleimide-sensitive fusion (NSF) protein function in *Drosophila melanogaster*: dNSF1 is required in the nervous system, and dNSF2 is required in mesoderm. *Genetics* **158**, 265–278.
- Golic, K. G., and Lindquist, S. (1989). The FLP recombinase of yeast catalyzes site-specific recombination in the *Drosophila* genome. *Cell* **59**, 499–509.
- Gonzalez-Gaitan, M., and Jackle, H. (1997). Role of *Drosophila* alpha-adaptin in presynaptic vesicle recycling. *Cell* **88**, 767–776.
- Goodman, C. S., Bastiani, M. J., Doe, C. Q., du Lac, S., Helfand, S. L., Kuwada, J. Y., and Thomas, J. B. (1984). Cell recognition during neuronal development. *Science* **225**(4668), 1271–1279.
- Goodman, C. S., and Doe, C. Q. (1993). Embryonic development of the *Drosophila* central nervous system. In “The Development of *Drosophila melanogaster*” (M. Bate and A. Martinez Arias, eds.), pp. 1131–1206. Cold Spring Harbor Laboratory Press, Cold Spring Harbor, NY.
- Gorzcyca, M. G., Budnik, V., White, K., and Wu, C.-F. (1991). Dual muscarinic and nicotinic action on a motor program in *Drosophila*. *J. Neurobiol.* **22**, 391–404.
- Greenspan, R. J. (1997). “Fly Pushing: The Theory and Practice of *Drosophila* Genetics,” Cold Spring Harbor Laboratory Press, Cold Spring Harbor, NY.
- Grieder, N. C., de Cuevas, M., and Spradling, A. C. (2000). The fusome organizes the microtubule network during oocyte differentiation in *Drosophila*. *Development* **127**, 4253–4264.
- Grigliatti, T. A. (1998). Mutagenesis. In “*Drosophila*: A Practical Approach” (D. B. Roberts, ed.), 2nd Ed., pp. 55–84. Oxford University Press, New York.

- Grigliatti, T. A., Hall, L., Rosenbluth, R., and Suzuki, D. T. (1973). Temperature-sensitive mutations in *Drosophila melanogaster*. XIV. A selection of immobile adults. *Mol. Genet.* **120**, 107–114.
- Grinnell, A. D. (1995). Dynamics of nerve-muscle interaction in developing and mature neuromuscular junctions. *Physiol. Rev.* **75**(4), 789–834.
- Grotewiel, M. S., Beck, C. D. O., Wu, K. H., Zhu, X.-R., and Davis, R. L. (1998). Integrin-mediated short-term memory in *Drosophila*. *Nature* **391**, 455–460.
- Grueber, W. B., Jan, L. Y., and Jan, Y. N. (2002). Tiling of the *Drosophila* epidermis by multidendritic sensory neurons. *Development* **129**, 2867–2878.
- Gubb, D. (1998). Chromosome mechanics; the genetic manipulation of aneuploid stocks. In “*Drosophila: A Practical Approach*” (D. B. Roberts, ed.), 2nd Ed., pp. 55–84. Oxford University Press, New York.
- Guichet, A., Wucherpennig, T., Dudu, V., Etter, S., Wilsch-Brauniger, M., Hellwig, A., Gonzalez-Gaitan, M., Huttner, W. B., and Schmidt, A. A. (2002). Essential role of endophilin A in synaptic vesicle budding at the *Drosophila* neuromuscular junction. *EMBO J.* **21**, 1661–1672.
- Gunawardena, S., and Goldstein, L. S. (2001). Disruption of axonal transport and neuronal viability by amyloid precursor protein mutations in *Drosophila*. *Neuron* **32**(3), 389–401.
- Guo, H. F., Tong, J., Hannan, F., Luo, L., and Zhong, Y. (2000). A neurofibromatosis-1-regulated pathway is required for learning in *Drosophila*. *Nature* **403**(6772), 895–898.
- Gutjahr, T., Patel, N. H., Li, X., Goodman, C. S., and Noll, N. (1993). Analysis of the *gooseberry* locus in *Drosophila* embryos: *gooseberry* determines the cuticular pattern and activates *gooseberry* neuro. *Development* **118**, 21–31.
- Hakeda-Suzuki, S., Ng, J., Tzu, J., Dietzl, G., Sun, Y., Harms, M., Nardine, T., Luo, L., and Dickson, B. J. (2002). Rac function and regulation during *Drosophila* development. *Nature* **416**(6879), 438–442.
- Halter, D. A., Uban, J., Rickert, C., Ner, S. S., Ito, K., Travers, A. A., and Technau, G. M. (1995). The homeobox gene *repo* is required for the differentiation and maintenance of glia function in the embryonic nervous system of *Drosophila melanogaster*. *Development* **121**, 317–332.
- Hamilton, B. A., and Zinn, K. (1994). From clone to mutant gene. *Methods Cell Bio.* **44**, 81–98.
- Harata, N., Ryan, T. A., Smith, S. J., Buchanan, J., and Tsien, R. W. (2001). Visualizing recycling synaptic vesicles in hippocampal neurons by FM 1-43 photoconversion. *Proc. Natl. Acad. Sci. USA* **98**(22), 12748–12753.
- Hardie, R. C. (1991a). Whole-cell recordings of the light-induced current in *Drosophila* photoreceptors: Evidence for feedback by calcium permeating the light sensitive channels. *Proc. R. Soc. Lond. B* **245**, 203–210.
- Hardie, R. C. (1991b). Voltage sensitive potassium channels in *Drosophila* photoreceptors. *J. Neurosci.* **11**, 3079–3095.
- Hardie, R. C. (1996). INDO-1 measurements of absolute resting and light-induced Ca²⁺ concentration in *Drosophila* photoreceptors. *J. Neurosci.* **16**(9), 2925–2933.
- Hardie, R. C., Raghu, P., Moore, S., Juusola, M., Baines, R. A., and Sweeney, S. T. (2001). Calcium influx via TRP channels is required to maintain PIP₂ levels in *Drosophila* photoreceptors. *Neuron* **30**, 149–159.
- Hardie, R. C., Voss, D., Pongs, O., and Laughlin, S. B. (1991). Novel potassium channels encoded by the Shaker locus in *Drosophila* photoreceptors. *Neuron* **6**, 477–486.
- Harlow, E., and Lane, D. (1999). “Using Antibodies: A Laboratory Manual.” Cold Spring Harbor Laboratory Press, Cold Spring Harbor, NY.
- Harris, R., Sabatelli, L. M., and Seeger, M. A. (1996). Guidance cues at the *Drosophila* CNS midline: Identification and characterization of two *Drosophila* Netrin/UNC-6 homologs. *Neuron* **17**, 217–228.
- Harrison, S. D., Broadie, K., van de Goor, J., and Rubin, G. M. (1994). Mutations in the *Drosophila* Rop gene suggest a function in general secretion and synaptic transmission. *Neuron* **13**, 555–566.
- Hassan, B. A., Bermingham, N. A., He, Y., Sun, Y., Jan, Y. N., Zoghbi, H. Y., and Bellen, H. J. (2000). Atonal regulates neurite arborization but does not act as a proneural gene in the *Drosophila* brain. *Neuron* **25**(3), 549–561.

- Hazelrigg, T. (2000). GFP and other reporters. In "Drosophila Protocols" (W. Sullivan, M. Ashburner, and R. Scott Hawley, eds.), pp. 313–344. Cold Spring Harbor Laboratory Press, Cold Spring Harbor, NY.
- Heisenberg, M., Borst, A., Wagner, S., and Byers, D. (1985). *Drosophila* mushroom body mutants are deficient in olfactory learning. *J. Neurogenet.* **2**, 1–30.
- Heisenberg, M., and Götz, K. G. (1975). The use of mutations for the partial degradation of vision in *Drosophila melanogaster*. *J. Comp. Physiol.* **98**, 217–241.
- Heitzler, P., Coulson, D., Saenz-Robles, M. T., Ashburner, M., Roote, J., Simpson, P., and Gubb, D. (1993). Genetic and cytogenetic analysis of the 43A-E region containing the segment polarity gene *costa* and the cellular polarity genes *prickle* and *spiny-legs* in *Drosophila melanogaster*. *Genetics* **135**, 105–115.
- Helfrich-Forster, C. (1995). The period clock gene is expressed in central nervous system neurons which also produce a neuropeptide that reveals the projections of circadian pacemaker cells within the brain of *Drosophila melanogaster*. *Proc. Natl. Acad. Sci. USA* **92**(2), 612–616.
- Henkel, A. W., Lübke, J., and Betz, W. J. (1996). FM1-43 dye ultrastructural localization in and release from frog motor nerve terminals. *Proc. Natl. Acad. Sci. USA* **93**, 1918–1923.
- Hevers, W., and Hardie, R. C. (1995). Serotonin modulates the voltage dependence of Shaker potassium channels in *Drosophila* photoreceptors. *Neuron* **14**, 845–856.
- Hidalgo, A., and Brand, A. H. (1997). Targeted neuronal ablation: The role of pioneer neurons in guidance and fasciculation in the CNS of *Drosophila*. *Development* **124**, 3253–3262.
- Hing, H., Xiao, J., Harden, N., Lim, L., and Zipursky, S. L. (1999). Pak functions downstream of Dock to regulate photoreceptor axon guidance in *Drosophila*. *Cell* **97**(7), 853–863.
- Hirsch, J. (2000). Exposing *Drosophila* to neuroactive drugs. In "Drosophila Protocols" (W. Sullivan, M. Ashburner, and R. S. Hawley, eds.), pp. 617–624. Cold Spring Harbor Laboratory Press, Cold Spring Harbor, NY.
- Hitier, R., Chaminade, M., and Preat, T. (2001). The *Drosophila* *castor* gene is involved in postembryonic brain development. *Mech. Dev.* **103**(1–2), 3–11.
- Hoang, B., and Chiba, A. (2001). Single-cell analysis of *Drosophila* larval neuromuscular synapses. *Dev. Biol.* **229**, 55–70.
- Hodges, D. D., Lee, D., Preston, C. F., Boswell, K., Hall, L. M., and O'Dowd, D. K. (2002). *tipE* regulates Na⁺-dependent repetitive firing in *Drosophila* neurons. *Mol. Cell Neurosci.* **19**(3), 402–416.
- Homyk, T. Jr., and Pye, Q. (1989). Some mutations affecting neural or muscular tissues alter the physiological components of the electroretinogram in *Drosophila*. *J. Neurogenet.* **5**, 37–48.
- Hong, K., Hinck, L., Nishiyama, M., Poo, M. M., Tessier-Lavigne, M., and Stein, E. (1999). A ligand-gated association between cytoplasmic domains of UNC5 and DCC family receptors converts netrin-induced growth cone attraction to repulsion. *Cell* **97**, 927–941.
- Hortsch, M., Bieber, A. J., Patel, N. H., and Goodman, C. S. (1990). Differential splicing generates a nervous system-specific form of *Drosophila* neuroglian. *Neuron* **4**(5), 697–709.
- Hortsch, M., and Goodman, C. S. (1990). *Drosophila* fasciclin I, a neural cell adhesion molecule, has a phosphatidylinositol lipid membrane anchor that is developmentally. *J. Biol. Chem.* **265**(25), 15104–15109.
- Hoshino, M., Suzuki, E., Nabeshima, Y., and Hama, C. (1996). Hikaru genki protein is secreted into synaptic clefts from an early stage of synapse formation in *Drosophila*. *Development* **122**(2), 589–597.
- Hoskins, R. A., Phan, A. C., Naemuddin, M., Mapa, F. A., Ruddy, D. A., Ryan, J. J., Young, L. M., Wells, T., Kopczynski, C., and Ellis, M. C. (2001). SNP markers for genetic mapping in *Drosophila melanogaster*. *Genome Res.* **11**, 1100–1113.
- Hotta, Y., and Benzer, S. (1969). Abnormal electroretinograms in visual mutants of *Drosophila*. *Nature* **222**, 354–356.
- Huang, A. M., Rehn, E. J., and Rubin, G. M. (2000). Recovery of DNA sequences flanking P-element insertions: Inverse PCR and plasmid rescue. In "Drosophila Protocols" (W. Sullivan, M. Ashburner,

- and R. S. Hawley, eds.), pp. 429–438. Cold Spring Harbor Laboratory Press, Cold Spring Harbor, NY.
- Huang, A. M., and Rubin, G. M. (2000). A misexpression screen identifies genes that can modulate RASI pathway signaling in *Drosophila melanogaster*. *Genetics* **156**(3), 1219–1230.
- Huet, F., Lu, J. T., Myrick, K. V., Baugh, L. R., Crosby, M. A., and Gelbart, W. M. (2002). A deletion-generator compound element allows deletion saturation analysis for genomewide phenotypic annotation. *Proc. Natl. Acad. Sci. USA* **99**, 9948–9953.
- Hummel, T., Krukkert, K., Roos, J., Davis, G., and Klambt, C. (2000). *Drosophila* Futsch/22C10 is a MAP1B-like protein required for dendritic and axonal development. *Neuron* **26**, 357–370.
- Huovila, A. P., Eder, A. M., and Fuller, S. D. (1992). Hepatitis B surface antigen assembles in a post-ER, pre-Golgi compartment. *J. Cell Biol.* **118**, 1305–1320.
- Hurd, D. D., and Saxton, W. M. (1996). Kinesin mutations cause motor neuron disease phenotypes by disrupting fast axonal transport in *Drosophila*. *Genetics* **144**(3), 1075–1085.
- Hutvagner, G., and Zamore, P. D. (2002). RNAi: Nature abhors a double-strand. *Curr. Opin. Genet. Dev.* **12**, 225–232.
- Hwang, J. R., Siekhaus, D. E., Fuller, R. S., Taghert, P. H., and Lindberg, I. (2000). Interaction of *Drosophila melanogaster* prohormone convertase 2 and 7B2: Insect cell-specific processing and secretion. *J. Biol. Chem.* **275**, 17886–17893.
- Ikeda, K., and Kaplan, W. D. (1974). Neurophysiological genetics in *Drosophila melanogaster*. *Am. Zool.* **14**, 1055–1066.
- Ikeda, K., and Koenig, J. H. (1988). Morphological identification of the motor neurons innervating the dorsal longitudinal flight muscles of *Drosophila melanogaster*. *J. Comp. Neurol.* **273**, 436–444.
- Ikeda, K., Koenig, J. H., and Tsuruhara, T. (1980). Organization of identified axons innervating the dorsal longitudinal flight muscle of *Drosophila melanogaster*. *J. Neurocytol.* **9**, 799–823.
- Ikeda, K., and Salvaterra, P. M. (1989). Immunocytochemical study of a temperature-sensitive choline acetyltransferase mutant of *Drosophila melanogaster*. *J. Comp. Neurol.* **280**(2), 283–290.
- Inoue, H., Yoshioka, T., and Hotta, Y. (1985). A genetic study of inositol trisphosphate involvement in phototransduction using *Drosophila* mutants. *Biochem. Biophys. Res. Commun.* **132**, 513–519.
- Inoue, H., Yoshioka, T., and Hotta, Y. (1989). Diacylglycerol kinase defect in a *Drosophila* retinal degeneration mutant rdgA. *J. Biol. Chem.* **264**, 5996–6000.
- Ito, K., Awano, W., Suzuki, K., Hiromi, Y., and Yamamoto, D. (1997). The *Drosophila* mushroom body is a quadruple structure of clonal units each of which contains a virtually identical set of neurones and glial cells. *Development* **124**, 761–771.
- Ito, K., and Hotta, Y. (1992). Proliferation pattern of postembryonic neuroblasts in the brain of *Drosophila melanogaster*. *Dev. Biol.* **149**, 134–148.
- Iwai, Y., Usui, T., Hirano, S., Steward, R., Takeichi, M., and Uemura, T. (1997). Axon patterning requires DN-cadherin, a novel neuronal adhesion receptor, in the *Drosophila* embryonic CNS. *Neuron* **19**(1), 77–89.
- Jan, L. Y., and Jan, Y. N. (1976a). Properties of the larval neuromuscular junction in *Drosophila melanogaster*. *J. Physiol.* **262**, 189–214.
- Jan, L. Y., and Jan, Y. N. (1976b). L-glutamate as an excitatory transmitter at the *Drosophila* larval neuromuscular junction. *J. Physiol.* **262**, 215–236.
- Jan, L. Y., and Jan, Y. N. (1982). Antibodies to horseradish peroxidase as specific neuronal markers in *Drosophila* and in grasshopper embryos. *Proc. Natl. Acad. Sci. USA* **79**(8), 2700–2704.
- Jan, Y. N., Jan, L. Y., and Dennis, M. J. (1977). Two mutations of synaptic transmission in *Drosophila*. *Proc. R. Soc. Lond. B* **198**, 87–108.
- Jarman, A. P., Sun, Y., Jan, L. Y., and Jan, Y. N. (1995). Role of the proneural gene, atonal, in formation of *Drosophila* chordotonal organs and photoreceptors. *Development* **121**(7), 2019–2030.
- Jefferis, G. S., Marin, E. C., Stocker, R. F., and Luo, L. (2001). Target neuron prespecification in the olfactory map of *Drosophila*. *Nature* **414**, 204–208.
- Jefferis, G. S., Marin, E. C., Watts, R. J., and Luo, L. (2002). Development of neuronal connectivity in *Drosophila* antennal lobes and mushroom bodies. *Curr. Opin. Neurobiol.* **12**(1), 80–86.

- Jhaveri, D., Sen, A., and Rodrigues, V. (2000). Mechanisms underlying olfactory neuronal connectivity in *Drosophila*: The atonal lineage organizes the periphery while sensory neurons and glia pattern the olfactory lobe. *Dev. Biol.* **226**, 73–87.
- Jia, X. X., Gorczyca, M., and Budnik, V. (1993). Ultrastructure of neuromuscular junctions in *Drosophila*: Comparison of wild type and mutants with increased excitability. *J. Neurobiol.* **24**, 1025–1044.
- Jin, P., Griffith, L. C., and Murphey, R. K. (1998). Presynaptic calcium/calmodulin-dependent protein kinase II regulates habituation of a simple reflex in adult *Drosophila*. *J. Neurosci.* **18**, 8955–8964.
- Jin, Y. (2002). Synaptogenesis: Insights from worm and fly. *Curr. Opin. Neurobiol.* **12**, 71–79.
- Johansen, J., Halpern, M. E., Johansen, K. M., and Keshishian, H. (1989a). Morphology of glutamatergic synapses on identified muscle cells of *Drosophila* larvae. *J. Neurosci.* **9**(2), 710–725.
- Johansen, J., Halpern, M. E., and Keshishian, H. (1989b). Axonal guidance and the development of muscle fiber-specific innervation in *Drosophila* embryos. *J. Neurosci.* **9**(12), 4318–4332.
- Kalidas, S., and Smith, D. P. (2002). Novel genomic cDNA hybrids produce effective RNA interference in adult *Drosophila*. *Neuron* **33**(2), 177–184.
- Karunanithi, S., Georgiou, J., Charlton, M. P., and Atwood, H. L. (1997). Imaging of calcium in *Drosophila* larval motor nerve terminals. *J. Neurophysiol.* **78**(6), 3465–3467.
- Katz, F., Moats, W., and Jan, Y. N. (1988). A carbohydrate epitope expressed uniquely on the cell surface of *Drosophila* neurons is altered in the mutant nac (neurally altered carbohydrate). *EMBO J.* **11**, 3471–3477.
- Kaufmann, N., DeProto, J., Ranjan, R., Wan, H., and Van Vactor, D. (2002). *Drosophila* liprin-alpha and the receptor phosphatase Dlar control synapse morphogenesis. *Neuron* **34**(1), 27–38.
- Kawasaki, F., Collins, S. C., and Ordway, R. W. (2002). Synaptic calcium-channel function in *Drosophila*: Analysis and transformation rescue of temperature-sensitive paralytic and lethal mutations of cacophony. *J. Neurosci.* **22**, 5856–5864.
- Kawasaki, F., Felling, R., and Ordway, R. W. (2000a). A temperature-sensitive paralytic mutant defines a primary synaptic calcium channel in *Drosophila*. *J. Neurosci.* **20**, 4885–4889.
- Kawasaki, F., Hazen, M., and Ordway, R. W. (2000b). Fast synaptic fatigue in shibire mutants reveals a rapid requirement for dynamin in synaptic vesicle membrane trafficking. *Nature Neurosci.* **3**, 859–860.
- Kawasaki, F., Mattiuz, A. M., and Ordway, R. W. (1998). Synaptic physiology and ultrastructure in comatose mutants define an in vivo role for NSF in neurotransmitter release. *J. Neurosci.* **18**, 10241–10249.
- Kawasaki, F., and Ordway, R. W. (1999). The *Drosophila* NSF protein, dNSF1, plays a similar role at neuromuscular and some central synapses. *J. Neurophysiol.* **82**, 123–130.
- Keleman, K., and Dickson, B. J. (2001). Short- and long-range repulsion by the *Drosophila* Unc5 netrin receptor. *Neuron* **32**(4), 605–617.
- Kelly, L. E., and Phillips, A. M. (1998). The effect of inositol hexaphosphate on the association of the *Drosophila* STNB protein with synaptotagmin. *Mol. Biol. Cell* **9**, 341a.
- Kelly, L. E., and Suzuki, D. T. (1974). The effects of increased temperature on electroretinograms of temperature-sensitive paralysis mutants of *Drosophila melanogaster*. *Proc. Natl. Acad. Sci. USA* **71**, 4906–4909.
- Kennerdell, J. R., and Carthew, R. W. (1998). Use of dsRNA-mediated genetic interference to demonstrate that frizzled and frizzled 2 act in the wingless pathway. **95**, 1017–1026.
- Kennerdell, J. R., and Carthew, R. W. (2000). Heritable gene silencing in *Drosophila* using double-stranded RNA. *Nature Biotechnol.* **18**, 896–898.
- Kernan, M., Cowan, D., and Zuker, C. (1994). Genetic dissection of mechanosensory transduction: Mechanoreception-defective mutations of *Drosophila*. *Neuron* **12**, 1195–1206.
- Kerr, R., Lev-Ram, V., Baird, G., Vincent, P., Tsien, R. Y., and Schafer, W. R. (2000). Optical imaging of calcium transients in neurons and pharyngeal muscle of *C. elegans*. *Neuron* **26**, 583–594.
- Keshishian, H., Broadie, K., Chiba, A., and Bate, M. (1996). The *Drosophila* neuromuscular junction: A model system for studying synaptic development and function. *Annu. Rev. Neurosci.* **19**, 545–575.

- Kidd, T., Bland, K. S., and Goodman, C. S. (1999). Slit is the midline repellent for the robo receptor in *Drosophila*. *Cell* **96**, 785–794.
- Kidd, T., Brose, K., Mitchell, K. J., Fetter, R. D., Tessier-Lavigne, M., Goodman, C. S., and Tear, G. (1998a). Roundabout controls axon crossing of the CNS midline and defines a novel subfamily of evolutionarily conserved guidance receptors. *Cell* **92**, 205–215.
- Kidd, T., Russell, C., Goodman, C. S., and Tear, G. (1998b). Dosage-sensitive and complementary functions of roundabout and commissureless control axon crossing of the CNS midline. *Neuron* **20**, 25–33.
- Kidokoro, Y., and Nishikawa, K.-I. (1994). Miniature endplate currents at the newly formed neuromuscular junction in *Drosophila* embryos and larvae. *Neurosci. Res.* **19**, 143–154.
- Kim, Y.-T., and Wu, C.-F. (1991). Distinctions in growth cone morphology and motility between monopolar and multipolar neurons in *Drosophila* CNS culture. *J. Neurobiol.* **22**, 263–275.
- Kitamoto, T. (2001). Conditional modification of behavior in *Drosophila* by targeted expression of a temperature-sensitive shibire allele in defined neurons. *J. Neurobiol.* **47**, 81–92.
- Klagges, B. R., Heimbeck, G., Godenschwege, T. A., Hofbauer, A., Pflugfelder, G. O., Reifegerste, R., Reisch, D., Schaupp, M., Buchner, S., and Buchner, E. (1996). Invertebrate synapsins: A single gene codes for several isoforms in *Drosophila*. *J. Neurosci.* **16**(10), 3154–3165.
- Klingauf, J., Kavalali, E. T., and Tsien, R. W. (1998). Kinetics and regulation of fast endocytosis at hippocampal synapses. *Nature* **394**(6693), 581–585.
- Koenig, J. H., and Ikeda, K. (1983). Characterization of the intracellularly recorded response of identified flight motor neurons in *Drosophila*. *J. Comp. Physiol.* **150**, 295–303.
- Koenig, J. H., and Ikeda, K. (1989). Disappearance and reformation of synaptic vesicle membrane upon transmitter release observed under reversible blockage of membrane retrieval. *J. Neurosci.* **9**, 3844–3860.
- Koenig, J. H., Kosaka, T., and Ikeda, K. (1989). The relationship between the number of synaptic vesicles and the amount of transmitter released. *J. Neurosci.* **9**, 1937–1942.
- Koh, Y. H., Popova, E., Thomas, U., Griffith, L. C., and Budnik, V. (1999). Regulation of DLG localization at synapses by CaMKII-dependent phosphorylation. *Cell* **6**; 98(3), 353–363.
- Kolhekar, A. S., Roberts, M. S., Jiang, N., Johnson, R. C., Mains, R. E., Eipper, B. A., and Taghert, P. H. (1997). Neuropeptide amidation in *Drosophila*: Separate genes encode the two enzymes catalyzing amidation. *J. Neurosci.* **17**, 1363–1376.
- Kolodkin, A. L., Matthes, D. J., and Goodman, C. S. (1993). The semaphorin genes encode a family of transmembrane and secreted growth cone guidance molecules. *Cell* **75**, 1389–1399.
- Kolodziej, P. A., Timpe, L. C., Mitchell, K. J., Fried, S. R., Goodman, C. S., Jan, L. Y., and Jan, Y. N. (1996). frazzled encodes a *Drosophila* member of the DCC immunoglobulin subfamily and is required for CNS and motor axon guidance. *Cell* **87**(2), 197–204.
- Korn, S., Mary, A., Connor, J., and Horn, R. (1991). Perforated patch recording. *Methods Neurosci.* **4**, 264–373.
- Koto, M., Tanouye, M. A., Ferrus, A., Thomas, J. B., and Wyman, R. J. (1981). The morphology of the cervical giant fiber neuron of *Drosophila*. *Brain Res.* **221**, 213–217.
- Kraut, R., Menon, K., and Zinn, K. (2001). A gain-of-function screen for genes controlling motor axon guidance and synaptogenesis in *Drosophila*. *Curr. Biol.* **20**(11), 417–430.
- Kuang, B., Wu, S. C., Shin, Y., Luo, L., and Kolodziej, P. (2000). split ends encodes large nuclear proteins that regulate neuronal cell fate and axon extension in the *Drosophila* embryo. *Development* **127**(7), 1517–1529.
- Kumar, J. P., and Moses, K. (2000). Cell fate specification in the *Drosophila* retina. *Results Probl. Cell Differ.* **31**, 93–114.
- Kurdyak, P., Atwood, H. L., Stewart, B. A., and Wu, C.-F. (1994). Differential physiology and morphology of motor axons to ventral longitudinal muscles in larval *Drosophila*. *J. Comp. Neurol.* **350**, 463–472.
- Kuromi, H., and Kidokoro, Y. (1998). Two distinct pools of synaptic vesicles in single presynaptic boutons in a temperature-sensitive *Drosophila* mutant, shibire. *Neuron* **20**, 917–925.

- Kuromi, H., and Kidokoro, Y. (1999). The optically determined size of exo/endo cycling vesicle pool correlates with the quantal content at the neuromuscular junction of *Drosophila* larvae. *J. Neurosci.* **19**, 1557–1565.
- Kuromi, H., and Kidokoro, Y. (2000). Tetanic stimulation recruits vesicles from reserve pool via a cAMP-mediated process in *Drosophila* synapses. *Neuron* **27**, 133–143.
- Kuromi, H., and Kidokoro, Y. (2002). Selective replenishment of two vesicle pools depends on the source of Ca^{2+} at the *Drosophila* synapse. *Neuron* **35**, 333.
- Kuromi, H., Yoshihara, M., and Kidokoro, Y. (1997). An inhibitory role of calcineurin in endocytosis of synaptic vesicles at nerve terminals of *Drosophila* larvae. *Neurosci. Res.* **27**, 101–113.
- Lahey, T., Gorczyca, M., Jia, X. X., and Budnik, V. (1994). The *Drosophila* tumor suppressor gene *dlg* is required for normal synaptic bouton structure. *Neuron* **13**(4), 823–835.
- Lam, G., and Thummel, C. S. (2000). Inducible expression of double-stranded RNA directs specific genetic interference in *Drosophila*. *Curr. Biol.* **10**, 957–963.
- Landgraf, M., Bossing, T., Technau, G. M., and Bate, M. (1997). The origin, location, and projections of the embryonic abdominal motoneurons of *Drosophila*. *J. Neurosci.* **17**, 9642–9655.
- Landis, G., Bhole, D., Lu, L., and Tower, J. (2001). High-frequency generation of conditional mutations affecting *Drosophila melanogaster* development and life span. *Genetics* **158**, 1167–1176.
- Lawrence, P. A., Casal, J., and Struhl, G. (1999). hedgehog and engrailed: Pattern formation and polarity in the *Drosophila* abdomen. *Development* **126**, 2431–2439.
- Lebovitz, R. M., Takeyasu, K., and Fambrough, D. M. (1989). Molecular characterization and expression of the (Na^{+} + K^{+})-ATPase alpha-subunit in *Drosophila melanogaster*. *EMBO J.* **8**(1), 193–202.
- Lee, C. H., Herman, T., Clandinin, T. R., Lee, R., and Zipursky, S. L. (2001). N-cadherin regulates target specificity in the *Drosophila* visual system. *Neuron* **30**(2), 437–450.
- Lee, D., and O'Dowd, D. K. (1999). Fast excitatory synaptic transmission mediated by nicotinic acetylcholine receptors in *Drosophila* neurons. *J. Neurosci.* **19**, 5311–5321.
- Lee, D., and O'Dowd, D. K. (2000). cAMP-dependent plasticity at excitatory cholinergic synapses in *Drosophila* neurons: Alterations in the memory mutant *dunce*. *J. Neurosci.* **20**, 2104–2111.
- Lee, T., Lee, A., and Luo, L. (1999). Development of the *Drosophila* mushroom bodies: Sequential generation of three distinct types of neurons from a neuroblast. *Development* **126**, 4065–4076.
- Lee, T., and Luo, L. (2001). Mosaic analysis with a repressible cell marker (MARCM) for *Drosophila* neural development. *Trends Neurosci.* **24**, 251–254.
- Lee, T., and Luo, L. (1999). Mosaic analysis with a repressible cell marker for studies of gene function in neuronal morphogenesis. *Neuron* **22**, 451–461.
- Lee, T., Marticke, S., Sung, C., Robinow, S., and Luo, L. (2000a). Cell-autonomous requirement of the USP/EcR-B ecdysone receptor for mushroom body neuronal remodeling in *Drosophila*. *Neuron* **28**(3), 807–818.
- Lee, T., Winter, C., Marticke, S. S., Lee, A., and Luo, L. (2000b). Essential roles of *Drosophila* RhoA in the regulation of neuroblast proliferation and dendritic but not axonal morphogenesis. *Neuron* **25**(2), 307–316.
- Lee, W. R. (1976). Chemical mutagenesis. In “The Genetics and Biology of *Drosophila*.” (M. Ashburner and E. Novitski, eds.), Academic Press, New York.
- Lee, W. R., Beranek, D. T., Byrne, B. J., and Tucker, A. B. (1990). Comparison of dose-response relationships for ethyl methanesulfonate and 1-ethyl-1-nitrosourea in *Drosophila melanogaster* spermatozoa. *Mutat. Res.* **231**(1), 31–45.
- Lehman, R., and Tautz, D. (1994). In situ hybridization to RNA. In “*Drosophila melanogaster*: Practical Uses in Cell and Molecular Biology” (L. S. B. Goldstein and E. A. Fryberg, eds.), Academic Press, New York.
- Leung, H. T., Branton, W. D., Phillips, H. S., Jan, L., and Byerly, L. (1989). Spider toxins selectively block calcium currents in *Drosophila*. *Neuron* **3**(6), 767–772.
- Leung, H.-T., and Byerly, L. (1991). Characterization of single calcium channels in *Drosophila* embryonic nerve and muscle cells. *J. Neurosci.* **11**, 3047–3059.

- Li, Y. X., Farrell, M. J., Liu, R., Mohanty, N., and Kirby, M. L. (2000). Double-stranded RNA injection produces null phenotypes in zebrafish. *Dev. Biol.* **217**, 394–405.
- Lindsley, D. L., and Zimm, G. (1992). *Drosophila melanogaster*. Academic Press, San Diego.
- Link, C. D. (2001). Transgenic invertebrate models of age-associated neurodegenerative diseases. *Mech. Aging Dev.* **122**, 1639–1649.
- Littleton, J. T., Barnard, R. J., Titus, S. A., Slind, J., Chapman, E. R., and Ganetzky, B. (2001). SNARE-complex disassembly by NSF follows synaptic-vesicle fusion. *Proc. Natl. Acad. Sci. USA* **98**(21), 12233–12238.
- Littleton, J. T., and Bellen, H. J. (1995). Synaptotagmin controls and modulates synaptic-vesicle fusion in a Ca²⁺-dependent manner. *Trends Neurosci.* **18**, 177–183.
- Littleton, J. T., Bellen, H. J., and Perin, M. S. (1993). Expression of synaptotagmin in *Drosophila* reveals transport and localization of synaptic vesicles to the synapse. *Development* **118**, 1077–1088.
- Littleton, J. T., Chapman, E. R., Kreber, R., Garment, M. B., Carlson, S. D., and Ganetzky, B. (1998). Temperature-sensitive paralytic mutations demonstrate that synaptic exocytosis requires SNARE complex assembly and disassembly. *Neuron* **21**, 401–413.
- Littleton, J. T., Serano, T. L., Rubin, G. M., Ganetzky, B., and Chapman, E. R. (1999). Synaptic function modulated by changes in the ratio of synaptotagmin I and IV. *Nature* **400**(6746), 757–760.
- Littleton, J. T., Upton, L., and Kania, A. (1995). Immunocytochemical analysis of axonal outgrowth in synaptotagmin mutations. *J. Neurochem.* **65**(1), 32–40.
- Liu, Z., Steward, R., and Luo, L. (2000). *Drosophila* Lis1 is required for neuroblast proliferation, dendritic elaboration and axonal transport. *Nature Cell Biol.* **2**, 776–783.
- Llinas, R., Sugimori, M., and Silver, R. B. (1992). Microdomains of high calcium concentration in a presynaptic terminal. *Science* **256**(5057), 677–679.
- Ludmerer, S. W., Warren, V. A., Williams, B. S., Zheng, Y., Hunt, D. C., Ayer, M. B., Wallace, M. A., Chaudhary, A. G., Egan, M. A., Meinke, P. T., Dean, D. C., Garcia, M. L., Cully, D. F., and Smith, M. M. (2002). Ivermectin and nodulisporic acid receptors in *Drosophila melanogaster* contain both gamma-aminobutyric acid-gated Rdl and glutamate-gated GluCl alpha chloride channel subunits. *Biochemistry* **41**(20), 6548–6560.
- Luer, K., and Technau, G. M. (1992). Primary culture of single ectodermal precursors of *Drosophila* reveals a dorsoventral prepattern of intrinsic neurogenic and epidermogenic capabilities at the early gastrula stage. *Development* **116**, 377–385.
- Luo, L. (2000). Trio quartet in *D. melanogaster*. *Neuron* **26**, 1–2.
- Luo, L., Hensch, T. K., Ackerman, L., Barbel, S., Jan, L. Y., and Jan, Y. N. (1996). Differential effects of the Rac GTPase on Purkinje cell axons and dendritic trunks and spines. *Nature* **379**(6568), 837–840.
- Luo, L., Lee, T., Tsai, L., Tang, G., Jan, L. Y., and Jan, Y. N. (1997). Genghis Khan (Gek) as a putative effector for *Drosophila* Cdc42 and regulator of actin polymerization. *Proc. Natl. Acad. Sci. USA* **94**, 12963–12968.
- Luo, L., Liao, Y. J., Jan, L. Y., and Jan, Y. N. (1996). Distinct morphogenetic functions of similar small GTPases: *Drosophila* Dracl is involved in axonal outgrowth and myoblast fusion. *Genes Dev.* **8**(15), 1787–1802.
- Luo, L., Tully, T., and White, K. (1992). Human amyloid precursor protein ameliorates behavioral deficit of flies deleted for Appl gene. *Neuron* **9**(4), 595–605.
- Luo, L. Q., Martin-Morris, L. E., and White, K. (1990). Identification, secretion, and neural expression of APPL, a *Drosophila* protein similar to human amyloid protein precursor. *J. Neurosci.* **10**(12), 3849–3861.
- Mallart, A., Angaut-Petit, D., Bourret-Poulain, C., and Ferrus, A. (1991). Nerve terminal excitability and neuromuscular transmission in T (X;Y)V7 and Shaker mutants of *Drosophila melanogaster*. *J. Neurogenet.* **7**, 75–84.
- Marin, E. C., Jefferis, G. S., Komiyama, T., Zhu, H., and Luo, L. (2002). Representation of the glomerular olfactory map in the *Drosophila* brain. *Cell* **109**(2), 243–255.

- Marsault, R., Murgia, M., Pozzan, T., and Rizzuto, R. (1997). Domains of high Ca²⁺ beneath the plasma membrane of living A7r5 cells. *EMBO J.* **1**, 16(7), 1575–1581.
- Martin, S. G., Dobi, K. C., and St. Johnston, D. (2001). A rapid method to map mutations in *Drosophila*. *Genome Biol.* **2**(9), .
- Martinez-Padron, M., and Ferrus, A. (1997). Presynaptic recordings from *Drosophila*: Correlation of macroscopic and single-channel K⁺ currents. *J. Neurosci.* **17**, 3412–3424.
- Matthes, D. J., Sink, H., Kolodkin, A. L., and Goodman, C. S. (1995). Protein Semaphorin II can function as a selective inhibitor of specific synaptic arborizations. *Cell* **81**(4), 631–639.
- Matthews, D. A., Salvaterra, P. M., Crawford, G. D., Houser, C. R., and Vaughn, J. E. (1987). An immunocytochemical study of choline acetyltransferase-containing neurons and axon terminals in normal and partially deafferented hippocampal formation. *Brain Res.* **402**(1), 30–43.
- McDonald, K. L., Sharp, D. L., and Rickoll, W. (2000). Preparation of thin sections of *Drosophila* for examination by transmission electron microscopy. In “*Drosophila* Protocols.” (W. Sullivan, M. Ashburner, and R. S. Hawley, eds.), Cold Spring Harbor Laboratory Press, Cold Spring Harbor, NY.
- McGrail, M., and Hays, T. S. (1997). The microtubule motor cytoplasmic dynein is required for spindle orientation during germline cell divisions and oocyte differentiation in *Drosophila*. *Development* **124**(12), 2409–2419.
- McNeil, G. P., Zhang, X., Genova, G., and Jackson, F. R. (1998). A molecular rhythm mediating circadian clock output in *Drosophila*. *Neuron* **20**(2), 297–303.
- Misquitta, L., and Paterson, B. M. (1999). Targeted disruption of gene function in *Drosophila* by RNA interference (RNAi): A role for nautilus in embryonic somatic muscle formation. *Proc. Natl. Acad. Sci. USA* **96**, 1451–1456.
- Misquitta, L., and Patterson, B. M. (2000). In “*Drosophila* Protocols.” (W. Sullivan, M. Ashburner, and R. S. Hawley, eds.), Cold Spring Harbor Laboratory, Cold Spring Harbor, NY.
- Mistra, S., Drosby, M. A., and Drysdale, R. A. (2000). Using *Drosophila* genome databases. In “*Drosophila* Protocols.” (W. Sullivan, M. Ashburner, and R. S. Hawley, eds.), pp. 509–524. Cold Spring Harbor Laboratory Press, Cold Spring Harbor, NY.
- Miyawaki, A., Griesbeck, O., Heim, R., and Tsien, R. Y. (1999). Dynamic and quantitative Ca²⁺ measurements using improved cameleons. *Proc. Natl. Acad. Sci. USA* **96**(5), 2135–2140.
- Monastirioti, M., Gorczyca, M., Rapus, J., Eckert, M., White, K., and Budnik, V. (1995). Octopamine immunoreactivity in the fruit fly *Drosophila*. *J. Comp. Neurol.* **356**(2), 275–287.
- Montell, D. J. (1999). The genetics of cell migration in *Drosophila melanogaster* and *Caenorhabditis elegans* development. *Development* **126**(14), 3035–3046.
- Munoz-Maines, V. J., Slemmon, J. R., Panicker, M. M., Neighbor, N., and Salvaterra, P. M. (1988). Production of polyclonal antisera to choline acetyltransferase using a fusion protein produced by a cDNA clone. *J. Neurochem.* **50**, 167–175.
- Nagai, T., Sawano, A., Park, E. S., and Miyawaki, A. (2001). Circularly permuted green fluorescent proteins engineered to sense Ca²⁺. *Proc. Natl. Acad. Sci. USA* **98**(6), 3197–3202.
- Newsome, T. P., Asling, B., and Dickson, B. J. (2000). Analysis of *Drosophila* photoreceptor axon guidance in eye-specific mosaics. *Development* **127**, 851–860.
- Ng, J., Nardine, T., Harms, M., Tzu, J., Goldstein, A., Sun, Y., Dietzl, G., Dickson, B. J., and Luo, L. (2002). Rac GTPases control axon growth, guidance and branching. *Nature* **416**(6879), 442–447.
- Niemeyer, B. A., and Schwarz, T. L. (2000). SNAP-24, a *Drosophila* SNAP-25 homologue on granule membranes, is a putative mediator of secretion and granule-granule fusion in salivary glands. *J. Cell Sci.* **113**, 4055–4064.
- Niemeyer, B. A., Suzuki, E., Scott, K., Jalink, K., and Zuker, C. S. (1996). The *Drosophila* light-activated conductance is composed of the two channels TRP and TRPL. *Cell* **85**, 651–659.
- Nighorn, A., Healy, M. J., and Davis, R. L. (1991). The cyclic AMP phosphodiesterase encoded by the *Drosophila* dunce gene is concentrated in the mushroom body neuropil. *Neuron* **6**(3), 455–467.
- Nishikawa, K-I., and Kidokoro, Y. (1995). Junctional and extrajunctional glutamate receptor channels in *Drosophila* embryos and larvae. *J. Neurosci.* **15**, 7905–7915.

- Noordermeer, J. N., Kopczynski, C. C., Fetter, R. D., Bland, K. S., Chen, W. Y., and Goodman, C. S. (1998). Wrapper, a novel member of the Ig superfamily, is expressed by midline glia and is required for them to ensheath commissural axons in *Drosophila*. *Neuron* **21**(5), 991–1001.
- Nordhoff, E., Egelhofer, V., Giavalisco, P., Eickhoff, H., Horn, M., Przewieslik, T., Theiss, D., Schneider, U., Lehrach, H., and Gobom, J. (2001). Large-gel two-dimensional electrophoresis-matrix assisted laser desorption/ionization-time of flight-mass spectrometry: An analytical challenge for studying complex protein mixtures. *Electrophoresis*. **22**, 2844–2855.
- O'Dowd, D. K. (1995). Voltage-gated currents and firing properties of embryonic *Drosophila* neurons grown in a chemically defined medium. *J. Neurobiol.* **27**(1), 113–126.
- O'Dowd, D. K., and Aldrich, R. W. (1988). Voltage-clamp analysis of sodium channels in wild-type and mutant *Drosophila* neurons. *J. Neurosci.* **8**, 3633–3643.
- O'Dowd, D. K., Gee, J. R., and Smith, M. A. (1995). Sodium current density correlates with expression of specific alternatively spliced sodium channel mRNAs in single neurons. *J. Neurosci.* **15**(5 Pt 2), 4005–4012.
- O'Dowd, D. K., Germeraad, S. E., and Aldrich, R. W. (1989). Alterations in the expression and gating of *Drosophila* sodium channels by mutations in the para gene. *Neuron* **2**(4), 1301–1311.
- Oleskevich, S. (1999). Cholinergic synaptic transmission in insect mushroom bodies in vitro. *J. Neurophysiol.* **82**, 1091–1096.
- Oleskevich, S., Clements, J. D., and Srinivasan, M. V. (1997). Long-term synaptic plasticity in the honeybee. *J. Neurophysiol.* **78**, 528–532.
- Ordway, R. W., Pallanck, L., and Ganetzky, B. (1994). Neurally expressed *Drosophila* genes encoding homologs of the NSF and SNAP secretory proteins. *Proc. Natl. Acad. Sci. USA* **91**, 5715–5719.
- Osterwalder, T., Yoon, K. S., White, B. H., and Keshishian, H. (2001). A conditional tissue-specific transgene expression system using inducible GAL4. *Proc. Natl. Acad. Sci. USA* **98**, 12596–12601.
- Otto, H., Hanson, P. I., and Jahn, R. (1997). Assembly and disassembly of a ternary complex of synaptobrevin, syntaxin, and SNAP-25 in the membrane of synaptic vesicles. *Proc. Natl. Acad. Sci. USA* **94**, 6197–6201.
- Pak, W. L., Grossfield, J., and White, N. V. (1969). Nonphototactic mutants in the study of vision of *Drosophila*. *Nature* **222**, 351–354.
- Palka, J., Malone, M. A., Ellison, R. L., and Wigston, D. J. (1986). Central projections of identified *Drosophila* sensory neurons in relation to their time of development. *J. Neurosci.* **6**, 1822–1830.
- Pallanck, L., Ordway, R. W., and Ganetzky, B. (1995). A *Drosophila* NSF mutant. *Nature* **376**, 25.
- Pascual, A., and Preat, T. (2001). Localization of long-term memory within the *Drosophila* mushroom body. *Science* **294**(5544), 1115–1117.
- Patel, N. (1994). Imaging neuronal subsets and other cell types in whole-mount *Drosophila* embryos and larvae using antibody probes. *Methods Cell Biol.* **44**, 445–487.
- Patel, N. H., Ball, E. E., and Goodman, C. S. (1992). Changing role of even-skipped during the evolution of insect pattern formation. *Nature* **357**(6376), 339–342.
- Patel, N. H., Condrón, B. G., and Zinn, K. (1994). Pair-rule expression patterns of even-skipped are found in both short- and long-germ beetles. *Nature* **367**(6462), 429–434.
- Patel, N. H., Martín-Blanco, E., Coleman, K. G., Poole, S. J., Ellis, M. C., Kornberg, T. B., and Goodman, C. S. (1989). Expression of engrailed proteins in arthropods, annelids, and chordates. *Cell* **58**(5), 955–968.
- Pauron, D., Qar, J., Barhanin, J., Fournier, D., Cuany, A., Pralavorio, M., Berge, J. B., and Lazdunski, M. (1987). Identification and affinity labeling of very high affinity binding sites for the phenylalkylamine series of Ca⁺ channel blockers in the *Drosophila* nervous system. *Biochemistry* **26**, 6311–6315.
- Pavlidis, P., Ramaswami, M., and Tanouye, M. A. (1994). The *Drosophila* easily shocked gene: A mutation in a phospholipid synthetic pathway causes seizure, neuronal failure, and paralysis. *Cell* **79**(1), 23–33.
- Pelzer, S., Barhanin, J., Pauron, D., Trautwein, W., Lazdunski, M., and Pelzer, D. (1989). Diversity and novel pharmacological properties of Ca²⁺ channels in *Drosophila* brain membranes. *EMBO J.* **8**, 2365–2371.

- Pennetta, G., Hiesinger, P. R., Fabian-Fine, R., Meinertzhagen, I. A., and Bellen, H. J. (2002). *Drosophila* VAP-33A directs bouton formation at neuromuscular junctions in a dosage-dependent manner. *Neuron* **35**, 291–306.
- Peretz, A., Suss-Toby, E., Rom-Glas, A., Arnon, A., Payne, R., and Minke, B. (1994). The light response of *Drosophila* photoreceptors is accompanied by an increase in cellular calcium: Effects of specific mutations. *Neuron* **12**, 1257–1267.
- Pesavento, P. A., Stewart, R. J., and Goldstein, L. S. (1994). Characterization of the KLP68D kinesin-like protein in *Drosophila*: Possible roles in axonal transport. *J. Cell Biol.* **127**, 1041–1048.
- Petersen, S. A., Fetter, R. D., Noordermeer, J. N., Goodman, C. S., and DiAntonio, A. (1997). Genetic analysis of glutamate receptors in *Drosophila* reveals a retrograde signal regulating presynaptic transmitter release. *Neuron* **19**(6), 1237–1248.
- Phelps, C. B., and Brand, A. H. (1998). Ectopic gene expression in *Drosophila* using GAL4 system. *Methods* **14**, 367–379.
- Phillips, A. M., Smith, M., Ramaswami, M., and Kelly, L. E. (2000). The products of the *Drosophila* stoned locus interact with synaptic vesicles via synaptotagmin. *J. Neurosci.* **20**, 8254–8261.
- Phillips, A. M., Salkoff, L. B., and Kelly, L. E. (1993). A neural gene from *Drosophila melanogaster* with homology to vertebrate and invertebrate glutamate decarboxylases. *J. Neurochem.* **61**(4), 1291–1301.
- Piccin, A., Salameh, A., Benna, C., Sandrelli, F., Mazzotta, G., Zordan, M., Rosato, E., Kyriacou, C. P., and Costa, R. (2001). Efficient and heritable functional knock-out of an adult phenotype in *Drosophila* using a GAL4-driven hairpin RNA incorporating a heterologous spacer. *Nucleic Acids Res.* **29**(12), E55.
- Pilling, A., and Saxton, W. M. (1999). Transport of GFP-mitochondria in living *Drosophila* neurons. *Dros. Res. Conf.* **40**, 93.
- Pongs, O., Lindemeier, J., Zhu, X. R., Theil, T., Engelkamp, D., Krah-Jentgens, I., Lambrecht, H. G., Koch, K. W., Schwemer, J., Rivosecchi, R., Mallart, A., Galceran, J., Canal, I., Barbas, J. A., and Ferrus, A. (1993). Frequentin: A novel calcium-binding protein that modulates synaptic efficacy in the *Drosophila* nervous system. *Neuron* **11**(1), 15–28.
- Poodry, C. A. (1990). Shibire, a neurogenic mutant of *Drosophila*. *Dev. Biol.* **138**, 464–472.
- Poodry, C. A., and Edgar, L. (1979). Reversible alteration in the neuromuscular junctions of *Drosophila melanogaster* bearing a temperature-sensitive mutation, shibire. *J. Cell Biol.* **81**, 520–527.
- Poodry, C. A., Hall, L., and Suzuki, D. T. (1973). Developmental properties of Shibire: A pleiotropic mutation affecting larval and adult locomotion and development. *Dev. Biol.* **32**, 373–386.
- Prokopenko, S. N., He, Y., Lu, Y., and Bellen, H. J. (2000). Mutations affecting the development of the peripheral nervous system in *Drosophila*: A molecular screen for novel proteins. *Genetics* **156**(4), 1691–1715.
- Pullikuth, A. K., and Gill, S. S. (1999). Identification of a *Manduca sexta* NSF ortholog, a member of the AAA family of ATPases. *Gene* **240**(2), 343–354.
- Pyle, J. L., Kavalali, E. T., Piedras-Renteria, E. S., and Tsien, R. W. (2000). Rapid reuse of readily releasable pool vesicles at hippocampal synapses. *Neuron* **28**(1), 221–231.
- Raghu, P., Colley, N. J., Webel, R., James, T., Hasan, G., Danin, M., Selinger, Z., and Hardie, R. C. (2000). Normal phototransduction in *Drosophila* photoreceptors lacking an InsP(3) receptor gene. *Mol. Cell Neurosci.* **15**(5), 429–445.
- Ramaswami, M., Krishnan, K. S., and Kelly, R. B. (1994). Intermediates in synaptic vesicle recycling revealed by optical imaging of *Drosophila* neuromuscular junctions. *Neuron* **13**, 363–375.
- Ranganathan, R., Bacskaï, B. J., Tsien, R. Y., and Zuker, C. S. (1994). Cytosolic calcium transients: Spatial localization and role in *Drosophila* photoreceptor cell function. *Neuron* **13**, 837–848.
- Ranjan, R., Bronk, P., and Zinsmaier, K. E. (1998). Cysteine string protein is required for calcium secretion coupling of evoked neurotransmission in *Drosophila* but not for vesicle recycling. *J. Neurosci.* **18**, 956–964.
- Rao, S., Lang, C., Levitan, E. S., and Deitcher, D. L. (2001a). Visualization of neuropeptide expression, transport, and exocytosis in *Drosophila melanogaster*. *J. Neurobiol.* **49**(3), 159–172.

- Rao, S. S., Stewart, B. A., Rivlin, P. K., Vilinsky, I., Watson, B. O., Lang, C., Boulianne, G., Salpeter, M. M., and Deitcher, D. L. (2001b). Two distinct effects on neurotransmission in a temperature-sensitive SNAP-25 mutant. *EMBO J.* **20**, 6761–6771.
- Ray, K., Perez, S. E., Yang, Z., Xu, J., Ritchings, B. W., Steller, H., and Goldstein, L. S. B. (1999). Kinesin-II is required for axonal transport of choline acetyltransferase in *Drosophila*. *J. Cell Biol.* **147**, 507–518.
- Reichmuth, C., Becker, S., Benz, M., Debel, K., Reisch, D., Heimbeck, G., Hofbauer, A., Klagges, B., Pflugfelder, G. O., and Buchner, E. (1995). The *sap47* gene of *Drosophila melanogaster* codes for a novel conserved neuronal protein associated with synaptic terminals. *Brain Res. Mol. Brain Res.* **32**(1), 45–54.
- Reiff, D. F., and Schuster, C. M. (2000). Imaging presynaptic calcium dynamics at wild type and mutant neuromuscular junctions of *Drosophila* using cameleon. *Abstr. Soc. Neurosci.* **26**, 233.14.
- Renden, R., Berwin, B., Davis, W., Ann, K., Chin, C. T., Kreber, R., Ganetzky, B., Martin, T. F., and Broadie, K. (2001). *Drosophila* CAPS is an essential gene that regulates dense-core vesicle release and synaptic vesicle fusion. *Neuron* **31**, 421–437.
- Requena, J., Whittembury, J., Scarpa, A., Brinley, J. F. Jr., and Mullins, L. J. (1991). Intracellular ionized calcium changes in squid giant axons monitored by Fura-2 and aequorin. *Ann. N.Y. Acad. Sci.* **639**, 112–125.
- Richards, D. A., Guatimosim, C., and Betz, W. J. (2000). Two endocytic recycling routes selectively fill two vesicle pools in frog motor nerve terminals. *Neuron* **27**, 551–559.
- Rivosecchi, R., Pogs, O., Theil, T., and Mallart, A. (1994). Implication of frequenin in the facilitation of transmitter release in *Drosophila*. *J. Physiol.* **474**, 223–232.
- Roberts, D. B. (ed.) (1998). “*Drosophila: A Practical Approach*,” 2nd Ed. Oxford University Press, New York.
- Robinow, S., Campos, A. R., Yao, K. M., and White, K. (1988). The *elav* gene product of *Drosophila*, required in neurons, has three RNP consensus motifs. *Science* **242**(4885), 1570–1572.
- Roche, J. P., Packard, M. C., Moeckel-Cole, S., and Budnik, V. (2002). Regulation of synaptic plasticity and synaptic vesicle dynamics by the PDZ protein Scribble. *J. Neurosci.* **22**, 6471–6479.
- Rodesch, C. K., and Broadie, K. (2000). Genetic studies in *Drosophila*: Vesicle pools and cytoskeleton-based regulation of synaptic transmission. *Neuroreport*. **11**, R45–53.
- Rohrbough, J., and Broadie, K. (2002). Electrophysiological analysis of synaptic transmission in central neurons of *Drosophila* larvae. *J. Neurophysiol.* **88**, 847–860.
- Rohrbough, J., Grotewiel, M. S., Davis, R. L., and Broadie, K. (2000). Integrin-mediated regulation of synaptic morphology, transmission, and plasticity. *J. Neurosci.* **20**(18), 6868–6878.
- Rohrbough, J., Pinto, S., Mihalek, R., Tully, T., and Broadie, K. (1999). *Latheo*, a *Drosophila* gene involved in learning, regulates functional synaptic plasticity. *Neuron* **23**, 55–70.
- Roman, G., and Davis, R. L. (2001). Molecular biology and anatomy of *Drosophila* olfactory associative learning. *Bioessays* **23**(7), 571–581.
- Roman, G., Endo, K., Zong, L., and Davis, R. L. (2001). P{Switch}, a novel system for spatial and temporal control of gene expression in *Drosophila melanogaster*. *Proc. Natl. Acad. Sci. USA* **98**, 12602–12607.
- Rong, Y. S., and Golio, K. G. (2000). Gene targeting by homologous recombination in *Drosophila*. *Science* **288**, 2013–2018.
- Rong, Y. S., and Golio, K. G. (2001). A targeted gene knockout in *Drosophila*. *Genetics* **157**, 1307–1312.
- Rong, Y. S., Titen, S. W., Xie, H. B., Golic, M. M., Bastiani, M., Bandyopadhyay, P., Olivera, B. M., Brodsky, M., Rubin, G. M., and Golic, K. G. (2002). Targeted mutagenesis by homologous recombination in *D. melanogaster*. *Genes Dev.* **16**(12), 1568–1581.
- Roos, J., and Kelly, R. B. (1998). Dap 160, a neural-specific Eps 15 homology and multiple SH3 domain-containing protein that interacts with *Drosophila* dynamin. *J. Biol. Chem.* **273**(30), 19108–19119.
- Roos, J., and Kelly, R. B. (1999). The endocytic machinery in nerve terminals surrounds sites of exocytosis. *Curr. Biol.* **9**(23), 1411–1414.

- Rosay, P., Armstrong, J. D., Wang, Z., and Kaiser, K. (2001). Synchronized neural activity in the *Drosophila* memory centers and its modulation by amnesiac. *Neuron* **30**, 759–770.
- Rosay, P., Davies, S. A., Yu, Y., Sozen, A., Kaiser, K., and Dow, J. A. (1997). Cell-type specific calcium signalling in a *Drosophila* epithelium. *J. Cell Sci.* **110**(15), 1683–1692.
- Rosen, D. R., Martin-Morris, L., Luo, L. Q., and White, K. (1989). A *Drosophila* gene encoding a protein resembling the human beta-amyloid protein precursor. *Proc. Natl. Acad. Sci. USA* **86**(7), 2478–2482.
- Rothberg, J. M., Hartley, D. A., Walther, Z., and Artavanis-Tsakonas, S. (1988). slit: An EGF-homologous locus of *D. melanogaster* involved in the development of the embryonic central nervous system. *Cell* **55**, 1047–1059.
- Rothberg, J. M., Jacobs, J. R., Goodman, C. S., and Artavanis-Tsakonas, S. (1990). slit: An extracellular protein necessary for development of midline glia and commissural axon pathways contains both EGF and LRR domains. *Genes Dev.* **4**(12A), 2169–2187.
- Ryan, T. A., Smith, S. J., and Reuter, H. (1996). The timing of synaptic vesicle endocytosis. *Proc. Natl. Acad. Sci. USA* **93**(11), 5567–5571.
- Saitoe, M., Schwarz, T. L., Umbach, J. A., Gundersen, C. B., and Kidokoro, Y. (2001). Absence of junctional glutamate receptor clusters in *Drosophila* mutants lacking spontaneous transmitter release. *Science* **293**(5529), 514–517.
- Saitoe, M., Tanaka, S., Takata, K., and Kidokoro, Y. (1997). Neural activity affects distribution of glutamate receptors during neuromuscular junction formation in *Drosophila* embryos. *Dev. Biol.* **184**(1), 48–60.
- Saito, M., and Wu, C.-F. (1991). Expression of ion channels and mutational effects in giant *Drosophila* neurons differentiated from cell division-arrested embryonic neuroblasts. *J. Neurosci.* **11**, 2135–2150.
- Salkoff, L., and Wyman, R. (1983). Ion currents in *Drosophila* flight muscle. *J. Physiol.* **337**, 687–709.
- Salkoff, L. B., and Kelly, L. E. (1978). Temperature-induced seizure and frequency-dependent neuromuscular block in a mutant of *Drosophila*. *Nature* **273**, 156–158.
- Salvaterra, P. M., Bournias-Vardiabasis, N., Nair, T., Hou, G., and Lieu, C. (1988). In vitro neuronal differentiation of *Drosophila* embryo cells. *J. Neurosci.* **7**, 10–22.
- Salzberg, A., Cohen, N., Halachmi, N., Kimchie, Z., and Lev, Z. (1993). The *Drosophila* Ras2 and rop gene pair: A dual homology with a yeast ras-like gene and a suppressor of its loss-of-function phenotype. *Development* **117**(4), 1309–1319.
- Salzberg, A., Prokopenko, S. N., He, Y., Tsai, P., Pal, M., Maroy, P., Glover, D. M., Deak, P., and Bellen, H. J. (1997). P-element insertion alleles of essential genes on the third chromosome of *Drosophila melanogaster*: Mutations affecting embryonic PNS development. *Genetics* **147**(4), 1723–1741.
- Sankaranarayanan, K., and Sobels, F. H. (1976). Radiation genetics. In “The Genetics and Biology of *Drosophila*.” (M. Ashburner and E. Novitski, eds.), Academic Press, New York.
- Saxton, W. M., Hicks, J., Goldstein, L. S. B., and Raff, E. C. (1991). Kinesin heavy chain is essential for viability and neuromuscular functions in *Drosophila*, but mutants show no defects in mitosis. *Cell* **64**, 1093–1102.
- Saxton, W. M., Porter, M. E., Cohn, S. A., Scholey, J. M., Raff, E. C., and McIntosh, J. R. (1988). *Drosophila* kinesin: Characterization of microtubule motility and ATPase. *Proc. Natl. Acad. Sci. USA* **85**(4), 1109–1113.
- Schikorski, T., and Stevens, C. F. (2001). Morphological correlates of functionally defined synaptic vesicle populations. *Nature Neurosci.* **4**, 391–395.
- Schmid, A., Chiba, A., and Doe, C. Q. (1999). Clonal analysis of *Drosophila* embryonic neuroblasts: Neural cell types, axon projections and muscle targets. *Development* **126**, 4653–4689.
- Schmid, A., Schindelhof, B., and Zinn, K. (2002). Combinatorial RNAi: A method for evaluating the functions of gene families in *Drosophila*. *Trends Neurosci.* **25**, 71–74.
- Schmidt, H., Luer, K., Hevers, W., and Technau, G. M. (2000). Ionic currents of *Drosophila* embryonic neurons derived from selectively cultured CNS midline precursors. *J. Neurobiol.* **44**(4), 392–413.

- Schmidt, H., Rickert, C., Bossing, T., Vef, O., Urban, J., and Technau, G. M. (1997). The embryonic central nervous system lineages of *Drosophila melanogaster*. II. Neuroblast lineages derived from the dorsal part of the neuroectoderm. *Dev. Biol.* **189**, 186–204.
- Schmidt-Nielsen, B. K., Gepner, J. I., Teng, N. N., and Hall, L. M. (1977). Characterization of an alpha-bungarotoxin binding component from *Drosophila melanogaster*. *J. Neurochem.* **29**, 1013–1029.
- Schmucker, D., Clemens, J. C., Shu, H., Worby, C. A., Xiao, J., Muda, M., Dixon, J. E., and Zipursky, S. L. (2000). *Drosophila* Dscam is an axon guidance receptor exhibiting extraordinary molecular diversity. *Cell* **101**, 671–684.
- Schneider, L. E., Sun, E. T., Garland, D. J., and Taghert, P. H. (1993). An immunocytochemical study of the FMRFamide neuropeptide gene products in *Drosophila*. *J. Comp. Neurol.* **337**, 446–460.
- Scholnick, S. B., Caruso, P. A., Klemencic, J., Mastick, G. S., Mauro, C., and Rotenberg, M. (1991). Mutations within the Ddc promoter alter its neuron-specific pattern of expression. *Dev. Biol.* **146**(2), 423–437.
- Schote, U., and Seelig, J. (1998). Interaction of the neuronal marker dye FM1-43 with lipid membranes: Thermodynamics and lipid ordering. *Biochim. Biophys Acta* **1415**(1), 135–146.
- Schulze, K. L., Littleton, J. T., Salzberg, A., Halachmi, N., Stern, M., Lev, Z., and Bellen, H. J. (1994). rop, a *Drosophila* homolog of yeast Sec 1 and vertebrate n-Sec1/Munc-18 proteins, is a negative regulator of neurotransmitter release in vivo. *Neuron* **13**, 1099–1108.
- Scott, E. K., Lee, T., and Luo, L. (2001). enok encodes a *Drosophila* putative histone acetyltransferase required for mushroom body neuroblast proliferation. *Curr. Biol.* **23**(11), 99–104.
- Seecof, R. L., Alleaume, N., Teplitz, R. L., and Gerson, I. (1971). Differentiation of neurons and myocytes in cell cultures made from *Drosophila gastrulae*. *Exp. Cell Res.* **69**, 161–173.
- Seecof, R. L. (1979). Preparation of cell cultures from *Drosophila melanogaster* embryos. *Tissue Culture Assoc. Manual* **5**, 1019–1022.
- Seecof, R. L., Donady, J. J., and Teplitz, R. L. (1973). Differentiation of *Drosophila* neuroblasts to form ganglion-like clusters of neurons in vitro. *Cell Differ.* **2**(3), 143–149.
- Seecof, R. L., Teplitz, R. L., Gerson, I., Ikeda, K., and Donady, J. J. (1972). Differentiation of neuromuscular junctions in cultures of embryonic *Drosophila* cells. *Proc. Natl. Acad. Sci. USA* **69**, 566–570.
- Seeger, M., Tear, G., Ferres-Marco, D., and Goodman, C. S. (1993). Mutations affecting growth cone guidance in *Drosophila*: Genes necessary for guidance toward or away from the midline. *Neuron* **10**, 409–426.
- Sharp, P. A. (2001). RNA interference. *Genes Dev.* **15**, 485–490.
- Shields, G., and Sang, J. (1977). Improved medium for culture of *Drosophila* embryonic cells. *Drosophila Inform. Serv.* **52**, 161.
- Siddiqi, O., and Benzer, S. (1976). Neurophysiological defects in temperature-sensitive paralytic mutants of *Drosophila melanogaster*. *Proc. Natl. Acad. Sci. USA* **73**, 3253–3257.
- Singh, S., and Wu, C.-F. (1990). Properties of potassium currents and their role in membrane excitability in *Drosophila* larval muscle fibers. *J. Exp. Biol.* **152**, 59–76.
- Sisson, J. C. (2000). Culturing large populations of *Drosophila* for protein biochemistry. In “*Drosophila* Protocols.” (W. Sullivan, M. Ashburner, and R. S. Hawley, eds.), pp. 541–552. Cold Spring Harbor Laboratory Press, Cold Spring Harbor, NY.
- Skeath, J. B., and Carroll, S. B. (1992). Regulation of proneural gene expression and cell fate during neuroblast segregation in the *Drosophila* embryo. *Development* **114**(4), 939–946.
- Skipski, V. P., and Barclay, M. (1969). Thin-layer chromatography of lipids. *Meth. Enzymol.* **14**, 530–598.
- Skoulakis, E. M., and Davis, R. L. (1996). Olfactory learning deficits in mutants for leonardo, a *Drosophila* gene encoding a 14–3–3 protein. *Neuron* **17**(5), 931–944.
- Smith, L. A., Wang, X., Peixoto, A. A., Neumann, E. K., Hall, L. M., and Hall, J. C. (1996). A *Drosophila* calcium channel 1 subunit gene maps to a genetic locus associated with behavioral and visual defects. *J. Neurosci.* **16**, 7868–7879.

- Smith, L. A., Peixoto, A. A., Kramer, E. M., Villela, A., and Hall, J. C. (1998). Courtship and visual defects of cacophony mutants reveal functional complexity of a calcium-channel 1 subunit in *Drosophila*. *Genetics* **149**, 1407–1426.
- Smith, M. M., Warren, V. A., Thomas, B. S., Brochu, R. M., Ertel, E. A., Rohrer, S., Schaeffer, J., Schmatz, D., Petuch, B. R., Tang, Y. S., Meinke, P. T., Kaczorowski, G. J., and Cohen, C. J. (2000). Nodulisporic acid opens insect glutamate-gated chloride channels: Identification of a new high affinity modulator. *Biochemistry* **39**, 5543–5554.
- Snow, P. M., Patel, N. H., Harrelson, A. L., and Goodman, C. S. (1987). Neural-specific carbohydrate moiety shared by many surface glycoproteins in *Drosophila* and grasshopper embryos. *J. Neurosci.* **7**(12), 4137–4144.
- Sokolowski, M. B. (2001). *Drosophila*: Genetics meets behaviour. *Nature Rev. Genet.* **2**(11), 879–890.
- Solc, C. K., and Aldrich, R. W. (1988). Voltage-gated potassium channels in larval CNS neurons of *Drosophila*. *J. Neurosci.* **8**, 2556–2570.
- Sone, M., Hoshino, M., Suzuki, E., Kuroda, S., Kaibuchi, K., Nakagoshi, H., Saigo, K., Nabeshima, Y., and Hama, C. (1997). Still life, a protein in synaptic terminals of *Drosophila* homologous to GDP-GTP exchangers. *Science* **275**(5299), 543–547.
- Spradling, A. C. (1986). P-element-mediated transformation. In “*Drosophila*: A Practical Approach” (D. B. Roberts, ed.), pp. 175–199. IRL Press, Oxford.
- Spradling, A. C., Stern, D., Beaton, A., Rhem, E. J., Laverly, T., Mozden, N., Misra, S., and Rusin, G. M. (1999). The Berkeley *Drosophila* Genome Project Gene Disruption Project: Single P-element insertions mutating 25% of vital *Drosophila* genes. *Genetics* **153**, 135–177.
- St. Johnston, D. (2002). The art and design of genetic screens: *Drosophila melanogaster*. *Nature Rev. Genet.* **3**, 176–188.
- Stanley, H., Botas, J., and Malhotra, V. (1997). The mechanism of Golgi segregation during mitosis is cell type-specific. *Proc. Natl. Acad. Sci. USA* **94**, 14467–14470.
- Stark, W. S., Lin, T. N., Brackhahn, D., Christianson, J. S., and Sun, G. Y. (1993). Phospholipids in *Drosophila* heads: Effects of visual mutants and phototransduction manipulations. *Lipids* **28**, 23–28.
- Stebbins, M. J., Urlinger, S., Byrne, G., Bello, B., Hillen, W., and Yin, J. C. (2001). Tetracycline-inducible systems for *Drosophila*. *Proc. Natl. Acad. Sci. USA* **98**, 10775–10780.
- Stebbins, M. J., and Yin, J. C. (2001). *Gene* **270**, 103–111.
- Stewart, B. A., Atwood, H. L., Renger, J. J., Wang, J., and Wu, C.-F. (1994). Improved stability of *Drosophila* larval neuromuscular preparations in haemolymph-like physiological solutions. *J. Comp. Physiol.* **175**, 179–191.
- Stimson, D. T., Estes, P. S., Rao, S., Krishnan, K. S., Kelly, L. E., and Ramaswami, M. (2001). *Drosophila* stoned proteins regulate the rate and fidelity of synaptic vesicle internalization. *J. Neurosci.* **21**, 3034–3044.
- Stimson, D. T., Estes, P. S., Smith, M., Kelly, L. E., and Ramaswami, M. (1998). A product of the *Drosophila* stoned locus regulates neurotransmitter release. *J. Neurosci.* **18**(23), 9638–9649.
- Stowers, R. S., and Schwarz, T. L. (1999). A genetic method for generating *Drosophila* eyes composed exclusively of mitotic clones of a single genotype. *Genetics* **152**(4), 1631–1639.
- Sun, B., and Salvaterra, P. M. (1995). Characterization of nervana, a *Drosophila melanogaster* neuron-specific glycoprotein antigen recognized by anti-horseradish peroxidase antibodies. *J. Neurochem.* **65**, 434–443.
- Sun, B., Wang, W., and Salvaterra, P. M. (1998). Functional analysis and tissue-specific expression of *Drosophila* Na⁺, K⁺-ATPase subunits. *J. Neurochem.* **71**, 142–151.
- Sun, J., and Tower, J. (1999). FLP recombinase-mediated induction of Cu/Zn-superoxide dismutase transgene expression can extend the lifespan of adult *Drosophila melanogaster* flies. *Mol. Cell. Biol.* **19**, 216–228.
- Sun, Q., Bahri, S., Schmid, A., Chia, W., and Zinn, K. (2000). Receptor tyrosine phosphatases regulate axon guidance across the midline of the *Drosophila* embryo. *Development* **127**, 801–881.
- Suzuki, D. T., Grigliatti, T. A., and Williamson, R. (1971). Temperature-sensitive mutations in *Drosophila melanogaster*. *Proc. Natl. Acad. Sci. USA* **68**, 890–893.

- Sweeney, N. T., Li, W., and Gao, F. B. (2002). Genetic manipulation of single neurons in vivo reveals specific roles of flamingo in neuronal morphogenesis. *Dev. Biol.* **247**, 76–88.
- Sweeney, S. T., Broadie, K., Keane, J., Niemann, H., and O’Kane, C. J. (1995). Targeted expression of tetanus toxin light chain in *Drosophila* specifically eliminates synaptic transmission and causes behavioral defects. *Neuron* **14**, 341–351.
- Sweeney, S. T., Hidalgo, A., deBelle, J. S., and Keshishian, H. (2000). In “*Drosophila* Protocols.” (W. Sullivan, M. Ashburner, and R. S. Hawley, eds.), pp. 449–478. Cold Spring Harbor Laboratory Press, Cold Spring Harbor, NY.
- Taghert, P. H., and Schneider, L. E. (1990). Inter-specific comparison of a *Drosophila* gene encoding FMRFamide-related neuropeptides. *J. Neurosci.* **10**, 1929–1942.
- Takagawa, K., and Salvaterra, P. (1996). Analysis of choline acetyltransferase protein in temperature sensitive mutant flies using newly generated monoclonal antibody. *Neurosci. Res.* **24**(3), 237–243.
- Takahashi, A., Camacho, P., Lechleiter, J. D., and Herman, B. (1999). Measurement of intracellular calcium. *Physiol. Rev.* **79**(4), 1089–1125.
- Takasu-Ishikawa, E., Yoshihara, M., Ueda, A., Rheuben, M. B., Hotta, Y., and Kidokoro, Y. (2001). Screening for synaptic defects revealed a locus involved in presynaptic and postsynaptic functions in *Drosophila* embryos. *J. Neurobiol.* **48**(2), 101–119.
- Tanouye, M. A., and Ferrus, A. (1985). Action potentials in normal and Shaker mutant *Drosophila*. *J. Neurogenet.* **2**, 253–271.
- Tanouye, M. A., and King, D. G. (1983). Giant fiber activation of direct flight muscles in *Drosophila*. *J. Exp. Biol.* **105**, 241–251.
- Tanouye, M. A., and Wyman, R. J. (1980). Motor outputs of giant nerve fiber in *Drosophila*. *J. Neurophysiol.* **44**, 405–421.
- Tautz, D., Lehmann, R., Schnurch, H., Schuh, R., Seifert, E., Kienlin, A., Jones, K., and Jaeckle, H. (1987). Finger protein of novel structure encoded by hunchback, a second member of the gap class of *Drosophila* segmentation genes. *Nature* **327**, 383–389.
- Tautz, D., and Pfeifle, C. (1989). A non-radioactive in situ hybridization method for the localization of specific RNAs in *Drosophila* embryos reveals translational control of the segmentation gene hunchback. *Chromosoma* **98**(2), 81–85.
- Teeter, K., Naemuddin, M., Gasperini, R., Zimmerman, E., White, K. P., Hoskins, R., and Gibson, G. (2000). Haplotype dimorphism in a SNP collection from *Drosophila melanogaster*. *J. Exp. Zool.* **288**, 63–75.
- Tiffert, T., Garcia-Sancho, J., and Lew, V. L. (1984). Irreversible ATP depletion caused by low concentrations of formaldehyde and of calcium-chelator esters in intact human red cells. *Biochim Biophys Acta* **773**(1), 143–156.
- Torroja, L., Luo, L., and White, K. (1996). APPL, the *Drosophila* member of the APP-family, exhibits differential trafficking and processing in CNS neurons. *J. Neurosci.* **16**(15), 4638–4650.
- Torroja, L., Packard, M., Gorczyca, M., White, K., and Budnik, V. (1999). The *Drosophila*-amyloid precursor protein homolog promotes synapse differentiation at the neuromuscular junction. *J. Neurosci.* **19**, 7793–7803.
- Toyoshima, S., Matsumoto, N., Wang, P., Inoue, H., Yoshioka, T., Hotta, Y., and Osawa, T. (1990). Purification and partial amino acid sequences of phosphoinositide-specific phospholipase C of *Drosophila* eye. *J. Biol. Chem.* **265**, 14842–14848.
- Trimarchi, J. R., and Murphey, R. K. (1997). The shaking-B mutation disrupts electrical synapses in a flight circuit in adult *Drosophila*. *J. Neurosci.* **17**, 4700–4710.
- Trimarchi, J. R., and Schneiderman, A. M. (1994). The motor neurons innervating the direct flight muscles of *Drosophila melanogaster* are morphologically specialized. *J. Comp. Neurol.* **340**, 427–443.
- Truong, K., Sawano, A., Mizuno, H., Hama, H., Tong, K. I., Mal, T. K., Miyawaki, A., and Ikura, M. (2001). FRET-based in vivo Ca²⁺ imaging by a new calmodulin-GFP fusion molecule. *Nature Struct. Biol.* **8**, 1069–1073.
- Tsien, R. Y. (1998). The green fluorescent protein. *Annu. Rev. Biochem.* **67**, 509–544.

- Tsunoda, S., and Salkoff, L. (1995). Genetic analysis of *Drosophila* neurons: Shal, Shaw, and Shab encode most embryonic potassium currents. *J. Neurosci.* **15**, 1741–1754.
- Ueda, A., and Kidokoro, Y. (1996). Longitudinal body wall muscles are electrically coupled across the segmental boundary in the third instar larva of *Drosophila melanogaster*. *Invertebr. Neurosci.* **1**, 315–322.
- Umbach, J. A., Grasso, A., Zurcher, S. D., Kornblum, H. I., Mastrogiacomo, A., and Gundersen, C. B. (1998a). Electrical and optical monitoring of alpha-latrotoxin action at *Drosophila* neuromuscular junctions. *Neuroscience* **87**, 913–924.
- Umbach, J. A., and Gundersen, C. B. (1997). Evidence that cysteine string proteins regulate an early step in the Ca²⁺-dependent secretion of neurotransmitter at *Drosophila* neuromuscular junctions. *J. Neurosci.* **17**, 7203–7209.
- Umbach, J. A., Saitoe, M., Kidokoro, Y., and Gundersen, C. B. (1998b). Attenuated influx of calcium ions at nerve endings of csp and shibire mutant *Drosophila*. *J. Neurosci.* **18**(9), 3233–3240.
- Usui, T., Shima, Y., Shimada, Y., Hirano, S., Burgess, R. W., Schwarz, T. L., Takeichi, M., and Uemura, T. (1999). Flamingo, a seven-pass transmembrane cadherin, regulates epithelial planar polarity under the control of Frizzled. *Cell* **98**, 585–595.
- van de Goor, J., Ramaswami, M., and Kelly, R. (1995). Redistribution of synaptic vesicles and their proteins in temperature-sensitive shibire(ts1) mutant *Drosophila*. *Proc. Natl. Acad. Sci. USA* **92**, 5739–5743.
- Van der Meer, J. M., and Jaffe, L. F. (1983). Elemental composition of the perivitelline fluid in early *Drosophila* embryos. *Dev. Biol.* **95**, 249–252.
- van Roessel, P., and Brand, A. H. (2000). Gal4-mediated ectopic gene expression in *Drosophila*. In “*Drosophila* Protocols.” (W. Sullivan, M. Ashburner, and R. S. Hawley, eds.), pp. 509–524. Cold Spring Harbor Laboratory Press, Cold Spring Harbor, NY.
- van Roessel, P., and Brand, A. H. (2002). Imaging into the future: Visualizing gene expression and protein interactions with fluorescent proteins. *Nature Cell Biol.* **4**, E15–E20.
- van Vactor, D., Krantz, D. E., Reinke, R., and Zipursky, S. L. (1988). Analysis of mutants in chaoptin, a photoreceptor cell-specific glycoprotein in *Drosophila*, reveals its role in cellular morphogenesis. *Cell* **52**, 281–290.
- Van Vactor, D., and Lorenz, L. J. (1999). Introduction: Invertebrate axons find their way. *Cell Mol. Life Sci.* **30**(55), 1355–1357.
- Van Vactor, D., Sink, H., Fambrough, D., Tsoo, R., and Goodman, C. S. (1993). Genes that control neuromuscular specificity in *Drosophila*. *Cell* **73**, 1137–1153.
- Verkhusha, V. V., Tsukita, S., and Oda, H. (1999). Actin dynamics in lamellipodia of migrating border cells in the *Drosophila* ovary revealed by a GFP-actin fusion protein. *FEBS Lett.* **445**(2–3), 395–401.
- Verstreken, P., Kjaerulf, O., Lloyd, T. E., Atkinson, R., Zhou, Y., Meinertzhagen, I. A., and Bellen, H. J. (2002). Endophilin mutations block clathrin-mediated endocytosis but not neurotransmitter release. *Cell* **109**, 101–112.
- Voets, T. (2000). Dissection of three Ca²⁺-dependent steps leading to secretion in chromaffin cells from mouse adrenal slices. *Neuron* **28**, 537–545.
- Vogel, E., and Natarajan, A. T. (1979). The relation between reaction kinetics and mutagenic action of mono-functional alkylating agents in higher eukaryotic systems. I. Recessive lethal mutations and translocations in *Drosophila*. *Mutat. Res.* **62**(1), 51–100.
- von Schilcher, F. (1976). The behavior of cacophony, a courtship song mutant in *Drosophila melanogaster*. *Behav. Biol.* **17**, 187–196.
- von Schilcher, F. (1977). A mutation which changes courtship song in *Drosophila melanogaster*. *Behav. Genet.* **7**, 251–259.
- Vorechovsky, I., Luo, L., Dyer, M. J., Catovsky, D., Amlot, P. L., Yaxley, J. C., Foroni, L., Hammarstrom, L., Webster, A. D., and Yuille, M. A. (1997). Clustering of missense mutations in the ataxia-telangiectasia gene in a sporadic T-cell leukaemia. *Nature Genet.* **17**(1), 96–99.

- Waddell, S., Armstrong, J. D., Kitamoto, T., Kaiser, K., and Quinn, W. G. (2000). The amnesiac gene product is expressed in two neurons in the *Drosophila* brain that are critical for memory. *Cell* **103**, 805–813.
- Waddell, S., and Quinn, W. G. (2001). Flies, genes, and learning. *Annu. Rev. Neurosci.* **24**, 1283–1309.
- Wager-Smith, K., and Kay, S. A. (2000). Circadian rhythm genetics: From flies to mice to humans. *Nature Genet.* **26**, 23–27.
- Wan, H. I., DiAntonio, A., Fetter, R. D., Bergstrom, K., Strauss, R., and Goodman, C. S. (2000). Protein Highwire regulates synaptic growth in *Drosophila*. *Neuron* **26**, 313–329.
- Wan, L., Dockendorff, T. C., Jongens, T. A., and Dreyfuss, G. (2001). Characterization of dFMR1, a *Drosophila melanogaster* homolog of the fragile X mental retardation protein. *Mol. Cell Biol.* **20**(22), 8536–8547.
- Wang, J., Renger, J. J., Griffith, L. C., Greenspan, R. J., and Wu, C.-F. (1994a). Concomitant alterations of physiological and developmental plasticity in *Drosophila* CaM kinase II-inhibited synapses. *Neuron* **13**, 1373–1384.
- Wang, X., Sun, B., Yasuyama, K., and Salvaterra, P. M. (1994b). Biochemical analysis of proteins recognized by antiHRP antibodies in *Drosophila melanogaster*: Identification and characterization of neuron specific and male specific glycoproteins. *Insect Biochem. Mol. Biol.* **24**, 233–242.
- Wang, Y., Wright, N. J., Guo, H., Xie, Z., Svoboda, K., Malinow, R., Smith, D. P., and Zhong, Y. (2001). Genetic manipulation of the odor-evoked distributed neural activity in the *Drosophila* mushroom body. *Neuron* **29**, 267–276.
- Waterman-Storer, C. M., and Holzbaaur, E. L. (1996). The product of the *Drosophila* gene, Glued, is the functional homologue of the p150Glued component of the vertebrate dynactin complex. *J. Biol. Chem.* **271**(2), 1153–1159.
- Waud, J. P., Bermudez Fajardo, A., Sudhaharan, T., Trimby, A. R., Jeffery, J., Jones, A., and Campbell, A. K. (2001). Measurement of proteases using chemiluminescence-resonance-energy-transfer chimaeras between green fluorescent protein and aequorin. *Biochem. J.* **357**(Pt 3), 687–697.
- White, B., Osterwalder, T., and Keshishian, H. (2001a). Molecular genetic approaches to the targeted suppression of neuronal activity. *Curr. Biol.* **11**, R1041–R1053.
- White, B. H., Osterwalder, T. P., Yoon, K. S., Joiner, W. J., Whim, M. D., Kaczmarek, L. K., and Keshishian, H. (2001b). Targeted attenuation of electrical activity in *Drosophila* using a genetically modified K(+) channel. *Neuron* **31**, 699–711.
- White, K., and Valles, A. M. (1985). Immunohistochemical and genetic studies of serotonin and neuropeptides in *Drosophila*. In “Molecular Bases of Neural Development; Annual Symposia of the Neurosciences Institute of the Neurosciences Research Program.”
- Wianny, F., and Zernicka-Goetz, M. (2000). Specific interference with gene function by double-stranded RNA in early mouse development. *Nature Cell Biol.* **2**, 70–75.
- Williams, D. W., Tyrer, M., and Shepherd, D. (2000). Tau and tau reporters disrupt central projections of sensory neurons in *Drosophila*. *J. Comp. Neurol.* **428**(4), 630–640.
- Winter, C. G., Wang, B., Ballew, A., Royou, A., Karess, R., Axelrod, J. D., and Luo (2001). *Drosophila* Rho-associated kinase (Drok) links Frizzled-mediated planar cell polarity signaling to the actin cytoskeleton. *Cell* **105**(1), 81–91.
- Wolff, T. (2000a). Histological techniques for the *Drosophila* eye. I. Larva and pupa. In “*Drosophila* Protocols.” (W. Sullivan, M. Ashburner, and R. S. Hawley, eds.), pp. 201–228. Cold Spring Harbor Laboratory Press, Cold Spring Harbor, NY.
- Wolff, T. (2000b). Histological techniques for the *Drosophila* eye. II. Adult. In “*Drosophila* Protocols” (W. Sullivan, M. Ashburner, and R. S. Hawley, eds.), pp. 229–244. Cold Spring Harbor Laboratory Press, Cold Spring Harbor, NY.
- Wolfner, M. F., and Goldberg, M. L. (1994). Harnessing the power of *Drosophila* genetics. *Methods Cell Biol.* **44**, 34–80.
- Woods, D. F., and Bryant, P. J. (1991). The discs-large tumor suppressor gene of *Drosophila* encodes a guanylate kinase homolog localized at septate junctions. *Cell* **9**, 66(3) 451–464.

- Worby, C. A., Simonson-Leff, N., Clemens, J. C., Huddler, D. Jr., Muda, M., and Dixon, J. E. (2002). *Drosophila* Ack targets its substrate, the sorting nexin DSH3PX1, to a protein complex involved in axonal guidance. *J. Biol. Chem.* **277**(11) 9422–9428.
- Worby, C. A., Simonson-Leff, N., Clemens, J. C., Kruger, R. P., Muda, M., and Dixon, J. E. (2001a). The sorting nexin, DSH3PX1, connects the axonal guidance receptor, Dscam, to the actin cytoskeleton. *J. Biol. Chem.* **276**(45), 41782–41789.
- Worby, C. A., Simonson-Leff, N., and Dixon, J. E. (2001b). RNA interference of gene expression (RNAi) in cultured *Drosophila* cells. *Sci STKE*. (95):PL1.
- Wright, N. J. D., and Zhong, Y. (1995). Characterization of K⁺ currents and the cAMP-dependent modulation in cultured *Drosophila* mushroom body neurons identified by lacZ expression. *J. Neurosci.* **15**, 1025–1034.
- Wu, C.-F., and Ganetzky, B. (1992). Neurogenetic studies of ion channels in *Drosophila*. *Ion Channels* **3**, 261–314.
- Wu, C.-F., Ganetzky, B., Jan, L. Y., Jan, Y. N., and Benzer, S. (1978). A *Drosophila* mutant with a temperature-sensitive block in nerve conduction. *Proc. Natl. Acad. Sci. USA* **75**, 4047–4051.
- Wu, C.-F., and Haugland, F. N. (1985). Voltage clamp analysis of membrane currents in larval muscle fibers of *Drosophila*. *J. Neurosci.* **5**, 2626–2640.
- Wu, C.-F., Sakai, M., and Hotta, Y. (1990). Giant *Drosophila* neurons differentiated from cytokinesis-arrested embryonic neuroblasts. *J. Neurobiol.* **21**, 499–507.
- Wu, C.-F., Suzuki, N., and Poo, M.-M (1983). Dissociated neurons from normal and mutant *Drosophila* larval central nervous system in cell culture. *J. Neurosci.* **3**, 1888–1899.
- Wu, M. N., Littleton, J. T., Bhat, M. A., Prokop, A., and Bellen, H. J. (1998). ROP, the *Drosophila* Sec1 homolog, interacts with syntaxin and regulates neurotransmitter release in a dosage-dependent manner. *EMBO J.* **17**, 127–139.
- Xia, Z., Zhou, Q., Lin, J., and Liu, Y. (2001). Stable SNARE complex prior to evoked synaptic vesicle fusion revealed by fluorescence resonance energy transfer. *J. Biol. Chem.* **276**, 1766–1771.
- Yang, M. Y., Armstrong, J. D., Vilinsky, I., Strausfeld, N. J., and Kaiser, K. (1995). Subdivision of the *Drosophila* mushroom bodies by enhancer-trap expression patterns. *Neuron* **15**(1), 45–54.
- Yao, W. D., Rusch, J., Poo, M., and Wu, C. F. (2000). Spontaneous acetylcholine secretion from developing growth cones of *Drosophila* central neurons in culture: Effects of cAMP-pathway mutations. *J. Neurosci.* **20**(7), 2626–2637.
- Yao, W. D., and Wu, C. F. (1999). Auxiliary hyperkinetic beta subunit of K⁺ channels: Regulation of firing properties and K⁺ currents in *Drosophila* neurons. *J. Neurophysiol.* **81**(5), 2472–2484.
- Yasuyama, K., Kitamoto, T., and Salvaterra, P. M. (1995). Localization of choline acetyltransferase-expressing neurons in the larval visual system of *Drosophila melanogaster*. *Cell Tissue Res.* **282**(2), 193–202.
- Yasuyama, K., Meinertzhagen, I. A., and Schurmann, F. W. (2002). Synaptic organization of the mushroom body calyx in *Drosophila melanogaster*. *J. Comp. Neurol.* **445**, 211–226.
- Yoshihara, M., Rheuben, M. B., and Kidokoro, Y. (1997). Transition from growth cone to functional motor nerve terminal in *Drosophila* embryos. *J. Neurosci.* **17**, 8408–8426.
- Yoshikami, D., and Okun, L. (1984). Staining of living presynaptic nerve terminals with selective fluorescent dyes. *Nature* **310**, 53–56.
- Yoshioka, T., Inoue, H., and Hotta, Y. (1983). Defective phospholipid metabolism in the reticular cell membrane of norpA (no receptor potential) visual transduction mutants of *Drosophila*. *Biochem. Biophys. Res. Commun.* **16**, 111(2), 567–573.
- Zagotta, W. N., Brainard, M. S., and Aldrich, R. W. (1988). Single-channel analysis of four distinct classes of potassium channels in *Drosophila* muscle. *J. Neurosci.* **8**, 4765–4779.
- Zhang, B., Koh, Y. H., Beckstead, R. B., Budnik, V., Ganetzky, B., and Bellen, H. J. (1998). Synaptic vesicle size and number are regulated by a clathrin adaptor protein required for endocytosis. *Neuron* **21**(6), 1465–1475.
- Zhang, B., and Zehlf, A. C. (2002). Amphiphysins: Raising the BAR for synaptic vesicle recycling and membrane dynamics. *Traffic* **3**, 452–460.

- Zhang, H.-G., Lee, H.-J., Rocheleau, T., French-Constant, R. H., and Jackson, M. B. (1995). Subunit composition determines picrotoxin and bicuculline sensitivity of *Drosophila* gamma-aminobutyric acid receptors. *Mol. Pharmacol.* **48**, 835–840.
- Zhang, Y. Q., Bailey, A. M., Matthies, H. J., Renden, R. B., Smith, M. A., Speese, S. D., Rubin, G. M., and Broadie, K. (2001). *Drosophila* fragile X-related gene regulates the MAP1B homolog Futsch to control synaptic structure and function. *Cell* **107**, 591–603.
- Zhang, Y. Q., Rodesch, C. K., and Broadie, K. (2002). A living synaptic vesicle marker: Synaptotagmin-GFP. *Genesis*.
- Zheng, W., Feng, G., Ren, D., Eberl, D. F., Hannan, F., Dubald, M., and Hall, L. M. (1995a). Cloning and characterization of a calcium channel alpha 1 subunit from *Drosophila melanogaster* with similarity to the rat brain type D isoform. *J. Neurosci.* **15**(2), 1132–1143.
- Zheng, Y., Wong, M. L., Alberts, B., and Mitchison, T. (1995b). Nucleation of microtubule assembly by a gamma-tubulin-containing ring complex. *Nature* **378**, 578–583.
- Zheng, Y., Wong, M. L., Alberts, B., and Mitchison, T. (1998). Purification and assay of gamma tubulin ring complex. *Methods Enzymol.* **298**, 218–228.
- Zhao, M.-L., and Wu, C.-F. (1997). Alterations in frequency coding and activity dependence of excitability in cultured neurons of *Drosophila* memory mutants. *J. Neurosci.* **17**, 2187–2199.
- Zhong, Y., Budnik, V., and Wu, C.-F. (1992). Synaptic plasticity in *Drosophila* memory and hyperexcitability mutants: Role of cAMP cascade. *J. Neurosci.* **12**, 644–665.
- Zhong, Y., and Wu, C.-F. (1991). Altered synaptic plasticity in *Drosophila* memory mutants with defective cyclic AMP cascade. *Science* **251**, 198–201.
- Zinsmaier, K. E., Eberle, K. K., Buchner, E., Walter, N., and Benzen, S. (1994). Paralysis and early death in cysteine string protein mutants of *Drosophila*. *Science* **18**, 263(5149), 977–980.
- Zinsmaier, K. E., Hofbauer, A., Heimbeck, G., Pflugfelder, G. O., Buchner, S., and Buchner, E. A. (1990). Cysteine-string protein is expressed in retina and brain of *Drosophila*. *J. Neurogenet.* **7**(1), 15–29.
- Zipursky, S. L., Venkatesh, T. R., Teplow, D. B., and Benzer, S. (1984). Neuronal development in the *Drosophila* retina: Monoclonal antibodies as molecular probes. *Cell* **36**, 15–26.
- Zito, K., Fetter, R. D., Goodman, C. S., and Isacoff, E. Y. (1997). Synaptic clustering of Fascilin II and Shaker: Essential targeting sequences and role of Dlg. *Neuron* **19**, 1007–1016.
- Zito, K., Parnas, D., Fetter, R. D., Isacoff, E. Y., and Goodman, C. S. (1999). Watching a synapse grow: Noninvasive confocal imaging of synaptic growth in *Drosophila*. *Neuron* **22**, 719–729.
- Zusman, S., Grinblat, Y., Yee, G., Kafatos, F. C., and Hynes, R. O. (1993). Analyses of PS-integrin functions during *Drosophila* development. *Development* **118**, 737–750.

This Page Intentionally Left Blank

CHAPTER 12

PC12 Cells as a Model for Studies of Regulated Secretion in Neuronal and Endocrine Cells

T. F. J. Martin and R. N. Grishanin

Department of Biochemistry
University of Wisconsin
Madison, Wisconsin 53706

-
- I. Introduction
 - II. Propagation and Culture of PC12 Cells
 - III. Studying Secretion Using PC12 Cells
 - A. Secretion Assays with Permeable PC12 Cells Using Radioactive Catecholamines
 - B. Secretion Assays with Permeable PC12 Cells Using Continuous Electrochemical Detection of Released Monoamines
 - C. Secretion Assays in Transfected Cells Using Human Growth Hormone
 - IV. Immunocytochemical Detection of Proteins in Intact and Permeable PC12 Cells
 - A. Immunostaining of Mechanically Permeabilized PC12 Cells
 - B. Immunocytochemical Detection of Cytosolic Proteins Interacting Transiently with Membranes in PC12 Cells
 - References

Pheochromocytoma-derived cell lines such as PC12 cells maintain a differentiated neuroendocrine phenotype and have been widely used as a convenient model system for a wide variety of cell biological studies on neurotrophin action, monoamine biogenesis, protein trafficking, and secretory vesicle dynamics. This chapter reviews a number of methods that are useful for studies of the regulated dense core vesicle secretory pathway. This includes protocols for maintaining cells and preserving their phenotype. A variety of assays are discussed for monitoring secretion in intact or permeable cells and in transfected cells. Specific methods for immunocytochemical studies in permeable cells are discussed. Finally, protocols

for high-efficiency PC12 cell transfections and the isolation of stably transfected cell lines are provided.

I. Introduction

The PC12 cell line was derived from a rat pheochromocytoma, an adrenal medullary tumor (Greene and Tischler, 1976). Soon after its derivation, this cell line was widely utilized for studies of different aspects of neuronal and endocrine cell physiology. Differentiation (arrested proliferation and neurite outgrowth) of PC12 cells into a neuronal phenotype by nerve growth factor (NGF) treatment was described in the first report on the cells (Greene and Tischler, 1976), and numerous subsequent studies of neurotrophin signaling were reported using this cell line (see Huang and Reichardt, 2001; Vaudry *et al.*, 2002). PC12 cells have also become an important model for studies of the mechanisms of regulated neuroendocrine secretion. The cells contain large (~100 nm) dense core vesicles (DCVs) that store monoamines as well as smaller (~40 nm) vesicles of endosomal origin termed synaptic vesicle-like microvesicles (SLMVs) that have been reported to contain acetylcholine (Greene and Tischler, 1976; Greene and Rein, 1977; Rebois *et al.*, 1980). Elevations in cytosolic Ca^{2+} trigger vesicle fusion with the plasma membrane and the secretion of catecholamines and neuropeptides from DCVs and acetylcholine from SLMVs (Rebois *et al.*, 1980; Schubert and Klier, 1977; Ninomiya *et al.*, 1997). The cholinergic neuronal phenotype is reported to be enhanced by NGF and retinoic acid treatment (Greene and Tischler, 1976; Matsuoka *et al.*, 1989), whereas the endocrine adrenergic phenotype is maintained in undifferentiated cells and is enhanced by dexamethazone treatment (Anderson, 1993), PC12 cells have also been used for studies on the biogenesis of DCVs in the Golgi and SLMVs at the plasma membrane (Bauerfeind *et al.*, 1993; Weihe *et al.*, 1996; Tooze and Huttner, 1990; de Wit *et al.*, 1999; Desnos *et al.*, 1995; Urbe *et al.*, 1998; Andrea *et al.*, 1997; Lichtenstein *et al.*, 1998).

The ability to grow PC12 cells in continuous culture with a well-defined secretory cell phenotype presents advantages for cell biological and biochemical studies of the secretory pathway. Facile transfection techniques and the ease of isolating stable cell lines harboring protein expression vectors provide another important set of experimental advantages. Our laboratory has developed a number of broken cell and membrane preparations for the *in vitro* study of cellular processes that, in combination with the preceding, have enabled mechanistic studies of the secretory pathway. A previous methods article (Klenchin *et al.*, 1998) described aspects of some of these techniques in detail and should be consulted. This chapter emphasizes some additional features and updates on several basic techniques, including cell culture that are useful for the study of Ca^{2+} -dependent exocytosis in PC12 cells.

PC12 cells are neuroendocrine in origin and exhibit a well-developed DCV secretory pathway, although it is less highly developed (fewer smaller DCVs) than in adrenal medullary progenitor cells. Undifferentiated as well as

NGF-treated PC12 cells exhibit a rudimentary version of a synaptic vesicle (SV)-mediated pathway for acetylcholine secretion, which is not readily observed in many PC12 cell sublines (Nishiki *et al.*, 1997). While there are overall a number of important mechanistic similarities between DCV and SV exocytosis, PC12 cells represent a more important model for neuroendocrine/endocrine DCV exocytosis than for neuronal SV exocytosis. Ca^{2+} -evoked DCV exocytosis is relatively slow in PC12 cells compared to the fastest components of DCV exocytosis in chromaffin cells and to synaptic SV exocytosis in neurons (Ninomiya *et al.*, 1997). The basis for the slow kinetics of Ca^{2+} -activated DCV exocytosis in PC12 cells will need to be explained in order to extrapolate the findings in this model system to the mechanisms underlying faster modes of exocytosis. Kinetic studies of catecholamine release in PC12 cells suggest that the many docked DCVs in the cells are mainly staged several steps removed from fusion and need to transit through priming steps (Ninomiya *et al.*, 1997; Ng *et al.*, 2002; Grishanin *et al.*, 2003).

PC12 cells offer a number of advantages for studies of regulated exocytosis because of the development of permeable cell and plasma membrane preparations in which Ca^{2+} -dependent exocytosis can be reconstituted (Martin, 1989; Martin and Kowalchuk, 1997; Walent *et al.*, 1992). These preparations, which provide macromolecular access to the exocytic machinery, have facilitated studies of protein identification (Walent *et al.*, 1992; Hay and Martin, 1993b; Hay *et al.*, 1995; Chen *et al.*, 1999a) and the use of probes such as toxins (Bannerjee *et al.*, 1996a; Gerona *et al.*, 2000; Banerjee *et al.*, 1996), recombinant proteins (Ann *et al.*, 1997; Desai *et al.*, 2000; Blackmer *et al.*, 2001; Earles *et al.*, 2001; Shin *et al.*, 2002; Sugita *et al.*, 2001, 2002) and antibodies (Fukuda *et al.*, 2002) for mechanistic studies. Many (40–60% of ~1000) of the DCVs in PC12 cells are docked at the plasma membrane and retain competence for Ca^{2+} -triggered fusion following permeabilization or homogenization of the cells. Cytosolic and peripheral membrane proteins required for exocytosis can be depleted by washing the permeable cell or membrane preparations, which can be reconstituted in *in vitro* incubations. This approach resulted in the discovery of several soluble proteins that are essential for ATP-dependent or Ca^{2+} -dependent stages of exocytosis (Walent *et al.*, 1992; Hay and Martin, 1993b; Hay *et al.*, 1995; Chen *et al.*, 1999a).

Advances in understanding molecular mechanisms involved in late stages of Ca^{2+} -triggered exocytosis have been facilitated by the accessibility of permeable PC12 cells to macromolecular probes. Functional roles for synaptotagmins I and IX were demonstrated using antibody Fab fragments specific for either synaptotagmin isoform (Fukuda *et al.*, 2002). Aspects of the mechanisms of synaptotagmin action (phospholipid binding, SNARE interactions, oligomerization) were inferred from the dominant inhibitory effects of recombinant synaptotagmin fusion proteins and mutants on Ca^{2+} -activated secretion (Desai *et al.*, 2000; Earles *et al.*, 2001; Sugita *et al.*, 2001, 2002). Evidence that soluble N-ethylmaleimide-sensitive factor attachment protein receptor (SNARE) complex formation was essential for Ca^{2+} -triggered exocytosis was provided by direct inhibition studies with botulinum neurotoxins (Gerona *et al.*, 2000) and reconstitution studies using C-terminal

SNAP-25 protein fragments to restore complex formation and exocytosis in permeable cells containing botulinum neurotoxin E (BoNTE)-cleaved SNAP-25 (Chen *et al.*, 1999). The specificity of SNARE protein interactions during DCV exocytosis was assessed by testing dominant interfering soluble fragments of SNARE proteins (Chen *et al.*, 2001). Overall, the use of macromolecular probes targeted at proteins essential for late stages of DCV exocytosis proximal to fusion have facilitated studies of the underlying mechanisms.

Many components of the exocytotic machinery are tightly membrane associated or are integral membrane proteins. While these are accessible in permeable cells to antibodies or fusion proteins that interact with them, the use of transfection methods provides a useful approach for reverse genetic manipulation in PC12 cells. Studies have shown that synaptotagmin protein overexpression alters the machinery for fusion pore formation (Wang *et al.*, 2001). Another very useful approach enables replacement of one protein with a mutated version. Zhang *et al.* (2002) expressed the light chain of BoNTE to proteolytically inactivate SNAP-25, which was replaced effectively with BoNTE-resistant SNAP-25 mutants. Replacement of SNAP-25 with mutants deficient in Ca^{2+} -dependent synaptotagmin binding revealed the importance of this interaction in the Ca^{2+} triggering of exocytosis. This approach can be generalized to other toxin light chains that target VAMP/synaptobrevin and syntaxin for studies of the physiological role of specific interactions reported for these SNARE proteins. The following section provides several protocols for culturing PC12 cells and studying the secretory pathway.

II. Propagation and Culture of PC12 Cells

PC12 cells are cultured in Dulbecco's modified Eagle's medium (DMEM) with high (10 g/liter) glucose supplemented with 5% iron-supplemented calf serum and 5% horse serum in a 10% CO_2 atmosphere. We do not employ antibiotics in the medium but prefer that any bacterial contaminants reveal themselves by growth. Propagation and replating PC12 cells require special attention because the cells tend to form cell aggregates that are associated with irreversible changes in cell physiology, which include a loss of secretory responsiveness. To prevent the progressive accumulation of cell aggregates through multiple passages, cell suspensions are triturated extensively prior to replating. The growth medium is aspirated from cultures that are 80% or less of maximal density, and the culture dish is rinsed with Hanks' basal salt solution containing 1 mM EDTA. Hanks'/EDTA is added to the dish (1 ml for a 10-cm dish), and the dish is incubated for less than 5 min in a 37°C incubator to loosen adherent cells. The loosened cells are dislodged by agitating the dish and adding growth medium (9 ml for a 10-cm dish). At this step, the cell suspension is triturated up to 10 times by passage through a 10-ml pipette fitted with a yellow pipetman tip attached to the end. Cell aggregates should be dispersed into mainly single cell suspension for replating onto new dishes containing fresh medium.

A large number of distinct PC12 cell lines are available from laboratories around the world as well as from the ATCC culture collection. Many of these exhibit a propensity to aggregate and exhibit poor properties, including a small number of DCVs, highly variable abilities to synthesize acetylcholine, a low density of Ca^{2+} channels, and extreme heterogeneity across the culture. Unfortunately, the diversity of properties reported for individual PC12 cell lines from different laboratories has resulted in conflicting results in the literature and the perception that the cells are too variable to support reproducible findings. It is the case for immortalized aneuploid cell lines that clonal lines with differing characteristics can be isolated (Clementi *et al.*, 1992), presumably due to accumulated chromosomal translocations, rearrangements, and loss. We strongly recommend isolating a number of single cell clones and characterizing each after expansion for desired properties prior to embarking upon a set of studies. This is extremely important when stably transfected cell lines will be isolated. Cultures maintained as described earlier will maintain reproducible properties for many passages and the passage number should be noted. Frozen stocks of a low passage number for desired clones can be stored in a liquid nitrogen freezer to retrieve cells with the original properties. Frozen stocks are prepared by subculturing a 10-cm dish with $\sim 10^7$ cells and resuspending the cells in 1 ml culture medium containing 10% dimethyl sulfoxide DMSO. After transferring to a sterile cryostatic vial, the cells are frozen by placing in an insulated container for 4 h at -20°C and overnight at -80° before transfer to liquid nitrogen.

III. Studying Secretion Using PC12 Cells

A. Secretion Assays with Permeable PC12 Cells Using Radioactive Catecholamines

Exocytosis of DCVs in intact as well as permeable PC12 cells can be assayed readily by the release of preloaded radioactive norepinephrine. This simple type of permeable cell assay was utilized to monitor the activity of required cytosolic factors during their purification (Walent *et al.*, 1992; Hay and Martin, 1993b; Hay *et al.*, 1995; Ahnart-Hilger *et al.*, 1987). Various methods for permeabilizing PC12 cells have been described previously (Schafer *et al.*, 1987; Ahnert-Hilger *et al.*, 1989). This section describes the techniques that have been used routinely in our laboratory.

1. Cell Labeling and Harvesting

Cells are labeled 12–20 h before an experiment. Cells at 70–80% of maximal density are fed with fresh growth medium to which [^3H]NE (norepinephrine) (Amersham Pharmacia Biotech, TRK 584, 45 Ci/mmol) to $1\ \mu\text{Ci/ml}$ and $0.5\ \text{mM}$ sodium ascorbate are added. Following overnight labeling, cells are washed and incubated for 60 min in DMEM containing $1\ \text{mg/ml}$ bovine serum albumin (BSA)

to remove unincorporated [^3H]NE. Then cells are rinsed with PC12 buffer (70 mM sucrose, 130 mM NaCl, 4.8 mM KCl, 1.3 mM CaCl_2 , 1.2 mM MgSO_4 , 25 mM HEPES, pH 7.3) or KGlu buffer (120 mM potassium glutamate, 20 mM HEPES, 20 mM potassium acetate, 2 mM EGTA, pH 7.2). Rinsed cells are dislodged from dishes by the repeated pipetting of ice-cold KGlu buffer and are collected by centrifugation in a 15-ml disposable plastic tube.

2. Cell Permeabilization

We use a mechanical permeabilization method of “cell cracking” that requires the use of a custom-built ball homogenizer. This can be made by a local machine shop based on a design given elsewhere (Martin, 1989) or from an alternative source (H&Y Enterprise). Cells are suspended in KGlu buffer containing 1% BSA and passed once through the prechilled ball homogenizer using 3- to 5-ml disposable syringes. With a proper clearance in the ball homogenizer (~ 0.0001 in.), a single pass yields $>95\%$ permeable cells as estimated by trypan blue staining. Permeable cells are collected in a 15-ml disposable plastic tube, and the buffer is adjusted to 10 mM EGTA by addition from a 100 mM potassium-EGTA stock solution. Cells are left on ice for 1–2 h to extract proteins from cell ghosts. After incubation, cell ghosts are washed three times with KGlu-BSA buffer at ~ 3 ml/dish, with centrifugation at $1000 \times g$ for 5 min. A freeze-thaw cracking method developed in our lab (Klenchin *et al.*, 1998) can be used successfully to permeabilize the cells as an alternative to using the ball homogenizer. Several cycles of freezing cell suspensions in KGlu buffer in liquid nitrogen followed by slow thawing at room temperature are used to rupture the plasma membrane (Klenchin *et al.*, 1998). Cells permeabilized by freeze-thaw are otherwise handled as described for mechanically permeabilized cells.

3. Secretion Assays

In the permeable cell format, the Ca^{2+} -dependent release of [^3H]NE exhibits requirements for MgATP and cytosolic factors (Hay and Martin, 1993a). It has been shown that the MgATP requirement can be fulfilled in preincubations (Ng *et al.*, 2002; Hay and Martin, 1993b; Hay *et al.*, 1995). Routine assays make use of either of two configurations: a single step combined assay containing Ca^{2+} , MgATP, and rat brain cytosol or a sequential two-stage assay employing “priming” incubations with MgATP and rat brain cytosol followed by “triggering” incubations that include Ca^{2+} and rat brain cytosol.

Cytosolic factors required for MgATP-dependent priming and Ca^{2+} -dependent triggering reactions have been purified and characterized. Priming factors in rat brain cytosol consist of phosphatidylinositol transfer protein (PITP) and phosphatidylinositol 4-monophosphate 5-kinase (PIP5K) (Hay *et al.*, 1995; Hay and Martin, 1993b). While purified or recombinant PITP and PIP5K can be used in the priming reactions, the use of crude cytosol will be more accessible and convenient

for general use by most laboratories. The factor required for Ca^{2+} -dependent triggering in rat brain cytosol was identified as Ca^{2+} -dependent activator protein secretion (CAPS) (Walent *et al.*, 1992), and the purified or recombinant protein can be employed in triggering reactions (Ann *et al.*, 1997). The exclusive expression of this protein in neural/endocrine cells (Walent *et al.*, 1992) necessitates the use of neural/endocrine tissue cytosols such as rat brain cytosol for triggering reactions. Alternatively, as described later, cytosols from COS cells expressing CAPS also fulfill this requirement readily.

For the *preparation of rat brain cytosol*, 50 fresh rat brains from animals weighing more than 200 g are homogenized in ice-cold buffer (20 mM HEPES, 2 mM EDTA, 2 mM EGTA, 250 mM sucrose, 1 mM dithiothreitol, pH 7.0) containing 1 mM phenylmethylsulfonyl fluoride (PMSF), 5 $\mu\text{g}/\text{ml}$ leupeptin, and 2 $\mu\text{g}/\text{ml}$ aprotinin (150 or 3 ml/brain) with a Polytron homogenizer. The homogenate is centrifuged for 30 min at $48,000 \times g$ (Beckman JA-20, 20,000 rpm), and the supernatant is clarified by centrifugation at $200,000 \times g$ for 90 min (Beckman 70Ti, 45,000 rpm). The resulting cytosol typically has a protein concentration of 10 mg/ml. Aliquots of 0.5 ml are flash frozen and stored at -70°C .

The *combined assay* is useful for screening the effects of various reagents (antibodies, fusion proteins, toxins) for their ability to inhibit exocytosis. Once a reagent is identified as useful, staged assays can distinguish whether the reagent acts at early ATP-dependent or later Ca^{2+} -triggered stages of DCV exocytosis. Combined assays are conveniently conducted in 1.5-ml microfuge tubes in a final volume of 200 μl , although this can be scaled down to 25 μl . The reactions contain $\sim 10^6$ permeable cells, 2 mM ATP, 2 mM MgCl_2 , 1 mg/ml rat brain cytosol, and 1.72 mM Ca^{2+} ($\sim 10 \mu\text{M}$ free ionic Ca^{2+}) in KGlu buffer. Reactions are assembled on an ice bath, and extended preincubations of permeable cells with reagents may be conducted (usually omitting Ca^{2+}) prior to incubating the tubes for 5–15 min in a water bath at 30°C . Unincubated control reactions and incubated reactions lacking Ca^{2+} are run in parallel to determine levels of carryover of free [^3H]NE and nonexocytic release, respectively. Reactions are terminated by chilling on an ice bath, and the tubes are centrifuged at 4°C for 10 min at $3000 \times g$. Supernatants are transferred to scintillation vials for liquid scintillation counting, and cell pellets are solubilized in 1% Triton X-100 for liquid scintillation counting. Secretion is determined as the percentage NE released by normalizing supernatant [^3H]NE to the total detected in pellet plus supernatant. In typical experiments, [^3H]NE release can reach 60–70% of the total in 15 min with the majority of this being Ca^{2+} dependent.

In the *two-stage assay*, ATP- and Ca^{2+} -dependent steps in regulated exocytosis are resolved experimentally as sequential reactions. This assay configuration is useful for determining whether a reagent of interest acts prior to or at the Ca^{2+} -triggered step of exocytosis. Priming reactions are carried out by incubating permeable cells with 1 mg/ml rat brain cytosol and 2 mM MgATP for 30 min at 30°C . Reactions are chilled on ice, and permeable cells are washed by low-speed centrifugation (usually three to four times) in KGlu buffer containing BSA. Cell

pellets are resuspended gently after centrifugation in 100–200 μl of KGlu buffer + BSA, and reactions are adjusted to 1.72 mM Ca^{2+} plus 0.5 mg/ml rat brain cytosol (or 20 nM recombinant CAPS). Samples are transferred to glass tubes, and $^3\text{H}[\text{NE}]$ release is triggered by placing the tubes at 30°C for 3 min. Reactions are terminated by chilling followed by centrifugation at 3000 $\times g$, and the relative amount of [^3H]NE in supernatants and Triton X-100-solubilized pellets is assessed by liquid scintillation counting.

Cytosols from heterologous expression systems can be employed in place of or in addition to rat brain cytosol in the secretion assays to test the activity of specific proteins in regulated exocytosis. This approach is quite useful when a protein of interest (e.g., a phosphoprotein or high molecular weight protein) cannot be produced in an active form or be purified readily from *Escherichia coli* expression. It is also quite useful for a high throughput analysis of mutant proteins that are not expressed readily in *E. coli* but can be expressed in a heterologous mammalian expression system (e.g., COS cell). This approach was utilized to determine the activity of a number of CAPS mutants for reconstituting the Ca^{2+} -triggering step of exocytosis (see Fig. 1 and Grishanin *et al.*, 2002). In this case, rat brain cytosol was employed in the first incubation of the two-stage assay, whereas cytosols prepared from COS-1 fibroblasts expressing the protein of interest were used in the second incubation. Cytosols prepared from nonexpressing COS-1 cells exhibit a low level of activity in the Ca^{2+} -triggering assay, which can be attributed to calmodulin (Chen *et al.*, 1999a). In contrast, the activity of cytosols from COS-1 cells expressing CAPS can greatly exceed that present in rat brain cytosol (Grishanin *et al.*, 2002). Thus, the activity of proteins involved in secretion, as well as cognate mutant forms, may be studied by complementing permeable PC12 cells with cytosols from transfected COS-1 cells.

The cDNA of the protein of interest is cloned into a mammalian expression vector containing the SV40 origin to allow amplification of the plasmid in COS-1 cells. COS-1 cells are cultured in DMEM supplemented with 10% fetal bovine serum in a 5% CO_2 atmosphere. Cells are transfected by electroporation at 1000 $\mu\text{F}/300\text{ V}$ using conditions described by Van den Hoff *et al.* (1992) (see later) with 10–50 μg plasmid DNA per 10^7 cells. Electroporated cells are plated in 10-cm dishes in growth medium and grow for 48 h. Cells are harvested in phosphate-buffered saline (PBS) containing 5 mM EDTA, washed three times with KGlu buffer, resuspended in KGlu buffer containing 10 $\mu\text{g}/\text{ml}$ aprotinin, 10 $\mu\text{g}/\text{ml}$ leupeptin, and 1 mM PMSF, and homogenized by multiple passes through a 10- μm clearance ball homogenizer. Cytosols are prepared by centrifugation at 80,000 $\times g$ and are concentrated to 2–5 mg/ml with Centricon 50 (Amicon) concentrator devices. The relative content of expressed proteins in cytosol is estimated by Western blot (conveniently using HA- or myc-tagged expression plasmids) and is used to adjust cytosols to a constant value by dilution with cytosols from nontransfected COS-1 cells. A range of concentrations of each cytosol is tested in the triggering assay with parallel positive (rat brain cytosol) and negative (nontransfected COS-1 cytosol) controls.

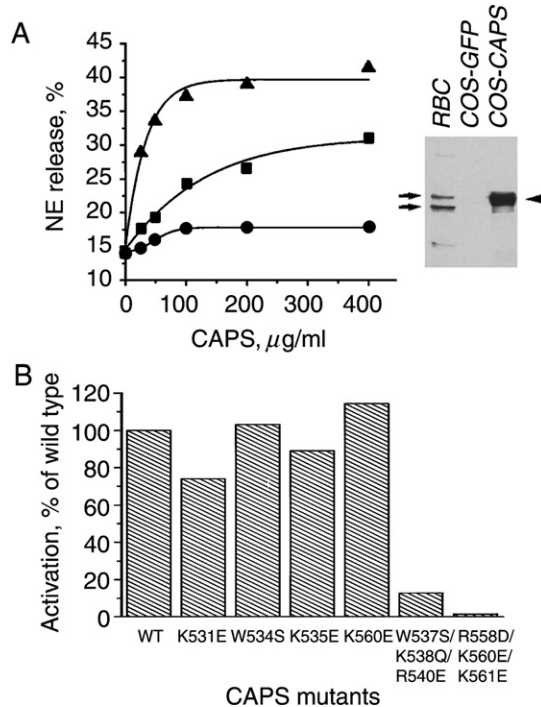


Fig. 1 Reconstitution of Ca^{2+} -dependent DCV exocytosis in permeable PC12 cells with cytosols from COS cells expressing wild-type and mutant forms of CAPS. (A) CAPS expression in COS cells confers reconstituting activity on cytosol for Ca^{2+} -triggered norepinephrine release. Indicated amounts of crude cytosol derived from rat brain (■), COS-1 cells expressing GFP (●), or COS-1 cells expressing CAPS(HA)₃ (▲) were tested in a 5-min triggering assay. (Insert) Western blot analysis of CAPS (arrows) in rat brain cytosol (RBC), cytosol from GFP-expressing COS-1 cells, and cytosol from CAPS-expressing COS-1 cells. (B) Mutations in the CAPS PH domain differentially affect the activity of CAPS in regulated exocytosis. COS-1 cells were transfected with constructs encoding wild-type and mutant forms of CAPS(HA)₃. Cytosols prepared from cells expressing CAPS were adjusted with cytosol from nontransfected COS-1 to equalize the amount of CAPS per milligram of cytosol protein. The Ca^{2+} -triggered release of [³H]NE from permeable PC12 cells was tested at 0.4 mg/ml of cytosol for each of the indicated CAPS proteins. Maximal cytosol-dependent activity from wild-type CAPS-expressing COS-1 cells was set at 100%. Methods: The COS-1 cytosol-based assay was used to facilitate the analysis of the effects of mutations on CAPS activity. COS-1 cells were transfected with 50 pCMVCAPS(HA)₃ encoding full-length CAPS C-terminally tagged with a triple HA tag under control of the CMV promoter or with PEGFP-N1 for the expression of GFP in control cells. Both transfections were done using 50 μg DNA per 10⁷ cells and cytosols were prepared as described. Cytosol from COS-1 cells expressing GFP had very low activity compared to rat brain cytosol. Expression of CAPS protein in COS-1 cells conferred greater activity (A) than that of rat brain cytosol due to higher amounts of CAPS per weight unit of cytosolic protein (insert). These methods were used to assess the activities of CAPS proteins containing mutations in the pleckstrin homology (PH) domain. While several PH domain mutants exhibited wild-type activity, the mutants (W537S/K538Q/R540E and R558D/K560E/K561E) exhibited strongly impaired activity in the secretion assay, which correlated with decreased interactions with liposomes containing acidic phospholipids and with cellular membranes (see Grishanin *et al.*, 2002). Reprinted from the Journal of Biological Chemistry.

B. Secretion Assays with Permeable PC12 Cells Using Continuous Electrochemical Detection of Released Monoamines

The preceding biochemical assay employing the release of [³H]NE can be performed readily in most laboratories for studies of factors that influence the final extent of exocytosis. However, this assay has limitations for kinetic studies of exocytosis because numerous tubes are required to determine multiple points in a time course of release. Kinetic studies on the Ca²⁺-triggered release of [³H]NE from permeable PC12 cells indicate that secretion reaches its final extent within 1–2 min following Ca²⁺ addition. Routine assays measure final extents, and factors that affect initial rates rather than final extents may be overlooked in this assay format. Previous studies of secretion in intact PC12 (or chromaffin) cells have employed carbon fiber electrode detection of catecholamines usually in single cells. This approach has provided important information about multiple kinetic components of exocytosis that reflect an apparent sequential multistep pathway through which DCVs transit toward fusion (Chow *et al.*, 1992; Ashery *et al.*, 2000) and detailed dynamics of fusion process of single secretory granule with plasma membrane (Wang *et al.*, 2001; Voets *et al.*, 2001). However, direct studies of individual stages in DCV exocytosis are somewhat limited to the analysis of single cells overexpressing proteins or derived from knockout animals (Voets *et al.*, 2002).

To couple the advantages of the permeable PC12 cell assay with higher time resolution kinetic methods for the detection of monoamine secretion, Earles *et al.* (2001) employed rotating disk electrode voltametry (RDE). Using this methodology, we have found that the initial rate of Ca²⁺-triggered DCV exocytosis is quite dependent on prior ATP-dependent priming and the concentration of CAPS protein, and is sensitive to inhibition by a variety of reagents directed at the SNARE fusion machinery (Grishanin *et al.*, 2003). Thus, the permeable PC12 cell assay combined with RDE represents a more refined method that will facilitate molecular studies on regulated exocytosis.

Methods for the detection of catecholamines by RDE, and a survey of the instrument setup, are described in detail by Earles and Schenk (1998). Permeable cells are incubated in a custom-built ~0.5-ml volume glass chamber containing a Ag/AgCl reference electrode and platinum auxiliary electrode (Earles and Schenk, 1998). The chamber is temperature controlled by a water jacket connected to a circulating water bath. Catecholamines released during the incubation are detected by electrooxidation on a 2-mm glassy carbon electrode driven by a precision rotator (Pine Instrument Co.). The rotator is connected to a potentiostat (e.g., Petit Ampere LC-3D, Bioanalytical Systems, Inc.) with an output to an analog-to-digital converter data acquisition board (e.g., DI-700, Dataq Instruments) with software for viewing voltage output on a personal computer. The electrode, with an applied potential of 500 mV (relative to the Ag/AgCl reference electrode), is placed into the cell suspension and rotated at 3000 rpm, which enables extremely rapid (millisecond) mixing.

In the original assay described by Earles *et al.* (2001), the authors relied on the detection of endogenous catecholamine, mainly dopamine. In addition, PC12 cells detached from culture dishes by pipetting were permeabilized to Ca^{2+} by centrifugation at $1600 \times g$ for 3 min (Earles *et al.*, 2001). We have instead utilized the RDE assay with PC12 cells permeabilized by the methods described in the preceding section, which enable full control over the incubation constituents that constitute the “intracellular” environment of the permeable cells. The permeable cells are utilized following ATP-dependent priming incubations in a modification of the two-stage secretion assay. While the Ca^{2+} -triggered release of endogenous dopamine is detected readily in these assays, we routinely preload cells with NE (1.5 mM plus 0.5 mM ascorbate) in overnight incubations to increase the quantal catecholamine content of DCVs to allow fewer permeable cells per incubation to be used. NE loading can also be conducted during the priming reactions with permeable cells by adding 0.5 mM NE during the last 15 min of the incubation.

Other methods utilized for these experiments are similar to those described for the [^3H]NE release assays. However, one important difference is that cytosols employed for Ca^{2+} -triggering reactions conducted in the RDE chamber must be dialyzed or gel filtered in order to eliminate small molecular weight oxidizable constituents that are detected by the electrode. In general, all reagents used in the assay need to be checked for possible oxidation at 500 mV to avoid generating spurious signals.

For the recording, a 350- μl suspension containing $\sim 2\text{--}10 \times 10^6$ permeable cells in KGlu buffer with 0.5–1 mg/ml dialyzed rat brain cytosol is loaded into the incubation chamber equilibrated at 35°C , and the glassy carbon electrode is placed into the chamber and rotated. Within 1 min, the electrode response stabilizes and the cells reach equilibration temperature. Ca^{2+} is injected in a small volume with a spring-loaded Hamilton syringe to initiate NE release. An experimental example in which the pleckstrin homology (PH) domain of phospholipase C (PLC) $\delta 1$ was used to inhibit Ca^{2+} -triggered NE release is shown in Fig. 2. Control incubations are conducted without cells to provide a trace that includes injection and dilution artifacts that can be subtracted from experimental records. At the end of a series of incubations, the cellular content of NE can be obtained by lysing cells by the addition of Triton X-100 to 0.1%. The total concentration obtained can be used to determine the percentage of NE released throughout the incubation. Experiments can be calibrated routinely by injecting small amounts of NE from a stock solution (Earles *et al.*, 2001).

The kinetics of Ca^{2+} -triggered NE secretion from permeable PC12 cells can be fitted to a single exponential except for an initial small (< 2 s) lag. The time constant of the exponential phase of the release and the final extent of exocytosis is determined from an exponential fit (Grishanin *et al.*, 2003). Tau values are observed to be 20–30 s, which is consistent with the reported slow kinetics for DCV exocytosis in intact PC12 cells (Ninomiya *et al.*, 1997; Wang *et al.*, 2001).

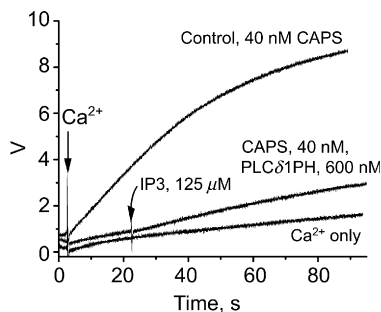


Fig. 2 A PH domain fusion protein inhibits CAPS-dependent, Ca^{2+} -triggered exocytosis detected by RDE. $\text{PtdIns}(4,5)\text{P}_2$ is known to be essential for Ca^{2+} -triggered LDCV exocytosis, as indicated by the inhibition of secretion by reagents that bind or hydrolyze $\text{PtdIns}(4,5)\text{P}_2$. A fusion protein corresponding to the $\text{PtdIns}(4,5)\text{P}_2$ -specific PH domain of phospholipase C (PLC)- $\delta 1$ strongly inhibits Ca^{2+} -triggered catecholamine release from permeable PC12 cells as detected in the RDE assay. Proteins (CAPS or PH domain) were added to permeable PC12 cells, and exocytosis was triggered by the injection of Ca^{2+} to generate $10 \mu\text{M}$ free Ca^{2+} . (Upper trace) Ca^{2+} -triggered catecholamine release in the presence of 40 nM CAPS. (Lower trace) Catecholamine release in the absence of CAPS. (Middle trace) Incubations containing 40 nM CAPS plus 600 nM PH domain in which the PH domain fully inhibited Ca^{2+} -triggered catecholamine release. $\text{Ins}(1,4,5)\text{P}_3$, to a final concentration of $125 \mu\text{M}$, was injected 20 s after the addition of Ca^{2+} . $\text{Ins}(1,4,5)\text{P}_3$, an antagonist of $\text{PtdIns}(4,5)\text{P}_2$ binding by the PH domain, reversed inhibition by the PH domain but secretion proceeded with slower kinetics. Methods: The phospholipase C- $\delta 1$ PH domain was expressed in *E. coli* as a GFP and 6xHis tag fusion and was purified by Ni^{2+} -NTA chromatography. PC12 cells were loaded with NE by preincubation, permeabilized with a ball homogenizer, and primed in incubations with MgATP and rat brain cytosol. Washed primed cells were incubated at 35°C in a water-jacketed chamber for RDE analysis.

C. Secretion Assays in Transfected Cells Using Human Growth Hormone

The permeable PC12 cell and membrane assays provide a valuable format for the study of soluble proteins that function in Ca^{2+} -dependent exocytosis (Walent *et al.*, 1992; Hay and Martin, 1993b; Hay *et al.*, 1995; Chen *et al.*, 1999). Cytoplasmic domains of membrane proteins can also be introduced readily for mechanistic studies in which dominant inhibitory effects can be assessed (e.g., for SNAREs; see Chen *et al.*, 2001). However, many of the protein components of the exocytotic machinery are intrinsic or tightly associated peripheral membrane proteins, the concentrations of which cannot be manipulated readily in the standard assays. However, it is quite feasible to use transfection techniques in PC12 cells to alter expression levels of wild-type or mutant forms of the proteins of interest. The effects of expression can subsequently be assessed in intact cell, permeable cell, or membrane secretion assays.

Transfection approaches in PC12 cells are somewhat limited by the reported low transfection efficiencies (but see later). One solution to this problem was provided by Wick *et al.* (1993) by coexpressing human growth hormone (hGH), which is targeted to DCVs and is used as a marker for regulated secretion in successfully transfected cells. In this case, hGH secretion is elicited in intact cells by K^+ depolar-

ization and Ca^{2+} influx or in permeable cells directly by Ca^{2+} addition (Wick *et al.*, 1993). One disadvantage of the hGH assay is the imprecise targeting of hGH to the regulated secretory pathway and potentially high levels of constitutive release; however, this can be lowered readily by acute treatment with brefeldin A (see later).

While transfection efficiencies of PC12 cells with $\text{Ca}_3(\text{PO}_4)_2$ or lipofection methods do not routinely exceed 10%, we have modified a high efficiency electroporation protocol for PC12 cells that overcomes this limitation (Grishanin *et al.*, 2002). Alternatively, the use of viral vectors (e.g., Semliki Forest virus, see Ashery *et al.*, 1999) and infection improves the efficiency of protein expression markedly; however, cell lysis during viral infection places limitations on these approaches. We provide protocols for the efficient electroporative transfection of PC12 cells with enhanced sensitivity hGH expression. These methods have been employed (Zhang *et al.*, 2002) in cotransfection studies with three plasmids for biochemical and functional studies of the effects of mutant SNAP-25 proteins (Fig. 3).

1. Transfection of PC12 Cells

We have adapted a protocol described by Van den Hoff *et al.* (1992) to PC12 cells that provides transfection efficiencies exceeding 60%, as estimated by the percentage of fluorescent cells expressing green fluorescent protein (GFP). DNA purified using the Qiagen DNA kit has sufficient purity for successful transfections. PC12 cells are cultured to ~80% of maximal density and removed from dishes in Hanks/EDTA buffer. Cells are pelleted at $500 \times g$, washed once with cytomix buffer (25 mM HEPES, 120 mM KCl, 10 mM KH_2PO_4 , 0.15 mM CaCl_2 , 5 mM MgCl_2 , 2 mM EGTA, pH 7.6), and resuspended in the cytomix at $\sim 6 \times 10^7$ cell/ml. Five hundred micro liters of cell suspension is transferred to a 4-mm electroporation cell, and ATP and reduced glutathione are added to 2 and 5 mM, respectively, from a $100 \times$ stock solution with pH adjusted with KOH to 7.6. Plasmid DNA (up to 100 μg plasmid DNA per transfection) resuspended in the cytomix or 20 mM Tris-HCl, pH 8.0, is added to the electroporation cell and mixed. Electroporation is conducted at room temperature at 1000 $\mu\text{F}/330$ V for 2 min in an exponential decay electroporator (e.g., Invitrogen Electroporator II) that exhibited a time constant ~12 ms. Cells are collected from the cuvette and plated in 10-cm dishes in growth medium supplemented additionally with 10% fetal bovine serum. On the next day, the medium is replaced with fresh unsupplemented growth medium, and the cells are grown usually for 48–72 h, although the expression of GFP-tagged proteins is detected readily within 4 h following electroporation.

2. Assays for Ca^{2+} -Dependent Human Growth Hormone Secretion

PC12 cells are transfected by electroporation with 10 μg of plasmid encoding hGH and 20 μg or more of other plasmids. While a number of studies employing hGH as a secreted marker utilized expression plasmids containing the metallothioneine promoter, increased levels of hGH expression and increased sensitivity of

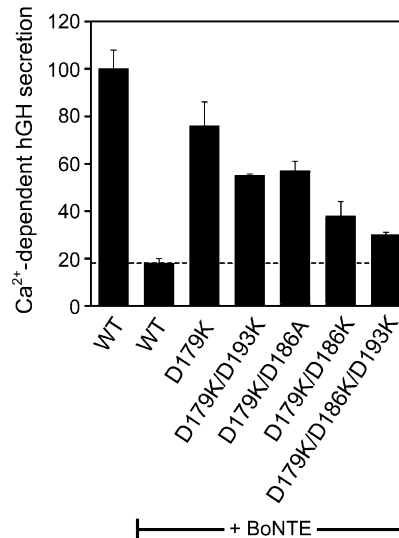


Fig. 3 C-terminal SNAP-25 mutants confer a loss of function in regulated exocytosis by decreasing Ca²⁺-dependent fusion rates. Single and double SNAP-25 mutants exhibit a progressive loss of function in Ca²⁺-dependent exocytosis. PC12 cells were cotransfected with a plasmid encoding botulinum neurotoxin E (BoNTE) light chain where indicated. Ca²⁺-dependent hGH secretion was determined as hGH secretion in 20 min at 37°C stimulated in a high K⁺ buffer minus hGH secretion in a low K⁺ buffer. A high K⁺ buffer increased the rate of hGH secretion 5- to 10-fold. Ca²⁺-dependent secretion was inhibited by more than 80% in cells expressing BoNTE with wild-type SNAP-25 (dotted line). Expression of the indicated BoNTE-resistant SNAP-25 proteins rescued Ca²⁺-dependent secretion. The extent of rescue corresponded to activity in synaptotagmin I binding. Values represent the mean of triplicate determinations with SD indicated by error bars. Methods: The hGH cotransfection assay was employed to test the function of BoNTE-resistant SNAP-25 mutants in regulated exocytosis. PC12 cells were transfected with 20 μg of DNA plasmid encoding SNAP-25 (wild-type or mutant), 40 μg plasmid encoding BoNTE light chain, and 10 μg plasmid encoding hGH. After 48 h of incubation in growth medium, cells were utilized in intact cell secretion assays by plating them into six-well cluster trays. Prior to secretion incubation, cells were incubated in medium containing 5 μg/ml brefeldin A for 30 min to eliminate constitutive hGH secretion. Depolarization with high K⁺-containing buffers was used to evoke Ca²⁺-dependent secretion. Coexpression of the BoNTE light chain strongly (>80%) inhibited Ca²⁺-dependent hGH release in cells expressing wild-type SNAP-25. In contrast, expression of the BoNTE-resistant D179K mutant SNAP-25 resulted in a rescue of Ca²⁺-dependent hGH secretion to ~70% of that observed without BoNTE. The inability to fully rescue Ca²⁺-dependent secretion is compatible with the partial loss of function for the D179K mutant in synaptotagmin binding. Expression of double mutants with replacement at Asp193 (D179K/D193K) or at Asp186 with Ala (D179K/D186A) resulted in less (40%) rescue of Ca²⁺-dependent secretion. Expression of the double mutant with a Lys replacement at Asp186 (D179K/D186K) resulted in a stronger loss of function with only ~25% rescue. Finally, a triple mutant containing both second site mutations (D179K/D186K/D193K) exhibited little (12%) rescue of Ca²⁺-dependent secretion. Overall, the progression in loss of function exhibited by SNAP-25 C-terminal mutants in Ca²⁺-dependent exocytosis was similar to the loss of Ca²⁺-dependent synaptotagmin binding to SNAP-25 *in vitro* (not shown, see Zhang *et al.*, 2002). Reprinted from Neuron.

secretion assays are obtained with plasmids employing the more powerful CMV promoter. The construct pCMVGH for the expression of hGH under the CMV promoter (Budker *et al.*, 1996) was generously provided by H. Herweijer. After 48 h of incubation in culture medium, cells are utilized in intact or permeable cell secretion assays. For the intact cell assay, transfected cells plated into six-well cluster trays are incubated in medium containing 5 $\mu\text{g/ml}$ brefeldin A for 30 min to eliminate constitutive hGH secretion. For the release assay, cells are incubated in basal medium [15 mM HEPES (pH 7.4), 145 mM NaCl, 5.6 mM KCl, 2.2 mM CaCl_2 , 0.5 mM MgCl_2 , 5.6 mM MgCl_2 , 5.6 mM glucose, 0.5 mM ascorbic acid, 0.1% bovine serum albumin] or depolarization medium (same as basal medium adjusted to 95 mM NaCl and 56 mM KCl) plus brefeldin A for various times at 37°C. Medium is removed and cells are solubilized in 0.1% sodium dodecyl sulfate containing a complete protease inhibitor cocktail (Roche). hGH in medium and solubilized cells is determined using the hGH radioisotopic assay (Nichols Institute Diagnostics). *In vitro* secretion assays with permeable cells or membrane fractions are conducted as described earlier. The percentage hGH released is calculated from the hGH in medium or supernatant divided by the total hGH obtained from solubilized cells plus medium or supernatant.

3. Isolation of Stable Transfectants

Transient transfection of PC12 cells has proven to be a very effective tool for cell biological studies. However, because the transfection efficiency is less than 100% and there is considerable variance in protein expression levels among transfected cells, this approach is largely limited to single cell assays or to biochemical assays in which a coexpressed protein (e.g., hGH) is used. Studies of catecholamine secretion in single transfected cells, while labor-intensive due to variability, have provided important results. In one study (Wang *et al.*, 2001), GFP was coexpressed from an internal ribosome entry site (IRES)-containing plasmid to locate fluorescent transfected cells for carbon fiber amperometric determinations of evoked catecholamine secretion and fusion pore kinetics. In these studies, cells expressing a midrange level of GFP were chosen for recordings in an effort to examine cells that coexpressed midrange levels of the protein under investigation, synaptotagmin (Wang *et al.*, 2001).

Especially for biochemical studies, it would be desirable to have homogeneous cell populations expressing different levels of a protein of interest. This can be approximated by isolating stably transfected cell lines from a heterogeneous population of transiently transfected cells. Expression vectors can integrate into chromosomal DNA and be stably inherited. Most available mammalian transfection vectors harbor drug resistance genes such as the neo gene encoding aminoglycoside 3'-phosphotransferase or the Sh Ble gene, which confer resistance to G418 or zeocine, respectively. Selection markers simplify the isolation of stably transfected clones by drug resistance, although the level of resistance and levels of expression of the gene of interest do not correlate readily.

An increased yield of stably transfected clones is obtained by linearizing DNA plasmids with restriction enzymes that cleave at noncoding sites. Linearized DNA with double strand breaks is recognized effectively by DNA repair mechanisms and integrated into chromosomal DNA. This also prevents the possible disruption of coding sequences during the process of integrating circular DNA. Integration at random chromosomal sites that differ in transcriptional activity and may affect expression of other genes, and the intrinsic clonal variation in PC12 cells (Clementi *et al.*, 1992) all necessitate that multiple independent stably transfected clones be isolated and characterized. Such clones will vary in the levels of expression of the transgene and it may be possible to correlate expression levels with the cellular phenotypes of interest (see Kim *et al.*, 2001).

To obtain stably transfected PC12 cell lines, we use the electroporation technique described previously. Plasmids are purified with the Qiagen DNA kit and are linearized by incubation with an appropriate restriction nuclease, and the sample is heated for 10 min at 65°C to inactivate the enzyme. Transfection by electroporation produces a very large number of clones surviving the selection with antibiotics.

Electroporated PC12 cells are plated on 10-cm dishes at 10×, 100×, and 1000× dilutions. On the next day, the growth medium is changed to fresh medium containing 500 µg/ml G418 for plasmids containing the neo gene. Medium is changed every 5 days, and the antibiotic concentration is reduced to 200 µg/ml when cell colonies are evident to the unaided eye. Colonies can be picked easily when they reach 1–2 mm in diameter. Dishes with well-separated colonies are marked on the bottom using a permanent marker. For clones expressing GFP fusion proteins, an inverted fluorescence microscope under low power is used to mark fluorescent colonies. To pick colonies, the dish is aspirated, rinsed twice, and refilled with culture medium. Colonies are picked with a yellow tip on a pipetman set at 30 µl and transferred to wells of a 24-well plate containing 0.5 ml culture medium and 200 µg/ml G418. The dish is washed and replaced with medium after picking 10 colonies to prevent contamination by detached cells. After colonies attach, wells on the multiwell plates are rinsed with Hanks'/EDTA, and the colonies are incubated in 100 µl Hanks'/EDTA for 5 min at 37°C followed by repeated pipetting to disperse the cells. One milliliter of culture medium with 200 µg/ml G418 is added, and the cells are grown to maximal density in the wells. At this point, cells are subcultured into 200 µl Hanks'/EDTA, and 180 µl is processed for PAGE and Western blotting to detect expression of the desired protein. The remaining 20 µl of cell suspension is plated on 10-cm dishes for propagating cell stocks in culture medium plus antibiotic. Dishes with clones with satisfactory levels of expression are left for the propagation of second-generation clones, which are again checked for levels of expression. This protocol has been used successfully to obtain clones of PC12 cells stably expressing HA-tagged and GFP-tagged CAPS, GFP-labeled atrial natriuretic factor (which is sorted to DCVs), GFP-labeled synaptotagmins I and IV, and cell lines stably expressing synaptotagmin I antisense RNA. These cell lines continue to stably

express the indicated constructs for extended time periods even in the absence of continuous antibiotic expression.

IV. Immunocytochemical Detection of Proteins in Intact and Permeable PC12 Cells

The secretion of DCV-stored constituents triggered by Ca^{2+} elevations in PC12 cells is an overall slow ($\tau_{1/2} \sim 10\text{--}30\text{ s}$) form of exocytosis compared to the much more rapid process of synaptic vesicle exocytosis in neuronal cells. While the basis for this relative slowness is incompletely understood, kinetic studies of the type shown in Fig. 2 indicate that PC12 cells may lack a substantial pool of DCVs that are rapidly releasable and that fusion rates may be rate limited at the step of priming vesicles (Grishanin *et al.*, 2003; also see Ninomiya *et al.*, 1997; Grishanin *et al.*, 2002). It has been shown that prior to stimulation with Ca^{2+} , PC12 cells do not contain detectable amounts of preassembled SNARE complexes (Chen *et al.*, 1999; Lang *et al.*, 2002). It has been suggested that SNARE complexes form in loose or tight complexes prior to Ca^{2+} -triggered membrane fusion and that preassembled SNARE complexes may be essential for fast exocytosis (Xu *et al.*, 1999). Conceivably, a slower step involving a Ca^{2+} -dependent assembly of SNARE complexes may rate limit the overall process of Ca^{2+} -dependent exocytosis in PC12 cells. The relative slowness of the fusion pathway in PC12 cells may prove to be a major advantage in enabling detection of a complex formation or of the membrane translocation of key proteins. It may be possible to use fluorescent probes (fusion proteins, antibodies) that can be applied rapidly to a preparation in which exocytosis has been triggered by Ca^{2+} . This section provides a protocol for antibody labeling fusion-competent permeable PC12 cells as well as a description of methods for detecting the membrane association of cytosolic proteins in cells permeabilized prior to fixation.

A. Immunostaining of Mechanically Permeabilized PC12 Cells

To conduct immunocytochemical studies on permeable PC12 cells, we adopted the method of Weidemann *et al.* (1993) to tether permeable cells to glass coverslips. This represents an alternative to the flat carrier supported PC12 cell membrane patches prepared by sonication (Lang *et al.*, 2002; Avery *et al.*, 2000). Both approaches allow efficient immunolabeling of SNARE and other proteins that function in exocytosis. Permeable PC12 cells can be incubated in secretion assays under a variety of conditions prior to quenching exocytosis by chilling prior to tethering by chemical cross-linking. Coverslips cleaned in 50% HNO_3 , rinsed extensively in distilled H_2O and airdried, are coated with 1 mg/ml poly-L-lysine (Sigma) for 30 min. Following four washes with 0.1 M KCl, the coverslips are activated by incubation with 1% glutaraldehyde in 0.1 M KCl for 10 min on a shaker at room temperature. Treated coverslips can be stored in 0.1 M KCl before

use at which point the KCl solution is aspirated and excess fluid is blotted with filter paper. A suspension of permeable PC12 cells is washed three times in PBS with 1 mM EDTA and is resuspended at $\sim 2 \times 10^7$ cells/ml (Weidman *et al.*, 1993), and 15 μ l is applied to the coverslip held on ice. Cells are allowed to attach for 30 min, and the coverslips are washed into buffers desired for antibody binding. Attached cells can be fixed prior to or following incubation with primary and secondary antibodies or left unfixed before mounting coverslips on microscopic slides.

B. Immunocytochemical Detection of Cytosolic Proteins Interacting Transiently with Membranes in PC12 Cells

Many cytosolic proteins function through transient interactions with membranes, organelles, or cytoskeletal elements. Mild permeabilization of the plasma membrane with digitonin or saponin prior to fixation can be used to remove the soluble cytosolic fraction of protein and reveal intracellular structures to which proteins have localized. Because permeabilization with digitonin does not impair

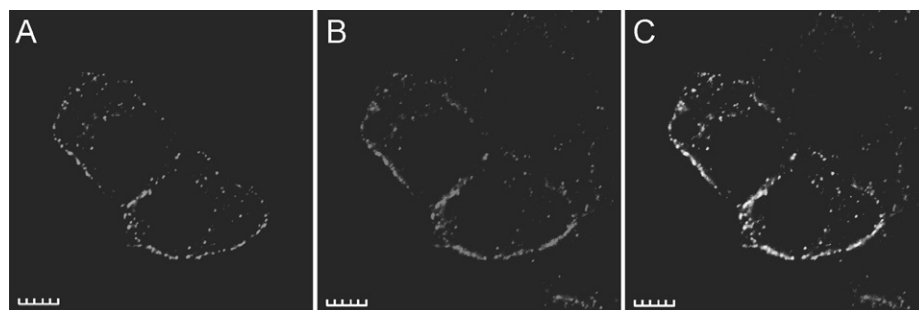


Fig. 4 CAPS localizes to dense core vesicles in transfected PC12 cells. CAPS proteins were expressed in PC12 cells by transfection and localized by immunocytochemistry following detergent permeabilization. (A) Fluorescein channel showing CAPS localization. (B) Rhodamine channel showing synaptotagmin I localization. (C) Merge of both channels. The wild-type CAPS protein was localized to DCVs indicated by colocalization with synaptotagmin I. Scale bar represents 10 μ m. Methods: Staining of intact cells first fixed and subsequently extracted with Triton X-100 with the CAPS antibody revealed that CAPS was localized diffusely throughout the cytoplasm as a soluble protein. To determine the membrane localization of CAPS, PC12 cells were transfected by electroporation with plasmid pCMVCAPS(HA)3 encoding full-length CAPS. Transfected cells were plated on tissue culture dishes and incubated at 37°C. Two hours later, cells were removed from the dish using Hanks'/EDTA buffer, resuspended in PC12 growth medium, and grown on poly-L-lysine-treated coverslips for 24 h. To visualize membrane structures to which CAPS bound, cells were permeabilized with 0.025% digitonin, fixed in 4% formaldehyde, and further extracted with 0.3% Triton X-100. Cells were incubated with an affinity-purified CAPS polyclonal antibody generated to the full-length protein. The synaptotagmin I monoclonal antibody (Synaptic Systems GMBH) was used to localize LDCVs. Secondary reagents used were fluorescein isothiocyanate-goat antirabbit and Texas red-goat antimouse antibodies (Sigma Chemical Corp.) at a dilution of 1:500. Fluorescence was imaged with a Bio-Rad MRC 600 confocal imaging system. A fraction of CAPS was retained on LDCVs upon permeabilization with digitonin and removal of the bulk cytosolic protein.

Ca²⁺-triggered exocytosis, this technique can be used to determine whether soluble proteins associate with membranes or whether membrane proteins colocalize at specific sites of exocytosis.

PC12 cells are grown on coverslips coated with poly-L-lysine. Culture medium is removed, the monolayer is washed with buffer, and cells are permeabilized by incubation with 0.05% saponin or 0.025% digitonin dissolved in the cytomix for 20 min on ice. Permeabilized cells are rinsed once with ice-cold cytomix and fixed in 4% paraformaldehyde dissolved in PBS at room temperature for 20 min. Cells are further fixed and permeabilized in cold (−20°C) methanol/acetone (2:1, v/v). Alternatively, fixed cells can be permeabilized by the extraction of lipids with 0.3% Triton X-100 in PBS for 10 min. Coverslips with fixed and permeabilized cells are washed four times with PBS, and standard immunocytochemical methods are used for the detection of proteins (Fig. 4).

References

- Ahnert-Hilger, G., Bader, M. F., Bhakdi, S., and Gratzl, M. (1989). *J. Neurochem.* **52**, 1751–1758.
- Ahnert-Hilger, G., and Gratzl, M. J. (1987). *Neurochemistry* **49**, 764–770.
- Anderson, D. J. (1993). *Annu. Rev. Neurosci.* **16**, 129–158.
- Andrea, S., Dittie, A. S., Thomas, L., Thomas, G., and Tooze, S. A. (1997). *EMBO J.* **16**, 4859–4870.
- Ann, K., Kowalchuk, J. A., Loyet, K. M., and Martin, T. F. (1997). *J. Biol. Chem.* **272**, 19637–19640.
- Ashery, U., Betz, A., Xu, T., Brose, N., and Rettig, J. (1999). *Eur. J. Cell Biol.* **78**, 525–532.
- Ashery, U., Varoqueaux, F., Voets, T., Betz, A., Thakur, P., Koch, H., Neher, E., Brose, N., and Rettig, J. (2000). *EMBO J.* **19**, 3586–3596.
- Avery, J., Ellis, D. J., Lang, T., Holroyd, P., Riedel, D., Henderson, R. M., Edwardson, J. M., and Jahn, R. (2000). *J. Cell Biol.* **148**, 317–324.
- Banerjee, A., Barry, V. A., DasGupta, B. R., and Martin, T. F. (1996a). *J. Biol. Chem.* **271**, 20223–20226.
- Banerjee, A., Kowalchuk, J. A., DasGupta, B. R., and Martin, T. F. (1996b). *J. Biol. Chem.* **271**, 20227–20230.
- Bauerfeind, R., Regnier-Vigouroux, A., Flatmark, T., and Huttner, W. B. (1993). *Neuron* **11**, 105–121.
- Blackmer, T., Larsen, E. C., Takahashi, M., Martin, T. F., Alford, S., and Hamm, H. E. (2001). *Science* **292**, 293–297.
- Budker, V., Zhang, G., Knechtle, S., and Wolff, J. A. (1996). *Gene Ther.* **3**, 593–598.
- Chen, Y. A., Duvvuri, V., Schulman, H., and Scheller, R. H. (1999a). *J. Biol. Chem.* **274**, 26469–26476.
- Chen, Y. A., Scales, S. J., Patel, S. M., Doung, Y.-C., and Scheller, R. H. (1999b). *Cell* **97**, 165–174.
- Chen, Y. A., Scales, S. J., and Scheller, R. H. (2001). *Neuron* **30**, 161–170.
- Chow, R. H., von Ruden, L., and Neher, E. (1992). *Nature* **356**, 60–63.
- Clementi, E., Racchetti, G., Zacchetti, D., Panzeri, M. C., and Meldolesi, J. (1992). *Eur. J. Neurosci.* **4**, 944–953.
- de Wit, H., Lichtenstein, Y., Geuze, H., Kelly, R. B., van der Sluijs, P., and Klumperman, J. (1999). *Mol. Biol. Cell* **10**, 4163–4176.
- Desai, R. D., Vyas, B., Earles, C. A., Littleton, J. T., Kowalchuk, J. A., Martin, T. F. J., and Chapman, E. R. (2000). *J. Cell Biol.* **150**, 1125–1135.
- Desnos, C., Clift-O'Grady, L., and Kelly, R. B. (1995). *J. Cell Biol.* **130**, 1041–1050.
- Earles, C. A., Bai, J., Wang, P., and Chapman, E. R. (2001). *J. Cell Biol.* **154**, 1117–1123.
- Earles, C., and Schenk, J. O. (1998). *Anal. Biochem.* **264**, 191–198.
- Fukuda, M., Kowalchuk, J. A., Zhang, X., Martin, T. F. J., and Mikoshiba, K. (2002). *J. Biol. Chem.* **277**, 4601–4604.

- Gerona, R. R., Larsen, E. C., Kowalchuk, J. A., and Martin, T. F. (2000). *J. Biol. Chem.* **275**, 6328–6336.
- Greene, L. A., and Rein, G. (1977). *Nature* **268**, 349–351.
- Greene, L. A., and Tischler, A. S. (1976). *Proc. Natl. Acad. Sci. USA* **73**, 2424–2528.
- Grishanin, R. N., Klenchin, V. A., Earles, C. A., Ann, K., Porter, B., Chapman, E. R., and Martin, T. F. J. (2003). Submitted for publication.
- Grishanin, R. N., Klenchin, V. A., Loyet, K. M., Kowalchuk, J. A., Ann, K., and Martin, T. F. J. (2002). *J. Biol. Chem.* **277**, 22025–22034.
- Hay, J. C., Fiset, P. L., Jenkins, G. H., Fukami, K., Takenawa, T., Anderson, R. A., and Martin, T. F. (1995). *Nature* **374**, 173–177.
- Hay, J. C., and Martin, T. F. J. (1993a). *J. Cell. Biol.* **119**, 139–151.
- Hay, J. C., and Martin, T. F. J. (1993b). *Nature* **336**, 572–575.
- Huang, E. J., and Reichardt, L. F. (2001). *Annu. Rev. Neurosci.* **24**, 677–736.
- Kim, T., Tao-Cheng, J. H., Eiden, L. E., and Loh, Y. P. (2001). *Cell* **106**, 499–509.
- Klenchin, V. A., Kowalchuk, J. A., and Martin, T. F. (1998). *Methods* **16**, 204–208.
- Lang, T., Margittai, M., Hölzler, H., and Jahn, R. (2002). *J. Cell. Biol.* **158**, 751–760.
- Lichtenstein, Y., Desnos, C., Faundez, V., Kelly, R. B., and Clift-O'Grady, L. (1998). *Proc. Natl. Acad. Sci. USA* **95**, 11223–11228.
- Martin, T. F., and Kowalchuk, J. A. (1997). *J. Biol. Chem.* **272**, 14447–14453.
- Martin, T. F. J. (1989). *Methods Enzymol.* **168**, 225–233.
- Matsuoka, I., Mizuno, N., Kurihara, K., Matsuoka, I., Mizuno, N., and Kurihara, K. (1989). *Brain Res.* **502**, 53–60.
- Ng, Y. K., Lu, X., Watkins, S. C., Ellis-Davies, G. C., and Levitan, E. S. (2002). *J. Neurosci.* **22**, 3890–3897.
- Ninomiya, Y., Kishimoto, T., Yamazawa, T., Ikeda, H., Miyashita, Y., and Kasai, H. (1997). *EMBO J.* **16**, 929–934.
- Nishiki, T., Shoji-Kasai, Y., Sekiguchi, M., Iwasaki, S., Kumakura, K., and Takahashi, M. (1997). *Biochem. Biophys. Res. Commun.* **239**, 57–62.
- Rebois, R. V., Reynolds, E. E., Toll, L., and Howard, B. D. (1980). *Biochemistry* **19**, 1240–1248.
- Schaefer, T., Karli, U. O., Gratwohl, E. K., Schweizer, F. E., and Burger, M. M. (1987). *J. Neurochem.* **49**, 1697–1707.
- Schubert, D., and Klier, F. G. (1977). *Proc. Natl. Acad. Sci. USA* **74**, 5184–5188.
- Shin, O. H., Rizo, J., and Sudhof, T. C. (2002). *Nature Neurosci.* **5**, 649–656.
- Sugita, S., Han, W., Butz, S., Liu, X., Fernandez-Chacon, R., Lao, Y., and Sudhof, T. C. (2001). *Neuron* **30**, 459–473.
- Sugita, S., Shin, O. H., Han, W., Lao, Y., and Sudhof, T. C. (2002). *EMBO J.* **21**, 270–280.
- Tooze, S. A., and Huttner, W. B. (1990). *Cell* **60**, 837–847.
- Urbe, S., Page, L. J., and Tooze, S. A. (1998). *J. Cell. Biol.* **143**, 1831–1844.
- Van den Hoff, M. J., Moorman, A. F., and Lamers, W. H. (1992). *Nucleic Acids Res.* **20**, 2902.
- Vaudry, D., Stork, P. J., Lazarovici, P., and Eiden, L. E. (2002). *Science* **296**, 1648–1649.
- Voets, T., Moser, T., Lund, P. E., Chow, R. H., Geppert, M., Sudhof, T. C., and Neher, E. (2002). *Proc. Natl. Acad. Sci. USA* **98**, 11680–11685.
- Walent, J. H., Porter, B. W., and Martin, T. F. (1992). *Cell* **70**, 765–775.
- Wang, C. T., Grishanin, R., Earles, C. A., Chang, P. Y., Martin, T. F., Chapman, E. R., and Jackson, M. B. (2001). *Science* **294**, 1111–1115.
- Weidman, P., Roth, R., and Heuser, J. (1993). *Cell* **75**, 123–133.
- Weihe, E., Tao-Cheng, J., Schaefer, M. K., and Erickson, J. D. (1996). *Proc. Natl. Acad. Sci. USA* **93**, 3547–3552.
- Wick, P. F., Senter, R. Z., Parsels, L. A., Uhler, M. D., and Holz, R. W. (1993). *J. Biol. Chem.* **268**, 10983–10989.
- Xu, T., Rammner, B., Margittai, M., Artalejo, A. R., Neher, E., and Jahn, R. (1999). *Cell* **99**, 713–722.
- Zhang, X., Kim-Miller, M. J., Fukuda, M., Kowalchuk, J. A., and Martin, T. F. J. (2002). *Neuron* **34**, 599–611.

CHAPTER 13

B35 Neuroblastoma Cells: An Easily Transfected, Cultured Cell Model of Central Nervous System Neurons

Carol A. Otey, Malika Boukhelifa,^{*} and Patricia Maness[†]

^{*}Departments of Cell and Molecular Physiology
University of North Carolina School of Medicine
Chapel Hill, North Carolina 27599

[†]Biochemistry and Biophysics
University of North Carolina School of Medicine
Chapel Hill, North Carolina 27599

-
- I. Introduction
 - II. Applications Utilizing B35 and B50 Cells
 - A. B35 and B50 Cells in Studies of Differentiation Toxicology, and Cell Death
 - B. B35 Cells as Models for Axon Growth and Cell Migration
 - C. Intracellular Signaling Mechanisms in B35 Cells
 - D. Endocytosis of Cell Adhesion Molecules in B35 Cells
 - III. Protocols
 - A. Using Antisense Constructs in B35 Cells
 - B. Exploring Protein Function with Stable Transfection and Motility Assays
 - C. Culturing and Transfection (Transient and Stable) of B35 Neuroblastoma Cells
 - D. Transwell Migration Assay to Monitor Motility in B35 Neuroblastoma Cells
 - E. Detecting Migrated/Nonmigrated and Expressing/Nonexpressing Cells by Immunocytochemistry
 - References

A panel of neuronal cell lines was derived from tumors of the neonatal rat central nervous system (CNS) in 1974, and two of these lines are in wide use today. Both the B35 and B50 lines offer a number of advantages to researchers who study CNS neurons in culture: they are simple to grow, to differentiate, and to transfect. B50 cells have been used extensively in the study of neuronal cell death, toxicology, and

differentiation, whereas B35 cells have proven useful in the molecular analysis of endocytosis and of signaling pathways, in particular those that guide axonal outgrowth and cell motility. This chapter provides protocols for growing and transfecting B35 cells, selecting stable transfectants, exploring protein function using an antisense approach, and assaying cell motility in a Transwell chamber. All of these protocols have been written for researchers who have some skill in basic cell culture techniques, but previous experience with cultured neurons is not required.

I. Introduction

Researchers who study cultured neurons of the central nervous system (CNS) face many challenges, as CNS neurons are resistant to transfection and finicky to culture. One option is to utilize neuroblastoma cell lines derived from CNS tumors. In 1974, Schubert and co-workers cloned multiple neuronal and glial cell lines using neoplasms induced in neonatal BDIX rats with nitrosoethylurea (Schubert *et al.*, 1974; Stallcup and Cohn, 1976a,b). Of the 14 cell lines characterized in their initial study, 2 are in wide use today: B35 and B50. B35 cells have a near-normal karyotype and display neuronal properties such as membrane excitability and expression of enzymes for neurotransmitter metabolism, but they do not appear to be highly differentiated. They express acetylcholinesterase, glutamic acid decarboxylase (GAD), and γ -aminobutyric acid (GABA), but not tyrosine hydroxylase, acetylcholine receptors, or glial markers such as S100 (Schubert *et al.*, 1974). B35 cells also express normal levels of neuron-specific enolase (Vinores *et al.*, 1984), and they upregulate α -amanitin-sensitive RNA synthesis upon treatment with methylmercury (Frenkel and Ducote, 1987). In culture, B35 cells grow loosely attached to culture dishes, probably due to only a low level of collagen production, and have phase-bright round cell bodies and short processes (Fig. 1A).

B35 cells can be induced to differentiate reversibly, extending long neurites when grown in low serum or treated with dibutyryl cAMP, so that they are particularly useful for studies of CNS neuronal differentiation and neurite outgrowth. Fig. 1 illustrates neurite extension in B35 cells during the period of 0–5 days following the withdrawal of serum and the addition of dibutyryl cAMP. Sodium butyrate also induces neurite extension in B35 cell cultures, concomitant with the slowing of cell division and induction of expression of rat brain types I, II, and III sodium channels (Baines *et al.*, 1992). The cells can be transfected readily with plasmids for either transient or stable expression (see protocols later) and have large, well-developed growth cones (see Fig. 2).

B50 cells (and the less widely used lines B65, B103, and B104) were also derived from the original cloning and possess neuron-like features. Each is able to produce action potentials and to extend neurites in culture; however, relative to B35, these lines express higher levels of neurotransmitters and acetylcholine receptors and exhibit a more flattened morphology, suggesting that they may represent a more differentiated state (Schubert *et al.*, 1974).

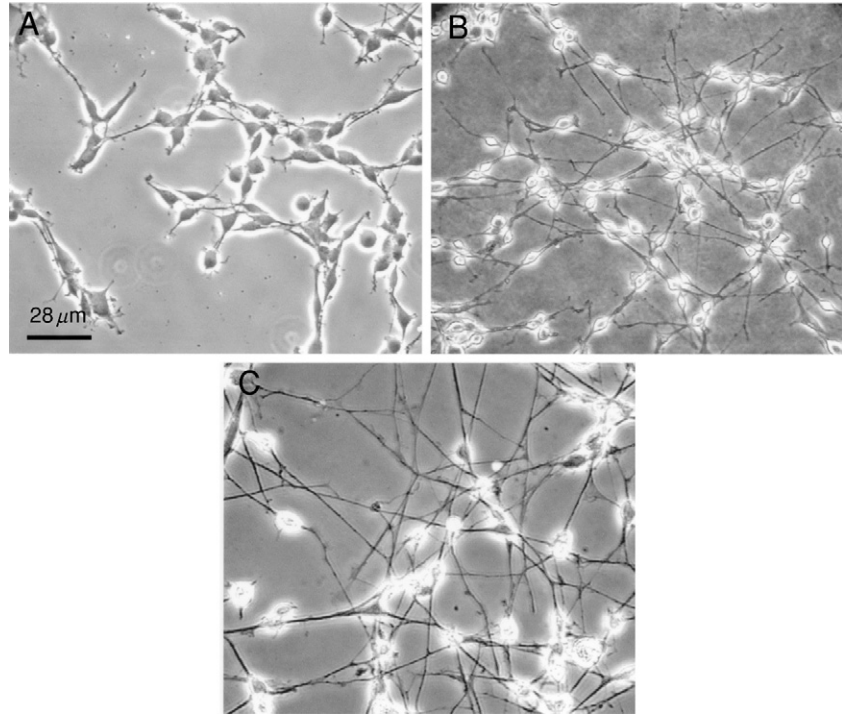


Fig. 1 B35 cells in culture, either untreated (A) or treated with 1 mM dibutyryl cAMP for 3 days (B) or 5 days (C), were photographed to illustrate neuronal differentiation.

II. Applications Utilizing B35 and B50 Cells

A. B35 and B50 Cells in Studies of Differentiation, Toxicology, and Cell Death

The B35 and B50 lines offer substantial advantages over primary CNS neurons for use in cell biology and biochemistry experiments, including ease of culture, efficiency of transfection, and ability to establish stable cell lines. Soon after their development, B50 cells came into wide use in the study of factors that control the morphological differentiation of CNS neurons. B50 cells can be grown at low density so that neurite outgrowth can be imaged easily in nonoverlapping cells and the rate of neurite extension can be measured unambiguously. Early studies with B50 cells explored the role of calcium influx in stimulating morphological differentiation and showed that inositol uptake decreased during the phase of active neurite outgrowth (Reboulleau 1986, 1990; Wu and Ledeen, 1991). Ease of culture also made it feasible to grow large numbers of B50 cells, sufficient for use in biochemical methods such as column chromatography. This facilitated the study of proteins that function in neurite extension and allowed the identification of

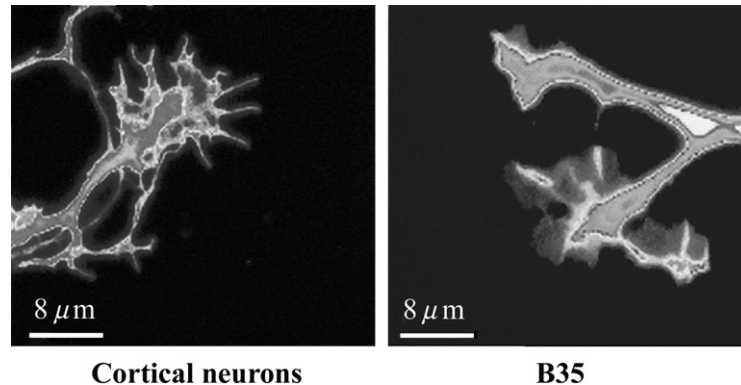


Fig. 2 Comparison of growth cones from a primary cortical neuron obtained from an embryonic rat (left) and from B35 cells allowed to differentiate for 3 days (right). Cells were imaged using the vital dye calcein AM. (See Color Insert.)

β 1-type integrins as the laminin receptors that mediate neuronal attachment and outgrowth (Ignatius and Reichardt, 1988).

B50 cells were also used in many toxicology experiments through the 1980s and 1990s (Frenkel *et al.*, 1988; Lai *et al.*, 1993; Miyazaki *et al.*, 1999). One interesting study focused on the detrimental effects of lead on the developing nervous system (Audesirk *et al.*, 1991). Because lead impacts on Ca^{+2} -dependent processes and neuronal differentiation is Ca^{+2} dependent, the authors explored the effects of inorganic lead on survival and differentiation of three different types of cultured cells: rat primary hippocampal neurons, N1E-115 mouse neuroblastoma cells (derived from peripheral neurons), and B50 cells. Results showed that lead altered neurite initiation, axonal length and branching, and dendrite number in hippocampal neurons and N1E-115 cells, but B50 cells were the least affected of the three cell types. This could be interpreted as an indication that B50 cells sequester or expel lead more efficiently than the other two cell types; however, it is also consistent with the idea that B50 cells are more differentiated than either embryonic primary neurons or other neuron-like cell lines, and thus less susceptible to the effects of lead.

Behl and co-workers (1993) used cultured cells to explore the idea that cell death in Alzheimer's disease and stroke may be mediated in part by amyloid β protein and glutamate, respectively. They tested the susceptibility of three neuron-like cell lines (B50, PC-12, and human neuroblastoma IMR-5) and obtained similar results in all three: Bcl-2 failed to protect the cells from killing by amyloid β protein but did protect all three cell lines from death induced by glutamate. More recently, specific caspase activities have been studied in B50 cells undergoing apoptosis. Capano and co-workers (2002) established that glutamate and the nitric oxide donor, nitroprusside, induce cell death in B50 cells synergistically via a caspase

cascade that was inhibited by cyclosporin A. Using an antisense approach, the authors showed that depletion of the cyclosporin A-binding protein CyP-A also inhibits activation of the apoptotic pathway by glutamate and nitroprusside, implicating CyP-A as a key player in regulating death and survival in neuronal cells.

B. B35 Cells as Models for Axon Growth and Cell Migration

The rat B35 neuroblastoma cell line has been particularly useful for studies of neural cell adhesion molecule (CAM) function. Neural CAMs of the immunoglobulin (Ig) superfamily are cell recognition molecules that mediate neuronal cell adhesion, migration, axon growth, and fasciculation important for neurodevelopment and plasticity in the adult (Schmid and Maness, 2001). B35 cells have been used to study the function of neural CAM (NCAM) and members of the L1-CAM family [L1 and CHL1 (Close Homolog of L1)]. Studies of NCAM have been complicated by the fact that a single NCAM gene undergoes complex alternative splicing, resulting in three principal splice forms (180, 140, and 120 kDa), each of which may include an extracellular sequence encoded by the VASE exon in the fourth Ig domain, which downregulates neurite growth (Doherty *et al.*, 1992). B35 cells express low levels of NCAM (2.5×10^5 molecules/cell) of which >95% lack the VASE exon (Akeson *et al.*, 1988). B35 cells also express low levels of CHL1 and no detectable L1. Parental B35 cells express mostly 140 kDa NCAM, with only low levels of 180 kDa NCAM. An NCAM-nonexpressing variant of B35 (clone 3) was derived by selection using complement-mediated cell lysis with NCAM antibodies (Liu *et al.*, 1993). These cells were used to derive stable cell lines expressing rat NCAM140 or NCAM180 isoforms, with and without VASE (Liu *et al.*, 1993). NCAM140 minus VASE expressed in B35 cells is more efficient at promoting neurite outgrowth on NCAM substrates than NCAM140 with VASE expressed in B35 cells (Liu *et al.*, 1993). Conversely, axon growth by retinal cells, which express NCAM, is greater on B35 cells expressing NCAM140 minus VASE as a substrate than on B35 cells expressing NCAM with VASE. NCAM-nonexpressing B35 cells (clone 3) express a cell surface heparan sulfate proteoglycan that binds heterophilically to the heparin-binding domain of NCAM (Kallapur and Akeson, 1992).

L1 on the human X chromosome is the target for mutation in a complex X-linked human mental retardation syndrome characterized by a variable phenotype that includes hydrocephalus, spastic paraplegia, aphasia, adducted thumbs, and cognitive impairment (Kenwrick *et al.*, 2000). Mutations are distributed throughout all of the extracellular domains, as well as the cytoplasmic domain of L1. To study how individual L1 mutations affect the functions of L1 and result in diverse pathologies, cell lines of B35 cells have been established that stably express the neuronal splice form of human L1 (containing the RSLE insert in the cytoplasmic domain) (Schmid *et al.*, 2000) and three-point mutations in the cytoplasmic domain of neuronal L1 found in human patients: S1194L, S1224L, and

Y1229H (Needham *et al.*, 2001). Analysis of these B35 cell lines by immunofluorescence staining and Western blotting showed expression of mutant L1 proteins on the B35 cell surface at levels equivalent to wild-type L1 (with RSLE). L1 is able to potentiate cell migration toward extracellular matrix molecules such as fibronectin and laminin by functionally interacting with $\beta 1$ integrins on the cell surface (Mechtersheimer *et al.*, 2001; Thelen *et al.*, 2002). In haptotactic Transwell migration assays, stable expression of L1 (with RSLE) in B35 cells potentiates their ability to migrate toward fibronectin compared to parental B35 cells (Thelen *et al.*, 2002). Strikingly, the stable expression of L1 cytoplasmic domain mutations S1194L, S1224L, and Y1229H in B35 cells did not potentiate migration to fibronectin, suggesting that impaired neuronal cell migration might contribute to the pathology of these L1 mutations.

A related rat tumor line B28 with glioblastoma characteristics that is negative for L1 was used for stably expressing human L1 and variant forms lacking specific extracellular domains from the plasmid pcDNA in order to identify determinants necessary to support neurite extension on L1-expressing B28 (Stallcup, 2000). The study revealed that the third fibronectin III domain of L1, which mediates integrin binding (Silletti *et al.*, 2000), plays a key role in promoting the neurite outgrowth of cerebellar neurons (Stallcup, 2000). Stable transfection of the B28 cell line with L1 cytoplasmic domain deletion and missense mutants was used also to identify a juxtamembrane segment of the L1 cytoplasmic domain as a site for organizing cell surface L1 into linear arrays codistributing with actin stress fibers (Dahlin-Huppe *et al.*, 1997).

A novel actin-associated protein named palladin has been implicated in neurite outgrowth in B35 cells. Palladin is detected in the axons, but not the dendrites, of cultured cortical neurons and is concentrated in the axonal growth cones (Boukhelifa *et al.*, 2001). Because the sequence of palladin contains binding sites for proteins that regulate actin polymerization at focal adhesions (Parast and Otey, 2000), it was hypothesized that palladin might play a role in promoting actin assembly in the growth cone. To test the idea that palladin is required for neurite outgrowth, both B35 cells and primary cortical neurons were transfected with antisense constructs to inhibit palladin expression, which resulted in a dramatic reduction in neurite extension (Boukhelifa *et al.*, 2001). The result is illustrated in Fig. 3, which shows B35 cells transfected with palladin antisense or control (sense) constructs and cotransfected with GFP to show the morphology of the cells. The antisense-treated cells remained unpolarized, even 3 days after induction of differentiation, at which time the control cells had extended long neurites. Qualitatively similar results were obtained with primary neurons, but with a smaller sample size due to their resistance to transfection (Boukhelifa *et al.*, 2001).

C. Intracellular Signaling Mechanisms in B35 Cells

The B35 cell line has been of immense utility in elucidating intracellular signaling mechanisms initiated by axon growth-promoting CAMs. Stable B35 cell lines

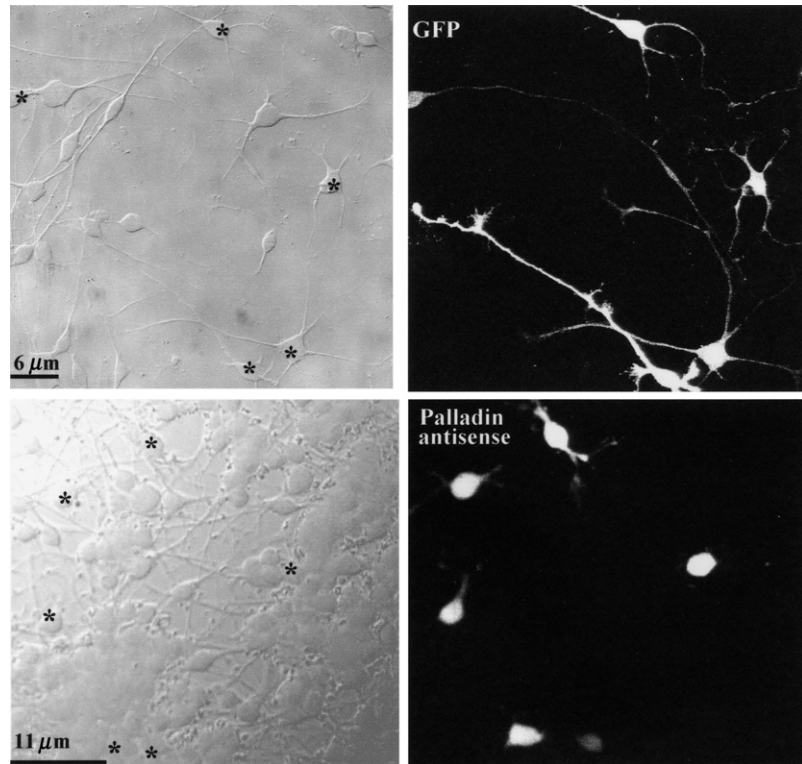


Fig. 3 B35 cells were transfected with GFP alone (top) or GFP plus palladin antisense construct (bottom). These images illustrate the failure of neurite outgrowth that results from inhibition of palladin expression and also show the high level of transfection that is typically achieved in B35 cells with lipofectamine.

expressing NCAM isoforms have been used to show that clustering of NCAM140, but not NCAM180, due to homophilic binding with NCAM-Fc fusion protein or treatment with divalent NCAM antibodies activates the nonreceptor tyrosine kinases p125^{fak} (focal adhesion kinase) and p59^{fyn} (Beggs *et al.*, 1997). These kinases are proximal members of a β 1 integrin signaling cascade. In B35 cells, p59^{fyn} constitutively associates with NCAM140, which upon clustering induces recruitment of p125^{fak} to the NCAM-p59^{fyn} complex. Similar results were found in mouse brain cerebellar extracts and in COS7 cells transiently expressing NCAM140, demonstrating that results in B35 neuroblastoma cells were representative of other cells. Clustering of the NCAM140 isoform in B35 cells subsequently induces transient activation of the MAP kinases ERK1 and ERK2 by a pathway regulated by p125^{fak}, p59^{fyn}, Ras, and MEK (Schmid *et al.*, 1999). This pathway is also regulated by the small GTPase RhoA and culminates in phosphorylation and activation of the transcription factor cAMP response

element binding protein (CREB) both in B35 cells and in primary cerebellar neurons (Schmid *et al.*, 1999). The MAP kinase pathway is required for NCAM-dependent neurite outgrowth. These results suggest that NCAM140 signaling taps into a p125^{fak}-dependent β 1 integrin pathway leading to expression of genes important for axon growth.

Cell surface clustering of L1 in B35 neuroblastoma cells stably expressing human L1 (with RSLE) with L1 antibodies or L1-Fc fusion proteins activates a MAP kinase signaling cascade that is distinct from that of NCAM (Schmid *et al.*, 2000). L1 signaling to MAP kinase proceeds through the activation of pp60^{c-src}, rather than p59^{lyn} (Ignelzi *et al.*, 1994), Rac1 GTPase, rather than RhoA, and is independent of p125^{fak} and c-Ras (Schmid *et al.*, 2000). Additional signaling intermediates include phosphatidylinositol-3-kinase, PAK1, MEK, and the guanine nucleotide exchange factor Vav-2. Interestingly, the L1 signaling pathway closely resembles early integrin signaling responsible for membrane ruffling, lamellipodia formation, and migration in non neural cells (Clark *et al.*, 1998; Meng and Lowell, 1998; Miranti *et al.*, 1998). MAP kinase activation is required for L1-dependent neurite outgrowth, as shown in primary cerebellar neurons (Schmid *et al.*, 2000). The importance of MAP kinase in L1 signaling through integrins leading to the potentiation of haptotactic migration toward extracellular matrix proteins is underscored by the coordinate inhibition of MAP kinase activation and migration toward fibronectin in Transwell assays in B35 cells transiently or stably expressing pathological L1 mutations in the cytoplasmic domain (Thelen *et al.*, 2002).

B35 cells have also been used to investigate signaling mechanisms of axon repellent molecules: ephrin-B ligands and their EphB tyrosine kinase receptors. B35 cells contain substantial levels of endogenous EphB2, as well as the nonreceptor tyrosine kinase Abl, which is a downstream signaling intermediate of ephrin-B stimulation. Treatment of B35 cells with ephrin-B1 activates EphB2 kinase activity, resulting in a subsequent decrease in the kinase activity of Abl (Yu *et al.*, 2001). It was also found that the transient expression of EphB2 in the related glioblastoma cell line B28 stably expressing human L1 led to tyrosine phosphorylation of L1, suggesting an interplay between L1 and EphB2 signaling (Zisch *et al.*, 1997). Proliferating B35 cells have also been found to undergo apoptosis in response to pressure as a model of pressure-induced cell death in glaucoma (Agar *et al.*, 2000).

D. Endocytosis of Cell Adhesion Molecules in B35 Cells

Antibody-mediated endocytosis of L1 appears to be an essential step in growth cone motility and cell signaling (Kamiguchi and Lemmon, 1998; Schaefer *et al.*, 1999; Schmid *et al.*, 2000). In cells expressing the neuronal form of L1 (with RSLE), L1 antibodies induce rapid dynamin I- and clathrin-dependent internalization of L1, as shown in B35 cells and dorsal root ganglion neurons. L1 internalization in B35 cells also requires a functional pp60^{c-src} kinase (Schmid *et al.*,

2000). Inhibition of either dynamin I or pp60^{c-src} by expression of dominant negative mutants blocks L1-induced endocytosis and MAP kinase activation; thus, L1 endocytosis is probably required for downstream signaling to ERKs necessary for neurite outgrowth. Because inhibition of dynamin I or pp60^{c-src} in B35 cells also blocks L1-potentiated cell migration toward extracellular matrix proteins (Thelen *et al.*, 2002), endocytosis also appears to be important for haptotactic migration.

In another study, B35 cell lines expressing L1 cytoplasmic domain mutations S1194L or S1224L were unimpaired for antibody-induced L1 endocytosis (Needham *et al.*, 2001). However, B35 cells expressing the L1 point mutation Y1229H showed enhanced endocytosis of this L1 mutant (Needham *et al.*, 2001), suggesting a critical role for tyrosine residue 1229 in the regulation of L1 endocytosis that probably affects neurodevelopmental functions of axon growth and neural migration dependent on L1.

III. Protocols

Because our own hands-on experience has been with B35 rather than B50 cells, our protocols have been optimized using this line. We provide protocols for growing B35 cells in culture and for exploring protein function through transient transfection with antisense constructs, establishing stable cell lines, and monitoring the effects of protein overexpression on B35 cell migration.

A. Using Antisense Constructs in B35 Cells

The function of a protein can be studied by reducing the amount of the protein in cultured cells and then assaying for phenotypic changes. This can be achieved with high specificity using an antisense approach, either with oligonucleotides or with longer antisense constructs. The goal is to introduce into the cytoplasm of cells an RNA or a single-stranded DNA complementary to the mRNA of the target gene. In order to produce high levels of antisense RNA, we have constructed plasmid vectors that contain the target gene (in this case, palladin) in an antisense orientation (or sense orientation for control). The “antisense” is the complementary strand to the mRNA sequence coding for palladin. When cells are transfected with the antisense construct, the endogenous mRNA and the transfected antisense RNA form a complex so that protein translation is inhibited.

We have used two different approaches to deliver the antisense construct: standard transient transfection and adenovirus infection. The advantage of adenovirus infection is its high efficiency, such that 100% of the cells in a plate can be infected with the construct. This makes it possible to confirm by Western blot that expression of the target protein is effectively inhibited (see, for example, Parast and Otey, 2000). In the case of neurons and neuron-like cell lines, there are problems with viral toxicity, so we recommend using transient transfection of

antisense constructs as described in the following detailed protocols. Immunofluorescence staining can be used to confirm that levels of the target protein are reduced in antisense-transfected cells.

There are no firm rules to guide the design of antisense constructs. In the case of palladin, we made three different constructs, corresponding to the full-length cDNA, or to the N-terminal or C-terminal halves. Somewhat surprisingly, the antisense construct corresponding to a partial sequence (the C-terminal half of the molecule) worked the best at inhibiting palladin translation, probably due to an optimal “fit” with the shape of the endogenous mRNA. Unless one has knowledge of the three-dimensional shape of a particular mRNA, it is probably best to test two or three different constructs and to determine empirically which one produces the greatest loss of signal in the immunofluorescence assay. Protocols are described for the transient transfection of B35 cells, which typically yield a transfection efficiency of ~40%.

B. Exploring Protein Function with Stable Transfection and Motility Assays

Much information on the function of neuronal cell adhesion molecules has been gained through the use of stably transfected B35 cells. The phenotype of cells expressing NCAM or wild-type or mutated L1 has been determined through the use of a variety of assays, including the Transwell motility assay, as shown in Fig. 4. Protocols for selecting and maintaining stably transfected B35 cells and for

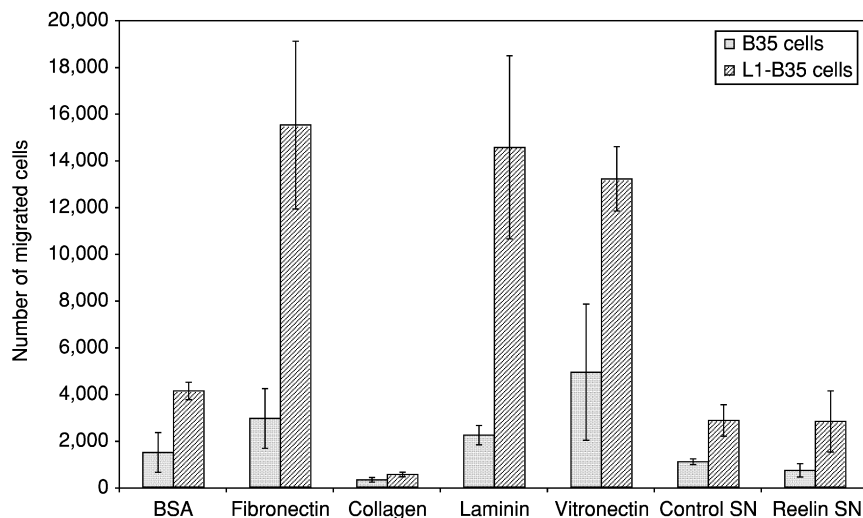


Fig. 4 L1 potentiates the migration of B35 neuroblastoma cells to extracellular matrix proteins. Haptotactic cell migration was measured in B35 cells (20,000 cells per chamber) expressing no L1 or L1(+RSLE) toward extracellular matrix proteins or BSA for 16 h. Each sample was assayed in triplicate, and experiments were repeated at least twice with similar results.

assaying their ability to migrate haptotactically through a filter in a Transwell chamber are as follows.

C. Culturing and Transfection (Transient and Stable) of B35 Neuroblastoma Cells

1. Materials

9-in. Pasteur pipettes
12-well culture plates
Dulbecco's Modified Eagle Medium, High Glucose (DMEM-H) with L-glutamine, with 4.5 g/liter glucose
Fetal bovine serum (FBS) or fetal clone II (Hyclone)
Geneticin G-418 sulfate, 100 × (25 mg/ml made from powder)
Gentamicin/kanamycin (G/K), 100 × (5 mg/ml gentamicin, 20 mg/ml kanamycin)
Hanks' Buffered Saline Solution (HBSS) without calcium and magnesium
Incubator, 37°C, 5% CO₂
Plasmid cDNA
Lipofectamine (2 mg/ml)
Opti-MEM I reduced serum medium
Polystyrene tubes, sterile, 12 × 75 mm, with snap cap
Polystyrene tubes, sterile, 15 ml conical, with screw cap
Timer
Tissue culture plates, 100 mm
Trypsin-EDTA, 1X (0.05% trypsin, 0.53 mM EDTA, liquid)
Water bath, 37°C

2. General Culture Conditions

B35s are elongated, neuronal cells with two neurites (usually). The length of the neurites depends on the time since passage and experimental stimuli. It is possible for neurites to be longer than 100 μm . Soma may be 10–20 μm in diameter, but should not appear spherical in shape. B35s may be differentiated with dibutyryl cyclic AMP. B35 cells are adherent, but not contact inhibited. They should be fed every 48 to 72 h and passaged when 75–85% confluent.

3. Transfection for Transient Expression

Maintain cell cultures for at least 1 week. The transfection phase requires 72 h from the addition of the cDNA to the splitting of cultures.

a. Day 0

Start with cells from one 100-mm plate at ~80% confluence. Pass one-third of the source culture to another 100-mm plate. Incubate for 24 h at 37°C. Ideally, cells should be split such that they will be 50–60% confluent when transfection begins.

b. Day 1

1.0. Prepare the following solutions in sterile polystyrene (NOT polypropylene) tubes for each 100 mm plate of cells. *Note:* Do not add serum or antibiotics to HBSS or Opti-MEM during transfection. Use the laminar flow hood and aerosol-barrier pipette tips: (A) 1–10 µg plasmid cDNA in Opti-MEM or serum-free medium to a final volume of 800 µl. (B) 15 µl Lipofectamine in Opti-MEM to a final volume of 800 µl. Gently mix all tubes, tap drops down. Combine solutions A and B for each plate and mix cautiously.

1.1. Incubate A+B mixture for 45 min at room temperature to allow DNA–liposome complexes to form.

1.2. Rinse cells once with warm (37°C), sterile HBSS or serum-free medium.

1.3. Add 4.8 ml of warm (37°C) Opti-MEM to the mixture containing the Lipofectamine–cDNA complexes and add to the corresponding plate with cells.

1.4. Incubate for 8 h at 37°C.

1.5. Add 6.4 ml of 2X warm (37°C) culture medium (i.e., DMEM-H + 20% FBS + 1:50 G/K) to each 100-mm plate, *but do not remove the transfection medium! DNA should remain on cells.* The total volume of medium on the plate is now 12.8 ml.

1.6. Incubate for 18 h at 37°C.

c. Day 2

2.0. Split the cells into two 100-mm plates (one should contain coverslips if you are planning to perform immunofluorescence staining). This time, use 8 ml warm (37°C) 1X culture medium (DMEM-H + 10% FBS + 1:100 G/K) for each 100-mm plate.

4. Posttransfection Establishment of Stable Cell Lines**a. Day 4**

4.0. Pass cells according to standard procedure. Distribute cells equally into seven 100-mm plates (1:7 for each plate).

4.1. Remove medium and wash cells once with HBSS (without calcium or magnesium).

4.2. Aspirate rinse medium and treat cells with trypsin–EDTA for 3 min at 37°C. Monitor in scope.

4.3. Collect free cells from plate with standard culture medium and centrifuge gently to pellet.

4.4. Remove supernatant and resuspend cells in selection medium (i.e., DMEM-H + 10% FBS + 1:100 G/K + 500 $\mu\text{g/ml}$ G-418) for distribution. Continue to use selection medium until colonies are visible on plates or until all cells die. This may take 10–14 days.

4.5. Distribute cells equally into labeled plates. Incubate at 37°C.

b. Postday 4

From day 4 to day 7, change medium every day, using 7 ml warm (37°C) selection medium for each 100-mm plate. Observe for colony formation on plates. From day 8 to day 14, change medium every other day.

D. Transwell Migration Assay to Monitor Motility in B35 Neuroblastoma Cells

1. Prepare the substrate. Dilute bovine serum albumin (BSA), fibronectin (FN), or the desired substrate in 100 μl phosphate-buffered saline (PBS) (3 μg FN per Transwell). *An alternative method is to dilute substrate in PBS to a concentration of 4 $\mu\text{g/ml}$. Prepare 500 μl for each Transwell to be coated.*

2. Invert the Transwell inserts and place them on a flat, level surface in the laminar flow hood. The top side of a 24-well culture dish (lid) or an open 150-mm plate may be used for this purpose. Coat the bottom surface of the membrane with 100 μl of the substrate solution. Observe the membranes frequently during the drying period. The substrate should remain on top of the membranes. Discard any membranes that leak. *An alternative method is to pipette 500 μl of substrate solution (e.g., 4 $\mu\text{g/ml}$ fibronectin) into each empty well of the 24-well tray and then place Transwells on top of the solution and cover the tray. Gently tilt the tray to eliminate any bubbles under the membranes.*

3. Incubate the coated Transwell membranes in the tissue culture hood until the substrate is completely dry. This should take 2–4 h, depending on the room temperature and humidity. *Another alternative method is to incubate the Transwells with substrate solution at 4°C overnight (~18 h). Gently transfer the tray with its contents to a plastic bag and seal it. Keep the tray level at all times. Transfer the sealed tray to a refrigerator or cold room.*

4. After coating the Transwells, prepare the lower chambers by adding 500 μl PBS-CMF to each well. In addition, prepare the same number of Transwell chambers by adding 500 μl blocking solution (2% BSA in PBS-CMF) to each well. Rinse the membranes by placing them in the wells with the PBS-CMF. After 5 min, transfer the membranes to the wells containing the blocking solution.

5. Block each membrane in 500 μl of blocking solution at room temperature (20–25°C) for at least 30 min. Do not block the top side of the membrane! If there is leakage of blocking solution through the membrane at this point, discard it, as cells will not attach to wells coated with BSA. Aspirate the PBS from the other 24-well plate and replace it with 750 μl cell migration medium per well. This is a good time to begin processing the cell cultures.

6. After blocking, rinse the bottom of the Transwells by placing them into the wells containing 750 μ l cell migration medium for about 5 min. Then transfer the membrane to wells containing 500 μ l cell migration medium. Prewarm this tray in the CO₂ incubator at 37°C while preparing the cells.
7. While blocking proceeds, rinse the cell cultures (50–80% confluence) gently with 1× HBSS-CMF. Immediately aspirate the liquid and begin detachment of the cells.
8. Detach cells with 1× HBSS-CMF + 5 mM EDTA. Triturate cells several times with a plugged, fire-polished Pasteur pipette to dissociate cells thoroughly.
9. Transfer the cells to 15- or 50-ml centrifuge tube, fill with serum-free medium (e.g., DMEM-H or OptiMEM I), and spin at ~ 1200 rpm (~500 × *g*) for a minimum of 5 min at 4°C.
10. Aspirate the supernatant. Resuspend the cell pellet in 1–5 ml freshly prepared cell migration medium, using a fire-polished, plugged Pasteur pipette.
11. Count cells with a Coulter counter or hemacytometer. Use the standard procedures described in other protocols.
12. Dilute 0.1–1 × 10⁶ cells in 1.0 ml DMEM-H + 1X gentamicin/kanamycin (optional) + 0.4 mM MnCl₂•4H₂O. Add 100 μ l of cell solution into the Transwell.
13. Incubate at 37°C, according to the experimental requirements (usually 16–18 h for B35 cells).
14. Remove the assay plate(s) from the incubator and process immediately.
15. Rinse each Transwell chamber twice in 1 ml PBS at room temperature (5 min per rinse). Transfer the membranes to wells containing PBS (first rinse). After 5 min, repeat this step (second rinse). Carefully aspirate liquid from the top of the membrane between rinses. Use a narrow-bore pipette tip connected to a vacuum source.
16. After the second rinse, remove cells from the side of the membrane you are *not* interested in. Wipe off this side of the membrane before staining with a cotton-tipped applicator. A folded Kimwipe may also be used to remove excess liquid if necessary.
17. Stain cells in membrane for 5–10 min in 1 ml hematoxylin. Alternatively, label the cells with the desired antibody and follow the appropriate staining procedure for indirect immunofluorescence (see Section III,E).
18. Wash again twice in 1 ml PBS. Repeat step 15.
19. Remove the Transwell membrane by cutting gently around the perimeter with a sharp scalpel and mount it on a glass slide using Gel Mount (Biomedica Corp). Seal the coverslip with quick-drying nail enamel.
20. Count cells from 5 to 10 fields of 20× objective of the Zeiss microscope. Count only cells within the 10×10 grid (one field). Average the number of cells per field. Multiply with factor 132 to obtain the cell number per whole membrane side. For transfection experiments, also count cells on top of selected membranes.

E. Detecting Migrated/Nonmigrated and Expressing/Nonexpressing Cells by Immunocytochemistry

1. Prepare 4% paraformaldehyde (PFA). Pipette 500 μ l–1.0 ml of the fixative into each well of a 24-well plate.
2. As soon as the Transwells are removed from the incubator (end of migration period), carefully place them directly into the wells with 4% PFA. Fix cells for 15–30 min at room temperature.
3. Carefully remove fixative from the upper sides of Transwells by gentle aspiration. We use a narrow, gel-loading pipette tip attached to a vacuum source. Tilt the Transwell about 45° while applying the tip to the inside wall of the Transwell housing. Try to avoid touching the membrane, but aspirate as much liquid as possible.
4. Place Transwells into blocking solution. We use PBS + 10% goat serum + 0.2% fish skin gelatin (Sigma) as our blocking solution for immunocytochemistry. Block Transwells for 1 h at room temperature or overnight at 4°C.
5. Prepare the primary antibody in blocking solution and dispense to a 24-well plate (500 μ l/well).
6. Omit cells from either upper or lower sides of Transwells, according to your analysis, by swabbing with cotton-tipped applicators or wiping with Kimwipes. Place Transwells into the wells with the primary antibody. Incubate cells with the primary antibody for 4 h at room temperature or overnight at 4°C.
7. Rinse Transwells carefully three times in PBS. Dispense PBS to a 24-well plate (1.0 ml/well). Then simply transfer the Transwells to those wells. Allow the Transwells to soak for 5 min per rinse. Carefully aspirate excess PBS from the upper sides of Transwells between each rinse.
8. Prepare the secondary antibody (e.g., FITC-conjugated goat antirabbit IgG) in blocking solution. Follow the manufacturer's recommendations regarding concentration. Dispense solution into a 24-well plate (500 μ l–1.0 ml/well).
9. Place the rinsed Transwells into the secondary antibody solution. Incubate cells with the secondary antibody for at least 1 h at room temperature.
10. For dual staining, we use the permeant DNA stain bis-benzimide (Molecular Probes). DAPI may be substituted for bis-benzimide. However, DAPI is only semipermeant and requires permeabilization of the cells. Dilute the bis-benzimide to a concentration of 10 μ M in HBSS. Dispense into a 24-well plate (1.0 ml/well). This will be the first rinse.
11. Carefully aspirate the secondary antibody solution from the upper sides of the Transwells. Place them into the bis-benzimide solution. After soaking for 5 min at room temperature, repeat step 11.
12. Prepare a slide with Vectashield mounting medium (one drop/membrane). Remove Transwells from the polystyrene housing by carefully cutting around the perimeter of each membrane and then use blunt forceps to pull the membrane free.

Place the membrane, cells side up, onto the Vectashield. Apply a No. 1 cover glass. Secure the cover glass with fingernail polish.

References

- Agar, A., Yip, S. S., Hill, M. A., and Coroneo, M. T. (2000). Pressure related apoptosis in neuronal cell lines. *J. Neurosci. Res.* **60**, 495–503.
- Akeson, R. A., Wujek, J. R., Roe, S., Warren, S. L., and Small, S. J. (1988). Smooth muscle cells transiently express NCAM. *Brain Res.* **464**, 107–120.
- Audesirk, T., Audesirk, G., Ferguson, C., and Shugarts, D. (1991). Effects of inorganic lead on the differentiation and growth of cultured hippocampal and neuroblastoma cells. *Neurotoxicology* **12**, 529–538.
- Baines, D., Mallon, B. S., and Love, S. (1992). Effects of sodium butyrate on the expression of sodium channels by neuronal cell lines derived from the rat CNS. *Brain Res. Mol. Brain Res.* **16**, 330–338.
- Beggs, H. E., Baragona, S. C., Hemperly, J. J., and Maness, P. F. (1997). NCAM140 interacts with the focal adhesion kinase p125(fak) and the SRC-related tyrosine kinase p59(fyn). *J. Biol. Chem.* **272**, 8310–8319.
- Behl, C., Hovey, L., Krajewski, S., Schubert, D., and Reed, J. C. (1993). BCL-2 prevents killing of neuronal cells by glutamate but not by amyloid beta protein. *Biochem. Biophys. Res. Commun.* **197**, 949–956.
- Boukhelifa, M., Parast, M. M., Valtschanoff, J. G., LaMantia, A. S., Meeker, R. B., and Otey, C. A. (2001). A role for the cytoskeleton-associated protein palladin in neurite outgrowth. *Mol. Biol. Cell* **12**, 2721–2729.
- Capano, M., Virji, S., and Crompton, M. (2002). Cyclophilin-A is involved in excitotoxin-induced caspase activation in rat neuronal B50 cells. *Biochem. J.* **363**, 29–36.
- Clark, E. A., King, W. G., Brugge, J. S., Symons, M., and Hynes, R. O. (1998). Integrin-mediated signals regulated by members of the rho family of GTPases. *J. Cell Biol.* **142**, 573–586.
- Dahlin-Huppe, K., Berglund, E. O., Ranscht, B., and Stallcup, W. B. (1997). Mutational analysis of the L1 neuronal cell adhesion molecule identifies membrane-proximal amino acids of the cytoplasmic domain that are required for cytoskeletal anchorage. *Mol. Cell. Neurosci.* **9**, 144–156.
- Doherty, P., Moolenaar, C. E., Ashton, S. V., Michalides, R. J., and Walsh, F. S. (1992). The VASE exon downregulates the neurite growth-promoting activity of NCAM 140. *Nature* **356**, 791–793.
- Frenkel, G. D., and Ducote, J. (1987). The enhanced rate of transcription of methyl mercury-exposed DNA by RNA polymerase is not sufficient to explain the stimulatory effect of methyl mercury on RNA synthesis in isolated nuclei. *J. Inorg. Biochem.* **31**, 95–102.
- Frenkel, G. D., Ducote, J., Reboulleau, C. P., and Gierthy, J. (1988). A cell line with decreased sensitivity to the methyl mercury-induced stimulation of alpha-amanitin sensitive RNA synthesis in isolated nuclei. *Comp. Biochem. Physiol. B* **91**, 477–482.
- Ignatius, M. J., and Reichardt, L. F. (1988). Identification of a neuronal laminin receptor: An Mr 200K/120K integrin heterodimer that binds laminin in a divalent cation-dependent manner. *Neuron* **1**, 713–725.
- Ignelzi, M. A., Miller, D. R., Soriano, P., and Maness, P. F. (1994). Impaired neurite outgrowth of src-minus cerebellar neurons on the cell adhesion molecule L1. *Neuron* **12**, 873–884.
- Kallapur, S. G., and Akeson, R. A. (1992). The neural cell adhesion molecule (NCAM) heparin binding domain binds to cell surface heparan sulfate proteoglycans. *J. Neurosci. Res.* **33**, 538–548.
- Kamiguchi, H., and Lemmon, V. (1998). A neuronal form of the cell adhesion molecule L1 contains a tyrosine-based signal required for sorting to the axonal growth cone. *J. Neurosci.* **18**, 3749–3756.

- Kenwrick, S., Watkins, A., and De Angelis, E. (2000). Neural cell recognition molecule L1: Relating biological complexity to human disease mutations. *Hum. Mol. Genet.* **9**, 879–886.
- Lai, M., Griffiths, H., Pall, H., Williams, A., and Lunec, J. (1993). An investigation into the role of reactive oxygen species in the mechanism of 1-methyl-4-phenyl-1,2,3,6-tetrahydropyridine toxicity using neuronal cell lines. *Biochem. Pharmacol.* **45**, 927–933.
- Liu, L., Haines, S., Shew, R., and Akeson, R. A. (1993). Axon growth is enhanced by NCAM lacking the VASE exon when expressed in either the growth substrate or the growing axon. *J. Neurosci. Res.* **35**, 327–345.
- Mechtersheimer, S., Gutwein, P., Agmon-Levin, N., Stoeck, A., Oleszewski, M., Riedle, S., Fogel, M., Lemmon, V., and Altevogt, P. (2001). Ectodomain shedding of L1 adhesion molecule promotes cell migration by autocrine binding to integrins. *J. Cell Biol.* **155**, 661–673.
- Meng, F., and Lowell, C. A. (1998). A beta 1 integrin signaling pathway involving Src-family kinases, Cbl and PI-3 kinase is required for macrophage spreading and migration. *EMBO J.* **17**, 4391–4403.
- Miranti, C. K., Leng, L., Maschberger, P., Brugge, J. S., and Shattil, S. J. (1998). Identification of a novel integrin signaling pathway involving the kinase Syk and the guanine nucleotide exchange factor Vav1. *Curr. Biol.* **8**, 1289–1299.
- Miyazaki, I., Iwata-Ichikawa, E., Asanuma, M., Iida, M., and Ogawa, N. (1999). Bifemelane hydrochloride protects against cytotoxicity of hydrogen peroxide on cultured rat neuroblastoma cell line. *Neurochem. Res.* **24**, 857–860.
- Needham, L. K., Thelen, K., and Maness, P. F. (2001). Cytoplasmic domain mutations of the L1 cell adhesion molecule reduce L1-ankyrin interactions. *J. Neurosci.* **21**, 1490–1500.
- Parast, M. M., and Otey, C. A. (2000). Characterization of palladin, a novel protein localized to stress fibers and cell adhesions. *J. Cell Biol.* **150**, 643–656.
- Reboulleau, C. P. (1986). Extracellular calcium-induced neuroblastoma cell differentiation: Involvement of phosphatidylinositol turnover. *J. Neurochem.* **46**, 920–930.
- Reboulleau, C. P. (1990). Inositol metabolism during neuroblastoma B50 cell differentiation: Effects of differentiating agents on inositol uptake. *J. Neurochem.* **55**, 641–650.
- Schaefer, A. W., Kamiguchi, H., Wong, E. V., Beach, C. M., Landreth, G., and Lemmon, V. (1999). Activation of the MAPK signal cascade by the neural cell adhesion molecule L1 requires L1 internalization. *J. Biol. Chem.* **274**, 37965–37973.
- Schmid, R.-S., Graff, R., Schaller, M. D., Chen, S., Schachner, M., Hemperley, J. J., and Maness, P. F. (1999). NCAM stimulates the Ras-MAPK pathway and CREB phosphorylation in neuronal cells. *J. Neurobiol.* **38**, 542–555.
- Schmid, R. S., and Maness, P. F. (2001). Cell recognition molecules and disorders of neurodevelopment. In “Int. Handbook on Brain and Behaviour in Human Development.” (A. F. Kalverboer and A. Gramsbergen, eds.), Kluwer, A Groningen, The Netherlands.
- Schmid, R. S., Pruitt, W. M., and Maness, P. F. (2000). A MAP kinase-signaling pathway mediates neurite outgrowth on L1 and requires Src-dependent endocytosis. *J. Neurosci.* **20**, 4177–4188.
- Schubert, D., Heinemann, S., Carlisle, W., Tarikas, H., Kimes, B., Patrick, J., Steinback, J. H., Culp, W., and Brandt, B. L. (1974). Clonal cell lines from the rat central nervous system. *Nature* **249**, 224–227.
- Silletti, S., Mei, F., Sheppard, D., and Montgomery, A. M. (2000). Plasmin-sensitive dibasic sequences in the third fibronectin-like domain of L1-cell adhesion molecule (CAM) facilitate homomultimerization and concomitant integrin recruitment. *J. Cell Biol.* **149**, 1485–1502.
- Stallcup, W. B. (2000). The third fibronectin type III repeat is required for L1 to serve as an optimal substratum for neurite extension. *J. Neurosci. Res.* **61**, 33–43.
- Stallcup, W. B., and Cohn, M. (1976a). Electrical properties of a clonal cell line as determined by measurement of ion fluxes. *Exp. Cell Res.* **98**, 277–284.
- Stallcup, W. B., and Cohn, M. (1976b). Correlation of surface antigens and cell type in cloned cell lines from the rat central nervous system. *Exp. Cell Res.* **98**, 285–297.
- Thelen, K., Kedar, V., Panicker, A. K., Schmid, R. S., Midkiff, B. R., and Maness, P. F. (2002). The neural cell adhesion molecule L1 potentiates integrin-dependent cell migration to extracellular matrix proteins. *J. Neurosci.* **22**, 4918–4931.

- Vinores, S. A., Marangos, P. J., Bonnín, J. M., and Rubinstein, L. J. (1984). Immunoradiometric and immunohistochemical demonstration of neuron-specific enolase in experimental rat gliomas. *Cancer Res.* **44**, 2595–2599.
- Wu, G., and Ledeen, R. W. (1991). Stimulation of neurite outgrowth in neuroblastoma cells by neuraminidase: Putative role of GM1 ganglioside in differentiation. *J. Neurochem.* **56**, 95–104.
- Yu, H. H., Zisch, A. H., Dodelet, V. C., and Pasquale, E. B. (2001). Multiple signaling interactions of Abl and Arg kinases with the EphB2 receptor. *Oncogene* **20**, 3995–4006.
- Zisch, A. H., Stallcup, W. B., Chong, L. D., Dahlin-Huppe, K., Voshol, J., Schachner, M., and Pasquale, E. B. (1997). Tyrosine phosphorylation of L1 family adhesion molecules: Implication of the Eph kinase Cdk5. *J. Neurosci Res.* **47**, 655–665.

CHAPTER 14

Live-Cell Imaging of Slow Axonal Transport in Cultured Neurons

Anthony Brown

Neurobiotechnology Center and Department of Neuroscience
Ohio State University
Columbus, Ohio 43210

- I. Introduction
 - II. Culturing Neurons from Superior Cervical Ganglia
 - A. Establishing Cultures
 - B. Culture Medium
 - C. Culture Dishes
 - III. Transfecting Neurons by Nuclear Injection
 - IV. Injecting Neurons with Fluorescent Proteins
 - V. Observing Movement
 - A. Naturally Occurring Gaps
 - B. Photobleaching
 - C. Live-Cell Imaging
 - D. Motion Analysis
 - VI. Conclusion
- References

Cytoskeletal polymers and other cytosolic protein complexes are transported along axons in the slow components of axonal transport. Studies on the movement of neurofilaments and microtubules in the axons of cultured neurons indicate that these polymers actually move at fast rates and that the movements are also infrequent and highly asynchronous. These observations indicate that the slow rate of slow axonal transport is due to rapid movements interrupted by prolonged pauses which presents special challenges for studies on the mechanism of movement. This chapter describes the procedures that the author's laboratory has used to observe and analyze the movement of neurofilaments and microtubules in axons of cultured neurons from the superior cervical ganglia of neonatal rats. In

particular, the author describes how to culture these neurons, how to transfect them by nuclear injection, and how to detect the rapid and infrequent movement of cytoskeletal polymers using time-lapse fluorescence imaging.

I. Introduction

Cytoskeletal and cytosolic proteins are synthesized in the neuronal cell body and are transported along axons in the slow components of axonal transport at average rates of approximately 0.3–3 mm/day (Lasek *et al.*, 1984). We and others have succeeded in observing the slow axonal transport of neurofilaments and microtubules directly in cultured nerve cells using live-cell fluorescence imaging (Wang *et al.*, 2000; Roy *et al.*, 2000; Wang and Brown, 2001, 2002). Contrary to expectations, these cytoskeletal polymers move at rapid rates, approaching the rate of fast axonal transport, but their movements are also infrequent and highly asynchronous. Based on these observations, we have proposed that slow axonal transport is powered by fast motors and that the overall slow rate is due to rapid movements interrupted by prolonged pauses (Brown, 2000).

Despite this progress, there is still a great deal to be learned about the mechanism of slow axonal transport. For example, what are the structural forms in which cytoskeletal and cytosolic proteins move, what are the motors that move them, what are the tracks along which they move, and how is their movement regulated? Cultured neurons offer researchers a special opportunity to address these questions because of their amenability to observation by live-cell fluorescence imaging. This chapter describes two approaches that allow observation of the axonal transport of cytoskeletal proteins in cultured neurons. One approach takes advantage of naturally occurring gaps in the axonal neurofilament array in certain types of cultured neuron, and the other employs fluorescence photobleaching. While the former approach is only applicable to studies on neurofilaments, the latter approach has also permitted us to observe the axonal transport of microtubules, and we believe that this technique should also be capable of detecting the movement of other cytoskeletal and cytosolic proteins in axons.

II. Culturing Neurons from Superior Cervical Ganglia

A. Establishing Cultures

All of our live-cell imaging studies on slow axonal transport have been performed using primary cultures of dissociated neurons from superior cervical ganglia (SCG). A more detailed discussion of the culture of these neurons can be found elsewhere (Hawrot and Patterson, 1979; Johnson *et al.*, 1981; Johnson and Argiro, 1983; Higgins *et al.*, 1991; Mahanthappa and Patterson, 1998). We have most experience with SCG neurons from rats, but the procedures described here work equally well for mice. We purchase timed pregnant female Sprague–

Dawley rats from Harlan on a weekly basis and sacrifice the newborn rat pups using carbon dioxide followed by cardiac puncture. We normally use neonatal pups, but older pups can also be used. The two ganglia obtained from a single pup are sufficient for one batch of cultures because we plate the cells at very low density in order to facilitate the tracing of individual axons along their length.

All procedures are performed under sterile conditions in a horizontal laminar flow hood. Hoods with a vertical flow design are not suitable because they cannot accommodate a stereo dissection microscope. The ganglia are dissected from the animal together with the associated carotid artery and vagus nerve as described by Higgins *et al.* (1991) and are then immersed in a 35-mm plastic dish containing Leibovitz's L-15 medium. The associated tissue is removed under the dissection microscope using fine forceps, and cleaned ganglia are transferred to a 15-ml disposable polystyrene centrifuge tube containing fresh L-15 and allowed to settle to the bottom of the tube under gravity. If any of the submerged ganglia adhere to the sides of the tube, they can be dislodged by squirting L-15 on them using a Pasteur pipette. Contamination of the cultures with nonneuronal cells can be reduced by removing the thin connective tissue capsule that ensheaths the ganglia, but we do not find this to be necessary when using L-15-based culture media (see later).

To dissociate the neurons, we rinse ganglia once with phosphate-buffered saline (PBS) and then incubate them in 2.5 mg/ml collagenase (type 3, Worthington Biochemicals) at 37°C for 1 h. We then rinse them twice with PBS and incubate them in 2.5 mg/ml trypsin (3× crystallized, Worthington Biochemicals) at 37°C for 30 min. The enzyme solutions are prepared fresh in PBS and sterilized by 0.2- μ m syringe filtration prior to use. For the rinses, ganglia are allowed to settle to the bottom of the tube under gravity and then the liquid is removed using a Pasteur pipette, leaving just enough to cover the ganglia so that they do not dry out. After trypsinization, ganglia are rinsed with L-15 containing 15–20% fetal bovine serum (to inactivate the trypsin) and are then triturated in 2 ml L-15 containing 0.5 mg/ml bovine serum albumin ("L-15 + BSA") using a Pasteur pipette (5–10 passages). The resulting cell suspension is diluted in L-15 + BSA to the desired concentration and is plated onto coverslips in the culture dish assemblies described later (150 μ l cell suspension per well). It is important not to triturate too much because this can reduce the yield of viable cells. The actual cell density can be determined using a hemocytometer, but we find it more convenient to estimate it in units of ganglia per milliliter. In our hands, a concentration of dissociated cells equivalent to 0.03 to 0.06 ganglia/ml yields approximately 25–50 neurons per dish. At this density, two ganglia yield enough cells to plate more than 100 dishes, although we typically plate only 8–12. The cells are allowed to settle onto the coverslip under gravity for 45 min in the incubator (37°C, atmospheric CO₂), and then 1.5 ml culture medium (see later) is added to each dish. Cells can be maintained for at least a week without changing the medium, providing that care is taken to minimize evaporation loss, but we generally replace the medium with fresh medium every 3–4 days. Prior to adding fresh medium, we aspirate the old medium from the dish but not the well (about 85 μ l) so as to avoid disturbing the

cells on the coverslip. More frequent feeding is not necessarily better, as some conditioning of the medium may occur with time in culture.

B. Culture Medium

The culture medium that we use is based on the formulation of Bray (1991) and contains 10% adult rat serum, 0.6% glucose, 2 mM L-glutamine, 0.5% hydroxypropylmethylcellulose (Methocel F4M-PREM, Dow Chemical Co.), and 50 ng/ml nerve growth factor (2.5S subunit purified from mouse salivary glands; Collaborative Research) in L-15 (phenol red free, Gibco). Because L-15 medium is designed to buffer its pH in atmospheric CO₂, it is more convenient for observation and microinjection of cells on the microscope stage than media with bicarbonate buffering systems. An additional benefit is that nonneuronal cells proliferate far less in this medium than in bicarbonate-buffered media, thereby eliminating the need for the addition of antimetabolic agents to the culture medium. We avoid using phenol red in the culture medium because it increases background fluorescence during live-cell imaging. The fluorescence of the culture medium may be reduced further by using a custom L-15 formulation lacking riboflavin, but we have not tried this ourselves. With a good sterile technique it is not necessary to use antibiotics. A defined serum-free L-15-based culture medium can also be used (Hawrot and Patterson, 1979; Mahanthappa and Patterson, 1998), but the neurons appear to do better in the presence of serum when cultured at low density. While it is possible to culture SCG neurons for many months, all of our own work has been performed within 1 week of plating.

Adult rat serum can be prepared by the method of Hawrot and Patterson (1979) or purchased from a commercial source such as Harlan. We sterilize the serum by 0.2- μ m syringe filtration and store it frozen in aliquots to minimize repeated freezing and thawing. Often the serum forms a fine precipitate after a few days at 37°C. This precipitate can be mistakenly identified as microbial contamination, but it is actually innocuous and does not harm the cells. With serum from some commercial sources, the precipitate can become so dense that it obscures the cells. In this case, switch to a different commercial source or prepare the serum yourself. Fetal bovine serum can also be used, but it is our impression that the cells are healthier and attach better to the substrate in the presence of adult rat serum.

The function of Methocel is to increase the viscosity of the culture medium. It is not critical, but the cells appear to attach better to the substrate when it is present. Because Methocel solutions are too viscous to sterilize by filtration, the powder must be autoclaved. We weigh out 200-mg aliquots of Methocel powder in 50-ml disposable polypropylene centrifuge tubes and then sterilize by autoclaving with the caps loosely attached. After cooling, the caps can be tightened and the tubes can be stored indefinitely at room temperature. To dissolve the Methocel, we add 40 ml sterile L-15 and shake the tube overnight at room temperature. The resulting solution contains insoluble particulate material, which we remove by filtration using a 5- μ m syringe filter (Millex-SV, Millipore).

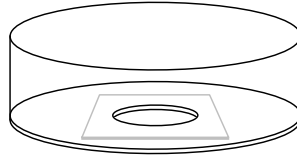


Fig. 1 Coverslip culture dish assembly. A hole is drilled in the bottom of a 35-mm culture dish and a glass coverslip is affixed to the base of the dish using paraffin wax. Cells are plated onto the coverslip in the shallow well created by the hole in the bottom of the dish.

C. Culture Dishes

The neurons are cultured on glass coverslips in the coverslip culture dish assembly described by Bray (1991) (Fig. 1). To prepare the dishes, we drill 13/32-in-diameter holes in 35-mm polystyrene culture dishes using a titanium-coated step drill (McMaster-Carr Supply Co.). The drill bit should be cleaned thoroughly before use because it contacts the culture dishes. We use Nunclon 35-mm culture dishes with vented lids (Nalge Nunc), but any similar dish should be suitable. It is important to use slow and steady pressure with a sharp drill bit and to support the dish from underneath to avoid cracking the plastic. We use a specially built jig milled out of aluminum to hold the dish in position on the drill press. The drill often leaves a slight burr, which must be removed by scraping around the holes gently with a scalpel blade in order to allow coverslips to be placed flush against the plastic (see later).

The coverslips are acid washed prior to use by soaking them in concentrated nitric acid for 18 h and are then rinsed extensively with water. We use 22×22 -mm No. 1.5 coverslips, which match the 0.17-mm coverslip thickness correction of our objectives. To dry the coverslips, we dip them in ethanol and then flame them. To attach the coverslips to the dishes, we invert the dishes so that the base faces upward and apply a circle of molten paraffin wax around the hole using a paint brush. After the paraffin has cooled, we place a coverslip over the hardened paraffin and hold the inverted dish with the coverslip on it close to the surface of an inverted hot plate. As the paraffin beneath the coverslip melts, it spreads out between the coverslip and the dish. Once the paraffin has melted fully, the dish is removed from the heat and cooled immediately using a gentle stream of compressed air. Be careful not to apply the paraffin too close to the hole or to use too much paraffin or too much heat because this may cause the paraffin to flow into the well. Paraffin works well because it is not toxic to the cells and it remains hard at 37°C , yet the coverslip can be removed if necessary using a thin razor blade. Silicone adhesives such as aquarium sealant can also be used (Challacombe *et al.*, 1997), but we have not tried this ourselves. Coverslip culture dishes are now also available commercially (World Precision Instruments and Warner Instruments).

On the day before dissection, the coverslip culture dishes and lids are sterilized with 70% ethanol for 45 min. After air drying in the hood, the coverslips are treated with 1 mg/ml poly-D-lysine HBr (M_w 70–150,000, Sigma) in sodium borate

buffer, pH 8.5, for 3 h (150 μ l per well) as described by Higgins *et al.* (1991). We make up a 10-mg/ml stock solution in borate buffer and freeze it in aliquots. Prior to use, aliquots are diluted in borate buffer and sterilized by 0.2- μ m syringe filtration. After the polylysine treatment, the coverslips are rinsed three times with sterile water to remove polylysine that is not bound to the glass. A few milliliters of sterile water is then added to each dish and they are stored overnight. On the morning of the dissection, the coverslips are rinsed three more times with sterile water and are then coated with 10 μ g/ml mouse laminin (BD Biosciences) in L-15 or 10 μ g/ml phenol red-free Matrigel (BD Biosciences) in L-15. Matrigel is a basement membrane extract that is produced by Engelbreth–Holm–Swarm mouse tumor cells. It is an excellent substrate for SCG neurons, but we prefer not to use it for immunofluorescence applications because it does tend to form sticky clumps. The laminin and Matrigel are stored in aliquots at -80°C . To prevent gelation, they are thawed on a slurry of ice and water on the day of the dissection and are diluted into ice-cold L-15. After dilution, the L-15 is allowed to warm to room temperature. We apply 150 μ l of laminin or Matrigel solution per coverslip well and incubate for 4 h in the incubator (37°C , atmospheric CO_2). The dissection is performed during this incubation period and then the coverslips are rinsed once with L-15 before plating.

III. Transfecting Neurons by Nuclear Injection

Primary neurons are not transfected readily using many of the protocols that work well for mitotic cells. For example, when we have attempted to transfect cultured SCG neurons with cationic lipid reagents (e.g., Lipofectamine 2000, Gibco), we have obtained far fewer than one fluorescent cell per dish (unpublished observations). The principal reason for this appears to be that plasmids are not taken up readily by interphase nuclei. Better transfection efficiencies may be obtained with other approaches, such as infection with viral or retroviral vectors or transfection using electroporation or biolistics (discussed elsewhere in this volume). Which method is most suitable for a particular application will depend on the number of transfected cells required for the study, the relative ease or difficulty of the procedure, and the extent to which it is tolerated by the particular neuronal cell type being used. For studies on slow axonal transport in cultured neurons, other researchers have had success using infection with adenoviral vectors (Roy *et al.*, 2000) and transfection with calcium phosphate (Ackerley *et al.*, 2000). In my laboratory, we have had good success with microinjection of expression constructs directly into the cell nucleus (Garcia *et al.*, 1992; Wang *et al.*, 2000; Wang and Brown, 2001). This procedure has the advantage that it is simple, direct, and reliable. By minimizing the number and relative proximity of the injected cells in each dish, we can ensure that we are able to trace single axons of expressing cells for long distances without ambiguity. The principal disadvantages of this approach are (1) that it requires an inverted microscope equipped

with a pressure injection apparatus and a micromanipulator and (2) that it requires a certain amount of practice to perfect the technique. Nuclear injection is also not suitable for the transfection of large numbers of cells, but this is not a limitation for our live-cell imaging studies because a considerable amount of data can be obtained from a small number of cells.

For studies on the axonal transport of neurofilaments, we use a plasmid (pEGFP-NFM) that directs the expression of a green fluorescent fusion protein. This plasmid was produced by cloning the full-length cDNA for rat neurofilament protein M (NFM) into the multiple cloning site of the Clontech pEGFP-C1 mammalian expression vector (Wang *et al.*, 2000). The resulting fusion protein (GFP-NFM) consists of green fluorescent protein (GFP) linked to the amino terminus of NFM by a short linker. For studies on microtubules, we have also experimented with a GFP-tubulin fusion protein construct that is available commercially from Clontech (pEGFP-Tub). Both vectors use the human cytomegalovirus (CMV) immediate early promoter and the SV40 early mRNA polyadenylation signal, and both express in cultured SCG neurons transfected by nuclear injection. We have no experience with other promoters or expression vectors at this time. The plasmids are purified using a Qiagen Endo-free Maxi Prep kit, and the purified DNA is stored at 1–2 mg/ml in TE buffer (10 mM Tris-HCl, 1 mM EDTA, pH 8.0) in aliquots at -20°C . Prior to injection, the DNA is diluted to 0.6 mg/ml in TE or 50 mM potassium glutamate, pH 7.2. The cells appear to tolerate injection of either buffer with no apparent adverse effects. During the plasmid preparation, we take care to use disposable plastic whenever possible. If it is necessary to reuse plasticware such as centrifuge tubes, care should be taken to remove all traces of detergent after washing. We wash our centrifuge tubes with ES-7X detergent (ICN Biomedicals) and rinse thoroughly.

We currently inject using an Eppendorf Injectman NI2 semiautomated injection system, but for many years we used a simpler and less expensive manual system composed of a Narashige three-axis hydraulic manipulator and a Medical Systems Corporation PLI-100 pressure injector (Harvard Apparatus). The Eppendorf system uses internally generated compressed air as the pressure source, and the Medical Systems Corporation system uses an external source of compressed nitrogen gas. Both systems work well. The Eppendorf system is more complex to operate, but, once mastered, it can result in more reliable penetration of the plasma and nuclear membranes because it can be programmed to advance into the cell at rates of up to 7.5 mm/s. We perform our injections using a Nikon TE300-inverted microscope situated on a vibration isolation table (Technical Manufacturing Corporation). We pull our own micropipettes from thick-wall borosilicate glass (1.0 mm O.D., 0.58 mm I.D., 4 in. long with internal filament; World Precision Instruments) using a Sutter P-97 Flaming-Brown micropipette puller (Sutter Instrument Co.). The internal glass filament facilitates back-loading of the micropipettes by capillary action. The puller settings must be determined empirically for a given filament geometry and may vary with ambient temperature and humidity. The goal is to obtain a tip that is fine enough to penetrate nuclei but not so fine

that it frequently becomes blocked. We pull micropipettes with a two-stage pull cycle in order to obtain a short taper. The glass can be sterilized with dry heat (170°C for 3 h) prior to pulling, but we do not find this to be necessary. A container to hold glass capillary tubing during dry heat sterilization is available commercially (World Precision Instruments). To load the micropipette, we place approximately 1 μ l of injection solution at the opening of the capillary (the end opposite to the micropipette tip) and then suspend the micropipette vertically in a moist environment for a few minutes to allow the solution to draw down the capillary to the tip.

The micromanipulator is orientated so that the micropipette can be advanced axially into the cell at an angle of about 45° to the horizontal. Because we mount the micromanipulator on the left-hand side of the microscope, it is easiest for us to inject nuclei that are located on the left side of the cell body. If necessary, the culture dish can be rotated on the microscope stage to reorientate the cell body prior to injection. We typically inject cells 18–48 h after plating and observe them 1–3 days later. We inject under phase-contrast optics using a 40 \times objective and a 0.52 NA long working distance condenser, which provides sufficient clearance for the micropipette. It is necessary to remove the lid from the culture dish for injection, but this rarely results in microbial contamination. If the cells are to be kept out of the incubator for more than 20 min, we warm the dish and microscope stage to 37°C using an air stream incubator (see Section V,C). To prevent evaporation loss, we pipette a layer of low viscosity silicone fluid (0.75 ml dimethylpolysiloxane, 5 centistokes, Sigma) over the culture medium. The silicone fluid is prewarmed to 37°C and sterilized using a 0.2- μ m nylon syringe filter. After injection, we generally remove the silicone fluid and the culture medium by aspiration and replace with fresh medium. This may reduce the chance of microbial contamination, but the condition of the cells does not appear to be compromised if the silicone fluid is not removed and the medium is not changed. If cells are cultured in bicarbonate-buffered media, then the medium will become alkaline in atmospheric CO₂. To solve this problem it is necessary to use a buffering agent such as HEPES or to maintain elevated CO₂ concentrations on the microscope stage (McKenna and Wang, 1989).

Micoinjection of adherent cells does require some practice, but once the technique is mastered, it is possible to routinely locate and inject 15 neurons in a single dish within 20 min. The principal challenges are to penetrate the nucleus with minimal damage to the cell and to minimize blockage of the injector. To minimize blockages, we routinely clarify the injection solution by centrifugation or by filtration using an Amicon Ultrafree-MC 0.1- μ m centrifugal concentrator (Millipore Corporation). It is essential to include a fluorescent marker in the injection solution so that the flow rate can be adjusted empirically for each micropipette. The fluorescent marker also provides immediate visual confirmation of a successful injection (Fig. 2). We generally use rhodamine-labeled dextran (M_w 10,000 or 70,000, Molecular Probes). The smaller dextran diffuses out of the nucleus within minutes after injection. To maximize cell survival, it is critical to

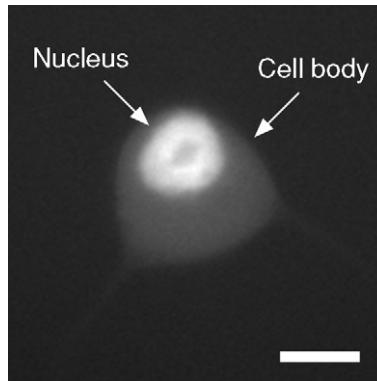


Fig. 2 Nucleus injected with fluorescent dextran. Cell body of a cultured SCG neuron imaged by epifluorescence microscopy immediately after microinjection of the nucleus with MW 70,000 rhodamine-labeled dextran. The dark spot within the nucleus represents the nucleolus, which excludes the fluorescent dextran. Scale bar: 10 μm .

use very low injection pressures. We typically use injection pressures of 7–14 hPa (0.1–0.2 psi) above the balance pressure (see later). Higher pressures result in damage to the nucleus. We have not measured the volume that is injected under these conditions, but it is small enough that we do not observe any noticeable increase in nuclear volume as judged by phase-contrast or differential interference contrast microscopy. Too much pressure or too much volume (e.g., sufficient to cause a visible increase in nuclear volume) will result in cell death.

It is important to use a pressure injection apparatus that can supply a constant balance pressure to the injector at all times in order to prevent medium being drawn into the micropipette tip by capillary action between injections. The magnitude of the balance pressure should be adjusted empirically for each pipette so that injection solution is trickling out into the medium at all times (the fluorescent dextran in the injection solution allows the flow rate to be observed directly). Cells can be injected by initiating the injection pressure before penetration and terminating the injection pressure after the tip is removed (“continuous flow technique”) or, alternatively, by initiating the injection pressure after the tip has penetrated the cell and terminating the injection pressure before it is removed. We generally use the latter method. The former method may reduce the chance of clogging during penetration, but it also results in more leakage of injection solution into the medium. This can temporarily obscure the fluorescence of the injected cell, making it difficult to determine whether the injection was successful.

In our studies using the GFP-NFM expression construct, about 20–30% of the injected cells typically survive and express GFP fluorescence, and the fusion protein becomes fully incorporated throughout the entire axonal neurofilament array within 3 days after microinjection (Wang *et al.*, 2000; Wang and Brown, 2001). The brightness of GFP fluorescence varies from cell to cell, depending on the expression level. Most of the cell death can be attributed to injury during the

injection or toxicity due to overexpression of the GFP-NFM fusion protein. We have not investigated how soon GFP fluorescence first appears, but some delay is expected because GFP is known to acquire its fluorescent properties through a slow posttranslational autocatalytic oxidative reaction that has been estimated to take several hours for wild-type GFP (Heim *et al.*, 1994).

IV. Injecting Neurons with Fluorescent Proteins

Slow axonal transport can also be studied by the direct injection of a fluorescently labeled protein into the cytoplasm of cultured neurons. For our studies on the axonal transport of microtubules, we injected rhodamine-labeled bovine brain tubulin (Cytoskeleton, Inc.) into the cytoplasm of cultured rat SCG neurons (Wang and Brown, 2002). The injection technique is similar to that described earlier except that we pull micropipettes with slightly broader tips (lower velocity trip point on the Sutter micropipette puller) and use higher injection pressures. In general, cultured neurons will tolerate the injection of significant volumes into their cytoplasm and the survival rate is much higher than for nuclear injection, even if the volume injected is sufficient to cause the cell to swell visibly.

V. Observing Movement

The study of slow axonal transport is challenging because of the small size and dynamic nature of the moving structures (macromolecular complexes of cytoskeletal and cytosolic proteins) and because of the rapid and intermittent nature of their movement. For example, observations on the slow axonal transport of cytoskeletal proteins require imaging strategies that are capable of detecting rapid, infrequent and asynchronous movements of cytoskeletal polymers (Brown, 2000). This section describes two such approaches that have enabled us to observe the rapid movement of neurofilaments and microtubules in axons of cultured SCG neurons.

A. Naturally Occurring Gaps

Cultured neurons from the SCG of neonatal rats express low levels of neurofilament protein and frequently exhibit short segments of axon that lack neurofilaments entirely. These “gaps” in the axonal neurofilament array arise naturally in these neurons and appear to have no functional significance, but they do present a unique opportunity for studies on the movement of neurofilaments in axons (Wang *et al.*, 2000; Roy *et al.*, 2000). To detect movement, a GFP-tagged neurofilament protein is expressed in cultured SCG neurons and is allowed to incorporate throughout the endogenous neurofilament array, and then gaps in the axonal neurofilament array are located and observed by live-cell time-lapse fluorescence

imaging. Rapidly moving neurofilaments can be detected as they move through these gaps because the gaps are devoid of other neurofilaments; essentially all of the neurofilament protein is polymerized in these neurons so there is negligible background fluorescence due to diffusible neurofilament subunits. We have also observed gaps in the neurofilament array of cultured rat brain cortical neurons, but not in cultures of rat dorsal root ganglion (DRG) neurons, which express much higher amounts of neurofilament protein. We have never observed gaps in the microtubule or microfilament array of any cultured neuron, which is consistent with the fact that the continuity of these cytoskeletal arrays is critical for axon survival. Thus, while gaps are unique to the axonal neurofilament array, they are not unique to SCG neurons.

B. Photobleaching

Slow axonal transport can also be observed in cultured neurons using fluorescence photobleaching. For example, to detect the movement of neurofilaments, a GFP-tagged neurofilament protein is expressed in cultured SCG neurons and is allowed to incorporate throughout the endogenous neurofilament array, and then the fluorescence is bleached in a segment of axon and the bleached region is observed by live-cell time-lapse fluorescence imaging. Neurofilaments that move into the bleached region are fluorescent (and can thus be detected) because they originate from the surrounding nonbleached regions of axon flanking the bleached region. In contrast to the observation of naturally occurring gaps in the neurofilament array, this approach can reveal the movement of neurofilaments in axons that do not exhibit gaps, and also the movement of other proteins that are distributed continuously along the axons. For example, we have used photobleaching to detect the movement of both GFP-tagged neurofilament proteins and rhodamine-labeled tubulins in axons of cultured SCG neurons (Wang and Brown, 2001, 2002). By comparing the kinetics of neurofilament movement in photobleached axons and in naturally occurring gaps, we have established that the bleaching process does not impair movement (Wang and Brown, 2001).

We perform the photobleaching using a standard Nikon TE300 or Nikon TE2000 inverted microscope equipped for epifluorescence and a Plan Apo 100×/1.4 NA phase-contrast or DIC oil-immersion objective. The region of axon to be bleached is positioned in the center of the field of view and then the field diaphragm in the epifluorescence illumination light path is closed down to illuminate only the area that is to be bleached. The fluorescence is then excited continuously for 30–120 s using a standard epifluorescence filter cube and epiillumination from a standard mercury arc lamp (HBO100W/2). While the long duration of this bleaching exposure makes this approach unsuitable for many photobleaching applications, it is not a problem for studies on slow axonal transport because of the asynchronous and infrequent nature of the movement. To obtain the maximum possible light intensity for photobleaching, we remove all neutral density filters from the epifluorescence illumination light path for the

bleaching exposure (radiant intensity = 600 kW/m^2) and then replace them prior to subsequent imaging. Because bleaching at this intensity is relatively slow, it is desirable to select thin axons, which can be bleached more readily than thicker axons. Imaging can begin immediately after bleaching—no recovery period appears to be necessary. However, care must be taken to watch for evidence of photodamage caused by the bleaching process. We can bleach GFP-tagged neurofilament protein in axons of cultured SCG neurons for up to 2 min without noticeable impairment of neurofilament movement, so we believe that there is minimal photodamage under these conditions (Wang and Brown, 2001). Longer bleach times, however, can cause blebbing and vesiculation of the axons, which is a clear sign of damage.

Many previous studies on slow axonal transport in cultured neurons have used laser photobleaching, but those studies did not detect movement (Lim *et al.*, 1989, 1990; Okabe and Hirokawa, 1990, 1993; Okabe *et al.*, 1993; Takeda *et al.*, 1994, 1995; Chang *et al.*, 1998; Sabry *et al.*, 1995). It now appears that those studies failed because they were designed with the expectation of a slow and synchronous movement and were not capable of detecting rapid asynchronous movements (Brown, 2000). For example, those studies bleached short regions of axon ($3\text{--}5 \mu\text{m}$ in length) and acquired images with long time-lapse intervals (typically 5 min or more). Our photobleaching strategy differs from previous strategies in that it is designed with the explicit expectation of rapid asynchronous movements (Wang and Brown, 2001). The key features of our approach are (1) the use of thin axons, which can be bleached sufficiently to allow the detection of the moving polymers without causing photodamage; (2) the use of short time-lapse intervals (2–5 s), which enables the detection of rapid movements (see Section V,C); and (3) the use of long bleached regions ($20\text{--}60 \mu\text{m}$ in length), which enables entire cytoskeletal polymers to be observed while they are moving.

Another difference between our photobleaching method and previous methods is that we use a mercury arc lamp to bleach the fluorescence. The principal advantage of this approach is that it can be performed with a standard epifluorescence microscope and that it is easy to bleach large areas of the field of view. However, a disadvantage of this method is that the relatively low energy of the mercury light source necessitates long bleaching times. More efficient bleaching could be accomplished using a laser, but lasers are not readily adapted to bleaching large areas of the field of view. A solution to this problem would be to bleach axons using a laser-scanning confocal microscope, although we have not tried this ourselves.

C. Live-Cell Imaging

One of the challenges associated with live-cell fluorescence imaging is to minimize photobleaching and photodamage. Because photobleaching and photodamage are enhanced in the presence of oxygen, we observe the neurons in a sealed chamber containing oxygen-depleted medium (see later), essentially as described by Dent *et al.* (1999) (see Fig. 3). Cultured neurons thrive for many hours under

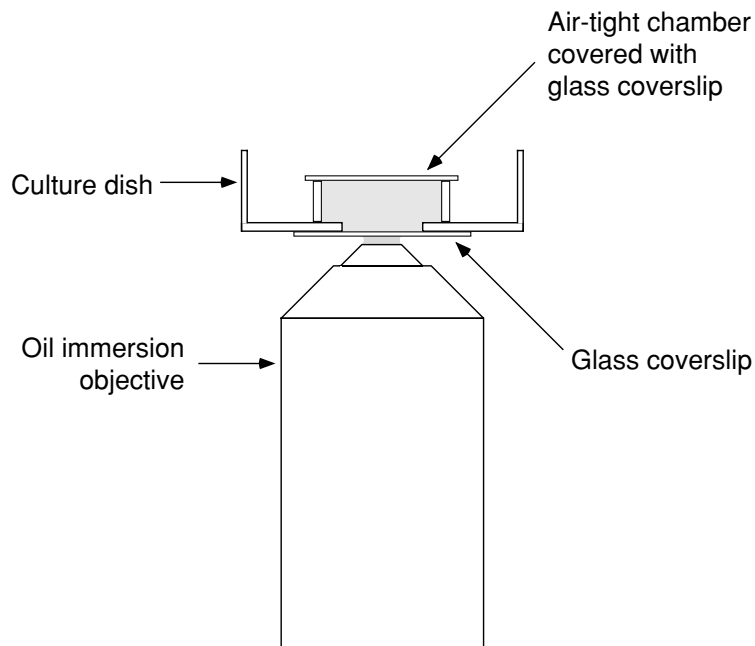


Fig. 3 Sealed imaging chamber for live-cell fluorescence imaging. The chamber is constructed by placing a cylindrical glass ring around the well, filling it with oxygen-depleted medium, and then covering it with a glass coverslip. The glass ring is sealed to the dish and to the top coverslip using silicone grease.

these conditions because their energy metabolism is predominantly glycolytic. To assemble the chamber, we aspirate the medium from the culture dish (leaving medium in the well), rinse with deoxygenated culture medium, and then seal a cylindrical glass ring (“micro slide ring,” 15 mm diameter, 5 mm high; Thomas Scientific) to the dish around the well using type 111 silicone grease (Dow Chemical Co.). The chamber created by this ring is then filled to the brim with deoxygenated culture medium (volume of 0.9 ml) and a coverslip is sealed to the top of the ring using silicone grease.

To deplete oxygen from the culture medium, we use Oxyrase (Oxyrase Inc.), which is a bacterial membrane fraction that contains enzymes of oxidative phosphorylation (Mikhailov and Gundersen, 1995). It is necessary to confirm the activity of the Oxyrase in the culture medium (e.g., using an oxygen electrode) because it may not be as active as expected; while Oxyrase can deplete oxygen from 50 mM phosphate buffer in a matter of minutes, we have found that it takes 2 h in our L-15-based medium. Thus we incubate the culture medium with Oxyrase at 37°C for at least 2 h prior to assembling the imaging chamber. It is also critical to include an adequate substrate for the Oxyrase enzymes. We supplement the medium with 20 mM sodium succinate and 20 mM sodium DL-lactate (Sigma).

We incubate the medium with Oxyrase in a disposable syringe, taking care to eliminate any air bubbles or spaces and to seal the opening with Parafilm. Because the membranes in the Oxyrase tend to aggregate during the incubation, we attach a 0.2- μm syringe filter to the syringe and filter the oxygen-depleted medium directly into the imaging chamber. We then seal the chamber immediately so as to minimize exposure of the oxygen-depleted medium to the air. Care should be taken to avoid leaving any trapped air bubbles in the chamber as these will interfere with observation and possibly also compromise the efficacy of the Oxyrase.

To maintain the temperature on the microscope stage, we use an air stream incubator (Nevtek). This approach has the advantage that it heats the dish, stage, and objective. Cells thrive on the microscope stage for many hours with this arrangement. We usually warm the microscope for 30–60 min before use. Because the fan generates vibration, it must be isolated mechanically from the microscope. We place it on an equipment shelf supported above the vibration isolation tabletop and direct the air stream under the stage of the inverted microscope so that it is angled up toward the base of the dish (in order to prevent vibration of the micropipette during microinjection).

To observe the cells, we use a Nikon TE300 or TE2000-inverted microscope. For fluorescence imaging, we try to use optics with the highest numerical aperture and light throughput. In our experience, Plan Apo DIC objectives are generally the best choice. We recommend that individual objectives be compared quantitatively because we have found significant differences that would not be apparent from the manufacturer's specifications. Fluorescent polystyrene beads (Molecular Probes) that fluoresce across the entire visible spectrum are excellent for such quantitative comparisons because they are bright, uniform, and very photostable. It is also desirable to use the most efficient light path on the microscope (minimizing any lens elements that might lead to loss of light) and to use the most sensitive detection device available.

In selecting a camera for live-cell fluorescence imaging, three features are of paramount importance: sensitivity, resolution, and speed. Generally there is a trade-off between speed and resolution on the one hand and sensitivity on the other. According to the Nyquist theorem, the best possible resolution is obtained when the pixel size of the camera chip is less than half the optical resolution of the microscope objective (Young, 1989). We are currently using two different cooled CCD cameras for live-cell imaging. For better sensitivity, we use a Princeton Instruments Micromax 512 BFT camera with 512×512 back-illuminated chip (Roper Scientific). The pixel size of this chip is $13.0 \times 13.0 \mu\text{m}$, which corresponds to $0.131 \mu\text{m}$ per pixel using a $100\times$ objective on our inverted Nikon microscopes. This camera has a full frame readout time of 350 ms, a quantum efficiency of about 85% in green light, and a read noise of eight electrons at 1 MHz. For better speed, we use a Photometrics CoolSNAP HQ camera with a 1392×1040 front-illuminated interline chip (Roper Scientific). The pixel size of this chip is $6.45 \times 6.45 \mu\text{m}$, which corresponds to $0.065 \mu\text{m}/\text{pixel}$ when using a $100\times$ objective on our inverted Nikon microscopes. This camera has a full frame readout time of 100 ms,

a quantum efficiency of about 60% in green light, and a read noise of six electrons at 10 MHz. Because our exposure times tend to be quite long (typically 1 s), we have found that the sensitivity of the camera (determined by quantum efficiency and read noise) can sometimes be a more critical determinant of the rate of image acquisition than the actual readout time. In other words, a camera with a shorter readout time may not necessarily result in faster image acquisition if longer exposures and/or frame averaging is required to detect the fluorescent signal.

To observe movement, fluorescent cells are located at low magnification using a 10 or 40 \times objective and then examined at high magnification using a Plan Apo 100 \times /1.4 NA DIC or phase-contrast oil-immersion objective. We avoid cells that are overly bright because of the potential for artifacts associated with high concentrations of exogenous protein. To find gaps in the neurofilament array or to locate axons that are suitable for photobleaching, we scan along the axons using epifluorescence and either phase contrast or DIC, always taking care to observe the fluorescence as little as possible. We stop down the field diaphragm in the epifluorescence illumination light path to prevent exposing areas outside the field of view. The neurons are cultured at low density (see Section II,A) so that axons can be traced from the cell body to the growth cone. This is necessary in order to establish the proximal and distal orientation of the axons in the time-lapse movies. The low density also helps minimize axonal fasciculation.

Time-lapse fluorescence images are acquired using the “acquire time-lapse” function in Metamorph software (Universal Imaging Corporation). We use electronic shutters on the mercury and halogen light sources, which can be controlled with foot switches (for hands-free manual operation) and from Metamorph software (for automated operation during image acquisition). To reduce photobleaching, it is necessary to minimize the intensity of the exciting light and the duration of the fluorescence exposures. Typically we attenuate the mercury light source by 85–90% using neutral density filters and use exposures of about 1 s. Under these conditions, we are typically able to acquire time-lapse movies that are 100–200 images in length. Because the movements are very infrequent, it is not unusual to acquire movies in which no movement is observed, especially if the movie is short. For example, in our studies on neurofilaments, we observed an average of one moving neurofilament every 5 min (Wang and Brown, 2001; Wang *et al.*, 2000). To maximize the duration of the movies, we use the longest time-lapse intervals that we can without sacrificing our ability to track the movements. For studies on neurofilaments, time-lapse intervals of 4 or 5 s are a good compromise, allowing us to acquire movies that are approximately 5–15 min in length. The principal factors limiting the duration of our time-lapse movies are the sensitivity of the camera and the brightness and photostability of the GFP. Fig. 4 shows an example of time-lapse imaging of a neurofilament moving through a photobleached axon obtained using the methods described in this chapter.

A problem that we often encounter during the acquisition of time-lapse movies is focus drift. The causes of focus drift are either mechanical (e.g., instability in the focusing mechanism of the microscope) or thermal (expansion and contraction of

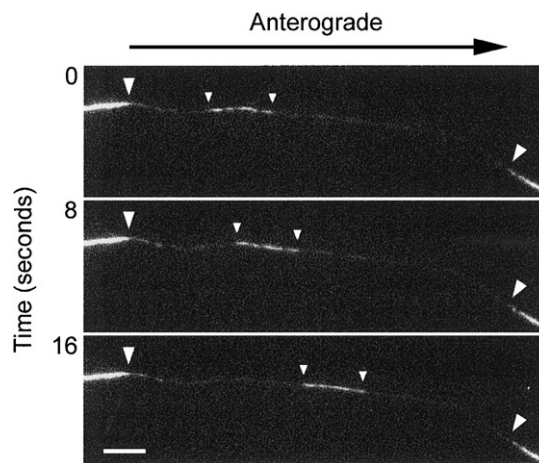


Fig. 4 Movement of a neurofilament through the photobleached region of an axon. Axon of a cultured SCG neuron expressing a GFP-tagged neurofilament protein. These images were selected from a time-lapse movie in which images were acquired at 4-s intervals. GFP fluorescence was bleached as described in Section V.B. A fluorescent neurofilament can be seen moving in an anterograde direction through the photobleached region. Small white arrowheads mark the leading and trailing ends of the moving neurofilament, and large white arrowheads mark the edges of the photobleached region. Proximal is left and distal is right. Data from Wang and Brown (2001). Scale bar: 5 μm .

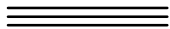
the microscope stage and/or optics). With practice, one can learn to anticipate and correct for this drift during image acquisition by making small adjustments to the fine focus on the microscope in between image acquisitions. We have found that a motorized Z axis (Prior Scientific) helps by giving the user more precise control over the fine focus movement. It is also helpful to keep the temperature of the microscope and room as stable as possible.

D. Motion Analysis

The movement of fluorescent structures can be tracked in successive frames of the time-lapse movies using the “track points” function in the Metamorph software and data can be logged directly to an Excel worksheet. It is important to establish objective criteria for the analysis. We generally exclude structures if they move less than a total distance of 10 μm during the course of the movie or if their location is ambiguous: this excludes objects that jiggle around but do not display directed movement. Ambiguity can arise due to poor focus, overlap with other moving or pausing structures, or loss of brightness due to photobleaching. When tracking the movement of neurofilaments or microtubules, we generally follow the position of the leading end. Fiduciary points in the field of view can be used to ensure that there is no stage drift during the movie, although this is rarely a problem. If stage drift does occur, planes in the stack can be registered using the “align stack” function in Metamorph. For presentation, we save the time-lapse

images in RGB tiff format using the “convert stack to TIFFs” feature in the Metamorph software and then import them into Adobe Premiere for movie construction and editing. QuickTime movies are created with a play-back rate of six to eight frames per second. If necessary, the movies can be compressed with a lossy compression algorithm (“codec”) such as Cinepak.

To facilitate detection of the moving structures in time-lapse movies, we sometimes perform difference imaging. To obtain a rolling difference image, each image in the time-lapse series is subtracted from the image that follows it. To obtain a fixed-frame difference image, a single reference image at the start of the time-lapse series is subtracted from all subsequent images in the series. Both methods selectively enhance changes in fluorescence intensity within the field of view, such as those associated with the movement of fluorescent structures. We have found difference imaging to be especially useful for photobleaching studies on microtubule movement in axons because the pool of unpolymerized tubulin recovers its fluorescence rapidly after bleaching due to the diffusion of fluorescent tubulin subunits from the adjacent unbleached regions, and this fluorescence is often sufficient to completely or partially obscure the moving polymers in the raw images (Wang and Brown, 2002).



VI. Conclusion

For many years it had been assumed that proteins conveyed by slow axonal transport move in a slow and synchronous manner, but attempts to observe this movement by live-cell imaging have been largely unsuccessful. Recent observations by ourselves and others on the movement of neurofilaments and microtubules in axons of cultured neurons have demonstrated that the movements are neither slow nor synchronous; both neurofilaments and microtubules actually move in a rapid and asynchronous manner, but the overall rate is slow because the movements are also very infrequent. In other words, these structures spend most of their time not moving during their journey down the axon. This remarkable motile behavior presents special challenges for live-cell imaging studies, but I hope that this chapter has demonstrated that they are not insurmountable and that movement can be detected if the experiments are designed with the expectation of rapid and infrequent movements.

Acknowledgments

I thank Yanping Yan and Kitty Jensen for their helpful comments on this manuscript and Reyna Martinez for the image used in Fig. 2. This work was supported by a grant from the NINDS to A.B.

References

- Ackerley, S., Grierson, A. J., Brownlee, J., Thornhill, P., Anderton, B. H., Leigh, P. N., Shaw, C. E., and Miller, C. C. (2000). Glutamate slows axonal transport of neurofilaments in transfected neurons. *J. Cell Biol.* **150**, 165–176.

- Bray, D. (1991). Isolated chick neurons for the study of axonal growth. In "Culturing Nerve Cells." (G. Banker and K. Goslin, eds.), pp. 119–135. MIT Press, Cambridge, MA.
- Brown, A. (2000). Slow axonal transport: Stop and go traffic in the axon. *Nature Rev. Mol. Cell Biol.* **1**, 153–156.
- Challacombe, J. F., Snow, D. M., and Letourneau, P. C. (1997). Dynamic microtubule ends are required for growth cone turning to avoid an inhibitory guidance cue. *J. Neurosci.* **17**, 3085–3095.
- Chang, S. H., Rodionov, V. I., Borisy, G. G., and Popov, S. V. (1998). Transport and turnover of microtubules in frog neurons depend on the pattern of axonal growth. *J. Neurosci.* **18**, 821–829.
- Dent, E. W., Callaway, J. L., Szebenyi, G., Baas, P. W., and Kalil, K. (1999). Reorganization and movement of microtubules in axonal growth cones and developing interstitial branches. *J. Neurosci.* **19**, 8894–8908.
- Garcia, I., Martinou, I., Tsujimoto, Y., and Martinou, J. C. (1992). Prevention of programmed cell death of sympathetic neurons by the bcl-2 proto-oncogene. *Science* **258**, 302–304.
- Hawrot, E., and Patterson, P. H. (1979). Long-term culture of dissociated sympathetic neurons. *Methods Enzymol.* **58**, 574–584.
- Heim, R., Prasher, D. C., and Tsien, R. Y. (1994). Wavelength mutations and posttranslational autoxidation of green fluorescent protein. *Proc. Nat. Acad. Sci. USA* **91**, 12501–12504.
- Higgins, D., Lein, P. J., Osterhout, D. J., and Johnson, M. I. (1991). Tissue culture of mammalian autonomic neurons. In "Culturing Nerve Cells." (G. Banker and K. Goslin, eds.), pp. 177–205. MIT Press, Cambridge, MA.
- Johnson, M. I., and Argiro, V. (1983). Techniques in the tissue culture of rat sympathetic neurons. *Methods Enzymol.* **103**, 334–347.
- Johnson, M. I., Iacovitti, L., Higgins, D., Bunge, R. P., and Burton, H. (1981). Growth and development of sympathetic neurons in tissue culture. *CIBA Found. Symp.* **83**, 108–122.
- Lasek, R. J., Garner, J. A., and Brady, S. T. (1984). Axonal transport of the cytoplasmic matrix. *J. Cell Biol.* **99**, 212s–221s.
- Lim, S.-S., Edson, K. J., Letourneau, P. C., and Borisy, G. G. (1990). A test of microtubule translocation during neurite elongation. *J. Cell Biol.* **111**, 123–130.
- Lim, S.-S., Sammak, P. J., and Borisy, G. G. (1989). Progressive and spatially differentiated stability of microtubules in developing neuronal cells. *J. Cell Biol.* **109**, 253–263.
- Mahanthappa, N. K., and Patterson, P. H. (1998). Culturing mammalian sympathoadrenal derivatives. In "Culturing Nerve Cells." (G. Banker and K. Goslin, eds.), pp. 289–307. MIT Press, Cambridge, MA.
- McKenna, N. M., and Wang, Y. L. (1989). Culturing cells on the microscope stage. *Methods Cell Biol.* **29**, 195–205.
- Mikhailov, A. V., and Gundersen, G. G. (1995). Centripetal transport of microtubules in motile cells. *Cell Motil. Cytoskel.* **32**, 173–186.
- Okabe, S., and Hirokawa, N. (1990). Turnover of fluorescently labelled tubulin and actin in the axon. *Nature* **343**, 479–482.
- Okabe, S., and Hirokawa, N. (1993). Do photobleached fluorescent microtubules move? Re-evaluation of fluorescence laser photobleaching both in vitro and in growing *Xenopus* axons. *J. Cell Biol.* **120**, 1177–1186.
- Okabe, S., Miyasaka, H., and Hirokawa, N. (1993). Dynamics of the neuronal intermediate filaments. *J. Cell Biol.* **121**, 375–386.
- Roy, S., Coffee, P., Smith, G., Liem, R. K. H., Brady, S. T., and Black, M. M. (2000). Neurofilaments are transported rapidly but intermittently in axons: Implications for slow axonal transport. *J. Neurosci.* **20**, 6849–6861.
- Sabry, J., O'Connor, T. P., and Kirschner, M. W. (1995). Axonal transport of tubulin in T1l pioneer neurons in situ. *Neuron* **14**, 1247–1256.
- Takeda, S., Funakoshi, T., and Hirokawa, N. (1995). Tubulin dynamics in neuronal axons of living zebrafish embryos. *Neuron* **14**, 1257–1264.

- Takeda, S., Okabe, S., Funakoshi, T., and Hirokawa, N. (1994). Differential dynamics of neurofilament-H protein and neurofilament-L protein in neurons. *J. Cell Biol.* **127**, 173–185.
- Wang, L., and Brown, A. (2001). Rapid intermittent movement of axonal neurofilaments observed by fluorescence photobleaching. *Mol. Biol. Cell* **12**, 3257–3267.
- Wang, L., and Brown, A. (2002). Rapid movement of microtubules in axons. *Curr. Biol.* **12**, 1496–1501.
- Wang, L., Ho, C.-L., Sun, D., Liem, R. K. H., and Brown, A. (2000). Rapid movement of axonal neurofilaments interrupted by prolonged pauses. *Nature Cell Biol.* **2**, 137–141.
- Young, I. T. (1989). Image fidelity: Characterizing the imaging transfer function. *Methods Cell Biol.* **30**, 1–45.

This Page Intentionally Left Blank

CHAPTER 15

Making Proteins into Drugs: Assisted Delivery of Proteins and Peptides into Living Neurons

Gianluca Gallo

Department of Neurobiology and Anatomy
Drexel University College of Medicine
Philadelphia, Pennsylvania 19129

- I. Introduction
- II. Principles
 - A. Peptide Sequences within Proteins That Promote Cellular Uptake
 - B. Noncovalently Associated Peptides That Promote Cellular Uptake
 - C. Circumventing the Endocytotic Degradation Pathway
 - D. Protein Transduction Domains (PTDs) and Protein Transduction Peptides (PTPs) Exhibit Minimal Toxicity
 - E. Specificity of Subcellular Delivery of PTP Cargo
 - F. Retention of Biological Activity by PTP-Delivered Cargo
 - G. Time Course of Cargo Delivery by PTPs
 - H. Molecular Handshakes between PTPs and Their Cargo
 - I. Serum Does Not Interfere with PTP-Mediated Cargo Delivery
- III. Materials
 - A. Purchasing and Producing Proteins and Peptides Containing PTDs
 - B. Chariot: A Commercially Available PTP
- IV. Methods
 - A. General Comments on the Introduction of Reagents to Neuronal Cultures
 - B. Use of Antennapedia-Conjugated Peptides
 - C. Use of Chariot PTP to Deliver Proteins and Peptides into Neurons
- V. Conclusions and Perspectives
 - A. Making Your Favorite Protein into a Drug: A Bonus for the Basic Research Scientist
 - B. Potential Applications of the Use of Peptide-Based Methodologies to the Development of *in Vivo* Therapies
- References

The introduction of exogenous proteins and peptides into cells is a valuable experimental approach. However, exogenous proteins are not internalized by living cells readily. This limitation has been overcome by the development of peptide-based methods that assist in the delivery of exogenous proteins into the cytoplasm and nucleus. These methods may facilitate the *in vivo* delivery of reagents in therapies aimed at neurodegenerative disorders and recovery from nervous system injury.

I. Introduction

The delivery of biologically active proteins, or inhibitors of protein function, into living primary neurons is an important approach to the study of the molecular machinery of neuronal cell biology. Unfortunately, the introduction of exogenous proteins and peptides into neurons is not a trivial matter. Thus, researchers have often relied upon pharmacological reagents (hereby referred to as drugs). Pharmacological inhibition, or activation, of cellular signaling pathways and cytoskeletal dynamics has allowed a number of fundamental discoveries in neurons. The use of drugs allows for a high degree of experimental control. Pharmacological analysis has a number of advantageous features: (1) many drugs are internalized by cells readily or are cell membrane permeable, (2) can be washed out, (3) large numbers of cells can be exposed simultaneously to the drug, and (4) the concentration of the drug is controlled easily, allowing for dose–response studies. These features are very important to the investigation of protein function in living cells. In recent years, novel techniques have been developed that allow the introduction of purified proteins and peptides into living neurons with relative ease. These new methods are beginning to allow investigators to apply the advantageous features of pharmacological analysis to studies utilizing purified proteins and peptides.

The purpose of this chapter is to introduce the reader to peptide-based methods that allow efficient protein internalization into living neurons *in vitro*. Two separate classes of peptides that promote the internalization of exogenously applied proteins are discussed: peptides that are incorporated into the sequence of a protein or attached to proteins covalently and peptides that bind noncovalently to purified proteins in solution and promote cellular uptake of the peptide–protein complex.

II. Principles

A. Peptide Sequences within Proteins That Promote Cellular Uptake

Some proteins are internalized by cells. These proteins contain amino acid sequences termed protein transduction domains (PTD). PTDs have been identified in proteins ranging from viral proteins (e.g., TAT from human HIV-1;

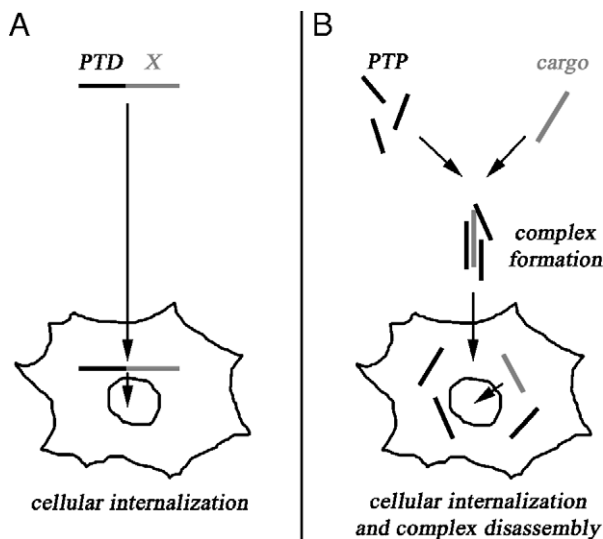


Fig. 1 Protein transduction domains (PTD) and protein transduction peptides (PTP). (A) PTDs are linked covalently to protein cargo (X) and are internalized into the cytosol and nucleus. (B) PTPs associate with the protein cargo noncovalently and allow delivery of the cargo into the cytosol. If the cargo contains a nuclear internalization domain, it can then be translocated into the nucleus.

Frankel and Pabo, 1988) to drosophila neuronal transcription factors (e.g., Antennapedia homeodomain, Perez *et al.*, 1992). Additional PTDs have been designed and tested (for a review, see Dunican and Doherty, 2001), and other homeodomain transcription factors contain PTDs (engrailed, Cosgaya *et al.*, 1998; islet-1, Kilk *et al.*, 2001). The Antennapedia PTD, also termed penetratin, has been used to deliver peptides inhibitory to signaling proteins into neurons (Williams *et al.*, 1996; Vastrik *et al.*, 1999; Aizawa *et al.*, 2001; Journey *et al.*, 2002). PTDs can be either linked to a protein covalently or inserted into its sequence in order to render it cell permeable (Fig. 1). Thus, proteins containing PTDs must be individually designed and produced using either molecular biology techniques, resulting in the production of PTD fusion proteins, or through the covalent attachment of PTDs to purified proteins. PTDs in tandem with short peptides can also be manufactured through standard peptide synthesis methodologies. Each of these approaches, and commercially available sources of reagents, will be presented in Section III,A.

B. Noncovalently Associated Peptides That Promote Cellular Uptake

A disadvantage of PTDs is that each PTD–protein conjugate must be developed individually. To overcome this methodological limitation, cell-permeable peptides that associate noncovalently with proteins have been developed (Fig. 1). This class

of protein transduction peptides (PTP) is designed to associate with cargo proteins through hydrophobic interactions. Additional domains in PTPs have been designed to increase solubility and intracellular delivery. Once complexed with the cargo protein, PTPs assist in internalization of the protein. Following internalization, the PTP–protein cargo complex dissociates within the cytoplasm, releasing the cargo protein into the cell (Fig. 1). A commercially available PTP, Chariot (ActiveMotif Inc., Carlsbad, CA), has been used to deliver the Rac1 GTPase (Journey *et al.*, 2002) and C3 transferase protein (Gallo *et al.*, 2002) into primary neurons.

The association of PTPs with proteins depends on the structure and biophysical properties of both components of the complex, and thus complex formation may vary between different combinations of PTPs and proteins. However, studies using Chariot found efficient association and intracellular delivery of disparate proteins and peptides [Morris *et al.*, 2001; The Pep-1 peptide described in Morris *et al.* (2001) has the same sequence as the commercially available Chariot peptide]. Even large molecules, such as IgGs, can be delivered efficiently using PTPs. A growing literature on the use and design of PTDs is already available (e.g., Lindgren *et al.*, 2000; Dunican and Doherty, 2001). Thus, this chapter focuses on the use of the Chariot PTP.

C. Circumventing the Endocytotic Degradation Pathway

Ideally, methods that promote the cellular internalization of proteins should bypass the degradation pathways normally associated with the uptake of extracellular proteins. The mode of action of both PTDs and PTPs does not appear to involve endocytosis or routing of proteins through the lysosomal degradation pathways (Derossi *et al.*, 1994; Morris *et al.*, 2001). This is an important feature of these delivery methods as it allows the internalized proteins to retain their biological activity for prolonged time periods.

D. Protein Transduction Domains (PTDs) and Protein Transduction Peptides (PTPs) Exhibit Minimal Toxicity

Ideal protein transfection reagents must not exhibit cellular toxicity within the range of concentrations required for protein internalization. The Chariot PTP is not toxic to cells at concentrations that effectively internalize proteins *in vitro* (Morris *et al.*, 2001). The full-length Antennapedia peptide (60 amino acids) exhibits neurotrophic action and is not toxic to neurons (Bloch-Gallego *et al.*, 1993). The Antennapedia PTD (minimal 16 amino acid sequence for internalization) is not toxic at concentrations that sufficiently deliver the conjugated cargo and have biological actions (Vastrik *et al.*, 1999; Aizawa *et al.*, 2001; Journey *et al.*, 2002). An intraperitoneal injection of the Antennapedia PTD (100 $\mu\text{g}/\text{day}$) in mice did not result in adverse effects, although the associated cargo had biological effects (Hotosani *et al.*, 2002). A study of the uptake and spread of the Antennapedia PTD revealed that injection of the PTD into the ventricles does not allow spread into the brain

(Bolton *et al.*, 2000). However, direct focal injection into the brain matter delivered the PTD effectively. Focal injections greater than 1 μg of the Antennapedia PTD in adult rat brain caused cytotoxicity and recruitment of inflammatory response cells. However, Antennapedia PTD-delivered cargo *in vitro* is capable of eliciting cell responses at concentrations of a few micrograms per milliliter, indicating that sufficient delivery of reagents in the intact brain is feasible.

E. Specificity of Subcellular Delivery of PTP Cargo

Following intracellular delivery by PTPs, peptides/proteins that contain nuclear localization domains are found within the nucleus (Morris *et al.*, 2001). In the absence of nuclear localization domains, the PTP cargo is released in the cytoplasm. These observations indicate that the PTP–cargo complex dissociates in the cytoplasm and that the final localization of the cargo is determined by its inherent intracellular targeting properties. Thus, it should be possible to specifically deliver protein cargo using PTPs to any subcellular region in conjunction with targeting sequences present in the cargo. Waizenegger *et al.* (2002) reported that the Antennapedia PTD, once internalized, distributes evenly between the cytosol and the nucleus, indicating that the protein attached to the PTD will be delivered to both cellular compartments. This feature of the Antennapedia PTD has been taken advantage of by coupling it to oligonucleotides in order to increase the delivery of oligonucleotides into the nucleus (Troy *et al.*, 1996; Fisher *et al.*, 2002). Similarly, a PTP that binds single- and double-stranded DNA and contains a nuclear localization signal has been used to transfect oligonucleotides and plasmids into living cells (Morris *et al.*, 1997).

F. Retention of Biological Activity by PTP-Delivered Cargo

A variety of enzymes have been introduced into cells using PTPs (e.g., β -Gal, Rho-family GTPases). Delivered enzymes have been shown to retain their activity through either biological assays or the visualization of reaction products (Morris *et al.*, 2001; Jurney *et al.*, 2002; Gallo *et al.*, 2002). While reports in the literature thus far are promising, the bioactivity of individual PTP cargo following delivery should be determined using proper positive and negative controls.

G. Time Course of Cargo Delivery by PTPs

An important feature of peptide-based protein delivery is that it allows for the relatively rapid introduction of proteins into cells. Using DNA-based transfection, a protein product is not usually observed until 8–24 h following transfection. Protein cargo delivered using Chariot is delivered within as short a time interval as 10 min (Morris *et al.*, 2001). However, treatment with the PTP–cargo complex of 1–3 h may be required depending on the nature of the cargo (<http://www.activemotif.com/products/cell/Chariot.html>), with the internalization of large cargo molecules (e.g., IgG) requiring longer time intervals.

H. Molecular Handshakes between PTPs and Their Cargo

The ratio of PTPs to cargo protein that results in the most efficient cargo delivery should be determined for each combination of PTP and cargo. In studies of the stoichiometry of PTP association with cargo, Morris *et al.* (2001) reported that multiple PTPs bind to each cargo molecule (protein or peptide). Data indicate that binding of PTPs to cargo will occur to saturation and that the majority of remaining PTPs stay in solution as monomers. At high ratios of PTP to protein, some aggregates of PTP–protein have been detected. However, as the development of PTPs approaches the second generation, efforts have been made to increase PTP solubility and decrease aggregate formation. For example, the Chariot PTP has been designed to exhibit greater solubility and requires less effort by the experimenter to minimize aggregate formation.

I. Serum Does Not Interfere with PTP-Mediated Cargo Delivery

One of the problems with most transfection methods is the sensitivity to serum, a common additive to the culturing medium. It is thus a great advantage that PTPs deliver their cargo effectively in the presence of serum (Morris *et al.*, 2001). However, the process of complex formation between the PTP and its cargo must be carried out in the absence of serum to prevent PTPs from complexing with serum proteins.

III. Materials

A. Purchasing and Producing Proteins and Peptides Containing PTDs

Although multiple PTDs have been discovered/developed (see Section II, A), the Antennapedia PTD has been used to successfully deliver inhibitory peptides into living neurons by multiple laboratories. Additionally, discovery of the Antennapedia PTD occurred during the course of studies on the internalization of homeodomain proteins by neurons (reviewed in Dunican and Doherty, 2001). Thus, this chapter mostly discusses approaches to obtaining Antennapedia PTD-based protein/peptide constructs for use in experiments involving neurons.

In the absence of an in-house peptide manufacturing facility, peptides can be obtained from commercial peptide synthesis companies. This route is suggested if the PTD is to be coupled to another bioactive/inhibitory peptide and the total length of the final peptide is less than approximately 30–40 amino acids. Most companies also offer a number of peptide modifications (e.g., biotin labeling, fluorochrome tagging, phosphorylated peptide production). One of the advantages of obtaining peptides from commercial sources is that they offer different grades of peptide purity with a certificate of analysis. The highest level of purity is recommended for applications involving living cells. For use in *in vitro* experiments, 1–5 mg of peptide will provide sufficient reagent for a large number

of experiments (depending on the total amount of medium in the cultures and the concentration at which the peptide is effective).

If the protein or peptide that a PTD is to be coupled to is readily available, Qbiogene (Carlsbad, CA) offers Antennapedia PTD (Penetratin; <http://www.qbiogene.com/products/transfection/penetratin.shtml>), which can be coupled to any protein/peptide at an available thiol group (i.e., a cystine residue). Alternatively, if the DNA coding for the protein is available, Qbiogene also offers the Trans Vector plasmid system (<http://www.qbiogene.com/products/transfection/transvector.shtml>) for the production of Penetratin–fusion proteins. In this system, the gene of interest is cloned downstream of the Penetratin coding region and the fusion protein is expressed in bacteria. The fusion protein can be purified due to the presence of an N-terminal polyhistidine tag.

B. Chariot: A Commercially Available PTP

Chariot is a PTP manufactured by ActiveMotif Inc. (Carlsbad, CA; <http://www.activemotif.com>). Presently, lyophilized Chariot is shipped as a component of a kit containing additional reagents necessary for the transfection protocol (e.g., phosphate-buffered saline and sterile deionized water). The kit also contains a vial of β -GAL enzyme as a positive control for the transfection protocol. Guidelines are provided by the manufacturer for the preparation and use of Chariot in a variety of transfection scenarios. In the author's experience, these guidelines have been appropriate for the delivery of proteins and peptides in embryonic chicken and mouse primary neurons. The protocol used for introducing proteins and peptides using Chariot in primary neurons is presented in Section IV,B. Using this protocol, Chariot effectively delivers proteins into fibroblasts, Schwann cells, and neurons (Fig. 2).

The sequence of Chariot has been published (KETWWETWWTEWSQ-PKKKRKV; identical to Pep-1 in [Morris *et al.*, 2001]). The peptide consists of three domains with specific functions. The Chariot–cargo interaction domain is delineated by the hydrophobic tryptophan-containing sequence (KETWWETWWTEW). This is followed by a spacer domain (SQP) that reportedly increases peptide stability and flexibility. The spacer domain is followed by a hydrophilic domain derived from the simian virus 40 (SV40) large T antigen (KKKRKV). This last domain improves cellular delivery and solubility of the peptide.

IV. Methods

A. General Comments on the Introduction of Reagents to Neuronal Cultures

Although the addition of reagents to a cell/explant culture may seem trivial, neuronal cultures are more sensitive to fluid shear forces and mechanical disturbances than other cell types (e.g., fibroblasts). It is not recommended that neuronal

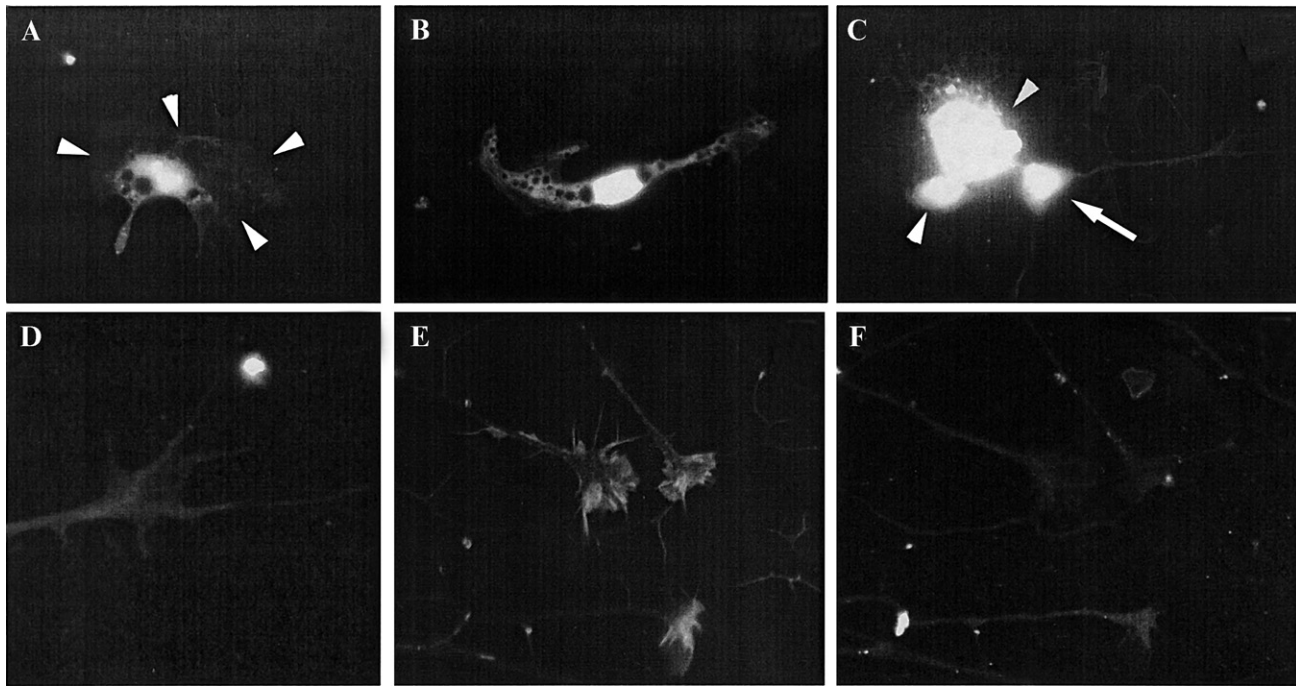


Fig. 2 Chariot-mediated protein transfection of cells in cultures of embryonic chicken dorsal root ganglion cultures. Rhodamine-labeled albumin (Sigma, $1 \mu\text{g}$ of protein from a stock solution prepared at 10 mg/ml in water) was introduced into cells using the protocol described in Section IV, B. (A–D) Examples of internalization into dissociated cells loaded with rhodamine-labeled albumin prior to plating (1 h with protein + Chariot + $400 \mu\text{l}$ of medium containing the cell suspension, followed by the addition of $400 \mu\text{l}$ of medium at the time of plating) and allowed to grow in culture for a total of 4 h. As determined by immunofluorescence, rhodamine-labeled albumin was internalized into fibroblasts (A, arrowheads point to the leading edge of the lamellipodium), Schwann cells (B), and neurons (C, arrow denotes soma of neuron that has initiated axon extension and arrowheads point to a cluster of neuron somas that have not yet initiated axon extension). (C) Note that the axon and growth cone of the neuron contain detectable levels of rhodamine-labeled albumin. (D) A higher magnification view of the tip of the axon in C. Cells treated with Chariot, or rhodamine-labeled albumin, alone did not have detectable fluorescence (not shown). (E) Fluorescein phalloidin staining to reveal growth cone morphology and (F) rhodamine-labeled albumin show internalization of albumin in axons extending from a dorsal root ganglion explant cultured for 1 day prior to loading with rhodamine-labeled albumin using Chariot for 3 h.

cultures be subjected to movement at any time during an experiment as this may cause the deformation of axonal processes and growth cone collapse. This is particularly important if the details of growth cone motility or morphology are being investigated. Also, the response of neurons to physical stress may vary between culturing substrata. For example, on highly adhesive but not biologically relevant substrata (e.g., polylysine), neurons may be relatively well attached. However, on biologically relevant substrata, such as the extracellular matrix molecules laminin or fibronectin, neurons are often less adherent and more subject to physical forces. These considerations are provided to assist in the selection of a substratum that is a best fit for the particular requirements of an experimental paradigm, e.g., when neurons need to remain firmly attached to the substratum through multiple medium replacements, in which case polylysine would be the recommended substratum.

Reagents are delivered with the greatest ease to cultures prepared in dishes with removable covers. When adding a reagent to a culture, it is important to ensure even dispersal throughout the culturing medium. If the experiments require live visualization of neurons, it is suggested that the culture be placed on a microscope stage for a minimum period of 30 min prior to the commencement of an experiment. Table I details a general protocol used routinely for the even addition of reagents to neuronal cell cultures containing 1 ml of medium.

The protocol presented in Table I works well for dissociated neuronal cultures. Ideally, each user should determine the efficiency of their reagent delivery method in “dry-run” experiments using a visible dye (e.g., methylene blue) to determine distribution of the dye in the culture medium. In the author’s experience, explant cultures (i.e., whole pieces of tissue placed in culture without prior dissociation) can produce artifacts due to the lack of sufficient delivery of reagents within 100–200 μm of the explant following short time intervals after treatment. This is most obvious when a short time interval is required between addition of the reagent

Table I
Delivery of Reagents to Neuronal Cultures

-
- i. Remove the cover to the culture dish without moving the culture from the incubator/microscope stage
 - ii. Using a pipette, gently remove 10% of the culturing medium. Keep the pipette tip just below the surface of the medium. Place the medium in a sterile microfuge tube
 - iii. Add the reagent to the medium removed from the culture. Mix by pipetting up and down
 - iv. Place the tip of the pipette in close apposition to the surface of the medium and gently dropwise add the medium + reagent mixture to the culture medium. Angle the pipette tip to approximately 45° relative to the surface of the medium. Move the pipette tip after each drop is released to a new location in the dish to deliver the mixture evenly. Pay attention not to create a constant stream of medium flow from the pipette tip. To further increase the even distribution of the reagent in the culturing medium, remove 10% of the culture medium (which now contains the reagent) and redistribute it as described (repeat four times)
 - v. Return the cover on the culture dish and observe the live culture, fix at the end of the experiment for further processing (e.g., immunocytochemistry), or prepare for biochemical/molecular analysis
-

and determination of the experimental result. For example, when explant cultures are treated with a high concentration of an actin depolymerizing drug for a short time interval (2 min or less), growth cones in the outer halo of the explant (600 μm or more from the explant) will collapse rapidly, but those within 100–200 μm of the explant will not. If the experiment is allowed to progress, all growth cones will eventually collapse. Qualitative observations of the distribution of dyes introduced into cultures support the idea that reagents are excluded from reaching the edges of explants during short time periods. This observation is provided to highlight the importance of the careful selection of the culturing system and experimental paradigm when determining the effects of reagents delivered to neuronal cultures.

B. Use of Antennapedia-Conjugated Peptides

The use of Antennapedia PTD-conjugated peptides to inhibit the function of the GTPase Rac1 and LIM kinase in neurons has been described previously (Vastrik *et al.*, 1999; Aizawa *et al.*, 2001; Journey *et al.*, 2002). Table II details a protocol for the use of the Antennapedia-Rac1(17–32) (Vastrik *et al.*, 1999) inhibitory peptide in cultures containing 1 ml of medium. The amino acid sequence of individual peptides determines solubility and stability. Thus, this protocol is intended to be a general starting point, but may need to be modified for each specific peptide.

In the author's experience, using the protocol shown in Table II to deliver an Antennapedia-Rac1 inhibitory peptide, changes in neuronal morphology consistent with the inactivation of Rac1 occur within 30–40 min of treatment (Journey *et al.*, 2002). For experiments using the Antennapedia-Rac1 inhibitory peptide to investigate the role of Rac1 signaling in mediating the effects of negative axon guidance cues (semaphorin IIA and ephrin-A2), we routinely used a 1-h pretreatment period with the peptide prior to the addition of guidance cues.

Table II
General Protocol for the Use of Antennapedia Peptides

-
- i. Peptide solubilization: If the peptide is in the form of a lyophilized powder, use sterile deionized water to bring the peptide to a concentration of 1 mg/ml. Additional solvents may be required if the peptide is not readily soluble in water
 - ii. Storage: Aliquot and store at -70°C in cryotubes. Do not freeze–thaw the peptide stock solution
 - iii. Preparation of the peptide for immediate use: Thaw the peptide stock solution at room temperature. Dilute the peptide 1:9 in sterile deionized water prior to the addition of cultures to prevent precipitation upon addition to the culture medium^a
 - iv. Adding the peptide to the culture: Remove a volume of medium from the culture equal to that prepared in step iii (100 μl in the example). Pipette the peptide-containing solution into the culture. Make sure to disperse the peptide solution evenly when adding it to the culture medium (see Protocol 1)
-

^aExample: If the desired final concentration of the peptide is 10 $\mu\text{g}/\text{ml}$, first add 90 μl of sterile deionized water to a microfuge tube. Next, add 10 μl of thawed 1-mg/ml stock to a microfuge tube. Mix gently by pipetting.

C. Use of Chariot PTP to Deliver Proteins and Peptides into Neurons

Chariot can be used to deliver both protein and peptide cargo into neurons. The amount of Chariot used in delivering proteins and peptides differs, with proteins requiring more Chariot. This difference is likely due to the fact that Chariot transfection is optimal when the ratio of Chariot molecules to the cargo is maximal (Morris *et al.*, 2001). Given that full-length proteins are larger than most commonly used peptides, the requirement of more Chariot to associate with protein cargo is not surprising. Importantly, using too much Chariot can result in the formation of insoluble protein–Chariot particles, decreasing the efficiency of transfection. The interaction of Chariot with individual species of cargo will differ based on the structure and hydrophobic properties of the cargo (Chariot associates with proteins through hydrophobic interactions). Thus, the quantity of Chariot used to deliver a specific cargo should be optimized empirically, utilizing either direct visualization of cargo internalization or a bioassay to determine the efficiency of the intracellular delivery of the cargo (e.g., enzymatic reaction product formation or bioassay).

One advantage of Chariot-mediated cargo delivery is that relatively small quantities of cargo are required for efficient internalization (0.5–1 μg). The ability to deliver biologically significant amounts of active cargo into neurons is dependent on the mode of action of the cargo. The introduction of relatively few molecules of an enzyme may have a significant cellular effect, whereas a similar number of molecules of an inhibitory, or activating, peptide may not be sufficient to produce a cellular effect. In the author's experience, Chariot can deliver sufficient amounts of an inhibitory myosin light chain kinase peptide to inhibit myosin driven axon retraction (Gallo *et al.*, 2002).

The protocol presented in Table III is designed to use Chariot to deliver proteins and peptides into established neuronal cultures (containing 1 ml of medium with 20,000–40,000 dissociated sensory neurons or one to two explants) and utilizes the kit components provided by ActiveMotif Inc. Although usually not an issue with primary neuronal cultures due to the relatively low number of cells plated, subconfluent (<50–60%) culturing conditions are suggested in using neuronal cell lines. The amount of protein introduced in step ii should be optimized based on an internalization assay or bioassay. If multiple cultures are being transfected at the same time, prepare one microfuge containing the Chariot–cargo complex for each culture instead of one tube containing enough complex to transfect multiple cultures.

Using the protocol shown in Table III, we have been able to introduce recombinant Rho-family GTPases in both chicken and mouse embryonic sensory and retinal cultures. To introduce peptides into neuronal cultures we used the same protocol, but as suggested by the manufacturer, we used a 1:10 dilution of the Chariot stock solution in step i. We found that 1 μg of peptide complexed with 12 μl of 1:10 Chariot produced optimal internalization of a myosin light chain inhibitory peptide, based on a bioassay. We have not attempted to introduce antibodies

Table III
Protocol for the Use of Chariot (1 ml Culture)

-
- i. Add 6 μl of Chariot to 94 μl of sterile water in a sterile microfuge tube. Sonicate for 3 min to disrupt Chariot complexes
 - ii. Add 0.5–1.0 μg of protein cargo to a sterile microfuge tube containing PBS for a final volume of 100 μl . Use a concentrated protein cargo solution to minimize the introduction of additional chemicals/salts that may be present in the protein cargo solution, as required for the storage of the cargo. Do not use cargo solutions that contain additional proteins/peptides other than the desired cargo molecule as these will decrease complex formation between Chariot and the intended cargo
 - iii. Add the 100 μl of PBS containing the protein cargo prepared in step ii to the microfuge tube containing the Chariot for a final volume of 200 μl . Mix gently by pipetting. Let the solution sit at room temperature for 30 min. During this time Chariot complexes to the protein cargo
 - iv. Remove and dispose of 600 μl of the culture medium. Add the 200 μl of the Chariot–cargo complex containing solution from step iii. Let stand in the incubator for 1 h
 - v. Add 400 μl of fresh prewarmed medium to the culture and keep in the incubator for an additional 2 h
 - vi. Process the culture for the desired experimental analysis or continue by performing additional experimental manipulations
-

into neurons using Chariot. However, antibodies can be delivered by Chariot in other cell types, indicating that this approach may also function in neurons. Morris *et al.* (2001) reported that, under optimal conditions, using Chariot greater than 80% of cells can be transfected with detectable levels of protein.

V. Conclusions and Perspectives

A. Making Your Favorite Protein into a Drug: A Bonus for the Basic Research Scientist

The ability to introduce biologically relevant amounts of protein or peptide into living cells through the use of PTDs or PTPs significantly expands the experimental repertoire of the basic research scientist interested in studying the cell biology of neurons. Although additional methods for the introduction of proteins in neurons exist (e.g., trituration loading and microinjection), none provide the ability to simultaneously deliver proteins to many neurons, while also allowing control over the time course of internalization. For example, trituration loading allows the introduction of proteins in many neurons, but it must be performed prior to plating the neurons. However, microinjection can be used to deliver proteins to neurons at any time after plating, but only a few cells can be injected in each experiment. Regardless, although peptide-based methods have advantages over these other methodologies, the optimal delivery method is ultimately determined by the nature of the experimental question and design.

The advantageous features of pharmacological analysis, outlined in Section I, can now be exploited in the context of delivering proteins into living neurons using PTDs and PTPs. This is a first step in the development of new tools for the controlled manipulation of cellular processes in neurons. Using these tools, neuro-

biologists and cell biologists should be able to, with relative ease, approach experimental questions that were previously technically demanding or time-consuming.

B. Potential Applications of the Use of Peptide-Based Methodologies to the Development of *in Vivo* Therapies

The ability to internalize peptides and proteins into cells using PTDs and PTPs is also being exploited in the development of therapeutic interventions aimed at stopping, or ameliorating, disease processes. Hosotani *et al.* (2002) used the Antennapedia PTD fused to a peptide from the tumor suppressor gene p16 to inhibit pancreatic cancer growth *in vivo* in a murine model. In this study, no hematological toxicity or body weight loss resulted as a function of treatment with either the Antennapedia peptide alone or the Antennapedia–p16 fusion peptide. Additionally, Antennapedia-coupled antisense oligonucleotides were found to be delivered efficiently *in vivo*, resulting in decreased galanin receptor expression in the rat spinal cord (Pooga *et al.*, 1988). These results demonstrate the potential application of peptide-based technologies to the development of therapeutic agents.

Promoting the regeneration of axons following injury is an important approach to the repair of nervous system damage. In recent years advances have been made in promoting the regeneration of injured axons by blocking the signals inhibitory to axon extension present in the damaged nervous system (reviewed in Wickelgren, 2002). One of these approaches has been to inhibit the function of the RhoA–GTPase using C3 exozyme, an enzyme that inactivates RhoA (Dergham *et al.*, 2002). Although cellular delivery of C3 *in vivo* has been accomplished without the assistance of additional factors to promote C3 internalization, peptide-based methods may serve useful in increasing the cellular delivery of C3 *in vivo*. Conjugation of C3 to PTDs, or using PTPs, may enhance the amount delivered and decrease the time course of internalization *in vivo*. It will be of great interest to further investigate the potential applications of peptide-based methods to the intracellular delivery of therapeutic proteinaceous reagents.

Acknowledgments

The author thanks Dr. G. Divita (CRBM-CNRS-UPR, Montpellier, France) and Dr. J. Archdeacon (ActiveMotif Inc. Carlsbad, CA) for discussion of Chariot. This work was supported in part by Spinal Cord Research Foundation Grant 2199 to G.G.

References

- Aizawa, H., Wakatsuki, S., Ishii, A., Moriyama, K., Sasaki, Y., Ohashi, K., Sekine-Aizawa, Y., Sehara-Fujisawa, A., Mizuno, K., Goshima, Y., and Yahara, I. (2001). Phosphorylation of cofilin by LIM-kinase is necessary for semaphorin 3A-induced growth cone collapse. *Nature Neurosci.* **4**, 367–373.
- Bloch-Gallego, E., Le Roux, I., Joliot, A. H., Volovitch, M., Henderson, C. E., and Prochiantz, A. (1993). Antennapedia homeobox peptide enhances growth and branching of embryonic chicken motoneurons in vitro. *J. Cell Biol.* **120**, 485–492.

- Bolton, S. J., Jones, D. N., Darker, J. G., Eggleston, D. S., Hunter, A. J., and Walsh, F. S. (2000). Cellular uptake and spread of the cell-permeable peptide penetration in adult brain. *Eur. J. Neurosci.* **12**, 2847–2855.
- Cosgaya, J. M., Aranda, A., Cruces, J., and Martin-Blanco, E. (1998). Neuronal differentiation of PC12 cells induced by engrailed homeodomain is DNA-binding specific and independent of MAP kinases. *J. Cell Sci.* **111**, 2377–2384.
- Dergham, P., Ellezam, B., Essagian, C., Avedissian, H., Lubell, W. D., and McKerracher, L. (2002). Rho signaling pathway targeted to promote spinal cord repair. *J. Neurosci.* **22**, 6570–6577.
- Derossi, D., Joliot, A. H., Chassaing, G., and Prochiantz, A. (1994). The third helix of the Antennapedia homeodomain translocates through biological membranes. *J. Biol. Chem.* **269**, 10444–10450.
- Dunican, D. J., and Doherty, P. (2001). Designing cell-permeant phosphopeptides to modulate intracellular signaling pathways. *Biopolymers* **60**, 45–60.
- Fisher, A. A., Ye, D., Sergueev, D. S., Fisher, M. H., Shaw, B. R., and Juliano, R. L. (2002). Evaluating the specificity of antisense oligonucleotides: A DNA array analysis. *J. Biol. Chem.* **277**, 22980–22984.
- Frankel, A. D., and Pabo, C. O. (1988). Cellular uptake of the tat protein from human immunodeficiency virus. *Cell* **55**, 1189–1193.
- Gallo, G., Yee, H. F. Jr., and Letourneau, P. C. (2002). Actin turnover is required to prevent axon retraction driven by endogenous actomyosin contractility. *J. Cell Biol.* **158**, 1219–1228.
- Hosotani, R., Miyamoto, Y., Fujimoto, K., Doi, R., Otaka, A., Fujii, N., and Imamura, M. (2002). Trojan p16 peptide suppresses pancreatic cancer growth and prolongs survival in mice. *Clin. Cancer Res.* **8**, 1271–1276.
- Jurney, W. M., Gallo, G., Letourneau, P. C., and McLoon, S. C. (2002). Rac1-mediated endocytosis during ephrin-A2 and semaphorin 3A-induced growth cone collapse. *J. Neurosci.* **22**, 6019–6028.
- Kilk, K., Magzoub, M., Pooga, M., Eriksson, L. E., Langel, U., and Graslund, A. (2001). Cellular internalization of a cargo complex with a novel peptide derived from the third helix of the islet-1 homeodomain: Comparison with the penetratin peptide. *Bioconjug. Chem.* **12**, 911–916.
- Lindgren, M., Hallbrink, M., Prochiantz, A., and Langel, U. (2000). Cell-penetrating peptides. *Trends Pharmacol. Sci.* **21**, 99–103.
- Morris, M. C., Depollier, J., Mery, J., Heitz, F., and Divita, G. (2001). A peptide carrier for the delivery of biologically active proteins into mammalian cells. *Nature Biotech.* **19**, 1173–1176.
- Morris, M. C., Vidal, P., Chaloin, L., Heitz, F., and Divita, G. (1997). A new peptide vector for efficient delivery of oligonucleotides into mammalian cells. *Nucleic Acids Res.* **25**, 2730–2736.
- Perez, F., Joliot, A., Bloch-Gallego, E., Zahraoui, A., Triller, A., and Prochiantz, A. (1992). Antennapedia homeobox as a signal for the cellular internalization and nuclear addressing of a small exogenous peptide. *J. Cell Sci.* **102**, 717–722.
- Pooga, M., Soomets, U., Hallbrink, M., Alkna, A., Saar, K., Rezaei, K., Kahl, U., Hao, J. X., Xu, X. J., Wiesenfeld-Hallin, Z., Hokfelt, T., Bartfai, T., and Langel, U. (1988). Cell penetrating PNA constructs regulate galanin receptor levels and modify pain transmission in vivo. *Nature Biotech.* **16**, 857–861.
- Troy, C. M., Derossi, D., Prochiantz, A., Greene, L. A., and Shelanski, M. L. (1996). Downregulation of Cu/Zu superoxide dismutase leads to cell death via the nitric oxide-peroxynitrite pathway. *J. Neurosci.* **16**, 253–261.
- Vastrik, I., Eickholt, B. J., Walsh, F. S., Ridley, A., and Doherty, P. (1999). Sema3A-induced growth cone collapse is mediated by Rac1 amino acids 17-32. *Curr. Biol.* **9**, 991–998.
- Waizenegger, T., Fischer, R., and Brock, R. (2002). Intracellular concentration measurements in adherent cells: A comparison of import efficiencies of cell-permeable peptides. *Biol. Chem.* **383**, 291–299.
- Wickelgren, I. (2002). Animal studies raise hope for spinal cord repair. *Science* **297**, 178–181.
- Williams, H. H., Moore, E. J., Walsh, F. S., Prochiantz, A., and Doherty, P. (1996). Inhibition of FGF-stimulated phosphatidylinositol hydrolysis and neurite outgrowth by a cell membrane permeable phosphopeptide. *Curr. Biol.* **6**, 587–590.

CHAPTER 16

Transfection of Primary Central and Peripheral Nervous System Neurons by Electroporation

Cecilia Y. Martinez and Peter J. Hollenbeck

Department of Biological Sciences
Purdue University
West Lafayette, Indiana 47906

-
- I. Introduction
 - II. Electroporation Theory and Principles
 - III. Electroporation Protocol for Chick Primary Neurons
 - A. Procedure
 - IV. Rationale for Setting Electroporation Parameters
 - A. Cell Density
 - B. Voltage and Duration of Pulse
 - C. Free Ca^{2+} in Electroporation Buffer
 - D. Temperature of Cell Suspension
 - E. Rest for Recovery
 - F. Buffer Composition
 - V. Discussion
 - References

Neurons are difficult cells to transfect. Many methods that work routinely for immortalized tissue culture cells or primary cultures of nonneuronal cells are ineffective, toxic, or both when applied to neurons. This chapter describes a protocol that optimizes electroporation-based transfection of chick embryonic peripheral and central neurons. The key features required for successful electroporation and recovery of transfected neurons are high cell density, correct applied voltage and pulse duration, and the presence of calcium ions in the electroporation medium. Less important features are temperature, postporation rest, and the general composition of the electroporation medium. We emphasize

the rationale for each element in our method and provide information useful for optimizing the procedure for other neurons.

I. Introduction

Transient transfection has become a routine and powerful technique to assess the effects of the expression of transgenes in eukaryotic cells. Perhaps the most rapid, efficient, and repeatable method of transient transfection is transient electrical permeabilization, or electroporation. Transfection by electroporation requires fewer steps than other transfection protocols and lacks the potential toxic effects of chemical transfection methods. Because of their simplicity, electroporation techniques tend to give highly reproducible results. This makes electroporation attractive not only as a primary experimental technique, but also as a rapid and inexpensive screening method to assess the behavior of fusion proteins within cells prior to using more costly *in vivo* transgenic methods. Although cells can be electroporated as adherent single cells or in explants, it is advantageous, for reasons described later, to electroporate cells such as neurons in suspension.

Electroporation was developed as a technique for introducing exogenous macromolecules into cells in the 1980s. Although its most common application has been to transform cells with DNA, it has also been used to introduce antibodies, enzymes, and other reagents into a variety of cell types (Weaver, 1993). Electroporation is generally carried out in one of two ways: using point electrodes positioned in embryonic tissues, organ culture, or cell culture or by placing a suspension of dissociated cells in a cuvette with parallel plate electrodes. Although virtually any cell exposed to a suitable external electric field will be transiently permeabilized, different cell types differ in their capacity to undergo and recover from electroporation. Neurons have proven to be challenging subjects for this procedure. Although individual adherent neurons (Tereul *et al.*, 1999) and retinal explants (Pu and Young, 1990; Li *et al.*, 1995) have been electroporated successfully using point electrodes, the most broadly useful application of electroporation—transfection of large numbers of primary neurons in suspension prior to plating out—has been difficult to achieve. While $\geq 50\%$ of typical fibroblastic cells can be transformed successfully by electroporation in suspension, the transfection efficiency of rat brain cells electroporated in cell suspension was reported to be 2% (Li *et al.*, 1997).

There are two major reasons why transfection by electroporation is more difficult to achieve in neurons than in many nonneuronal cells: neurons recover more poorly from permeabilization and they subsequently express transgenes less efficiently. The lower recovery rate is no surprise: how successfully cells survive electroporation tends to vary inversely with the cell diameter (Potter, 1993), and neurons are larger than most nonneuronal cells. While the diameter of the cells cannot be changed, electroporation conditions for neurons can be tailored to provide the gentlest possible treatment consistent with permeabilization.

However, even after neurons recover from transfection by electroporation, the efficiency of transgene expression tends to be lower than in nonneuronal cells, probably due to their terminally differentiated state. In a mitotic cell, the plasmid can access the nucleus easily during each cell cycle, whereas in postmitotic cells such as neurons, it can only reach the nucleus through the nuclear pores. This has been observed in nonneuronal cells as well: Anderson *et al.* (1991) reported that lymphoid cells in stationary growth phase had a two-fold decrease of gene expression following electroporation compared to cells treated during logarithmic growth. In addition, microinjection of DNA directly into the nucleus of individual sympathetic neurons in culture (see Chapter 14) results in a higher transfection efficiency than bulk treatment techniques such as electroporation.

II. Electroporation Theory and Principles

During electroporation, the electric field applied to the cells induces an abrupt increase in transmembrane potential. This results in the formation in the plasma membrane of transient, metastable aqueous pores of varying diameters. Once pores form, additional current will be shunted through the cytoplasm, which tends to limit additional increases in transmembrane potential. Pores of adequate diameter will allow exogenous material such as DNA to electrodiffuse into the cytoplasm during the transient permeable state, but if pores become too large and numerous the result will be irreversible breakdown of the membrane and cell death. Because pores originate in the membrane at the location that experiences the largest transmembrane potential, their distribution on the membrane surface is not uniform: membrane sites facing the electrodes will form pores whereas sites furthest from the electrodes will not (Tekle *et al.*, 1994). In addition, pore formation is apparently asymmetric in the field: it has been reported that the membrane surface facing the anode develops pores that have a smaller diameter but higher density, whereas the surface facing the cathode has pores of larger radius and lower density (Tekle *et al.*, 1994). Not surprisingly, the actual fraction of the surface area of the cell that is open varies with field strength, and the fraction of the total area that is open is thought to be small. Theoretical modeling of planar bilayer membranes has predicted that even at a transmembrane potential of 1000 mV, less than 0.1% of the total membrane area would be porated (Ho and Mittal, 1996).

A primary advantage of cell suspension electroporation over other transfection procedures is its reproducibility, and this relies on very precise control of the physical parameters of the electrical pulse. Thus, the electroporation apparatus and its proper use are critical for good results. We electroporate neurons in suspension in a standard cuvette with parallel plate electrodes designed for the application of a uniform electric pulse by a solid-state generator. Two physical parameters of the apparatus whose selection is critical for electroporation efficiency and cell survival are field strength and pulse duration. The electrical environment within the electroporation chamber is described by the applied *field*

strength, E , which depends on the applied voltage, V , and the distance between the electrodes, d . Thus, $E = V/d$ and is usually expressed in volts/cm. Note that the distance between electrodes is determined by the choice of electroporation cuvettes, which are available commercially with gaps between the electrodes of 1–4 mm. The arrangement of parallel plates found in an electroporation cuvette gives the homogeneous field that is necessary to produce accurate and repeatable electroporation conditions.

The type of waveform experienced by intact cells during electroporation depends on the electroporation apparatus used. Square wave and exponential decay pulses are used most commonly to electroporate cells. Electrical pulses generated by square wave electroporation apparatuses sustain a constant voltage for a specific amount of time. Square wave generators are essentially a high-voltage power supply connected to a switch. Thus, field strength, E , and duration, t , fully characterize the pulse, which is usually described by $E \times t$ in volts/cm \times ms. Our procedures were developed and will be described for square wave generators.

However, many existing electroporation apparatuses are exponential wave generators. In order to convert electroporation parameters between square wave and exponential generators, it is necessary to understand that the latter apparatuses consist of capacitors whose properties can be manipulated. A capacitor stores a characteristic amount of electrical charge Q at a voltage V such that $C = Q/V$, where C is the capacitance in farads (F), usually given in μF . From the moment of release, the voltage discharged from a capacitor decreases exponentially with time according to the equation:

$$V = V_0 e^{-t/RC}$$

where V_0 is the voltage at time 0, e is the base of the natural logarithm, and R is the resistance. The discharge of a capacitor is usually described by its time constant, τ , which equals the time required for the voltage to decay to V_0/e , or approximately $0.37 \times V_0$. Thus, from the decay equation:

$$\tau = R \times C$$

Because both R and C are known (and one or both are adjustable) for exponential decay wave generators, it is simple to set these parameters to give the desired time constant τ for a particular application. Note that if R is expressed in ohms and C in farads, τ will have the units of seconds; i.e., if $R = 1000 \Omega$ and $C = 200 \mu\text{F}$, then $\tau = 10^3 \Omega \times (2 \times 10^{-4} \text{ farads}) = 0.2 \text{ s}$, or 200 ms. A simple and reasonably accurate way to convert an electroporation protocol for a square wave apparatus to one suitable for an exponential decay apparatus is this: use identical conditions, including an identical value for E , but set the time constant, τ , for the exponential wave protocol equal to twice the time, t , used in the square wave protocol. For example, a square wave protocol with $t = 100 \text{ ms}$ would be approximately equivalent to an exponential wave protocol (using the same E) with $\tau = 200 \text{ ms}$ (see Fig. 1). The desired τ value could be achieved for this apparatus by setting $R = 500 \Omega$ and $C = 400 \mu\text{F}$ ($500 \Omega \times 400 \mu\text{F} = 200 \text{ ms}$). In the primary research

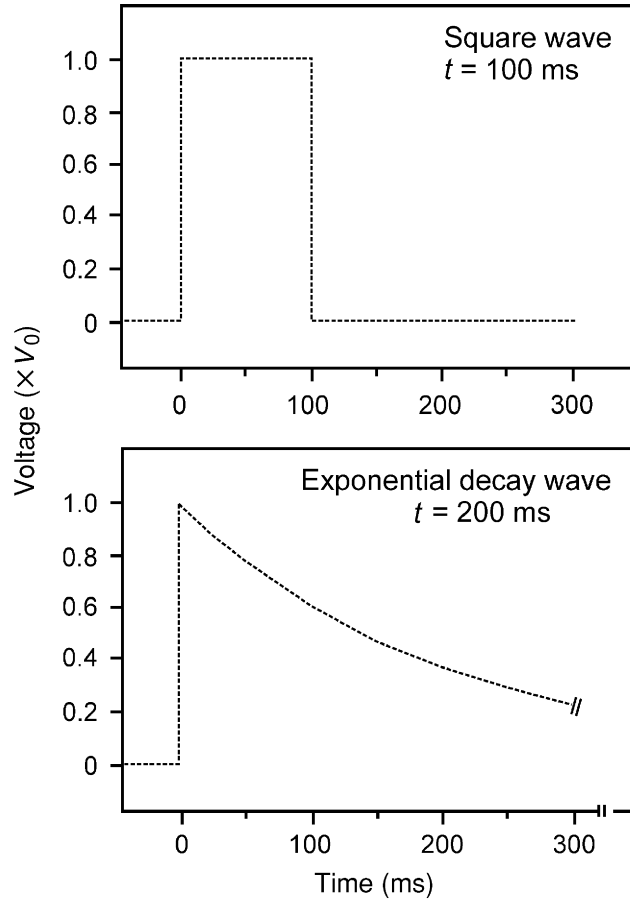


Fig. 1 Plots of voltage versus time for the discharge of a square wave (top) and exponential decay wave (bottom) generator. In this illustration, the square wave generator is shown to produce a voltage of V_0 for exactly 100 ms. The exponential decay wave generator is set to produce an approximately equivalent effect to the square wave generator: τ has been set to 200 m, twice the time setting of the square wave generator. Upon discharge, the exponential decay wave generator initially produces a voltage of V_0 , which falls off quickly according to the equation $V = V_0 e^{-t/RC} = V_0 e^{-t/\tau}$. Note that when $t = \tau$, $V = V_0/e \approx 0.37V_0$. Although the areas ($V \times t$) under the two plots are clearly not equivalent, the right tail of the exponential plot that includes $V < V_0/e$ is thought to make a negligible contribution to the effect of the pulse on the cells. For most applications, particularly for methods development, the use of a square wave electroporation apparatus is recommended.

literature, electroporation protocols for exponential decay wave generators are often described (inadequately) by the R value or C value alone; it is obviously important that both the R and the C settings — or simply the value of τ — be specified in order to fully describe the conditions used.

It should be noted that cells can also be electroporated by an electric field oscillating at a radio frequency (Chang and Reese, 1990; Chang, 1992) but this form of electroporation is not used commonly and is not discussed here.

III. Electroporation Protocol for Chick Primary Neurons

The following protocol has been developed for the electroporation transfection of chick sensory (dorsal root ganglion, DRG), sympathetic (paravertebral ganglia), and forebrain neurons. Details of dissection and cell culture can be found elsewhere in this volume. Representative images of neurons transfected by this procedure are shown in Fig. 2. The rationale for each parameter is discussed in Section IV.

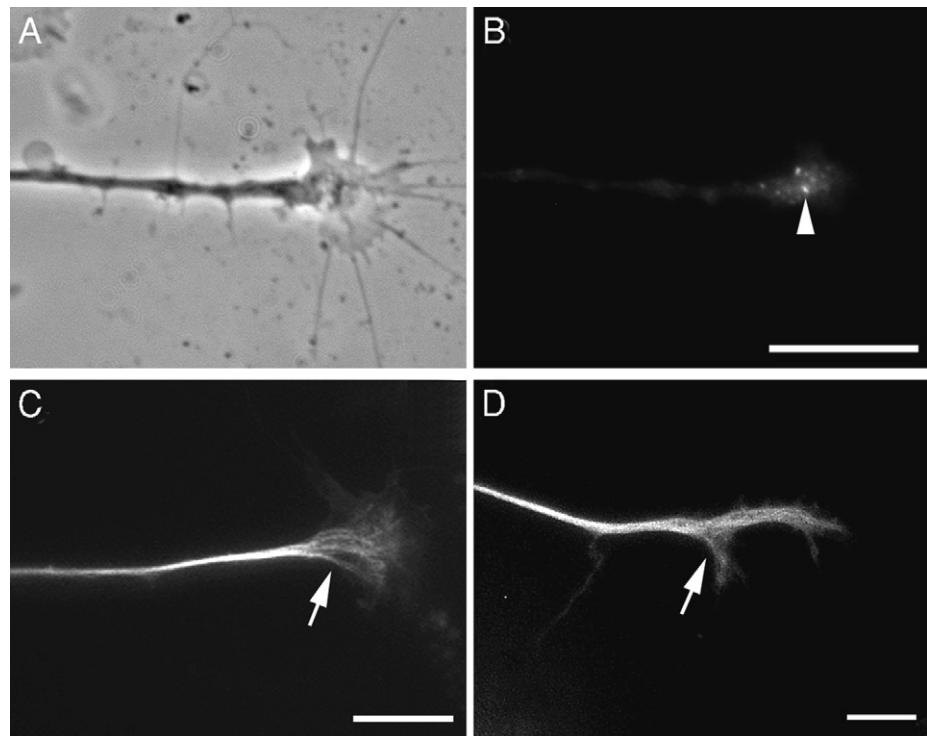


Fig. 2 Examples of cultured chick neurons transfected by electroporation. Phase-contrast (A) and epifluorescence images of the growth cone region of a neuron transfected with a pEGFP::rab11a vector show endosomes containing rab11a (arrowhead). Fluorescence images of the growth cone region of two neurons (C and D) transfected with a pEGFP::tubulin vector show individual microtubules or microtubule bundles (arrows). Scale bars: 10 μm .

A. Procedure

1. Dissect out chick sensory or sympathetic ganglia (from E9 to E12) or forebrain hemispheres (from E7 to E8) as per standard procedures (see relevant chapters in this volume). Each electroporation requires ≥ 50 DRGs or one to two forebrain hemispheres.

2. Dissociate tissue by incubation in 0.025% trypsin in Ca^{2+} / Mg^{2+} -free Hanks' balanced salt solution (HBSS) in a 1.5-ml Eppendorf tube at 37°C for 20 min for forebrain tissue and 17 min for DRGs and sympathetic ganglia.

3. For ganglia, allow them to settle to the bottom of the tube, carefully remove the trypsin, wash the tissue once gently with $150\ \mu\text{l}$ HBSS, and then resuspend in $25\text{--}50\ \mu\text{l}$ electroporation buffer: standard phosphate-buffered saline (PBS) plus (added just before use) $1\ \text{mM}$ CaCl_2 and $5.5\ \text{mM}$ glucose. Dissociate into a suspension of single cells by trituration with a yellow ($200\ \mu\text{l}$) pipette tip. For forebrain neurons, wash the tissue with $500\ \mu\text{l}$ of FB growth medium (see Chapter 4), resuspend in $100\ \mu\text{l}$ of the same medium, and dissociate by trituration with a glass pipette followed by trituration with a yellow pipette tip. Take a small sample (a few μl) of the suspension of neurons, dilute $100\times$ with PBS or medium, and count the cells in a hemocytometer. Once the typical yield of cells per ganglion or per forebrain hemisphere has been determined, this step can be omitted. After cell density has been determined for forebrain neurons, make the appropriate dilution (if any) of the cells to yield a density of $10^8\text{--}10^9$ cells/ml.

4. Add the optimal concentration of the DNA plasmid (determined empirically) to the suspension of neurons. We have used $20\text{--}50\ \mu\text{g/ml}$ for a variety of expression plasmids. Load the suspension gently into a 1-mm gap cuvette (BTX Electroporation Cuvettes Plus Model 610). Chill to 4°C for 10 min.

5. Place the cuvette into the safety stand (BTX Safety Stand 630B) of the electroporation generator (BTX Electro Square Porator T820, Genetronics, etc.). Pulse the cell suspension with the following settings: voltage, 112 V; duration, 5 ms; and pulse number, 1. Allow cells to rest at 37°C for 5 min in the cuvette and then recover cells from the cuvette gently into $500\ \mu\text{l}$ of warm culture medium.

6. Dilute with the appropriate volume of culture medium for the desired plating density and set out over appropriate culture substrata.

IV. Rationale for Setting Electroporation Parameters

There are several major variables in transfection of neurons by electroporation. We have tested many of them and found that the three most important are cell density, free Ca^{2+} levels, and field strength/pulse duration. The temperature of the pulse and the recovery period are of minor importance, and the exact composition of the physiological buffer is less important still. The following is a brief description of our observations on these factors.

A. Cell Density

We found that the density of neurons in the suspension during electroporation was one of the most important variables for achieving good cell survival and transfection efficiency. Nonneuronal cells such as lymphoid and Chinese hamster ovary (CHO) cells have been electroporated successfully at densities of 10^6 cells/ml, whereas HT-5 and HeLa cells have good transfection efficiencies at densities of 10^7 cells/ml (Lambert *et al.*, 1990; Chakrabarti *et al.*, 1989). We found that the optimal density for good survival and transfection of neurons was higher still. The best results were obtained at cell densities of $1-5 \times 10^8$ cells/ml for sympathetic chain (SC) and DRG neurons and 10^9 cells/ml for forebrain neurons. Lower densities resulted in significantly lower survival and transfection rates. Even higher densities can be used, but this will cause an increase in the percentage of fused cells. Attaining these densities with primary neurons may seem intimidating, but commercially available electroporation cuvettes with a 1-mm gap allow the use of as little as $25 \mu\text{l}$ of cell suspension for each poration. Thus, 10^8 cells/ml requires only around 2.5×10^6 cells, and so a quantity of cells obtainable in a fairly brief dissection of DRGs from E9 to E11 chick embryos will suffice for one electroporation experiment. For central neurons, obtaining adequate quantities of neurons is trivial: a typical E7 chick embryo forebrain will yield approximately 10^8 cells/hemisphere. Workers employing mouse or rat primary neurons will also have no difficulty in obtaining these cell densities. The first few times that a particular source of tissue is used, the yield of cells should be checked with a hemocytometer; after that a good estimate of cell density can be made based on the number of ganglia or forebrain hemispheres.

B. Voltage and Duration of Pulse

The physiological transmembrane voltage of most cells ranges from 60 to 100 mV. When an electrical field is applied to induce a threshold transmembrane potential of 1 V, the transmembrane voltage of a typical cell reaches values 5 to 15 times that of resting membrane potential. When the threshold is reached, the membrane forms pores and becomes permeable. We found that electroporating neuronal cells with a combination of long duration pulses between 5 and 100 ms and low applied electric fields between 25 and 500 V/cm resulted in little or no transfection. For example, the highest transfection efficiency that we obtained with a long duration–low field strength combination was with forebrain neurons that were electroporated with one 50-ms pulse of 200 V/cm (2.5% expression after 6 days in culture). Transfection efficiency was much higher when a larger field strength and shorter duration were utilized. Forebrain or sensory neurons electroporated with one 5-ms pulse of 1120 V/cm yielded an average transfection efficiency of 12%, judged by the expression of transgene-encoded proteins 36–48 h after electroporation. By applying fields ranging from 25 to 1500 V/cm and durations of 5–100 msec, we have found that a field strength of 1000 V/cm is necessary to permeabilize neuronal cells efficiently. It should be noted that

applying several pulses in rapid succession, as often done to transfect *Escherichia coli*, gives almost 100% cell death with the neurons and nonneuronal cells, such as fibroblasts, that we have tried.

C. Free Ca^{2+} in Electroporation Buffer

Transfection by electroporation can be viewed as taking the cells perilously close to death by breaching the plasma membrane and then relying on their ability to recover from membrane wounding and survive. However, it is important to realize that the formation of plasma membrane pores during electroporation and the subsequent recovery of membrane integrity are not qualitatively different from the mechanical wounding and recovery that occur routinely in eukaryotic cells in many tissues (McNeil and Steinhardt, 1997). A large body of data on both physiological and experimentally induced membrane wounding and resealing shows that the ability of a wounded plasma membrane to recover depends on the cell type, the extent of the injury, and the presence of divalent cations. Many cell types containing an endomembrane system have been shown to be capable of rapid resealing after membrane wounds, provided that 0.1–1.0 mM Ca^{2+} is present in the surrounding medium (McNeil and Terasaki, 2001). The Ca^{2+} is required to stimulate organelle motility, exocytosis, and membrane fusion events by which cells patch and seal membrane wounds, a process that requires between a few seconds and 1 min (McNeil and Terasaki, 2001; McNeil, 2002). Thus, it was no surprise that the addition of 1 mM CaCl_2 to our electroporation buffer led to a significantly higher survival and transfection efficiency in neurons and in chick embryonic fibroblasts. In experiments with chick forebrain neurons, we found that the omission of CaCl_2 from the electroporation buffer caused a fourfold reduction in the percentage of transfected cells. This is most likely because cells that had been permeabilized by the pulse in the absence of Ca^{2+} did not reseal and survive, and those that were not permeabilized did not take up plasmid. Many electroporation protocols lack enough free Ca^{2+} in the buffer to stimulate membrane recovery, which is likely to be a critical cause for failure to achieve good results.

D. Temperature of Cell Suspension

There are good reasons to expect temperature to be an important variable in electroporation procedures, but in our experience with neurons it does not seem to matter significantly. Electroporation itself is a nonthermal phenomenon because aqueous pore formation induced by the applied electrical field occurs very rapidly, before a significant change in temperature is experienced by the cell. However, heat will be generated in the extracellular medium during the pulse, with the amount depending on the electroporation buffer and the applied voltage. If microsecond pulses are used for electroporation, then cells should experience negligible thermal heating. As the pulse duration increases, so does the likelihood of decreased cell viability due to thermal heating. The extent of membrane

breakdown induced by an external field that is passed through a cell suspension is determined by the conductivity of the medium. In fact, evidence suggests that an increase in the ionic conductivity of the electroporation buffer alters or decreases the uptake and transport of molecules into cells (Djuzenova *et al.*, 1996; Dimitrov and Sowers, 1990). To prevent decreased cell viability due to buffer heating immediately after electroporation, it is commonly suggested to incubate cells at low temperatures prior to electroporation (Potter, 1993).

Despite this recommendation, we observed that prepulse temperature was not a significant factor affecting transfection efficiency or neuronal survival. When forebrain neurons were preincubated on ice and electroporated at low temperatures, neuronal survival was not observed to increase significantly as compared to neuronal cell suspensions electroporated at room temperature.

E. Rest for Recovery

Upon exposure to an electric field, membrane pores form very rapidly—within $0.5\ \mu\text{s}$ to 3 ms (Chang, 1992; Hibino *et al.*, 1993)—but membrane recovery is a slower process. Normal plasma membrane permeability is generally recovered within seconds to 1 min (Steinhardt *et al.*, 1994). Along with the presence of free Ca^{2+} , an important factor in recovery is thought to be temperature. The intracellular processes that mediate membrane recovery—organelle motility and membrane fusion—operate slower at lower temperatures. Thus, an elevated temperature during the period immediately following the application of an electric pulse should speed membrane recovery and improve cell survival. However, it is commonly recommended in the literature to incubate cells at low temperatures after electroporation. This is because slowing the process of membrane resealing should, in principle, allow a longer time for the influx of DNA through the pores, which should lead to a higher transfection efficiency as long as cell survival is adequate (Mir *et al.*, 1988; Potter, 1993). Rols *et al.* (1994) have reported that optimal transfection efficiency was obtained when CHO cells were subjected to the electrical pulse at 4°C and then allowed to recover at 37°C . This suggests that optimal transfection depends not on reducing the resealing rate of the pores to increase DNA influx, but rather on promoting the rapid resealing of pores and restoration of the membrane to produce a higher number of viable cells.

In our hands, there was only a small increase in the transfection efficiency of forebrain neurons when cells recovered for 5 min at 37°C as opposed to 30 min at 4°C . It is also notable that in the absence of CaCl_2 , the recovery temperature made no difference in transfection efficiency, presumably because the cell recovery was so poor.

F. Buffer Composition

Selection of an appropriate electroporation medium is usually assumed to be a critical factor influencing the applied electric field experience by cells.

Physiological buffers such as PBS, which have a relatively high ionic strength, offer low resistance during electroporation. Lower ionic strength buffers such as iso-osmolar phosphate buffer (PB) have approximately 10 times greater resistance. This is important to keep in mind when using an exponential decay electroporation apparatus, as the electrical resistance of medium is a major factor in determining the time constant, or the length of the pulse delivered by exponential wave generators. Cells electroporated in a low ionic strength medium will experience a longer time constant than cells in a high ionic strength medium. If a square wave electroporation apparatus is used, then longer pulses for cells in low ionic strength must be utilized. If the electroporation medium is supplemented with serum, it may be necessary to consider that the variation in different batches of serum may lead to inconsistent electrical resistance. In our hands, different physiological buffers with similar ionic strengths, e.g., PBS vs HBSS, yielded almost identical transfection results. Nonetheless, the buffer composition is a variable that should be considered and perhaps manipulated when developing a new procedure.

Glucose or sucrose has been added to electroporation buffers in studies of how osmotic pressure influences electroporation efficiency. Variations in transfection results with sucrose buffers of different osmolarity are presumably due to changes in the hydrodynamic influx of plasmid DNA caused by cell swelling (Golzio *et al.*, 1998). However, the inclusion of low levels of glucose (5.5 mM) in our electroporation buffer was solely for nutritive purposes and not to control the osmolarity of the electroporation buffer. The effect of this low concentration of glucose on transfection efficiency was not significant, and we conclude that it is not a necessary ingredient for electroporation of neurons.

V. Discussion

Neurons have been among the most difficult of cells to transfect. Only infection with viral vectors has yielded high transfection rates (see Chapter 19) and cloning into viral vectors and preparing active virus can be costly and time-consuming. For this reason, we sought to improve the available methods for the transient transfection of primary neurons with conventional expression vectors. The electroporation protocol that we devised for chick embryonic peripheral and central neurons gave an average transfection efficiency of 12%, sixfold higher than previously reported methods. This level of transfection provides an adequate number of transgene-expressing cells for light microscopy studies of many phenomena in neurons.

Workers using other primary neurons should be able to modify our procedures to suit other types of neurons. To this end we emphasize the importance of using high-cell density, including free Ca^{+2} in the electroporation buffer, and using a high-voltage/short-duration pulse. Previously reported electroporation methods have used cell densities two orders of magnitude lower than those that we found to

be optimal for chick neurons, which probably explains much of the sixfold difference in transfection efficiency. Likewise, most reported electroporation buffers contain little or no Ca^{+2} , and this is likely to be a consistent source of poor results, as our systematic examination of the effect of Ca^{+2} showed that including it in the buffer resulted in a substantial improvement in transfection efficiency. Finally, we found that identifying the optimal pulse parameters was critically important, although these are likely to vary among different types of neurons. Because we found little or no transfection at field strengths below 1000 V/cm or at pulse lengths above 10 ms, we suggest that these be used as starting points for developing new procedures.

Although prepulse temperature, postpulse temperature, and buffer composition were not important in obtaining optimal transfection efficiencies for chick neurons, it is possible that they are significant for other cell types. There is good reason to believe that the prepulse temperature influences the degree of wounding by the pulse, whereas the postpulse temperature can affect the rate of resealing. Thus, cells with significantly different membrane properties or intracellular machinery for membrane wound healing could require more specific temperatures than chick neurons.

Acknowledgments

This work was supported by NIH Grant NS27073 (PJH) and a DOE GAANN predoctoral fellowship (CYM).

References

- Anderson, M. L. M., Spandidos, D. A., and Coggins, J. R. (1991). Electroporation of lymphoid cells: Factors affecting the efficiency of transfection. *J. Biochem. Biophys. Methods* **22**, 207–222.
- Chakrabarti, R., Wylie, D. E., and Schuster, S. M. (1989). Transfer of monoclonal antibodies into mammalian cells by electroporation. *J. Biol. Chem.* **264**(26), 15494–15500.
- Chang, D. C. (1992). Structure and dynamics of electric field-induced membrane pores are revealed by rapid-freezing electron microscopy. In "Guide to Electroporation and Electrofusion." (D. C. Chang, B. M. Chassy, J. A. Saunders, and A. E. Sowers, eds.), pp. 9–28. Academic Press, San Diego.
- Chang, D. C., and Reese, T. S. (1990). Changes in membrane structure induced by electroporation as revealed by rapid-freezing electron microscopy. *Biophys. J.* **58**, 1–12.
- Dimitrov, D. S., and Sowers, A. E. (1990). Membrane electroporation-fast molecular exchange by electroosmosis. *Biochem. Biophys. Acta* **1022**, 381–392.
- Djuzenova, C. S., Zimmerman, U., Frank, H., Sukhorukov, V. L., Richter, E., and Fuhr, G. (1996). Effect of medium conductivity and composition on the uptake of propidium iodide into electropermeabilized myeloma cells. *Biochem. Biophys. Acta* **1284**, 143–152.
- Golzio, M., Mora, M. P., Raynaud, C., Delteil, C., Teissie, J., and Rols, M. P. (1998). Control by osmotic pressure of voltage-induced permeabilization and gene transfer in mammalian cells. *Biophys. J.* **749**(6), 3015–3022.
- Hibino, M., Itoh, H., and Kinoshita, K. Jr. (1993). Time courses of cell electroporation as revealed by submicrosecond imaging of transmembrane potential. *Biophys. J.* **64**, 1789–1800.
- Ho, S. Y., and Mittal, G. S. (1996). Electroporation of cell membranes: A review. *Crit. Rev. Biotechnol.* **16**, 349–362.

- Lambert, H., Pankov, R., Gauthier, J., and Hancock, R. (1990). Electroporation-mediated uptake of proteins into mammalian cells. *Biochem. Cell Biol.* **68**, 729–734.
- Li, H., Chan, S. T. H., and Tang, F. (1997). Transfection of rat brain cells by electroporation. *J. Neurosci. Methods* **75**, 29–32.
- Li, Y.-C., Beard, D., Hayes, S., and Young, A. P. (1995). A transcriptional enhancer of the glutamine synthetase gene that is selective for retinal Müller glial cells. *J. Mol. Neurosci.* **6**, 169–183.
- McNeil, P. L. (2002). Repairing a torn cell surface: Make way, lysosomes to the rescue. *J. Cell Biol.* **115**, 873–879.
- McNeil, P. L., and Steinhardt, R. A. (1997). Loss, restoration and maintenance of plasma membrane integrity. *J. Cell Biol.* **137**, 1–4.
- McNeil, P. L., and Terasaki, M. (2001). Coping with the inevitable: How cells repair a torn surface membrane. *Nature Cell Biol.* **3**, E124–E128.
- Mir, L. M., Banoun, H., and Paoletti, C. (1988). Introduction of definite amounts of nonpermeant molecules into living cells after electroporation: Direct access to the cytosol. *Exp. Cell Res.* **175**, 15–25.
- Potter, H. (1993). Application of electroporation in recombinant DNA technology. *Methods Enzymol.* **217**, 461–478.
- Pu, H., and Young, A. P. (1990). Glucocorticoid-inducible expression of glutamine synthetase-CAT-encoding fusion plasmid after transfection of intact chicken retinal explant cultures. *Gene* **89**, 259–263.
- Rols, M.-P., Delteil, C., Serin, G., and Teissié, J. (1994). Temperature effects on electrotransfection of mammalian cells. *Nucleic Acids Res.* **22**(3), 540–540.
- Steinhardt, R. A., Bi, G., and Alderton, J. M. (1994). Cell membrane resealing by a vesicular mechanism similar to neurotransmitter release. *Science* **263**, 390–393.
- Tekle, E., Astumian, D., and Chock, P. B. (1994). Selective and asymmetric molecular transport across electroporated cell membranes. *Proc. Natl. Acad. Sci. USA* **91**, 11512–11516.
- Teruel, M. N., Blanpied, T. A., Shen, K., Augustine, G. J., and Meyer, T. (1999). A versatile microporation technique for the transfection of cultured CNS neurons. *J. Neurosci. Methods* **93**, 37–48.
- Weaver, J. C. (1993). Electroporation: A general phenomenon for manipulating cells and tissues. *J. Cell. Biochem.* **51**, 426–435.

This Page Intentionally Left Blank

CHAPTER 17

Biolistic Transfection

Paul C. Bridgman, Michael E. Brown, and Irina Balan

Department of Anatomy and Neurobiology
Washington University School of Medicine
St. Louis, Missouri 63110

- I. Introduction
 - A. Background
 - B. Overview of the Method
- II. Parameters that Affect Success of the Method
 - A. Particle Size and Composition
 - B. DNA Coating
 - C. Particle Immobilization on a Carrier
 - D. Particle Propulsion
 - E. Particle Speed, Spread, and Penetration Depth
 - F. Fluid Level
 - G. Particle and Cell Density
 - H. Levels and Timing of Expression
- III. Factors that May Affect Performance but Have Not Been Tested
 - A. Damage to Cell or Nucleus
 - B. Damage to DNA on the Particle
- IV. Future Developments or Improvements
 - A. Particle Design
 - B. DNA Coating Efficiency
 - C. Improved Barrel Design
 - D. Focused Transfection of Single or Small Groups of Cells
 - E. Application to Related Techniques
- V. Conclusion
- References

Recent improvements in the biolistic technique and devices have increased its usefulness for transfection of neurons. With these recent advances, both dissociated and slice cultures can be transfected at reasonably high rates. This

chapter focuses on the parameters that determine the successful biolistic transfection of neurons in both types of cultures.

I. Introduction

A. Back ground

Biological ballistics (biolistics) was developed as a method for the transformation of plant cells in the late 1980s (Klein *et al.*, 1987; Sanford *et al.*, 1993). Because the cell wall of plant cells resists chemical methods of transformation, an alternative physical method became necessary. The use of biolistics to transfect plant cells has been successful and has subsequently been used with increased frequency. Soon after the development of biolistics for plant cell transfection, the method was tried for other difficult to transfect cells, including primary neuronal cultures and brain slices (Yang *et al.*, 1990; Klein *et al.*, 1992; Jiao *et al.*, 1993; Lo *et al.*, 1994). The method has met with mixed success. However, recent modifications have improved its reliability and utility for neuronal cultures. For studies requiring transfection of primary cultured neurons, biolistics has become a useful technique (Bridgman, 1999; Malin and Nerbonne, 2001; Cummins *et al.*, 2001). McAllister (2000) has described details of the basic procedure used for neurons. This chapter focuses on understanding the parameters that can influence the success of the method and how these relate to custom adaptations of the technique or devices for specific experimental purposes.

A physical method of transfection, such as biolistics, has several advantages over chemical transfection or viral infection methods when used for neurons or brain tissue. Biolistics appears to be less toxic than certain chemical procedures (lipophilic transfection agents). It requires less preparation time and may be less toxic than some types of viral infection (Ehrengreuber *et al.*, 2001). Although, as discussed later, the biolistic procedure must be adapted to different culture conditions (dissociated cells versus slices) or target cell size, it appears to be less dependent on specific cell type or location in the nervous system (peripheral versus central) for success. Biolistic procedures can be standardized to give reproducible rates of transfection. The maximum rates of transfection compare favorably to those obtained with chemical methods or viral infection (Wellmann *et al.*, 1999; Murphy and Messer, 2001; O'Brien *et al.*, 2001; Klimashewski *et al.*, 2002). In addition, biolistics can be modified easily to give different rates of transfection for different types of experiments (Wellmann *et al.*, 1999; O'Brien *et al.*, 2001; unpublished observations). One drawback of the biolistic method in its current form is that it has not been adapted to allow transfection of single cells as has been done with transfection using electroporation (Haas *et al.*, 2001). Therefore, if a cell type in a mixed dissociated culture or slice is rare, then the frequency of obtaining transfection of that specific type of cell is low. However, this deficiency might be met by a further custom adaptation of the method.

B. Overview of the Method

Biolistics is based on a simple concept. DNA (usually plasmid DNA)-coated particles are forced into cells using high-speed physical propulsion. Particles that enter and remain in the nucleus presumably release DNA from their surfaces, which results in production of the protein encoded by that DNA through normal transcriptional and translational mechanisms. Because of the physical basis of the method it depends on several defined parameters, each of which is relatively simple. Each parameter can determine the success or failure of the method, but can also be changed to adapt to different cellular, tissue, or experimental requirements. Parameters include (1) particle density and size; (2) DNA coating density; (3) particle attachment strength and degree of dispersal on the carrier; (4) particle speed, spread, and distance of travel; (5) particle and cell density; (6) cell size or tissue thickness; and (7) thickness of the fluid level covering the cells or tissue. These parameters depend on the physical characteristics of the biolistic device in combination with the preparation of “bullets” and the setup of the device for shooting. Each of these is discussed, focusing on the adaptations that have led to the successful transfection of cultured neuronal cells or brain slices.

II. Parameters that Affect Success of the Method

A. Particle Size and Composition

Particle size is limited by several factors. These are the minimum surface area needed for DNA absorption, the minimum mass necessary for particles to penetrate fluid and cells, and the maximum size allowable without causing excessive cell damage. The most frequent sizes used are between 0.6 and 1.6 μM . These have proven to be the most useful. Small (0.6–1.0) particles have been used most frequently for cell culture monolayers. The larger particles have been used with most success in tissue slices where the goal is to transform relatively large cells. A larger particle mass gives greater penetration, as the particles have greater momentum. However, particles that are too large may cause cell damage. Gold particles are used most frequently because they are inert, nontoxic, spherical, and relatively dense. Gold particles can be purchased in different sizes from Bio-Rad. These particles have been sized so that they are relatively uniform in diameter. Less uniform gold particles are also available from Technic, Inc. In our hands, the transformation rates obtained with particles from Technic (average 1 μm diameter) are very similar to those obtained with 1- μm particles from Bio-Rad.

Tungsten has also been used for biolistics, but has been reported to cause changes in culture medium pH and may cause neuronal apoptosis (O'Brien *et al.*, 2001; Sanford *et al.*, 1993). It is our experience that tungsten particles also tend to be shaped more irregularly and tend to clump.

B. DNA Coating

Highly pure plasmid DNA free of protein, genomic DNA, or RNA is recommended for particle coating. It is important that any resin residue that may result from plasmid DNA column purification be removed completely, as small amounts of residual resin can cause particle aggregation (Wellmann *et al.*, 1999). DNA coating to the gold particles is usually facilitated by precoating the gold with the highly charged polycationic molecule spermidine. Other polymers have also been used with success (Prokop *et al.*, 2002). DNA apparently can bind directly to gold particles because successful transfection has also been obtained without using precoating materials (Sato *et al.*, 2000). The amount of DNA coating is usually expressed as the ratio of DNA mass to particle mass or DNA loading ratio (DLR). Typical ratios range from 1 to 4 $\mu\text{g}/\text{mg}$. Too high of a DNA-to-gold ratio can lead to gold particle aggregation, which is most apparent with the smaller sizes of gold (Wellmann *et al.*, 1999).

1. Gold Coating Procedure

Purify plasmid DNA using (Qiagen) plasmid Midi (or Maxi) prep kits. Spin the purified DNA for 5 min at the maximum speed in a microfuge. Remove supernatant carefully, leaving a small amount of fluid (and any residual resin) in the tube. Precipitate DNA with cold ethanol (overnight) and resuspend in water at a concentration of about 1 $\mu\text{g}/\mu\text{l}$. The following is very similar to the procedure outlined in the Bio-Rad gene gun instruction manual. Weigh out 50 mg of gold. Add 100 μl spermidine and then vortex. Sonicate for 5–10 s. Add 100 μl DNA and vortex. Precipitate onto gold by adding 100 μl 1 M CaCl_2 dropwise during low-speed vortexing (let settle 10 min). Wash three times with fresh 100% ethanol (1 ml). Resuspend in fresh ethanol containing polyvinylpyrrolidone (PVP) (we use a low concentration: 2.5–5 $\mu\text{g}/\text{ml}$). We have found that PVP is not necessary for some types of plastic carriers (polypropylene), but improves adherence to Teflon. The final volume determines the density of particle coating the carrier. It is best to error on the side of being too concentrated initially, as the solution can always be diluted further. To coat the carrier, add the gold particle solution to the carrier tube. Let the gold settle and then draw off fluid slowly using a syringe. Immediately rotate tube to evenly disperse gold particles over the entire inner surface of the carrier. Let dry completely before shooting.

C. Particle Immobilization on a Carrier

DNA-coated particles need to be attached to an immobile inert carrier to allow their acceleration by the means of propulsion. For acceleration by a pressure gradient, PVP has been used as a gluing agent to attach the particles to the inner surface of Teflon (tefzel) tubing. It is important to disperse the particles as much as possible on the wall of the tubing or carrier to avoid clumps. Clumping leads to decreased transfection rates (Wellmann *et al.*, 1999). For tube carriers,

this is accomplished by adding the particles to the inside of the tubing as a ethanol PVP suspension followed by quick rotation of the tubing or carrier immediately after removal of the liquid. It is difficult to obtain even coating. However, as long as clumping is minimized, this does not appear to influence transfection rates. More even distribution of particles and a wider target area can be achieved using different types of carriers, such as those made from flat porous materials. However, we have found that tube type carriers are the most efficient. Fewer particles are left behind after the blast and the particles disperse to different degrees depending on the barrel design.

D. Particle Propulsion

The means of accelerating particles has varied with devices of different design. The original commercial device used the high-speed impact of a “macrocarrier” driven by a bullet or helium gas burst to accelerate particles off a surface through a partial vacuum. Other impact-driven acceleration methods have also been used (Sato *et al.*, 2000). The latest commercially available device (Bio-Rad Helios gene gun) uses a high-pressure helium gas burst to directly carry the particles through air. A high-speed gas valve releases a short (tens of milliseconds) burst of pressurized helium. The pressure gradient formed within a small diameter tube creates a high velocity wave or wind that sweeps the particles off the internal surface of a Teflon carrier. The gas carrying the particles is directed along a barrel toward the sample. This is an efficient and simple means of accelerating particles over relatively large distances, but suffers from the detrimental affects of damage caused by the impact of the particles and gas itself at the specimen surface. Recent custom refinements have minimized these affects using improved screens or filters that allow many of the single particles to pass, but block aggregates and much of the wind created by the steep pressure gradient. The degree of the screening affect is determined by pore size and total open area.

We use a 50-ms burst of compressed gas to propel gold particles from a custom-made device (Fig. 1). A minimum pressure is needed to strip the particles from the carrier, but the exact setting used depends on the sample and barrel configuration (see later). We have used both high-purity-compressed helium and nitrogen as the gas propellant. The type of nonflammable gas used should have little or no affect on propulsion provided it is dry and free from contaminants. We have not detected any observable differences between high-purity helium and nitrogen when used for biolistic transfection.

E. Particle Speed, Spread, and Penetration Depth

For pressure gradient-induced propulsion, particle velocity is determined by the difference between atmospheric pressure and the helium (or other gas) pressure prior to release, in combination with the size and geometry of the exit chamber or barrel. Thus, assuming a fixed valve opening time, setting a higher starting

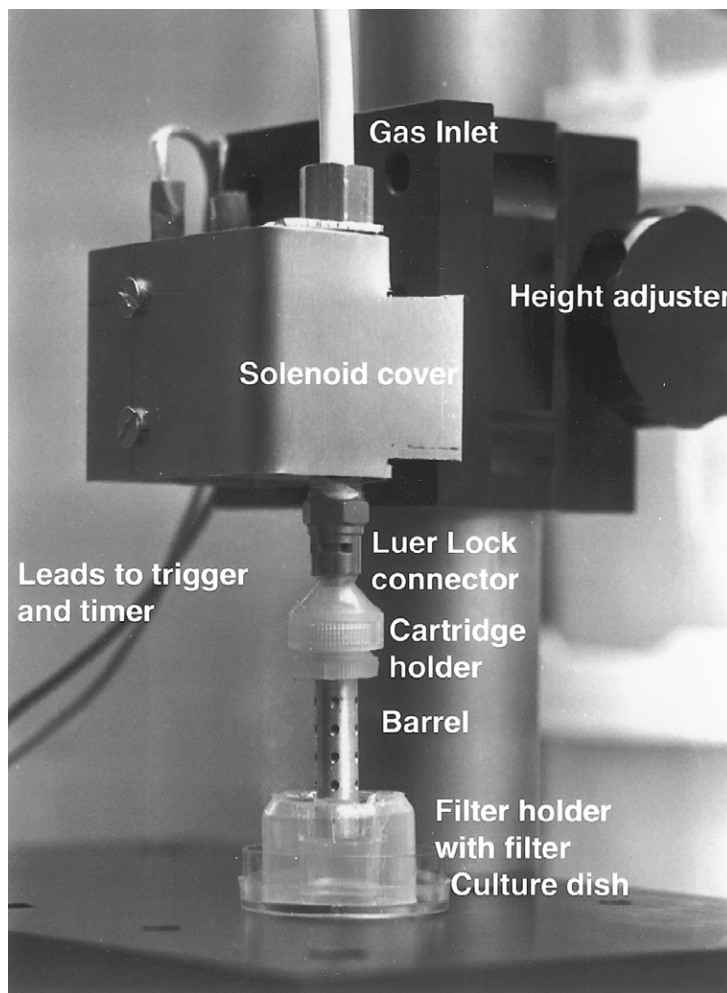


Fig. 1 An image of our custom-designed biologics device. The main features that contribute to its reliability and reproducibility include a precisely timed trigger for the solenoid valve, a precise height adjustment system, a narrow-diameter baffled barrel, and a small pore size filter. Particle carriers (cartridges) are supported by a plastic ring that fits inside a modified Millipore filter holder (cartridge holder). The particle carriers are cut-off yellow pipette tips (200- μ l tips). The gold particle solution is drawn into the pipette tip using an Eppendorf pipettman. The solution is allowed to settle for about 30 s and is then expelled slowly. The tip is removed, inverted quickly, and rotated by hand. The middle part of the tip containing the adhering gold particles is cut out and mounted for shooting. The narrow part of the tip is oriented toward the sample. The straight baffled barrel was based on the design described by O'Brien *et al.* (2001). The tapered barrel is made from an inverted, cut-off (narrow end) yellow tip.

pressure on a compressed gas tank or using a smaller diameter particle chamber and barrel produces higher velocities. This is because the mass of the gas bolus released depends on the starting pressure. Higher pressures result in a larger mass being released that expands to a greater volume at atmospheric pressure. The flow of the expanding gas through the chamber and barrel is similar to other propulsion devices and is defined by the physics of compressible mass flow rates. The velocity that a fluid (a liquid or gas) mass flows through a tube is dependent on the cross-sectional area of the tube. Thus, for a set mass, narrow tubes (or constrictions within tubes) produce higher velocities (within limits; flow choking can occur).

The extent of the pressure gradient, size, and geometry of the barrel could also potentially determine the distance that the particles are carried before being slowed or halted by air resistance or other factors (pressure equalization or wall friction). In practice, the mass of gas released is set large enough that internal pressure equalization is not a factor and internal frictional or air resistance effects are minimal. However, air resistance does cause spreading of the particles as they exit the barrel. This affects distribution of the gold particles so that the particles are spread over a larger target area with increasing distance from their site of exit (Fig. 2). An appropriate analogy is the air rifle. High pressure combined with a long narrow barrel (internal ballistics) maximizes the speed that the projectile exits the barrel. The speed of exit, in combination with other factors, such as wind resistance (external ballistics), determines the distance (or speed of impact) and path that a projectile is shot. The speed and spreading of the particles is important because it determines the ability of the particles to penetrate the overlying fluid layer and into cells or tissue. Minimizing the spread using a small-diameter barrel positioned close to the specimen gives better sample penetration at a given pressure gradient, but it reduces the area hit by particles and can increase the amount of blast damage due to the impact of the propulsive gas.

One recent modification that helps circumvent blast damage is the incorporation of baffles along the barrel (O'Brien *et al.*, 2001). The baffles reduce the impact of the pressure gradient by allowing venting along the length of the barrel without causing significant particle dispersal. Another modification that we have found effective is to use a continuously tapered chamber/barrel. The narrow end contains the immobilized particles and the wide end is the barrel exit. The result is high velocities at the start of the chamber needed to sweep the particles from the internal surface followed by a continually decreasing gas velocity until the barrel exit. The particles are spread more evenly than with a uniform diameter barrel (Fig. 2). It is important to note that even at its widest diameter the taper barrel we have tested is smaller in diameter (see later) than those used in commercial devices (Bio-Rad Helios gene gun).

We use different pressure settings, barrels, and screens for different samples. To determine the pressure range and distance from the barrel to the sample, we did a series of tests using 0.5% agarose as a target (without filters or screens). The consistency of 0.5% agarose is close to that of P0 mouse brain. After the shot,

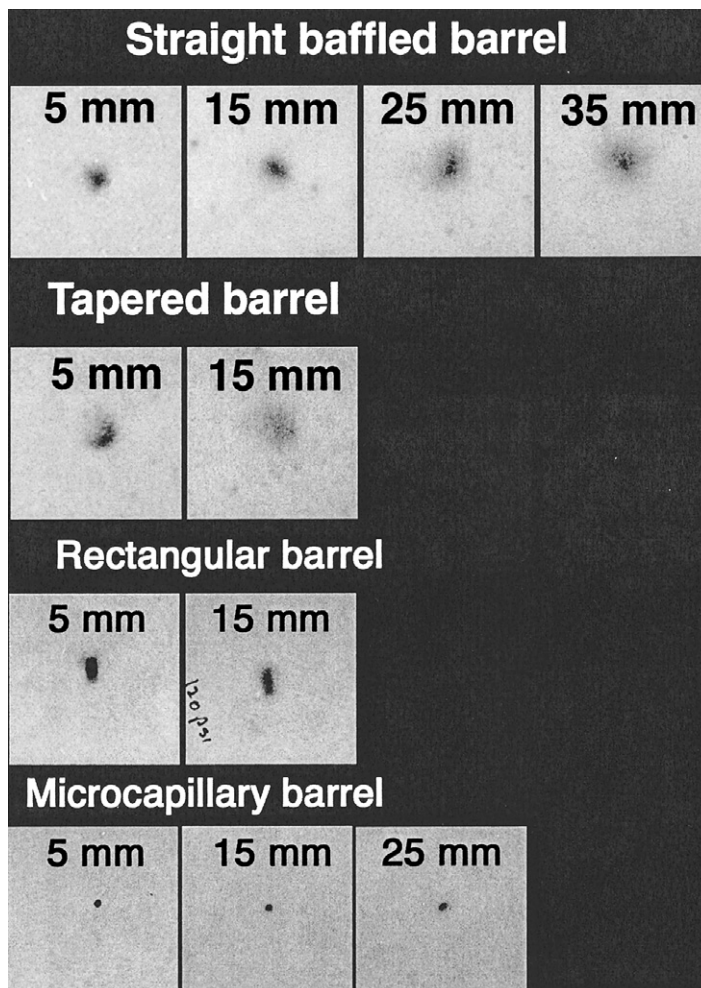


Fig. 2 (Top) A series of images showing particles (tungsten) spread on pieces of filter paper following shots at 120 psi from our custom gun at different heights (numbers in millimeters). A baffled straight barrel was used. Note that although the particles show some spreading with increasing distance from the paper, the central target area remains relatively concentrated. This is presumably a product of the straight relatively narrow barrel. The slight asymmetries result from uneven coating of the carrier. (Top middle) Two images showing the spread of particles, but using a tapered barrel. Particles show greater spread and a more even distribution at equivalent distances compared to the straight barrel. (Bottom middle) Two images showing the spread of particles from a rectangular barrel (3 cm length, 6.5 × 3 mm O.D., 5.5 × 2.5 mm I.D.) following shots at 120 psi. The particles are distributed evenly within the rectangle and tend to spread little with increasing distance from the paper. (Bottom) Several images showing the particle distribution that occurs upon shots (60 psi) from a barrel made from microcapillary glass (7 cm length, 1.5 mm O.D., 1.0 mm I.D.). Particles spread relatively little at increasing distances and are confined to a small area. Bar: 170 mm.

we cut the target area of the agarose on a vibratome (50- μm sections) perpendicular to the surface. The depth of particle penetration and surface of the agarose was viewed by microscopy. Greater numbers of particles penetrate to greater depths with increasing pressure or short distances from the barrel to the sample, similar to observations made by others using a modified commercially available gene gun (O'Brien *et al.*, 2001). However, high pressure and short distances also caused surface damage. Too low a pressure setting leaves too many of the particles bound to the carrier. We found that the best approach was to find a minimum pressure setting that resulted in the majority of particles being swept from the carrier and then to vary the distance between the barrel and the sample. With pressure settings between 110 and 140 psi and a distance between 10 and 20 mm from the end of the barrel to the sample surface, there was little or no detectable surface damage. There were only minor differences in degree of surface damage and particle penetration depth between the straight and tapered barrels (see later). It appears that the most critical factor is the distance of the barrel to the sample (assuming barrels of similar diameters). A series of tests using the aforementioned pressure and distance ranges was then performed on dissociated cultures and brain slices. These tests resulted in the following optimal set of parameters for our device. For dissociated cultures, we use an aluminum baffled barrel 35 mm in length and an internal diameter of 6 mm. The pressure setting is 120 psi. We use 3- to 12- μm pore size tissue culture insert filters [Costar brand Transwell-clear inserts (12 mm diameter) normally used for tissue culture of slices or organotypic cultures] as screens. The distance from the end of the barrel to the sample is 15 mm. Using this configuration, we typically achieve up to a 25% transfection rate in the central target area in dissociated cultures of peripheral nerve (superior cervical ganglion or dorsal root ganglion neurons) (Fig. 3A). Dissociated cultures of central nervous system neurons give similar results (Fig. 3B). For brain slices, we use either the baffled barrel or a nonbaffled tapered barrel (30 mm length, entry 3 mm I.D., exit 5.5 mm I.D.). The starting pressure setting is 120–140 psi. For slices, we use either a 12- μm pore size filter or a nylon mesh with a 35- μm pore size (27% open area) as a screen. Both glia and neurons are transfected with both types of barrels (Fig. 4).

For a simple monolayer cell culture (assuming a minimal fluid level of 5–10 μm), penetration depth needed for particle entry into a cell nucleus is minimal (in the range of 20–30 μm). However, for a brain slice or organotypic culture, penetrations of 40–100 μm may be necessary. Thus, the pressures and barrel diameters for optimal performance are different (Wellmann *et al.*, 1999; O'Brien *et al.*, 2001). In addition, the optimal means of screening the blast are different. We have found that filters with relatively small-diameter pores and minimal open areas protect monolayer cultures better. Because of varying gene gun designs or modifications and means of screening the blast, these have to be determined empirically. However, once determined they should remain unchanged and reproducible for that sample type. One main disadvantage of the commercially available biolistic device (Bio-Rad Helios gene gun) is that most of the parameters that affect transfection

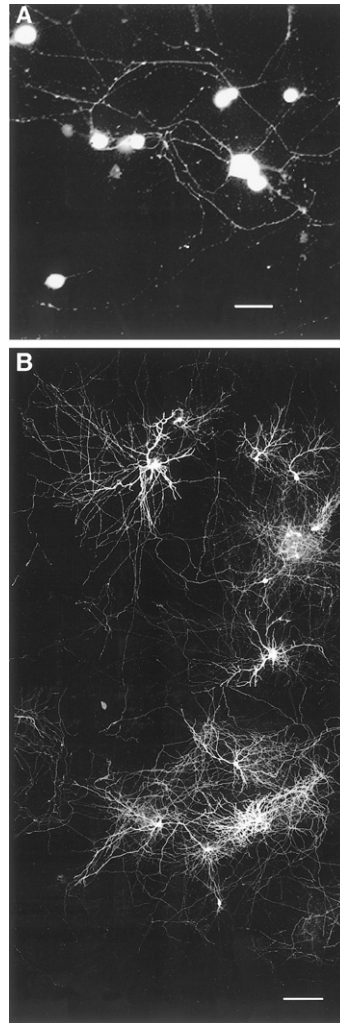


Fig. 3 (A) An image from a dissociated culture of mouse dorsal root ganglion neurons expressing EGFP. The culture was shot using our standard condition (120 psi, straight, baffled barrel, 15 mm distance, 3- μ m filter) for dissociated cultures. Twenty-five percent of the cells in the field showed EGFP expression 34 h after transfection. Bar: 35 μ m. (B) An image (a merged confocal stack) of a dissociated culture of mouse hippocampal neurons 24 h after transfection. The culture was shot using the standard condition. Bar: 210 μ m.

rates cannot be varied without custom alteration. In addition, it is difficult to precisely position and maintain a hand-held gun at a set distance that is exactly perpendicular to the sample. This reduces its effective reproducible transfection capability.

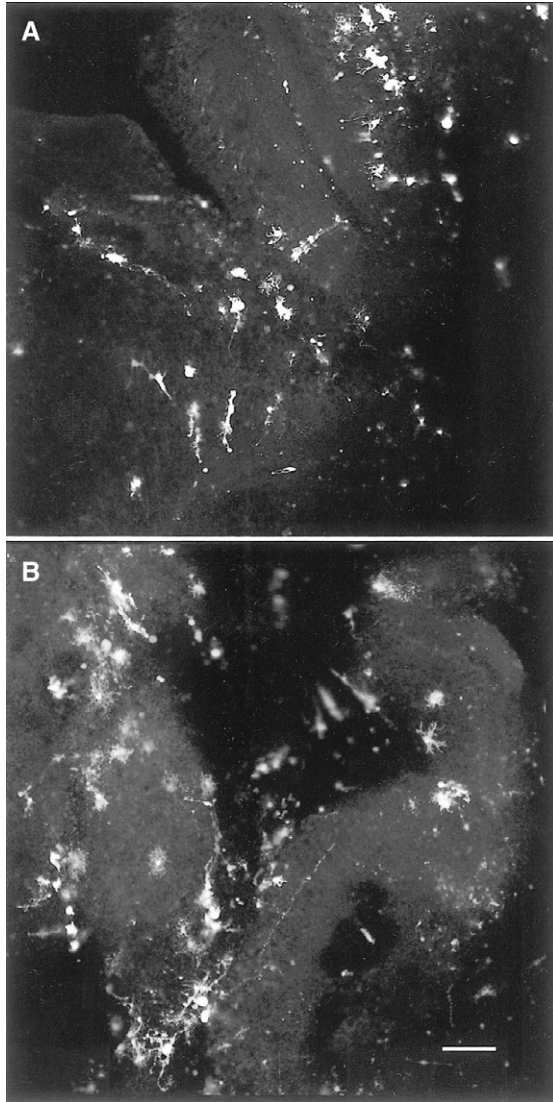


Fig. 4 (A) A low-magnification confocal merged stack of a cerebellar slice culture from a P8 mouse showing transfected neurons and glia expressing EGFP. The culture was shot with a baffled barrel under the same conditions used for dissociated cultures. (B) A confocal merged stack of a cerebellar slice shot at 120 psi with a tapered barrel using a 12- μm filter. Not all the cells fall with the focal range that was scanned because they are deeper within the section. The frequency of transfection is similar to the area shown in A, but EGFP-positive cells were distributed over a wider area in B (outside the field shown). Bar: 135 μm .

F. Fluid Level

The level of fluid covering the surface of the sample is the most difficult parameter to reproduce from sample to sample because it must be decreased to a thin layer just prior to shooting the particles. It is essential to keep a covering layer of fluid over all cultured cells or slices. If the fluid layer is too low, there is a danger of cell lysis resulting from surface tension forces at the air–fluid interface. In addition, as the volume of fluid decreases, there is a danger of changes in osmolarity due to water evaporation and, in extreme cases, total desiccation of cells or tissue. However, if the fluid layer covering the sample is too thick, then the penetration of particles into cells can be severely hampered or eliminated. One can imagine the loss of speed that occurs when a solid metal particle traveling through air hits a fluid surface. Depending on the angle that the particle hits the surface, this can potentially be accompanied by skipping of the particle over the surface followed by slow settling. Thus it is an advantage to minimize both the thickness of the fluid level covering the sample and the spread of particles so that they hit at approximately a 90° angle with the fluid surface. To prevent evaporation (especially when working under a culture hood), it is important to work fast. Fluid covering the sample must be drawn off and then returned as quickly as possible. To minimize surface tension affects, it is an advantage to use fluid such as culture medium that contains relatively high protein levels. The protein acts as a surfactant to help in wetting the sample surface and minimizing beading of the fluid. However, if the sample has an uneven surface contour (i.e., hills and valleys), it will be impossible to achieve an even layer of fluid over the surface and uneven penetration into cells will occur.

G. Particle and Cell Density

The rate of transfection is dependent on the density of particles shot relative to the density of target cells. Loading carriers with low numbers of particles reduces the number of cells transfected. The opposite is also true (provided the particles are dispersed and not clumped) except that too high a particle density can result in cell damage. For monolayer cultures, reducing the plating density results in fewer transfected cells. For organotypic cultures or brain slices, the cell density is not a variable. However, a greater penetration depth of particles results in more cells being transfected, assuming that blast damage is minimized.

H. Levels and Timing of Expression

The typical levels of expression achieved using biolistics are similar to those observed with other transfection methods (Klimaschewski *et al.*, 2002). Expression of enhanced green fluorescent protein (EGFP) in neurons produces very bright fluorescence, whereas expression of EGFP fusion proteins produces varying levels of fluorescence depending on the size of the construct used for transfection. For instance, large EGFP fusion proteins such as EGFP–myosin II are distinctly less

bright than EGFP. Coexpression of two constructs usually results in reduced levels of expression, but has the advantage that it can be used for quantitative assessments of relative expression levels (Thomas *et al.*, 1998).

The timing of detectable expression using fluorescent proteins also varies with construct. In our hands, EGFP can be detected as early as 4 h after transfection. Larger constructs may require 12–24 h.

III. Factors that May Affect Performance but Have Not Been Tested

A. Damage to Cell or Nucleus

It is clear that monolayer cultures are particularly susceptible to damage if the blast of the gas or the impact of particles is too intense. Usually this can be seen at the light microscopic level as a central area of high particle density containing dead cells (or no cells if very intense) surrounded by a ring of decreasing particle density and undamaged cells. In some cases there is a complete absence of cells (they have been blown off the substrate) if the blast is much too intense.

Less clear is how the impact of particles that does not noticeably affect cell morphology may influence long-term viability. It is unclear if individual particles that enter cells and stop in the nucleus cause cell damage. Presumably, particles entering the nucleus are coming to a halt rapidly. This suggests that it is unlikely that they cause fragmentation of genomic DNA. However, this has not been tested directly. If other cellular damage does occur, it is apparently repaired rapidly. Cells survive for at least 48 h after transfection as indicated by the expression of marker proteins such as GFP (O'Brien *et al.*, 2001). Stable cell lines of PC12 cultures have been made from cells transformed by biolistics (Wellmann *et al.*, 1999). Presumably, if cells are damaged irreversibly by a shot, they do not show expression and die quickly.

B. Damage to DNA on the Particle

The impact of gold particles onto the fluid surface could damage or strip DNA from the particle surface. Occasionally, spurious expression of proteins is observed that could result from DNA damage. However, no direct assays of DNA damage after biolistic procedures have been reported.

IV. Future Developments or Improvements

A. Particle Design

Designing particles with different shapes and compositions has been proposed as a means of improving penetration and DNA loading of particles (Ho *et al.*,

1998). For instance, using more streamlined particle shapes might enhance penetration. The DNA loaded onto particle could potentially be protected if it were attached within a protected pocket at the rear of a streamlined particle. To date, no studies have been reported using such designer particles.

B. DNA Coating Efficiency

The amount of DNA coating particles can potentially be increased using improved adhering reagents. This would be particularly valuable when coating particles with two or more types of DNA. Several different polymers have been tested for their ability to bind DNA to gold particles (Prokop *et al.*, 2002). At least one type of synthetic polymer (Tetronic, a trademark of BASF, Mount Olive, NJ) derived from propylene oxide, ethylene oxide, and ethylenediamine could produce a higher level of protein expression than spermidine in two of its formulations. This suggests that increasing the amount of DNA adhering to particles is possible and that this can result in higher levels of gene expression. However, it has already been observed with current coating protocols that adding large amounts of DNA can result in increased particle aggregation. Thus increasing coating density further may be counterproductive in some instances. This will need further investigation.

C. Improved Barrel Design

One drawback of a tubular barrel is that the particles at the site of impact are not distributed evenly. Usually, one observes a roughly radial distribution (asymmetry results from uneven coating of the carrier) with increased particle density in the center and gradually decreasing density with increasing distance from the center point (see Fig. 2). If one draws a line through the center of the particle field and measures the density of particles along this line the distribution appears to be roughly gaussian. The reason for this distribution is not entirely clear, but is likely to result from the characteristics of the airflow through the barrel combined with the tendency of the particles to show a radial spread upon exiting the barrel. An uneven distribution of particles can be detrimental for several reasons. If the particle density or pressure is too high, then the cells in the middle of impact field are destroyed or damaged. Transfected cells showing expression are then observed in a ring surrounding the center of the impact area. If damage does not occur, then transfection rates will decline with increasing distance from the center of the field.

We have tested alternative barrel shapes (Fig. 2). A tapered barrel shows a more even spread of particles with much less tendency for concentration at the central site of impact. Surprisingly, a straight barrel with a rectangular cross section also gives a more even distribution of particles than a straight cylindrical barrel.

D. Focused Transfection of Single or Small Groups of Cells

Very small-diameter barrels made from capillary glass may allow the transfection of single or small groups of cells (Fig. 2). The challenge is aiming such small-diameter barrels to precise areas of a culture or slice. It will be essential to view the sample and barrel end under a microscope for precise positioning.

E. Application to Related Techniques

Particle bombardment of cells and tissue has been adapted to allow staining of neurons with membrane dyes such as DiI (Gan *et al.*, 2000). This variation has been designated “DiOlistics.” Multicolored membrane dye-coated particles allow visualization of complex neural networks. We have also found that particles coated with Alexa 488 phalloidin can be used to stain actin in localized regions of cells such as neuronal dendritic spines. Other variations are likely to be developed and could potentially be used in various combinations.

V. Conclusion

Ten years after biolistics was first used with neurons, gradual improvements have finally made it a viable alternative as a routine transfection method. When optimized it is a reliable, efficient, and rapid method of transfection. Further improvements and custom alterations to the devices used for biolistics will only add to its usefulness and versatility in the future.

Acknowledgment

This work was supported by NIH Grants NS26150 and NS35162 to P.C.B. Dr. Michael Nonet developed the original prototype for the custom gene gun that we describe.

References

- Bridgman, P. C. (1999). Myosin Va movements in normal and dilute-lethal axons provide support for a dual filament motor complex. *J. Cell Biol.* **146**, 1045–1060.
- Cummins, T. R., Aglieco, F., Renganathan, M., Herzog, R. I., Dib-Hajj, S. D., and Waxman, S. G. (2001). Nav1.3 sodium channels: Rapid repriming and slow closed-state inactivation display quantitative differences after expression in a mammalian cell line and in spinal sensory neurons. *J. Neurosci.* **21**, 5952–5961.
- Ehrenguber, M. U., Hennou, S., Bueler, H., Naim, H. Y., Deglon, N., and Lundstrom, K. (2001). Gene transfer into neurons from hippocampal slices: Comparison of recombinant Semliki Forest virus, adenovirus, adeno-associated virus, lentivirus and measles virus. *Mol. Cell. Neurosci.* **17**, 855–871.
- Gan, W. B., Grutzendler, J., Wong, W. T., Wong, R. O., and Lichtman, J. W. (2000). Multicolor “DiOlistic” labeling of the nervous system using lipophilic dye combinations. *Neuron* **27**, 219–225.
- Haas, K., Sin, W. C., Javaherian, A., Li, Z., and Cline, H. T. (2001). Single cell electroporation for gene transfer in vivo. *Neuron* **29**, 583–591.

- Ho, T. H., Ruoff, R. S., Nemchuk, N. I., Zhang, P., and Amin, C. (1998). Use of designer particles in biolistics plant-transformation studies. *Am. Phys. Soc. Abst.* 138.11.
- Jiao, S., Cheng, L., Wolff, J. A., and Yang, N. S. (1993). Particle-bombardment mediated gene transfer and expression in rat brain tissues. *Bio Technology* **11**, 497–502.
- Klein, T. M., Arentzen, R., Lewi, P. A., and Fitzpatrick-McElligott, S. (1992). Transformation of microbes, plants, and animals by particle bombardment. *Bio Technology* **10**, 286–291.
- Klein, T. M., Wolf, E. D., Wu, R., and Sanford, J. C. (1987). High-velocity microprojectiles for delivering nuclei acids into living cells. *Nature* **327**, 70–73.
- Klimaschewski, L., Nindl, W., Pimpl, M., Waltinger, P., and Pfaller, K. (2002). Biolistic transfection and morphological analysis of cultured sympathetic neurons. *J. Neurosci. Methods* **113**, 63–71.
- Lo, D. C., McAllister, A. K., and Katz, L. C. (1994). Neuronal transfection in brain slices using particle-mediated gene transfer. *Neuron* **13**, 1263–1268.
- Malin, S. A., and Nerbonne, J. M. (2001). Molecular heterogeneity of the voltage-gated fast transient outward K⁺ current, I-Af, in mammalian neurons. *J. Neurosci.* **21**, 8004–8014.
- McAllister, A. K. (2000). Biolistic transfection of neurons: Science's STKE signal transduction knowledge environment. 2000:PL1.
- Murphy, R. C., and Messer, A. (2001). Gene transfer methods for CNS organotypic cultures: A comparison of three nonviral methods. *J. Am. Soc. Gene Ther.* **3**, 113–121.
- O'Brien, J. A., Holt, M., Whiteside, G., Lummis, S. C.R., and Hastings, M. H. (2001). Modifications to the hand-held gene gun: Improvements for in vitro biolistic transfection of organotypic neuronal tissue. *J. Neurosci. Methods* **112**, 57–64.
- Prokop, A., Kozlov, E., Moore, W., and Davidson, J. M. (2002). Maximizing the in vivo efficiency of gene transfer by means of nonviral polymeric gene delivery vehicles. *J. Pharm. Sci.* **91**, 67–76.
- Sanford, J. C., Smith, F. D., and Russell, J. A. (1993). Optimizing the biolistic process for different biological applications. *Methods Enzymol.* **217**, 483–509.
- Sato, H., Hattori, S., Kawamoto, S., Kudoh, I., Hayashi, A., Yamamoto, I., Yoshinari, M., Minami, M., and Kanno, H. (2000). In vivo gene gun-mediated DNA delivery into rodent brain tissue. *Biochem. Biophys. Res. Commun.* **270**, 163–170.
- Thomas, A., Kim, D. S., Fields, R. L., Chin, H., and Gainer, H. (1998). Quantitative analysis of gene expression in organotypic slice-explant cultures by particle-mediated gene transfer. *J. Neurosci. Methods* **84**, 181–191.
- Wellmann, H., Kaltschmidt, B., and Kaltschmidt, C. (1999). Optimized protocol for biolistic transfection of brain slices and dissociated cultured neurons with a hand-held gene gun. *J. Neurosci. Methods* **92**, 55–64.

CHAPTER 18

Expression of Transgenes in Primary Neurons from Chick Peripheral and Central Nervous Systems by Retroviral Infection of Early Embryos

Peter. J. Hollenbeck and D. M. Fekete

Department of Biological Sciences
Purdue University
West Lafayette, Indiana 47907

- I. Introduction
- II. Building Retroviral Vectors and Growing Functional Virus
 - A. Insert Size and Cloning Sites
 - B. Selecting and Modifying the Transgene for Insertion: SLAX 12 NCO
 - C. Confirming the Orientation and Sequence of the Insert
 - D. Producing Functional Virus
- III. Infecting Early Chick Embryos by Injection
 - A. Preparing Eggs
 - B. Injection into the Neural Tube
 - C. Postinjection Incubation
- IV. Dissecting Embryos and Culturing Neurons
 - A. Dissection and Selection of Ganglia
 - B. Culture and Microscopy
- V. Conclusions
- References

Many cell biological studies require the expression of transgenes in cells in culture, but it is difficult to obtain uniform, stable, and efficient expression of transgenes in primary neurons. We have approached this problem by adapting from developmental biologists the avian retroviral vector, RCAS. This vector allows the introduction of a transgene by infection early in chick embryonic development. Transgenes that are less than 2.6 kb in size can be cloned through an adapter

vector, SLAX 12 NCO, and into the RCAS retroviral vector with relative ease. The vector is then used to produce active virus, and the virus is injected into the neural tube or ventricles of stage 10 embryos. By infecting the neuronal precursor cells while they are still mitotic, the retrovirus and accompanying transgene are introduced into the genome and subsequently spread by replication, shedding of new virus, and infection of other cells. Embryos are incubated from the time of injection until E9–E12 and peripheral and central nervous system neurons are dissected out and grown in culture using standard techniques. In this manner, the majority of the sympathetic and dorsal root ganglion neurons can be induced to express the transgene. A similar result, at lower efficiencies, is obtained for central nervous system neurons.

I. Introduction

Several chapters in this volume address the difficulties of expressing transgenes in primary neurons in culture. In recent years, a number of methods have been developed that allow the transfection of primary neurons at reasonable efficiency in relatively large numbers. However, with the exception of adenovirus infection (see Chapter 19), most transfection methods remain best suited for the transient expression of transgenes in a relatively small fraction of a sample of neurons in culture. While this is adequate for studies using light microscopy to study individual neurons (e.g., see Chapter 14), analyses that require transgene expression by a high percentage of neurons in culture require a different approach. We have addressed this problem by adapting from developmental biologists the use of avian retroviral vectors for expressing transgenes in chick neurons. Properly used, these vectors allow the strong expression of transgenes at high efficiency starting from early in development and continuing through the period of cell culture.

Avian retroviral vectors have allowed developmental biologists to perform many of the same sorts of gene gain-of-function and loss-of-function experiments in the chick embryo that transgenic methods have made possible in the mouse. Vectors based on the genome of Rous sarcoma virus/avian leukemia virus (RSV/ALV) have now been used for more than a decade both to study the role of specific genes in chick embryonic development and to follow cell lineage during embryogenesis (Cepko *et al.*, 1995; Morgan and Fekete, 1996; Satoh and Fekete, 2003). Most of these studies utilize the RCAS vector, developed by Hughes and co-workers (Hughes and Kosik, 1984; Petropoulos and Hughes, 1991; Boerkoel *et al.*, 1993). A detailed treatment of the construction of RCAS vectors has been published in this series (Morgan and Fekete, 1996), and this chapter focuses on the use of these vectors for studies of chick neurons in culture.

The use of RCAS vectors to express transgenes is not a transient transfection method, but an infection method. An RCAS virus is introduced into the early chick embryo where it binds to host cells, is internalized, integrates into the genome, and is thus transmitted to all of the descendants of infected cells during

embryonic development. In addition, the use of replication-competent vectors ensures additional spread of the virus throughout the embryo due to viral replication, release, and infection of nearby cells. Replication-competent RCAS vectors can carry out all aspects of the retroviral life cycle, and cells infected by them show strong expression of viral proteins (and introduced transgenes) due to an efficient viral promoter. We have also found that, compared to transfected cells, populations of RCAS-infected neurons in culture show a level of transgene expression that is both more moderate and more consistent from cell to cell.

In order to use avian retroviral vectors to produce neurons expressing transgenes, it is important to appreciate three aspects of the retrovirus life cycle. First, a retrovirus can only integrate into the genome of a cell during the M phase of the cell cycle (Roe *et al.*, 1993). This places temporal limits on the accessibility of the virus to a cell population of interest and is particularly important for terminally differentiated cell types such as neurons. The vector must be introduced into the embryo well before the bulk of the precursors of the targeted neuronal population exits mitosis. Second, the ability of the retrovirus to spread is limited by diffusion of the introduced virus and the virus that has reproduced in cells and been released to the extracellular space. Thus, it is necessary to be aware of the location of the precursor cells of the targeted neurons, the position and nature of the embryonic compartment boundaries near them, and the routes of migration that they will take during development. As described later, our main sites of injection in the chick embryo have been the neural tube and the developing brain ventricles. Finally, the retrovirus enters the cell via a surface receptor that exists in four groups for the RCAS vectors. These ALV subgroups, designated A, B, D, and E, are not all present in all strains of chickens, and the viral susceptibility of the flock must be determined for each supplier. Because most commercial chicken flocks are resistant to subgroup E retrovirus, vectors are not usually built with this subgroup. The procedures described in this chapter were carried out using a subgroup A vector, but they are equally applicable to other subgroups.

II. Building Retroviral Vectors and Growing Functional Virus

A. Insert Sizes and Cloning Sites

Although both replication-competent and replication-incompetent vectors are used in developmental studies, replication-competent ones are the most useful for cell biological experiments. The spread of replication-competent virus from cell to cell within the embryo is essential to obtain the highest possible fraction of infected neurons. In fact, the replication-competent virus, introduced into an embryo before the last birthday of the neurons of interest, has the capacity to infect 100% of the neurons in the infected region or compartment of the embryo. The major limitation of the replication-competent virus is that because replication requires a full set of retroviral genes (Morgan and Fekete, 1996), there is an upper limit on the size of the transgene that can be inserted without compromising the

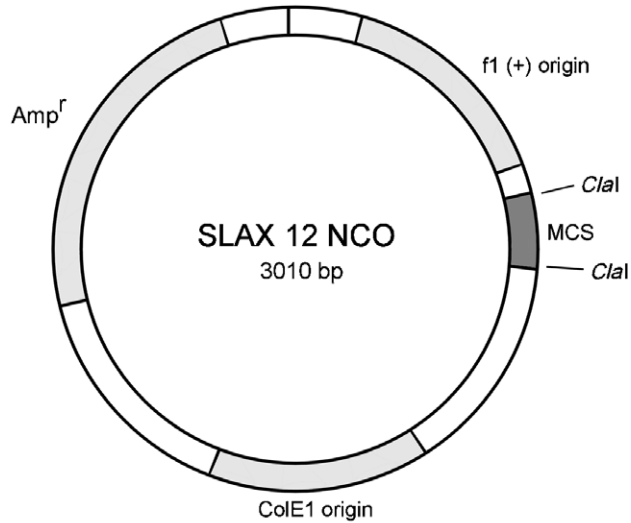
viability of the virus. Another limitation of replication-competent RCAS is that its size (11.6 kb) can make it difficult to clone into it directly. For routine use, the transgene is first subcloned into a shuttle vector, then excised with *Cla*I, and then inserted into RCAS at the virus' single *Cla*I site. RCAS vectors should be obtained by material transfer agreement (MTA) request from S. Hughes (NCI-Frederick Cancer Research and Development Center, Frederick, MD).

B. Selecting and Modifying the Transgene for Insertion: SLAX 12 NCO

Although an insert can be cloned into RCAS with no more than its coding region bearing a *Cla*I site at each end, several other factors are important in maximizing expression of the transgene in virus-infected cells. First, because expression of a transgene in the retroviral genome requires termination and reinitiation of translation, it is best to use inserts with the minimum possible amount of an 5'-untranslated sequence. Second, the total size of the insert cannot exceed 2.6 kb or expression drops off precipitously.

Cloning into RCAS and obtaining a functional virus with good transgene expression have been made easier by the development of shuttle vectors that contain a multicloning sequence flanked on either side by *Cla*I sites, thus facilitating the construction of an insert with *Cla*I ends. Although several shuttle vectors can be used, we strongly recommend the use of SLAX 12 NCO (Morgan and Fekete, 1996) for virus construction (see Fig. 1). SLAX 12 NCO contains the *Cla*I-*Cla*I region of a shuttle vector designed previously by Hughes and co-workers (1987), Cla 12 NCO, transferred to a pBluescript backbone. Within the *Cla*I-*Cla*I region is a multicloning sequence and, upstream of that, the src 5'-untranslated region. An insert can be placed in the correct frame by cloning it into SLAX 12 NCO with its start codon at the ATG of the *Nco*I site (CCATGG). When the insert is finally cloned out of SLAX 12 NCO and into the retroviral vector, the position of this *Nco*I site relative to the src 5' UTR promotes strong expression of the transgene in infected cells. SLAX 12 NCO can be obtained by MTA request from Bruce Morgan (Cutaneous Biology Research Center, Harvard Medical School, Charlestown, MA)

The best strategy for cloning an insert into SLAX 12 NCO at the *Nco*I site depends on the base sequence around the start codon of the insert gene (see Morgan and Fekete, 1996). If the start codon of the gene to be inserted sits in the context of an *Nco*I site (CCATGG), it can be cloned directly into SLAX 12 NCO using *Nco*I and a convenient 3' cloning site. If the start codon is not within an *Nco*I site, there are two approaches to getting the insert into SLAX 12 NCO. If the two bases upstream of the ATG are not CC, but the downstream base is a G, polymerase chain reaction (PCR) mutagenesis with an appropriate 5' primer (CCATGG...) can be used to produce the insert gene with a *Nco*I site around the start codon without changing the coding region. If a convenient 3' cloning site is not present in the insert gene, this can also be introduced in the same PCR procedure using an appropriate 3' primer. The final PCR product can then be



Multicloning sequence of SLAX 12 NCO:

```

AAT AAC CCT TAA AGG GAA CAA AAG CTG GAG CTC ATC GAT TCT AGA CCA
          ↑                                     ↓
          T3 primer                             ClaI

CTG TGG CCA GGC GGT ACG TGG GAC GTG CAG CCG ACC ACC ATG GCC ATG
                                               NcoI

ATT ACG AAT TCG AGC TCG CCC GGG GAT CCT CTA GAG TCG ACC TGC AGC
      Eco RI          Sma I BamH I          PstI

CCA AGC TTA TCG ATA CCG TCG ACC TCG AGG GGG GGC CCG GTA CCC AAT
      HindIII ClaI          Xho I          Apa I          Kpn I

TCG CCC TAT AGT GAG TCG TAT T
          ↓
          T7 primer
  
```

Fig. 1 (Top) A graphic representation of the SLAX 12 NCO vector, which contains the *ClaI*–*ClaI* region of the adapter plasmid Cla 12 NCO (Hughes *et al.*, 1987) transferred to a pBluescript derivative. This places the versatile multicloning sequence (MCS) of Cla 12 NCO in a high-copy number plasmid with universal primers to facilitate sequencing and other PCR procedures. (Bottom) The multicloning sequence is flanked by T3 and T7 primers and the two *ClaI* sites. It includes several 3' sites for insertion of the transgene, including *PstI*, which generates a 3' overhang and is essential for inserting transgenes that lack a G immediately 3' to their start codon (see text).

cloned easily into SLAX 12 NCO using *NcoI* and the chosen 3 site. However, if the base downstream of the start codon is not a G, it is necessary to generate an *NcoI*-compatible overhang (CATG) in order to clone into the *NcoI* site. This is accomplished by using PCR mutagenesis with an appropriate 5' primer to produce a CATG 5' end, followed by digestion with exonuclease III to generate a *NcoI*-compatible 5' overhang. Prior to exo III digestion, the 3' end should be cut at a convenient restriction site that produces a 3' overhang that is resistant to exo III, such as *PstI*. Once modified in this manner, the insert can then be cloned into SLAX 12 NCO at *NcoI/PstI*, with the loss of a functional *NcoI* site (see Morgan and Fekete, 1996).

An additional potential problem with cloning an insert into SLAX 12 NCO at the *NcoI* site is the presence of one or more internal *NcoI* sites in the insert. We have dealt with one internal *NcoI* site by partial digestion of the insert and selection of the fragment that is cut only at the *NcoI* start codon. The presence of two or more *NcoI* sites, or of an internal *NcoI* site very close to the 5' end, in the insert would make the cloning of an insert into SLAX 12 NCO more difficult, although this problem could be solved using PCR mutagenesis.

Once the insert is cloned into SLAX 12 NCO at the *NcoI* site and a convenient 3' cloning site, the new vector can be amplified in bacteria, and the insert can be excised from the shuttle vector (along with the src 5' UTR) by *ClaI* digestion, gel purified, and ligated into RCAS at its unique *ClaI* site. We are careful to conserve and safely store each insert-containing SLAX 12 NCO vector that we construct for future analysis or virus construction, with or without additional modification of the transgene.

C. Confirming the Orientation and Sequence of the Insert

The mandatory use of the single RCAS *ClaI* site to clone in the transgene insert means that both orientations of the transgene in the viral vector are equally likely. Thus, PCR and/or sequencing must be used to select RCAS clones with the correct insert orientation. Primers specific for sites on the RCAS vector that are close to the *ClaI* site are paired with primers designed for the specific insert so as to bind within the insert sequence, close to each end, and to amplify toward the *ClaI* site. If the insert has the correct orientation for sense transcription, then a PCR reaction using the 5' to 3' internal primer and the RCAS DMF04 primer will produce a characteristic PCR product several hundred base pairs in length (depending on the position of the internal primer), as will a reaction using the 3' to 5' internal primer and the RCAS primer, *rcas5'* (see Fig. 2). If these two PCR reactions do not produce one distinct product each, and the reciprocal primer combinations do, then the insert is in the reverse orientation. Once one or more clones with the correct orientation have been selected, both the orientation and the sequence of the transgene should be confirmed by sequencing using the DMF-04 and *rcas5'* primers. Once the correct vector has been identified it can be amplified in bacteria and purified.

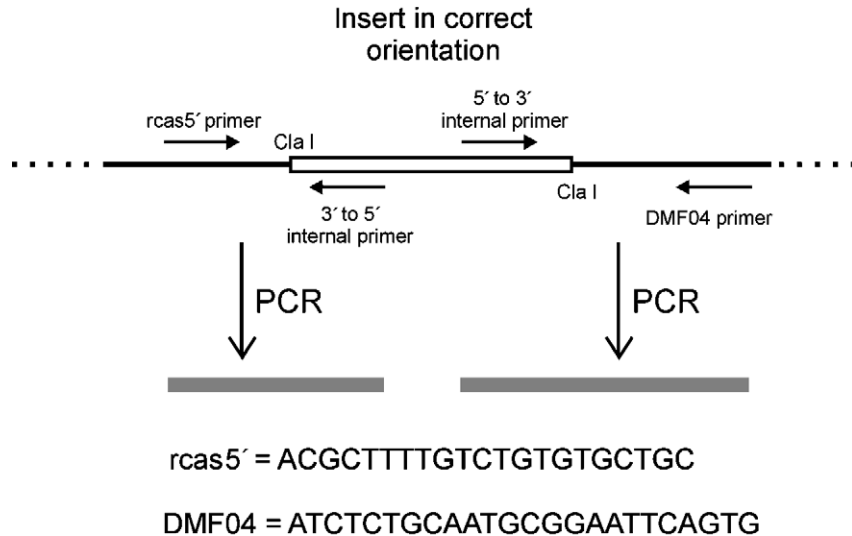


Fig. 2 A schematic representation of the PCR reactions used to determine the orientation of the inserted transgene in RCAS. Because both orientations are equally likely, several clones from the insert + RCAS ligation reaction are picked and subjected to PCR reactions with two sets of primer pairs. Because the primer *rcas5'* reads from the 5' side toward the *ClaI* site, a paired reaction with a 3' to 5' internal primer should give one distinct product if the insert is oriented correctly. The same is true for the combination of the primer DMF04 and a 5' to 3' internal primer. The reciprocal primer pairs—*rcas5'* plus 5' to 3' internal and DMF04 plus 3' to 5' internal—will each yield one distinct PCR product if the insert is in the opposite orientation. Each of the RCAS primers binds the retroviral vector 300–500 bases from its respective *ClaI* site.

D. Producing Functional Virus

Once the RCAS vector has been built and a clone with the correct insert orientation has been selected, the proviral vector is transfected into a chicken embryo fibroblast cell line to generate producer cells, in which active virus forms and is shed into the culture medium. This virus-containing supernatant is collected and the virus is harvested, concentrated, titered, and stored under liquid N₂.

1. Transfecting Cells and Growing Virus (see Fig. 3)

Materials

Proviral DNA (0.5–1.5 μg/μl)

DF-1 cells (UMNSAH/DF-1 cells, ATCC, CRL-12203)

Superfect transfection reagent (Qiagen)

Dulbecco's modified Eagle's medium (DMEM) (Sigma)

Fetal bovine serum (FBS; batch test it from several suppliers, choose the one that best supports growth of CEFs and purchase several years' supply)

RCAS Virus Preparation

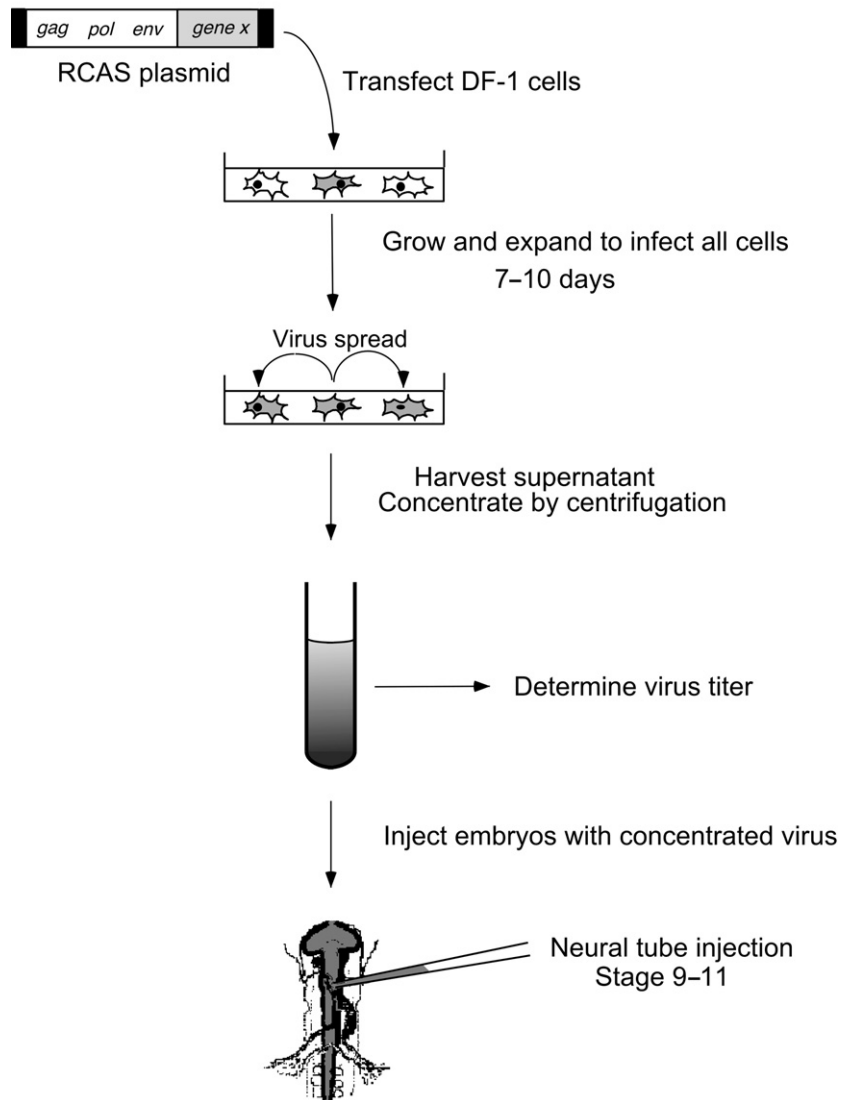


Fig. 3 Production of a retrovirus stock from a proviral RCAS DNA plasmid is shown schematically. First, the plasmid is transfected into a small percentage of DF-1 cells, where it integrates into the genome and produces new virus, which is shed into the culture medium. The cell cultures are grown and expanded for 7–10 days to produce many plates of fully infected cells (shown in gray). The culture supernatant from these plates, containing functional virions, is harvested and concentrated, and the retroviral titer is determined. Concentrated retrovirus stocks are frozen for use in neural tube injections.

Chick serum (CS; Sigma)

NuSerum (Collaborative Biomedical Products)

AMV-3C2 antibody (Developmental Studies Hybridoma Bank, University of Iowa)

60- and 100-mm tissue culture dishes

Ten microliters of Superfect reagent, 100 μ l of DMEM, and 2 μ g of DNA are vortexed together for 10 s, allowed to rest for 10 min at room temperature, and then diluted to 1 ml with DMEM containing 10% FBS and 2% CS. This is then placed onto a 60-mm culture dish of 70% confluent DF-1 cells, and the dish is incubated in a standard 5% CO₂, 37°C incubator for 3–4 h. The provirus-containing medium is then removed and, after rinsing the cells with phosphate-buffered saline (PBS), replaced with 2 ml of fresh DMEM/10% FBS/2% CS. After 18–24 h cells in the 60-mm dish are passaged into a 100-mm dish and subsequently split into four dishes as soon as they are 70–80% confluent. If the inserted transgene is a fluorescent fusion protein, the progress of infection can be gauged during this period by inspecting a plate of cells using epifluorescent illumination at low power (Fig. 4). In 7–10 days, when the culture has expanded to 10 or more 100-mm dishes, the cells are allowed to reach 100% confluence. The medium is removed and replaced with 5 ml/dish of DMEM plus 10% NuSerum (a low-serum substitute). Fix one plate and immunostain with AMV-3C2 antibody to confirm that all cells are infected with virus. The remaining plates are incubated overnight and then the medium is harvested. The incubation with DMEM/NuSerum can be repeated every 24 h, and additional virus can be harvested and concentrated separately. We recommend concentrating each batch fresh rather than pooling and freezing before concentrating, as this ensures the highest possible titers.

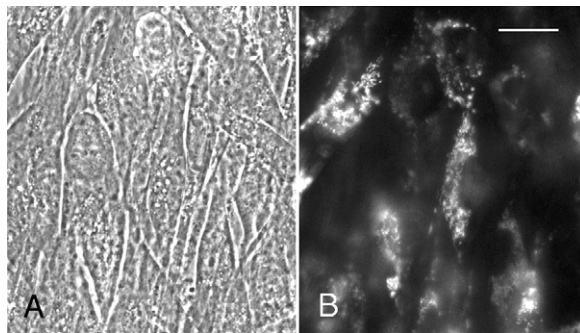


Fig. 4 Preparation of functional virus containing a fluorescent transgene can be monitored by simple inspection using low-power epifluorescent illumination. Here a plate of fibroblasts (A) infected with RCAS containing mitochondrially targeted EGFP has begun to produce virus and express the transgene, as is apparent from mitochondrial fluorescence (B). Nonfluorescent transgenes can be detected using cytochemical or immunocytochemical methods (see text). Bar: 20 μ m.

2. Concentrating, Titering, and Storing Virus

Materials

Stericup vacuum-driven disposable filtration units, 0.45 μm (Millipore)

Ultracentrifuge rotor (Beckman SW 28 or comparable)

Autoclaved polyallomer ultracentrifuge tubes

The pooled medium is cleared of cell debris by centrifugation at $2000 \times g$, for 15 min at 4°C . The supernatant is filtered through a 0.45- μm cellulose acetate filter. A small aliquot (<1 ml) of the filtrate should be saved frozen for subsequent titering. The remainder of the filtrate is transferred to sterile polyallomer ultracentrifuge tubes on ice. The virions are pelleted by centrifugation at 20,000 rpm ($72,000 \times g$) for 2.5 hr at 4°C . The supernate is poured off leaving only the residual volume of liquid from the wall of the tube over the pellet ($<200 \mu\text{l}$). The supernate may be frozen for subsequent processing in case pelleting was not efficient. Each pellet is then resuspended by gentle but persistent trituration, on ice, through a 200- μl pipette tip as follows: A sterile tip is lowered into each tube, the solution over the pellet is trituated for 10 strokes of the pipetter, being careful to minimize the generation of bubbles, and the tip is left in the tube while each subsequent tube is treated in the same manner. When the fluid in each tube has been trituated for 10 strokes, the process is repeated for the set of tubes until each has been trituated for 5–10 separate rounds over a 1-h period. The resuspended virus is then pooled. We have found that this gentle repeated trituration recovers the maximum amount of viable virus. The virus solution is then divided into aliquots of 10–20 μl and stored under liquid N_2 until needed. As an alternative, retrovirus stocks can be stored at -80°C , but their titer can drop with storage of ≥ 1 year.

To determine the titer of the virus and the efficiency of the concentration procedure, DF-1 cells are infected with a serial dilution of virus stock. A convenient method is to split 80% confluent cells at 1:6 dilution into six-well plates. The next day, add 1 ml of virus diluted in culture medium at 10^{-4} to 10^{-8} for concentrated stocks and 10^{-2} to 10^{-6} for unconcentrated virus. After several hrs, add 1 ml of warm medium to each well. After 36–48 h, remove the medium, fix the cells with 4% paraformaldehyde, and detect the expression of protein in one of three ways: perform indirect immunostaining with a primary antibody directed against the viral protein gag (AMV-3C2); indirect immunostaining with an antibody against the transgene product or its epitope tag, if appropriate; or for fluorescent transgene products, observe directly with epifluorescence illumination (see Fig. 4). Note that the first approach will indicate the titer of the virus independent of the efficiency of transgene protein expression. Typical titers are 10^6 to 10^7 IU/ml for unconcentrated virus and 10^8 to 10^9 IU/ml for concentrated virus. The efficiency of the concentration procedure can be determined by comparing the titers of unconcentrated and concentrated virus; this protocol typically yields 100–200 \times concentration.

III. Infecting Early Chick Embryos by Injection

A. Preparing Eggs

Materials

Fertilized specific pathogen-free (SPF) eggs (SPAFAS, Inc.)

Humidified 37°C egg incubator, a stationary (not rocking) model

Egg holder (can be fabricated from plastic)

Small curved dissecting scissors

Standard and wide transparent tape

3-ml syringe and 21-gauge needle

Stereodissecting microscope with adjustable oblique fiber optic illumination

If possible, eggs should be incubated for 32–36 h at 37°C before being windowed to judge their stage of development. Earlier windowing leads to decreased viability, whereas later windowing is difficult because the embryos stick to the shell. Windowing a number of eggs allows the worker to determine and record the stage of development for each in rapid succession and to return each to the incubator until it has reached the appropriate age for injection. By noting the exact stage of development of each embryo, they can be retrieved for injection later in order of their small differences in age. This allows the efficient injection of many embryos in one session, each at the appropriate stage of development. For neural tube injections to infect sensory and sympathetic ganglia, the ideal time to inject is early stage 10 (Hamburger and Hamilton, 1951; Bellairs and Osmond, 1998), which is reached after approximately 36 h of incubation at 37°C. At this stage the neural tube is almost, but not completely closed—the posterior end remains open (see Fig. 5). In order to avoid leakage out of this opening and retain all of the injected virus within the tube, it would be ideal to wait until the tube had closed completely (stage 11), but this would delay the exposure to virus until after many of the targeted neuronal precursor cells had already exited mitosis or migrated out of the spinal cord. Thus, injection at early stage 10 is a compromise between obtaining the maximum amount of virus in the neural tube and exposing the maximum number of susceptible neuronal precursors. For infection of forebrain neurons the injection must be performed earlier, at stage 9 if possible. Although the anterior neural tube is also open, the enlarged forebrain vesicle can be filled by direct injection so that most of the introduced virus is retained there.

1. Setting Eggs and Removing Albumen

When day 0 fertilized eggs arrive from the supplier, they should be placed into the incubator or stored at 4–12°C until the appropriate time for incubation. Eggs should be maintained on their sides in a humidified egg incubator without rocking or turning. The top surface should be marked with an ink dot or initial so that their orientation can be maintained through all of the following procedures.

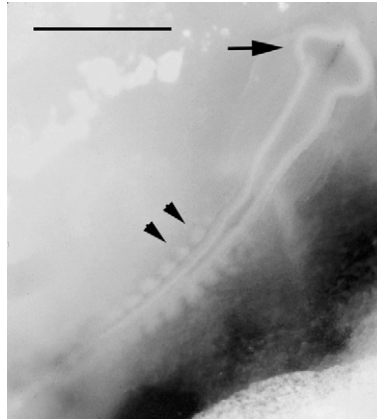


Fig. 5 An early stage 10 chick embryo is recognizable by the characteristic oval shape of the forming brain and optic vesicles (arrow), its obvious neural tube, and the appearance of eight large somites (examples denoted with arrowheads; two smaller, posterior somites are difficult to see in this plane of focus). The contrast of this embryo with the underlying yolk has been improved by an injection of India ink (mixed 1:1 with chick Ringers solution) under the superficial membrane of the yolk sac near the embryo. The neural tube has been injected with virus solution as described in the text, and the Fast Green dye clearly delineates the lumen of the neural tube and ventricles and allows the progress of the injection to be monitored closely. Bar: 1 mm. (See Color Insert.)

Approximately 36 h after they are set, they should be carefully opened and staged as follows: Remove about 18 eggs from the incubator, being careful to maintain the surface that was facing upward in that position. Place them in a plastic egg tray, squirt them with 70% ethanol, and allow to dry a few minutes. Then, one egg at a time, use a sterile 21-gauge syringe needle to barely poke through the upper surface of the egg, and then insert the same needle, on a 3-ml syringe, into the narrow end of the egg pointing nearly straight down. Remove approximately 1.5 ml of albumen from the egg and then cover the needle hole with a small piece of transparent tape. Next, using fine dissecting scissors, remove an oval section of the shell from the top surface of the egg, opening a window approximately 2 cm long and 1.5 cm wide, oriented along the long axis of the egg. Start with a smaller hole, look inside the egg as soon as the embryo is visible, and enlarge the opening to its full size so to expose the embryo. Use a fine forceps to remove any pieces of the shell that drop inside the egg.

2. Staging Eggs

Using a stereodissecting microscope, observe the embryo, which is located on the surface of the yolk, using oblique optical fiber illumination and an intermediate magnification. Although the embryo has rather poor contrast with the background yolk at these early stages, with practice it is possible to quickly distinguish

its stage of development. This is aided by comparing the image that is obtained through the stereoscope to a standard set of chick embryonic stage illustrations (Hamburger and Hamilton, 1951; Bellairs and Osmond, 1998). Some workers find it helpful to enhance the contrast of the embryo image by one or more of the following methods: using an opaque card in front of the illuminator to cast a crisp shadow along the embryo; using a green filter on the light source; or injecting India ink (Pelican brand; 50% in chick Ringers solution) under the embryo (see Fig. 5). After the stage has been noted and recorded, the egg is labeled, the window in the shell is carefully sealed with wide transparent tape, and the egg is returned to the incubator.

B. Injection into the Neural Tube

Materials

Freshly thawed retrovirus stock

Fast Green dye stock (10 \times , 0.25% stored on ice)

Borosilicate fiber capillary pipettes, 1.5 mm O.D., 1.17 mm I.D. (Warner Instrument Corp.)

Micropipette puller (Sachs-Flaming Model PC-84)

Micromanipulator (Narishige MN-151 or any simple direct mechanical system)

N₂ pressure microinjection apparatus (Parker PicoSpritzer II)

Micropipette beveler (Sutter Instrument BV-10)

The retrovirus stock should be freshly thawed from storage under liquid N₂. Fast Green dye is added from a 0.05% (10 \times) stock to a final concentration of 0.005%. The solution is then clarified by centrifugation in a 0.5-ml microfuge tube at 13,000 \times g, 4°C, for 15 min. Once diluted, the virus stock can be held on ice and used for several hours.

Micropipettes are pulled from fiber capillary glass using a Sachs-Flaming micropipette puller set to produce a tip with an outer diameter of $\leq 10 \mu\text{m}$ and a moderate taper. We also bevel the pipette tips to an angle of 30–45° using a micropipette beveler with a rotating abrasive pad. The pipette can be filled from the back by introducing 2–3 μl of virus solution with a narrow gel-loading pipette tip and allowing capillary action to draw it to the micropipette tip. A micropipette loaded with virus solution is used in successive injections for approximately 30 min, the remaining virus solution is blown out into a small container of chick Ringers solution, and the pipette is refilled with fresh solution from the stock that has been held on ice.

For infection of sensory and sympathetic ganglia, previously staged eggs are removed from the incubator at early stage 10 and placed in a plastic holder under the stereodissecting microscope with oblique illumination. The embryo should be oriented such that the micropipette approaches it parallel to the long axis of the body and neural tube. The pipette should be angled in the holder so as to

approach the embryo from the posterior aspect and to enter the neural tube at an acute angle ($\leq 45^\circ$). The pipette is brought very close to the embryo using the coarse control and is then guided into the neural tube using the fine control. For spinal cord injections, the pipette should penetrate the neural tube at a point approximately one-third of the way down the neural tube from the head. If a small amount of pressure is applied with the injector, it will be apparent when the pipette tip is within the neural tube due to the appearance of Fast Green within the tube. At this point the virus solution is injected in a series of approximately 10 pulses of 5–10 ms each at 40 psi until it fills the lumen of the neural tube (see Fig. 5). Some retrovirus solution may be leaking from the open posterior end of the tube by this point. The pipette is then smoothly removed from the neural tube. The procedure and approach are very similar for the infection of forebrain neurons, except that the best stage for injection is stage 9 and here the pipette must penetrate the forebrain at the front end of the neural tube. In between injections the tip of the micropipette should be rested in a small beaker of PBS or chick Ringers solution in order to prevent clogging.

C. Postinjection Incubation

After injection, the window in the egg must be resealed carefully with wide tape and the egg labeled and returned to the incubator. In order to perfect the injection technique and subsequent treatment of the embryos, it is essential to record the details of each egg injection and to track the progress of each embryo from the time of injection until it develops to the desired stage, or dies. Careful recording can also help the investigator to anticipate which embryos are likely to have the highest percentage of successfully infected neurons at later stages based on the quality of the initial injection. Embryos should be checked daily and those that die should be noted and removed from the incubator as soon as possible.

IV. Dissecting Embryos and Culturing Neurons

A. Dissection and Selection of Ganglia

When the embryos have developed to E9–E11, the sympathetic and dorsal root ganglia (DR6) are dissected out and cultured as whole explants or dissociated cells using standard procedures (Bray, 1991). Depending on the virus titer, the exact stage at which the embryo was injected, and the quality of the injection, the typical embryo will provide a population of peripheral neurons with 25–95% of the cells expressing the transgene at detectable levels. However, if the experimental application demands the highest possible percentage of infected cells, and if the transgene encodes a fluorescent fusion protein, then an additional screening step can be applied before ganglia are removed for culture. In this case the embryo is dissected to the point of exposing the posterior body wall, and ganglia are examined *in situ* using a stereomicroscope with epifluorescent illumination (Fig. 6). This allows

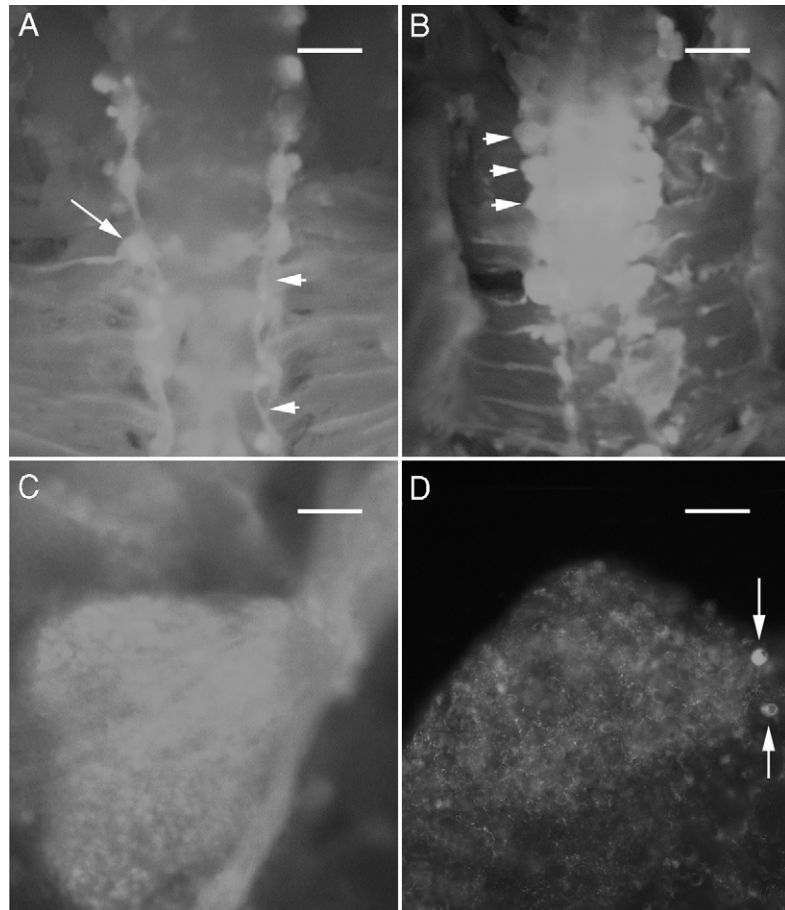


Fig. 6 The expression of fluorescent fusion proteins is easily detectable in dissected embryo and peripheral ganglia using a stereodissecting microscope equipped with epifluorescent illumination. These images show embryos infected with RCAS-GFP at stage 10, incubated until day 10, and dissected. (A) An embryo dissected to reveal the spinal column and paravertebral ganglia. Both dorsal root ganglia with attached spinal nerves (arrow at left) and sympathetic chain ganglia (arrowheads at right) show high levels of GFP expression. Bar: 1 mm. (B) An embryo similar to the one in A, but with sympathetic chain ganglia removed and the plane of focus lowered to make the expression of GFP in the dorsal root ganglia clear. Individual ganglia are obvious even at low magnification (arrowheads). Differences in the percentage of neurons expressing the transgene and in the level of expression can be judged quickly and easily during dissection, and the brightest ganglia can be selected for experiments requiring high levels of expression. Bar: 1 mm. (C) A higher magnification view of a dorsal root ganglion shows cell bodies expressing and not expressing GFP. Bar: 0.1 mm. (D) Higher magnification than C reveals individual cell bodies expressing GFP, with the nucleus forming a region of exclusion. Several cell bodies fall in the narrow plane of focus here, including two denoted by arrows. Bar: 50 μ m. (See Color Insert.)

sensory or sympathetic ganglia with the brightest fluorescence to be selected specifically and removed for culture. The brightness of a ganglion typically depends not on the level of expression of the transgene in individual cells, but on the percentage of expressing cells. This can be appreciated by examining the successive steps up in magnification shown in Fig. 6.

Forebrain neurons can be obtained by dissecting the embryos at E9 using the procedure of Heidemann and colleagues (Chapter 4). Because the population of forebrain neuron precursors exits mitosis earlier in development than those of peripheral ganglia, the percentage of forebrain neurons that can be infected successfully with retrovirus is lower on average. Nonetheless, retroviral infection can provide stable transgene expression in forebrain neurons at frequencies more than high enough for light microscope applications.

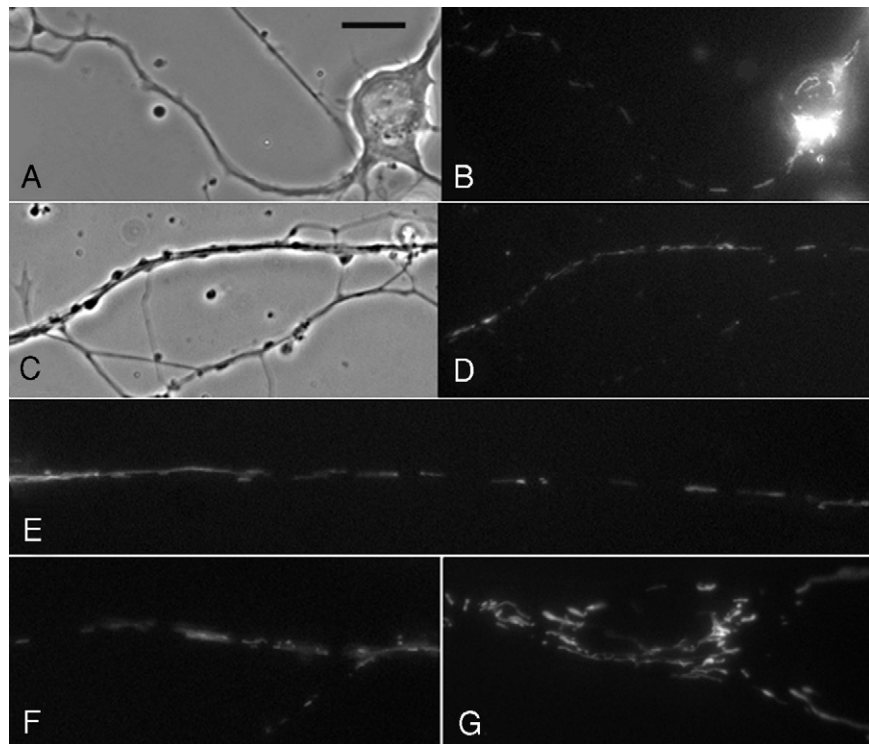


Fig. 7 Cultured peripheral neurons and nonneuronal cells from embryos infected with RCAS virus containing the EGFP gene fused to a mitochondrial localization sequence. An isolated sympathetic neuron (A) shows bright mitochondrial fluorescence in the cell body and axon (B). A bundle of sympathetic axons (C) also show bright mitochondrial fluorescence (D), as do the axons of dorsal root ganglion neurons (E and F). Fibroblastic cells in the culture also express the transgene (G). Bar: 10 μ m.

B. Culture and Microscopy

Retrovirus-infected embryos are dissected and DRG, sympathetic, or forebrain neurons are obtained and grown in culture by standard procedures (Bray, 1991; see Chapter 4). Figure 7 shows high-magnification views of sympathetic and DRG neurons from an embryo infected with an RCAS vector containing the EGFP gene fused to a mitochondrial localization sequence. Mitochondria are clearly visible using standard epifluorescence microscopy and can be observed for longer periods without photodamage than is possible using fluorescent mitochondrial dyes (e.g., Morris and Hollenbeck, 1995). In our hands, this procedure has also provided excellent expression in primary neurons of a soluble protein, EGFP, a cytoskeletal protein, actin depolymerizing factor, and an organelle-associated protein, rab 11a. In addition, nonneuronal cells in many tissues also express the transgenes (see Fig. 7G), and the RCAS method could be extended easily to other cell types that are difficult to transfect.

V. Conclusions

Similar to transgenic mouse technology, the manipulation of gene expression and the introduction of transgenes using replication-competent retroviral vectors have been powerful tools for developmental studies (Morgan and Fekete, 1996; Satoh and Fekete, 2003; Cepko *et al.*, 1995). By further analogy with transgenic mouse techniques, we have exploited the widespread and stable expression of transgenes in the early embryo to remove and study the properties of individual transfected neurons in culture.

This technique has some disadvantages compared to other methods of transfecting neurons. It is more complex and time-consuming than transient transfection of these cells. Electroporation, for instance, is a very simple and quick procedure once a suitable expression vector has been constructed or obtained, and it provides 10–15% transfected neurons (see Chapter 16). In addition, in the construction of retroviral vectors the properties of the transgene are limited: it cannot exceed 2.6 kb in size and its expression cannot be deleterious during early development even when it is expressed widely within the nervous system and other tissues. However, for many applications the advantages of retroviral infection far outweigh these shortcomings. If an experimental application requires construction of a standard expression vector, then building an RCAS vector is often not much additional work. For high-frequency, stable, consistent, and moderate transgene expression in primary neurons, retroviral infection is probably the best available technique, and for some applications, the only practical technique. In addition, the widespread cell and tissue expression of transgenes that is attainable using retroviral infection can ultimately allow some cellular studies to be carried to the developmental level.

Acknowledgments

We thank Brian DeGrush for images used in Fig. 6 and 7. The work described here was supported by grants from the NIH to PJH (NS-27073) and DMF (DC-02756).

References

- Bellairs, R., and Osmond, M. (1998). "The Atlas of Chick Development." Academic Press, San Diego.
- Boerkoel, C. F., Federspiel, M. J., Salter, D. W., Payne, W., Crittenden, L. B., Kung, S.-J., and Hughes, S. H. (1993). A new defective retroviral vector system based on the Bryan strain or Rous sarcoma virus. *Virology* **195**, 669–679.
- Bray, D. (1991). Isolated chick neurons for the study of axonal growth. In "Culturing Nerve Cells". (G. Banker and K. Goslin, eds.), pp.119–135. MIT Press, Cambridge, MA.
- Cepko, C., Ryder, E. F., Austin, C. P., Walsh, C., and Fekete, D. M. (1995). Lineage analysis using retroviral vectors. *Methods Enzymol.* **254**, 387–419.
- Hamburger, V., and Hamilton, H. L. (1951). A series of normal stages in the development of the chick embryo. *J. Morphol.* **88**, 49–91.
- Hughes, S. H., and Kosik, E. (1984). Mutagenesis of the region between *env* and *src* of the SR-A strain of Rous sarcoma virus for the purpose of constructing helper-independent vectors. *Virology* **136**, 88–99.
- Morgan, B. A., and Fekete, D. M. (1996). Manipulating gene expression with replication-competent retroviruses. In "Methods in Cell Biology". (M. Bronner-Fase, ed.), Vol. 51, pp. 185–218. Academic Press, San Diego.
- Morris, R. L., and Hollenbeck, P. J. (1995). Axonal transport of mitochondria along microtubules and F-actin in living vertebrate neurons. *J. Cell Biol.* **131**, 1315–1326.
- Petropoulos, C. J., and Hughes, S. H. (1991). Replication-competent retroviral vectors for the transfer and expression of gene cassettes in avian cells. *J. Virol.* **65**, 3728–3737.
- Roe, T. Y., Reynolds, T. C., Yu, G., and Brown, P. O. (1993). Integration of murine leukemia virus DNA depends on mitosis. *EMBO J.* **12**, 2099–2108.
- Satoh, T., and Fekete, D. M. (2003). Retroviral vectors to study cell differentiation. *Front. Biosci.* **8**, 183–192.

CHAPTER 19

Production and Use of Replication-Deficient Adenovirus for Transgene Expression in Neurons

**L. S. Minamide, A. E. Shaw, P. D. Sarmiere, O. Wiggan,
M. T. Maloney, Barbara W. Bernstein, J. M. Sneider,
J. A. Gonzalez, and James R. Bamberg**

Department of Biochemistry and Molecular Biology
Program in Molecular
Cellular and Integrative Neuroscience
Colorado State University
Fort Collins, Colorado 80523

-
- I. Introduction
 - A. Structure, Modification, and Replication of the Type 5 Adenovirus
 - B. Overview of Methods for Making Recombinant Adenovirus
 - II. Preparing Adenoviral Expression Vectors
 - A. Materials
 - B. Selecting Vectors
 - C. Inserting the Gene of Interest into a Shuttle Vector
 - D. Preparing Electrocompetent BJ5183 *Escherichia coli*
 - E. Preparing Electrocompetent BJ5183 Containing pAdEasy-1
 - F. Homologous Recombination in BJ5183
 - III. Production of Adenovirus in HEK293 Cells
 - A. Materials
 - B. Maintaining HEK293 Cells
 - C. Transfection of HEK293 Cells with Adenovirus DNA
 - D. Expansion of Transfection Harvests
 - IV. Purification and Storage of Adenovirus Stocks
 - A. Materials
 - B. Overview of Methods
 - C. CsCl Gradient Purification of Adenovirus
 - D. Virakit Purification

- V. Titer Assays
 - A. Materials
 - B. Overview of Plaque Assay and Immunoassay
 - C. Adenoviral Titers with Two-Day Immunoassay
- VI. Safety Issues
 - A. General Concerns
 - B. Testing Viral Stocks for Replication-Competent Virus
- VII. Infection of Primary Neurons
 - A. Overview
 - B. Infectivity of Different Neuronal Cultures
 - C. Infection of Neuronal Tissues in Suspension before Dissociation
 - D. Viral Toxicity
 - E. Reducing Nonneuronal Cell Contamination
- VIII. Conclusions and Perspectives
- References

Adenoviruses infect a wide range of cell types, do not require integration into the host cell genome, and can be produced as replication-deficient viruses capable of expressing transgenes behind any desired promoter. Thus, they are ideal for use in expressing transgenes in the postmitotic neuron. This chapter describes simplifications in the protocols for making recombinant adenoviruses and their use in expressing transgenes in primary neurons of several different types.

I. Introduction

Chapters in two previous volumes in this series have dealt with the preparation and use of recombinant adenoviruses (Ad) for gene transfer studies (Becker *et al.*, 1994; Leber *et al.*, 1996), and thus one might ask why another chapter on this subject is needed at this time. The main advantages in using adenoviral vectors are the ability to produce high titers of recombinant viruses, the ability to infect a wide range of cell types, and the ability to infect both dividing and postmitotic cells. The latter is particularly important when designing a system to be used with primary neuronal cultures. Additionally, high levels of transgene expression can be obtained by use of these viruses, and because the adenovirus DNA remains episomal, no host genes will be interrupted through chromosomal integration as occurs with most other viruses, including retroviruses. Simplifications in the procedures for generating recombinant adenoviruses have contributed to the significant increase in the use of adenoviral vectors for gene transfer into mammalian cells. It is worthwhile, therefore, to explain these recent advances that make the preparation of adenoviral vectors so much easier and faster. In addition, more information on adenovirus structure and the ability to alter viral infectivity now permit more detailed and specific information to be presented that will further aid researchers in using adenoviruses in neuronal systems.

A. Structure, Modification, and Replication of the Type 5 Adenovirus

Adenovirus type 5 is one of the most extensively studied and characterized adenovirus and is the one used most frequently in generating recombinant adenoviruses. Human Ad5 possess a linear double-stranded DNA genome of approximately 36 kb. The viral genome has been grouped into different transcriptional units, such as early (E1, E2, E3, E4), intermediate, and late transcription units. The E1 gene is essential for activation of other viral genes and for viral replication. Generation of recombinant adenoviruses is accomplished by deleting certain viral genes and replacing these deleted sequences with the gene(s) of interest. The majority of viral vectors presently in use contain deletions of the E1 and E3 genes. The E3 gene is nonessential for either viral replication or infection. Deletion of both E1 and E3 genes allows for insertion and packaging of up to 7.5 kb of foreign DNA into Ad vectors (Leber *et al.*, 1996). Deletion of the E1 gene results in viruses that are replication incompetent in normal cells. However, replication-competent viral particles can be produced from E1-deleted viral vectors by providing the E1 gene *in trans*. Because adenoviruses are endemic in the general population and cause respiratory diseases in humans (Grunhaus and Horwitz, 1992), protection against virus exposure should be taken when using recombinant adenoviruses for gene transfer studies.

One advantage to the use of recombinant adenoviruses for gene transfer in mammalian cells is the wide range of cell types that can be infected by Ad5 viruses. Ad5 viruses utilize several different cellular receptors for uptake, including integrins, MHC class 1 molecules, and the coxsackievirus and adenovirus receptor (CAR), a member of the immunoglobulin superfamily (Bergelson *et al.*, 1997; Tomko *et al.*, 1997; Davison *et al.*, 1997; Hong *et al.*, 1997; Wickham *et al.*, 1994). CAR mRNA has been detected in many tissues, including brain, in both humans and mice (Tomko *et al.*, 1997; Bergelson *et al.*, 1998), and CAR has been localized on neurons in rodent brain and spinal cord as well as on cultured cells (Soudais *et al.*, 2001). However, CAR is undetectable on many nonneuronal cells, which are readily infected in culture with Ad5 viruses, suggesting that efficient virus uptake is not CAR dependent. No systematic study has been done until now to compare the ability of a single batch of Ad5 adenovirus to infect many different types of neurons in culture. This chapter shows that recombinant Ad5 viruses can be used for gene expression studies in central and peripheral neuronal cultures from embryonic rat and chick.

B. Overview of Methods for Making Recombinant Adenovirus

Several different techniques have been described for generating recombinant adenoviral vectors (Mizuguchi *et al.*, 2001a). One early method employed direct *in vitro* ligation of foreign DNA sequences into the viral genome. This procedure was, however, highly inefficient. Bett *et al.* (1994) developed another procedure employing homologous recombination in human embryonic kidney (HEK) 293 cells (Graham *et al.*, 1977), which possess cell genome-integrated Ad E1 sequences.

Major drawbacks of this procedure are the low frequency of recombination and the requirement to perform several rounds of plaque purification to produce replication-incompetent and clonally selected recombinant adenovirus. More recently, He *et al.* (1998) developed an efficient procedure for generating recombinant Ad vectors in bacterial cells (Fig. 1). This procedure utilizes homologous

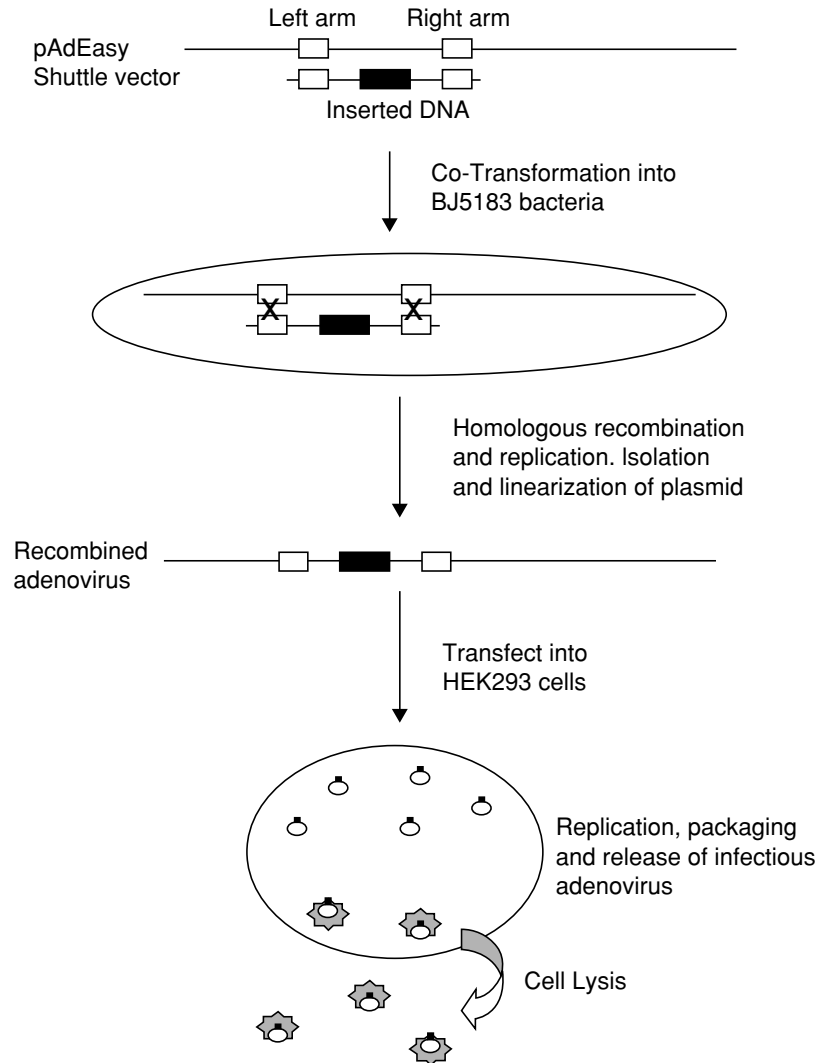


Fig. 1 Schematic diagram for the manufacture of replication-deficient adenoviral vectors using the AdEasy system. The black box represents the inserted gene for expression, and open boxes represent the homologous adenoviral sequences through which homologous recombination will occur in BJ5183 bacteria.

recombination between a shuttle plasmid containing the gene or cDNA of interest flanked by regions of homologous sequences to the viral genome and a second plasmid, pAdEasy-1, containing the E1/E3-deleted Ad genome. Recombinant viral plasmids are isolated from specialized BJ5183 *Escherichia coli* cells that are recombination competent. After selection of colonies containing the recombined virus, the DNA is isolated, linearized, and transfected into HEK293 cells to obtain packaged infectious, but replication-deficient viral particles. The high specificity of this bacterial recombination system eliminates the need to perform time-consuming plaque purifications. We have found this system to be highly efficient and have used it to generate numerous recombinant adenoviruses.

One advantage of the AdEasy system (He *et al.*, 1998) is the choice of shuttle vectors into which to insert the transgene. Two shuttle vectors (pShuttle and pAdTrack) were developed for expressing genes that have their own promoters, one of which (pAdTrack) expresses green fluorescent protein (GFP) driven by a separate cytomegalovirus (CMV) immediate-early promoter that permits rapid identification of infected cells. Two other shuttle vectors (pShuttle-CMV and pAdTrack-CMV) were developed for cloning the gene or cDNA of interest behind the CMV promoter. Again, the pAdTrack-CMV will express GFP from a separate CMV promoter, allowing identification of infected cells. If one is interested in expressing proteins without GFP or proteins that are chimeras with GFP, use of the pShuttle vectors is recommended.

This chapter describes the procedures used to generate, purify, and titer adenoviruses and their use for infecting and expressing transgenes in a variety of primary central and peripheral neurons in culture. In conclusion, we also describe an alternative approach to adenoviral construction that has appeared recently in the literature, which utilizes a two-plasmid *in vitro* ligation method that does not require a recombination step (Mizuguchi *et al.*, 2001a). This approach offers many interesting possibilities that also make it easier to alter the viral backbone and hence the cell receptor binding domain for adenovirus uptake.

II. Preparing Adenoviral Expression Vectors

A. Materials

BJ5183 *E. coli* [pick colony, grow in 10 ml Luria broth (LB)–streptomycin overnight; add 0.15 ml sterile glycerol to 0.85 ml bacterial culture, freeze in liquid nitrogen or dry ice/ethanol, and store at -80°C]

LB medium (Invitrogen Corporation, Carlsbad, CA)

LB-streptomycin (30 $\mu\text{g}/\text{ml}$); LB-ampicillin (100 $\mu\text{g}/\text{ml}$); LB-kanamycin (50 $\mu\text{g}/\text{ml}$) (cool all autoclaved medium to below 48°C before adding filter-sterilized antibiotics)

Shakerincubator at 37°C for growing bacteria

Visible spectrophotometer and cuvette
Refrigerated centrifuge
Sterile 10% glycerol (made up in H₂O and autoclaved 20 min)
Sterile 1.5-ml storage vials
pAdEasy-1 DNA
Electrocompetent BJ5183 *E. coli*
Electroporation cuvettes (0.1 cm, Bio-Rad Laboratories, Hercules, CA)
Electroporator (e.g., Bio-Rad Laboratories gene pulser)
Sterile 1.5- and 0.5-ml microfuge tubes
10 cm LB-agar plates containing ampicillin (100 µg/ml) or kanamycin (50 µg/ml)
(1.5% agar in LB, autoclave, cool to 48°C before adding filter-sterilized antibiotic
and pouring 20 ml per 10-cm sterile petri dish)
PmeI, *PacI*
37°C water bath
Phenol/chloroform/isoamyl alcohol (25:24:1 by volume)
Absolute ethanol
Sterile water
Electrocompetent BJ5183 *E. coli* containing pAdEasy-1
Agarose gel electrophoresis equipment
RecA⁻ bacteria (e.g., DH5α and DH10B)
Sterile glycerol (autoclave 20 min)

B. Selecting Vectors

Vectors and sequences for the AdEasy adenoviral system, as well as complete instructions for adenovirus construction, are available from Dr. Bert Vogelstein at www.coloncancer.org/adeasy.htm and Stratagene (La Jolla, CA). The AdTrack and AdTrack-CMV vectors are available only from the Vogelstein laboratory. The pShuttle vector will accommodate the largest inserts (up to 7.5 kb). The pAdTrack-CMV, pAdTrack, and pShuttle-CMV vectors accommodate slightly smaller DNA fragments (5, 5.9, and 6.6 kb, respectively) because the GFP gene (~0.7 kb), each CMV promoter (~0.6 kb), and other necessary expression sequences, such as the polyadenylation signal sequence, decrease the available cloning space. For insertion of larger fragments (up to 10 kb), pAdEasy-2, in which the adenoviral genes E1, E3, and E4 have been deleted, should be used for homologous recombination, and 911E4 cells, which provide the necessary proteins required for viral replication and packaging, should be substituted for HEK293 cells (He *et al.*, 1998).

The pShuttle and pAdTrack vectors confer resistance to kanamycin. The pAdEasy-1 vector confers resistance to ampicillin. All of the plasmids can be

maintained in standard cloning bacteria such as DH5 α or DH10B (He *et al.*, 1998) and grown in LB medium (Sambrook and Russell, 2001) or Terrific broth (Tartof and Hobbs, 1987) (see later for special bacteria requirements for the homologous recombination step). The plasmids can be isolated using standard purification columns (e.g., Qiagen maxi kit) or by CsCl gradient (Sambrook and Russell, 2001). Because of its large size, care must be taken when handling the pAdEasy-1 DNA (33.4 kb). It should never be vortexed as this may cause shearing. Mix by inversion when necessary.

C. Inserting the Gene of Interest into a Shuttle Vector

Prior to beginning cloning, it should be first confirmed that the gene of interest (up to 7.5 kb) does not contain any *PmeI* or *PacI* sites. These restriction endonuclease cleavage sites are used to linearize the DNA constructs prior to homologous recombination with the pAdEasy-1 and again prior to transfection of the HEK293 cells. If these sites are present, their removal by site-directed mutagenesis will simplify later steps. However, if *PmeI* or *PacI* sites are unavoidable, partial restriction digests or *EcoRI* and *recA*-assisted restriction endonuclease cleavage can be used for linearization (www.coloncancer.org/adeasy.htm).

The gene of interest is first inserted into one of the shuttle vectors using the appropriate restriction site(s) in the multicloning site (MCS) (Table I) by standard restriction digest, ligation, and CaCl₂ transformation procedures and selection with kanamycin (Sambrook and Russell, 2001). If the shuttle vectors with the CMV promoters are chosen, the gene of interest must include both translation initiation and stop codons. Confirmation of the presence of insert in the shuttle vector is done by restriction digest and electrophoresis on 0.6–0.8% agarose gels (Sambrook and Russell, 2001) or by sequencing using primers that bind outside the multicloning site. Table II lists sequencing primers that bind outside the MCS that have been used successfully for forward and reverse sequencing in the pAdtrack, pShuttle, and pShuttle-CMV vectors.

Table I
Multicloning Restriction Endonuclease Sites of pAdTrack and pShuttle Vectors

Direction-independent insertion	
pShuttle	<i>KpnI NotI XhoI XbaI EcoRV HindIII SalI BgIII</i>
pAdTrack	<i>BgIII KpnI SalI NotI EcoRV XhoI HindIII XbaI</i>
Direction-dependent (5'-3') insertion behind CMV promoter	
pShuttle-CMV	<i>BgIII KpnI SalI NotI^a XhoI^a HindIII XbaI EcoRV</i>
pAdTrack-CMV	<i>BgIII KpnI SalI NotI^a XhoI^a HindIII XbaI EcoRV</i>

^a*NotI* and *XhoI* sites overlap by one base and cannot be used in a single insertion+ligation.

Table II
Primers for Sequencing Inserts into the MCS of pAdTrack and pShuttle

pAdTrack forward: 5'-GGGCCATTTACCGTAAGTTATG-3'
pAdTrack reverse: 5'-CTCACAATGCTTCCATCAAACG-3'
pShuttle forward: 5'-CGGAAGTGTGATGTTGCA-3'
pShuttle reverse: 5'-CCCCACCTTATATATTCTTTCCC-3'
pShuttle-CMV forward: 5'-GGTCTATATAAGCAGAGCTG-3'
pShuttle-CMV reverse: 5'-GGTATGGCTGATTATGATCAG-3'

D. Preparing Electrocompetent BJ5183 *Escherichia coli*

BJ5183 *E. coli* are streptomycin resistant and can be maintained as glycerol stocks (Sambrook and Russell, 2001). Inoculate 250 ml LB-streptomycin with 250 μ l of an overnight culture. Grow on a shaker/incubator to an OD₅₅₀ of ~0.6–0.8. Transfer the culture to a sterile 250-ml centrifuge bottle and chill on ice for 30 min. Centrifuge the culture at 2600 $\times g$ for 15 min at 4°C. Resuspend the bacterial pellet in 250 ml of sterile, ice-cold 10% glycerol (ultrapure) in water. Centrifuge for 20 min at 4°C. Repeat the resuspension in 250 ml of sterile, ice-cold 10% glycerol and centrifugation. Remove all but ~0.6 ml of the 10% glycerol supernatant and resuspend the bacteria in this remaining volume. Divide the cell suspension into 20- to 50- μ l aliquots into sterile tubes that have been prechilled to –80°C. Keep the tubes on ice or in a –20°C cold block while making the aliquots and store them at –80°C.

E. Preparing Electrocompetent BJ5183 Containing pAdEasy-1

To prepare electrocompetent BJ5183 cells containing pAdEasy-1, add 20–100 ng (in no more than 5 μ l water) of pAdEasy-1 DNA to 20–25 μ l electrocompetent BJ5183 in an electroporation cuvette prechilled on ice. Electroporate at 2.25 kV, 200 Ω , 25 μ F. Immediately after electroporation, place the cuvette back on ice. Add 1 ml cold LB medium to the cuvette and transfer the bacteria to a 1.5-ml microfuge tube. Incubate the bacteria for 45 min at 37°C and then pellet the cells by centrifugation for 10 s at 10,000 $\times g$. Discard most of the supernatant, leaving behind 100–150 μ l to resuspend the bacteria. Plate the resuspended bacteria on two ampicillin-containing agar plates and incubate at 37°C overnight. Inoculate 250 ml LB containing ampicillin with four BJ5183-AdEasy-1 colonies or 0.25 ml of an overnight culture (one colony in 10 ml LB-amp) and prepare electrocompetent cells as described in Section II,D. BJ5183 cells containing pAdEasy-1 are also now available from Stratagene.

F. Homologous Recombination in BJ5183

Digest overnight at 37°C with *Pme*I a few micrograms (5–10 units/ μ g DNA) of high-quality (e.g., Qiagen column or CsCl gradient purified) shuttle vector DNA

containing the gene of interest. This digest must be complete (a small portion of the digest can be tested on an agarose gel) because incomplete digestion reduces considerably the recombination event with the pAdEasy-1 DNA. The linearized DNA is phenol/chloroform/isoamyl alcohol extracted, ethanol precipitated (Sambrook and Russell, 2001), and redissolved in sterile water at $0.1 \mu\text{g}/\mu\text{l}$. Linearized DNA ($0.1\text{--}0.2 \mu\text{g}$) is then added to $20\text{--}25 \mu\text{l}$ electrocompetent BJ5183 pretransformed with pAdEasy-1 DNA and electroporated as described earlier. Sequential transformation of BJ5183 first with pAdEasy-1 and second with the shuttle vectors results in $90\text{--}100\%$ recombination positive clones as compared to performing cotransformation with both DNAs simultaneously, which yields only $20\text{--}30\%$ recombination positive clones. Plate one-fourth of the bacterial suspension on a 10-cm kanamycin-containing agar plate and three-fourths on a second plate to enhance the probability of obtaining isolated colonies on at least one plate. Incubate the plates at 37°C for approximately 20 h. Both large (1.5 mm) and small ($0.5\text{--}0.8 \text{ mm}$) colonies will develop (Fig. 2). Bacteria containing recombinant DNA take longer to develop and usually form smaller colonies. Pick small colonies and isolate plasmid DNA using standard miniprep methods (Sambrook

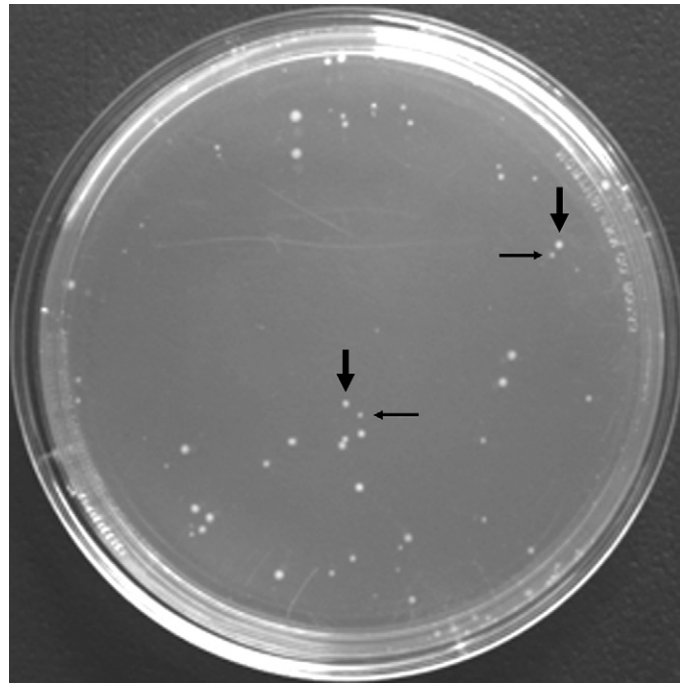


Fig. 2 Kanamycin-containing agar plate on which large and small colonies of BJ5183 *E. coli* have grown after the homologous recombination between the shuttle vector and the pAdEasy-1. Small colonies ($0.5\text{--}0.8 \text{ mm}$, small arrows) are potential recombinant clones. Large colonies (1.5 mm) often contain only the shuttle vector.

and Russell, 2001), being careful to never vortex the DNA, as this may cause shearing of the large DNA. Mix by gentle inversion when necessary.

Examination of the recombinated Ad plasmid DNA is done by digestion with *PacI* (5–10 units/ μ g DNA). One large fragment of \sim 30 kb should be present along with one smaller fragment of either 3.0 kb or 4.5 kb, depending on whether homologous recombination took place between the left flanking regions or at the origins of replication, both of which often occur and either of which will yield identical viruses. Occasionally, extra bands are observed in the *PacI* digest. These may be due to contaminating shuttle plasmid, spurious rearrangements of the pAdEasy-1 vector, or undesired recombination events. Fig. 3 shows digests containing the expected band sizes and digests with extra bands. We have not obtained successful adenovirus production from clones containing extra bands. Because BJ5183 *E. coli* are recombination competent, properly recombinated DNA should not be stored in this bacteria and must be removed as soon as possible. Miniprep DNA from clones that show no extra bands may be stored at -20°C or used to transform *recA*⁻ bacteria (e.g., DH5 α and DH10B) by CaCl_2

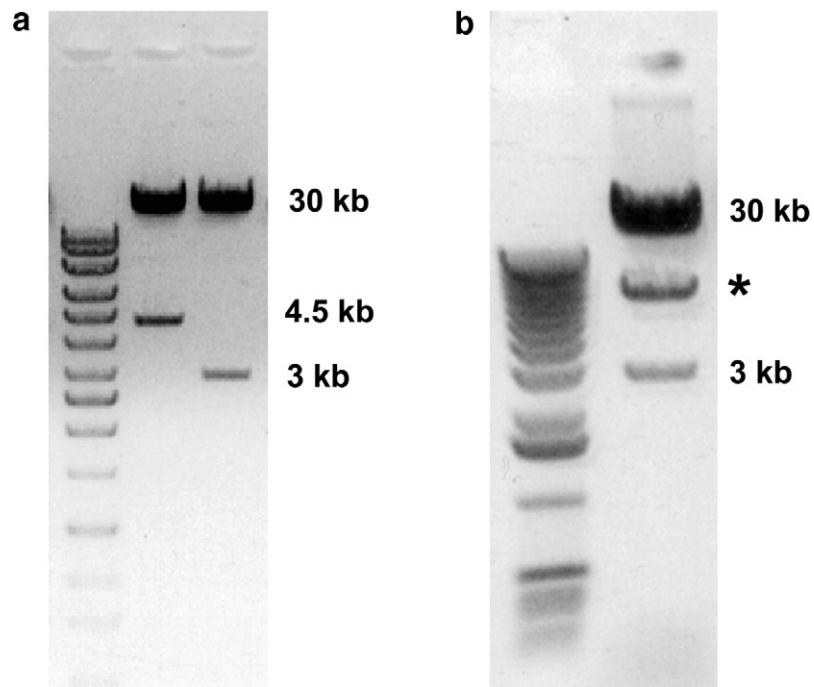


Fig. 3 (a) Band sizes obtained from successfully recombinated clones digested with *PacI*. The expected band sizes are \sim 30 kb and either 4.5 or 3 kb, depending on whether the recombination utilized the homologous left arms of the adenovirus or the origin of replication of the two plasmids. (b) A clone containing an extra band (*), which suggests abnormal or lack of recombination that will likely interfere with viral production.

transformation. For long-term storage and production of recombinant viral DNA, these recA^- bacteria should be used. Restriction digests of miniprep DNA obtained from the new clones should be performed to confirm that no additional recombination events have occurred. Glycerol stocks can be made from recA^- clones by taking a portion of an overnight culture and adding sterile glycerol to 15%. Store 1-ml aliquots at -80°C .

III. Production of Adenovirus in HEK293 Cells

A. Materials

HEK293 cells (ATCC CRL-1573)
High-glucose (4.5 g/liter) Dulbecco's modified Eagles medium (HGDMEM)
Fetal bovine serum (FBS)
 37°C 5% CO_2 /95% air incubator
T25 and T75 cell culture flasks
PacI-digested recombinant pAdenoviral DNA
 37°C water bath
Phenol/chloroform/isoamyl alcohol (25:24:1 by volume)
Absolute ethanol
Microfuge
Sterile 0.5-ml microfuge tubes
Class II biological safety cabinet in BL2 facility approved for adenovirus
Sterile water
Opti-MEM 1 (Invitrogen Corporation, Carlsbad, CA)
Lipofectamine (Invitrogen Corporation)
Sterile cell scraper (Sarstedt, Newton, NC)
Sterile 50-ml polypropylene tube
Clinical centrifuge
Phosphate-buffered saline (PBS) (1.104 g $\text{NaH}_2\text{PO}_4 \cdot \text{H}_2\text{O}$, 8.18 g NaCl, 0.202 g KCl at pH 7.2 with NaOH per liter)
Freezing bath (dry ice in 95% ethanol; or liquid nitrogen)
Ultracold freezer
Sterile 10-ml syringe
Sterile 0.45- μm syringe filter

B. Maintaining HEK293 Cells

HEK293 cells are human embryonic kidney cells that have been stably transformed by sheared Ad type 5 DNA (Graham *et al.*, 1977). These cells express the

adenoviral E1 gene product and produce packaged infectious particles when they are transfected with E1-deleted pAdEasy-1 recombinant DNA. HEK293 are maintained as adherent cultures in HGMEM supplemented with 10% FBS in a 5% CO₂/air incubator at 37°C. Cell clumping can be minimized by repetitive pipetting of the suspension following trypsinization by standard procedures. Because cells can be dislodged from the tissue culture plastic by mechanical shear, care must be taken to avoid pipetting medium directly onto them. If adherence of the standard HEK293 cells causes problems, Stratagene sells a more adherent 293 cell line (AD-293 cells) that can be used instead. It is important that the cells be healthy and passaged regularly at a maximum of 75% confluency no more than 20 times (approximately 2 months in culture) prior to transfection with the pAdEasy-1 recombinant DNA. One of the single major causes of lack of viral production is the use of HEK293 cells that have been passaged too many times or allowed to reach and remain confluent for too long. When HEK293 cells are first obtained, make many vials of low passage number of cells so that fresh cultures can be started every 4–6 weeks.

C. Transfection of HEK293 Cells with Adenovirus DNA

Inoculate a T25 flask with 1×10^6 HEK293 cells about 24 h prior to transfection. Before transfection, digest 4 μ g pAdEasy-1 recombinant DNA with *PacI* (40 units) for 2–4 h at 37°C. The quality of the DNA for transfection needs to be high (e.g., Qiagen column or CsCl purified). Extract the digest with phenol/chloroform/isoamyl alcohol and ethanol precipitate the DNA at room temperature. Centrifuge the DNA at $10,000 \times g$ for 5 min at 4°C. **From here on, all manipulations should be performed in a class II biological safety cabinet.** Carefully remove and discard the ethanol and briefly air dry the pellet to remove traces of ethanol. Resuspend the DNA in 10 μ l sterile water. HEK293 cells are transfected with *PacI*-linearized pAdEasy-1 recombinant DNA using cationic lipids (e.g., Lipofectamine) as per the manufacturer's instructions.

Incubate the transfection flask in a CO₂/air incubator at 37°C for 6–7 days. For cells transfected with vectors expressing GFP, fluorescence can be monitored on fluorescence microscopes equipped with GFP or fluorescein excitation and emission filters. Signs of viral infection [rounded up cells and clear areas (plaques) surrounded by rounded cells or GFP expression] must be present before harvesting the cells. These may be visible by 7 days posttransfection. If GFP is expressed, approximately 10% of the cells should be GFP positive before harvest. Occasionally, this can take an additional few days to a week. If the cells are left for periods longer than 7 days posttransfection, remove 2 ml of medium and replace with fresh medium every 3–4 days. When the cells are ready to harvest, use a sterile cell scraper to scrape the cells off the flask. Transfer the cells and medium to a 50-ml polypropylene tube. The larger volume tube makes it easier to shell-freeze the sample and to insert pipettors without touching the sides. Pellet the cells by centrifugation at $1000 \times g$ for 3 min. Discard the supernatant and suspend the

cell pellet in 2 ml PBS. Quick freeze the cells in a dry ice/95% ethanol bath or liquid nitrogen. Thaw the sample in a 37°C water bath, but remove it before the sample is completely thawed so that it does not get warm. Vortex the thawed sample. Repeat the freeze/thaw/vortexing three additional times. Centrifuge the sample at $1500 \times g$ for 5 min to remove large cell debris. Make 0.5-ml aliquots of the virus-containing supernatant and store them at -80°C . These are the original viral harvests that should be used for the expansion of stocks. Make sure they are well labeled and logged for future reference.

D. Expansion of Transfection Harvests

Add 0.5 ml (or more if very few GFP-positive cells or no rounded cells were visible in the transfection flask) of the primary viral harvest to a T25 flask inoculated 24 h earlier with $1\text{--}1.5 \times 10^6$ HEK293 cells. Within 2–3 days, infected cells should begin to round up and lift off the flask (Fig. 4). Harvest this first expansion flask as described for the transfection plate using four freeze–thaw cycles. If the cells do not round up within a few days, they can be left up to a week. If the cells have not rounded up by this time, the expansion may need to be repeated with a larger inoculum of primary viral harvest. For viruses expressing GFP (AdTrack) or GFP-chimeric proteins, fluorescence can also be monitored to determine if the virus is being replicated and is infectious. This is achieved most easily using a dissection microscope equipped for epifluorescence, but cells can also be observed with low-power objectives on an inverted fluorescence microscope.

Add 0.1 ml of the first expansion viral harvest to a T75 flask inoculated 24 h earlier with $3\text{--}4 \times 10^6$ HEK293 cells. In 2–3 days, cells from the second amplification should round up and can be harvested as described earlier, except that

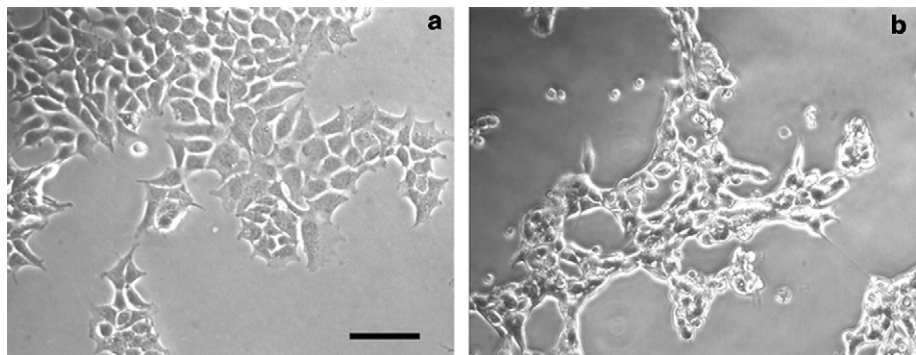


Fig. 4 Infection of HEK293 cells. (a) Noninfected HEK293 cells growing as an adherent monolayer. (b) HEK293 cells 2 days after infection with adenovirus. Cells have rounded up and are lifting off the tissue culture plastic. Bar: 100 μm .

the volume of the PBS used in the freeze–thaw cycles should be 5 ml. The virus-containing supernatants can be further separated from cell debris by passing them through a 0.45- μ m filter.

The standard protocol for amplification of the adenovirus is to infect HEK293 cells at 80% confluence with a multiplicity of infection (MOI) of 1–10. The MOI is defined as the number of infectious particles added per cell. The cells should round up within 24 h and lift off by 48 h after infection. Many procedures suggest infection in minimal amounts of medium. We have found that infecting cells cultured in a T75 flask in 10–12 ml complete medium works well.

Large-scale cultures can be grown in 850-cm² surface area roller bottles. The roller bottles should be inoculated with at least $1.5\text{--}3 \times 10^7$ HEK293 cells in 75–100 ml medium and rotated at 0.5 rpm. If the incubator is not supplied with CO₂, the bottles can be gassed with 5% CO₂/95% air before closing the lids tightly and placing them in a roller bottle incubator. When the cells have reached ~75% confluency (which takes several days), they can be infected at a MOI of 1–3. Harvest the cells when they have rounded up and lifted off the sides of the bottle. Pipetting the cell culture medium over the sides of the bottle is usually sufficient for dislodging the cells.

IV. Purification and Storage of Adenovirus Stocks

A. Materials

CsCl (ultrapure)
SW41 swinging bucket rotor (Beckman Coulter Instruments, Fullerton, CA)
SW41, Vti65.2 polyallomer tubes (Beckman Coulter Instruments)
VTi65.2 vertical rotor (Beckman Coulter Instruments)
Ultracentrifuge
70% ethanol
2-ml sterile syringe
23-gauge sterile needle
PBS
Virakit adenovirus purification kit (Virapur, LLC, Carlsbad, CA)

B. Overview of Methods

The freeze/thaw viral lysate is usually adequate for the infection of most cells. However, some cells may be sensitive to the cellular contaminants in this preparation. In addition, not all of the viral particles produced are functional and some cells may suffer from the toxic effects of these empty particles. Purification of virus is generally done by one of two methods. The first involves banding of the adenovirus in a CsCl gradient. The second involves the use of a commercially

available but proprietary filter disk (Virakit) to bind adenovirus, which can then be eluted. The CsCl gradient method (Kanegae *et al.*, 1994) is more time-consuming, requires an ultracentrifuge, rotors, and generates CsCl waste. The commercial kit is rapid, but relatively expensive.

C. CsCl Gradient Purification of Adenovirus

Infect T75 flasks or one roller bottle (850 cm² surface area) of HEK293 cells with virus. After releasing the virus particles from the HEK293 cells by freeze/thaw and centrifugation to remove most of the membranous contaminants, overlay the virus solution (8 ml) on a CsCl step gradient consisting of 1.4 and 1.25 g/ml CsCl. To prepare the 1.25-g/ml solution, add 9.04 g CsCl to 25 ml PBS. To prepare the 1.4 g/ml CsCl, add 15.5 g CsCl to 25 ml PBS. Pipette 1.5 ml 1.25 g/ml CsCl in an SW41 polyallomer tube. Underlay this solution with 1 ml 1.4 g/ml CsCl. Overlay with the virus solution and centrifuge at 20°C for 1 h at 36,000 rpm. Virus particles containing DNA will form a white band at the interface between the two CsCl steps. In a biological safety cabinet, wipe the outside of the centrifuge tube with 70% ethanol, puncture the top of the tube, and then withdraw the virus by side puncture of the tube with a needle and syringe, working over a collection container to catch leakage (see Section VI). Additional bands can sometimes be seen, including a band of empty particles within the 1.25-g/ml CsCl step. Place the collected virus band in a VTi65.2 tube and fill with 1.35 g/ml CsCl prepared by adding 12.8 g CsCl to 25 ml PBS. Heat seal the tube and centrifuge at 60,000 rpm overnight. Wipe the outside of the tube with 70% ethanol and collect the virus band, which should be close to the middle of the tube, by side puncture using a 3-ml syringe and 21-gauge needle. Dilute the virus stock with 4 volumes of PBS. The adenoviruses are stable in PBS even after repeated freeze/thaws. Buffers such as 10 mM Tris, pH 8, 100 mM NaCl, 0.1 mg/ml bovine serum albumin, and 50% glycerol (the glycerol is autoclaved and the other reagents are sterile filtered) have also been used for adenoviral storage. The viral stock may need to be dialyzed if the concentration of CsCl remaining is toxic to your cells. Dialysis should be done immediately before use, as the virus is less stable in low salt. Alternatively, the CsCl can be removed and virus particles concentrated with Ultrafree (Millipore Corp., Bedford, MA) centrifugal filters, but the virus particles should not be concentrated to greater than 10¹² particles/ml or they may aggregate irreversibly. The virus particles can also be concentrated by centrifugation in microfuge tubes at 14,500 × *g* at 4°C for 30 min (see Virakit protocol later). The pelleted virus must then be resuspended quickly to prevent irreversible aggregation. Aliquot and store the virus at -80°C at no greater than 10¹² particles/ml.

To estimate the concentration of virus particles, a sample of the virus is diluted and the absorbance measured at 260 nm. One *A*₂₆₀ unit is equivalent to 10¹² viral particles/ml, and there are 50–100 viral particles per plaque-forming unit. Even after CsCl banding, not all of the particles are functional. Titer assays must be done to determine the actual plaque-forming units per milliliter. The absorbance

measurements are adequate for estimating particle density to determine storage volumes before performing titer assays.

D. Virakit Purification

This method utilizes a commercial kit from Virapur, LLC. Each binding disk can handle the viral production from about 850 cm² of growth surface (11 T75 flasks or one roller bottle). After releasing virus particles from HEK293 cells by freeze/thaw in 2–5 ml PBS and centrifugation to remove most of the membranous contaminants, dilute the virus suspension to 20 ml with PBS. Alternatively, if the serum in the cell culture medium is reduced to 2% during infection, the cells may be lysed by freeze/thaw directly in the growth medium. Medium components will not interfere with the virus binding to the disk, but cellular DNA will interfere so do not exceed the cell numbers obtained from one roller bottle. The virus suspension is then filtered and diluted, and the virus is then bound to the Virakit disk by pulling the virus solution through the disk and then washing and eluting as per the manufacturer's directions. Store the virus in small aliquots (0.5 ml or less) at –80°C. Viral stocks are stable for at least 6 months stored at 4°C and indefinitely at –80°C.

V. Titer Assays

A. Materials

Six-well culture plate

B6-8 monoclonal antibody (hybridoma supernatant) (Reich *et al.*, 1983)

HEK293 cells

High glucose DMEM serum free

High glucose DMEM plus 2% FBS

37°C incubator with 5% CO₂/95% air

PBS

EM grade formaldehyde (Tousimis Research Corporation, Rockville, MD)

90% methanol/10% PBS

1% bovine serum albumin (fraction V) in PBS

Goat antimouse IgG–alkaline phosphatase conjugate (Sigma-Aldrich, St. Louis, MO)

High pH wash buffer (50 mM Tris, pH 9.5, 100 mM NaCl, 1 mM MgCl₂; adjust pH of this buffer before adding MgCl₂)

Nitroblue tetrazolium chloride (NBT) (75 mg/ml in 70% dimethylformamide)

5-Bromo-4-chloro-3-indolylphosphate *p*-toluidine salt (BCIP) [50 mg/ml in dimethylformamide (NBT and BCIP stocks should be stored at –20°C)]

Inverted microscope (tissue culture grade)

B. Overview of Plaque Assay and Immunoassay

Until recently, viral stock solutions were titered by plaque assays. HEK293 cells grown in 12-well tissue culture dishes were infected with serial dilutions of virus and then overlaid with agar. Viral replication occurred in infected cells and the cells lysed. Released virus infected neighboring cells, eventually resulting in a cleared area or plaque. The number of plaques per well was counted and related back to the dilution of the original stock, and the volumes used to infect the cells, thus getting plaque-forming units per milliliter. The difficulty with this assay is largely in performing the agar overlay. The agar needs to be warm enough to flow, but not too hot or it kills the HEK293 cells. The speed at which the agar is overlaid on the cells also has to be controlled carefully. In addition, the assay typically requires 7–10 days for the plaques to develop and be visible. Furthermore, variations in the agar due to bubbles or ripples in the surface make it difficult to find and count all of the plaques. The assay of choice is now a 2-day immunoassay (modified from Nevins *et al.*, 1997), which utilizes a monoclonal antibody (B6-8, Reich *et al.*, 1983) to the adenovirus E2a antigen, a nuclear protein made in infected cells. This assay is rapid but does require that cells be fixed and stained exactly 16 h after viral infection. This timing is sufficient to allow production of the E2a antigen in every infected cell but short enough to prevent the packaging and release of new virus to infect additional cells, which starts 18–24 h after infection.

We have compared the titers of several viruses done by the two different procedures and we usually get values that are two- to fourfold greater using the immunoassay than for the plaque assay. Thus the MOI that we use currently is approximately two- to fourfold higher than what we would report if we used plaque assay results.

C. Adenoviral Titers with Two-Day Immunoassay

Plate HEK293 cells in six-well plates at 6×10^5 cells per well. The next day, the cells should cover 70–95% of the area of the wells. Make dilutions of the virus to be titered in serum-free HGD MEM. Dilutions of $1:10^4$, 10^5 , and 10^6 are good starting points for virus made from cell lysates and not purified or concentrated further. Aspirate the medium off the HEK293 cells and apply 0.5 ml virus per well. When adding solutions to the wells, pipette the solutions gently down the sides of the wells so as not to dislodge the cells. Incubate the plate at 37°C in 5% CO_2 /95% air for 45 min with occasional rocking to obtain the best viral dispersion over the cells. Pipette off the virus solutions and add 2 ml HGD MEM/2% FBS to each well. Return the plate to the incubator for exactly 16 h (timing is important, so this incubation should be started late in the day).

Pipette the medium off the cells and wash the cells once with 2 ml PBS. Fix the cells in 3.7% EM grade formaldehyde in PBS for 5 min at room temperature using 2 ml fixative per well. Wash the cells twice with PBS. Permeabilize the cells in 90% methanol/10% PBS for 2 min at room temperature. Wash the cells twice in PBS and once in 1% bovine serum albumin (BSA) in PBS.

Dilute the mouse anti-E2a antibody (B6-8 hybridoma culture supernatant) 1:10 in 1% BSA in PBS. Apply 1 ml per well and incubate the plate for 45 min at room temperature with occasional gentle rocking by hand. Do not place the plate on a rocker or shaker as this may dislodge the HEK293 cells. Wash the cells twice with 2 ml PBS and once with 1 ml 1% BSA in PBS.

Dilute goat antimouse IgG-alkaline phosphatase conjugate 1:1000 in 1% BSA in PBS. Apply 1 ml per well and incubate for 45 min at room temperature with occasional rocking. Gently wash the cells three times with 2 ml PBS and then once with 2 ml high pH wash buffer. Dilute 44 μ l NBT and 33 μ l BCIP in 10 ml of the high pH wash buffer. Apply 1 ml diluted NBT/BCIP to each well and incubate at room temperature for 30–60 min. Nuclei of infected cells begin to turn blue and, when fully stained, they appear very dark blue (Fig. 5). Count the number of positive nuclei in 10 fields using a 20 \times objective and 10 \times eyepieces. [A horseradish peroxidase (HRP)-conjugated secondary antibody can be substituted for the alkaline phosphatase-conjugated antibody and diaminobenzidine (DAB) (Pierce Metal Enhanced DAB) used as the substrate for the HRP. The color reaction develops faster with DAB than with NBT/BCIP. However, DAB is a known carcinogen and requires hazardous waste disposal.]

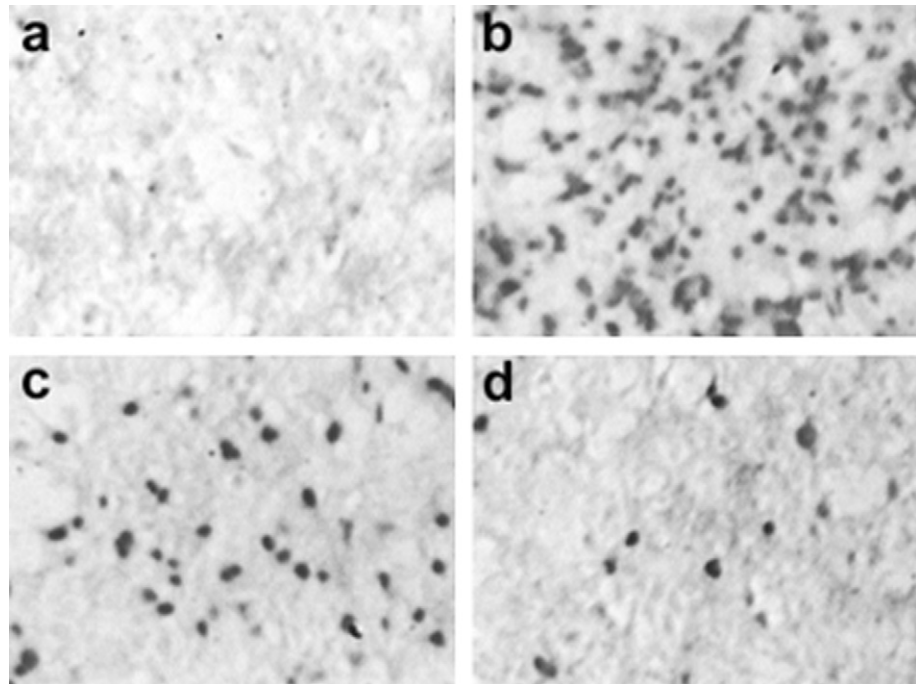


Fig. 5 Viral titer assay using a monoclonal antibody to the E2a DNA-binding protein. Three dilutions of the virus were tested: (a) control (uninfected), (b) 1:10³, (c) 1:10⁴, and (d) 1:10⁵. Nuclei of infected cells appear dark blue.

The titer or number of focus-forming units (ffu) per milliliter can be calculated as follows: average number of positive cells/field \times area conversion factor $\times 2 \times$ dilution. The area conversion factor is based on the area of the field viewed through the microscope versus the area of a well in the six-well plate. Typically, this number is ~ 3500 but can be calculated for any microscope by using a stage micrometer for obtaining the full field diameter of the $20\times$ objective and dividing this into the calculated area of a single well on a six-well plate. Multiplying by 2 adjusts for using 0.5 ml of virus per well. The titer of the virus used in Fig. 5 was calculated by this method to be 3×10^9 ffu/ml.

VI. Safety Issues

A. General Concerns

Adenovirus is a pathogen of respiratory and gastrointestinal mucosa and eye membranes and does not have to be replication competent to cause corneal and conjunctival damage. Biosafety level 2+ (BL2+) safety procedures must be in place for adenovirus work and no open benchwork should be performed. Goggles (not safety glasses) and gloves should be worn. Disposable pipettes and aerosol-resistant tips (e.g., ART pipette tips, Molecular Bioproducts Inc., San Diego, CA) are recommended to avoid contamination of pipettors and the accidental infection of cultured cells or cross-contamination of viral stocks. Primary decontamination of all infected disposables with 10% bleach or another disinfectant such as Coverage Plus (Calgon Vestal Laboratories, St. Louis, MO) within the biological safety cabinet is recommended before removing the waste to autoclaving bins. Centrifugation should be in closed containers using sealed rotors. Dishes should be sealed (e.g., wrapped with Parafilm M, American National Can, Neenah, WI) before microscopy. If possible, viruses remaining in the medium should be removed by washing the cells prior to performing microscopy. The toxicity of the proteins being expressed by the adenoviruses must also be understood. Obviously, adenoviruses engineered to express a known oncogene are more dangerous to work with than viruses expressing only GFP.

The recombinant adenoviruses are still infectious despite being replication incompetent. In addition, at any particular time, a significant fraction of the general population is infected with the wild-type adenovirus and there is potential for the production of replication-competent adenovirus due to E1 expression *in trans* after one is infected with the replication-incompetent adenovirus. Furthermore, because HEK293 cells produce the deleted E1 gene, there is the potential for low-frequency homologous recombination between the E1-deleted pAdEasy-1 vector and the host DNA, resulting in the production of some replication-competent adenovirus. The primary virus stock always contains the lowest number of replication-competent adenovirus. Thus, expansion of stocks should always be done from the earliest stocks available.

B. Testing Viral Stocks for Replication-Competent Virus

Some biosafety offices require proof that recombinant replication-incompetent viruses are indeed replication incompetent. There are two methods we have used to test a viral preparation for replication-competent viruses. The first method uses cultures of a nonpermissive cell line (almost any fibroblast or epithelial cell line but not HEK293 cells) grown in 60-mm culture dishes and infected with a MOI of the virus that will give a high percentage of infected cells over a 2-day period. Cells are then washed several times with medium and are then allowed to grow for another 2 days in fresh medium. If the virus can replicate in these cells, the medium should contain infectious particles by 48 h after infection. After about 2 days of growth, the medium is removed from the infected cells, centrifuged to pellet any floating cells, and the supernatant is added to a new uninfected culture of the same cell type. After 2 days in culture the expression of the exogenous protein from the recombinant adenovirus is measured. If the virus expresses a fluorescent protein (AdTrack) or a fluorescent protein chimera, the assay simply quantifies the percentage of infected cells by direct observation on a fluorescence microscope. If the exogenous protein must be detected by immunofluorescence staining or immunocytochemistry, cells are fixed and stained for the protein using standard methods. If viruses are replication competent, there should be a significant number of infected cells in the dish. If none or very few (<0.1%) of the cells are expressing the exogenous protein then the virus was unable to replicate. Because a small number of virions can carry over into the second dish, a small number of infected cells does not imply that viral replication has occurred.

The E2a protein is necessary for viral replication. Its synthesis is controlled by the E1a gene product that is deleted in the replication-deficient virus. Therefore, a simple method to test for a replication-competent virus is to infect nonpermissive-cultured cells with the adenovirus, wait until expression of the exogenous gene is high, and then fix and stain the cells with the monoclonal antibody to E2a, as described earlier for the viral titer assay. A control dish of uninfected cells should be fixed and stained along with the infected cells in case the cells carry a wild-type adenovirus or have a cross-reactive nuclear protein. This assay can be done to screen a large number of viral stocks by using 12-well culture dishes into which the test cells are plated. One well is left uninfected as a control and 11 virus preparations can be screened at their optimal MOI for infecting the test cells. Cultures should be allowed to grow for 2–3 days before they are fixed and stained for the E2a gene product.

VII. Infection of Primary Neurons

A. Overview

Postmitotic, primary neurons transfect with low efficiency using traditional transfection methods such as calcium phosphate precipitation. At most, only a

few percent of cells are transfected successfully. Other methods described elsewhere in this volume have improved transfection efficiency, and many of these methods work well for a single cell type of analysis, but none have achieved the high levels of transfection that are required to perform biochemical analyses of the effects of expressed proteins in neurons. The advantage of adenoviral expression of proteins is that the expression of exogenous proteins can be obtained in a very high percentage of cells, often reported at 90% or greater. Furthermore, the viruses can and have been used successfully *in vivo* for expressing proteins in animal tissues (Davidson *et al.*, 1993; Bilang-Bleuel *et al.*, 1997; Soudais *et al.*, 2001). For cell biological studies, a much lower level of infectivity is often more desirable, because in such cultures an abundance of uninfected cells can serve as observational controls. Furthermore, lower amounts of virus can be used for infection, decreasing the biohazard. The coexpression of GFP from a separate CMV promoter allows the investigator to select infected cells prior to making observations or measurements.

In selecting to use adenoviral methods for gene transfer into cultured neurons, several points need to be considered that will aid in selecting the best system and establishing the optimal conditions for its use. First it is necessary to define the end points that one wishes to measure and to determine that viral infection and expression can achieve the level of expression of the exogenous protein to affect the measured end point. For example, if one were interested in studying the effect of a specific protein on neurite initiation, one needs to have a system in which expression from the virus can be significant even before the cells are dissociated and placed in culture. If one is interested in effects of an exogenous protein on growth cone motility and process outgrowth, levels of expression would have to be sufficient to exert an effect during the early stages of outgrowth when individual neurites are identifiable and lengths can be measured. If one is interested in looking at the function of an exogenous protein on dendritic spine formation or synapse function in hippocampal neurons, infection can be carried out at a much later time in culture.

For every neuronal culture system one needs to know the optimal MOI of virus to use to achieve maximal infectivity with minimal toxicity. This type of information is often dependent on the specific adenovirus used, the toxicity of the protein encoded by the transgene (and GFP if it is also expressed), and the length of the observational period required. If the infectivity of certain neuronal cell types is low, methods for dissociating neuronal tissue for culture can be modified to use enzymes that may result in a greater preservation of receptors for adenovirus uptake. The extracellular environment (use of serum or growth factors) is important for maximizing viral infection, and optimal conditions will be different between neuronal types. In all dissociated neuronal cultures we have studied, Ad5 adenoviruses infect nonneuronal cells much more efficiently than they infect neurons. Therefore, if one wants to look at biochemical effects of exogenous protein expression in neurons, the number of nonneuronal cells needs to be kept to a minimum.

B. Infectivity of Different Neuronal Cultures

To examine many of the aforementioned characteristics of adenoviral infection in neurons, an adenovirus was constructed that expressed GFP behind the CMV promoter. Viruses obtained from crude HEK293 cell lysates or purified by Virakit filter disks were tested on a variety of different cultured neurons infected at different times after plating with different MOI of each virus in the presence and (for some neurons) in the absence of serum. We compared the fraction of cells expressing GFP 24, 48, 72, and, in some cases, 96 h after infecting the neurons. The neurons we tested were prepared and grown as described elsewhere in this volume and included E18 rat hippocampal and E18 rat cortical, E12 chick superior cervical ganglia, E8 chick dorsal root ganglia, E7 chick forebrain, and E10 chick ciliary ganglia. In addition, we have used other adenoviruses made in our laboratory for infecting spinal motor neurons (Kuhn *et al.*, 1999). The results of some of these expression studies for which we obtained approximate numbers for percentage of neurons expressing GFP are presented in Table III. Because we found no significant differences in using virus released from HEK293 cells by freeze/thaw and virus that was further purified on Virakit disks, the results presented in Table III do not distinguish between the two. Most of these values are from a single experiment in which we used a fixed exposure time on a digital camera with a 20 \times objective to record images of random fields in both phase and fluorescence. The numbers in Table III are presented only to show the general trends among infection conditions, ages of cultures *in vitro* when cells were infected, and the dependence on MOI. It is quite likely that the numbers are lower than would be obtained if the fluorescence were measured using oil immersion.

As a general finding, virtually all of the different neuronal types were infected better after the cells had been plated for 1–3 days than they did if the virus was added within 4 h after plating. Rat E18 hippocampal and cortical neurons were infected with greater efficiency in the presence of 10% serum than in its absence, but the presence of serum had no effect on the infection efficiency of chick forebrain neurons. In Fig. 6, fluorescence images of GFP-expressing hippocampal neurons are shown at 24, 48, 72, and 96 h after infection with the GFP adenovirus added 72 h after plating. At an MOI of 20, about 25% of the neurons became GFP positive by 48 h and that percentage did not change over the next 2 days. Even at an MOI of 400 we observed no toxicity over the 4-day observational period. Wilkemeyer *et al.* (1996) used adenovirus at a MOI of 1, 10, and 100 to infect hippocampal neurons and reported between 30 and 70% infectivity with an MOI of 1 using β -gal expression and X-gal staining as an end point. They reported toxicity after 5–10 days at the higher MOI. The infectivity of E18 rat cortical neurons has been reported to be greater than 90% in cultures examined 48 h after infection in the presence of serum when a membrane-associated and modified form of GFP was expressed (Moriyoshi *et al.*, 1996). Although we only obtained 21% GFP-expressing cells after 48 hr using serum during infection, our lower

Table III
Percentage of Neurons Expressing Transgene at Various Times after Infection

Observation times	Neuron ^a	Infected 4 h after plating (MOI)						Infected 24 h after plating (MOI)						Infected 72 h after plating (MOI)					
		20	60	100	150	200	400	20	60	100	150	200	400	20	60	100	150	200	400
24	H-n	0	0		5			0	0	0	0	0	0	17	19	0	17	4	6
	H-s			3		7	24			34		34	53						
	C-n	0	0		2			0	2		4			0	2		3		
	C-s			7		2	19			5		11	11						
	F-n	0	2		4			0	0		6			0	0		4		
	F-s			2		1	2			0		1	2						
	Fsu	6	0		0														
	DR	0	2		2			1	1		1			1	0		8		
SM																			38 ^b
48	H-n	0	0		2			6	4	0	0	0	2	25	33	8	39	12	11
	H-s			20		32	37			28		26	54						
	C-n	0	2		1			0	2		5			2	6		9		
	C-s			5		5	9			3		21	15						
	F-n	4	4		3			1	1		8			2	13		8		
	F-s			5		5	6			3		4	9						
	Fsu	10	3		5														
	DR	2	4		3			5	4		5			2	4		12		
SM																			60 ^b
72	H-n	2	3		11			3	7	7	17	4	11	25	49	12	45	12	13
	H-s			29		19	29			64		42	50						
	C-n	0	0		0			0	2		2			0	2		6		
	C-s			6		4	8			13		18	16						
	F-n	0	2		12			2	0		9			7	12		0		
	F-s			7		5	9			7		12	17						
	Fsu	9	3		6														
	DR	5	8		14			6	5		12			24	26		31		
SM																			86 ^b
96	H-n	4	3		14		3	2	16	13	27	16	18	23	30	27	52	20	22
	C-n	2	3		3									4	8		26		
	F-n	0	5		8			27			11			9	4		4		
	DR	6	10					4	24		26			10	23		25		
	SM																		

^aH-n, hippocampal neurons without serum; H-s, hippocampal neurons infected in 10% serum; C-n, cortical neurons without serum; C-s, cortical neurons infected in 10% serum; F-n, chick forebrain neurons without serum; F-s, chick forebrain neurons infected in 10% serum; Fsu, chick forebrain neurons infected in suspension without serum; DR, chick sensory ganglia infected in serum; SM, chick spinal motor neurons infected in serum. ^bData from Kuhn *et al.* (1999).

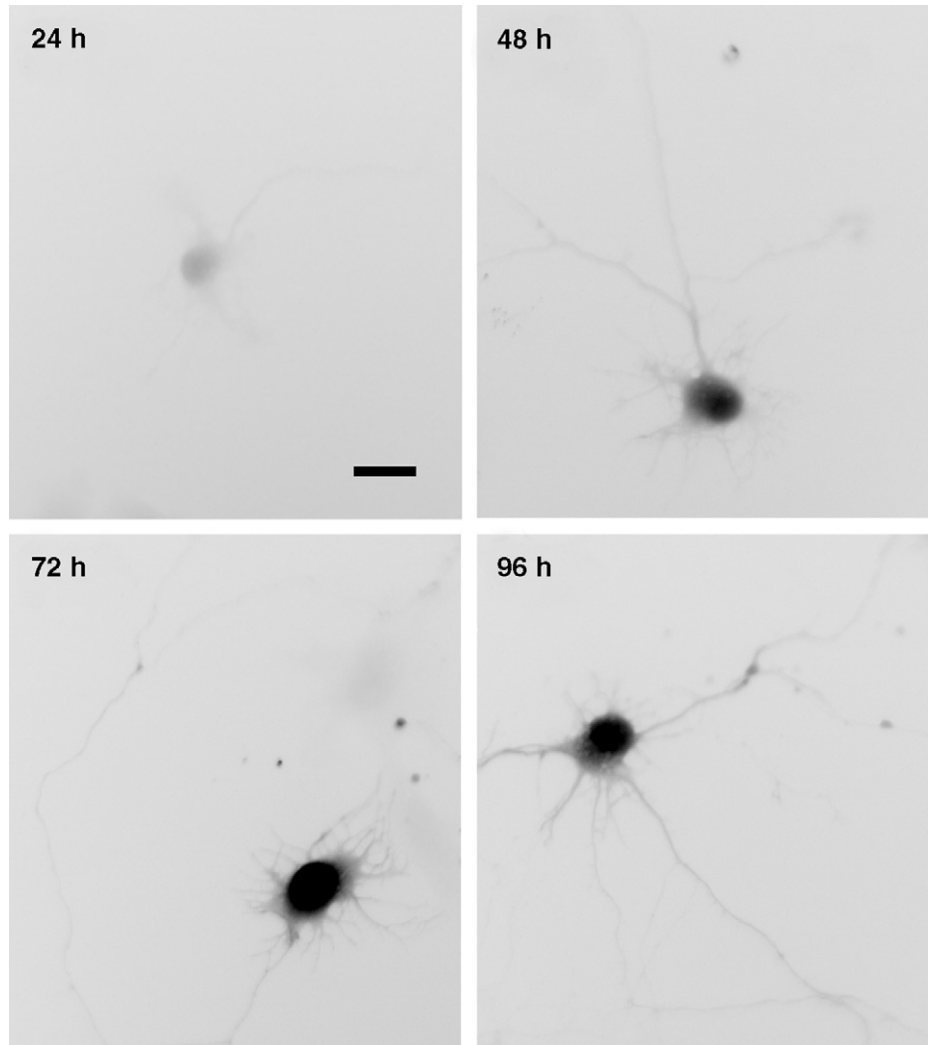


Fig. 6 Inverted fluorescent image of hippocampal neurons infected (MOI 400) 3 days after plating. GFP-positive cells are visible within 24 h of infection, and GFP fluorescence levels continue to increase until 72 h. GFP is detectable throughout the neurites of infected neurons. Bar: 20 μm .

values reflect in part the sensitivity of our imaging protocol that would exclude cells expressing low amounts of GFP.

For neurons from dorsal root ganglia, the enzymatic method of dissociation made a large difference in the number of cells infected and the time course of expression. Infectivity of neurons from collagenase-dissociated ganglia (not shown

in Table III) was two to three times greater than that obtained from trypsin-dissociated ganglia, with greater than 8% of the cells expressing GFP by 24 h and 30% by 72 h. Thus, altering dissociation methods can protect receptors needed for viral uptake on some cells. However, collagenase dissociation did not alter the infectivity of hippocampal or cortical neurons. Sympathetic neurons dissociated with trypsin gave even lower percentages of infected cells than DRG neurons, but at a MOI of 150 some labeled cells were present and thus cell biological studies on these cells could be performed. Others have found it possible to infect 80% of cultured sympathetic neurons with adenovirus at an MOI of 10 (Slack and Miller, 1996). Chick ciliary ganglion neurons also could be infected with adenovirus with about 10% of the neurons expressing GFP by 48 h after infection.

C. Infection of Neuronal Tissues in Suspension before Dissociation

To determine if chick sensory and ciliary ganglia, chick forebrain, or rat hippocampal cells could be infected in the tissue held in suspension for 24 h before dissociation, pieces of hippocampus, forebrain, or bisected ganglia were suspended in medium (Neurobasal plus B27 supplements for hippocampus, HEPES-buffered DMEM for ganglia, and HEPES-buffered Hams F12 with B27 supplements for chick forebrain) in the presence of the GFP-expressing adenovirus. Use of the vibrating platform device described in Section VII,E for overnight incubations increased the cell yield and infectivity of the chick forebrain pieces, probably because it kept the pieces in suspension and enhanced viral penetration of the tissue. Surprisingly, most of the cultures made from these dissociated cells looked very good with many healthy cells in yields comparable to those obtained when dissociation was done immediately after dissection. Some GFP-positive neurons were observed in sensory and ciliary neuronal cultures and these were fluorescent within 24 h after plating, suggesting that this method could be further developed to give labeled DRG and ciliary neurons very early in the process of neurite initiation.

D. Viral Toxicity

In general, neurons tolerate well adenovirus addition up to 400 MOI (determined by immunoassay; equal to a MOI of 100–150 by plaque assay), the highest values we tested in our studies. There was no significant difference in the survival or appearance of any of the different neuronal cell types infected with equal MOIs of the crude virus, obtained from repetitive freeze/thaws of the 293 cells, and the virus purified on Virapur disks over the 4-day period of observation. However, there are reports in the literature of adenoviral toxicity to neurons over longer times in culture. In our experience, unless transgene expression is under a regulatable or weak promoter, toxicity from most transgene products, including GFP, expressed behind strong promoters will occur as expression levels increase, which begins about 3–4 days postinfection in cultured neurons.

E. Reducing Nonneuronal Cell Contamination

Because nonneuronal cells in every dissociated cell culture system infected with greater efficiency and showed more rapid expression of the exogenous gene than the neurons, it is important to keep numbers of nonneuronal cells to a minimum. This is especially important if the infected cells are to be harvested for biochemical studies to look at the effects of the expressed protein on other proteins by blotting methods. If care is not taken to keep nonneuronal cell proliferation under control, neurons can rapidly become a minor component in the culture.

The best first method for reducing nonneuronal cell contamination is to be exceptionally careful in the removal of extraneous tissues when dissecting neuronal-containing tissue. Connective tissue and capsule material that surround ganglia give rise to a dividing fibroblast population. Three general strategies are used to decrease nonneuronal cells in every type of primary neuronal culture system. First, if nonserum-containing growth medium can be used, the proliferation of nonneuronal cells is usually retarded severely or stopped entirely due to the lack of supporting growth factors. Second, additives that kill proliferating cells are often used in culture because these agents should be nontoxic to neurons, which are nondividing. The most commonly used drug for this application is cytosine 1- β -D-arabinofuranoside (AraC), which at 2–4 μ g/ml inhibits most nonneuronal cell proliferation in chick sensory and sympathetic neuronal cultures (Mizel and Bamberg, 1976). Third, following enzymatic dissociation of neuronal tissue, separation of neurons from nonneuronal cells is often performed. Two methods used successfully for removing nonneuronal cells are density gradient centrifugation and preplating of cells. Density gradient centrifugation is more technically demanding but has been used successfully for enriching neurons from several tissues, including sympathetic ganglia (Bray *et al.*, 1987). Because nonneuronal cells adhere faster to tissue culture plastic or glass than neurons, allowing the cell suspension to settle onto a surface and decanting the nonadhered neurons after 0.5 to 2 h often removes most of the contaminating fibroblasts and glia.

A simple and inexpensive vibrating platform allows us to maintain neurons in suspension while allowing nonneuronal cells to adhere. This vibration system is made using a vibrating toothbrush motor unit (placed in the on position) squeezed tightly into a small cardboard box and plugged into a 5-min interval timer set to activate the motor for 30 s out of every 5-min period. A glass plate is taped tightly over the box to transduce the vibrations to an attached (with double sticky tape) 20 \times 20-cm tissue culture plate, used as a tray. Cultures containing our dissociated tissue are placed on this tray. The entire box vibrator is placed in a 37°C tissue culture incubator with the cord exiting to the interval timer. The box is secured to the shelf to prevent it from moving around the incubator. Holes punched in the side and bottom of the box permit it to be attached to the shelf using pipe cleaners or wire. Nonneuronal cells are allowed to attach for 1–4 h under these vibration conditions before we remove the neurons in suspension and plate them. Using this

method, we have achieved cultures containing greater than 99% neuronal cells from both sensory and sympathetic ganglia, similar to what has been reported using a much more sophisticated apparatus (Clark *et al.*, 1983).

VIII. Conclusions and Perspectives

Several things could be improved in the modification and manufacture of adenoviruses, as well as in their specificity, and in the regulation of their transgene expression. To improve the ease of adenoviral vector construction, a method for direct ligation-based cloning of foreign genes into the viral genome has been described (Mizuguchi *et al.*, 2001a). This approach has developed shuttle vectors in which separate genes can be inserted into the E1 and E3 regions of the adenoviral genome and has eliminated promoter interference that often occurs when heterologous gene expression cassettes are inserted into the E1 region. The direct ligation-based cloning methods also have been used to specifically modify the H1 loop of the expressed fiber knob domain, which is the component on the surface of the adenovirus that is used in cell surface receptor binding (Mizuguchi *et al.*, 2001c). Coding regions for different peptide sequence motifs that are specific for cell surface receptors (e.g., RGD peptides such as CDCRGDCFC, which binds with high affinities to integrins $\alpha v\beta 3$ and $\alpha v\beta 5$) have been inserted and their expression dramatically alters the efficiency of infection of targeted and hard to infect cell populations (e.g., microglia) (Omori *et al.*, 2002). Furthermore, a new serotype 2 strain of canine adenovirus that has almost a complete dependence on CAR for cellular uptake has been identified (Soudais *et al.*, 2001). Within the nervous system, CAR, which can be immunostained with monoclonal antibody RmcB (Hsu *et al.*, 1988; ATCC CRL-2379), is found almost exclusively on neurons, and these Ad2 canine adenoviruses could become the vector of the future in targeting genes specifically to neurons, especially *in vivo*.

One disadvantage to adenovirus-mediated gene expression behind the CMV promoter is that the expression is not regulated. For most proteins there is probably a defined window of opportunity between having sufficient expression and lethal expression of the virally expressed protein. However, pAdTrack and pShuttle vectors can be used for cloning the gene of interest behind other promoters. Alternatively, direct ligation-based methods can also be used to make viral vectors with desired promoters. Several studies have utilized the tetracycline controllable expression system in adenoviral vectors. Initially these were performed as a two virus infection system where a second adenovirus was used to express the tetracycline-controlled transcriptional activator or silencer (Harding *et al.*, 1997; Ghersa *et al.*, 1998). More recently, single adenoviral vectors for either tet-on or tet-off regulated control of gene expression have been developed (Corti *et al.*, 1999; Mizuguchi and Hayakawa, 2001; Mizuguchi *et al.*, 2001b). The tet-off Ad vector showed tightly regulated transgene expression even at low MOI, whereas the tet-on system had a higher background and lower inducibility

(Mizuguchi and Hayakawa, 2001). In addition the tet-off system could be regulated at much lower tet levels.

Given all of these recent developments, new generations of adenoviral vectors and reagents for modifying them will soon be widely available. Vectors will soon be selected for the specific type of cell one wishes to infect, avoiding some of the problems imparted by nonneuronal cell contamination. With regulatable promoters already available to control the level of transgene expression, adenoviral-mediated gene delivery will likely become the method of choice for many cell biological studies.

Acknowledgments

We thank Dr. C. L. Wilcox for introducing us to the applications of adenoviral technology, Drs. T. B. Kuhn and P. J. Meberg for getting this technology operational in our laboratory, and Dr. J. Schaack for many helpful hints. P. D. S. is supported by grant SB2-0110-2 from the Christopher Reeve Paralysis Foundation. We are grateful for research support from the Alzheimer's Association (Grant IIRG-01-2730) and from the National Institutes of Health (Grants GM35126, NS40371, and NS43115).

References

- Becker, T. C., Noel, R. J., Coats, W. S., Gómez-Foix, A. M., Alam, T., Gerard, R. D., and Newgard, C. B. (1994). Use of recombinant adenoviruses for metabolic engineering of mammalian cells. *Methods Cell Biol.* **43**, 161–189.
- Bergelson, J. M., Cunningham, J. A., Droguett, G., Kurt-Jones, E. A., Krithivas, A., Hong, J. S., Horwitz, M. S., Crowell, R. L., and Finberg, R. W. (1997). Isolation of a common receptor for coxsackie B viruses and adenoviruses 2 and 5. *Science* **275**, 1320–1323.
- Bergelson, J. M., Krithivas, A., Celi, L., Droguett, G., Horwitz, M. S., Wickham, T., Crowell, R. L., and Finberg, R. W. (1998). The murine CAR homolog is a receptor for coxsackie B viruses and adenoviruses. *J. Virol.* **72**, 415–419.
- Bett, A. J., Haddara, W., Prevec, L., and Graham, F. L. (1994). An efficient and flexible system for construction of adenovirus vectors with insertions or deletions in early regions 1 and 3. *Proc. Natl. Acad. Sci. USA* **91**, 8802–8806.
- Bilang-Bleuel, A., Revah, F., Colin, P., Locquet, I., Robert, J. J., Mallet, J., and Horellou, P. (1997). Intrastratial injection of an adenoviral vector expressing glial-cell-line-derived neurotrophic factor prevents dopaminergic neuron degeneration and behavioral impairment in a rat model of Parkinson disease. *Proc. Natl. Acad. Sci. USA* **94**, 8818–8823.
- Bray, D., Bunge, M. B., and Chapman, K. (1987). Geometry of isolated sensory neurons in culture: Effects of embryonic age and culture substratum. *Exp. Cell Res.* **168**, 127–137.
- Clark, S. E., Moss, D. J., and Bray, D. (1983). Actin polymerization and synthesis in cultured neurones. *Exp. Cell Res.* **147**, 303–314.
- Corti, O., Sabate, O., Horellou, P., Colin, P., Dumas, S., Buchet, D., Buc-Caron, M. H., and Mallet, J. (1999). A single adenovirus vector mediates doxycycline-controlled expression of tyrosine hydroxylase in brain grafts of human neural progenitors. *Nature Biotech.* **17**, 349–354.
- Davidson, B. L., Allen, E. D., Kozarsky, K. F., Wilson, J. M., and Roessler, B. J. (1993). A model system for *in vivo* gene transfer into the central nervous system using an adenoviral vector. *Nature Genet.* **3**, 219–223.
- Davison, E., Diaz, R. M., Hart, I. R., Santis, G., and Marshall, J. F. (1997). Integrin $\alpha 5\beta 1$ -mediated adenovirus infection is enhanced by the integrin-activating antibody TS2/16. *J. Virol.* **71**, 6204–6207.

- Ghersa, P., Gobert, R. P., Sattonnet-Roche, P., Richards, C. A., Merlo Pich, E., and van Huijsduijnen, R. H. (1998). Highly controlled gene expression using combination of a tissue specific promoter, recombinant adenovirus and a tetracycline-regulatable transcription factor. *Gene Ther.* **5**, 1213–1220.
- Graham, F. L., Smiley, J., Russell, W. C., and Nairn, R. (1977). Characteristics of a human cell line transformed by DNA from human adenovirus type 5. *J. Gen. Virol.* **36**, 59–72.
- Grunhaus, A., and Horwitz, M. S. (1992). Adenoviruses as cloning vectors. *Semin. Virol.* **3**, 237–252.
- Harding, T. C., Geddes, B. J., Noel, J. D., Murphy, D., and Uney, J. B. (1997). Tetracycline-regulated transgene expression in hippocampal neurones following transfection with adenoviral vectors. *J. Neurochem.* **69**, 2620–2623.
- He, T.-C., Zhou, S., Da Costa, L. T., Yu, J., Kinzler, K. W., and Vogelstein, B. (1998). A simplified system for generating recombinant adenoviruses. *Proc. Natl. Acad. Sci. USA* **95**, 2509–2514.
- Hong, S. S., Karayan, L., Tournier, J., Curiel, D. T., and Boulanger, P. A. (1997). Adenovirus type 5 fiber knob binds to MHC class I $\alpha 2$ domain at the surface of human epithelial and B lymphoblastoid cells. *EMBO J.* **16**, 2294–2306.
- Hsu, K.-H. L., Lonberg-Holm, K., Alstein, B., and Crowell, R. L. (1988). A monoclonal antibody specific for the cellular receptor for the group B coxsackieviruses. *J. Virol.* **62**, 1647–1652.
- Kanegae, Y., Makimura, M., and Saito, I. (1994). A simple and efficient method for purification of infectious recombinant adenovirus. *Jpn. J. Med. Sci. Biol.* **47**, 157–166.
- Kuhn, T. B., Brown, M. D., Wilcox, C. L., Raper, J. A., and Bamberg, J. R. (1999). Myelin and collapsin-1 induce motor neuron growth cone collapse through different pathways: Inhibition of collapse by opposing mutants of *rac1*. *J. Neurosci.* **19**, 1965–1975.
- Leber, S. M., Yamagata, M., and Sanes, J. R. (1996). Gene transfer using replication-defective retroviral and adenoviral vectors. *Methods Cell Biol.* **51**, 161–183.
- Mizel, S. B., and Bamberg, J. R. (1976). Studies on the action of nerve growth factor. I. Characterization of a simplified in vitro culture system for dorsal root and sympathetic ganglia. *Dev. Biol.* **49**, 11–19.
- Mizuguchi, H., and Hayakawa, T. (2001). Characteristics of adenovirus-mediated tetracycline-controllable expression system. *Biochim. Biophys. Acta* **1568**, 21–29.
- Mizuguchi, H., Kay, M. A., and Hayakawa, T. (2001a). Approaches for generating recombinant adenovirus vectors. *Adv. Drug Deliv. Rev.* **52**, 165–176.
- Mizuguchi, H., Kay, M. A., and Hayakawa, T. (2001b). *In vitro* ligation-based cloning of foreign DNAs into the E3 and E1 deletion regions for generation of recombinant adenoviral vectors. *Biotechniques* **30**, 1112–1116.
- Mizuguchi, H., Koizumi, N., Hosono, T., Utoguchi, N., Watanabe, Y., Kay, M. A., and Hayakawa, T. (2001c). A simplified system for constructing recombinant adenoviral vectors containing heterologous peptides in the H1 loop of their fiber knob. *Gene Ther.* **8**, 730–735.
- Moriyoshi, K., Richards, L. J., Akazawa, C., O'Leary, D. D. M., and Nakanishi, S. (1996). Labeling neuronal cells using adenoviral gene transfer of membrane-targeted GFP. *Neuron* **16**, 255–260.
- Nevins, J. R., DeGregori, J., Jakoi, L., and Leone, G. (1997). Functional analysis of E2F transcription factor. *Methods Enzymol.* **283**, 205–219.
- Omori, N., Mizuguchi, H., Ohsawa, K., Kohsaka, S., Hayakawa, T., Abe, K., and Shibasaki, F. (2002). Modification of a fiber protein in an adenovirus vector improves in vitro gene transfer efficiency to the mouse microglial cell line. *Neurosci. Lett.* **324**, 145–148.
- Reich, N. C., Sarnow, P., Duprey, E., and Levine, A. J. (1983). Monoclonal antibodies which recognize native and denatured forms of the adenovirus DNA-binding protein. *Virology* **128**, 480–484.
- Sambrook, J., and Russell, D. W. (2001). "Molecular Cloning: A Laboratory Manual" 3rd Ed. Cold Spring Harbor Laboratory Press, Cold Spring Harbor, NY.
- Slack, R. S., and Miller, F. D. (1996). Viral vectors for modulating gene expression in neurons. *Curr. Opin. Neurobiol.* **6**, 576–583.
- Soudais, C., Laplace-Builhe, C., Kissa, K., and Kremer, E. J. (2001). Preferential transduction of neurons by canine adenovirus vectors and their efficient retrograde transport *in vivo*. *FASEB J.* **15**, 2283–2285.

- Tartof, K. D., and Hobbs, C. A. (1987). Improved media for growing plasmid and cosmid clones. *Bethesda Res. Lab. Focus* **9**, 12.
- Tomko, R. P., Xu, R., and Philipson, L. (1997). HCAR and MCAR: The human and mouse cellular receptors for subgroup C adenoviruses and group B coxsackieviruses. *Proc. Natl. Acad. Sci. USA* **94**, 3352–3356.
- Wickham, T. J., Filardo, E. J., Cheresch, D. A., and Nemerow, G. R. (1994). Integrin $\alpha v\beta 5$ selectively promotes adenovirus mediated cell membrane permeabilization. *J. Cell Biol.* **127**, 257–264.
- Wilkemeyer, M. F., Smith, K. L., Zarei, M. M., Benke, T. A., Swann, J. W., Angelides, K. J., and Eisensmith, R. C. (1996). Adenovirus-mediated gene transfer into dissociated and explant cultures of rat hippocampal neurons. *J. Neurosci. Res.* **43**, 161–174.

INDEX

- 5-fluorodeoxyuridine (FDUR), in glial contamination, 120–121
- A**
- Acetic acid, dissolving rat collagen in, 22
- ActiveMotif Inc., 328
- AdEasy system, 390
- advantages of, 391
- Adenoviral expression of proteins
- advantages of, 407
 - disadvantage of, 392
- Adenoviral titers, with two-day immunoassay, 403–405
- Adenoviral vectors
- advantages of, 388
 - amplification of, 400
 - materials for making, 391–392
 - preparing, 391–397
 - producing in HEK293 cells, 397–400
 - safety issues regarding, 405–407
 - selecting, 386
 - titer assays for, 402–405
 - transfection of HEK293 cells with, 367
- Adenovirus mediation, 310–314
- in cortical and hippocampal neuronal cultures, 113
 - replication-deficient, 388
- Adenovirus stocks, purification and storage of, 400–401
- Adhesion, slow vs. fast in *Heliosoma* cultures, 169
- Adrenal medullary tumor, 268
- Agricultural guidelines and practices, 57
- Agriculture schools, ease of obtaining species through, 13, 57
- Air resistance, as factor in biolistics, 357–359
- Ajuba* cytoplasmic protein, 92
- Albumen, removing in preparation for retroviral infection, 379–380
- Alkaline phosphatase, in Purkinje neuronal cultures, 95
- Alzheimer's disease
- associated with Purkinje neurons, 91
 - cortical and hippocampal involvement in, 112
 - toxicologic effects of lead on, 290
- Amersham Australia, 95
- Amicon Ultrafree-MC centrifugal concentrator, 313
- Amyotrophic lateral sclerosis, GluT in spines of patients with, 92
- Animal-holding facilities, 10
- Animal-use issues, 14, 57
- Annulin, 182
- Antennapedia PTD, 327
- peptides conjugated by, 334
- Antibodies
- affinity purified, 213
 - and specific species, 9
 - blocking, in Tibia-1 pathway studies, 191
 - in *Drosophila* cultures, 208–212
 - screening in PC12 cell lines, 272
 - staining protocols, 217
- Anticytoskeletal drugs, applying to peripheral neurons, 18
- Antimitotic agents, reducing nonneuronal contamination with, 31
- Antiproliferative agents, 10–11
- Antisense RNA
- and specific species, 9
 - in B35 cells, 295
 - in *Xenopus* spinal neuron cultures, 131
- Aphasia, 291
- Aplysia*, 3
- organelle transport in, 8
- AraC, in long-term hippocampal cultures, 121–122
- Argon ion gas laser, 151
- Aristotle, 68
- Astrocytes
- contaminating cortical cultures, 120
 - effects on Purkinje neurons, 101
 - GFAP as marker of, 119
 - in Purkinje neuronal cultures, 93
- Ataxia telangiectasia (AT), associated with Purkinje neuron degeneration, 91
- Atmosphere, and choice of neuronal culture, 12
- Autosomal recessive disorders, ataxia telangiectasia (AT), 91
- Avian leukemia virus vectors, 370
- Avian Purkinje neuronal cultures, 89–105
- Avian retroviral vector RCAS, 369

- Axon guidance
 B35 cell lines in study of, 287, 291–292
 in chick embryos, 67
 in *Heliosoma* cultures, 158
in vivo study of, 154
 in *Xenopus* cultures, 130–131
 lipofection for studies of, 136
 Tibia-1 pathway studies in, 172–191
 toxicologic effect of lead on, 290
- Axon regeneration, Purkinje neuronal culture studies of, 91
- Axon size, 8–9
- Axonal and dendritic length, neural-enriched cultures for study of, 143
- Axonal development
 chick forebrain neuron studies of, 53–62
 examining with fluorescent tracing, 132–133
 in hippocampal and cortical neurons, 111
 in long-term cortical and hippocampal cultures, 124
 observing in *Heliosoma* neurons, 157
 slow in cortical neuronal cultures, 119–121
 speeded by glia-conditioned medium, 120
 studies in *Xenopus* spinal neurons, 130
 variable according to substrate, 146–147
- Axonal growth cones, properties of, *versus* dendritic growth cones, 2
- Axonal halo, and peripheral neuron explant cultures, 29
- Axonal morphogenesis, chick forebrain neurons, 52
- Axonal retraction experiments, peripheral neuron cultures and, 25
- Axonal transport, 18
 live-cell imaging in cultured neurons, 305–321
 observing, 314–321
- Axotomy, peripheral neurons and, 18
- B**
- B27 supplement, 12
- B35 neuroblastoma cell lines, 3, 8
 antisense RNA use in, 295
 as models for axon growth and cell migration, 291–292
 cell death studies using, 289–290
 compared with B50 cell lines, 287–288
 detecting migration and expression via immunocytochemistry, 301
 developmental properties of, 5
 differentiation studies, 289–290
 intracellular signaling mechanisms in, 292
 protocols for working with, 295–302
 research applications for, 289–290
 toxicology studies using, 289–290
- B50 cell lines, compared with B35 cell lines, 287–288
- Bacterial cells, making efficient recombinant adenovirus vectors in, 390
- Baffles, use in limiting blast damage in biolistics, 359
- Banker method, 112–121
- Barrel design, improvements in biolistics, 366
- Basal lamina
 adhesive role of, 177
 establishment, in Tibia-1 pathway, 181
 in grasshopper limb bud studies, 165
- Beckman airfuge, 132
- Beckman Instruments, 137–138
- Biochemical procedures, 11
- Biolistics, 353–367
 advantages over chemical transfection or viral infection methods, 354
 compared with nuclear injection, 310–314
 disadvantages of, 354
 future improvements to, 365–367
 parameters of, 355
 untested parameters of, 365
- Biolistics device, 358
- Biological activity, retained by PTP-delivered cargo, 329
- Biological ballistics. *see* Biolistics
- Biological properties, of neurons, 8–10
- Biological responsiveness, as criterion for choice of neuronal cultural culture, 2
- Biological safety cabinet, 398, 401
- Biosafety level 2+ safety procedures, for adenovirus work, 405–406
- Biospherix, 12
- BJ5183 *Escherichia coli*, 394
 preparing electrocompetent vector containing pAdEasy-1, 394
- Blast damage, in biolistics, 359
- Blastomere injections
 compared with lipofection, 136
 with *Xenopus* cultures, 131, 133–135
- Bloomington stock center
 (<http://flystocks.bio.indiana.edu/>), 202
- Bouton development, in *Drosophila* studies, 228
- BSA fraction V, 84
- Buccal ganglion, of freshwater snail *Heliosoma*, 3
- Buffer composition, as electroporation parameter, 349
- Bureaucracy, in neuronal culture systems, 14

- C
- Caged Ca^{2+} , 152–154
 - in PC12 cell line studies, 278–282
 - Caged-FITC dextrans, 132
 - Calcium dynamics
 - imaging and manipulating in *Drosophila* neurons, 224–226
 - in *Drosophila* studies, 206–207
 - neural-enriched cultures for study of, 143
 - Calcium indicator dextrans, 131
 - Calcium phosphate, transfection with, 310
 - Calcium signaling, examining with dextran tracing, 132
 - Calyx terminals, applications of chick ciliary neuron, 38–42
 - Carolina Biological (www.carolina.com), 70
 - Carotid artery, bifurcation of rat, 26
 - Cell adhesion molecules, endocytosis of, in B35 cells, 294–295
 - Cell behavior, and choice of neuronal culture, 2–5
 - Cell biological mechanisms
 - correlating with growth cone motility, 157
 - in *Drosophila* studies, 216
 - monoamine biogenesis, 267
 - neurotrophin action, 267
 - protein trafficking, 267
 - secretory vessel dynamics, 267
 - Cell body size, 8–9
 - Cell cracking methods, 272
 - Cell crawling and navigation, 2–3
 - Cell damage, affecting biolistics
 - performance, 365–367
 - Cell death
 - in B35 and B50 cell line studies, 289–291
 - regulated by CyP-A, 291
 - target-driven vs. programmed, 38
 - Cell debris, in cortical neuronal cultures, 119
 - Cell density
 - as biolistics parameter, 354
 - as electroporation parameter, 345–346
 - as parameter of biolistics, 355
 - Cell diameter, affecting survival of electroporation, 340
 - Cell differentiations, and choice of neuronal culture, 2–5
 - Cell dissociation solution, 77
 - in spinal and motor neuron cultures, 82
 - Cell extraction medium, in *Heliosoma* cultures, 160
 - Cell fate, in chick embryos, 68
 - Cell lines, 3
 - with stable expression of transgenes, 8
 - Cell motility
 - B35 cells as models for, 291–292
 - examining with fluorescent tracing, 132
 - study via ultraviolet photolysis, 152–154
 - Cell polarity
 - development of, 4
 - in hippocampal and cortical neurons, 112
 - Cell size
 - as criterion for choice of neuronal culture, 2
 - as parameter of biolistics, 355
 - Cell suspension temperature, as electroporation parameter, 347
 - Cell-cell attractions/repulsions, 3, 10
 - Cellular uptake
 - promoted by noncovalently associated peptides, 327–328
 - promoted by peptide sequences, 326–327
 - Central motor neurons
 - B35 neuroblastoma cells as models of, 287–288
 - recording in *Drosophila*, 230
 - Central nervous system neurons, 3, 90
 - limitations of, in transfection, 288
 - quantity of yield from, 11
 - transfection via electroporation, 288
 - Cerebellum, 90
 - Chariot PTP, 328
 - delivering proteins and peptides into neurons with, 335–336
 - Charles River Laboratories, 113
 - Chemical mutagens
 - advantages of, 201–202
 - point mutations induced by, 202
 - Chemical transfection, disadvantages compared with biolistics, 354
 - Chick ciliary neurons
 - advantages of, 38
 - applications of, 38
 - culturing methods, 46–47
 - developmental properties of, 5
 - disadvantages of, 41
 - dissection and culturing of, 37–49
 - endocytosis and recycling in, 5–8
 - materials for dissection of, 42
 - materials for dissociation and culturing of, 42–43
 - methods of dissecting and dissociating, 43–47
 - neuroanatomy and development of, 38
 - neuronal types of, 38
 - synapses formed in, 10
 - Chick dorsal root ganglia (DRG)
 - ease of dissection of, 18
 - endocytosis and recycling in, 5–8

- Chick dorsal root ganglia (DRG) (*continued*)
 - quantity of yield from, 11
 - relative infectivity of, 408
 - short-term cultures of, 32–33
- Chick embryo extract, 8
- Chick embryos
 - as sources of spinal motor neurons, 67–68
 - infecting by retroviral injection, 379–382
 - obtaining and maintaining, 57
 - preparation of, 71–73
- Chick forebrain neurons, 4
 - axonal development studies in, 53
 - axonal morphogenesis, 52
 - contrasting with rat hippocampal neurons, 54–56
 - culture conditions for, 57–63
 - culturing, 51–64
 - developmental properties of, 5
 - dissection of, 13, 57–58
 - dissociation of, 59
 - elongation behaviors in, 54
 - future improvements in culturing, 63–64
 - growth and development characteristics of, 53–56
 - in toxicological assays, 53
 - isolation of single, 56–59
 - plating efficiency and culture density of, 63
 - pyramidal shape of, 59
 - relative purity of, 11
 - small size of, 8–9
- Chick motor neurons, as basis of injury models, 69–70
- Chick peripheral neurons, expression of transgenes via retroviral infection, 369–385
- Chick primary neurons, electroporation protocol for, 344–345
- Chick Purkinje neuron cultures, 90
- Chick sensory ganglia, dissection of, 25
- Chick sensory neurons, 17
 - developmental properties of, 5
 - organelle transport in, 8
- Chick serum, 377
- Chick spinal motor neurons, 4
 - developmental properties of, 5
 - quantity of yield from, 11
 - relative purity of, 11
- Chick sympathetic neurons, 4
 - axonal-somatic synapses in, 10
 - developmental properties of, 5
 - endocytosis and recycling in, 5–8
 - organelle transport in, 8
- Cholinergic motor neurons, 140
- Choroid neurons, of chick ciliary ganglia, 38
- Chromosomal aberrations, inducing, 202
- Ciliary neurons, 3
- Cloning applications, 11
 - Drosophila* mutant analyses, 222–223
- Cloning sites, retroviral vectors, 371–378
- Clumping, of neuronal cell bodies, 24
- CO₂-dependent or-independent media, culturing
 - chick forebrain neurons with, 52
- Coculture systems
 - in Purkinje neuronal cultures, 93
 - Xenopus* spinal neurons, 145
- Cognitive impairment, 291
- Collagen, 21
 - as culture substrate, 11–12
 - as substrate for explant cultures, 29–30
 - rat tail, as substrate, 17
- Collagenase treatment, in neural-enriched *Xenopus* cultures, 144
- Confocal laser-scanning microscope, 96, 152
 - in *Xenopus* live-cell imaging studies, 151–152
- Constitutively active (CA) mutant proteins, in *Xenopus* cultures, 131
- Corneal damage, from adenovirus, 415–416
- Cortical neurons, 3
 - acquisition of, 113–117
 - culture characteristics, 119–121
 - culturing, 119–121
 - long-term culture of, 121–126
 - short-term culture methods, 117–121
- Cost, of obtaining/maintaining neurons, 2
- Coverage Plus disinfectant, 405
- Coverslips
 - cleaning of, 118
 - growing hippocampal neurons on, 112
 - plating of hippocampal and cortical neurons on, 117–119
- Creutzfeldt-Jakob disease, association with Purkinje neurons, 191
- Cross-reactivity, as limitation of *Heliosoma* antigens, 169
- CsCl gradient purification of adenovirus, 401–402
- Culture density, chick forebrain neurons, 63
- Culture dishes
 - for spinal and motor neuron cultures, 82–85
 - for superior cervical ganglia, 309–310
 - plating of hippocampal and cortical neurons on, 117–119
- Culture media
 - chick forebrain neurons, 49–60
 - for superior cervical ganglia, 306–308
 - simplified for *Heliosoma* cultures, 158

- Culture methods
 - chick ciliary neurons, 46–47
 - chick forebrain neurons, 60–64
 - cocultures, 145
 - dissociated mixed cultures of *Xenopus* spinal neurons, 141–143
 - neural-enriched cultures, 143–145
 - substrata, for *Xenopus* cultures, 145–148
- Culture properties, 11–12
- Culture substrates, 11–12
 - in *Xenopus* neuronal cultures, 139–148
- Cultured neurons, experimental properties of, 6–7
- CyP-A, regulating death and survival in neuronal cells, 291
- Cytosine arabinoside, reducing nonneuronal contamination with, 30
- Cytosine beta-arabino-furanoside (AraC), 10, 92, 121
- Cytoskeletal organization, 18
- Cytoskeletal polymers, transport of, 305
- Cytoskeletal proteins, fluorescently tagged, 39
- Cytoskeletal transport and dynamics, 5, 9
- Cytoskeleton, Inc., 132
- Cytosolic proteins
 - immunocytochemical detection in PC12 cell lines, 284
 - transport of, 314
- D**
- Defined medium, for spinal and motor neuron cultures, 84
- Deletions, chromosomal, 202
- Dendrites
 - in long-term cortical and hippocampal cultures, 124
 - organelle traffic in, 8
 - production of, 10
- Dendritic growth cones, properties of, *versus* axonal growth cones, 2
- Dendritic spines, in long-term cortical and hippocampal cultures, 120
- Density, of neuron yield in culture, 11
- Density gradient centrifugation, 79–80
- Developmental properties, 10–11
 - of cultured neurons, 5
- Developmental stages, advantageous in study of Tibia-1 pathway, 173
- Dextrans and proteins, preparing injection samples of, 132–133
- Dichroic mirror, 153
- Differentiation of neurons, epigenetic factors in, 102–104
- Difficulty of preparation, 6–7
- Digitization, of electrophysiological data, 234
- Dimensions, of neurons, 8–9
- Directional cues, 172
- Dissecting microscope, 42
- Dissection
 - ease of, 13
 - in Tibia-1 pathway studies, 172
 - enzymatic, of intact spinal cords or ventral halves, 77–79
 - intact chick spinal cords, 73–77
 - isolation of chick ciliary ganglion, 43–44
 - mechanical, 77–79
 - of chick ciliary ganglion neurons, 37–49
 - of chick forebrain neurons, 57–58
 - of *Drosophila* embryos and larvae for immunolabeling, 218–220
 - of grasshopper embryos, 186–187
 - of hippocampal and cortical neurons, 113–117
 - of peripheral neurons, 25–27
 - of retrovirally infected chick embryos, 382–385
- Dissociated cultures
 - biolistic transfection of, 354
 - chick ciliary ganglia, 46
 - chick forebrain tissue, 57–59
 - Drosophila* retina, 236
 - Heliosoma* ganglia, 166
 - hippocampal and cortical neurons, 117
 - in Purkinje neuron studies, 90
 - of *Xenopus* spinal neurons, 140–143
 - preparation of, 27–28
 - transfection of, 333
- DNA
 - as *Xenopus* culture injections, 132
 - preparing injection samples of, 132–134
- DNA coating density
 - and future biolistics improvements, 365
 - as parameter of biolistics, 355–356
- DNA constructs, species and, 9
- DNA damage, affecting biolistics performance, 365
- DNA plasmids, transfection of chick ciliary neurons with, 39
- DNase I, 83, 92
- Dominant-negative (DN) mutant proteins, in *Xenopus* cultures, 131
- Dorsal root ganglia, advantages of, 18
- Dose-response studies, 326
- DOTAP liposomal transfection reagent, 137
- Dow Corning, 119

- Down syndrome cell adhesion molecule, 214
- Drilled dishes, in spinal and motor neuron cultures, 83
- Drosophila melanogaster*, 3, 196
- antibodies found in, 208–212
 - as genetic model system for molecular neurobiology, 199–203
 - background references for, 196–199
 - cell biology techniques in, 216–222
 - central motor neuron recording, 232–234
 - clonal techniques for mutant analysis, 222–223
 - coimmunoprecipitation to identify interacting proteins, 213–214
 - compared with *Xenopus* cultures, 130
 - dissection of embryos and larvae for immunolabeling, 206–213
 - electrophysiology in, 228–238
 - embryo, small size of, 8
 - excitatory junctional current (EJC) recordings, 231
 - functional analysis techniques, 224–228
 - giant fiber system of, 234–235
 - head extracts, 203
 - identifying the phenotype of, 203
 - imaging and manipulating calcium levels, 224–226
 - immunolabeling nervous system cells, 217–218
 - isolation and extraction of heads, 205–206
 - life cycle, 216
 - lipid analysis in, 214–215
 - monitoring membrane dynamics with strylyl dyes, 226–227
 - monitoring protein dynamics in, 227–228
 - nervous system biochemistry, 203–215
 - neuromuscular junction recording in, 230–232
 - online database, 198
 - optic lobe of fly brain, 203
 - phospholipid metabolism in the eye of, 203
 - recording
 - from adult brain, 237
 - from cultured neurons, 228–229
 - from sensory systems, 236–238
 - shibire mutation in, 204
 - species advantages in gene expression, 10
 - synaptic transmission studies, 203
 - temperature dependency in, 216
 - transgenic protein expression studies in, 220–222
 - vesicle recycling in, 204
- Drugs, using proteins as, 325–328
- Dulbecco's modified Eagle's medium (DMEM), 43, 77, 83, 92, 376
- E**
- Ease of culture, peripheral neurons, 18
- Ectopic genes
 - in axonal pathfinding, 136
 - overexpression in grasshopper limb bud, 190–191
- Ectopic vectors, in *Drosophila*, 220–222
- Egg incubator, 10, 13, 42, 57
- postinjection, 382
- Eggs, staging for retroviral infection, 380
- Electrocompetence, of adenoviral vectors, 394
- Electrophysiology
 - cerebellum as study mutants for, 91
 - in *Drosophila*, 227–238
- Electroporation parameters
 - buffer composition, 349
 - cell density, 345–346
 - Free Ca²⁺ in electroporation buffer, 347–348
 - rest for recovery, 348
 - temperature of cell suspension, 348
 - voltage and duration of pulse, 346
- Electroporation technique
 - compared with nuclear injection, 311
 - compared with retroviral infection, 385
 - for chick primary neurons, 344–345
 - in PC12 cell lines, 282
 - transfection of primary and peripheral nervous system neurons with, 339–350
- Electroretinogram, 236–237
- Elongation behaviors, chick forebrain and rat hippocampal neurons, 52
- Embryonic chick brain (cerebellum), 3
- Embryonic chick ciliary ganglion, 3
- Embryonic chick dorsal root ganglia, 3
- Embryonic chick paravertebral chain ganglia, 3
- Embryonic development, avian ganglion as subject for study of, 38–42
- Embryonic rat brain neurons, 3
- Embryos
 - dejellying for blastomere injections, 133
 - staging for Tibia-1 pathway studies, 182–183
- Endocytosis, 5–8
 - B35 cell line analysis and, 288
 - circumventing degradation pathway of, 328
 - in *Drosophila* studies, 196
 - of cell adhesion molecules in B35 cells, 294–295
 - synaptic vesicle pathway in *Drosophila*, 204
- Enzymatic treatments, in *Heliosoma* cultures, 158

- Epilepsy, cortical and hippocampal involvement
in, 354
- Eppendorf Injectman N12 semiautomated
injection system, 311
- Eppendorf transjector 5246, 138
- Ernst, Karl, 68
- Excitotoxicity, in hippocampal and cortical
neurons, 111, 112
- Exocytosis, 5–8
in *Drosophila* studies, 196
inhibition in PC12 cell lines, 26
PC12 studies of, 269
- Exogenous molecules
assisted delivery into live neurons, 326
use with *Xenopus* spinal neurons, 130
- Experimental manipulations
choice of species based on, 17
motor neuron and spinal cord cultures, 80–82
- Experimental needs, choosing neuronal cultures
according to, 2–8
- Experimental properties, of cultured neurons, 6–7
- Experimental techniques, accessibility of specific
neurons to, 2
- Explant cultures
in *Xenopus* spinal neurons, 130
preparing, of peripheral neurons, 29–30
Xenopus cocultured, 145–147
- Expression, levels and timing of, in
biolistics, 364–365
- Extracellular matrix molecules, as culture
substrate, 11–12
- Extracellular matrix proteins, in *Xenopus*
cultures, 139–141
- Extrinsic cues
experimental studies of, 80
in avian Purkinje neuronal cultures, 89–105
- F**
- Facilities, animal, 13
- Fast axonal transport, 8
- Fast Green dye, 381
- Fel cell, in Tibia-1 pathway studies, 174–176
- Fertilized chicken eggs
incubation of, 67–69
storage length vs. fertility, 68
- Fetal bovine serum, 77, 374
for peripheral neuron cultures, 23
for spinal and motor neuron cultures, 83
- Fetal calf serum, 92
- Fibroblasts, contaminating neuronal
cultures, 30
- Fibronectin
as culture substrate, 12
in *Xenopus* cultures, 139, 145
- Filopodial extensions
ability to sense guidance cues, 176–177
chick forebrain neurons, 52
extension and retraction, in Tibia-1
pathway, 172
in embryonic grasshopper limb bud, 173–176
in *Xenopus* cultures, 146–147
- Fine Science tools (www.finescience.com), 71
- FITC-dextran, 132
monitoring untagged ciliary ganglion cultures
with, 38
- Fluid level, in biolistics, 354–367
- Fluorescence microscopy, in chick ciliary neuron
cultures, 39
- Fluorescence resonance energy transfer (FRET)
reported proteins, 132
- Fluorescent dextrans, 131
as single-cell injections, 138–139
nucleus injected with, 313
- Fluorescent fusion proteins, 131
expression of, 383
in *Xenopus* cultures, 130, 148
injecting neurons with, 314
- Fluorescent tagging
in *Xenopus* spinal neurons, 130
of cell motility, axon outgrowth, and calcium
signaling, 132
of cytoskeletal proteins, 39
- Fluoro-2'-deoxyuridine (FdUr), 84
- Fluorsave Reagent, 96
- Fly heads
isolation and extraction of, 205–206
lipid analysis of, 214–215
subcellular fractionation of, 206–207
- Fly nervous system. *See Drosophila*
- Flybase, 221
- Focus drift, in time-lapse fluorescence
imaging, 319
- Forebrain, 3
- Forward genetic systems, 216–228
and *Drosophila* electrophysiology, 228–238
- Free Ca²⁺ in electroporation buffer, as
electroporation parameter, 347
- Freezing cells, 13
- Frog neuromuscular junction neurons,
endocytosis and recycling in, 5–8
- Frog sensory neurons, endocytosis and
recycling in, 5–8
- Function-blocking antibodies, 130, 148

- Functional analysis techniques, in *Drosophila* nervous system, 224–228
- Functional proteins (peptides), 131
- Functional redundancy studies, 200–201
- Functional viruses
- growing, 369–375
 - producing, 375–378
- Fusion proteins, screening in PC12 cell lines, 283
- G**
- G-innexin-1, 182
- GABA-gated channels, 213
- and B35 cell lines, 288
- GABAergic and glycinergic inhibitory interneurons, 213
- Gallus gallus* (common domestic chick), 68
- Gaps, in axonal neurofilament array, 315
- Gene gain-of-function experiments, 370
- Gene of interest
- generating mutations in, 201–202
 - inserting into a shuttle vector, 393
- Gene targeting methods, 216
- Gene translocations, 202
- Genome sequencing, *Drosophila*, 198–202
- Genomic vectors, in *Drosophila*, 220–222
- GFP expression, 134
- in B35 neuroblastoma cell lines, 291
- GFP-alpha5 integrin receptors, 152
- Giant fiber system (*Drosophila*), 234
- Gilbert-Developmental Biology (www.devbio.com), 85
- Glass, as culture substrate, 12
- Glass coverslips
- for peripheral neurons, 19
 - for spinal and motor neuron cultures, 80
 - preparation of,
- Glass-bottom dishes
- for *Heliosoma* cultures, 169
 - for time-lapse imaging, 187
- Glia contamination, 30
- in cortical neuronal cultures, 121
 - in hippocampal neuron studies, 112
- Glia stocks, for long-term hippocampal and cortical neuronal cultures, 121
- Glia-conditioned medium
- and speed of axonal development in cortical cultures, 120
 - in long-term hippocampal cultures, 117–121
- Glial coculture, chick forebrain neurons, 63
- Glial fibrillary acidic protein (GFAP) immunoreactivity, 119
- Glutamate
- as extrinsic factor in Purkinje neuronal cultures, 90
 - gated channels in *Drosophila* studies, 213
 - neuronal sensitivity to, 91
 - uptake studies of, 91, 97–100
- Glutamate transporters, 91
- in developing Purkinje neurons, 102–105
- Glutamatergic excitatory interneurons, 140
- Glutamine, in chick ciliary neuron cultures, 43
- Glycosaminoglycans, 12
- Gold coating procedure, in biolistics, 356
- Gold particles, use in biolistics, 355
- Government agricultural agents, as sources for chick neuronal cultures, 57
- Granule cells
- effects on Purkinje neurons, 101
 - in Purkinje neuronal cultures, 91–92
- Grasshopper (*Schistocerca*) limb bud, 3
- advantages for axonal guidance studies, 172–173
 - culturing, 183
 - developmental properties of, 5
 - ectopic expression in embryo, 185–186
 - filleting to access the Tibia-1 pathway, 188–189
 - study of extracellular guidance cues in, 172
 - Tibia-1 pathway study of, 173–187
- Green helium neon laser, 151
- Growth conditions, 6–7
- Growth cone
- formation, *Heliosoma* advantageous for study of, 158
 - motile vs. nonmotile, 159
 - motility
 - correlating with cell biological mechanisms, 157
 - in *Xenopus* cultures, 130
 - ultraviolet photolysis study of, 152–154 - protrusive activity of, 3
 - rate of advance, as criterion for choice of neuronal culture, 2
 - responses, experimental studies of, 80
 - size, 8–9
 - as criterion for choice of neuronal culture, 2
- Growth medium, in dissociating chick ciliary ganglia, 46–48
- Growth rate, neural-enriched cultures for study of, 143
- Guidance cues, repulsive, 177
- guidance cues, 2
- exemplified in Tibia-1 pathway, 172

- Guidance molecules
 annulin, 182
 G-innexin-1, 182–183
 laminin, 181–182
 REGA-1, 182–183
 semaphorins, 171–181
- H**
- Hamburger, Viktor, 68
 Handling properties, 11–12
 Hank's balanced salt solution, 71
 in spinal and motor neuron cultures, 82
 Harvey, William, 68
 HeK293 cells
 maintaining, 397–398
 producing adenovirus in, 397–400
 transfection with adenovirus DNA, 398–399
Heliosoma buccal ganglion neurons, 165
 large size of, 8
Heliosoma saline, 160
Heliosoma trivolvis, 3
 advantages of culturing, 159
 conditioned medium cultures, 168–169
 culturing neurons of, 157–169
 developmental properties of, 5
 dissociation of whole ganglia, 166
 extracting single neurons from ganglia
 of, 164–167
 freshwater aquaria required for, 13
 initial dissection of, 160–163
 maintaining animals, 159
 nerve cell culture protocols, 163–169
 polylysine-attached cultures, 168
 speed of culture adhesion, 169
 time-consuming nature of initial dissection, 163
 HEPES, as media buffer, 22
 High-spatial resolution
 in *Heliosoma* studies, 157
 in live-cell imaging, 151
 High-temporal resolution, in live-cell imaging, 151
 Hippocampal neurons, 3
 acquisition of, 113–117
 advantages of, 18
 culture characteristics, 119–121
 culturing, 111–126
 long-term culture methods, 121–126
 organelle traffic in dendrites of, 8
 oxidative stress on, 12
 short-term culture methods, 117–121
 Homogeneity
 desirable in PC12 cell lines, 282
 of chick ciliary ganglion neurons, 38
 Homologous recombination
 in BJ5183 *E. coli*, 394–397
 in human kidney, 389
 Horse serum, 77, 83, 122
 Horseradish peroxidase, in Purkinje neuronal
 cultures, 96
 Hsp72, 91
 Human growth hormone, secretion assays
 using, 278–283
 Hydrocephalus, 291
- I**
- Imaging, advantageous in large neurons of
 grasshopper limb bud, 173
 Imaging chambers, in *Xenopus* live cell
 cultures, 148–150
 Immunoassay, 403
 Immunoblotting, 11
 Immunocytochemistry
 detecting migration and expression in B35
 cells, 301–302
 detection of cytosolic proteins in PC12 cell
 lines, 283
 in intact and permeable PC12 cell lines, 283–285
 in Tibia-1 pathway studies, 187
 limitations in *Heliosoma* cultures, 169
 with protein expression studies in *Drosophila*,
 216
 Immunohistochemistry, Purkinje neuronal
 cultures, 97–98
In vitro neuron morphology, 97
In vivo neuron morphology, 97
In vivo protein dynamics, *Drosophila*, 227–228
In vivo therapies, potential applications for, 337
 Incubation
 of fertilized chicken eggs, 69–71
 postinjection with retroviral vectors, 382
 Infection methods, vs. transfection methods, 370
 Inhibition, of high-affinity glutamate
 transport, 102–105
 Injection sample, preparation of, in *Xenopus*
 cultures, 131–133
 Injection volume, calibrating, 135
 Injury models, chick motor neurons as basis
 for, 69
 Insert sizes, retroviral vectors, 371–378
 Internal granule cell layer, Purkinje neuronal
 cultures, 90
 Intracellular events, as criteria for neuronal
 culture choice, 5–8

- Intracellular protein localization, neural-enriched cultures for study of, 143
- Intracellular signalling, in B35 cells, 291–292
- Intrasegmental epithelium, in Tibia-1 pathway studies, 174
- Inverted microscope, required for transfection, 311
- Ion channel function, in *Drosophila* studies, 196
- Ionizing radiation, mutagenesis via, 198
- Isolated neurons, culturing with *Xenopus*, 140
- L**
- L-15-based media, 27, 34
- for chick forebrain cultures, 52, 61
 - for peripheral neurons, 22–23
 - in *Heliosoma* cultures, 161
 - in studies of spinal and motor neuron cultures, 82
- L-glutamate transport (GluT), 92, 102–103
- Lamellipodial extensions
- chick forebrain neurons, 52
 - extension and retraction of, in Tibia-1 pathway, 173
 - in embryonic grasshopper limb bud, 175–176
 - in *Xenopus* cultures, 146–147
- Laminar flow hood, in chick embryo preparation, 71
- Laminin, 21, 92–93, 181–182
- as chick ciliary neuron substrate, 37
 - as culture substrate, 12
 - for peripheral neurons, 19
 - in *Xenopus* cultures, 140, 145
 - inducing rapid outgrowth of axons with, 33–34
- Large invertebrate neurons, 3
- Lead, toxicological effects on nervous system, 290
- Levels of expression, in biolistics, 364
- Lifetime in culture, as criterion for choice of neuronal culture, 2
- Ligation-based cloning methods, 413–414
- Light microscope studies, 3
- Lillie, Frank Rattray, 68
- Lipid biochemistry
- analysis in *Drosophila*, 214–215
 - in *Drosophila*, 204
- Lipofection, with *Xenopus* cultures, 136–138
- Liquid chromatography, 199
- Liquid N₂, 13
- Listerine, use in *Heliosoma* cultures, 162
- Live cell imaging
- fluorescent, 316–320
 - in superior cervical ganglia neurons, 306–321
 - in *Xenopus* cultures, 148–154
- Long-term cultures
- advantageous in study of Tibia-1 pathway, 172–173
 - characteristics of hippocampal and neuronal, 124–126
 - media for, 23
 - reducing nonneuronal contamination in, 30
- Low-density cultures, chick forebrain neurons, 53–54
- Lumbosacral dorsal root ganglia (DRGs), dissecting, 25
- M**
- Maintenance, of peripheral neuron cultures, 28
- Malpighi, Marcello, 68
- Matrigel matrix (BD Biosciences), 34, 46, 47, 92
- as culture substrate, 11–12
 - in chick ciliary neuron cultures, 42
- Media
- for chick forebrain neurons, 59–62
 - for long-term cultures, 23
 - for peripheral neurons, 22–25
 - for spinal and motor neuron cultures, 80–85
- Media supplements, for spinal and motor neuron cultures, 80–85
- Membrane dynamics
- B35 cell lines, 288
 - monitoring with stryl dyes, 226–227
- Membrane fraction, in protein function studies, 206–213
- Membrane potential, neural-enriched cultures for study of, 143–144
- Membrane recovery, speed of, 348
- Memory
- regulated in *Drosophila*, 237–238
 - storage in hippocampus and cortex, 112
- Metabolic labeling, 11–12
- Metamorph software, 319
- Methocel, 308
- Methods
- culturing of chick ciliary neurons, 46–47
 - dissection of chick ciliary ganglion, 43–44
 - dissociation of chick ciliary ganglion, 46
 - introducing reagents to neuronal cultures, 331–336
- Methylcellulose, for peripheral neuron cultures, 24–25
- Metrizamide, 85
- Microexudates, 12

- Microinjection
 - affecting choice of neuronal culture, 2
 - of adherent cells, 312
 - of Tibia-1 pathway neurons, 185–186, 190
 - preparation of glass-bottom culture dishes for, 187–188
 - studies of, in chick ciliary cultures, 41
 - suitability of peripheral neurons to, 139
 - survival of, 18
- Millicell inserts, 92
- Millipore Corporation, 312
- Mixed cultures, in *Xenopus* spinal neurons, 139
- Molecular handshakes, between PTPs and their cargo, 329–330
- Molecular Probes, 132
- Molluscan phylum, large neuron size in, 158
- Monoamine biogenesis, 267
- Morphological analysis
 - neural-enriched cultures for, 143
 - Purkinje neuronal cultures, 96–100
- Morphological similarity, chick
 - forebrain and rat hippocampal neurons, 54–56
- Morphological types
 - identifying, 98
 - Purkinje neurons, 96–97
 - quantitating, 99
 - Xenopus* varieties, 143
- Morphology, control of, in avian Purkinje cultures, 90–104
- Mosaic analysis with repressible cell marker (MARCM), 222–223
- Motility
 - assays, in B35 cell lines, 299–300
 - comparison among neuronal cultures, 9
 - monitoring via Transwel migration assays in B35 cells, 299–300
- Motion analysis, 320–321
- Motor neurons
 - enrichment by density gradient centrifugation, 79–80
 - experimental uses of, 80–82
 - induction via notochord, in chick embryos, 68
- Mouse cortical neurons, 5
 - culturing, 111–126
- Mouse hippocampal neurons, culturing, 111–126
- Mouse mutants, cerebellum as study
 - model for, 91
- Movement
 - mechanism of axonal, 305
 - observing axonal, 314–321
- mRNA and protein trafficking and targeting, 112
- Mutagenesis, in flies, 202
- Mutant screens, 196
 - Drosophila*, 199
- Mutations
 - chemically induced, 199, 202
 - clonal techniques for analyzing, 222–223
 - generating in genes of interest, 201–202
 - phenotypes of early lethal, 216
- N
- N-cadherin, in *Xenopus* cultures, 146
- N2-based media, 34
 - for peripheral neuron cultures, 23
- N3 supplement, 84
- N9 neuronal growth supplement, 61
- Names
 - of cell lines, 3
 - of neurons, 3
- Nanosep microconcentrators, 138
- Narishege IM-200 microinjector, 138
- NCI-Frederick Cancer Research and Development Center, 372
- Neonatal rat
 - central nervous system, 287
 - superior cervical sympathetic ganglia, dissection of, 25–27
- Nerve growth factor
 - for peripheral neuron cultures, 22
 - in PC12 cell line development, 268
- Nervous system injury, *in vivo* delivery of reagents in therapy, 326
- Neural cell adhesion molecule (CAM)
 - function, 291–292
- Neural induction, in chick embryos, 68
- Neural tube, injection of retrovirus into, 381–382
- Neural-enriched cultures, *Xenopus* spinal neurons, 143–145
- Neurite branching
 - studies of, 9
 - using motor and spinal cord neuron cultures, 80–82
 - toxicologic effect of lead on, 290
- Neurite diameter, as criterion for choice of neuronal culture, 2
- Neurite initiation and extension, in hippocampal and cortical neurons, 112
- Neurite length, as criterion for choice of neuronal culture, 2
- Neurites, length and number of, 9–10
- Neuroanatomy, of chick ciliary ganglion, 38

- Neurobasal medium, in chick ciliary neuron cultures, 43
- Neuroblastoma, 3
- Neurodegenerative diseases, cortical and hippocampal involvement in, 112
- Neurofilament 200 monoclonal antibodies, 95
- Neuromuscular junction studies, 41
in *Drosophila*, 230–232
- Neuron choice, factors influencing, 2
- Neuron properties, affecting
choice of culture, 2
- Neuron size
advantages of *Heliosoma* species, 157
in Tibia-1 pathway, 172
problematic in *Drosophila*
recording, 228–230
- Neuron-specific enolase (NSE), 95
- Neuronal cell death, 287–288
- Neuronal characterization, Purkinje neuronal cultures, 95–96
- Neuronal culture systems
choosing, 8–14
properties of, 2
relative infectivity of, 408–411
- Neuronal fate, in *Drosophila* studies, 196
- Neuronal guidepost cells, in Tibia-1 pathway studies, 174–176
- Neuronal labeling
immunolabeling in *Drosophila*, 217–218
in *Xenopus* cultures, 131–139
of Tibia-1 pathway neurons, 185–186, 190
- Neuronal migration, cerebellum as study model for, 91
- Neuronal morphology, neural-enriched cultures for study of, 143
- Neuronal outgrowth, Tibia-1 pathway studies in, 171–191
- Neuronal properties, study through hippocampal and cortical neurons, 111
- Neurons
ease and cost of obtaining and growing, 13–15
purity of, 11–12
- Neurotransmission, in *Drosophila* studies, 196
- Neurotransmitter metabolism, 91
- Neurotrophin action, 267
- Nichols Institute Diagnostics, 281
- Nikon TE300 inverted microscope, 318
- Nitrocellulose, use in *Xenopus* cultures, 147
- Nonneuronal contamination,
reducing, 412–413
in peripheral neuron cultures, 29–33
- Notochord, in chick embryos, 68
- Nuclear damage, affecting biolistics
performance, 364–366
- Nuclear injection, transfection of neurons by, 310–313
- Nucleic acids, injection into *Xenopus* spinal neurons, 130, 137–138
- Nucleus size, chick ciliary neurons, 39
- Number of neurons, disadvantage of chick ciliary ganglia, 41
- NuSerum, 377
- O**
- Olfactory learning, in *Drosophila*, 237
- Olympus Fluoview 500 laser-scanning confocal microscope, 150–151
- Optical properties, 6–7
- Oregon green BAPTA dextran, 132
- Organelle traffic, in dendrites, 8
- Organelle transport, 8
- Outgrowth rates, comparison of, 9
- Oxidative stress, on hippocampal neurons, 13
- Oxygen level, specific to neuronal species, 13
- Oxygen monitors, 13
- Oxyrase, 317
- P**
- P-element-generated mutants, 200
- pAdTrack shuttle vector, 391–392
- Pal Filtron, 138
- Pancreatic cancer, inhibition via *in vivo* therapies, 337
- Particle attachment strength, as parameter of biolistics, 355
- Particle damage, affecting biolistics
performance, 355
- Particle density, affecting biolistics
performance, 355, 364
- Particle design improvements, in biolistics, 365
- Particle immobilization, in biolistics, 356
- Particle propulsion, in biolistics, 357
- Particle size and composition, as parameter of biolistics, 355
- Particle speed and spread, as parameter of biolistics, 355, 357
- Pathfinding, 172
in *Drosophila* studies, 196
- Pattern formation, cerebellum as study model for, 91

- PC12 cell lines, 3, 8
 cell biological studies based on, 267
 cell labeling and harvesting, 271
 cell permeabilization, 272
 developmental properties of, 5
 high-efficiency transfection of, 268
 immunocytochemical detection of cytosolic proteins in, 284–285
 immunostaining of, 283
 isolation of stable transfectants in, 281
 propagation and culture of, 270
 secretion assays
 using continuous electrochemical detection of released monoamines, 276–278
 using human growth hormone, 278–279
 using radioactive catecholamines, 271
- pCS2 expression vector, 132
- Penetration depth, required for ballistics, 361
- Peptide sequences, promoting cellular uptake, 326
- Peptides
 assisted delivery into live neurons, 325–337
 blocking, in Tibia-1 pathway cultures, 191
 injection into *Xenopus* cultures, 131
 noncovalently associated, promoting cellular uptake, 327
- Peripheral ganglia, dissection of, 13
- Peripheral neurons
 and microinjection, 17
 and quantity of yield, 11
 buccal ganglion, 3
 chick sensory, 17
 culture maintenance, 28–29
 culture types, 31–34
 growing and working with, 17–34
 methods for working with, 19–30
 rat sympathetic, 17
 sensory, 3
 stereotyped in Tibia-1 pathway, 172
 sympathetic, 3
 transfection via electroporation, 339–350
- Petri dishes, untreated, for peripheral neurons, 19
- Pharmacological agents. *See* Drugs
 delivery to neuronal cultures, 333
 use in *Xenopus* live cell cultures, 148
- Pheochromocytoma, 3
- Pheochromocytoma-derived cell lines. *See* PC12 cell lines
- Photobleaching, 305–321
- Phototransduction studies, in *Drosophila*, 238
- Pipette tips, preparing for blastomere injections, 136–139
- Plaque assay, 403
- Plasmid DNA, 133
 coated particles in biolistics, 354–355
- Plasmid RNA, 133
- Plating efficiency
 chick forebrain neuronal cultures, 62
 hippocampal and cortical neurons, 117–119
 in neural-enriched cultures, 145
 long-term glia feeder cultures, 123
- Point mutations, 202
- Polarity, establishment of, 4
- Poly-D-lysine, 48, 92
 in hippocampal and cortical neuron cultures, 118
 promoting neuron adhesion with, 19
- Poly-D-ornithine, 47
- Poly-DL-ornithine, 47
- Poly-L-lysine, 92
 preparing coverslips for Tibia-1 pathway studies, 188
- Polycation-coated substrates, 11–12
- Polylinkers, in *Xenopus* spinal cultures, 132
- Polylysine
 as coverslip coating for *Heliosoma* cultures, 163
 as culture surface for chick forebrain neurons, 52, 59
 in *Xenopus* cultures, 145
- Polymerase chain reaction (PCR), 11, 199
- Poultry connection
 (www.poultryconnection.com), 70
- Preaxogenesis neurons, as guidepost cells, 176
- Preparation requirements, 6–7
- Preparation time, reduced in biolistic transfection, 354
- Presynaptic terminal research, 39
- Primary neurons, infection with replication-deficient adenovirus, 406–413
- Pro-ox model 110 (Biospherix), 12
- Production
 of dendrites, 10
 of synapses, 10
- Programmed cell death, 69
- Protease activity, neural-enriched cultures for study of, 143
- Protein dynamics
 immunocytochemical detection in PC12 cell lines, 283–285
 monitoring in *Drosophila*, 226–228
- Protein expression, in *Drosophila*, 203, 216–220
- Protein function
 blocking, in Tibia-1 pathway studies, 191
 studying with B35 cell transfection and motility assays, 295–297

- Protein loading
 affecting choice of neuronal culture, 2
 and specific species, 9
 as single-cell injections, 134–135
 in *Xenopus* spinal cultures, 130, 131
- Protein trafficking, 267
- Protein transduction domains, 327
 exhibiting minimal toxicity, 328
- Protein transduction peptides, exhibiting minimal toxicity, 320
- Proteins
 assisted delivery into live neurons, 325–337
 containing PTDs, purchasing and producing, 330
- Proteoglycans, 12
- Protrusive activity, of growth cone, 3–4
- pShuttle shuttle vector, 391, 392
- Pulse duration, as electroporation parameter, 345
- Purity of neurons, 10–11
 importance for biochemical studies, 130
- Purkinje neuron monolayer, 90
- Purkinje neuronal cultures, 3, 89–105
 astrocytes in, 93
 astrocyte effects on, 101–102
 cerebellar cell culture of, 92
 coculture variations, 94
 glutamate transport in, 105
 granule cells in, 93–94
 identifying, 96
 immunohistochemistry of, 94
 materials for culturing, 92
 procedures for culturing, 92–93
- Pyramidal neurons, 112
 in chick forebrain cultures, 53–54
 in hippocampal cultures, 119
- Q**
- Quantity, of neurons by species, 11
- R**
- Radioactive catecholamines, in PC12 cell studies, 271
- Rapid fixation and staining, in live-cell imaging studies, 151
- Rat brain cytosol, 272
- Rat cerebellum, Purkinje neuron cultures from, 90
- Rat cortical neurons
 developmental properties of, 5
 relative infective efficiency of, 48
- Rat dorsal root ganglia, quantity of yield from, 11
- Rat hippocampal neurons, 4
 contrasting with chick forebrain neurons, 54–57
 culturing, 111–126
 developmental properties of, 5
 growth and development characteristics of, 53
 infective efficiency of, 48
 quantity of yield from, 11
 small size of, 8
- Rat sympathetic neurons, 17
 developmental properties of, 5
 long-term cultures of, 33–34
 organelle transport in, 8
 quantity of yield from, 11
 short-term cultures of, 32–34
- Rate of development, 10
- RCAS virus preparation, 376
- Reagents
 effectiveness and cross-reactivity of, by species, 9–10
 screening, in PC12 cell lines, 273
- Receptor-mediated signalling, 12
- Recombinant adenovirus, methods for making, 389–391
- Recombinant Rho-family GTPases, 335
- Recovering cells, 13
- Recycling of neurons, 5–8
- Red helium neon laser, 151
- REGA-1, 182–183
- Released monoamines, secretion assays of, in PC12 cell lines, 276–277
- Replication-competent viruses, testing viral stocks for, 406
- Replication-deficient adenovirus, 387
- Reproducibility, as advantage of transfection by electroporation, 341
- Repulsive guidance cues, 177
- Research applications
 for B35 and B50 cell lines, 289–294
 for Purkinje neurons, 100–105
 making proteins into drugs, 336–337
- Rest for recovery, as electroporation parameter, 348
- Retroviral vectors
 building, 371–378
 compared with electroporation, 385
 concentrating, titrating, and storing, 378
 confirming orientation and sequence of insert, 374
 disadvantages of, 385

- expressing transgenes through, 369–387
- infecting chick embryos via injection, 379–382
- transfection with, 310–314
- Reverse genetics, 196, 200–201
 - in PC12 cell lines, 270
- RNA
 - as *Xenopus* culture injections, 131
 - metabolism studies in *Drosophila*, 203
 - preparing injection samples of, 132–133
- Robon-Beard cells, 140
- Roche Laboratories, 137
- Rodent cortical neurons, 4
- Rodent sensory neurons, 3
- Rous sarcoma virus vectors, 370

- S**
- Schistocerca americana*, 3
- Secof-type cultures, 228
- Secretion assays, in PC12 cell lines, 272–274
- Secretory vessel dynamics, 267
 - PC12 studies of, 271–283
 - PC12 usefulness for, 268
- Segment boundary epithelium, in Tibia-1
 - pathway studies, 174–176
- Semaphorins, 177–181
- Sensory system, recording from, in *Drosophila*, 236–237
- Shibire mutation, 204
- Shuttle vectors, 372
 - choice of, with AdEasy system, 391
 - inserting genes of interest into, 393
- Signaling mechanisms, 113
 - B35 cell lines in study of, 288
 - in hippocampal and cortical neurons, 112
 - studies of, 9
- Signalling, receptor mediated, 12
- Silicone aquarium sealant, 119
- Single neurons, extracting in *Heliosoma*, 164
- Single nucleotide polymorphism (SNP)
 - mapping, 200
- Single-cell injection, of *Xenopus* cultures, 138–139
- SIAX 12 NCO adapter vector, 369–370
 - selecting and modifying for
 - insertion, 372–374
- Slice cultures
 - biolistic transfection of, 354
 - in Purkinje neuron studies, 90
- Slow axonal transport, mechanism of, 306
- SlowFade antifade, 187
- Snail dissection, 158
- Snails (*Aplysia*), 3
- Snails (*Heliosoma*), 157–169
- Society for Developmental Biology
 - (<http://sdb.bio.purdue.edu/>), 85
- Solutions, for spinal and motor neuron
 - cultures, 82–85
- Source properties, 11–12
- Spastic paraplegia, 291
- Species
 - criteria for choosing, 9–10
 - quantity of neuron yields, 11
- Spinal cord medium, 84
- Spinal cord neurons
 - experimental uses of, 80–82
 - plating, 78–79
- Spinal motor neurons, 3
 - chick embryo access procedures, 71–72
 - chick embryo sources for, 67–68
 - dissection of spinal cords for, 72–75
 - enrichment by density gradient
 - centrifugation, 79–80
 - growing and working with, 67–85
 - incubation procedure, 70
 - isolation of chick embryos for, 72
 - isolation of ventral halves for, 73–77
 - materials needed for culture, 70
 - plating, 78–79
- Spinal neurons, 3
- Spinocerebellar ataxia, associated with Purkinje
 - neurons, 91
- Sprague-Dawley rates, 113
- Squid giant axon, diameters of, 9
- Stable transfectants
 - in B35 cells, 295–296
 - isolation of, 281
- Stage drift, 320
- Sterilization procedures, spinal and motor neuron
 - cultures, 82
- Stochastic interactions, between neurons and
 - target cells, 145
- Stoelting (www.stoeltingco.com), 71
- StonedB protein, in *Drosophila* vesicle
 - recycling, 204
- Stroke, cortical and hippocampal involvement
 - in, 112
- Subcellular delivery, of PTP cargo, 329
- Subcellular fractionation, of fly heads, 206–207
- Substance P immunoreactive sensory neurons, 140
- Substrate
 - for chick ciliary ganglion neurons, 37
 - for peripheral neurons, 19–22
- Substrate coatings, 21
 - for spinal and motor neuron cultures, 84

- Substratum-bound molecules, as guidance cues, 2–3
 - Superior cervical ganglia, culturing neurons from, 306–310
 - Suppliers, of neuron species, 13
 - Surface tension, affecting success of biolistics, 364
 - Survivability
 - enhancing, of hippocampal and cortical neuronal cultures, 124
 - of *Xenopus* cultures, 138–139
 - Suspension, infection of neuronal tissues in, 411
 - Sutter P-97 Flaming-Brown micropipette puller, 311
 - Sympathetic explant culture, 29
 - Sympathetic ganglion, rat, dissection of, 26
 - Sympathetic neuronal culture, maintenance of, 23
 - Synapses, production of, 10
 - Synaptic interactions
 - cerebellum as study model for, 91
 - enhanced via cocultures, 145
 - in *Drosophila* studies, 203
 - in hippocampal and cortical neurons, 111, 112
 - Synaptic vesicles, 205
 - Synaptogenesis
 - enhancing, 124
 - in *Drosophila* studies, 196
 - in hippocampal and cortical neurons, 112
- T**
- Target interactions
 - altered in mutations, 224–228
 - in chick embryos, 68
 - study of Tibia-1 pathway, 172
 - Targeted gene disruptions, 196
 - Technic, Inc., 355
 - Temperature
 - and choice of neuronal culture, 12
 - of cell suspension, as electroporation parameter, 347
 - Temperature-sensitive paralytics, 204
 - Tenascin, in *Xenopus* cultures, 140, 146
 - Tet-off and tet-on adenoviral vector systems, 413
 - Thickening agents, for peripheral neuron cultures, 24
 - Throughput, enhanced in neural-enriched cultures, 143–144
 - Tibia-1 pathway
 - advantages of studying, 172
 - axon guidance mechanisms in, 176–183
 - blocking antibody/peptide molecules in culture, 185
 - ectopic expression in developing limb bud, 185, 190–191
 - embryo cultures, 186–187
 - embryonic development of, 173–176
 - embryonic dissection, 186
 - filleting limb buds to access, 188–189
 - guidance molecules in, 177–183
 - immunochemistry protocols, 187
 - laboratory protocols for studying, 186–191
 - neuronal anatomy of, 173–176
 - neuronal labeling protocol, 190
 - peripheral to central nervous system direction, 174
 - procedures for analyzing, 183–186
 - staging grasshopper embryos for, 183
 - Time-lapse imaging
 - fluorescence, 319
 - in Tibia-1 pathway studies, 185, 187
 - Timing of expression, in biolistics, 364
 - Tissue culture dishes
 - for peripheral neurons, 19
 - in *Xenopus* cultures, 145
 - Tissue culture plastic, as substrate, 11–12
 - Tissue explants, culturing in *Xenopus*, 139
 - Tissue thickness, as parameter of
 - biolistics, 355
 - Titer assays, for adenovirus vectors, 400–402
 - Toxicity, reduced in biolistic transfection, 354
 - Toxicological assays, 287–288
 - chick forebrain neurons in, 53
 - of protein transduction domains and peptides, 328–329
 - Tr1 cell, in Tibia-1 pathway studies, 174
 - Transcription control, 201
 - Transfection
 - affecting choice of neuronal culture, 2
 - biolistic, 354–367
 - by nuclear injection, 310–314
 - chick ciliary neurons, with DNA plasmids, 39
 - focused on single or small groups of cells, 367
 - in B35 cell lines, 295–297
 - low efficiencies in PC12 cell lines, 278
 - mediated by Chariot PTP, 328–329
 - of B35 neuroblastoma cells, 287
 - with GFP, 293
 - of PC12 cell lines, 268
 - of primary central and peripheral nervous system neurons by
 - electroporation, 339–349
 - peripheral neurons and, 18
 - secretion assays with human growth hormone, 271–283

- transient electrical permeabilization, 340
 - vs. infection methods, 370
 - Transfection harvests, expanding, 399–400
 - Transgenes
 - expression not regulated with adenoviruses, 413
 - expression via replication-deficient adenovirus, 388–413
 - expression via retroviral infection, 369–385
 - in *Drosophila* studies, 220–222
 - stable expression of, 8
 - upper limit on usable size, 371
 - use in *Xenopus* cultures, 130
 - Transgenic flies, 201
 - Transmembrane potential, increase during electroporation, 341
 - Transwell migration assay, in B35 cell lines, 299–300
 - TRITC-dextran, 132
 - Trophic factors, in chick embryos, 68
 - Trypsin, in chick ciliary neuron cultures, 42
 - Type 5 adenovirus, structure, modification, and replication of, 389
- U**
- Ultracentrifuge, 138
 - Ultraviolet photolysis, in live-cell imaging studies, 152–154
 - Universal Imaging Corporation, 319
 - Untreated glass, as substrate in *Xenopus* cultures, 146
- V**
- Ventral spinal cord (chick), isolation of, 76
 - Vertebrate axon guidance mechanisms, similarity with grasshopper Tibia-1 pathway, 172
 - Vertebrate growth cones, compared with *Heliosoma* growth cones, 159
 - Vertebrate retinal ganglion cells, 3
 - Vesicle dynamics, 226–227
 - Virakit purification, 402
 - Viral toxicity, 411
 - Viral vectors
 - and species specificity, 9
 - disadvantages compared with biolistics, 354
 - transfection by, 310–313
 - Virtual Embryo (<http://www.ucalgary.ca>), 85
 - Viruses, methods for purification of, 401
 - Vitronectin, in *Xenopus* cultures, 146
- Voltage, as parameter of electroporation, 346
- Voltage-gate ionic currents, 232
- W**
- Web sites, for spinal and motor neuron cultures, 85
 - Whole cell patch-clamp recording, 229–232
 - Wild Leitz Instrument, 96
 - Wild-type adenovirus infection issues, 405–406
 - Wild-type reference lines, 202
 - Wolff, Kaspar Friedrich, 68
 - World Precision Instruments (www.wpiinc.com), 71
- X**
- Xenopus laevis*, 130
 - Xenopus* motor neurons, 5
 - ambient laboratory temperatures for, 12
 - high rate of outgrowth in, 9
 - quantity of yield from, 11
 - size of, 9
 - suppliers of, 13
 - Xenopus* neural tube, 3
 - Xenopus* species, facilities for, 13
 - Xenopus* spinal neurons
 - advantages of using, 130, 139–140
 - cocultures of, 145
 - culture substrata for, 145–148
 - culturing, 139–148
 - developmental properties of, 5
 - dissociated mixed cultures of, 141–143
 - easy culture of, 130
 - lipofection of, 136–138
 - live cell culture of, 129–154, 148–154
 - neural-enriched cultures of, 143–145
 - neuronal labeling of, 131–139
 - preparation of injection samples for, 132–133
 - protracted generation time of, 130
 - rapid rostral-to-caudal development of, 130
 - RNA/DNA injections of, 132–133
 - simple anatomy of, 130
 - single-cell injections into, 138–139
- Z**
- Zebrafish, 3
 - as forward genetic system, 228
 - compared with *Xenopus* culture, 130
 - Zygote (<http://zygote.swarthmore.edu/>), 85

This Page Intentionally Left Blank

VOLUMES IN SERIES

Founding Series Editor
DAVID M. PRESCOTT

Volume 1 (1964)
Methods in Cell Physiology
Edited by David M. Prescott

Volume 2 (1966)
Methods in Cell Physiology
Edited by David M. Prescott

Volume 3 (1968)
Methods in Cell Physiology
Edited by David M. Prescott

Volume 4 (1970)
Methods in Cell Physiology
Edited by David M. Prescott

Volume 5 (1972)
Methods in Cell Physiology
Edited by David M. Prescott

Volume 6 (1973)
Methods in Cell Physiology
Edited by David M. Prescott

Volume 7 (1973)
Methods in Cell Biology
Edited by David M. Prescott

Volume 8 (1974)
Methods in Cell Biology
Edited by David M. Prescott

Volume 9 (1975)
Methods in Cell Biology
Edited by David M. Prescott

Volume 10 (1975)
Methods in Cell Biology
Edited by David M. Prescott

Volume 11 (1975)
Yeast Cells
Edited by David M. Prescott

Volume 12 (1975)
Yeast Cells
Edited by David M. Prescott

Volume 13 (1976)
Methods in Cell Biology
Edited by David M. Prescott

Volume 14 (1976)
Methods in Cell Biology
Edited by David M. Prescott

Volume 15 (1977)
Methods in Cell Biology
Edited by David M. Prescott

Volume 16 (1977)
Chromatin and Chromosomal Protein Research I
Edited by Gary Stein, Janet Stein, and Lewis J. Kleinsmith

Volume 17 (1978)
Chromatin and Chromosomal Protein Research II
Edited by Gary Stein, Janet Stein, and Lewis J. Kleinsmith

Volume 18 (1978)
Chromatin and Chromosomal Protein Research III
Edited by Gary Stein, Janet Stein, and Lewis J. Kleinsmith

Volume 19 (1978)
Chromatin and Chromosomal Protein Research IV
Edited by Gary Stein, Janet Stein, and Lewis J. Kleinsmith

Volume 20 (1978)
Methods in Cell Biology
Edited by David M. Prescott

Advisory Board Chairman

KEITH R. PORTER

Volume 21A (1980)

Normal Human Tissue and Cell Culture, Part A: Respiratory, Cardiovascular, and Integumentary Systems

Edited by Curtis C. Harris, Benjamin F. Trump, and Gary D. Stoner

Volume 21B (1980)

Normal Human Tissue and Cell Culture, Part B: Endocrine, Urogenital, and Gastrointestinal Systems

Edited by Curtis C. Harris, Benjamin F. Trump, and Gray D. Stoner

Volume 22 (1981)

Three-Dimensional Ultrastructure in Biology

Edited by James N. Turner

Volume 23 (1981)

Basic Mechanisms of Cellular Secretion

Edited by Arthur R. Hand and Constance Oliver

Volume 24 (1982)

The Cytoskeleton, Part A: Cytoskeletal Proteins, Isolation and Characterization

Edited by Leslie Wilson

Volume 25 (1982)

The Cytoskeleton, Part B: Biological Systems and *in Vitro* Models

Edited by Leslie Wilson

Volume 26 (1982)

Prenatal Diagnosis: Cell Biological Approaches

Edited by Samuel A. Latt and Gretchen J. Darlington

Series Editor

LESLIE WILSON

Volume 27 (1986)

Echinoderm Gametes and Embryos

Edited by Thomas E. Schroeder

Volume 28 (1987)

***Dictyostelium discoideum*: Molecular Approaches to Cell Biology**

Edited by James A. Spudich

Volume 29 (1989)
**Fluorescence Microscopy of Living Cells in Culture, Part A: Fluorescent Analogs,
Labeling Cells, and Basic Microscopy**

Edited by Yu-Li Wang and D. Lansing Taylor

Volume 30 (1989)
**Fluorescence Microscopy of Living Cells in Culture, Part B: Quantitative
Fluorescence Microscopy—Imaging and Spectroscopy**

Edited by D. Lansing Taylor and Yu-Li Wang

Volume 31 (1989)
Vesicular Transport, Part A

Edited by Alan M. Tartakoff

Volume 32 (1989)
Vesicular Transport, Part B

Edited by Alan M. Tartakoff

Volume 33 (1990)
Flow Cytometry

Edited by Zbigniew Darzynkiewicz and Harry A. Crissman

Volume 34 (1991)
Vectorial Transport of Proteins into and across Membranes

Edited by Alan M. Tartakoff

Selected from Volumes 31, 32, and 34 (1991)
Laboratory Methods for Vesicular and Vectorial Transport

Edited by Alan M. Tartakoff

Volume 35 (1991)
Functional Organization of the Nucleus: A Laboratory Guide

Edited by Barbara A. Hamkalo and Sarah C. R. Elgin

Volume 36 (1991)
***Xenopus laevis*: Practical Uses in Cell and Molecular Biology**

Edited by Brian K. Kay and H. Benjamin Peng

Series Editors

LESLIE WILSON AND PAUL MATSUDAIRA

Volume 37 (1993)
Antibodies in Cell Biology

Edited by David J. Asai

Volume 38 (1993)**Cell Biological Applications of Confocal Microscopy***Edited by Brian Matsumoto***Volume 39 (1993)****Motility Assays for Motor Proteins***Edited by Jonathan M. Scholey***Volume 40 (1994)****A Practical Guide to the Study of Calcium in Living Cells***Edited by Richard Nuccitelli***Volume 41 (1994)****Flow Cytometry, Second Edition, Part A***Edited by Zbigniew Darzynkiewicz, J. Paul Robinson, and Harry A. Crissman***Volume 42 (1994)****Flow Cytometry, Second Edition, Part B***Edited by Zbigniew Darzynkiewicz, J. Paul Robinson, and Harry A. Crissman***Volume 43 (1994)****Protein Expression in Animal Cells***Edited by Michael G. Roth***Volume 44 (1994)*****Drosophila melanogaster*: Practical Uses in Cell and Molecular Biology***Edited by Lawrence S. B. Goldstein and Eric A. Fyrberg***Volume 45 (1994)****Microbes as Tools for Cell Biology***Edited by David G. Russell***Volume 46 (1995) (in preparation)****Cell Death***Edited by Lawrence M. Schwartz and Barbara A. Osborne***Volume 47 (1995)****Cilia and Flagella***Edited by William Dentler and George Witman***Volume 48 (1995)*****Caenorhabditis elegans*: Modern Biological Analysis of an Organism***Edited by Henry F. Epstein and Diane C. Shakes***Volume 49 (1995)****Methods in Plant Cell Biology, Part A***Edited by David W. Galbraith, Hans J. Bohnert, and Don P. Bourque*

Volume 50 (1995)**Methods in Plant Cell Biology, Part B**

Edited by David W. Galbraith, Don P. Bourque, and Hans J. Bohnert

Volume 51 (1996)**Methods in Avian Embryology**

Edited by Marianne Bronner-Fraser

Volume 52 (1997)**Methods in Muscle Biology**

Edited by Charles P. Emerson, Jr. and H. Lee Sweeney

Volume 53 (1997)**Nuclear Structure and Function**

Edited by Miguel Berrios

Volume 54 (1997)**Cumulative Index****Volume 55 (1997)****Laser Tweezers in Cell Biology**

Edited by Michael P. Sheez

Volume 56 (1998)**Video Microscopy**

Edited by Greenfield Sluder and David E. Wolf

Volume 57 (1998)**Animal Cell Culture Methods**

Edited by Jennie P. Mather and David Barnes

Volume 58 (1998)**Green Fluorescent Protein**

Edited by Kevin F. Sullivan and Steve A. Kay

Volume 59 (1998)**The Zebrafish: Biology**

Edited by H. William Detrich III, Monte Westerfield, and Leonard I. Zon

Volume 60 (1998)**The Zebrafish: Genetics and Genomics**

Edited by H. William Detrich III, Monte Westerfield, and Leonard I. Zon

Volume 61 (1998)**Mitosis and Meiosis***Edited by Conly L. Rieder***Volume 62 (1999)*****Tetrahymena thermophila****Edited by David J. Asai and James D. Forney***Volume 63 (2000)****Cytometry, Third Edition, Part A***Edited by Zbigniew Darzynkiewicz, J. Paul Robinson, and Harry Crissman***Volume 64 (2000)****Cytometry, Third Edition, Part B***Edited by Zbigniew Darzynkiewicz, J. Paul Robinson, and Harry Crissman***Volume 65 (2001)****Mitochondria***Edited by Liza A. Pon and Eric A. Schon***Volume 66 (2001)****Apoptosis***Edited by Lawrence M. Schwartz and Jonathan D. Ashwell***Volume 67 (2001)****Centrosomes and Spindle Pole Bodies***Edited by Robert E. Palazzo and Trisha N. Davis***Volume 68 (2002)****Atomic Force Microscopy in Cell Biology***Edited by Bhanu P. Jena and J. K. Heinrich Hörber***Volume 69 (2002)****Methods in Cell–Matrix Adhesion***Edited by Josephine C. Adams***Volume 70 (2002)****Cell Biological Applications of Confocal Microscopy***Edited by Brian Matsumoto*

This Page Intentionally Left Blank